

**Design and Synthesis of Quinoline and Quinazolinone
Derivatives through Transition Metal-Catalyzed
Cascade Protocols**

THESIS

Submitted in partial fulfillment of the requirements for degree of
DOCTOR OF PHILOSOPHY

by

SHIV DHIMAN

ID No. 2013PHXF0406P

Under the supervision of

Prof. Anil Kumar

and

Under the co-supervision of

Prof. Dalip Kumar



**BIRLA INSTITUTE OF TECHNOLOGY AND SCIENCE
PILANI (RAJASTHAN) INDIA-2019**

Dedicated to
My beloved parents

**BIRLA INSTITUTE OF TECHNOLOGY AND SCIENCE
PILANI (RAJASTHAN)**

CERTIFICATE

This is to certify that the thesis entitled “**Design and Synthesis of Quinoline and Quinazolinone Derivatives through Transition Metal-Catalyzed Cascade Protocols**” submitted by **Mr. Shiv Dhiman** ID No **2013PHXF0406P** for the award of Ph. D. Degree of the Institute embodies the original work done by him under our supervision.

Signature in full of the Supervisors:

Name in capital block letters: **Prof. ANIL KUMAR**

Designation: Professor

Date:

Name in capital block letters: **Prof. DALIP KUMAR**

Designation: Professor

Date:

ACKNOWLEDGMENTS

It is a moment of pleasure to recapture the several memorable moments, numerous people, who joined me in this long journey, whose continuous guidance, support, help, motivation, and blessing at the different stages helped to achieve this milestone of my life.

First and foremost, I would like to express my deep sense of gratefulness to my research supervisor Prof. Anil Kumar and co-supervisor Prof. Dalip Kumar for their constant guidance and support throughout my Ph.D. tenure. Without their enthusiastic motivation and expertise in organic synthesis achievement of this research work would have remained a dream. I am indebted to Prof. Anil Kumar for mentoring me and teaching me necessary things, endless chemistry discussions and allowing me to work in a laboratory without any pressure. His inspiration and supportive conversations with no time boundaries have helped me to become a successful researcher. His continued motivation and suggestions in technical writing resulted in the form of high-quality publications which are unprecedented in such a less period. I am also highly thankful to Prof. Anil Kumar for providing opportunities to work central NMR facility and to teach and mentor undergraduate and newcomer students in his laboratory which added valuable experience in my Ph.D. life.

I am greatly thankful to the former and present Vice-Chancellors, Directors, Deans and Associate Deans of Birla Institute of Technology & Science, Pilani (BITS Pilani) for allowing me to pursue my doctoral studies by providing necessary facilities and financial support.

I am profoundly grateful for the cooperation and affection extended by all the respected teachers: Prof. S. C. Sivasubramanian, Prof. Subit K. Saha, Prof. Ram. K. Roy, Prof. Saumi Ray, Prof. Bharti Khungar, Prof. Inamur R. Laskar, Prof. Surojit Pande, Prof. Shamik Chakraborty, Prof. Madhushree Sarkar, Prof. Ajay K. Sah, Dr. Prashant U. Manohar, Dr. Bibhas R. Sarkar, and staff members of Department of Chemistry, BITS Pilani, Pilani Campus for their constant guidance and substantial support at different stages during my research period. I am grateful to the members of my Doctoral Advisory Committee, Prof. Indresh Kumar and Prof. Rajeev Sakhuja for their excellent cooperation in refining my research proposal and thesis. My special thank is also extended to Mrs. Pusplata Ji for teaching me how to perform lab experiments in Gen. Chem. Lab, even access to use lab equipment and providing some required general chemicals.

I also acknowledge department of chemistry, BITS Pilani for providing me Institute fellowship during the tenure of my Ph.D. Also, DST-FIST is also sincerely acknowledged for providing instrumentation facilities in the department. My sincere thanks to Mr. Giridhar Kunkur, Librarian and other staff of library BITS Pilani for their support and help rendered while utilizing the library services.

I am grateful to Prof. Mukund Jha for giving me an opportunity to visit his lab at Nipissing University, Ontario, Canada and allowing me to work with their group for six months with the financial support. I wish to acknowledge Prof. R. Krishnan from Department of Chemistry, BITS Pilani, Hyderabad Campus, and Dr. Katherine N. Robertson, Department of Chemistry, Saint Mary University, Halifax for providing us single X-ray crystal analysis. I also thank our biology collaborators Dr. Rajnish Singh (Postdoc., Israel) for studying antimicrobial activity, Prof Benu Brata (IACS, Kolkata) and his student Ms. Srijita for studying leishmanial parasite activity of synthesized series of imidazopyridine fused heterocycles. I am also delighted to thank Dr. Om Prakash S. Patel, Dr. Kiran Bajaj, and Dr. Dinesh Kumar Sengottuvelu for their support and inspiration during my research work.

My special thanks to Dr. Sushil Pandey (Group Leader, Jubilant Chemsys Ltd., Noida) without his motivation, I would not have joined BITS Pilani. My sincere thanks to Dr. Arunendra Pathak (Associate Director, Jubilant Chemsys Ltd.) and Prashant Deb (Director, Jubilant Chemsys Ltd.) for their support and motivation. The words are inadequate to express my gratitude to my friends like a brothers Mr. Abhishek Sharma (Science Teacher, Kendriya Vidyalaya) and Mr. Ravi Pratap Singh (Research Scientist II, Jubilant Chemsys Ltd.) for their continuous support in all situations of my Ph.D. tenure. Their positive energy and ideal thoughts always gave exterior help to overcome struggles.

My special thanks to my senior lab colleague Dr. Kamesh Rao, Dr. Manoj Muthyala, Dr. Kasiviswanadharaju Pericherla Dr. Ganesh Shelke, Dr. Poonam Kedar, Dr. Sunita, and Dr. Pinku Kaswan, for their continued help and friendly atmosphere which always inspired me to work hard and together in one team at BITS Pilani. I would not find enough word of gratitude for my dear labmates Mr. Hitesh Kumar Saini, Mrs. Khima Pandey, Ms. Saroj Budania, Mr. Nitesh Kumar Nandwana, Mrs. Vaishali Saini, Mr. Vikki Shinde Ms. Sonam Jaspal, Ms. Neha Meena and Mr. Ram Prasad Bhatta for their support and love. I have learned a lot of essential things which are very important for my research and professional life. I thank all of you guys individually for your cooperation, caring and a charming company that made my Ph.D. life a bit easier in BITS Pilani. I am grateful to BITS graduate students Ms. Shreemala Dayal (BITS Alumni), Mr. Dhruv Agarwal, Ms. Megha Saini and Nipissing University undergraduate student Mr. Ben, Mr. Jordan, Mr. Steven, Mr. Eric and Ms. Laura with whom I have worked.

I am highly thankful to Dr. Hemant Joshi for discussion on palladium complex and helping in the design and synthesis of these compounds. His positive energy always motivated me to work smartly.

I extend my heartfelt thanks to research scholars and friends belonging from BITS Pilani, Dr. Amrith Sarmah, Dr. Rituparna, Dr. Nisar Ahmed Mir, Dr. Noorulla Baig, Dr. Mukund Tantak, Dr. V. Arun, Dr. Meenakashi Pilania, Dr. Ashok Sharma, Dr. Pankaj Nehra, Dr. Archana, Dr. Santosh Kumari, Dr. Fayaz Baig, Dr. P. O Venkata Ramana Reddy, Dr. Roshan Nazir, Dr. Sunita

Poonia, Dr. Sourab Mundra, Dr. Pankaj Wadhwa, Dr. Subhash Saini, Dr. Paakaj Munjal, Ms. Pallavi Rao, Mrs. Rajendra Shivran, Mr. Anoop Singh, Mrs. Sushila Poonia, Ms. Sonam Sharma, Mr. Vishal, and Mr. Vimal for their valuable help and charming company during my Ph.D. I am also thanking to my departmental juniors Ms. Bijoya, Ms. Moyna, Mr. Aabid, Mrs. Megha, Ms. Mamta Sharma, Ms. Mamta, Ms. Krishma, Mr. Mahesha, Mr. Dhritabrata, Mr. Amol, Mr. Bintu, Mr. Pramod, Mr. Santosh, Ms. Ashwariya, and Ms. Prachi, Ms. Gurpreet Kaur, Mr. Sumit, and Ms. Soumona whose positive response and help .

My acknowledgment can never be complete without the special mention of my roommates and Ph.D. friends Mr. Nitesh Kumar Nandwana, Mr. Devesh Agarwal and Mr. Manish Mehra for their continuous support in course work, brainstorming discussion and cheering me up all the time.

I extend my heartfelt gratitude to my best friends: Mr Arun Sharma, Mr. Varun Kohli (IT engineer, Paris), Mr. Rishi Chaudhary, Mr. Raman Sharma (QC executive, Sun Pharma), Mr. Raghu Sharma (Sr. RS, Fresenius Kabi Oncology), Mr. Pritpal Singh (RS, Mankind Research Center), Mr. Ranbir Rana (QC executive, Sun Pharma) for their extreme support.

I am fortunate to say thanks to many of my friends Mr. Navnath Kadam (Scientist E2, Lupin), Mr. Shyamsunder Pal (SRA, Jubilant Chemsys), Mr. Dipankar Roy (SRA, PI Industry), Mr. Dibendu Mahapatra (SRA, Jubilant Chemsys) Mr. Ramakrishana (RS-II, Jubilant Chemsys), Mr. Shri Hari (SRA, Jubilant Chemsys), Dr. Chatarsal (RS-II, Jubilant Chemsys), Mr. Sunil Khamkar (Scientist, BASF), Mr D. N. Chiranjeevi (RS, Syngene), Mr. Narender Rawat, Mr. Raghuram (Ph.D student, NIT Manipur), Mr. Nagaraju (Ph.D student, NIT Manipur), Dr. Dharmender (Ph.D student, NIT Jalandhar), Mr. Ranjeet Singh (Ph.D student, PU, Chandigarh), Ms. Priyanka Dhiman (Ph.D student, IIT-Roorkee), Dr. Seema Dhiman (Postdoc. fellow, Israel), Mr. Anish Nair (Sr. Engineer, Bruker), Mr. Manmohan Vyas (Sr. Engineer, Bruker), Dr. Muthamil (Ph.D student, CMST, Chennai), Mr. Arjun (Postdoc. fellow, Purdue University, USA), Dr. Suresh (BITS Alumni), Mr. Ramesh (Assistant Professor, Haryana) for their continuous support and charming company.

It is beyond the words to express my deep sense of gratitude to my parents Sh. Gurmeet Singh and Smt. Veena Dhiman for their moral support, endless inspiration and make my education very comfortably and enjoyable from the very beginning till the end. My special thanks and love to my younger brothers Sunny and Amit, I won't find enough words for their kind support, care, and love.

I deeply acknowledge a very special person who entered in my life during my research journey and will continue the journey with me, my beloved wife, Ritika Sembhi. Her indispensable support, high level of patience and unstopping flow of love in my endeavors which motivated me to reach my destination. During my research, God has given a very special gift when I become a father of little angel Saanvi. Her beautiful smile and cheerful activities always remove my

tiredness and reboot me automatically. I extended my heartfelt thanks to my Father-in-Law Sh. Ram Lal Sembhi for his endless patience, encouragement and constant support in all circumstances.

I duly acknowledge valuable financial support in the form of a research fellowship from Ranbaxy Project, BITS Pilani, and CSIR-New Delhi.

Last but not least, I bow my head to Almighty who gave me enough strength to work hard and cross the toughest situations.

Shiv Dhiman

ABSTRACT

Over the last few years, significant attention has been focus towards the development of biologically relevant *N*-heterocycles such as Indoles, quinolines, isoquinolines, and quinazolines by employing transition metal-catalyst. Because of these *N*-heterocyclic framework exhibits a variety of biological activity, found in various natural products, marketed drugs and in material science.

The thesis entitled “**Design and Synthesis of Quinoline and Quinazolinone Derivatives through Transition Metal-Catalyzed Cascade Protocols**” deals with the synthesis of selected *N*-heterocycles such as quinolines, imidazopyridine fused quinoline, quinazolines, and aza-fused isoquinolines by using transition metal-catalyst.

The first chapter of the thesis describes a brief overview on azides as one nitrogen source in the synthesis of various nitrogen-containing heterocycles and provide new innovative strategies towards the synthesis of *N*-heterocycles in the presence of transition metal-catalysts.

The second chapter of the thesis describes the synthesis of *N*-heterocycles using sodium azide as one nitrogen source and chapter is divided into three parts. **Part-A** deals with the synthesis of functionalized quinolines using transition metal-catalyst with recent literature survey. After that, describe the synthetic protocol for the synthesis of 2-aminoquinoline-3-carboxylates and 2-arylquinoline-3-carbonitriles by multicomponent reaction of 2-bromobenzaldehydes, active methylene nitriles and sodium azide as a nitrogen source in the presence of copper-catalysis. The developed methodology further utilized for one-pot synthesis of pyrimido[4,5-*b*]quinolin-4(3*H*)-ones in good yield. **Part-B** presents the simple and efficient protocol for the rapid synthesis of pyrido[2',1':2,3]imidazo[4,5-*c*]quinolones through Cu(I)-catalyzed three component, one-pot reaction of 2-(2-bromophenyl)imidazo[1,2-*a*]pyridines, aldehydes, and sodium azide. A series of twenty-seven compounds were prepared by varying different substituents on substrates in moderate to good yields (45-75%) and evaluated for their *in-vitro* antibacterial activity against three Gram-negative bacteria *S. typhi*, *K. pneumoniae*, *P. putida* and two Gram-positive bacteria *B. cereus*, *S. aureus*. Compounds, **3ae**, **3ai**, and **3cc**, exhibited moderate antibacterial activity against Gram-negative bacteria *S. typhi* and *P. putida*. **Part-C** described the synthesis of quinazolinones from 2-bromobenzamides, aldehydes and sodium azide *via* one-pot copper-catalyzed amination, condensation, and oxidative amidation. The reaction pathway proposed by performing series of control experiments. Good functional group tolerance, mild condition, readily

available starting materials and user friendly procedure makes this protocol practically good and attractive method for the synthesis of quinazolin-4(3*H*)-ones.

The third chapter of the thesis disclose a concise overview of the transition metal-catalyzed arylation strategies towards the synthesis of non-benzodiazepine drug azole-fused isoquinolines. Later on, this chapter focus on the synthetic method of imidazole and benzimidazole fused isoquinolines *via* Pd(II)-catalyzed intramolecular C-H arylation from 2-bromobenzaldehydes and 2-(1*H*-imidazol-1-yl/benzimidazolyl-1-yl)-1-arylethanones. The developed method proceeded through cross Knoevenagel condensation of 2-(1*H*-imidazol-1-yl/benzimidazolyl-1-yl)-1-arylethanones with 2-bromobenzaldehyde followed by Pd(II)-catalyzed intramolecular C-H arylation.

The fourth chapter of the thesis deals the synthesis of aroyl functionalized pyrazolo[5,1-*a*]isoquinolines by reaction of 1-aryl-2-(1*H*-pyrazol-1-yl)ethan-1-ones and 2-bromo aldehydes under Ni(II)-catalysis. This process involves, Initially Knoevenagel condensation followed by Ni(II)-catalyzed intramolecular arylation at C5 of pyrazole.

Finally, in **the fifth chapter** of the thesis, a summary of the thesis work is presented along with the future scope of the research work.

TABLE OF CONTENTS

	Page No	
Certificate	i	
Acknowledgments	ii	
Abstract	vi	
List of tables	xi	
List of figures	xiii	
List of abbreviations and symbols	xv	
Chapter 1: Synthesis of <i>N</i>-Heterocycles Using Azides as One Nitrogen Source: An Overview		
1.1	Introduction	2
1.2	Synthesis of <i>N</i> -heterocycles using azides as one <i>N</i> -source	4
1.2.1	Pyrroles	4
1.2.2	Indoles	5
1.2.3	Quinoline and isoquinoline derivatives	8
1.2.4	Carbazoles and acridines	10
1.2.5	Benzimidazoles and indazoles analogues	12
1.2.6	Quinazoline derivatives	15
1.2.7	<i>N</i> -fused heterocycles	17
1.2.8	Miscellaneous <i>N</i> -heterocycles	18
1.3	Conclusions	19
1.4	References	19
Chapter 2A: Copper-Catalyzed One-Pot Synthesis of Quinoline Derivatives		
2A.1	Introduction	24
2A.2	Different approaches for the synthesis of quinolines	25
2A.2.1	Ruthenium and Rhodium catalyst	27
2A.2.2	Palladium catalyst	32
2A.2.3	Copper catalyst	36
2A.2.4	Miscellaneous transition metal-catalyzed synthesis of quinolines	41
2A.3	Results and discussion	45
2A.4	Conclusions	55
2A.5	Experimental section	55

2A.6	References	70
Chapter 2B: One-Pot Synthesis of Pyrido[2',1':2,3]imidazo[4,5-<i>c</i>]quinoline Derivatives and their Antimicrobial Activity		
2B.1	Introduction	76
2B.2	Results and discussion	80
2B.2.1	Chemistry	80
2B.2.2	Biology	86
2B.2.2.1	Antibacterial activity	86
2B.2.2.2	Evaluation of cell death	88
2B.2.2.3	Bactericidal kinetics	88
2B.2.2.4	Live dead cell screening	89
2B.3	Conclusions	90
2B.4	Experimental section	90
2B.4.1	Biological studies	99
2B.5	References	101
Chapter 2C: Cu(I)-Catalyzed Three-Component Cascade Synthesis of Quinazolin-4(3<i>H</i>)-Ones		
2C.1	Introduction	105
2C.1.1	Synthesis of quinazolinones from 2-aminobenzamides	106
2C.1.2	Synthesis of quinazolinones from 2-bromobenzamides	111
2C.2	Results and discussion	116
2C.3	Conclusions	123
2C.4	Experimental section	123
2C.5	References	135
Chapter 3: Pd(II)-Catalyzed One-Pot Synthesis of Benzimidazo/Imidazo[1,2-<i>a</i>]-isoquinolines		
3.1	Introduction	141
3.2	Results and discussion	152
3.3	Conclusions	162
3.4	Experimental section	163
3.5	References	169

Chapter 4: Nickel-Catalyzed One-Pot Cascade Synthesis of Pyrazolo[5,1-<i>a</i>]-isoquinolines		
4.1	Introduction	173
4.1.1	Synthetic routes for the construction of pyrazolo[5,1- <i>a</i>]isoquinolines	173
4.1.2	Nickel-catalyzed direct C-H arylation using haloarenes/pseudohaloarenes	178
4.2	Results and discussion	182
4.3	Conclusions	194
4.4	Experimental section	194
4.5	References	211
Chapter 5: Conclusions		
5.1	General conclusions	215
5.2	Specific conclusions	216
5.3	Future scope of the research work	220
Appendices		
	List of publications	A-1
	Publication abstracts	A-2
	List of Poster Presented in Conferences/Workshop	A-3
	Brief Biography of the candidate	A-4
	Brief Biography of the supervisor	A-5
	Brief Biography of the co-supervisor	A-6

LIST OF TABLES

No	Title	Page No
2A.1	Optimization of reaction condition for the synthesis of ethyl 2-aminoquinoline-3-carboxylate.	49
2A.2	Substrate scope for the synthesis of 2-aminoquinoline derivatives	50
2A.3	Substrate scope for the synthesis of 2-arylquinoline-3-carbonitriles	51
2A.4	Sample and crystal data of 104af	65
2A.5	Data collection and structure refinement of 104af	65
2A.6	Atomic coordinated and equivalent isotropic displacement parameters (Å)	66
2A.7	Bond angle (Å)	67
2A.8	Bond angle (°)	68
2A.9	Anisotropic atomic displacement parameters (Å)	69
2B.1	Optimization of reaction condition for copper catalyzed one-pot reaction.	82
2B.2	Substrate scope of PIQs (4)	84
2B.3	<i>In vitro</i> antibacterial activity of pyrido[2',1':2,3]imidazo[4,5- <i>c</i>]quinolines	87
2C.1	Optimization of reaction condition for the synthesis of 3aa	117
2C.2	Substrate scope for the synthesis of 2,3-disubstituted quinazolin-4(3 <i>H</i>)-ones	119
3.1	Optimization of reaction conditions	155
3.2	Substrate scope for the Pd-catalyzed tandem synthesis of azole fused isoquinolines	157
4.1	Optimization of reaction condition for the synthesis of pyrazolo[5,1- <i>a</i>]isoquinoline	187

4.2	Substrate scope of pyrazolo[5,1- <i>a</i>]isoquinolines (56)	190
4.3	Crystal data and structure refinement for 56ae	209
4.4	Crystal data and structure refinement for 57a'	210

LIST OF FIGURES

Figure No.	Caption	Page No
2A.1	Antimalarial drugs containing quinoline framework	24
2A.2	Selective compounds containing a quinoline scaffold	25
2A.3	¹ H NMR spectrum of 96aa	46
2A.4	¹³ C NMR spectrum of 96aa	46
2A.5	IR spectrum of 96aa	47
2A.6	HRMS spectrum of 96aa	47
2A.7	ORTAP diagram of 104aa (CCDC 1433055)	54
2B.1	Selective examples of imidazo[1,2- <i>a</i>]pyridine based molecules	76
2B.2	¹ H NMR spectrum of 4ab	81
2B.3	¹³ C NMR spectrum of 4ab	81
2B.4	A) and B) Killing efficacy of 4ae , 4ai , and 4cc against <i>S. typhi</i> and <i>P. putida</i> , respectively	88
2B.5	A) and B) Kinetic study of 4ae , 4ai , and 4cc for inhibition of bacterial growth of <i>S. typhi</i> and <i>P. putida</i> , respectively	89
B.6	Fluorescence images of <i>S. typhi</i> A) without treatment; B) on treatment with 4ae ; C) on treatment with 4cc ; D) on treatment with 4ai	89
2C.1	Selected examples of natural product containing quinazolin-4(3 <i>H</i>)-one	105
2C.2	Quinazolin-4(3 <i>H</i>)-one based drugs and synthetic bioactive compounds	106
2C.3	IR spectrum of 3ac	120
2C.4	¹ H NMR spectrum of 3ac	120
2C.5	¹³ C NMR spectrum of 3ac	121
3.1	General strategy of C-H activation and functionalization	142
3.2	Representative molecules containing isoquinoline framework	143
3.3	Inhibition against h-NPP-1 and h-NPP-3 by compounds 36a and 36b , respectively	149
3.4	IR spectrum of 46aa	152
3.5	¹ H NMR spectrum of 46aa	153

3.6	¹³ C NMR spectrum of 46aa	153
3.7	HRMS spectrum of 46aa	154
3.8	Mass analysis of reaction mixture	158
3.9	¹ H NMR spectrum of 47aa	159
3.10	¹³ C NMR spectrum of 47aa	160
3.11	HMBC spectrum of 47aa	161
3.12	2D NOESY spectrum of 47aa	161
4.1	Representative examples of some bioactive pyrazolo[5,1- <i>a</i>]isoquinolines	173
4.2	¹ H NMR spectrum of 54a	183
4.3	¹³ C NMR spectrum of 54a	183
4.4	IR spectrum of 54a	184
4.5	¹ H NMR spectrum of 56aa	185
4.6	¹³ C NMR spectrum of 56aa	185
4.7	IR spectrum of 56aa	186
4.8	HRMS spectrum of 56aa	186
4.9	ORTEP diagram of 56ae	191
4.10	ORTEP diagram of 57a'	192
5.1	Systematically representation of thesis	215
5.2	Graphical representation to access various <i>N</i> -heterocycles using azides	216
5.3	Some quinoline-base heterocycles	221

LIST OF ABBREVIATIONS/SYMBOLS

Abbreviation/Symbol	Description
α	Alpha
β	Beta
δ	Delta
μW	Microwave
$^{\circ}\text{C}$	Degree centigrade
\AA	Angstrom
AcOH	Acetic acid
ACN	Acetonitrile
Ar	Aryl
Aq.	Aqueous
Bn	Benzyl
Bu	Butyl
$t\text{BuOK}$	Potassium <i>tert</i> -butoxide
$t\text{BuOLi}$	Lithium <i>tert</i> -butoxide
Calcd.	Calculated
^{13}C	Carbon-13
CDC	Cross-dehydrogenative coupling
CDCl_3	Deuterated chloroform

CNS	Central nervous system
Conc.	Concentration
CuAAC	Copper catalyzed azide-alkyne cycloaddition
^c Pr	Cyclopropyl
d	Doublet
dd	Doublet of doublet
DABCO	1,4-Diazabicyclo[2.2.2]octane
DBU	1,8-Diazabicyclo[5.4.0]undec-7-ene
DCE	Dichloroethane
DCM	Dichloromethane
DCPM	Bis(dicyclohexylphosphino)methane
DDQ	2,3-Dichloro-5,6-dicyanobenzoquinone
DMA	<i>N,N</i> -Dimethylacetamide
DME	1,2-Dimethoxyethane
DMF	<i>N,N</i> -Dimethylformamide
DMSO- <i>d</i> ₆	Deuterated dimethylsulfoxide
DPPE	1,2-Bis(diphenylphosphino)ethane
ESI	Electron spray ionization mass spectrometry
ESIPT	Excited state intramolecular proton transfer
EtOAc	Ethyl acetate
Et	Ethyl

EtOH	Ethanol
Eq.	Equivalent
g	Gram
h	Hours
HRMS	High resolution mass spectrometry
HMBC	Heteronuclear multiple bond correlation
IR	Infrared
ⁱ Pr	Isopropyl
Hz	Hertz
<i>J</i>	Coupling constant
Lit.	Literature
MCR	Multi component reaction
Me	Methyl
MS	Mass spectrometry
mp	Melting point
m	Multiplet
mg	Milligram
MHz	Mega hertz
min	Minutes
mL	Milliliter

mmol	Millimole
N ₂	Nitrogen gas
NBS	<i>N</i> -bromosuccinimide
NIS	<i>N</i> -iodosuccinimide
NMR	Nuclear magnetic resonance
NMP	<i>N</i> -methylpyrrolidone
NOESY	Nuclear overhauser effect spectroscopy
O ₂	Oxygen gas
PEG	Polyethylene glycol
PivOH	Pivalic acid
PIDA	Phenyl iodonium diacetate
Ph	Phenyl
1,10-Phen	1,10-Phenanthroline
ppm	Parts per million
Pr	Propyl
%	Percentage
<i>p</i> -TsOH	<i>p</i> -Toluenesulfonic acid
rt	Room temperature
s	Singlet
SET	Single electron transfer

t	Triplet
TBAB	Tetrabutylammonium bromide
TBAI	Tetrabutylammonium iodide
TBHP	<i>tert</i> -Butyl hydroperoxide
TEA	Triethylamine
TEMPO	2,2,6,6-tetramethylpiperidine-1-oxyl
TEMDA	<i>N,N,N,N</i> -Tetramethyl ethylenediamine
TFA	Trifluoroacetic acid
TFE	Tri(2-furyl)phosphine
TfOH	Trifluoromethanesulfonic acid
THF	Tetrahydrofuran
TLC	Thin layer chromatography
TMS	Tetramethylsilane
TMSN ₃	Trimethylsilyl azide
TPP	Triphenylphosphine
OTf	Trifluoromethanesulfonate

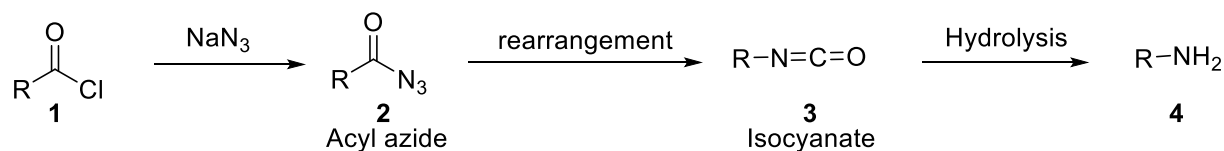
CHAPTER 1

Synthesis of *N*-Heterocycles Using Azides as One Nitrogen Source: An Overview

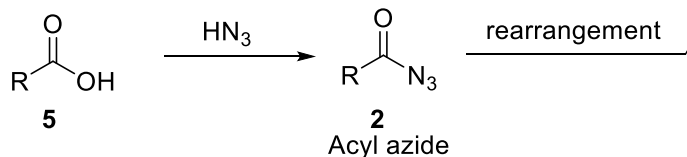
1.1 INTRODUCTION

Nitrogen-containing heterocycles are abundant in natural products, pharmacophores and many bioactive motifs as compared to other heterocycles and carbocycles.^[1-5] Most of the nitrogen-containing heterocycles (indoles, quinolines, quinazolines, benzimidazoles, etc.) have been synthesized using anilines, which are prepared by reduction of their nitroarene analogues.^[6-7] Since the synthesis of first phenyl azide by Peter Grieb, the organic azide intermediates have gained significant interest.^[8-9] Later on, Curtius^[10] and Schmidt^[11-12] discovered the rearrangement of acyl azides (**2**) to isocyanates (**3**), which further transformed into various organic molecules such as amines, amides, ureas and urethanes (**Scheme 1.1**).^[13] Multiple methods can synthesize organic azides; the traditional way of azide formation is the reaction of diazonium salts with hydrazines.^[8-9, 14] The most common and widely used method for the formation of azide derivatives is a nucleophilic substitution reaction of haloarenes/alkyl halides with sodium azide which produces corresponding azide in quantitative yields.^[8-9, 15-16]

Curtius Rearrangement



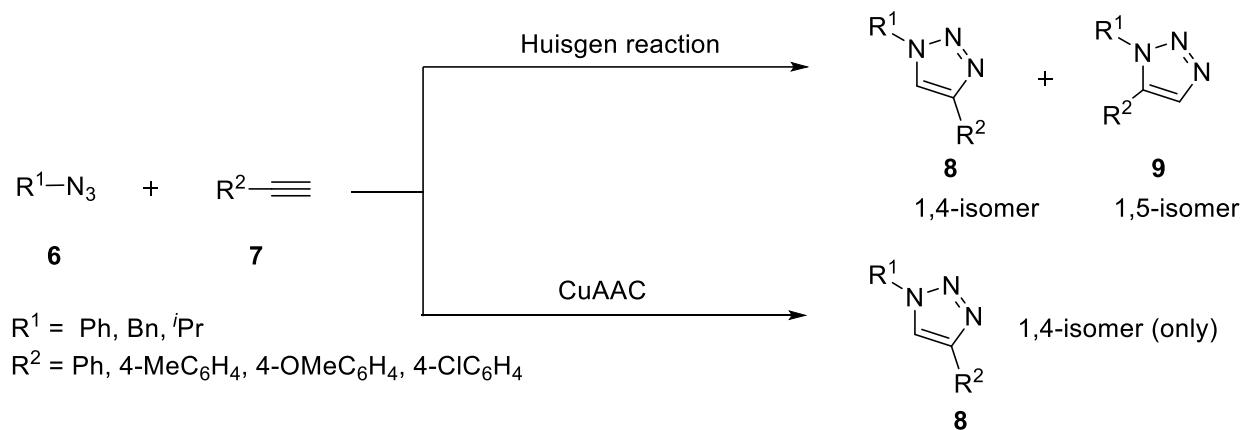
Schmidt Rearrangement



Scheme 1.1: Synthesis of amines using acyl azide

Azides readily decompose and release the nitrogen molecule by the input of external pressure and heat, and thus result in the explosion.^[8-9] Heavy metal azides are primarily used in explosive technology. Ionic azide such as sodium azide is more stable as compared to organic azides. It decomposes thermally by heating above 275 °C. However, organic azides have been used as pharmacophore in drug design such as azidothymidine (AZT) for the treatment of HIV^[17] and as valuable substrates in various organic synthesis, for example, Hassner reaction,^[18] Staudinger reaction,^[19] Boyer rearrangement^[20] and Hemetsberger rearrangement^[21].

The reactivity of azide varies in different reaction conditions used. Azides can be used as three N-atom synthons or one N-atom synthon according to reaction condition. Rolf Huisgen developed the first 1,3-dipolar cycloaddition reaction for the synthesis of triazoles (**8** and **9**) by using organic azides as three N-atom source (**6**) and alkynes (**7**) (**Scheme 1.2a**).^[22] However, this reaction has a regioselectivity issue, producing both disubstituted triazole isomers (1,4 and 1,5). Later on, Barry Sharpless and Meldal group independently reported the copper-catalyzed Huisgen's cycloaddition reaction and exclusively produced regioselectively 1,4-disubstituted triazoles (**8**).^[23] This 1,3-dipolar cycloaddition reaction further referred as copper-catalyzed azide-alkyne cycloaddition (CuAAC) click reaction (**Scheme 1.2b**).^[24] The click reaction is that reaction where reactants efficiently consumed and produce products in quantitatively yield under mild reaction condition. Over the last few years, AAC click reaction has been extended to other metal-catalyst such as Ni, Zn Ru, Ag and Au, although CuAAC click reactions extensively used for the synthesis of substituted triazoles.^[25-26]



Scheme 1.2: Synthesis of disubstituted triazoles using azides and alkynes

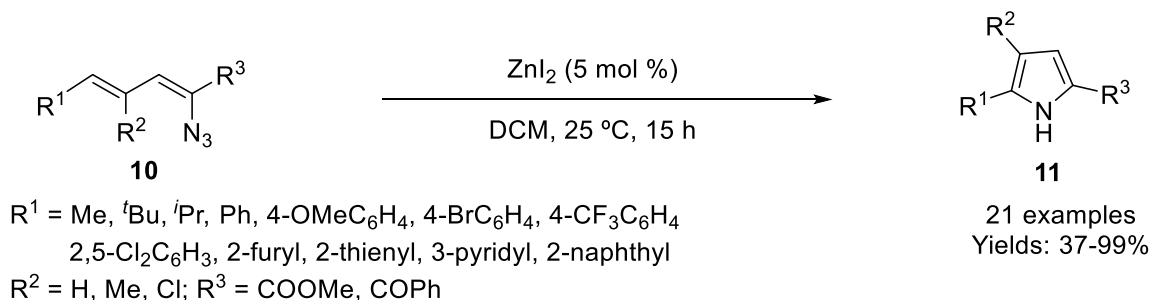
Azides have been used extensively as three N-atom sources for the synthesis of various N-heterocycles using different metal-catalyst,^[25] metal nanoparticles^[27-28] and metal-free reaction condition^[29] in the last few decades. Nowadays, synthetic chemists use azides as a pivotal one N-atom synthon for the formation of diverse nitrogen-containing heterocycles in the presence of transition metal catalysts. Transition metal reacts with azide and form nitrenoid with the release of N₂ molecule, for further transformation.^[8, 30] Azides also thermally decompose in the presence of transition metal and generated nitrenes, which react with others reactive species.^[30] This chapter

mainly focuses on transition metal-catalyzed synthesis of *N*-heterocycles using azides as one N-atom synthon.

1.2 Synthesis of *N*-heterocycles using azides as one N-source

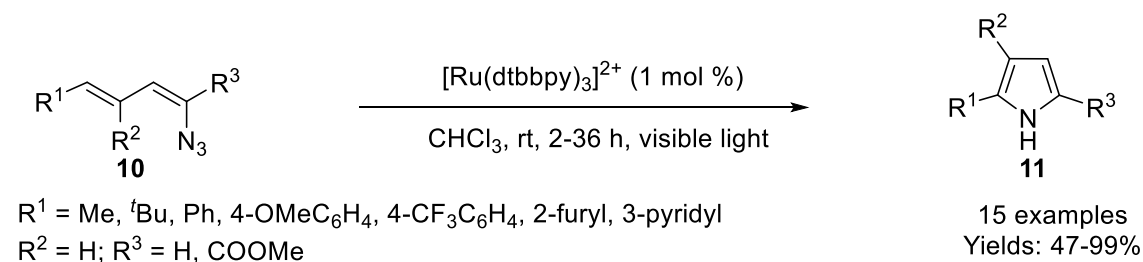
1.2.1 Pyrroles

Driver and coworkers reported the synthesis of poly-substituted pyrroles (**11**) using vinyl azides (**10**) under ZnI₂ catalyst in DCM at room temperature (**Scheme 1.3**).^[31] Various types of aromatic and aliphatic dienylazides were evaluated in this protocol and found that aromatic vinyl azides gave corresponding pyrroles in higher yields as compared to aliphatic vinyl azide. It was also observed that product yields were increased in the presence of SiO₂ (200 wt %) along with ZnI₂ and also converted both *E/Z* isomers gave the desired products (**11**). On the other hand, only *Z*-isomers was transformed into products in the presence of ZnI₂.



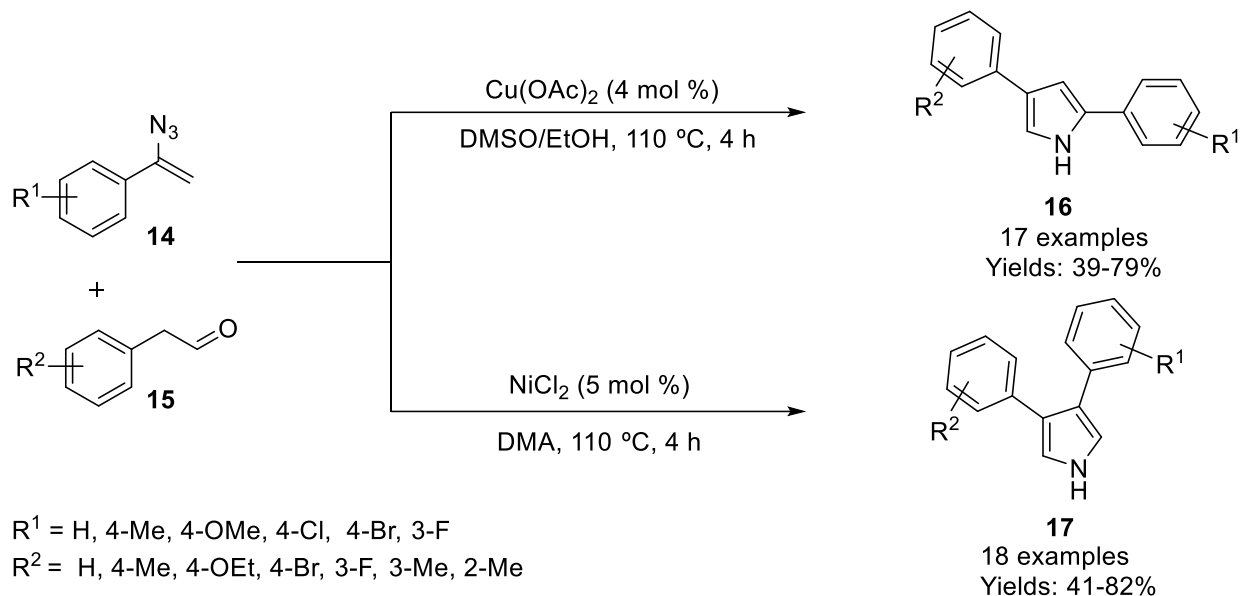
Scheme 1.3: Zn(II)-catalyzed synthesis of pyrrole using vinyl azide

In extension, Yoon group also demonstrated the synthesis of pyrroles (**11**) using Ru(II)-photoredox catalyst from dienylazides (**10**) under visible light in chloroform at room temperature (**Scheme 1.3**).^[32]



Scheme 1.4: Ru(II)-catalyzed synthesis of pyrroles using vinyl azide under visible light

Jiao *et al.* reported a new and efficient strategy for the synthesis of 2,4-disubstituted and 3,4-disubstituted pyrroles (**16** and **17**) by switching the transition metal (copper and nickel) from vinyl azides (**14**) and acetaldehydes (**15**) (**Scheme 1.5**).^[33]

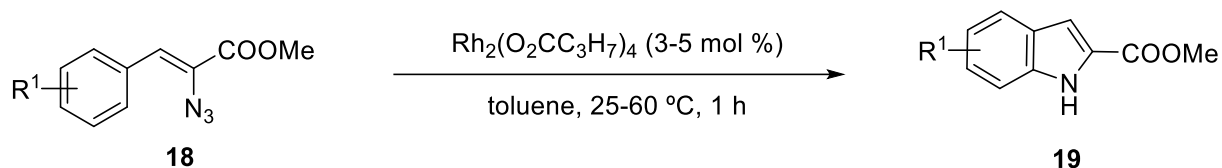


Scheme 1.5: Synthesis of 2,4 and 3,4-disubstituted pyrroles from vinyl azides (**14**)

A series of control experiments were conducted and suggested that nitrenoid was key intermediate for Cu(II)-catalyzed formation of 2,4-disubstituted pyrroles. The nucleophilic attack of enol- tautomers of phenylacetaldehyde to nitrenoid intermediate, followed by condensation, dehydration and aromatization afforded the target 2,4-disubstituted pyrroles. While in the case of Ni(II)-catalyzed reaction, initially thermal decomposition of azide forms azirine. Subsequently, nucleophilic attacks of enol-form of phenylacetaldehyde to azirine followed by azirine ring-opening generates a five-membered ring. Finally, elimination and aromatization led to the desired product (**16**).

1.2.2 Indoles

Driver and coworkers disclosed the formation of functionalized indole derivatives (**19**) by using vinyl azides (**18**) as starting materials in the presence of Rh-catalyst (**Scheme 1.6**).^[34] Variety of electron-releasing and electron-withdrawing substituents on aryl ring were well tolerated in this protocol to afford the products in 71-98% yields.

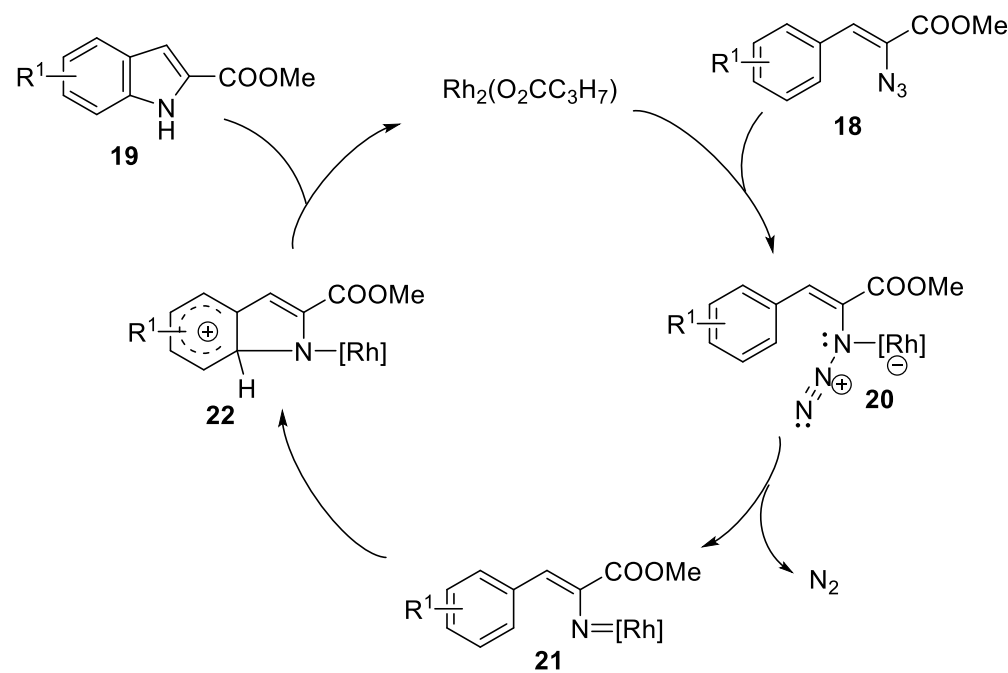


$R^1 = \text{H}, 2\text{-OMe}, 2\text{-Cl}, 2\text{-Br}, 3\text{-Me}, 3\text{-}i\text{Pr}$
 $3\text{-Cl}, 3\text{-Br}, 3\text{-CF}_3, 4\text{-Me}, 4\text{-OMe}, 4\text{-Cl}$

20 examples
 Yields: 71-98%

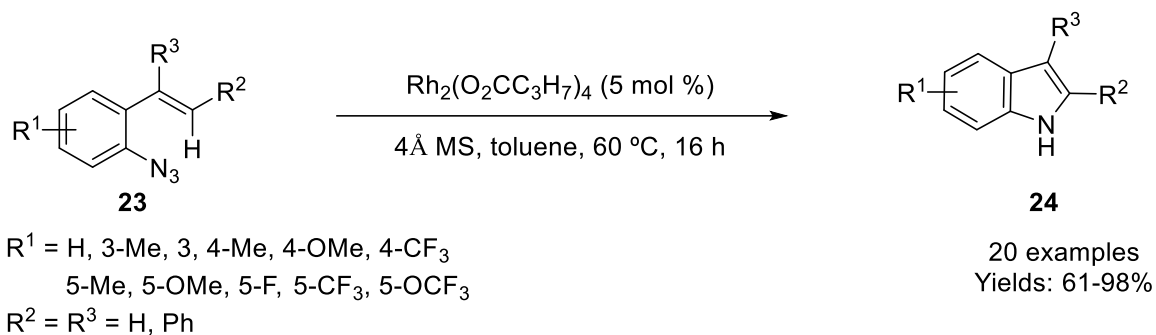
Scheme 1.6: Rh(II)-catalyzed synthesis of functionalized indoles from **18**

The reaction was proposed to proceed *via* Rh(II)-catalyzed C-H functionalization of vinyl azide ester. Initially, coordination of Rh(II)-catalyst with azides (**18**) produced rhodium nitrenoid (**20**) with the release of N_2 . Finally, the electrophilic aromatic substitution reaction led to the desired indole products (**19**). This has been confirmed by isotopic labelling experiment (**Scheme 1.7**).



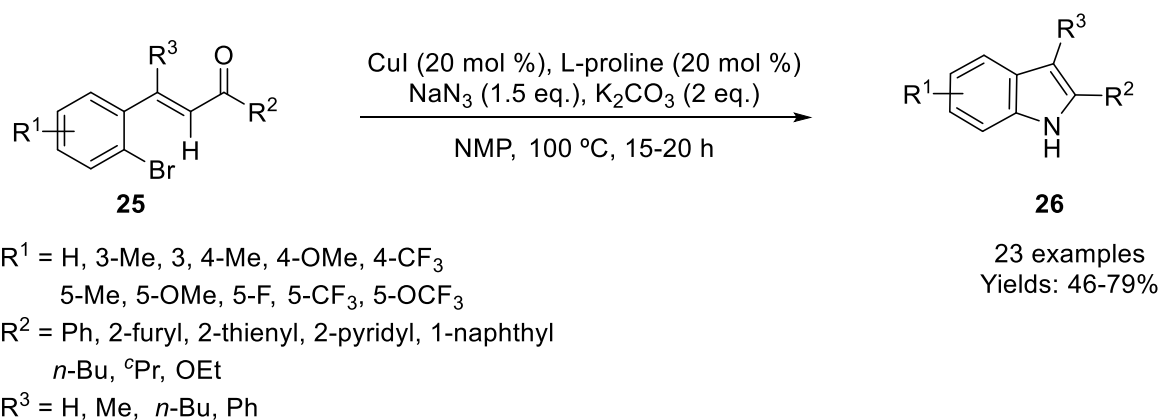
Scheme 1.7: Proposed catalytic cycle for the formation of indole from vinyl azide (**18**)

In extension, the same group reported the Rh(II)-catalyzed synthesis of indoles from arylazides (**Scheme 1.8**).^[35] This time they proposed that reaction proceeds through vinylic C-H functionalization by performing isotopic labelling experiment.



Scheme 1.8: Rh(II)-catalyzed synthesis of indoles *via* vinylic C-H functionalization

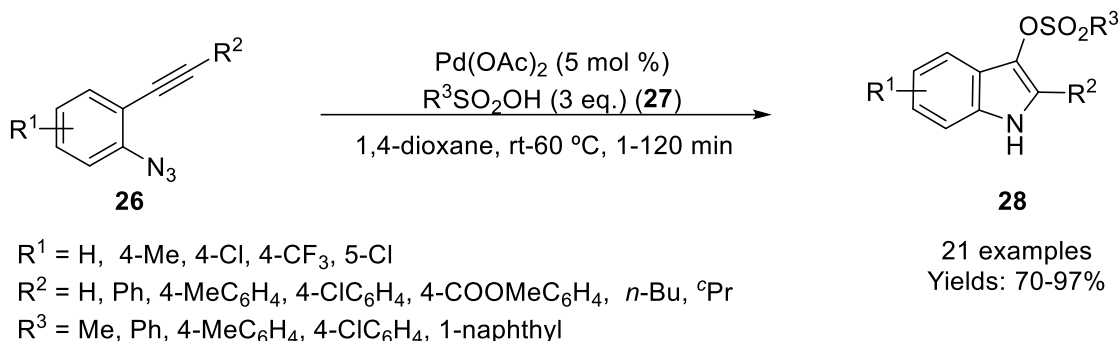
Alternatively, Ramana group disclosed the inexpensive and straightforward one-pot tandem protocol for the construction of functionalized indoles (**26**) from 2-bromochalcones (**25**) and sodium azide as one N-atom source under the copper catalysis (**Scheme 1.9**).^[36] Moreover, 2-bromocinnamates also well tolerated in the developed protocol and gave corresponding indole-2-carboxylates in good yields (57-74%). Bromochalcones with various aryl and heteroaryl ring were investigated such as phenyl, naphthyl, pyridyl, furyl, thienyl and benzofuran reacted smoothly. The developed strategy proceeded through a set of three reactions, *i.e.* (a) copper-catalyzed nucleophilic aromatic substitution reaction with azide (S_NAr); (b) conversion of azide to reactive nitrene intermediate; and (c) intramolecular C-N bond formation *via* insertion of nitrene to C-H bond.



Scheme 1.9: Synthesis of functionalized indoles from 2-bromochalcones

Rao and team also developed the method for the synthesis of 2,3-disubstituted indoles (**28**) through Pd(II)-catalyzed domino reaction of *o*-alkynyl arylazides (**26**) with sulfonic acids (**27**) (**Scheme 1.20**).^[37] Alkynes and sulfonic acids having various electron-rich and electron-poor substituents

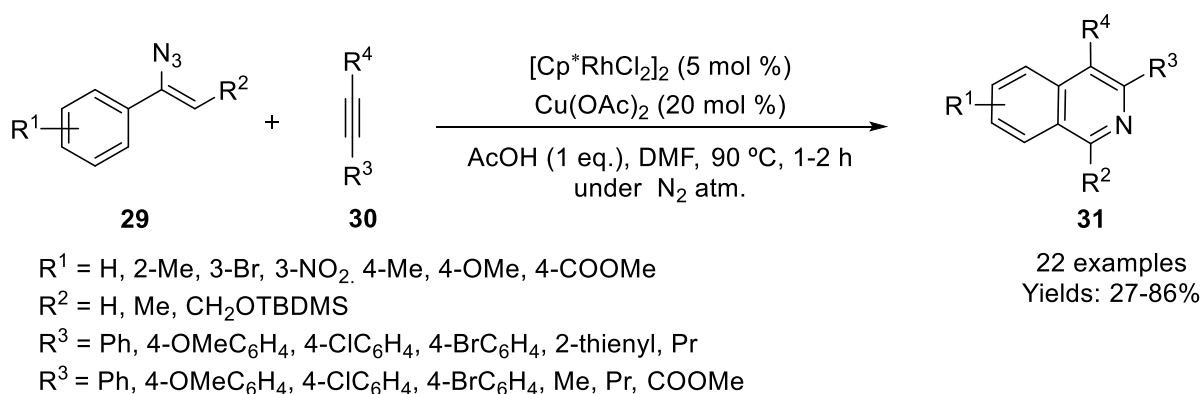
reacted smoothly under these conditions and afforded corresponding functionalized indoles in good to excellent yields (70-97%).



Scheme 1.20: Synthesis of indoles from *o*-alkynyl arylazides and sulfonic acids

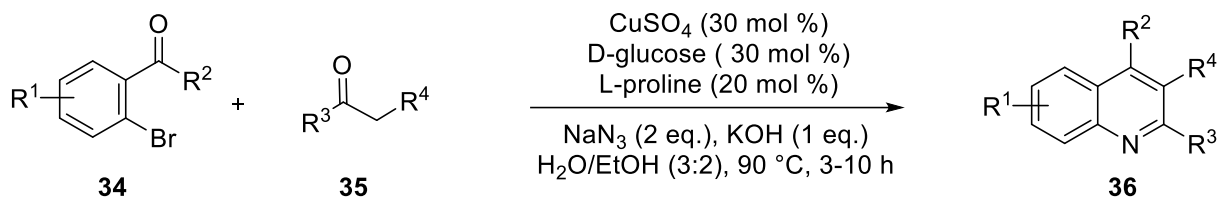
1.2.3 Quinoline and Isoquinoline Derivatives

Chiba group disclosed the synthesis of multi-substituted isoquinoline derivatives (**31**) from readily available vinyl azides (**29**) and internal alkynes (**30**) by the cooperative catalytic system of Rh(III) and Cu(II) in the presence of AcOH (**Scheme 1.21**).^[38]



Scheme 1.21: Rh(III)-catalyzed synthesis of polysubstituted isoquinolines from vinyl azides

Later on, Cheng group reported an alternate method for quinoline (**33**) synthesis from benzylic azides (**32**) and internal alkynes (**30**) via Cu(II)-catalyzed Schmidt rearrangement (**Scheme 1.22**).^[39-40]



$\text{R}^1 = \text{H}, \text{R}^2 = \text{H}, \text{Ph}$

$\text{R}^3 = \text{Ph}, 2\text{-ClC}_6\text{H}_4, 3\text{-OMeC}_6\text{H}_4, 3\text{-ClC}_6\text{H}_4$

$4\text{-MeC}_6\text{H}_4, 4\text{-OMeC}_6\text{H}_4, 4\text{-ClC}_6\text{H}_4$

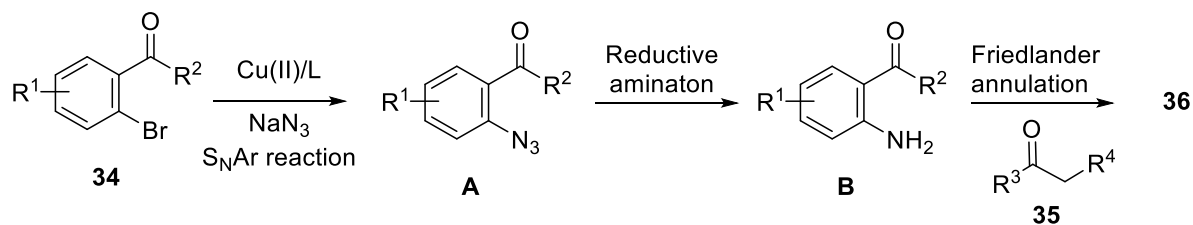
$2\text{-furyl}, 2\text{-thienyl}$

$\text{R}^4 = \text{H}, \text{Me}, \text{Et}$

16 examples
Yields: 52-95%

Scheme 1.24: Cu(II)-catalyzed synthesis of quinolines from 2-bromobenzaldehydes/ketones

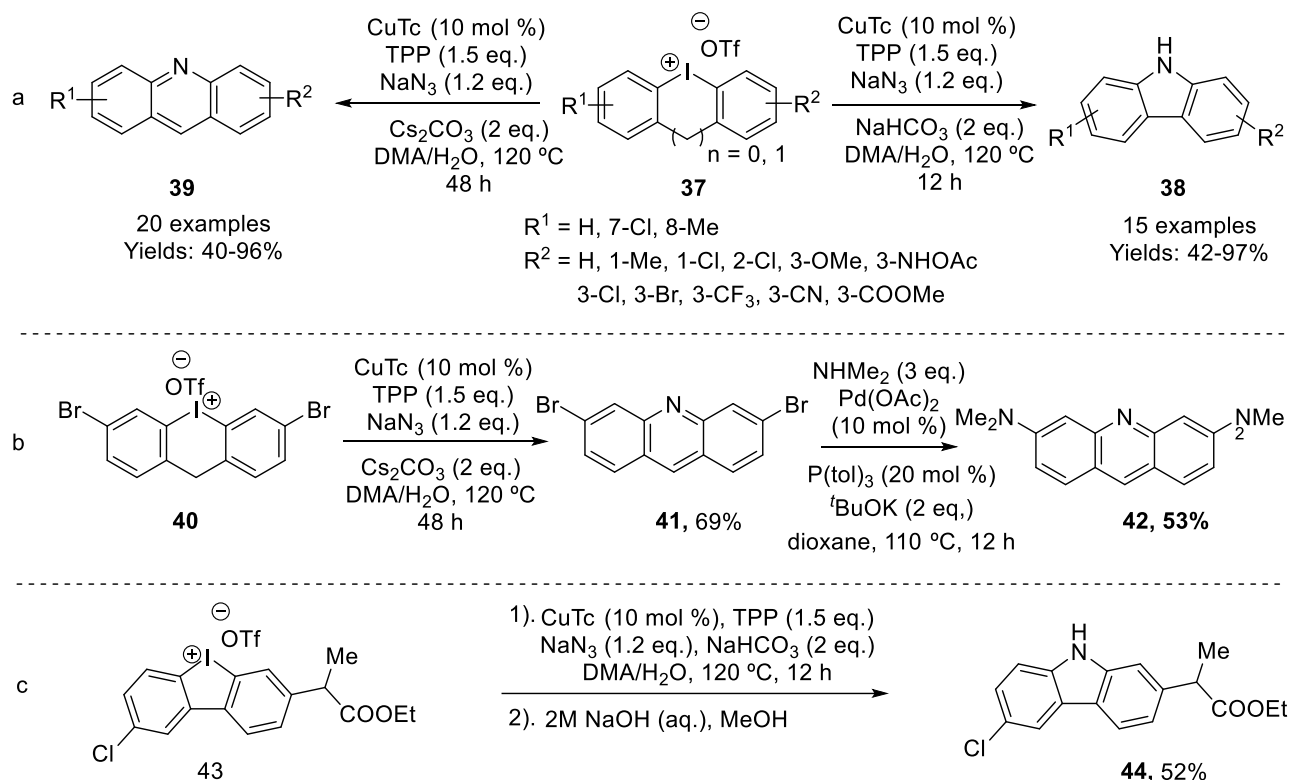
In this strategy, initially, copper-catalyzed nucleophilic aromatic substitution of 2-bromobenzaldehydes (**34**) with sodium azide generated azido intermediate (**A**) followed by reductive amination of **A** produced 2-aminobenzaldehydes (**B**). Finally, Friedlander annulation afforded the corresponding quinolines (**36**) (**Scheme 1.25**).



Scheme 1.25: Mechanism for the synthesis of quinolines from 2-bromobenzaldehydes/ketones

1.2.4 Carbazoles and Acridines

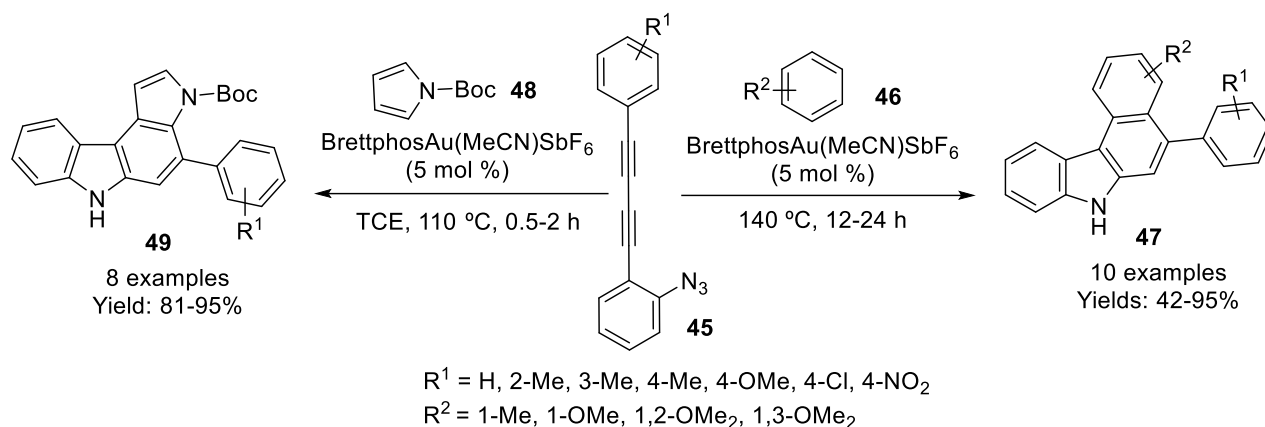
Jiang group established new synthetic route for the preparation of carbazole derivatives (**38**) from diaryliodonium salts (**37**) via copper(I) thiophene-2-carboxylate(CuTc)-catalyzed nitrogen-iodine exchange reaction in the presence of sodium azide (**Scheme 1.26a**).^[42] Further, this protocol further extended for the synthesis of acridine derivatives (**39**) by introducing one more carbon-atom in the diaryliodonium salts (**37**).



Scheme 1.26: Synthesis of carbazoles and acridines using diaryliodonium salts (**37**)

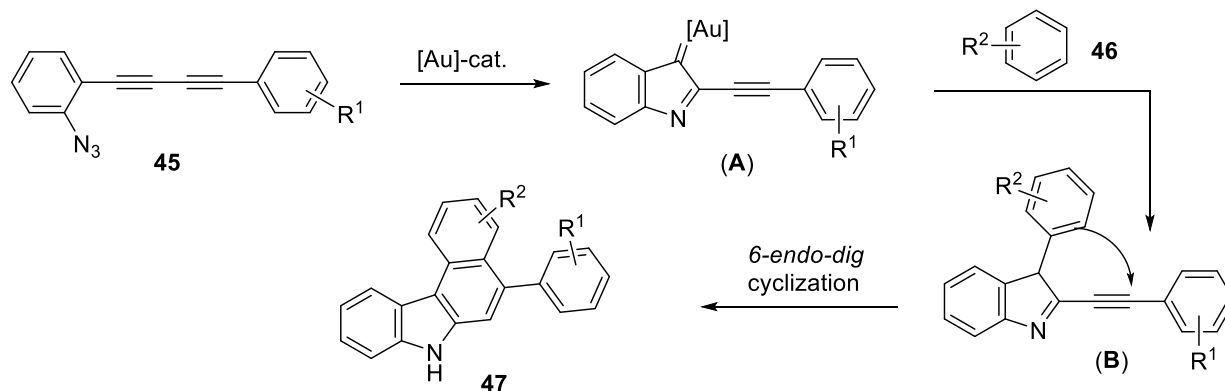
For practicability of this nitrogen-iodine protocol, synthesized acridine orange (**42**) from diaryliodonium salt (**40**) in a two-step (**Scheme 1.26b**). Furthermore, non-steroidal anti-inflammatory drug Carprofen (**44**) was synthesized using this protocol in a single step from diaryliodonium salt (**43**) (**Scheme 1.26c**).

Very recently, Ohno group achieved the carbazole (**47**) synthesis through gold-catalyzed domino annulation of conjugated alkyne (**45**) having azido functionality on aryl ring (**46**) (**Scheme 1.27**).^[43] This strategy was further extended for the synthesis of pyrrole fused carbazoles (**49**) by replacing arenes (**46**) with Boc protected pyrroles (**48**).



Scheme 1.27: Synthesis of carbazoles and pyrrole-fused carbazoles under Au-gold catalysis

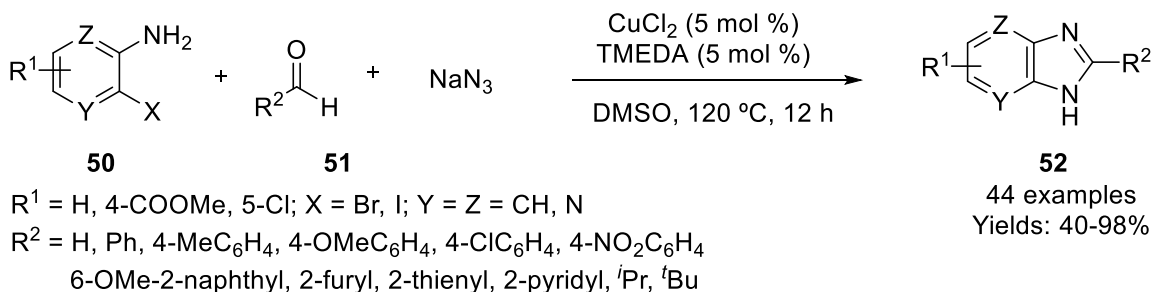
The developed method was proceeded *via* intramolecular nucleophilic attack of the azido group on the closed proximal alkyne group to form indole-gold carbenoid species (**A**). Subsequently, nucleophilic attack of arenes on indole-gold carbenoid produced intermediate (**B**), intermediate **B** on *6-endo-dig* cyclization by arenes to another alkyne group afforded desired carbazole derivatives (**47**) (**Scheme 1.28**). The proposed mechanism was supported by DFT calculation.



Scheme 1.28: Reaction mechanism for the synthesis of carbazoles *via* Au-catalyst

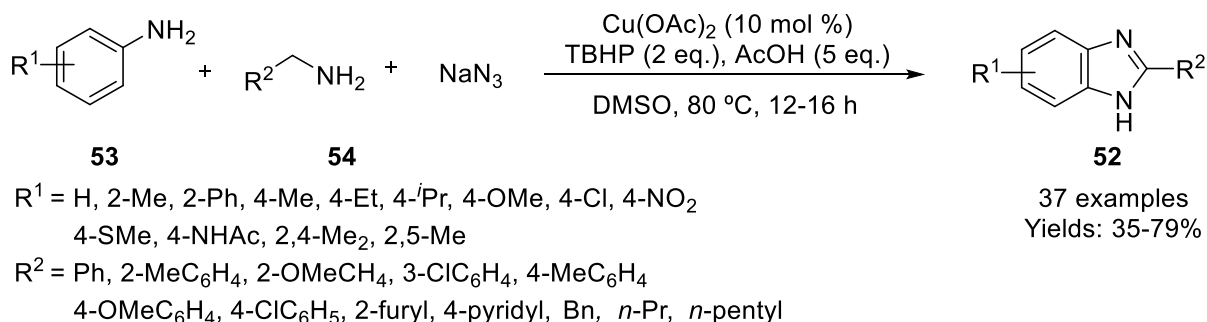
1.2.5 Benzimidazoles and Indazoles Analogues

Lee and coworkers disclosed Cu-catalyzed one-pot three-component tandem process for the synthesis of benzimidazole derivatives from *o*-haloanilines, aldehydes and sodium azide in the presence of TEMDA as a ligand in DMSO at 120 °C (**Scheme 1.29**).^[44] Both aromatic/heteroaromatic and aliphatic aldehydes reacted smoothly under these conditions and afforded corresponding benzimidazoles in moderate to excellent yields (40-98%).



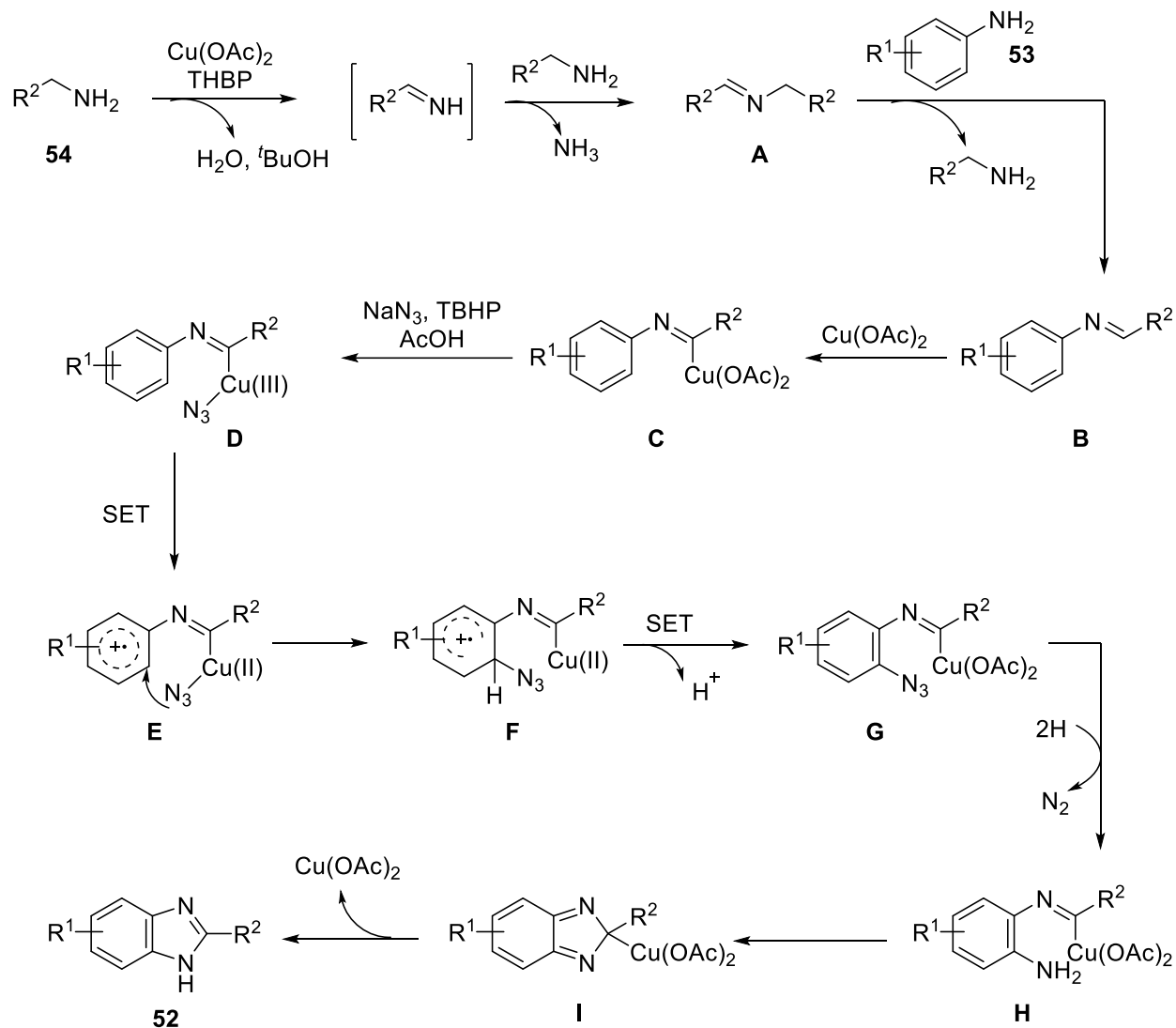
Scheme 1.29: Cu(II)-catalyzed three-component synthesis of benzimidazole derivatives

Later on, Punniyamurthy group further improved the benzimidazole synthesis by the reaction of anilines, benzylamines and sodium azide in the presence of $\text{Cu}(\text{OAc})_2$ as a catalyst, TBHP as oxidant and acetic acid as additives in DMSO at 80 °C (**Scheme 1.30**).^[45] Different anilines and benzylamines/aliphatic amines were well tolerated give desired benzimidazole derivatives in 35-79% yields. Few control experiments such as isotopic labelling and radical scavenger experiments were conducted to probe the reaction mechanism. These control experiments suggested that C-H bond was not cleaved during reaction and reaction proceeded *via* radical fashion.



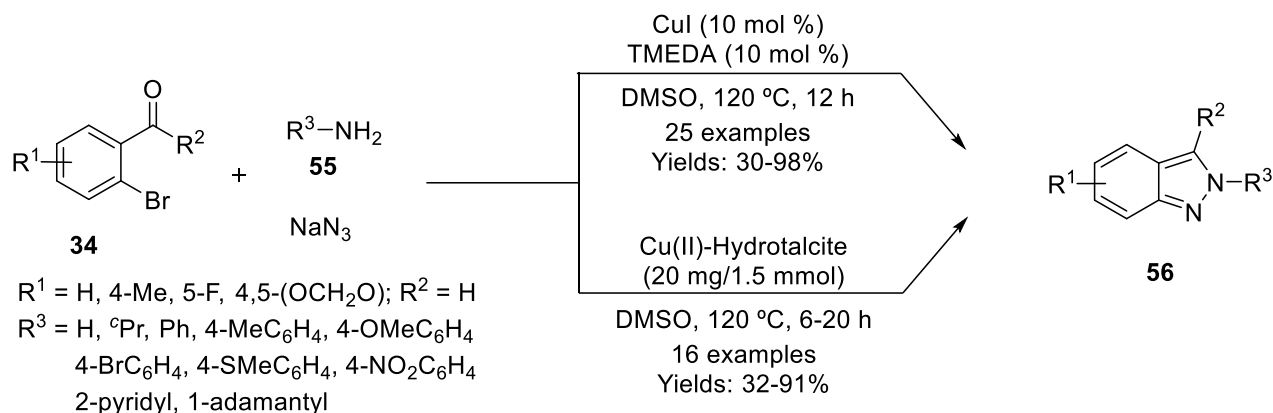
Scheme 1.30: Synthesis of benzimidazoles *via* Cu(II)-catalyzed multicomponent reaction

The proposed reaction mechanism was illustrated in **Scheme 1.31**. Initially, imine intermediate (**A**) was formed by oxidation of amines (**54**) in the presence of Cu(II) which on transamination with anilines (**53**) produced imine intermediate (**B**). Coordination of $\text{Cu}(\text{OAc})_2$ with intermediate (**B**) generated intermediate (**C**), which subsequently reacted with sodium azide in the presence of TBHP and AcOH to produce intermediate (**D**). The single electron transferred from aryl ring of aniline to metal centre further facilitated the transfer of azido group to aryl ring to form intermediate (**F**). The single electron transfer from intermediate (**F**) generated intermediate (**G**). Finally, reduction, oxidative cyclization, and aromatization led to desired benzimidazole derivatives (**52**).



Scheme 1.31: Reaction pathway for the synthesis of benzimidazoles

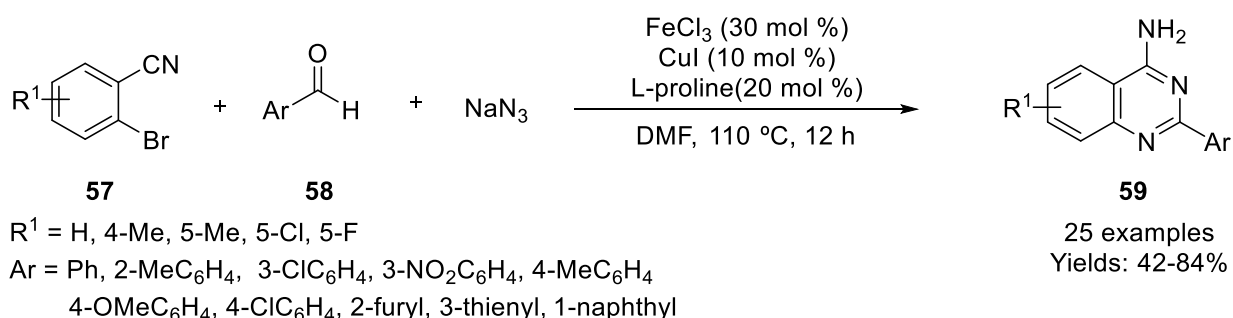
Lee and Reddy group independently reported the synthesis of indazole derivatives *via* Cu-catalyzed three-component cascade reaction of 2-bromobenzaldehydes (34), amines (55), and sodium azide (Scheme 1.32).^[46-47]



Scheme 1.32: Synthesis of indazoles through Cu-catalyzed multicomponent reaction of **34**, **55** and NaN₃

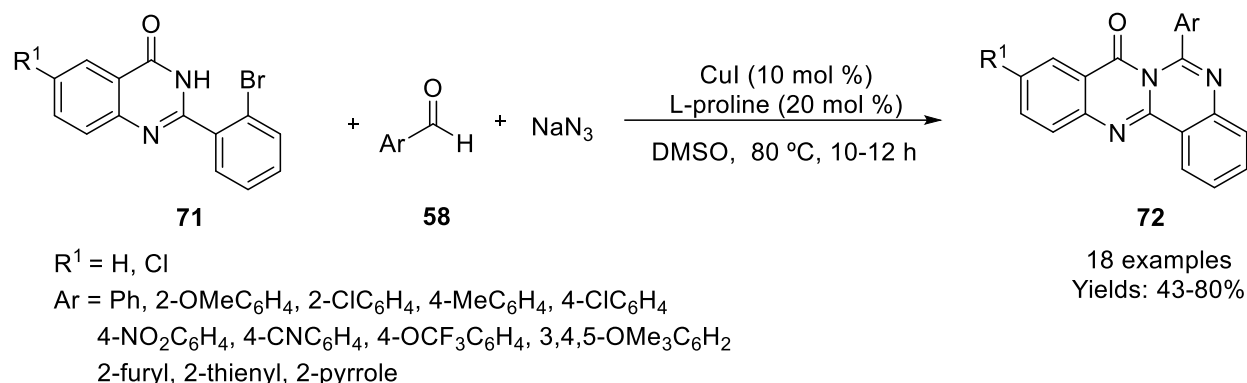
1.2.6 Quinazoline Derivatives

Wu *et al.* successfully employed the Fe(III)/Cu(I)-relay multi-component cascade process for the synthesis of 2-aryl-4-amino quinazoline derivatives from readily available 2-bromobenzonitrile, benzaldehydes and sodium azide (**Scheme 1.33**).^[48] The developed reaction proceeded through a set of reactions. i) Fe(III)-catalyzed [3+2] cycloaddition reaction between nitriles and sodium azide; ii) Cu(I)-catalyzed nucleophilic aromatic substitution with NaN₃; iii) reductive amination; iv) condensation with aldehydes; v) oxidative C-N bond formation; vi) aerobic oxidation; vii) finally, Cu(I)-catalyzed denitrogenation of tetrazoles.



Scheme 1.33: Fe/Cu-dual-catalyzed the synthesis of 2-aryl-4-amino quinazoline derivatives. Consecutively, the same group further developed a new method for the formation of substituted quinazolines through copper-catalyzed multi-component reaction of 2-bromoaldehydes, benzylamines and sodium azide (**Scheme 1.34**).^[49] In this method, benzylamines are used as a surrogate of benzaldehydes

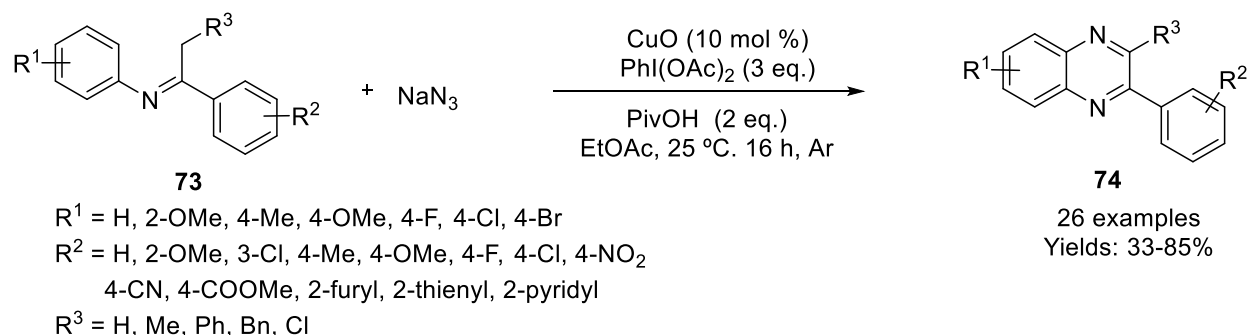
(Scheme 1.39).^[54] Different benzaldehydes having both electron-releasing and electron-withdrawing substituents were reacted smoothly in the developed optimized reaction conditions.



Scheme 1.39: Cu(I)-catalyzed one-pot synthesis of tetracyclic quinazolino[4,3-*b*]quinazolines

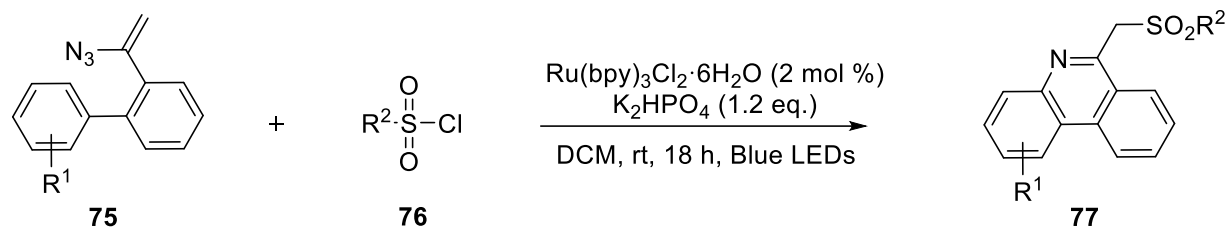
1.2.8 Miscellaneous *N*-heterocycles

The preparation of quinoxalines from *N*-aryl ketimines and NaN_3 in the presence of Cu-catalyst have achieved by Zeng *et al.* (Scheme 1.40).^[55] A variety of *N*-aryl ketimines gave the desired products in moderate to good yields (33-85%).



Scheme 1.40: Cu-catalyzed synthesis of quinoxalines from *N*-arylketimines (73)

Mao group applied the photoredox catalysis for the synthesis of functionalized phenanthridines starting from vinyl azides under visible light (Scheme 1.41).^[56] In the developed method, new C-N and C-S bonds are formed, and sulfonyl chlorides were used as the source of sulfonylation under mild reaction condition to get 6-sulfonylmethylated phenanthridine derivatives in moderate to excellent yields (28-93%).



R¹ = H, 2-OMe, 2-Me, 2-Ph, 4-Me, 4-OMe, 4-Cl, 4-CF₃

R² = Ph, 4-MeC₆H₄, 4-FC₆H₄, 4-NO₂C₆H₄, 4-CNC₆H₄

3-NO₂C₆H₄, 2,4,6-Me₃C₆H₂, 2-furyl, Bn, Me, ^cPr

27 examples
Yield: 28-93%

Scheme 1.41: Synthesis of functionalized phenanthridines from vinyl azides under visible light

1.3 CONCLUSIONS

Azides have proven to be alternative and powerful one nitrogen source in organic chemistry for the preparation on *N*-heterocycles. Recent application of azides in the development of numerous synthetic pathway for nitrogen-containing heterocycles has been described in this chapter with appropriate mechanistic details. There is a great scope to develop novel reaction methodologies for the synthesis of nitrogen-containing heterocycles using azide as a single nitrogen source.

1.4 REFERENCES

- [1] N. Chadha, O. Silakari, *European Journal of Medicinal Chemistry*, **2017**, *134*, 159-184.
- [2] L. Zhang, X.-M. Peng, G. L. V. Damu, R.-X. Geng, C.-H. Zhou, *Medicinal Research Reviews*, **2014**, *34*, 340-437.
- [3] K. Pericherla, P. Kaswan, K. Pandey, A. Kumar, *Synthesis*, **2015**, *47*, 887-912.
- [4] I. Khan, A. Ibrar, W. Ahmed, A. Saeed, *European Journal of Medicinal Chemistry*, **2015**, *90*, 124-169.
- [5] Y.-Q. Hu, C. Gao, S. Zhang, L. Xu, Z. Xu, L.-S. Feng, X. Wu, F. Zhao, *European Journal of Medicinal Chemistry*, **2017**, *139*, 22-47.
- [6] N. Ono, *The Nitro Group in Organic Synthesis, Vol. 9*, John Wiley & Sons, **2003**.
- [7] S. A. Lawrence, *Amines: Synthesis, Properties and Applications*, Cambridge University Press, **2004**.
- [8] S. Bräse, C. Gil, K. Knepper, V. Zimmermann, *Angewandte Chemie International Edition*, **2005**, *44*, 5188-5240.
- [9] E. F. Scriven, K. Turnbull, *Chemical Reviews*, **1988**, *88*, 297-368.

- [10] T. Curtius, *Journal für Praktische Chemie*, **1894**, 50, 275-294.
- [11] K. Schmidt, *Angewandte Chemie*, **1923**, 36, 511.
- [12] K. F. Schmidt, *Berichte der Deutschen Chemischen Gesellschaft (A and B Series)*, **1924**, 57, 704-706.
- [13] P. A. Smith, *Organic Reaction*, **1946**, 3, 337-449.
- [14] E. Noelting, O. Michel, *Berichte der Deutschen Chemischen Gesellschaft*, **1893**, 26, 86-87.
- [15] C. K. Lowe-Ma, R. A. Nissan, W. S. Wilson, *The Journal of Organic Chemistry*, **1990**, 55, 3755-3761.
- [16] D. Enders, D. Klein, *Synlett*, **1999**, 6, 719-720.
- [17] T.-S. Lin, W. H. Prusoff, *Journal of Medicinal Chemistry*, **1978**, 21, 109-112.
- [18] A. Hassner, C. Stumer, *Organic Syntheses Based on Name Reactions*, Vol. 22, Elsevier, **2002**.
- [19] J. Xiong, X. Wei, Z.-M. Liu, M.-W. Ding, *The Journal of Organic Chemistry*, **2017**, 82, 13735-13739.
- [20] J. H. Boyer, J. Hamer, *Journal of the American Chemical Society*, **1955**, 77, 951-954.
- [21] H. Hemetsberger, D. Knittel, *Monatshefte für Chemie/Chemical Monthly*, **1972**, 103, 194-204.
- [22] R. Huisgen, *Angewandte Chemie International Edition*, **1963**, 2, 565-598.
- [23] V. V. Rostovtsev, L. G. Green, V. V. Fokin, K. B. Sharpless, *Angewandte Chemie*, **2002**, 114, 2708-2711.
- [24] H. C. Kolb, K. B. Sharpless, *Drug Discovery Today*, **2003**, 8, 1128-1137.
- [25] C. Wang, D. Ikhlef, S. Kahlal, J.-Y. Saillard, D. Astruc, *Coordination Chemistry Reviews*, **2016**, 316, 1-20.
- [26] N. V. Sokolova, V. G. Nenajdenko, *RSC Advances*, **2013**, 3, 16212-16242.
- [27] B. Kaboudin, R. Mostafalu, T. Yokomatsu, *Green Chemistry*, **2013**, 15, 2266-2274.
- [28] M. Tavassoli, A. Landarani-Isfahani, M. Moghadam, S. Tangestaninejad, V. Mirkhani, I. Mohammadpoor-Baltork, *ACS Sustainable Chemistry & Engineering*, **2016**, 4, 1454-1462.
- [29] W. Chen, W. Yang, R. Wu, D. Yang, *Green Chemistry*, **2018**, 20, 2512-2518.
- [30] B. Hu, S. G. DiMagno, *Organic & Biomolecular Chemistry*, **2015**, 13, 3844-3855.

- [31] H. Dong, M. Shen, J. E. Redford, B. J. Stokes, A. L. Pumphrey, T. G. Driver, *Organic Letters*, **2007**, *9*, 5191-5194.
- [32] E. P. Farney, T. P. Yoon, *Angewandte Chemie International Edition*, **2014**, *53*, 793-797.
- [33] F. Chen, T. Shen, Y. Cui, N. Jiao, *Organic Letters*, **2012**, *14*, 4926-4929.
- [34] B. J. Stokes, H. Dong, B. E. Leslie, A. L. Pumphrey, T. G. Driver, *Journal of the American Chemical Society*, **2007**, *129*, 7500-7501.
- [35] M. Shen, B. E. Leslie, T. G. Driver, *Angewandte Chemie International Edition*, **2008**, *47*, 5056-5059.
- [36] Y. Goriya, C. V. Ramana, *Chemical Communications*, **2014**, *50*, 7790-7792.
- [37] X. Zhang, P. Li, C. Lyu, W. Yong, J. Li, X. Zhu, W. Rao, *Organic & Biomolecular Chemistry*, **2017**, *15*, 6080-6083.
- [38] Y.-F. Wang, K. K. Toh, J.-Y. Lee, S. Chiba, *Angewandte Chemie International Edition*, **2011**, *50*, 5927-5931.
- [39] C.-Z. Luo, P. Gandeepan, Y.-C. Wu, W.-C. Chen, C.-H. Cheng, *RSC Advances*, **2015**, *5*, 106012-106018.
- [40] W.-C. Chen, P. Gandeepan, C.-H. Tsai, C.-Z. Luo, P. Rajamalli, C.-H. Cheng, *RSC Advances*, **2016**, *6*, 63390-63397.
- [41] N. Anand, T. Chanda, S. Koley, S. Chowdhury, M. S. Singh, *RSC Advances*, **2015**, *5*, 7654-7660.
- [42] M. Wang, Q. Fan, X. Jiang, *Organic Letters*, **2018**, *20*, 216-219.
- [43] Y. Kawada, S. Ohmura, M. Kobayashi, W. Nojo, M. Kondo, Y. Matsuda, J. Matsuoka, S. Inuki, S. Oishi, C. Wang, T. Saito, M. Uchiyama, T. Suzuki, H. Ohno, *Chemical Science*, **2018**, *9*, 8416-8425.
- [44] Y. Kim, M. R. Kumar, N. Park, Y. Heo, S. Lee, *The Journal of Organic Chemistry*, **2011**, *76*, 9577-9583.
- [45] D. Mahesh, P. Sadhu, T. Punniyamurthy, *The Journal of Organic Chemistry*, **2016**, *81*, 3227-3234.
- [46] A. N. Prasad, R. Srinivas, B. M. Reddy, *Catalysis Science & Technology*, **2013**, *3*, 654-658.
- [47] M. R. Kumar, A. Park, N. Park, S. Lee, *Organic Letters*, **2011**, *13*, 3542-3545.

-
- [48] F.-C. Jia, Z.-W. Zhou, C. Xu, Q. Cai, D.-K. Li, A.-X. Wu, *Organic Letters*, **2015**, *17*, 4236-4239.
- [49] C. Xu, F.-C. Jia, Z.-W. Zhou, S.-J. Zheng, H. Li, A.-X. Wu, *The Journal of Organic Chemistry*, **2016**, *81*, 3000-3006.
- [50] M. H. Shinde, U. A. Kshirsagar, *RSC Advances*, **2016**, *6*, 52884-52887.
- [51] M. H. Sayahi, S. J. Saghanezhad, S. Bahadorikhalili, M. Mahdavi, *Applied Organometallic Chemistry*, **2019**, *33*, e4635.
- [52] B. Rai, P. Kumar, A. Kumar, *RSC Advances*, **2015**, *5*, 85915-85918.
- [53] N. K. Nandwana, S. Dhiman, H. K. Saini, I. Kumar, A. Kumar, *European Journal of Organic Chemistry*, **2017**, *2017*, 514-522.
- [54] G. R. Potuganti, D. R. Indukuri, M. Alla, *Synlett*, **2018**, *29*, 1717-1722.
- [55] T. Chen, X. Chen, J. Wei, D. Lin, Y. Xie, W. Zeng, *Organic Letters*, **2016**, *18*, 2078-2081.
- [56] L.-L. Mao, D.-G. Zheng, X.-H. Zhu, A.-X. Zhou, S.-D. Yang, *Organic Chemistry Frontiers*, **2018**, *5*, 232-236.

CHAPTER 2: PART-A

Copper-Catalyzed One-Pot Synthesis of Quinoline Derivatives

2A.1 INTRODUCTION

Quinoline is a privilege nitrogen-containing aromatic heterocycle which contains benzene ring fused with pyridine ring, and its systematic IUPAC name is benzo[*b*]pyridine.^[1-3] Quinoline skeleton is ubiquitous molecules found in various natural products, and many of quinoline derivatives act as intermediate and precursor in drug discovery, dye and pharmaceutical industries.^[4] Quinoline derivatives (such as quinine, quinidine, mefloquine, ferroquine, chloroquine, amodiaquine, and primaquine) have been exclusively used as antimalarial drugs (**Figure 2A.1**).^[5-8] Moreover, quinoline and their derivatives have also shown a variety of bioactivities, for example, antibacterial, antitumor, cardiotoxic and antifungal activities (**Figure 2A.2**).^[9-11]

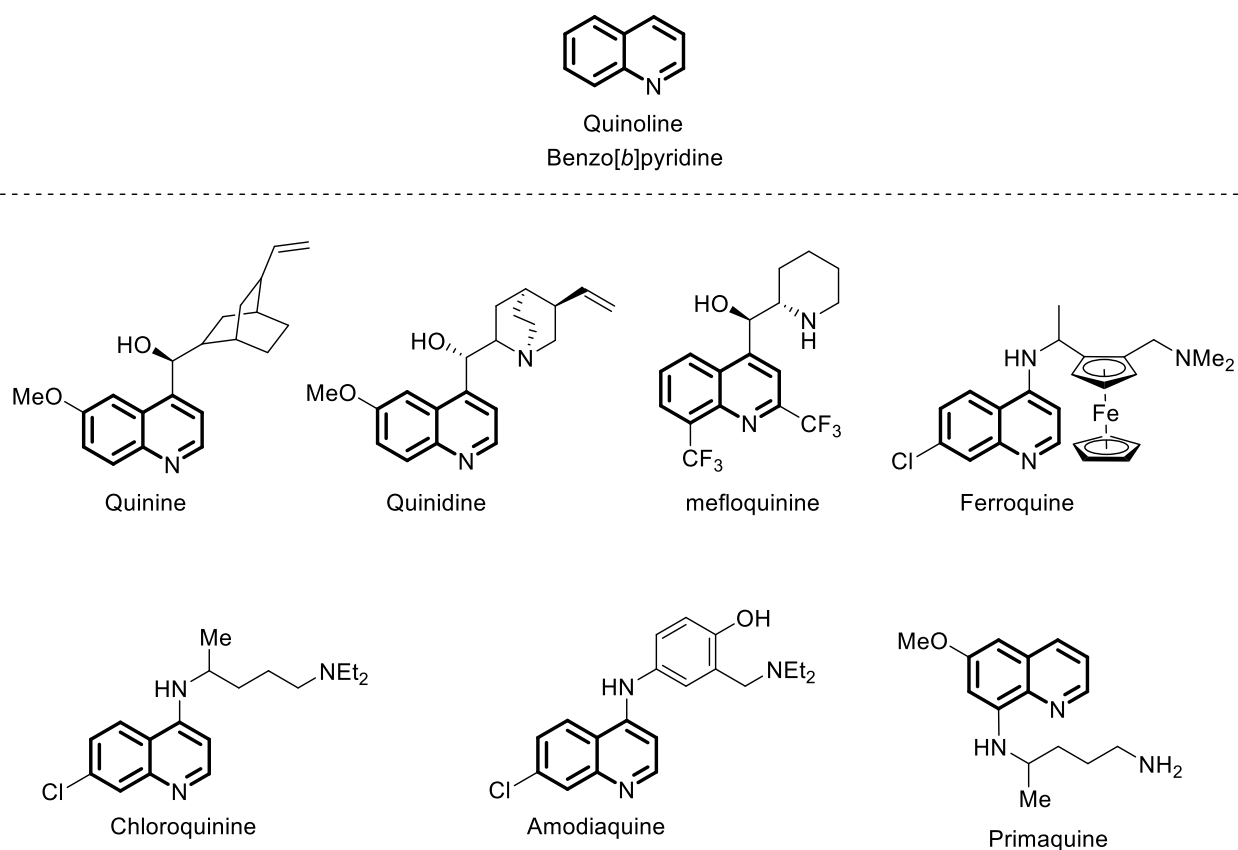


Figure 2A.1: Antimalarial drugs containing quinoline framework

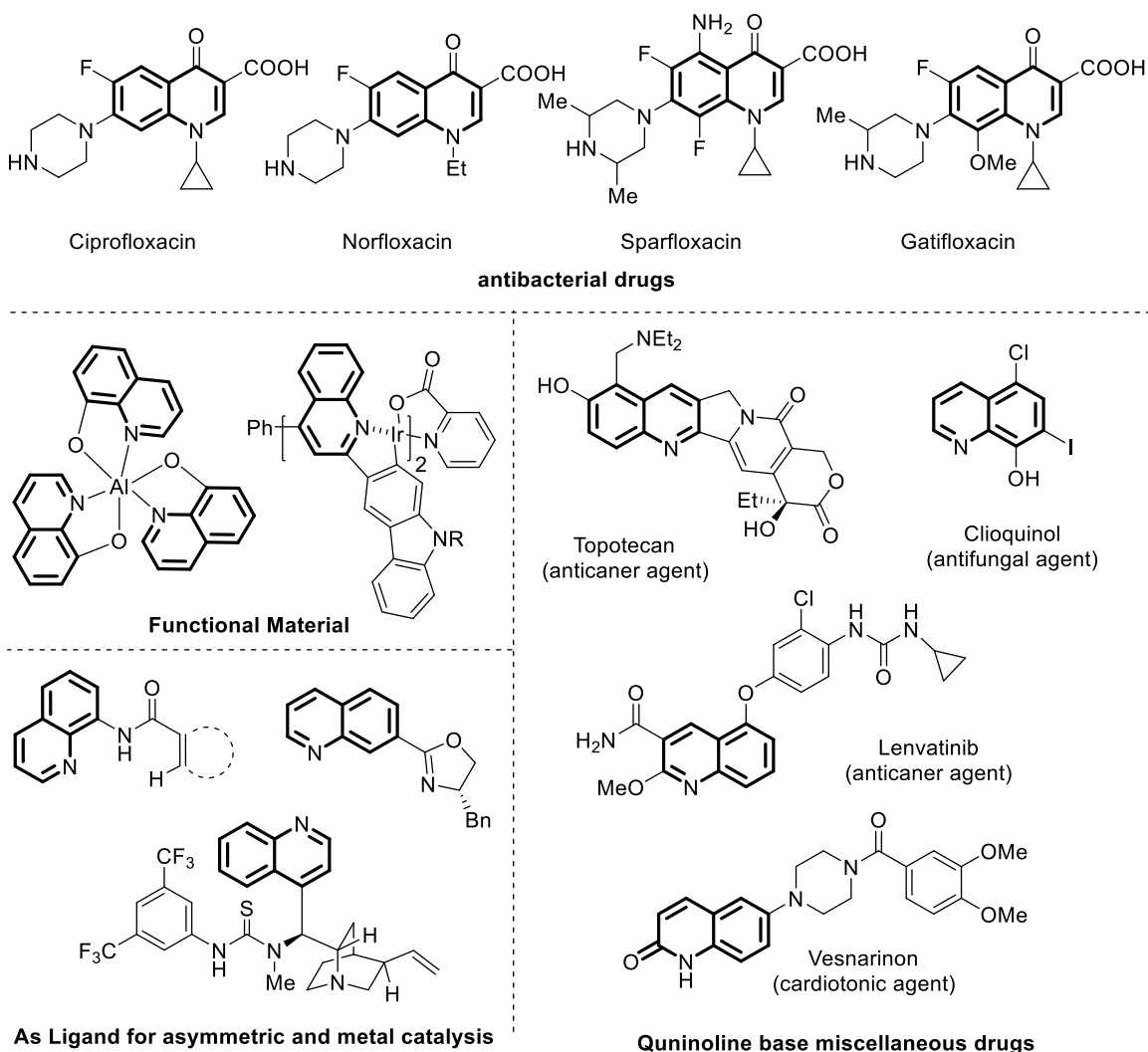


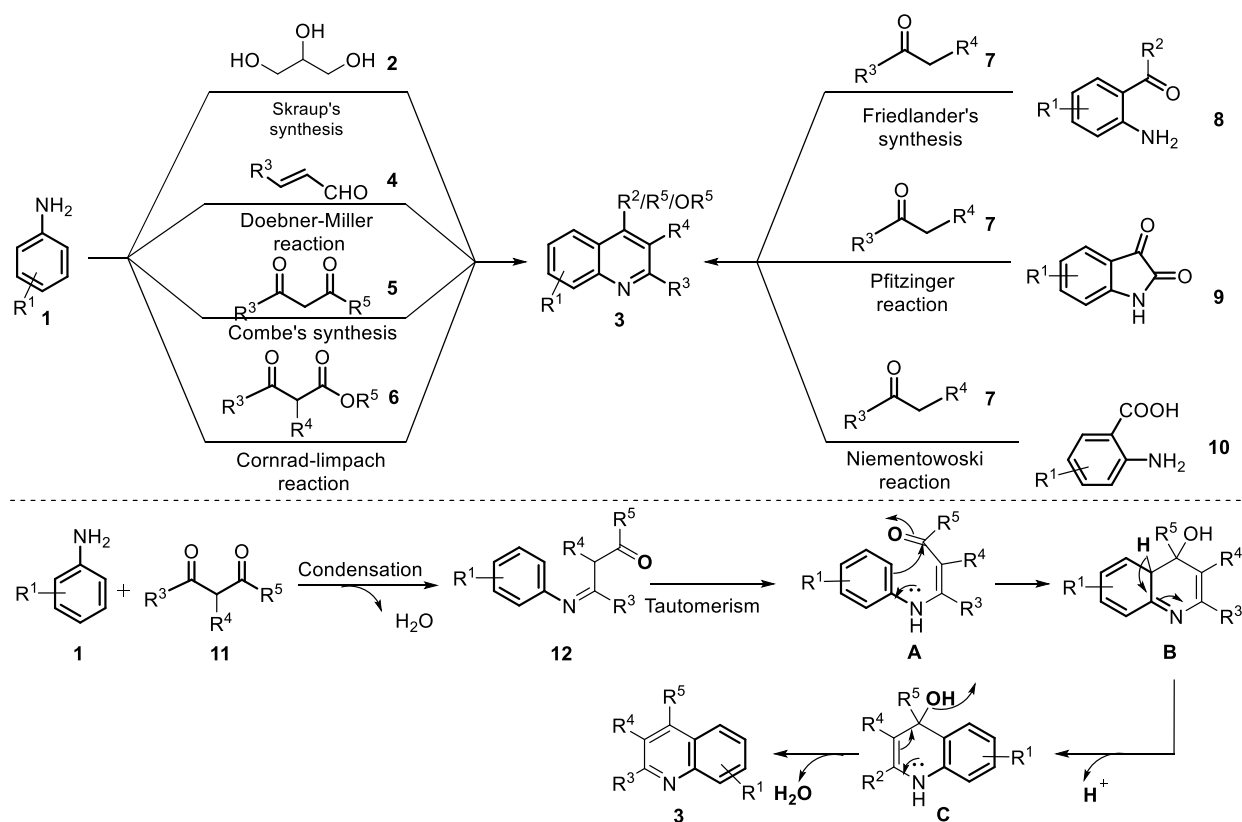
Figure 2A.2: Selective compounds containing a quinoline scaffold

Additionally, quinoline-based compounds also act as an asymmetric catalyst, a ligand as well as directing group in C–H activation under transition metal catalysis. Quinoline ring system incorporating with metal is also used in functional materials.^[12-13]

2A.2 Different approaches for the synthesis of quinolines

Several traditional methods such as Combes, Skraup, Friedlander, Niementowski, Doebner-von Miller, Pfitzinger and Conrad-limpach reactions have been developed for the synthesis of quinolines (**Scheme 2A.1**).^[14-15] In these conventional methods, first imine formation (**12**) occur in between aniline (**1**) and α -methylene aldehyde/ketone (**11**) which on tautomerization led to formation intermediate (**A**) and followed by intramolecular cyclization to afford intermediate (**B**)

which on dehydration result in the formation of quinoline derivative (**3**). Although these traditional methods have been successfully utilized in quinoline synthesis, they required harsh reaction condition and a stoichiometric amount of acid. These limitations restrict their application for the synthesis of functionalized quinolines. To overcome these limitations, several different methods have been developed in the last few decades employing multicomponent/ tandem reaction, use of transition metals and alternative starting materials.^[15-17] Among alternate route for quinoline synthesis, the multicomponent/tandem reactions using transition metals (such as Ru, Rh, Pd, and Cu) has received more attention because this strategy involves multiple bonds formation in one-pot, avoids isolation and purification of intermediates and it is a step- and atom-economical. The method allows to generate more functional substituted quinoline molecules.^[18-20]

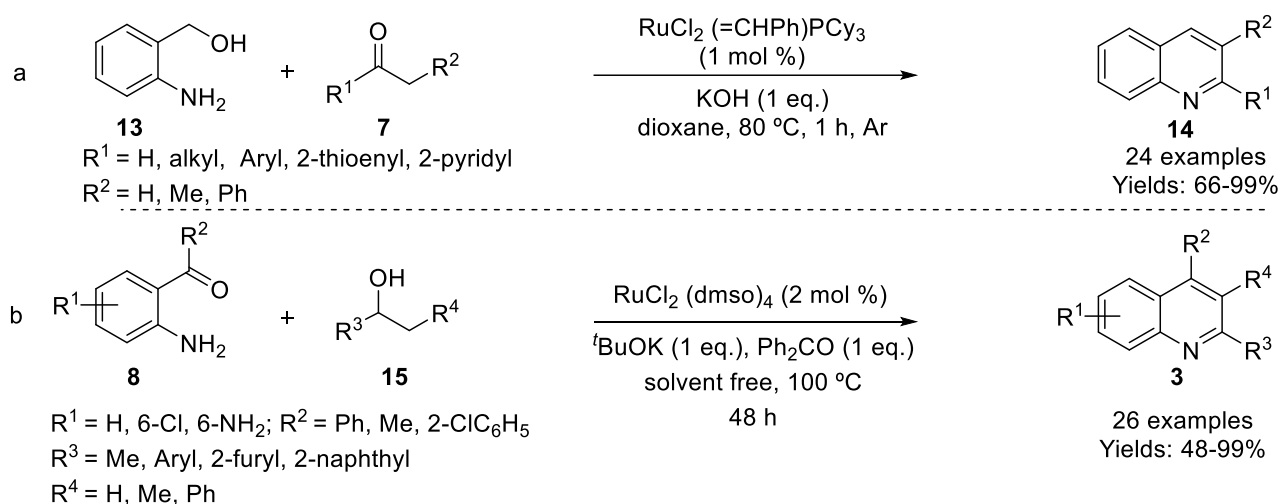


Scheme 2A.1: Different conventional approaches and general mechanism for quinoline synthesis

In this chapter, transition-metal catalyzed construction of substituted quinolines using multicomponent/tandem/domino approaches in recent years have been summarized. Subsections are based on the transition-metal used in the reactions.

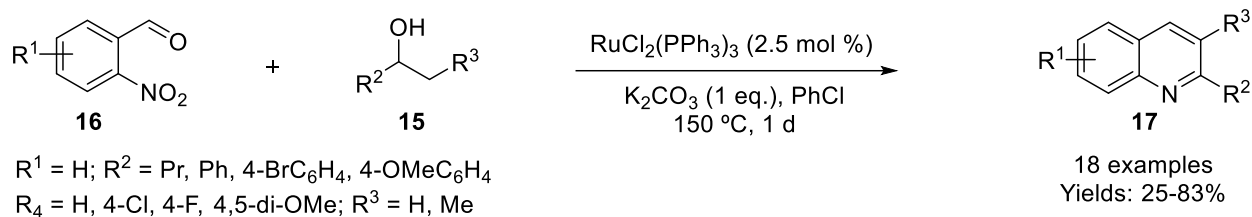
2A.2.1 Ruthenium and Rhodium catalyst

Shim group developed and modified the Friedlander quinoline synthesis through Grubb's Ru-complex catalyzed oxidative cyclization of 2-aminobenzyl alcohol (**13**) with ketones (**7**) (**Scheme 2A.2a**).^[21] The key step in this strategy is oxidation of 2-aminobenzyl alcohol to 2-aminobenzaldehyde *via* oxidative addition of Ru-complex followed by β -hydrogen elimination which undergoes imine formation with ketone followed by intramolecular cyclization as described in Friedlander synthesis. Friedlander quinoline synthesis has also been improved by Yus's group where they used alcohols (**15**) first time as a reagent in quinoline synthesis instead of ketones with *o*-aminocarbonyls (**8**) using $\text{RuCl}_2(\text{dmsO})_4$ complex as catalyst under solvent-free condition (**Scheme 2A.2b**).^[22]



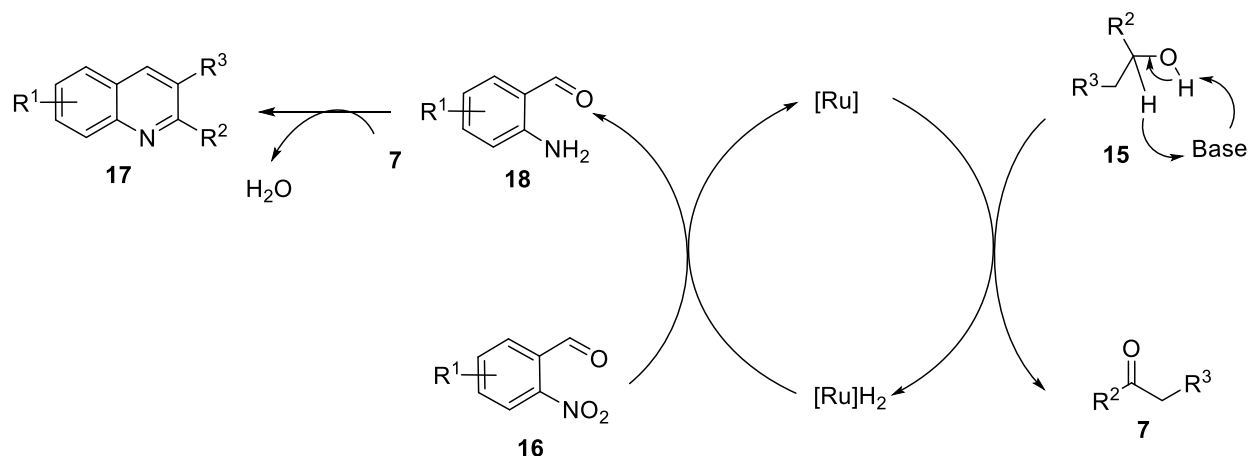
Scheme 2A.2: Modification of Friedlander quinoline synthesis using Ruthenium complex

Most of the reported methods required *o*-aminocarbonyl (**8**) as starting materials in quinoline synthesis, which are relatively unstable because of readily undergo self-condensation. One of the main disadvantages of these *o*-aminocarbonyl compounds (**8**) is that they are prepared by the typical reduction of *o*-nitrocarbonyls (**16**), which restrict the substrate scope of the quinoline synthesis. To overcome this inherent problem, Wu and coworker used *o*-nitrocarbonyls (**16**) as starting material which was *insitu* converted to *o*-aminocarbonyls (**8**) using alcohol (**15**) in the presence of Ru-catalyst *via* cascade process and gave a useful solution in Friedlander quinoline synthesis (**Scheme 2A.3**).^[23]



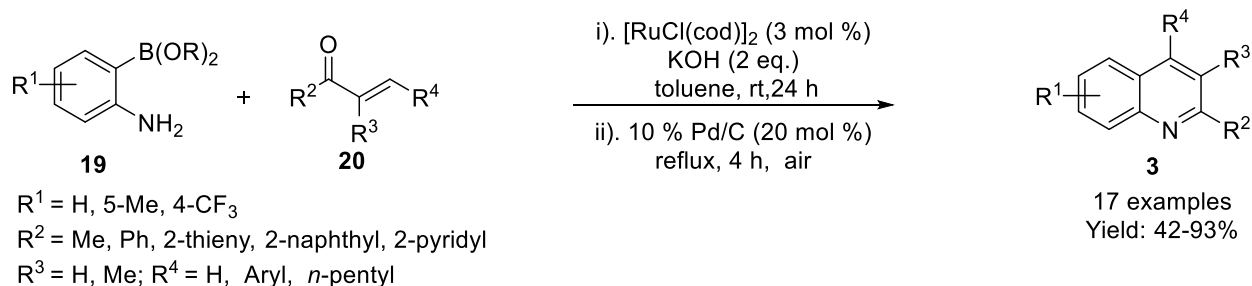
Scheme 2A.3: Ru-Catalyzed synthesis of substituted quinolines using *o*-nitrocarbonyls

The reaction pathway proposed by Wu was showed in **Scheme 2A.4**. In this approach, unreactive *o*-nitrobenzaldehyde (**16**) and alcohols (**15**) simultaneously converted into reactive *o*-aminobenzaldehyde (**18**) and α -methyl carbonyl compound (**7**) respectively by hydrogen transfer with the help of [Ru(PPh₃)₃Cl₂] catalyst. Initially, [Ru(PPh₃)₃Cl₂] complex takes away hydrogen with the help of base from alcohol (**15**) to form reactive carbonyl compound (**7**) and also [Ru] converted to [Ru]H₂. Subsequently [Ru]H₂ reduced the *o*-nitrobenzaldehyde (**16**) to *o*-aminobenzaldehyde (**18**) by hydrogen transfer which borrows from alcohol (**15**) and [Ru]H₂ converted back to [Ru]. Immediately *o*-aminobenzaldehyde (**18**) reacted with α -methyl carbonyl compound (**7**) to produce imine intermediate, which undergo cyclization as described in Friedlander synthesis (**Scheme 2A.4**)



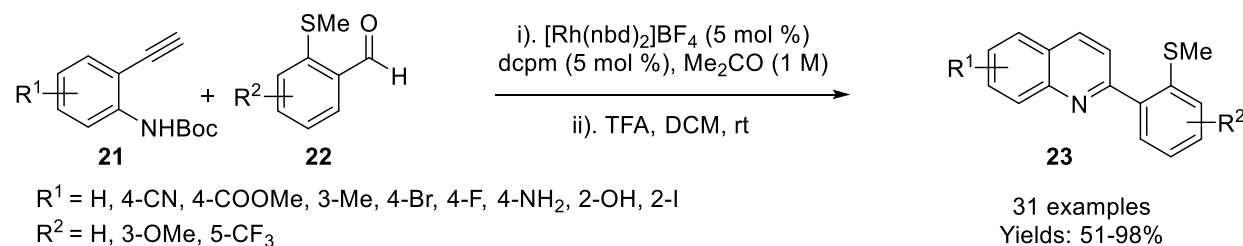
Scheme 2A.4: Mechanism of hydrogen transfer by [Ru(PPh₃)₃Cl₂] complex

Weingarten and coworkers presented a complementary method to the classical Skraup-Doebner-von Miller reaction for the synthesis of quinolines by using of *o*-aminophenyl boronic acid (**19**) and α , β -unsaturated ketones (**20**) in the presence of [RhCl(cod)]₂ catalyst under basic rather than acidic condition (**Scheme 2A.5**).^[24]



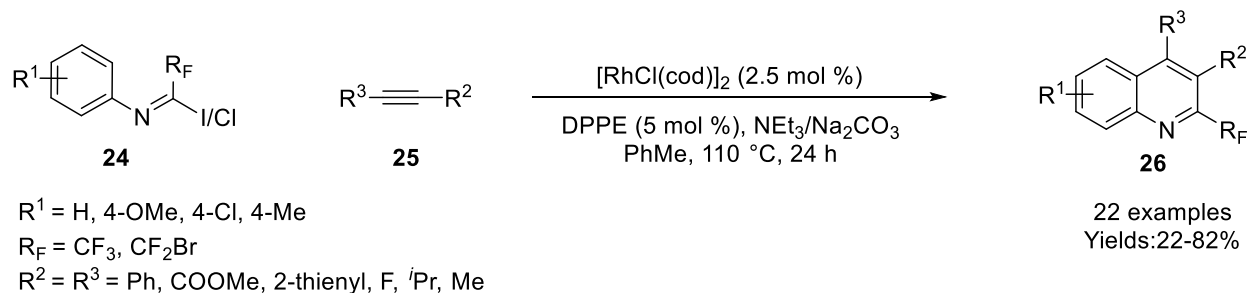
Scheme 2A.5: Ru-catalyzed synthesis of polysubstituted quinolines from 2-aminophenyl boronic acids

Willis also reported the synthesis of 2-aryl quinolines (**23**) by using *o*-alkenylanilines (**21**) through Rh-catalyzed hydroacylation with SMe-benzaldehydes (**22**) followed by deprotection of Boc using TFA (**Scheme 2A.6**).^[25] Furthermore, the SMe group on the aryl ring of quinoline was transformed into the aryl ring by the reaction of boronic acid to form sulfide-free quinolines.



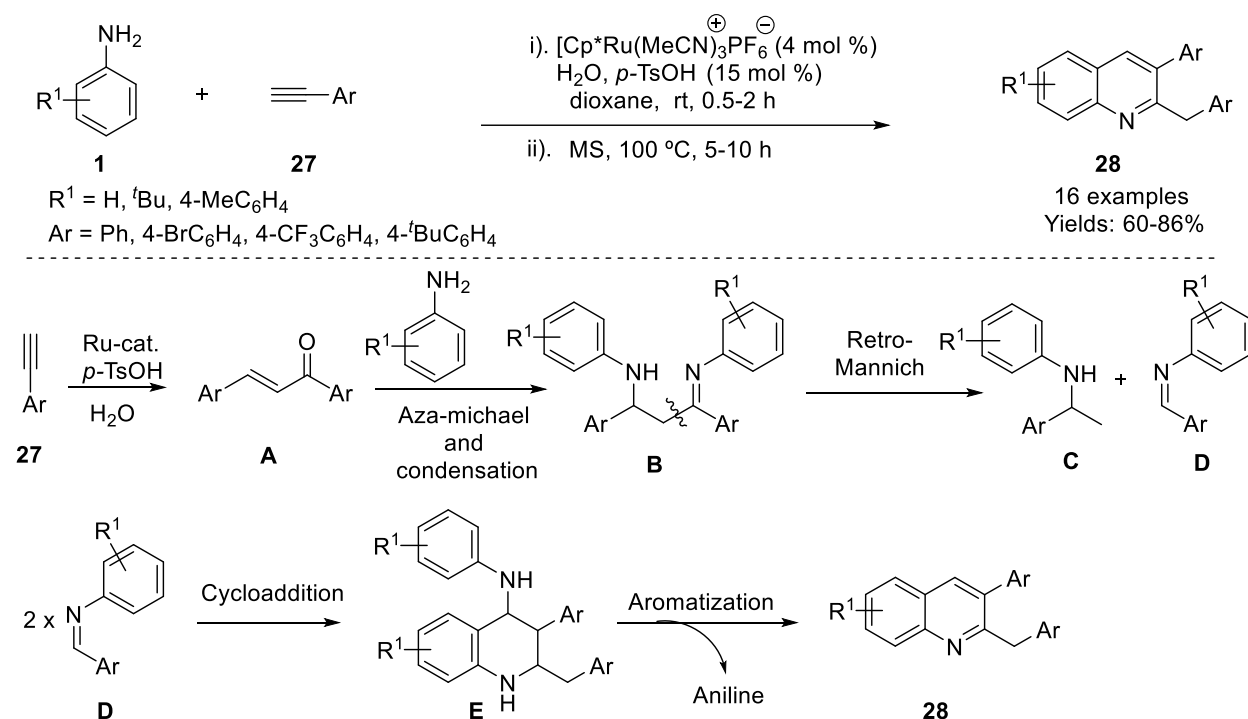
Scheme 2A.6: Rh-catalyzed synthesis of polysubstituted quinolines from *o*-alkenylanilines

Despite the various route for the quinoline synthesis, these methods were limited to α -methyl ketones and α, β -aldehydes/ketones.^[26] An alternate elegant and attractive approach has appeared by using alkenes and terminal/internal alkynes since Povarov reaction has been discovered. In the continuation of this Uneyama and team disclosed an attractive 2-fluorinated quinolines (**26**) synthesis from *N*-aryl trifluoroacetimidoyl chloride (**24**) and internal alkyne (**25**) in the presence of Rh(I)-catalyst (**Scheme 2A.7**).^[27]



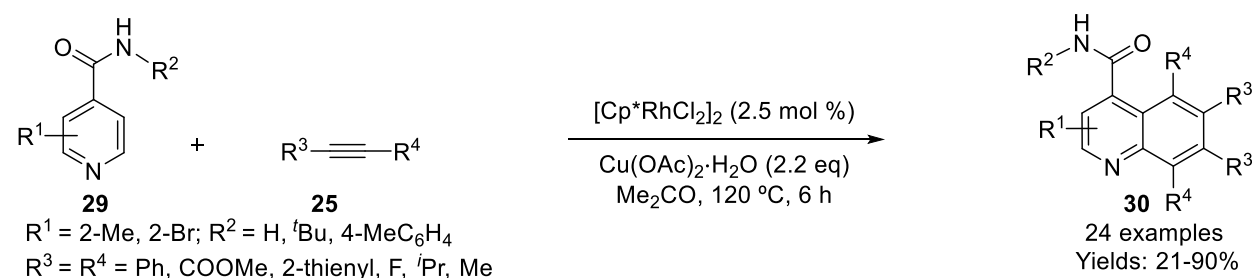
Scheme 2A.7: Rh-catalyzed synthesis of substituted quinolines from imines and alkynes

Dixneuf *et al.* reported new methodology for quinolines synthesis *via* sequential Ru(II)-catalyst and *p*-TsOH as co-catalyst from aniline and terminal alkynes (**27**) (**Scheme 2A.8**).^[28] The formation of quinolines were achieved from intermediate allyl ketones (**A**) which is produced by the reaction of a terminal alkyne with water under the co-operative catalytic process of Ru(II) and *p*-TsOH. Then condensation and aza-Michael addition of anilines to allyl ketones followed by retro-Mannich type fragmentation to generate ketamine (**C**) and imine (**D**). Then reactive imine undergoes self-condensation followed by oxidation to afford the desired quinolines (**28**).



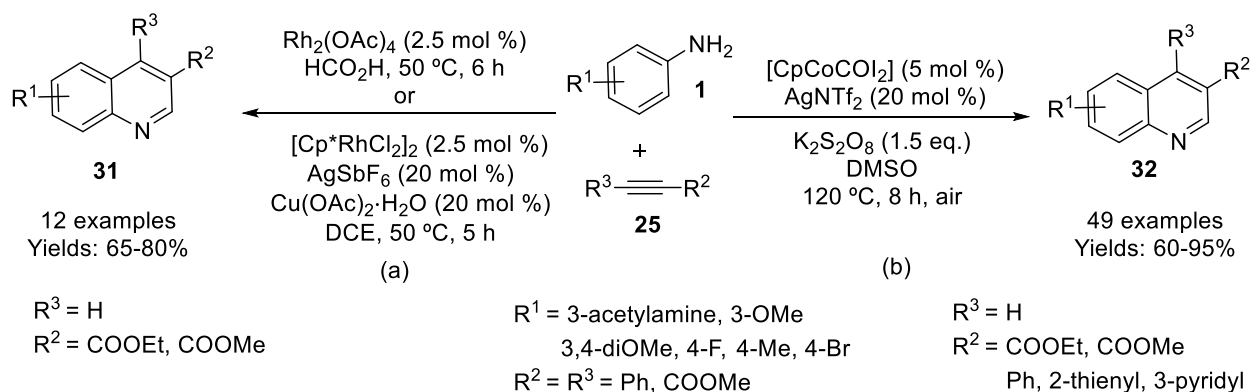
Scheme 2A.8: Synthesis of 2,3-disubstituted quinolines from aniline and alkynes

Li group documented chelation-assisted Rh(III)-catalyzed oxidative annulation of isonicotinamide (**29**) with 2 moles of internal alkynes (**25**) to achieve quinolines (**30**) in moderate to excellent yield (21-90%) *via* 2-fold C-H activation with broad functional group tolerance (**Scheme 2A.9**).^[29]



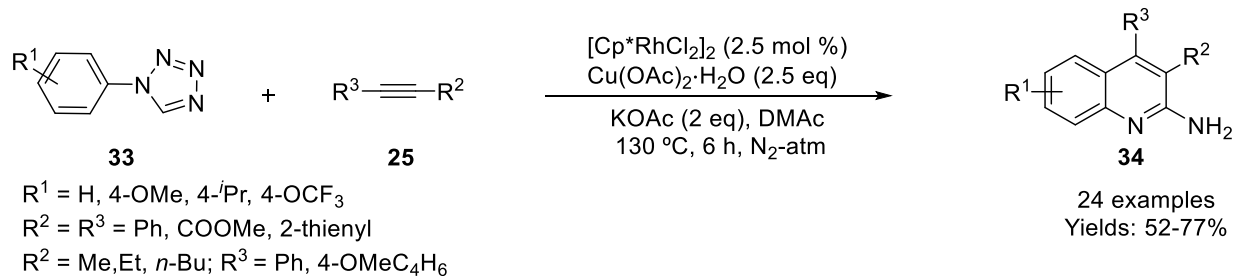
Scheme 2A.9: Rh-catalyzed synthesis of quinolines using alkynes

A one-pot oxidative annulation of anilines (**1**) with alkynyl ester (**25**) to access quinoline 3-carboxylates (**31**) catalyzed by $\text{Rh}_2(\text{OAc})_4$ have been described by Sudalai and coworkers with the use of formic acid as C1 synthon in quinoline product (**31**) (Scheme 2A.10a).^[30] The authors also observed that a combination of $[\text{RhCp}^*\text{Cl}_2]_2/\text{AgSbF}_6/\text{Cu}(\text{OAc})_2$ was the most suitable catalyst to access 3,4-disubstituted quinolines in case of internal alkynyl ester (**25**) with good to excellent yields. Very recently, Yi *et al.* employed DMSO as one carbon atom source as well as reaction medium in the quinoline (**32**) synthesis catalyzed by Co(III) using similar building blocks (Scheme 2A.10b).^[31] A series of 49 compounds were synthesized in 65-90% yield by varying different substituent on both anilines and internal alkynes.



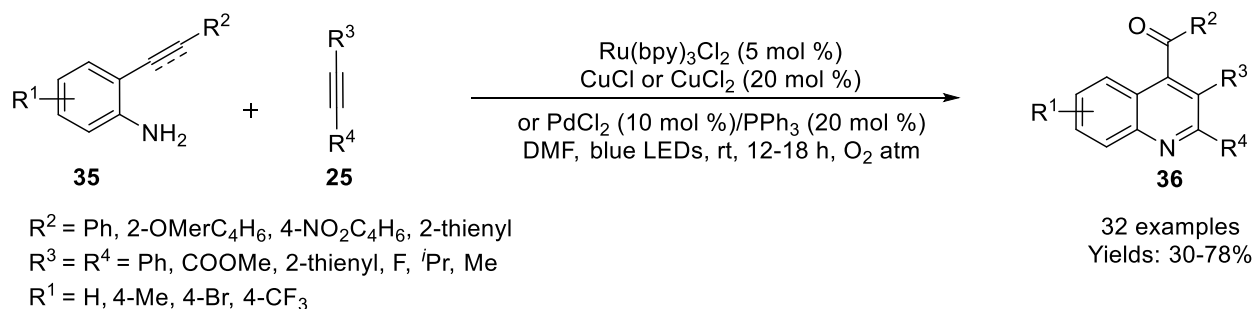
Scheme 2A.10: Formation of substituted quinolines from anilines and alkynes

A simple and elegant one-pot synthesis of 2-amino substituted quinolines (**34**) has been reported by Hua *et al.* from 1-aryl tetrazoles (**33**) and internal alkynes (**25**) under Rh(III) and Cu(II) catalysis (Scheme 2A.11).^[32] The reaction proceeds *via* initial formation of tetrazole fused quinolines by the reaction of 1-aryltetrazoles (**33**) with alkynes (**25**) through double C-H activation in the presence of Rh(III)-catalyst followed by Cu(II)-mediated denitrogenation to afford 2-aminoquinolines (**34**).



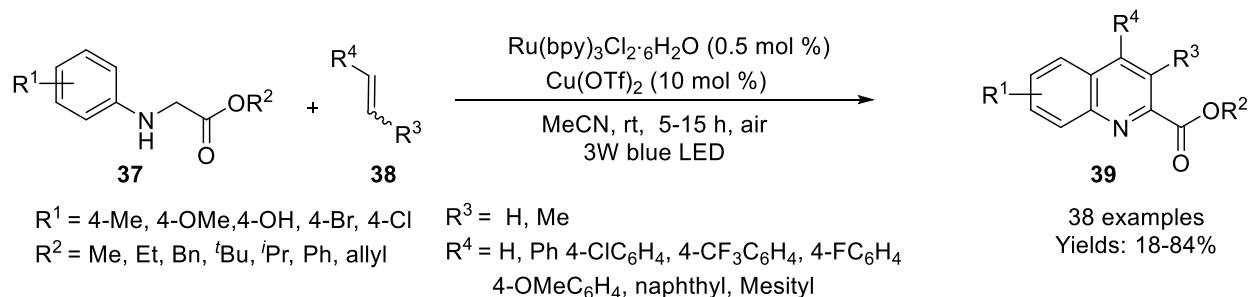
Scheme 2A.11: Rh(III)-catalyzed synthesis of 2-aminoquinolines from 1-aryltetrazoles

The oxidative cyclization of *o*-alkynyl/alkenyl anilines (**35**) with internal alkynes (**25**) to achieve substituted 4-keto quinolines (**36**) by dual transition metal photoredox catalyst has been developed by Zhu group (**Scheme 2A.12**).^[33] The molecular oxygen act as a source of oxygen in the carbonyl group was confirmed by isotopic labeling effect.



Scheme 2A.12: Synthesis of 4-carbonylquinolines by the photoredox catalyst

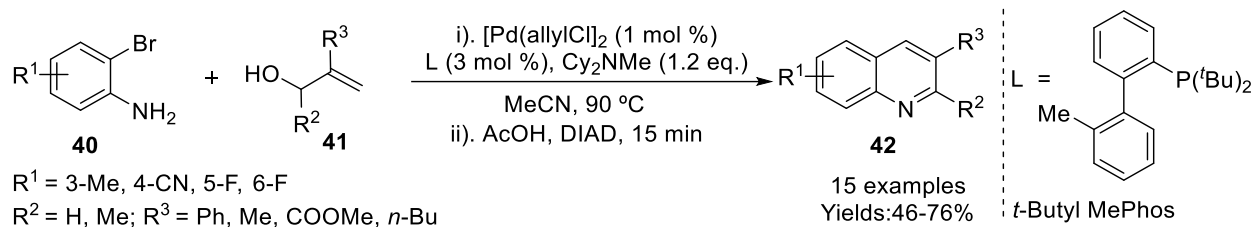
Zhang group also achieved quinoline (**39**) synthesis by visible-light-induced photocatalytic oxidative C-C cross-coupling followed by aromatization of functionalized anilines (**37**) with alkenes (**38**) at room temperature under aerobic conditions (**Scheme 2A.13**).^[34]



Scheme 2A.13: Synthesis of functionalized quinolines by visible-light induced photoredox catalyst

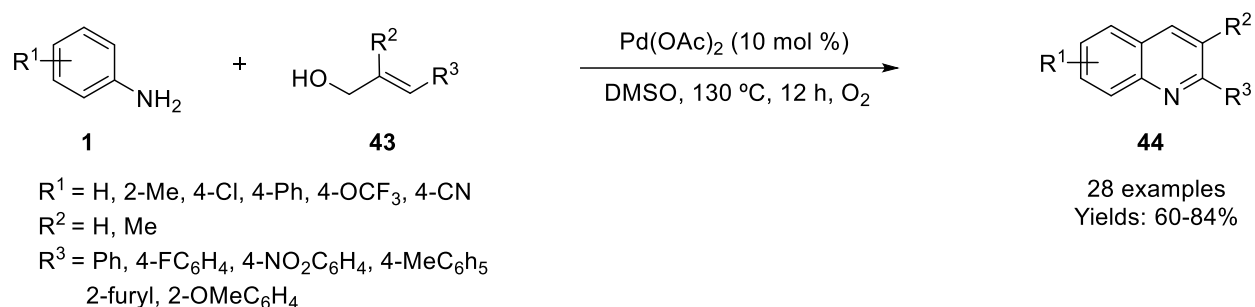
2A.2.2 Palladium catalyst

Palladium-catalyzed synthesis of substituted quinolines (**42**) *via* domino Heck coupling of *o*-bromoaniline (**40**) with allyl alcohol (**41**) followed by condensation and dehydrogenation in one-pot have been achieved by Stone and Larock independently (**Scheme 2A.14**).^[35-36] In Larock approach dehydrogenation happened by palladium itself to give corresponding quinolines which also lead to disproportion reaction of dihydroquinoline to tetrahydroquinoline. Stone further improved the Larock strategy by using diisopropyl azodicarboxylate (DIAD) for dehydrogenation reaction.



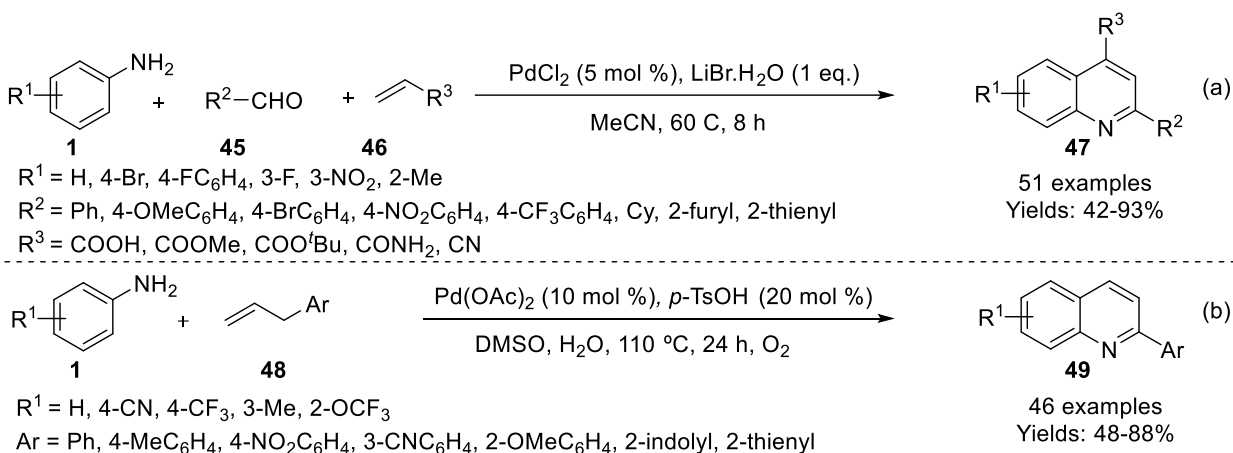
Scheme 2A.14: Pd-catalyzed synthesis of quinoline derivatives from 2-bromoanilines and allyl alcohols

Recently, Pd(II)-catalyzed synthesis of disubstituted quinolines (**44**) in moderate to good yield (60-84%) by oxidative cyclization of aryl allyl alcohol (**43**) with anilines (**1**) have been disclosed by Sun group under O_2 atmosphere without the use of acid and base (**Scheme 2A.15**).^[37]



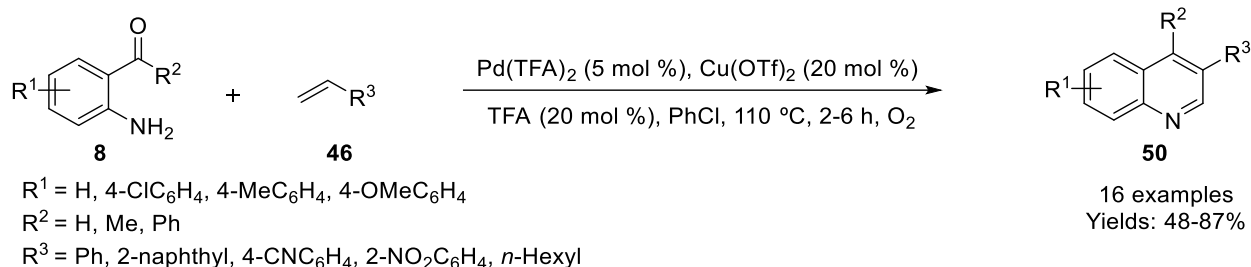
Scheme 2A.15: Pd(II)-catalyzed formation of quinolines from allyl alcohols and anilines

Jiang *et al.* modified Povarov's method by using electron-deficient terminal alkenes (**46**) under Pd-catalysis (**Scheme 2A.16a**).^[38] The modified method is compatible with both electron-releasing and withdrawing substituents on aldehydes (**45**) and anilines (**1**) to furnish corresponding 2,4-disubstituted quinolines (**47**) in good to excellent yield (42-93%). Furthermore, various terminal olefins (**46**) such as acrylamides, acrylonitriles, and aliphatic olefins also underwent the reaction smoothly in this protocol whereas in the case of acrylic acid underwent decarboxylation happened to produce 2-substituted quinolines. Subsequently, the same group established Pd-catalyzed synthesis of 2-substituted quinoline derivatives (**49**) from allylbenzenes (**48**) and anilines (**1**) *via* aerobic oxidative C-H coupling (**Scheme 2A.16b**).^[39] By the control experiments, the authors proved that allylbenzene (**48**) act as α, β -aldehydes (**4**) surrogate and water played an important role in the oxidative coupling.



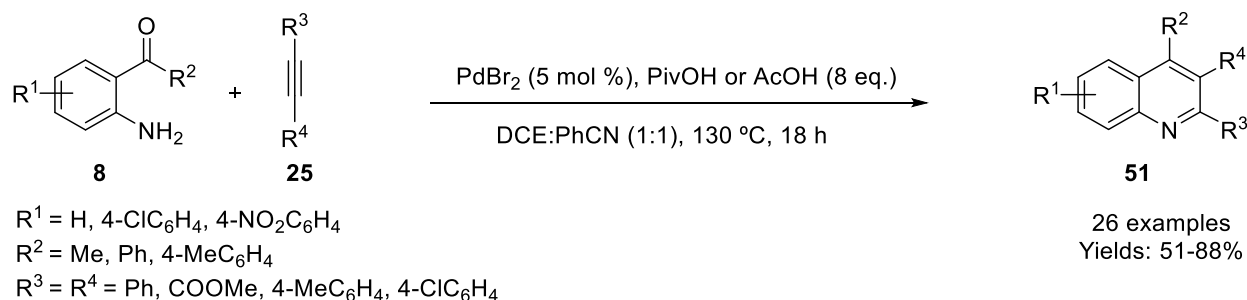
Scheme 2A.16: Synthesis of quinoline derivatives through Pd-catalyst using alkenes and anilines

Wang and coworkers demonstrated the construction of 3,4-disubstituted quinolines (**50**) from alkenes (**46**) and *o*-aminocarbonyls (**8**) using Pd(TFA)_2 as a catalyst in the presence Cu(OTf)_2 as oxidant under an oxygen atmosphere (**Scheme 2A.17**).^[40]



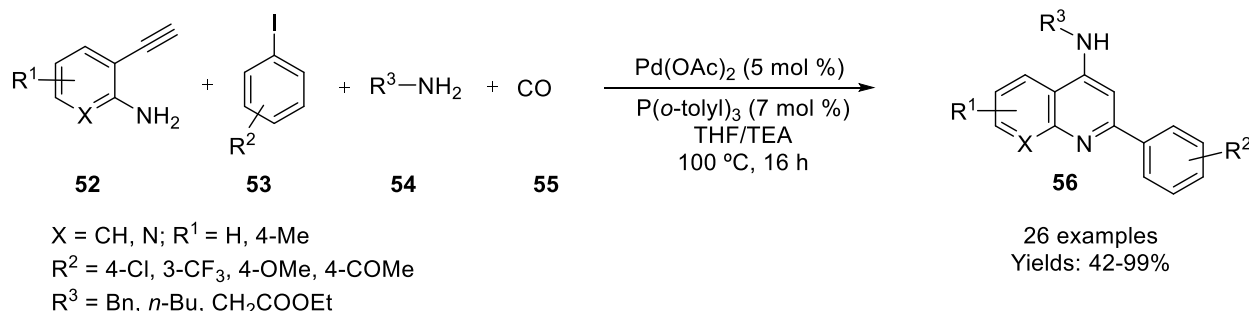
Scheme 2A.17: Synthesis of 3,4-disubstituted quinolines achieved by Pd(II)-catalyst

Lei *et al.* reported the first palladium-catalyzed synthesis of multi-substituted quinolines (**51**) from commercially available *o*-aminocarbonyls (**8**) and internal alkynes (**25**) in moderate to good product yield (51-88%) (**Scheme 2A.18**).^[41]



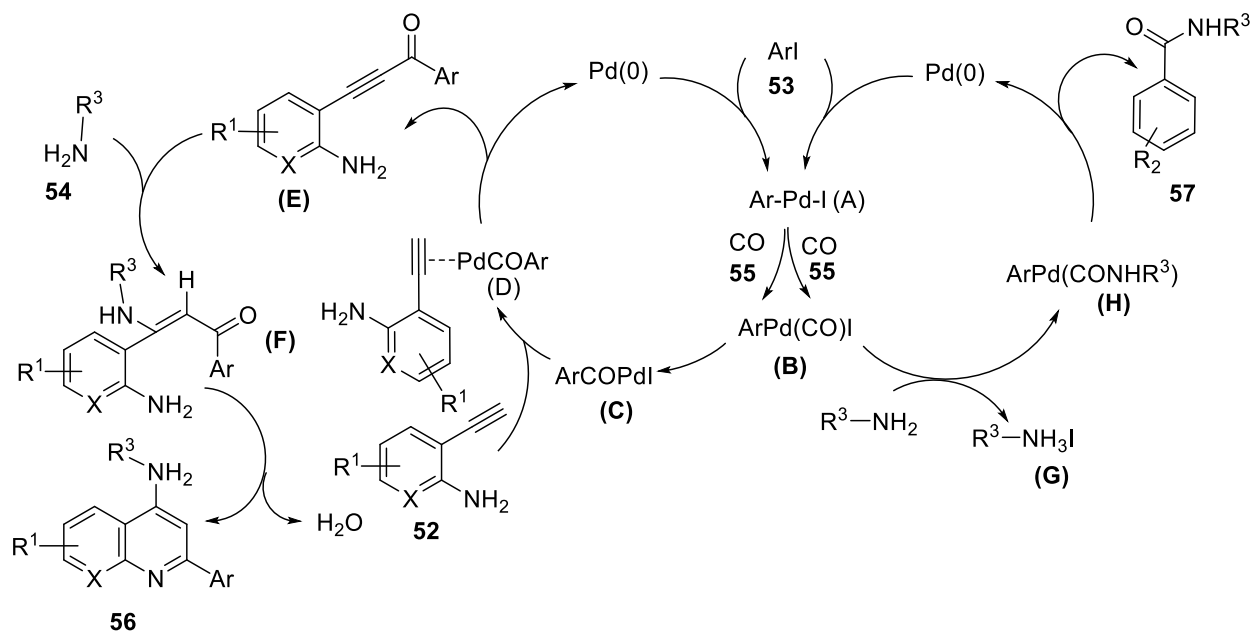
Scheme 2.18: Pd-catalyzed synthesis of poly-substituted quinolines from *o*-aminoketones and internal alkynes

Interestingly, Rossi and coworkers established an efficient route for the formation of 4-aminoquinoline derivatives (**56**) by four component reaction between *o*-alkenylamines (**52**), iodoarenes (**53**), amines (**54**), and carbon monoxide (**55**) under Pd-catalysis (**Scheme 2A.19**).^[42]



Scheme 2A.19: Pd(II)-catalyzed synthesis of 4-aminoquinolines *via* four-component reaction

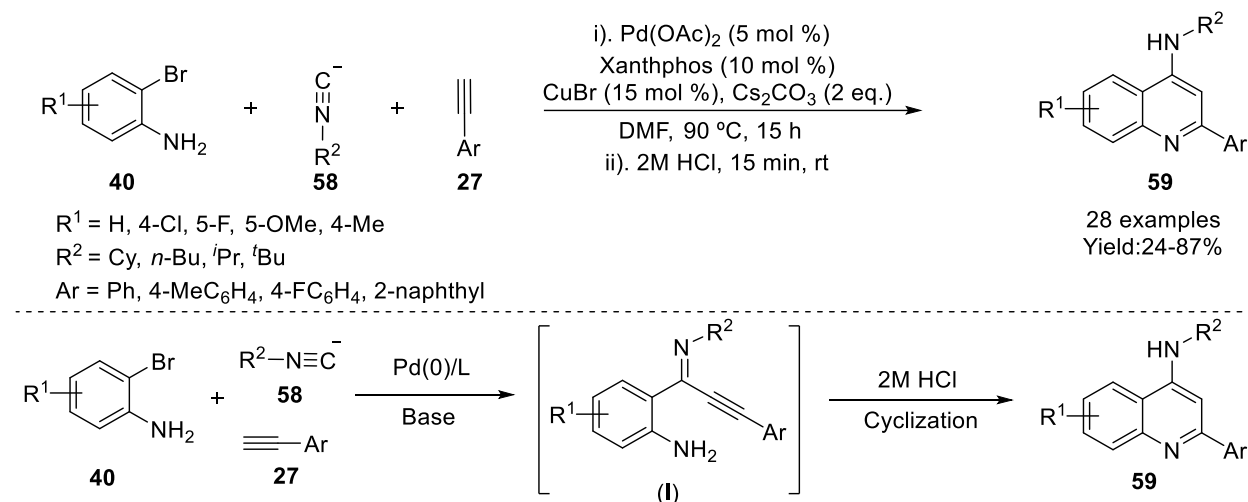
The synthesis of quinolines was carried out *via* triple tandem sequence where first carbonylative coupling of *o*-alkenylamines (**52**) with iodoarenes (**53**) followed by inter and intramolecular attack of amine (**54**) to the carbonyl couple product (**E**) (**Scheme 2A.20**). Initially, oxidative addition of Pd(0) to iodoarenes (**53**) gives intermediate (**A**) followed by insertion of CO to produce arylcarbonyl palladium complex (**B**), which undergoes 1,2 migration of aryl group gives complex (**C**). Then the addition of *o*-alkenylamines (**52**) to complex (**C**) followed by reductive elimination of complex (**D**) affords the ynones (**E**).



Scheme 2A.20: Mechanism for Pd-catalyzed synthesis of 4-aminoquinolines from *o*-alkylamines

Intermolecular nucleophilic attack of primary amine (**54**) to give intermediate (**F**) followed by intramolecular nucleophilic addition of arylamine to afford 4-amino substituted quinolines (**56**). Simultaneously, intermolecular nucleophilic attack of amines to arylcarbonyl palladium complex (**B**) to give arylcarbamoyl palladium complex (**H**) followed by reductive elimination give benzamide derivatives (**57**).

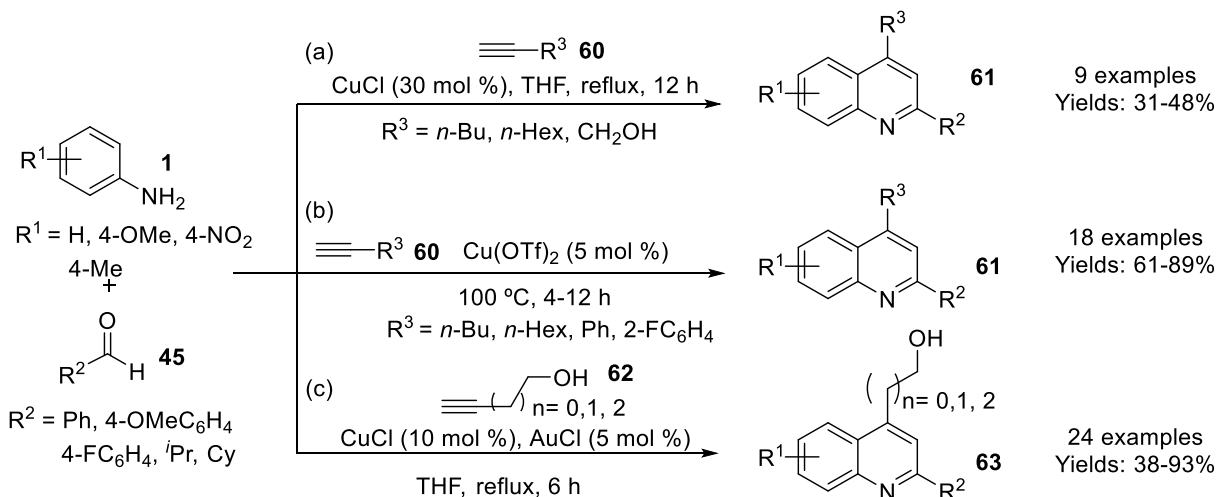
In extension, palladium-catalyzed domino three-component synthesis of 4-aminoquinolines (**59**) has been presented by Ruijter group from *o*-bromoanilines (**40**), isocyanides (**58**), and terminal alkynes (**27**) (**Scheme 2A.21**).^[43] The developed protocol proceeds *via* imidoylative Sonogashira coupling (**I**) followed by acid-mediated cyclization. This three-component protocol is highly compatible with diverse substituents on *o*-bromoanilines (**40**) and primary, secondary or tertiary aliphatic isocyanides (**58**).



Scheme 2A.21: Pd-catalyzed synthesis of 4-amino substituted quinolines from 2-bromoanilines

2A.2.3 Copper catalyst

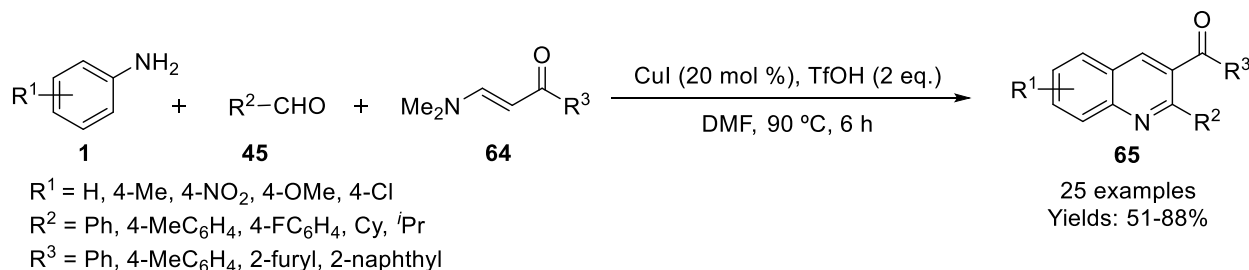
A simple, efficient and inexpensive strategy for quinoline synthesis is highly desirable for organic chemists. With this requirement, Iqbal and his coworkers successfully developed 2,4-disubstituted quinolines (**61**) by three component coupling reaction of anilines (**1**), arylaldehydes (**45**), and terminal alkynes (**60**) through copper-mediated *via* Povarov type reaction (**Scheme 2A.22a**).^[44] This three-component reaction also referred to as A³-coupling reaction^[45]. Wang group applied a similar strategy for quinoline synthesis (**61**) by using the combination of both AuCl₃ and CuBr catalyst.^[46]



Scheme 2A.22: Cu-catalyzed synthesis of substituted quinolines *via* Pavorov-type reaction

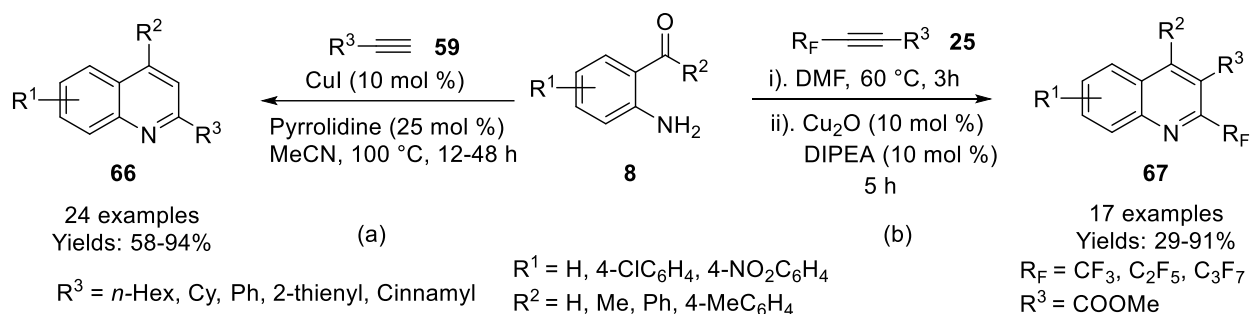
Larsen *et al.* further improved the Iqbal and wang's synthesis for the quinolines (**60**) by using 5 mol % of Cu(OTf)₂ without the use of ligand, additive, and solvent (**Scheme 2A.22b**).^[47] The improved methodology was also applied on both aromatic and aliphatic aldehydes (**45**) and provided quinolines (**61**) in good to excellent yield (61-89%). Later, an alternate route for the formation of functionalized quinolines by A³-coupling reaction was disclosed by Lin group under CuCl and AuCl as dual sequential catalysis. The developed transformation involves hydroxyalkylated terminal alkynes (**62**) to produce 4-hydroxyalkyl substituted quinolines (**62**) (**Scheme 2A.22c**).^[48]

Inspired by the above multi-component reaction using alkynes (**60**), Wan and coworkers examined the *N,N*-dimethyl enaminones (**64**) instead of the terminal alkynes (**60**) with amines (**1**) and aldehydes (**45**) under Cu-catalysis for the synthesis of functionalized quinolines (**65**) (**Scheme 2A.23**).^[49] Various analogue containing electron-releasing and withdrawing substituents have been achieved to explore the generality of the reaction.



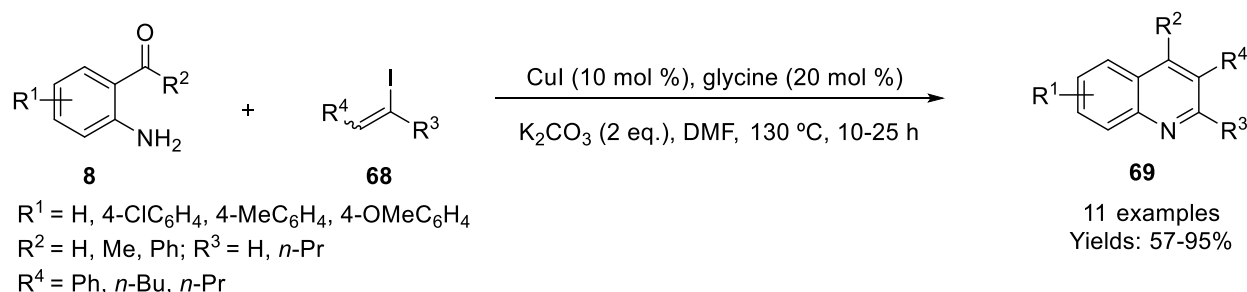
Scheme 2A.23: CuI catalyzed the synthesis of substituted quinolines from enaminones

Patil *et al.* disclosed an efficient strategy for substituted quinolines (**66**) *via* domino approach from readily accessible terminal alkynes (**60**) and *o*-aminobenzaldehydes (**8**) catalyzed by CuI and pyrrolidine co-operative catalytic system (**Scheme 2A.24a**).^[50] This co-operative catalytic process showed broad substrate scope with large functional group tolerance such as -NO₂, -CN, -COOMe and -Br on *o*-aminobenzaldehydes. Another example of Cu-catalyzed quinoline formation (**67**) with internal alkynes (**25**) and *o*-aminocarboxyls (**8**) was reported by Cao and coworkers (**Scheme 2A.24b**).^[51] This developed strategy, offered an inexpensive, easier and mild reaction condition to synthesize quinolines (**67**) having perfluoroalkyl group at the C2 position.



Scheme 2A.24: Cu-catalyzed synthesis of quinolines from 2-aminocarboxyls and alkynes

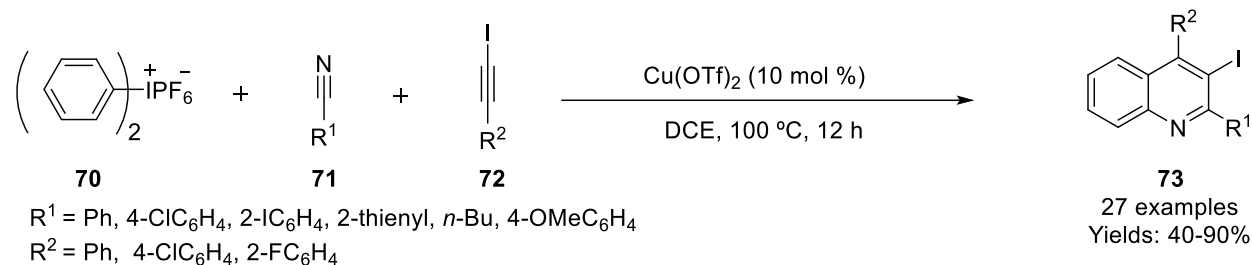
Formation of highly complex quinolines (**69**) *via* Cu-catalyzed domino reaction of alkenyl iodides (**68**) with *o*-aminocarboxyls (**8**) has been disclosed by Li group. The developed methodology proceed *via* Cu-catalyzed Ullman-type C-N coupling between alkenyl iodides (**68**) and *o*-aminocarboxyls (**8**) followed by an enamine condensation reaction (**Scheme 2A.25**).^[52]



Scheme 2A.25: Cu(I)-catalyzed synthesis of quinolines using alkenyl iodide and *o*-aminocarboxyls

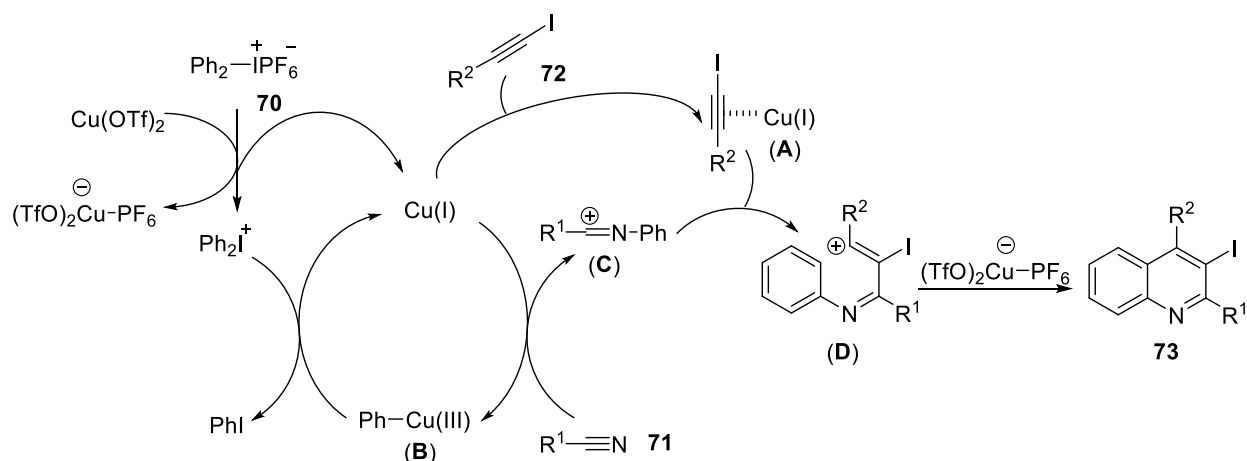
Hu *et al.* first time documented an attractive approach for the direct 3-iodosubstituted quinolines (**73**) *via* three-component reaction of 1-iodoalkynes (**72**), nitriles (**71**), and diaryliodonium salt (**70**) in the presence of Cu(OTf)₂ as catalyst (**Scheme 2A.26**).^[53] This method described good generality

to both iodoalkynes (**72**), and nitriles (**71**), thus providing the wide molecular diversity of 3-iodo functionalized quinoline derivatives (**73**) in moderate to excellent yields (40-90%).



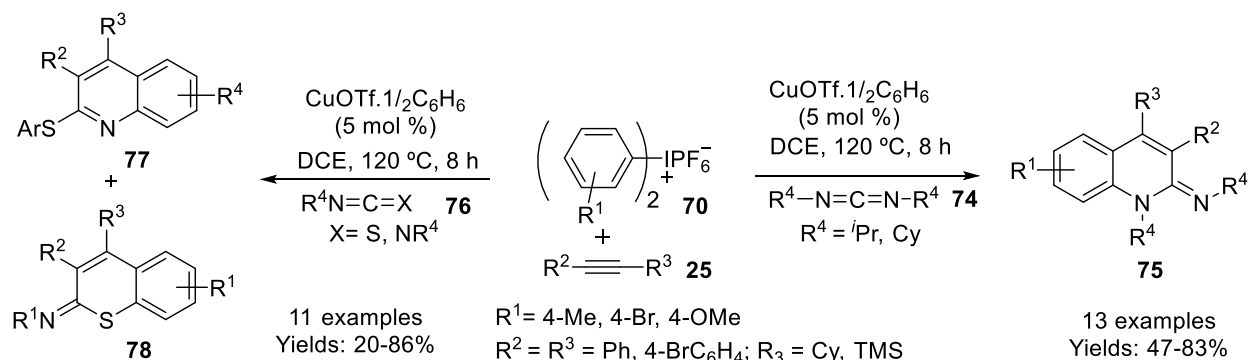
Scheme 2A.26: Synthesis of substituted 3-iodoquinoline by using aryliodonium salt

In this methodology, $\text{Cu}(\text{OTf})_2$ reacts with diaryliodonium salt (**70**) to give Lewis base $\text{PF}_6^- \text{Cu}(\text{OTf})_2$ and Ph_2I^+ . $\text{Cu}(\text{OTf})_2$ also undergoes disproportionation reaction *in situ* to produce $\text{Cu}(\text{I})$ and $\text{Cu}(\text{III})$ which plays an important role in reaction mechanism as shown in **Scheme 2A.27**. $\text{Cu}(\text{I})$ acts as a dual catalyst in this method: first, the diaryliodonium salt (**70**) converts into $\text{PhCu}(\text{III})$ complex (**B**), and second, it activates 1-iodoalkyne (**72**) by forming π -complex (**A**). Then nitriles (**71**) attack on $\text{PhCu}(\text{III})$ complex (**B**) to convert *N*-phenylnitrilium salt (**C**), subsequently **C** reacts with (**A**) to form intermediate (**D**). Finally, **D** undergoes electrophilic annulation to afford 3-iodoquinoline (**73**) in the presence of Lewis base $\text{PF}_6^- \text{Cu}(\text{OTf})_2$.



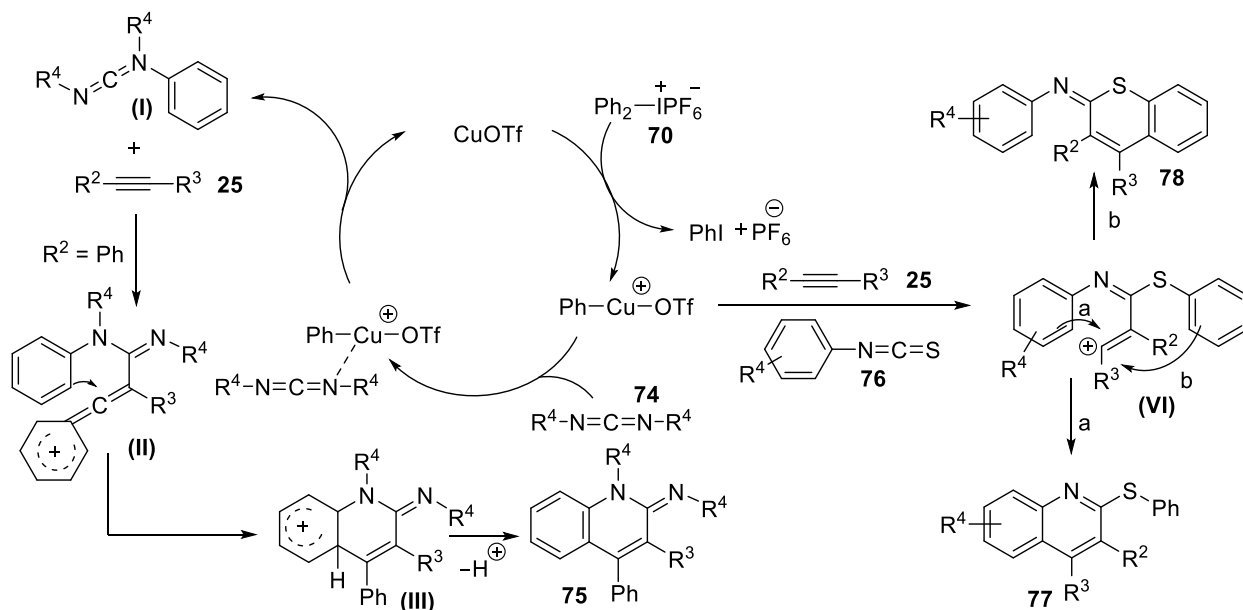
Scheme 2A.27: Proposed mechanism for quinoline synthesis using diaryliodonium salt through copper triflate.

Later on, Xi group reported CuOTf catalyzed the synthesis of substituted quinolines (**75**, **77** and **78**) using the multi-component reaction of diaryliodonium salts (**70**), internal alkynes (**25**), and heterocumulenes (**74** and **76**) via [2+2+2] and [4+2] cycloaddition (**Scheme 2A.28**).^[54]



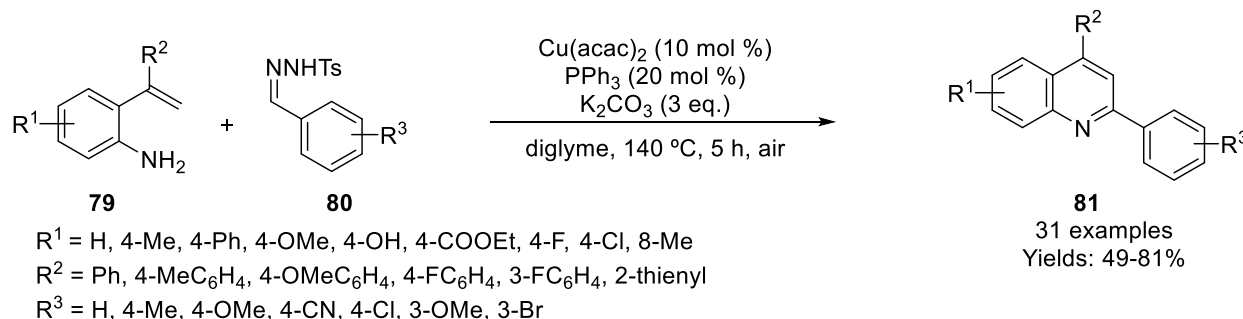
Scheme 2A.28: Cu(I)-catalyzed three-component synthesis of functionalized quinolines

The developed reaction proposed to proceed initially, aza-allene cation intermediate (**I**) is formed by the reaction of carbodiimide (**74**) diphenyliodonium salt (**70**) and CuOTf catalyst. Then the nucleophilic attack on reactive aza-allene cation (**I**) by internal alkyne (**25**) produced intermediate (**II**). Subsequently, Friedel-Crafts type reaction and aromatization led to corresponding quinolines (**75**). On the other hand, when isothiocyanates (**76**) were employed instead of carbodiimide (**74**), then selectivity was observed which is achieved in Friedel-Crafts step wherein the path (a) nucleophilic attack of the phenyl ring of isothiocyanate on a cationic intermediate (**IV**) produced 2-sulfurydrylquinolines (**77**) via [4+2] annulation. Another path (b) involved attack of the phenyl ring of diaryliodonium salt on a cationic intermediate (**IV**) through [2+2+2] annulation in generating thiacyclics (**78**).



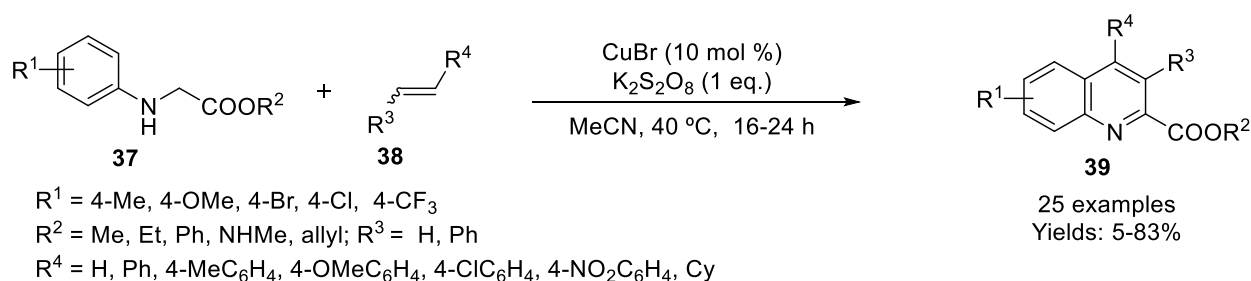
Scheme 2A.29: Mechanism of Cu(I)-catalyzed three-components synthesis of quinolines

Anbarasan group applied a Cu(II)-catalyzed oxidative cross-coupling approach for the synthesis of substituted quinoline derivatives (**81**) in moderate to good yields (49-81%) from *o*-vinylanilines (**79**) and *N*-tosylhydrazone (**80**) (Scheme 2A.30).^[55]



Scheme 2A.30: Cu(II)-catalyzed formation of quinolines from 2-vinylanilines

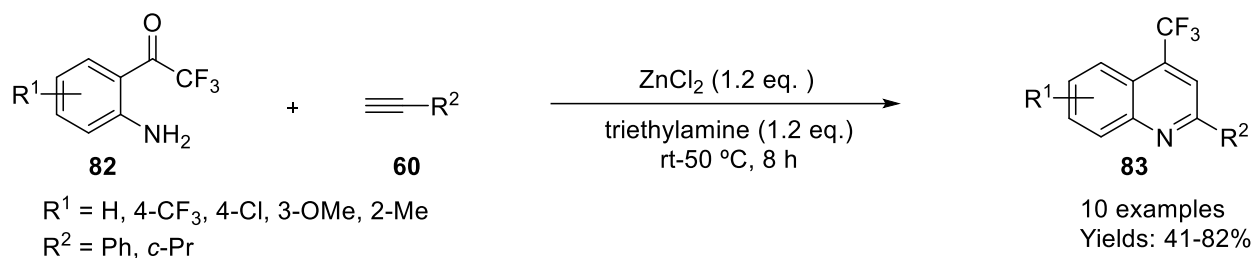
Liu *et al.* also established an economically viable CuBr-catalyzed cross-dehydrogenative coupling (CDC) of *N*-arylglycine derivatives (**37**) with a variety of olefins (**38**) for the synthesis of carboxylate functionalized quinolines (**39**) using K₂S₂O₈ as an oxidant under mild condition (Scheme 2A.31).^[56]



Scheme 2A.31: Cu(I)-catalyzed synthesis of substituted quinolines from glycines and alkenes

2A.2.4 Miscellaneous transition metal-catalyzed synthesis of quinolines

The first efficient and convenient Zn(II)-mediated synthesis of substituted quinolines (**83**) has been achieved by Jiang group from *o*-trifluoroacetyl anilines (**82**) and terminal alkynes (**60**). (Scheme 2A.32).^[57]



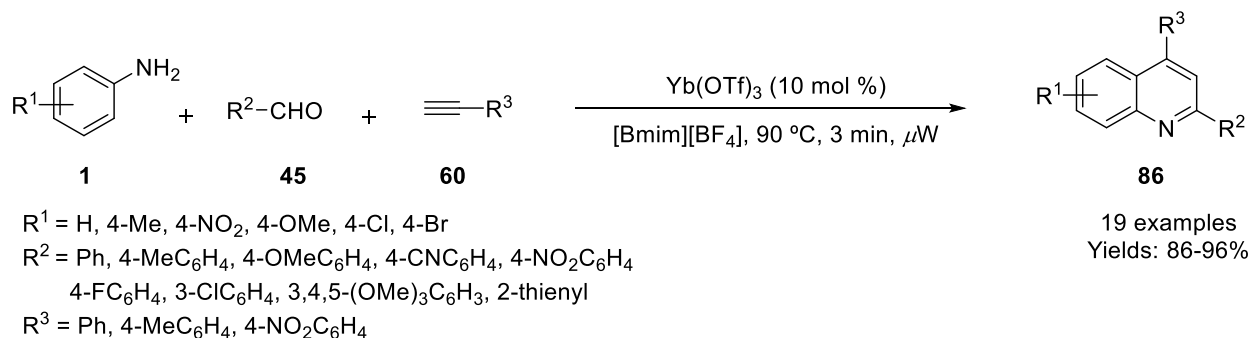
Scheme 2A.32: Zn(II)-mediated synthesis of functionalized quinolines from 2-aminocarbonyls

The preparation of polyfunctionalized quinolines (**83**) has been reported by Liu group from *o*-aminocarbonyls (**8**) and keto-alkynes (**84**) with a combination of Au(PPh₃)Cl and AgOTf-catalysts (**Scheme 2A.33**).^[58] This approach allowed the preparation of a large array of quinolines bearing keto-functional group at C3 in moderate to excellent yields.



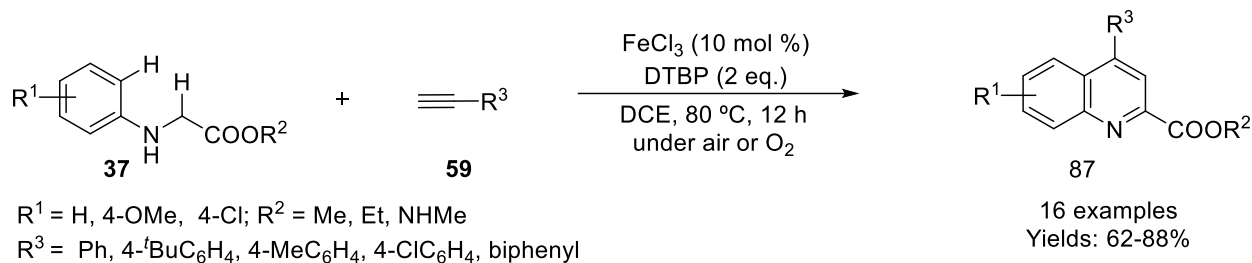
Scheme 2A.33: Au(I)/Ag(I)-catalyzed synthesis of substituted quinolines using 2-aminocarbonyls and keto-alkynes

Our group also synthesized multi-substituted quinoline derivatives (**86**) *via* Yb(OTf)₃ catalyzed three-component reaction between anilines (**1**), aldehydes (**45**) and terminal alkynes (**60**) using an ionic liquid as reaction media under microwave irradiation (**Scheme 2A.34**).^[59] A variety of quinoline derivatives were synthesized in good to excellent yield (86-96%).



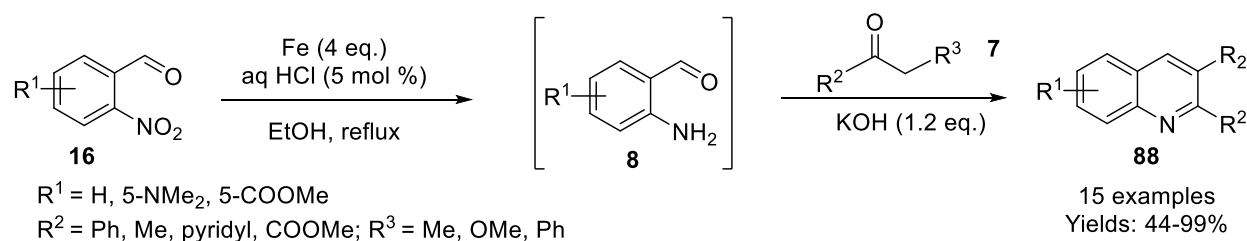
Scheme 2A.34: Yb(OTf)₃-catalyzed one-pot synthesis of quinolines from aniline

Hu group applied the Fe(III)-catalyzed cross-dehydrogenative coupling (CDC) strategy between *N*-arylglycines (**37**) and terminal alkynes (**59**) for the synthesis of functionalized quinolines (**87**) using DTBP as an oxidant in the presence of air or oxygen atmosphere (Scheme 2A.35).



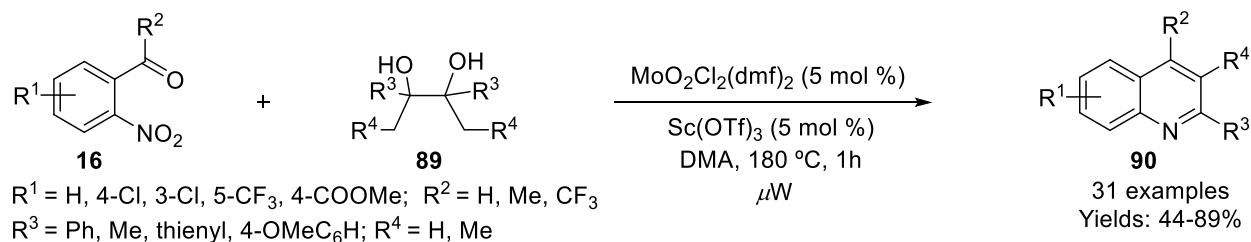
Scheme 2A.35: Fe(III)-catalyzed synthesis of quinoline derivatives *via* CDC of *N*-arylated glycines

Li *et al.* developed a simple and efficient one-pot synthesis of quinoline (**88**) by using readily available inexpensive *o*-nitrobenzaldehyde (**16**) which were reduced to *o*-aminobenzaldehyde (**8**) with Fe in the presence of 5 mol % of aq. HCl and subsequently reacted with α -methylene carbonyls (**7**) to give substituted quinolines (**88**) (Scheme 2A.36).^[60]



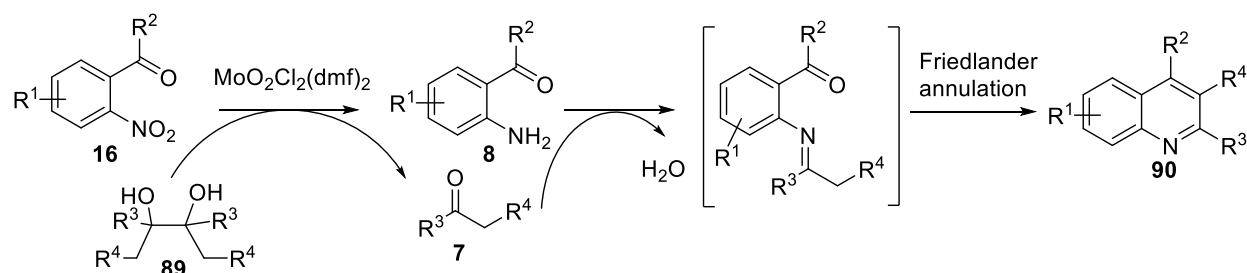
Scheme 2A.36: Fe-catalyzed construction of quinolines from *o*-nitrobenzaldehydes

Very recently, a synthetically reliable one-pot tandem route for Friedlander annulation has been developed by Sanz group by the reaction of *o*-nitrobenzaldehydes (**16**) and glycols (**89**) in the presence of Mo-catalyst under microwave radiation (Scheme 2A.37).^[61] Moreover, authors also observed that the addition of Sc(OTf)₃ (5 mol %) as co-catalyst improved the productivity of reaction with *o*-nitroacetophenones



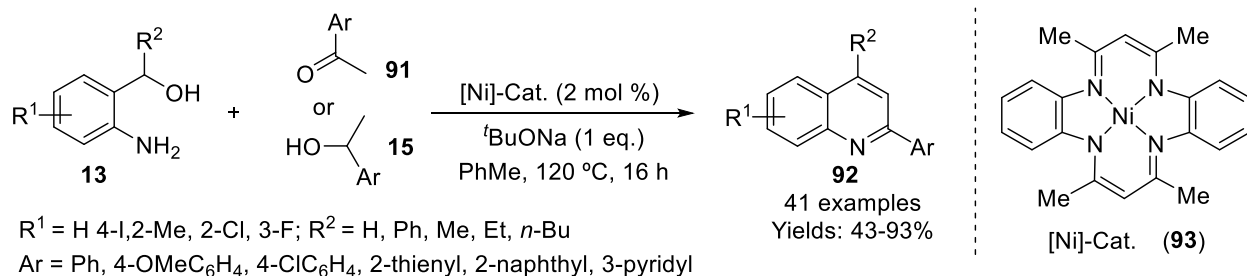
Scheme 2A.37: Mo-catalyzed Friedlander quinoline synthesis using *o*-nitrocarbonyls and glycols

In this strategy, $[\text{MoO}_2]^{2+}$ reduced *o*-nitrobenzaldehydes (**16**) to *o*-aminobenzaldehydes (**8**) with the help of glycols (**89**). Glycols (**89**) were converted to carbonyl compounds (**7**). Finally, Friedlander annulation led to polysubstituted quinolines (**90**) (**Scheme 2A.38**).



Scheme 2A.38: Mechanism of Mo-catalyzed synthesis of substituted quinolines

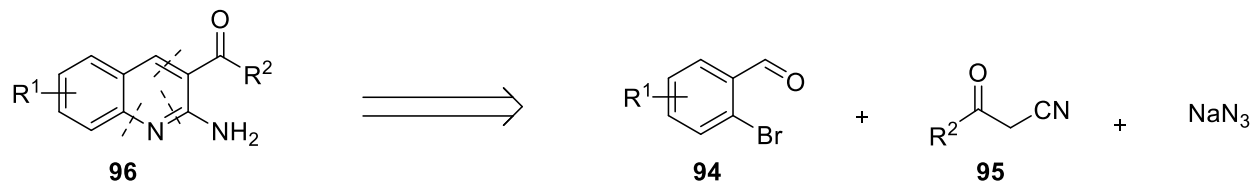
Sarkar group reported a simple and sustainable synthesis of polysubstituted quinolines (**92**) through Ni-catalyst (**93**) from *ortho*-aminobenzylalcohols (**13**) and carbonyl compounds (**91**) or secondary alcohols (**15**) (**Scheme 2A.39**).^[62] A variety of quinoline compounds were synthesized *via* sequential dehydrogenation and condensation process for C-C and C-N bond formation, respectively.



Scheme 2A.39: Ni-catalyzed synthesis of quinolines by dehydrogenative coupling

Mostly quinoline synthesis developed under transition metal catalysis rely on *o*-aminosubstituted carbonyl compounds or anilines. Thus, in this chapter, we described a simple and efficient

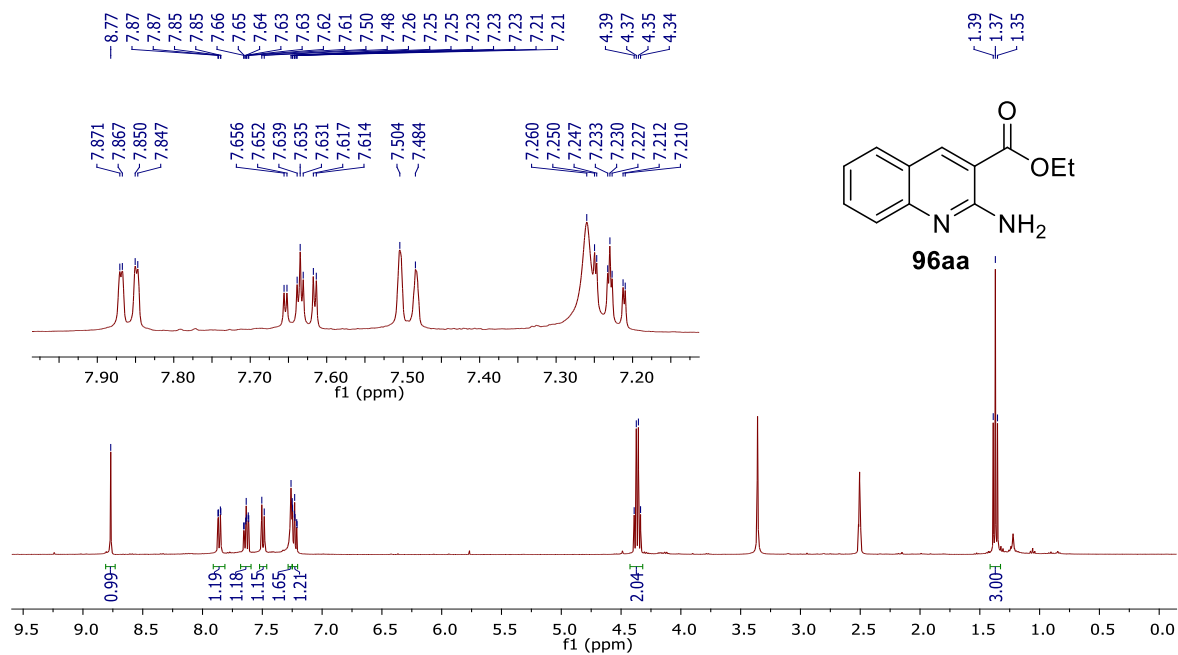
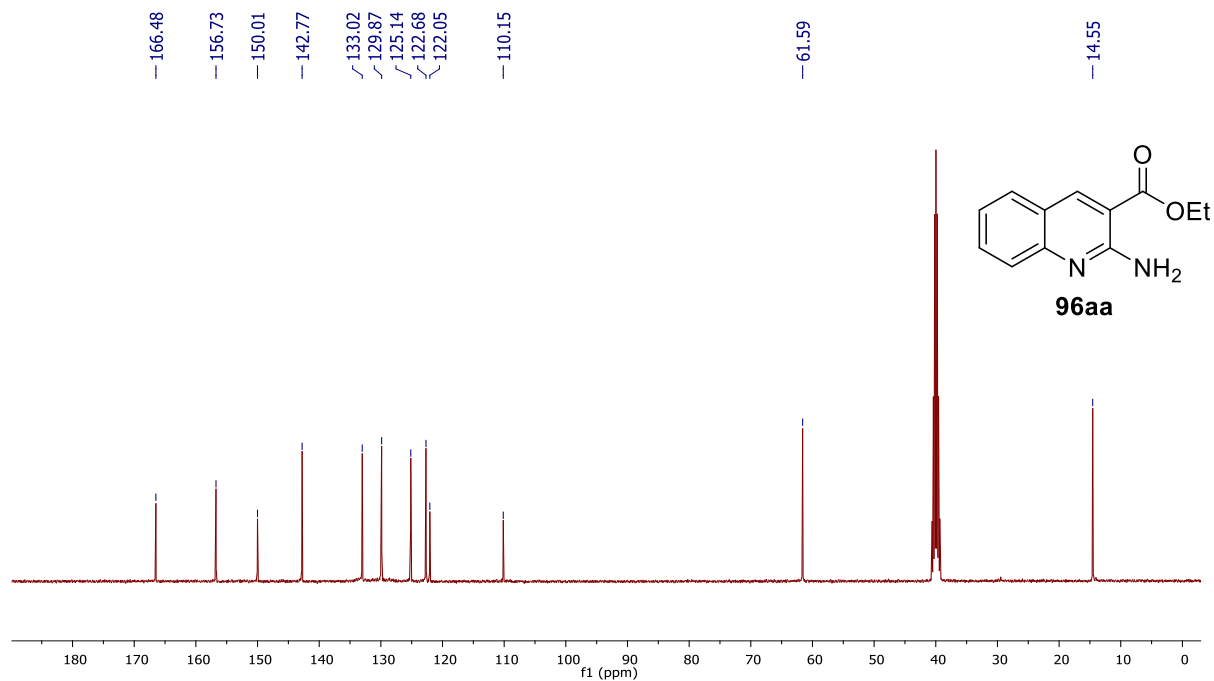
multicomponent reaction of *o*-bromobenzaldehydes (**94**), active methylene nitriles (**95**), and sodium azide as nitrogen surrogate under copper catalysis to access 2-amino-3-cabonylquinolines (**96**) (Scheme 2A.40).



Scheme 2A.40: Retrosynthesis for 2,3-disubstituted quinolines *via* multicomponent reaction

2A.3 RESULTS AND DISCUSSION

Our initial study began with the reaction of 2-bromobenzaldehyde (**94a**), ethyl cyanoacetate (**95a**), and NaN_3 using 10 mol % CuI as a catalyst, 20 mol % L-proline as ligand and 2.5 eq. of K_2CO_3 as a base in *N,N*-dimethylformamide (DMF) at 150 °C for 3.0 h under air atmosphere. Gratifyingly, expected ethyl 2-aminoquinoline-3-carboxylate (**96aa**) was isolated in 35% yield (Table 2A.1, entry 1). The structure of **96aa** was characterized by using various spectroscopic techniques such as IR, NMR, and MS. In ^1H NMR spectrum, characteristic deshielded singlet appeared at δ 8.77 ppm for $\text{C}_4\text{-H}$ and one broad singlet at δ 7.26 ppm for NH_2 group, quartet at δ 4.36 ppm for CH_2 and triplet at δ 1.37 ppm for CH_3 of ester group along with other expected protons at their respective positions were observed (Figure 2A.3). The carbonyl carbon of ester appeared at δ 166.48 ppm along with all other expected peaks in the ^{13}C NMR spectrum (Figure 2A.4). In the IR spectrum of **96aa**, a strong peak appeared at 1697 and 3418 cm^{-1} which confirmed the presence of $\text{C}=\text{O}$ and NH_2 functionality in the molecule respectively (Figure 2A.5). Also, the peak at m/z 217.0956 for the $[\text{M}+\text{H}]^+$ ion in HRMS further confirms the structure of **96aa** (Figure 2A.6).

Figure 2A.3: ^1H NMR spectrum of **96aa**Figure 2A.4: ^{13}C NMR spectrum of **96aa**

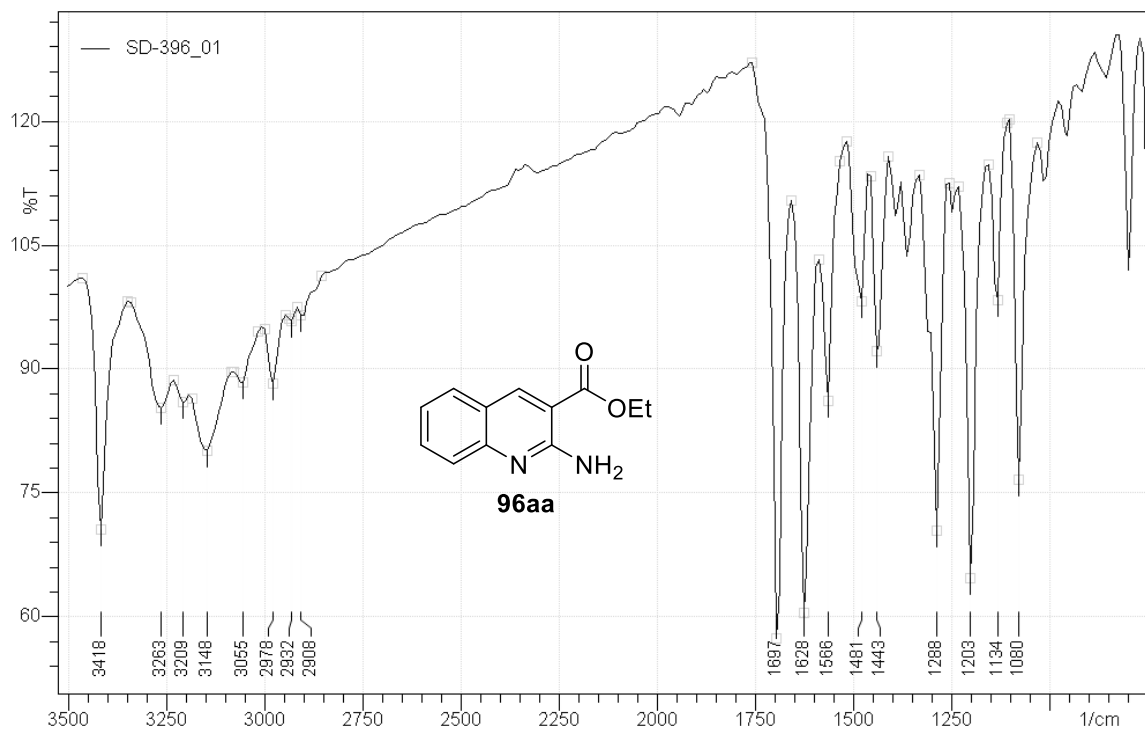


Figure 2A.5: IR spectrum of 96aa

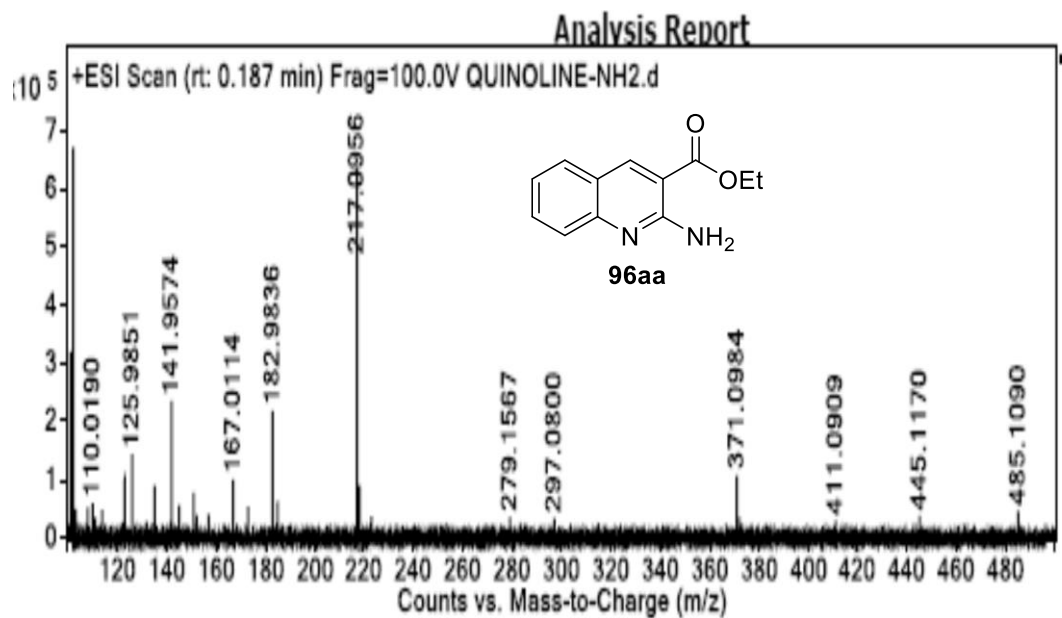
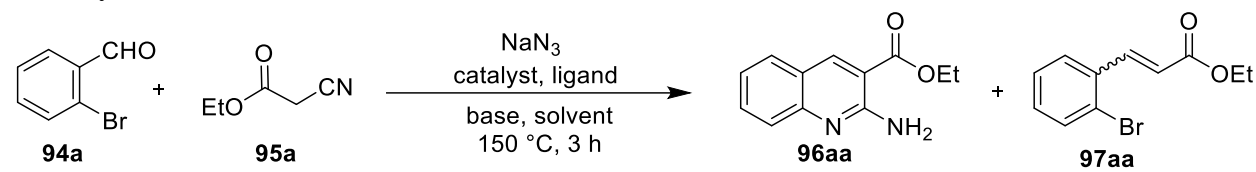


Figure 2A.6: HRMS spectrum of 96aa

To further improve the yield of tandem product **96aa**, various experimental conditions were screened by evaluating copper catalysts, ligands, bases and solvents (**Table 2A.1**). First, various copper salts were tested such as CuI, CuCl₂, CuBr, Cu(OAc)₂·H₂O, CuOTf.DCM and CuSO₄·5H₂O revealed that CuI was the efficient catalyst for this transformation giving the highest yield (**Table 2A.1**, entries 1-6). We further investigated the mole % of CuI suggested that 20 mole % CuI salt is suitable for the reaction which afforded product **96aa** in 55% yield (**Table 2A.1**, entry 7). Among various bases (K₂CO₃, K₃PO₄, ^tBuOK, Cs₂CO₃, Na₂CO₃, NaOMe, Et₃N, and DBU) examined (**Table 2A.1**, entries 7, 9–15), K₂CO₃ was found to be the most suitable base. In the case of trimethylamine (Et₃N), the reaction exclusively led to Knoevenagel product (**97aa**) (**Table 2A.1**, entry 14).

Reactions in different solvents namely DMSO, *N,N*-dimethylacetamide (DMA), toluene, *N*-methyl-2-pyrrolidone (NMP), 1,4-dioxane and PEG-400 (**Table 2A.1**, entries 16–21) revealed DMSO as a solvent of choice for this reaction. When the reaction was performed in toluene at 120 °C only Knoevenagel intermediate (**97aa**) was obtained in 45% yield (**Table 2A.1**, entry 20). Finally, by a screening of different ligands (**Table 2A.1**, entries 16 and 22-25), L-proline was found to be the most effective ligand. The reaction was ceased at the Knoevenagel adduct (**97aa**) in the absence of a catalyst (**Table 2A.1**, entry 26) and yield of desired product **96aa** was diminished in the absence of L-proline (**Table 2A.1**, entry 27).

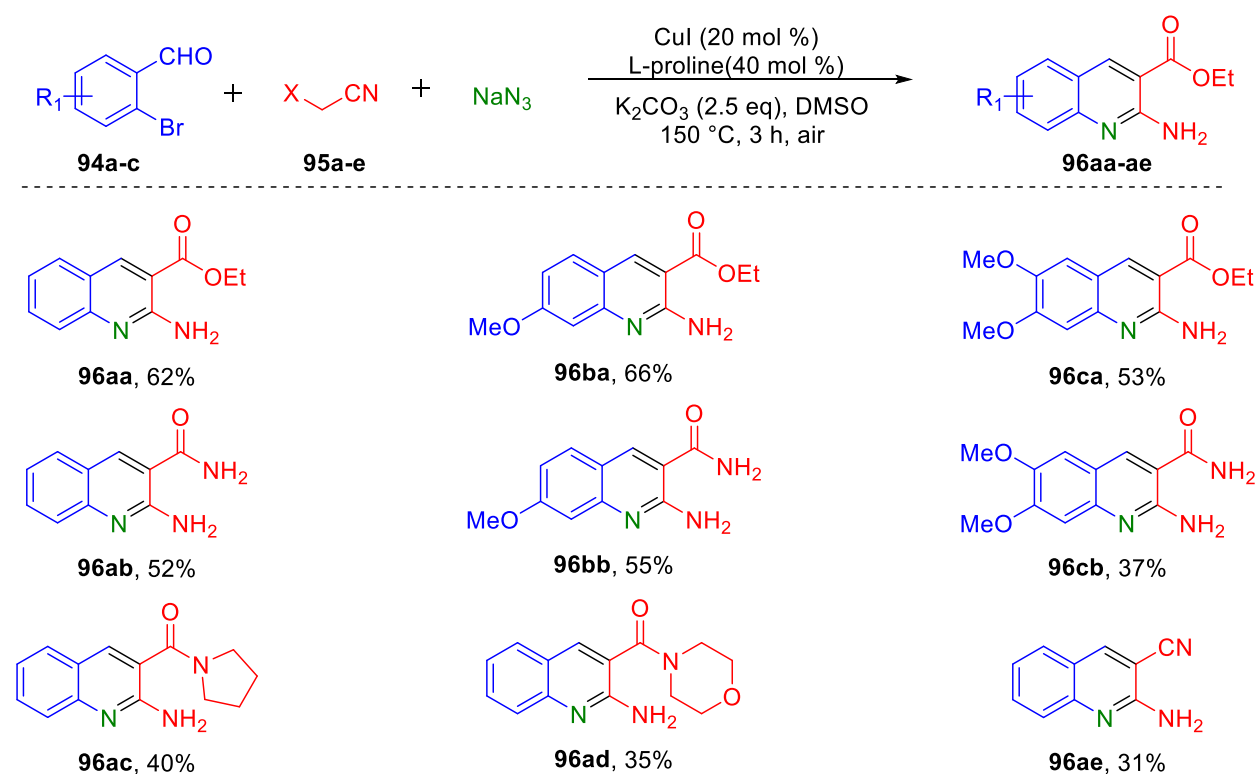
Table 2A.1: Optimization of reaction condition for the synthesis of ethyl 2-aminoquinoline-3-carboxylate.^a


Entry	Catalyst (mol %)	Ligand (mol %)	Base (2.5 eq.)	Solvent	Yield ^b (%)
1	CuI (10)	L-proline(20)	K ₂ CO ₃	DMF	35
2	CuCl ₂ (10)	L-proline(20)	K ₂ CO ₃	DMF	9
3	CuBr(10)	L-proline(20)	K ₂ CO ₃	DMF	20
4	Cu(OAc) ₂ ·H ₂ O(10)	L-proline(20)	K ₂ CO ₃	DMF	13
5	CuOTf.DCM (10)	L-proline(20)	K ₂ CO ₃	DMF	31
6	CuSO ₄ ·5H ₂ O(10)	L-proline(20)	K ₂ CO ₃	DMF	26
7	CuI(20)	L-proline(40)	K ₂ CO ₃	DMF	55
8	CuI(30)	L-proline(60)	K ₂ CO ₃	DMF	50
9	CuI(20)	L-proline(40)	K ₃ PO ₄	DMF	38
10	CuI(20)	L-proline(40)	^t BuOK	DMF	30
11	CuI(20)	L-proline(40)	CsCO ₃	DMF	10
12	CuI(20)	L-proline(40)	Na ₂ CO ₃	DMF	8
13	CuI(20)	L-proline(40)	NaOMe	DMF	11
14	CuI(20)	L-proline(40)	Et ₃ N	DMF	- ^c
15	CuI(20)	L-proline(40)	DBU	DMF	6
16	CuI(20)	L-proline(40)	K₂CO₃	DMSO	62
17	CuI(20)	L-proline(40)	K ₂ CO ₃	NMP	28
18	CuI(20)	L-proline(40)	K ₂ CO ₃	DMA	37
19	CuI(20)	L-proline(40)	K ₂ CO ₃	Dioxane ^d	10
20	CuI(20)	L-proline(40)	K ₂ CO ₃	Toluene ^e	- ^c
21	CuI(20)	L-proline(40)	K ₂ CO ₃	PEG-400	trace
22	CuI(20)	Glycine(40)	K ₂ CO ₃	DMSO	38
23	CuI(20)	DMEDA(40) ^f	K ₂ CO ₃	DMSO	42
24	CuI(20)	1,10-Phen(40) ^g	K ₂ CO ₃	DMSO	12
25	CuI(20)	8-HQ(40) ^h	K ₂ CO ₃	DMSO	9
26	-	L-proline(40)	K ₂ CO ₃	DMSO	trace ^c
27	CuI(20)	-	K ₂ CO ₃	DMSO	20

^aReactions conditions: **94a** (0.54 mmol), **95a** (0.65 mmol), NaN₃ (0.810 mmol), catalyst (20 mol %), ligand (40 mol %) and K₂CO₃ (2.5 eq.) were heated in DMSO (2 mL) at 150 °C for 3 h under air atmosphere. ^bIsolated yields. ^cOnly knoevenagel adduct (**97aa**) was observed after 16 h. ^dAt 110 °C. ^eAt 120 °C. ^fDMEDA= N, N-dimethylethylenediamine. ^g1,10-Phen= 1,10-phenanthroline. ^h8-HQ= 8-hydroxyquinolone

With the standard reaction condition in hand (Table 2A.1, entry 16), we explored the substrate generality for this tandem reaction by employing the differently substituted 2-bromobenzaldehydes and active methylene nitriles (Table 2A.2). Reactions of substituted 2-bromobenzaldehydes **94a-c** with different active methylene nitriles **95a-e** gave corresponding 2-aminoquinolines (**96aa-ae**) in moderate to good yields (31-66%). The method tolerated different functional groups such as cyano, methoxy, ester, and amide. It is worth to mentioned that the reaction of 2-bromo-5-chlorobenzaldehyde with ethyl cyanoacetate produced corresponding product only in trace amount.

Table 2A.2: Substrate scope for the synthesis of 2-aminoquinoline derivatives.^{a,b}

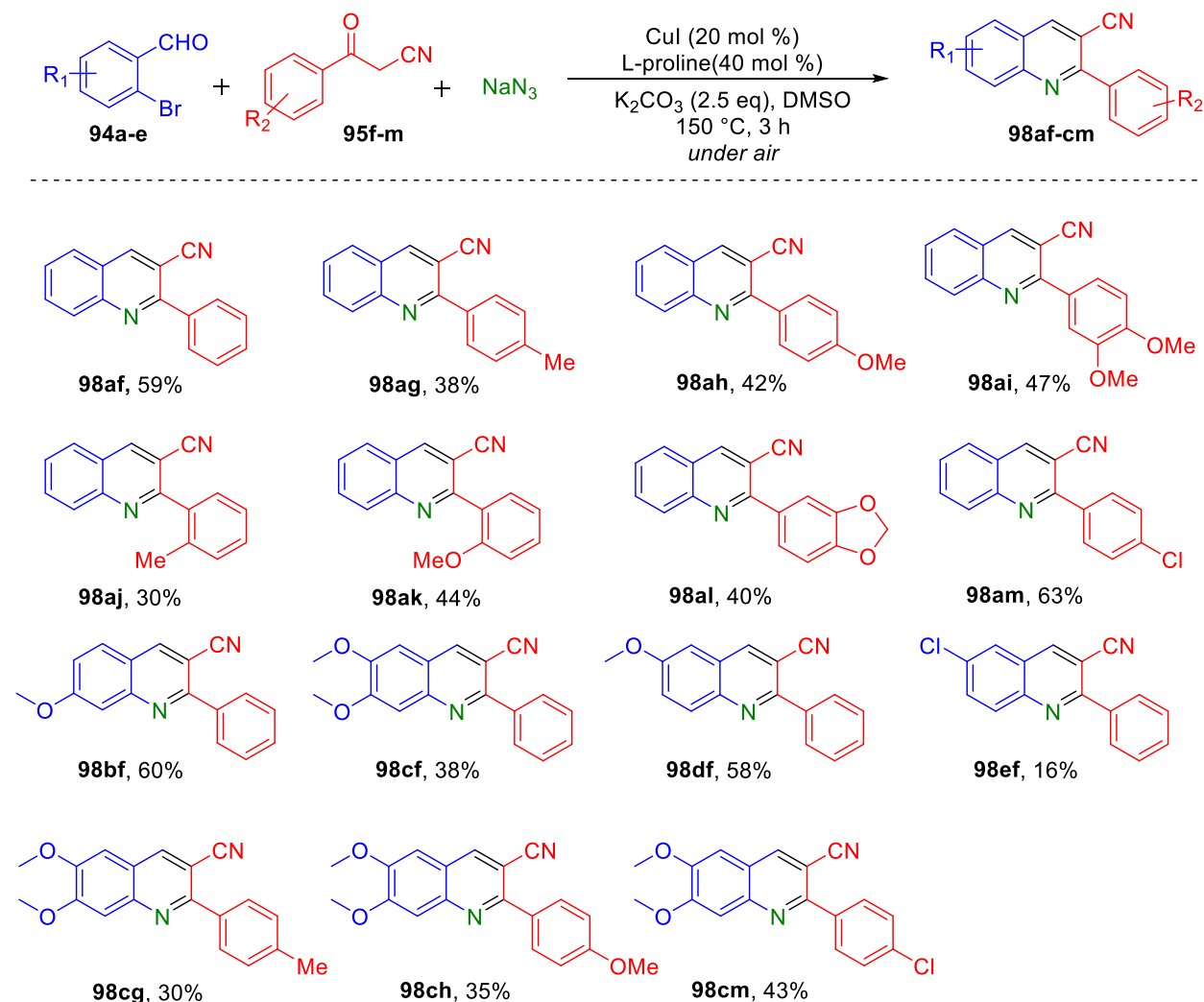


^aReactions conditions: **94** (0.54 mmol), **95** (0.65 mmol), NaN_3 (0.810 mmol), catalyst (20 mol %), ligand (40 mol %) and K_2CO_3 (1.35 mmol) were heated in DMSO (2 mL) at 150 °C for 3 h under air atmosphere. ^bIsolated yields.

Notably, when benzoylacetonitrile (R = ArCO, **95f-m**) was used as an active methylene nitrile, instead of expected 2-aminoquinoline, 2-phenylquinoline-3-carbonitrile (**98af**) was obtained in

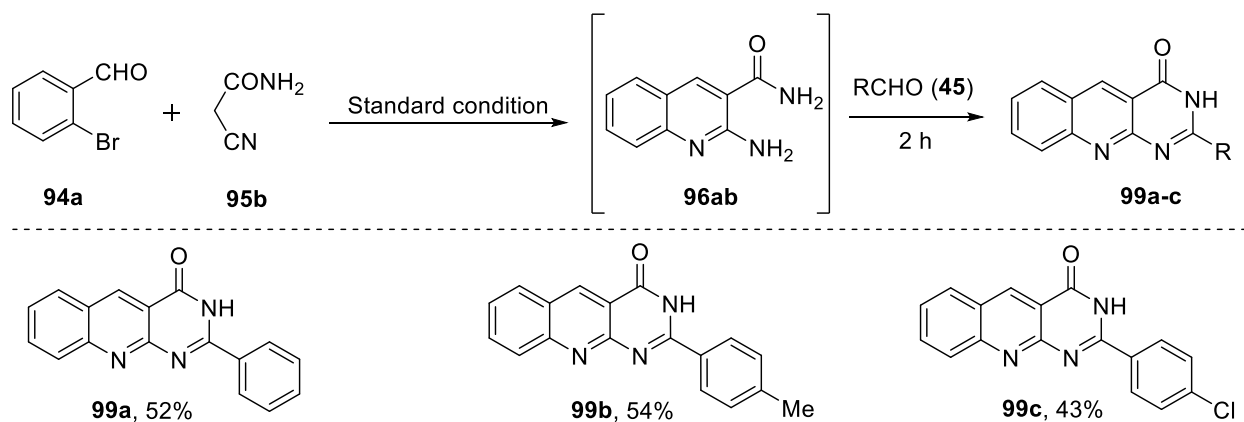
59% yield. Formation of **98af** prompted us to evaluate the chemoselectivity of this reaction for benzoylacetonitriles. As can be seen from **Table 2A.3**, benzoylacetonitriles containing methyl, methoxy, dioxole, and chloro substituent reacted efficiently with 2-bromobenzaldehydes (**94a**) to give corresponding quinoline-3-carbonitriles (**98af–am**) in moderate to good yields (30-63%). Similarly, 2-bromobenzaldehydes bearing methoxy and chloro groups were treated with differently substituted benzoylacetonitriles to give corresponding 2-arylquinoline-3-carbonitriles (**98bf–cm**) in moderate to good yields (30-60%).

Table 2A.3: Substrate scope for the synthesis of 2-Arylquinoline-3-carbonitrile.^{a,b}



^aReactions conditions: **94** (0.54 mmol), **95** (0.65 mmol), NaN_3 (0.810 mmol), catalyst (20 mol %), ligand (40 mol %) and K_2CO_3 (1.35 mmol) were heated in DMSO (2 mL) at 150 °C for 3 h under air. ^bIsolated yields.

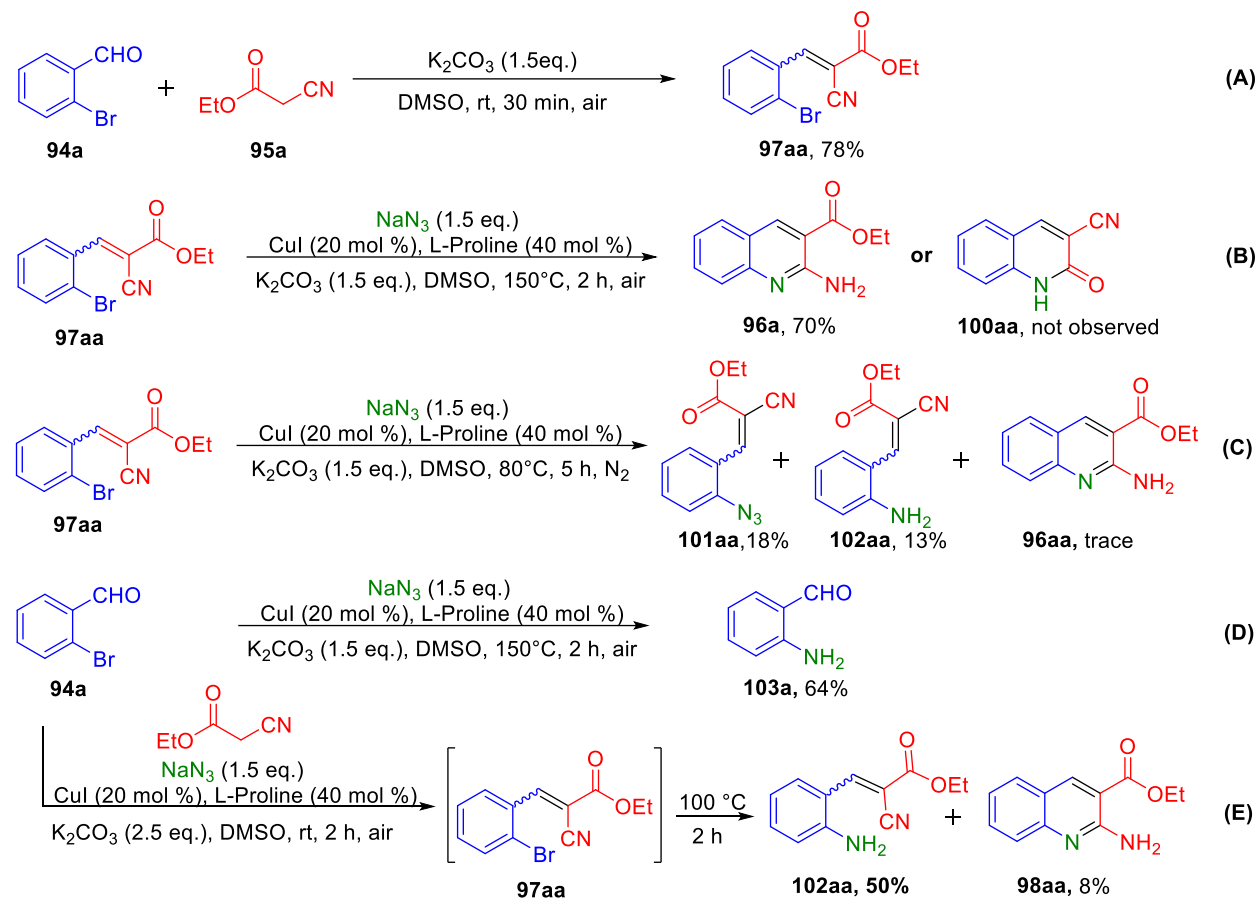
Next, the synthetic application of this developed methodology was demonstrated by the one-pot synthesis of pyrimido[4,5-*b*]quinolin-4(3*H*)-one derivatives (**99a-c**). In all the cases, reactions underwent smooth conversion to afford the corresponding pyrimido[4,5-*b*]quinolin-4(3*H*)-ones **99a-c** in moderate (52-43%) yields (**Scheme 2A.41**).



Scheme 2A.41: One-pot synthesis of pyrimido[4,5-*b*]quinolin-4(3*H*)-ones

Series of control experiments were performed to evaluate the possible reaction pathway for the tandem sequences to produce **96aa** and **98aa** (**Scheme 2A.42**). Initially, 2-bromobenzaldehyde (**94a**) was reacted with ethyl cyanoacetate using K_2CO_3 (1.5 eq.) in DMSO at room temperature for 30 min, only Knoevenagel adduct (**97aa**) was obtained in 78% yield (**Scheme 2A.42A**). When Knoevenagel adduct (**97aa**), NaN_3 , CuI, L-proline, and K_2CO_3 were heated at 150 °C for 2 h, only the desired product **96aa** was isolated in 70% yield (**Scheme 2A.42B**). Exclusive formation of **96aa** can be due to the relative reactivity of cyano-group over ester in **97aa**. Again, Knoevenagel adduct **97aa** was heated at 80 °C with NaN_3 , CuI, L-proline and K_2CO_3 under inert atmosphere, obtained ethyl 3-(2-azidophenyl)-2-cyanoacrylate (**101aa**) in 18% yield and ethyl 3-(2-aminophenyl)-2-cyanoacrylate (**102aa**) in 13% yield along with trace amount of desired product (**Scheme 2A.42C**). The reaction of *o*-bromobenzaldehyde (**94a**) with NaN_3 , CuI, L-proline, and K_2CO_3 at 120 °C gave 2-aminobenzaldehyde (**103a**) in 64% yield (**Scheme 2A.42D**). However, treatment of **94a** with ethyl cyanoacetate (**95a**) in the presence of NaN_3 , CuI, L-proline, and K_2CO_3 at room temperature exclusively resulted in intermediate **97aa**. When the same reaction mixture was heated at 100 °C, ethyl 3-(2-aminophenyl)-2-cyanoacrylate (**102aa**) was obtained in 50% yield along with the desired product **96aa** in 8% yield (**Scheme 2A.42E**). From these control

experiments, we concluded that ethyl 3-(2-bromophenyl)-2-cyanoacrylate (**97aa**) and ethyl 3-(2-azidophenyl)-2-cyanoacrylate (**101aa**) ethyl 3-(2-aminophenyl)-2-cyanoacrylate (**102aa**) are the key intermediates for the formation of 2-aminoquinoline (**96aa**).



Scheme 2A.42: Control experiments for the formation of 2-aminoquinoline derivatives

Similarly, the reaction of **94a** with **95f** in the absence of copper catalyst gave 2-benzoyl-3-(2-bromophenyl)acrylonitrile (**104aa**) which on reaction with NaN_3 , CuI , L-proline, and K_2CO_3 at 150°C after 2 h resulted in the exclusive formation of **98aa** (Scheme 2A.43A & B). This may be attributed to the relative electrophilicity of the carbonyl group over the nitrile group. Structure of **104aa** was further confirmed by single X-ray analysis (Figure 2A.7, CCDC 1433055) and suggested that intermediate **104aa** exist as *E*-isomer.

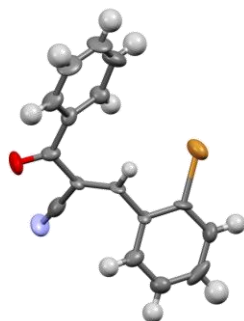
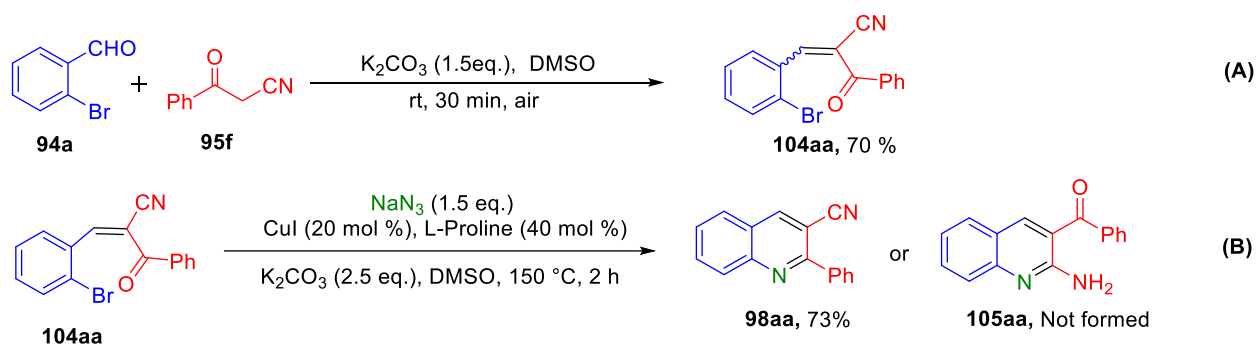
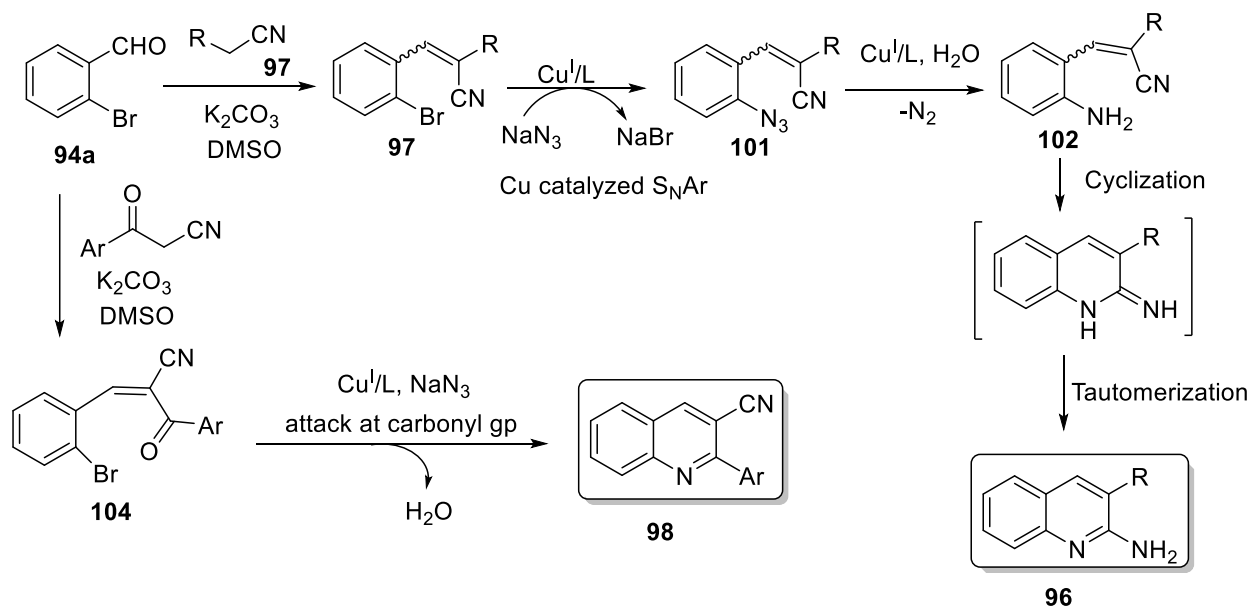


Figure 2A.7: ORTAP diagram of **104aa** (CCDC 1433055)



Scheme 2A.43: Control experiments for the synthesis of 2-phenyl-3-cyanoquinolines

Based on control experiments and literature reports,^[63-68] a possible mechanism for the copper-catalyzed multicomponent reaction has been described (Scheme 2A.44). Initially, the reaction of 2-bromobenzaldehyde (**94**) and ethyl cyanoacetate (**95**) produced Knoevenagel adduct (**97**). The azidation of **101** using sodium azide in the presence of a copper catalyst followed by reductive amination of **101** produced 2-(2-aminobenzylidene)malononitrile (**102**). This is in accordance with earlier reports wherein sodium azide has been used as ammonia surrogate to prepare primary amines and nitrogen-containing heterocycles in a copper-catalyzed reductive amination of aryl halides.^[69-70] Subsequently, intramolecular cyclization of **102** led to the formation of ethyl 2-aminoquinoline-3-carboxylate (**96**) via nucleophilic attack of amine onto nitrile followed by tautomerization.



Scheme 2A.44: Proposed mechanism for the synthesis of functionalized quinolines

In the case of aroylacetonitrile (**95**), intermediate **104** formed after Knoevenagel condensation underwent reductive amination followed by intramolecular condensation to afford 2-arylquinoline-3-carbonitrile (**98**).

2A.4 CONCLUSIONS

In summary, we have successfully developed an efficient and straightforward copper-catalyzed chemoselective synthesis of 2-aminoquinolines (**96**) and 2-arylquinoline-3-carbonitriles (**98**) from readily available 2-bromobenzaldehydes (**94**), active methylene nitriles (**95**) and sodium azide. The developed three-component, one-pot tandem protocol displays broad substrate scope with good functional group tolerance and gives quinolone derivatives in moderate to good yields. The developed methodology can further be utilized for the one-pot synthesis of pyrimido[4,5-*b*]quinolin-4(3*H*)-ones (**99**) in good yield.

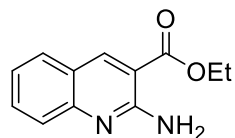
2A.5 EXPERIMENTAL SECTION

General information: Melting points were determined in open capillary tubes on an automated melting point apparatus and are uncorrected. Reactions were monitored by using thin layer chromatography (TLC) on 0.2 mm silica gel F₂₅₄ plates. The chemical structures of final products were determined by their NMR spectra (¹H and ¹³C NMR). Chemical shifts are reported in parts

per million (ppm) using deuterated solvent peak or tetramethylsilane as an internal standard. The HRMS data were recorded on a mass spectrometer with electrospray ionization and TOF mass analyzer. Some of the benzoyl acetonitriles and 2-cyano acetamides were synthesized according to the published procedure.^[71-72] All other chemicals were obtained from the commercial suppliers and used without further purification.

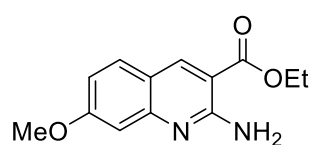
Representative procedure for synthesis of 2-aminoquinolines (96): A mixture of 2-bromobenzaldehyde (**94a**) (100 mg, 0.54 mmol), ethyl cyanoacetate (**95a**) (73 mg, 0.65 mmol), sodium azide (52 mg, 0.81 mmol), CuI (20 mol %), L-proline (40 mol %) and K₂CO₃ (186 mg, 2.5 eq.) in DMSO (2 mL) was mixed under air atmosphere at room temperature and then heated to 150 °C for 3 h. After cooling to ambient temperature, the reaction mass was quenched with ice-cold aqueous solution of NH₄Cl (30 mL), filtered through a bed of celite and the plug washed with ethyl acetate (20 mL). The resulting filtrate was extracted with ethyl acetate (2 × 20 mL) and the combined organic layers dried over anhydrous Na₂SO₄ and concentrated under reduced pressure. Desired product **96aa** (72 mg, 62%) was isolated by column chromatography on silica gel (100-200 mesh) using ethyl acetate/hexane (30%, v/v) as eluant.

Ethyl 2-aminoquinoline-3-carboxylate (**96aa**)



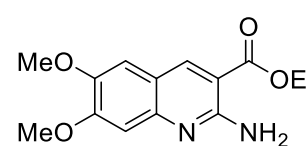
Yellow solid (72 mg, 62%); mp 134–136 °C; ¹H NMR (400 MHz, DMSO-*d*₆) δ 8.77 (s, 1H), 7.86 (dd, *J* = 8.1, 1.3 Hz, 1H), 7.63 (ddd, *J* = 8.4, 6.8, 1.5 Hz, 1H), 7.49 (d, *J* = 8.2 Hz, 1H), 7.26 (bs, 2H), 7.25 – 7.21 (m, 1H), 4.36 (q, *J* = 7.1 Hz, 2H), 1.37 (t, *J* = 7.1 Hz, 3H); ¹³C NMR (100 MHz, DMSO-*d*₆) δ 166.5, 156.7, 150.0, 142.8, 133.0, 129.9, 125.1, 122.7, 122.0, 110.5, 61.6, 14.6; IR (KBr): 3418, 1697, 1628, 1288, 1080 cm⁻¹; HRMS for C₁₂H₁₃N₂O₂ [M+H]⁺ calcd 217.0972, found 217.0956.

Ethyl 2-amino-7-methoxyquinoline-3-carboxylate (**96ba**)

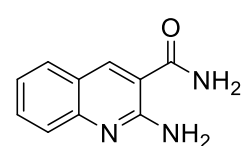


Yellow solid (87 mg, 66%); mp 138–140 °C; ¹H NMR (400 MHz, DMSO-*d*₆) δ 8.65 (s, 1H), 7.74 (d, *J* = 9.5 Hz, 1H), 7.23 (bs, 2H), 6.86 (d, *J* = 6.2 Hz, 2H), 4.33 (q, *J* = 7.0 Hz, 2H), 3.86 (s, 3H), 1.35 (t, *J* = 7.0 Hz, 3H); ¹³C NMR (100 MHz, DMSO-*d*₆) δ 166.8, 163.5, 157.4, 152.5, 142.1, 131.2, 117.1, 115.1, 107.1, 104.5, 61.3, 55.8, 14.6; IR (KBr): 3433, 1697, 1620, 1257, 1080 cm⁻¹; HRMS for C₁₃H₁₅N₂O₃ [M+H]⁺ calcd 247.1077, found 247.1087.

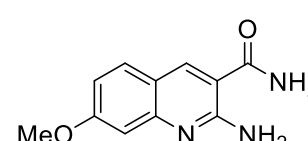
Ethyl 2-amino-6,7-dimethoxyquinoline-3-carboxylate (96ca)


 Brown solid (79 mg, 53%); mp 190–193 °C; ¹H NMR (400 MHz, DMSO-*d*₆) δ 8.60 (s, 1H), 7.28 (s, 1H), 6.99 (bs, 2H), 6.89 (s, 1H), 4.33 (q, *J* = 7.1 Hz, 2H), 3.88 (s, 3H), 3.82 (s, 3H), 1.35 (t, *J* = 7.1 Hz, 3H); ¹³C NMR (100 MHz, DMSO-*d*₆) δ 166.9, 156.3, 155.3, 148.0, 146.9, 140.4, 116.7, 107.8, 106.8, 105.0, 61.2, 56.1, 56.0, 14.6; IR (KBr): 3410, 1697, 1628, 1227, 1080 cm⁻¹; HRMS for C₁₄H₁₇N₂O₄ [M+H]⁺ calcd 277.1183, found 277.1189.

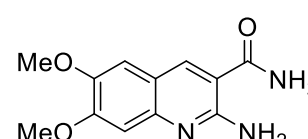
2-Aminoquinoline-3-carboxamide (96ab)

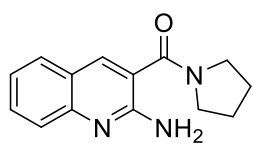

 Light orange solid (53 mg, 52%); mp 195–196 °C; ¹H NMR (400 MHz, DMSO-*d*₆) δ 8.48 (s, 1H), 8.24 (bs, 1H), 7.68 (d, *J* = 8.0 Hz, 1H), 7.61 (bs, 1H), 7.57 (ddd, *J* = 8.4, 6.9, 1.5 Hz, 1H), 7.47 (d, *J* = 8.4 Hz, 1H), 7.29–7.17 (m, 3H); ¹³C NMR (100 MHz, DMSO-*d*₆) δ 170.4, 157.1, 149.2, 138.6, 131.6, 129.1, 125.3, 122.3, 122.2, 114.6; IR (KBr): 3410, 3194, 1636, 1389, 1227 cm⁻¹; HRMS for C₁₀H₁₀N₃O [M+H]⁺ calcd 188.0818, found 188.0824.

2-Amino-7-methoxyquinoline-3-carboxamide (96bb)

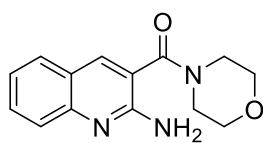

 Orange solid (64 mg, 55%); mp 221–224 °C; ¹H NMR (400 MHz, DMSO-*d*₆) δ 8.42 (s, 1H), 8.14 (bs, 1H), 7.56 (d, *J* = 8.6 Hz, 1H), 7.50 (bs, 1H), 7.27 (bs, 2H), 6.91–6.81 (m, 2H), 3.85 (s, 3H); ¹³C NMR (100 MHz, DMSO-*d*₆) δ 170.2, 162.4, 157.6, 151.3, 138.3, 130.3, 117.0, 114.4, 111.6, 104.7, 55.7; IR (KBr): 3378, 3209, 1620, 1381, 1227 cm⁻¹; HRMS for C₁₁H₁₂N₃O₂ [M+H]⁺ calcd 218.0924, found 218.0930.

2-Amino-6,7-dimethoxyquinoline-3-carboxamide (96cb)

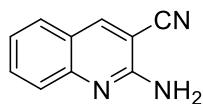

 Yellow solid (73 mg, 55%); mp 232–234 °C; ¹H NMR (400 MHz, DMSO-*d*₆) δ 8.33 (s, 1H), 8.07 (bs, 1H), 7.43 (bs, 1H), 7.02 (s, 1H), 6.98 (bs, 2H), 6.89 (s, 1H), 3.87 (s, 3H), 3.82 (s, 3H); ¹³C NMR (100 MHz, DMSO-*d*₆) δ 170.4, 156.3, 154.1, 146.6, 146.3, 137.0, 116.4, 111.5, 107.2, 105.3, 56.0; IR (KBr): 3380, 3210, 1623, 1381, 1225 cm⁻¹; HRMS for C₁₂H₁₄N₃O₃ [M+H]⁺ calcd 248.1030, found 248.1037.

(2-Aminoquinolin-3-yl)(pyrrolidin-1-yl)methanone (96ac)

Brown oil (52 mg, 40%); ^1H NMR (400 MHz, $\text{DMSO-}d_6$) δ 8.07 (s, 1H), 7.71 (d, $J = 7.7$ Hz, 1H), 7.57 – 7.46 (m, 2H), 7.20 (t, $J = 7.2$ Hz, 1H), 6.49 (s, 2H), 3.52 (t, $J = 6.7$ Hz, 2H), 3.38 (t, $J = 6.3$ Hz, 2H), 1.92 – 1.80 (m, 4H); ^{13}C NMR (100 MHz, $\text{DMSO-}d_6$) δ 166.6, 155.1, 148.1, 136.2, 130.7, 128.6, 125.4, 122.3, 120.1, 48.7, 46.2, 26.2, 24.4; IR (KBr): 3410, 1651, 1457, 1380 cm^{-1} ; HRMS for $\text{C}_{14}\text{H}_{16}\text{N}_3\text{O}$ $[\text{M}+\text{H}]^+$ calcd 242.1288, found 242.1292.

(2-Aminoquinolin-3-yl)(morpholino)methanone (96ad)

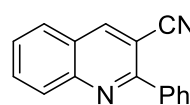
Yellow semisolid (49 mg, 35%); ^1H NMR (400 MHz, $\text{DMSO-}d_6$) δ 7.94 (s, 1H), 7.72 (d, $J = 7.4$ Hz, 1H), 7.57 – 7.49 (m, 2H), 7.22 (t, $J = 7.9$ Hz, 1H), 6.38 (bs, 2H), 3.62 (bs, 2H), 3.26 (bs, 2H), 1.60 (bs, 4H); ^{13}C NMR (100 MHz, $\text{DMSO-}d_6$) δ 167.8, 155.0, 147.6, 136.0, 130.9, 127.9, 125.8, 123.2, 122.6, 118.0, 65.9, 24.5; IR (KBr): 3410, 1653, 1458, 1381 cm^{-1} ; HRMS for $\text{C}_{10}\text{H}_8\text{N}_3$ $[\text{M}+\text{H}]^+$ calcd 258.1237, found 258.1243.

2-Aminoquinoline-3-carbonitrile (96ae)

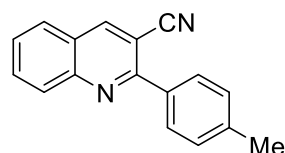
Yellow semisolid (28 mg, 31%); ^1H NMR (400 MHz, $\text{DMSO-}d_6$) δ 8.69 (s, 1H), 7.75 (dd, $J = 8.1, 1.2$ Hz, 1H), 7.66 (ddd, $J = 8.4, 6.9, 1.5$ Hz, 1H), 7.51 (d, $J = 8.6$ Hz, 1H), 7.28 (ddd, $J = 8.0, 6.9, 1.1$ Hz, 1H), 6.98 (bs, 2H); ^{13}C NMR (100 MHz, $\text{DMSO-}d_6$) δ 156.2, 149.6, 145.8, 133.3, 129.0, 125.9, 123.2, 121.4, 117.0, 95.0; IR (KBr): 3444, 2253, 1659, 1480, 1373 cm^{-1} ; HRMS for $\text{C}_{10}\text{H}_8\text{N}_3$ $[\text{M}+\text{H}]^+$ calcd 170.0713, found 170.0719.

Representative procedure for the synthesis of 2-phenylquinoline-3-carbonitriles (98af)

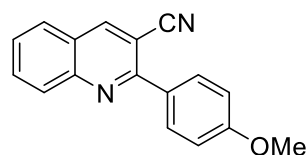
A mixture of 2-bromobenzaldehyde (**94a**) (100 mg, 0.54 mmol), benzoylacetonitriles (**95f**) (94 mg, 0.65 mmol), sodium azide (52 mg, 0.81 mmol), CuI (20 mol %), L-proline (40 mol %) and K_2CO_3 (186 mg, 2.5 eq.) in DMSO (2 mL) was mixed under air atmosphere at room temperature and then heated to 150 $^\circ\text{C}$ for 3 h. After cooling to ambient temperature, the reaction mass was quenched with ice-cold aqueous solution of NH_4Cl (30 mL), filtered through a bed of celite and the plug washed with ethyl acetate (20 mL). The resulting filtrate was extracted with ethyl acetate (2×20 mL) and the combined organic layers dried over anhydrous Na_2SO_4 and concentrated under reduced pressure. Desired product **98af** (73 mg, 59%) was isolated by column chromatography on silica gel (100-200 mesh) using ethyl acetate/hexane (10%, v/v) as eluant.

2-Phenylquinoline-3-carbonitrile (98af)

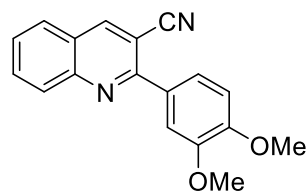
Off white solid (73 mg, 59%); mp 193–195 °C; ^1H NMR (400 MHz, CDCl_3) δ 8.70 (s, 1H), 8.23 (d, $J = 8.4$ Hz, 1H), 8.02 (dd, $J = 7.8, 1.7$ Hz, 2H), 7.97–7.89 (m, 2H), 7.75–7.66 (m, 1H), 7.64–7.52 (m, 3H); ^{13}C NMR (100 MHz, CDCl_3) δ 158.1, 148.7, 144.3, 137.7, 133.1, 130.1, 129.9, 129.2, 128.8, 128.1, 127.8, 125.0, 117.9, 105.5; IR (KBr): 3055, 2222, 1620, 1450, 1373 cm^{-1} ; HRMS for $\text{C}_{16}\text{H}_{11}\text{N}_2$ $[\text{M}+\text{H}]^+$ calcd 231.0917, found 231.0920.

2-*p*-Tolylquinoline-3-carbonitrile (98ag)

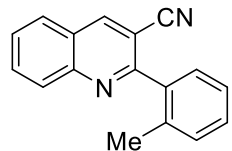
Pale yellow solid (54 mg, 41%); mp 174–177 °C; ^1H NMR (400 MHz, CDCl_3) δ 8.67 (s, 1H), 8.21 (d, $J = 9.1$ Hz, 1H), 8.01–7.84 (m, 4H), 7.67 (td, $J = 7.4, 1.0$ Hz, 1H), 7.40 (d, $J = 7.9$ Hz, 2H), 2.48 (s, 3H); ^{13}C NMR (100 MHz, CDCl_3) δ 158.0, 148.7, 144.2, 140.6, 134.9, 132.9, 129.9, 129.5, 129.1, 127.9, 127.7, 124.9, 118.1, 105.5, 21.4; IR (KBr): 2916, 2222, 1612, 1481, 1188 cm^{-1} ; HRMS for $\text{C}_{17}\text{H}_{13}\text{N}_2$ $[\text{M}+\text{H}]^+$ calcd 245.1073, found 245.1070.

2-(4-Methoxyphenyl)quinoline-3-carbonitrile (98ah)

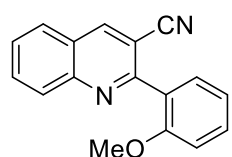
Off white solid (63 mg, 45%); mp 178–180 °C; ^1H NMR (400 MHz, CDCl_3) δ 8.65 (s, 1H), 8.19 (d, $J = 9.0$ Hz, 1H), 8.07–7.99 (m, 2H), 7.95–7.87 (m, 2H), 7.69–7.61 (m, 1H), 7.14–7.06 (m, 2H), 3.92 (s, 3H); ^{13}C NMR (100 MHz, CDCl_3) δ 161.5, 157.5, 148.7, 144.3, 132.9, 130.7, 130.2, 129.8, 127.8, 127.7, 124.8, 118.3, 114.2, 105.3, 55.5; IR (KBr): 2914, 2221, 1612, 1481, 1173 cm^{-1} ; HRMS for $\text{C}_{17}\text{H}_{13}\text{N}_2\text{O}$ $[\text{M}+\text{H}]^+$ calcd 261.1022, found 261.1028.

2-(3,4-Dimethoxyphenyl)quinoline-3-carbonitrile (98ai)

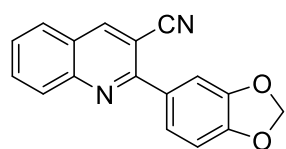
Off white solid (78 mg, 50%); mp 170–172 °C; ^1H NMR (400 MHz, CDCl_3) δ 8.67 (s, 1H), 8.21 (d, $J = 9.0$ Hz, 1H), 7.92 (s, 1H), 7.89 (dd, $J = 7.5, 1.2$ Hz, 1H), 7.67 (ddd, $J = 9.2, 8.2, 1.6$ Hz, 2H), 7.62 (d, $J = 2.1$ Hz, 1H), 7.07 (d, $J = 8.4$ Hz, 1H), 4.04 (s, 3H), 4.00 (s, 3H); ^{13}C NMR (100 MHz, CDCl_3) δ 157.4, 150.8, 149.1, 148.7, 144.4, 133.0, 130.2, 129.8, 127.8, 127.7, 124.8, 122.4, 118.3, 112.1, 111.0, 105.3, 56.1, 56.0; IR (KBr): 2916, 2222, 1615, 1483, 1180 cm^{-1} ; HRMS for $\text{C}_{18}\text{H}_{15}\text{N}_2\text{O}_2$ $[\text{M}+\text{H}]^+$ calcd 291.1128, found 291.1124.

2-*o*-Tolylquinoline-3-carbonitrile (98aj)

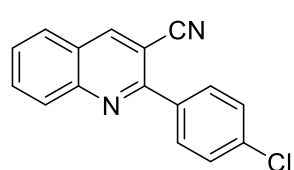
Yellow solid (42 mg, 32%); mp 163–164 °C; ^1H NMR (400 MHz, CDCl_3) δ 8.56 (s, 1H), 8.11 (d, $J = 8.5$ Hz, 1H), 7.84 (d, $J = 7.5$ Hz, 1H), 7.82 – 7.78 (m, 1H), 7.60 (ddd, $J = 8.1, 7.0, 1.1$ Hz, 1H), 7.33 (ddd, $J = 9.6, 6.4, 2.7$ Hz, 2H), 7.27 (d, $J = 7.0$ Hz, 2H), 2.22 (s, 3H); ^{13}C NMR (100 MHz, CDCl_3) δ 159.9, 148.3, 142.5, 137.6, 136.1, 132.9, 130.8, 129.8, 129.6, 129.2, 128.2, 127.9, 126.0, 125.1, 117.1, 107.5, 19.7; IR (KBr): 3015, 2222, 1616, 1473, 1170 cm^{-1} ; HRMS for $\text{C}_{17}\text{H}_{13}\text{N}_2$ $[\text{M}+\text{H}]^+$ calcd 245.1073, found 245.1076.

2-(2-Methoxyphenyl)quinoline-3-carbonitrile (98ak)

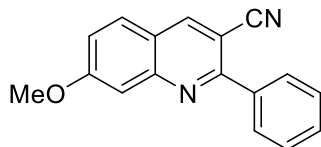
Pale yellow solid (63 mg, 45%); mp 150–153 °C; ^1H NMR (400 MHz, CDCl_3) δ 8.61 (s, 1H), 8.23 (d, $J = 9.3$ Hz, 1H), 7.93 (d, $J = 8.1$ Hz, 1H), 7.89 (ddd, $J = 8.5, 7.0, 1.5$ Hz, 1H), 7.69 (ddd, $J = 8.1, 7.0, 1.1$ Hz, 1H), 7.59 – 7.49 (m, 2H), 7.17 (td, $J = 7.5, 0.9$ Hz, 1H), 7.09 (d, $J = 8.3$ Hz, 1H), 3.91 (s, 3H); ^{13}C NMR (100 MHz, CDCl_3) δ 157.3, 157.0, 148.7, 142.3, 132.5, 131.5, 131.0, 130.0, 128.0, 127.3, 125.1, 121.2, 117.7, 111.3, 108.8, 55.4; IR (KBr): 3015, 2222, 1616, 1473, 1170 cm^{-1} ; HRMS for $\text{C}_{17}\text{H}_{13}\text{N}_2\text{O}$ $[\text{M}+\text{H}]^+$ calcd 261.1022, found 261.1032.

2-(Benzo[*d*][1,3]dioxol-5-yl)quinoline-3-carbonitrile (98al)

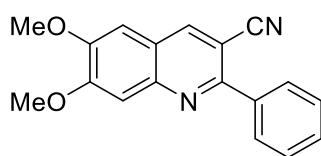
Light brown solid (62 mg, 42%); mp 187–189 °C; ^1H NMR (400 MHz, CDCl_3) δ 8.64 (s, 1H), 8.16 (d, $J = 8.9$ Hz, 1H), 7.88 (t, $J = 7.4$ Hz, 2H), 7.64 (t, $J = 7.2$ Hz, 1H), 7.55 (dd, $J = 8.1, 1.7$ Hz, 1H), 7.50 (d, $J = 1.6$ Hz, 1H), 6.99 (d, $J = 8.1$ Hz, 1H), 6.07 (s, 2H); ^{13}C NMR (100 MHz, CDCl_3) δ 157.3, 149.4, 148.6, 148.2, 144.4, 133.0, 131.7, 129.8, 127.9, 127.7, 124.9, 123.9, 118.1, 109.5, 108.5, 105.3, 101.6; IR (KBr): 3015, 2222, 1616, 1473, 1170 cm^{-1} ; HRMS for $\text{C}_{17}\text{H}_{11}\text{N}_2\text{O}_2$ $[\text{M}+\text{H}]^+$ calcd 275.0815, found 275.0820.

2-(4-Chlorophenyl)quinoline-3-carbonitrile (98am)

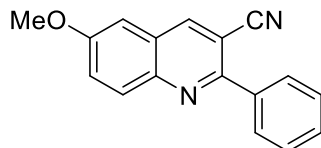
White solid (93 mg, 65%); mp 188–190 °C; ^1H NMR (400 MHz, CDCl_3) δ 8.69 (s, 1H), 8.21 (d, $J = 8.8$ Hz, 1H), 7.99 (d, $J = 8.5$ Hz, 2H), 7.93 (t, $J = 7.1$ Hz, 2H), 7.70 (t, $J = 7.5$ Hz, 1H), 7.56 (d, $J = 8.5$ Hz, 2H); ^{13}C NMR (100 MHz, CDCl_3) δ 156.7, 148.6, 144.3, 136.5, 136.1, 133.2, 130.5, 129.9, 129.0, 128.3, 127.8, 125.1, 117.8, 105.3; IR (KBr): 2914, 2221, 1612, 1481, 1173 cm^{-1} ; HRMS for $\text{C}_{16}\text{H}_{10}\text{ClN}_2$ $[\text{M}+\text{H}]^+$ calcd 265.0527, found 265.0524.

7-Methoxy-2-phenylquinoline-3-carbonitrile (98bf)

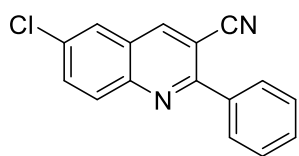
Off white solid 87 mg, 62%); mp 164–166 °C; ^1H NMR (400 MHz, CDCl_3) δ 8.56 (s, 1H), 7.99 (d, $J = 6.2$ Hz, 2H), 7.80 (d, $J = 9.0$ Hz, 1H), 7.60 – 7.51 (m, $J = 5.8$ Hz, 3H), 7.52 (d, $J = 1.9$ Hz, 1H), 7.31 (dd, $J = 9.0, 2.3$ Hz, 1H), 4.01 (s, 3H); ^{13}C NMR (100 MHz, CDCl_3) δ 163.6, 158.8, 150.9, 143.3, 137.9, 130.0, 129.1, 128.9, 128.7, 121.7, 120.4, 118.4, 107.7, 102.9, 55.9; IR (KBr): 3015, 2214, 1620, 1443, 1142 cm^{-1} ; HRMS for $\text{C}_{17}\text{H}_{13}\text{N}_2\text{O}$ $[\text{M}+\text{H}]^+$ calcd 261.1022, found 261.1028.

6,7-Dimethoxy-2-phenylquinoline-3-carbonitrile (98cf)

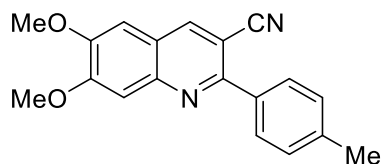
Pale yellow solid (64 mg, 41%); mp 196–199 °C; ^1H NMR (400 MHz, CDCl_3) δ 8.45 (s, 1H), 7.97 (dd, $J = 8.0, 1.4$ Hz, 2H), 7.59 – 7.52 (m, 3H), 7.51 (s, 1H), 7.10 (s, 1H), 4.08 (s, 3H), 4.06 (s, 3H); ^{13}C NMR (100 MHz, CDCl_3) δ 156.6, 155.3, 151.0, 146.5, 141.2, 138.0, 129.7, 129.0, 128.7, 121.0, 118.6, 108.3, 104.6, 103.2, 56.5, 56.3; IR (KBr): 2924, 2222, 1620, 1504, 1185 cm^{-1} ; HRMS for $\text{C}_{18}\text{H}_{15}\text{N}_2\text{O}_2$ $[\text{M}+\text{H}]^+$ calcd 291.1128, found 291.1125.

6-Methoxy-2-phenylquinoline-3-carbonitrile (98df)

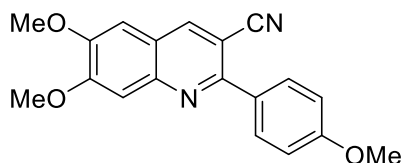
Yellow solid (84 mg, 60%); mp 167–168 °C; ^1H NMR (400 MHz, CDCl_3) δ 8.54 (s, 1H), 8.11 (d, $J = 9.2$ Hz, 1H), 8.00 (dd, $J = 8.0, 1.5$ Hz, 2H), 7.63 – 7.50 (m, 4H), 7.13 (d, $J = 2.7$ Hz, 1H), 3.99 (s, 3H); ^{13}C NMR (101 MHz, CDCl_3) δ 158.9, 155.7, 145.0, 142.5, 137.8, 131.3, 129.8, 129.0, 128.7, 126.2, 126.1, 118.2, 105.7, 104.6, 55.8; IR (KBr): 2945, 2222, 1620, 1489, 1034 cm^{-1} ; HRMS for $\text{C}_{17}\text{H}_{13}\text{N}_2\text{O}$ $[\text{M}+\text{H}]^+$ calcd 261.1022, found 261.1025.

6-Chloro-2-phenylquinoline-3-carbonitrile (98ef)

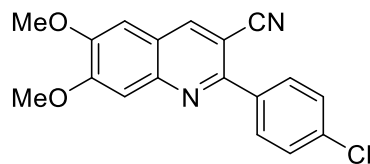
Pale yellow solid (36 mg, 25%); mp 190–193 °C; ^1H NMR (400 MHz, CDCl_3) δ 8.61 (s, 1H), 8.17 (d, $J = 9.0$ Hz, 1H), 8.04 – 8.00 (m, 2H), 7.92 (d, $J = 2.3$ Hz, 1H), 7.85 (dd, $J = 9.0, 2.3$ Hz, 1H), 7.62 – 7.57 (m, 3H); ^{13}C NMR (101 MHz, CDCl_3) δ 158.2, 147.1, 143.2, 137.3, 134.1, 133.9, 131.5, 130.4, 129.1, 128.8, 126.3, 125.6, 117.6, 106.6; IR (KBr): 3053, 2222, 1597, 1489, 1026, 764 cm^{-1} ; HRMS for $\text{C}_{16}\text{H}_{10}\text{ClN}_2$ $[\text{M}+\text{H}]^+$ calcd 265.0527, found 265.0524.

6,7-Dimethoxy-2-*p*-tolylquinoline-3-carbonitrile (98cg)

Pale yellow solid (49 mg, 30%); mp 198–200 °C; ^1H NMR (400 MHz, CDCl_3) δ 8.44 (s, 1H), 7.88 (d, $J = 8.2$ Hz, 2H), 7.51 (s, 1H), 7.37 (d, $J = 7.9$ Hz, 2H), 7.09 (s, 1H), 4.08 (s, 3H), 4.06 (s, 3H), 2.46 (s, 4H); ^{13}C NMR (101 MHz, CDCl_3) δ 156.6, 155.3, 150.9, 146.5, 141.3, 139.9, 135.1, 129.4, 128.9, 120.9, 118.7, 108.3, 104.6, 103.1, 56.5, 56.3, 21.4; IR (KBr): 2924, 2214, 1690, 1504, 1211 cm^{-1} ; HRMS for $\text{C}_{19}\text{H}_{17}\text{N}_2\text{O}_2$ $[\text{M}+\text{H}]^+$ calcd 305.1285, found 305.1291.

6,7-Dimethoxy-2-(4-methoxyphenyl)quinoline-3-carbonitrile (98ch)

Pale yellow solid (60 mg, 35%); mp 178–180 °C; ^1H NMR (400 MHz, CDCl_3) δ 8.41 (s, 1H), 7.96 (d, $J = 8.8$ Hz, 2H), 7.48 (s, 1H), 7.08 (d, $J = 5.0$ Hz, 2H), 7.06 (s, 1H), 4.07 (s, 3H), 4.05 (s, 3H), 3.90 (s, 3H); ^{13}C NMR (100 MHz, CDCl_3) δ 160.9, 156.1, 155.2, 150.8, 146.5, 141.3, 130.5, 130.4, 120.7, 118.8, 114.1, 108.2, 104.5, 102.9, 56.5, 56.3, 55.4; IR (KBr): 2925, 2213, 1612, 1494, 1173 cm^{-1} ; HRMS for $\text{C}_{19}\text{H}_{17}\text{N}_2\text{O}_3$ $[\text{M}+\text{H}]^+$ calcd 321.1234, found 321.1238.

2-(4-Chlorophenyl)-6,7-dimethoxyquinoline-3-carbonitrile (98cm)

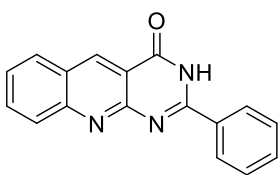
White solid (75 mg, 43%); mp 234–235 °C; ^1H NMR (400 MHz, CDCl_3) δ 8.45 (s, 1H), 7.98 – 7.90 (m, 2H), 7.57 – 7.51 (m, 2H), 7.49 (s, 1H), 7.11 (s, 1H), 4.09 (s, 3H), 4.08 (s, 3H); ^{13}C NMR (100 MHz, CDCl_3) δ 155.5, 155.2, 151.2, 146.5, 141.3, 136.4, 136.1, 130.3, 128.9, 121.2, 118.4, 108.2, 104.5, 102.9, 56.54, 56.3; IR (KBr): 2947, 2222, 1697, 1504, 1165 cm^{-1} ; HRMS for $\text{C}_{18}\text{H}_{14}\text{ClN}_2\text{O}_2$ $[\text{M}+\text{H}]^+$ calcd 325.0738, found 325.0734.

Representative procedure for synthesis of pyrimido[4,5-*b*]quinolin-4(3*H*)-ones (99)

A mixture of 2-bromobenzaldehyde (**94a**) (100 mg, 0.54 mmol), 2-cyanoacetamide (**95b**) (54 mg, 0.65 mmol), sodium azide (52 mg, 0.81 mmol), CuI (20 mol %), L-proline (40 mol %) and K_2CO_3 (186 mg, 2.5 eq.) in DMSO (2 mL) was mixed under air atmosphere at room temperature and then heated to 150 °C for 3 h. After cooling to ambient temperature, benzaldehyde (**45**) (69 mg, 0.65 mmol) was added and reaction mixture was then again heated to 150 °C for 2 h. After cooling to ambient temperature, the reaction mass was quenched with ice-cold aqueous solution of NH_4Cl (30 mL), filtered through a bed of celite and the plug washed with ethyl acetate (20 mL). The

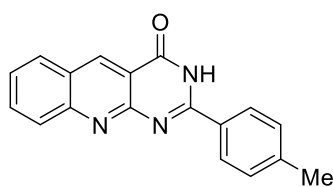
resulting filtrate was extracted with ethyl acetate (2 × 20 mL) and the combined organic layers dried over anhydrous Na₂SO₄ and concentrated under reduced pressure. Desired product **99a** (77 mg, 52%) was isolated by column chromatography on silica gel (100-200 mesh) using ethyl acetate/hexane (30%, v/v) as eluent.

2-Phenylpyrimido[4,5-*b*]quinolin-4(3*H*)-one (**99a**)



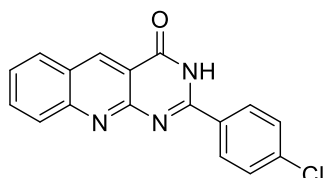
Yellow solid (77 mg, 52%); mp 356–357 °C; ¹H NMR (400 MHz, DMSO-*d*₆) δ 12.71 (s, 1H), 9.32 (s, 1H), 8.30 – 8.27 (m, 3H), 8.10 (d, *J* = 8.6 Hz, 1H), 7.96 (t, *J* = 7.6 Hz, 1H), 7.72 – 7.57 (m, 4H); ¹³C NMR (100 MHz, DMSO-*d*₆) δ 163.7, 156.8, 156.3, 151.6, 138.6, 133.3, 133.1, 132.6, 130.0, 129.2, 128.9, 128.6, 126.9, 126.7, 116.1; HRMS for C₁₇H₁₂N₃O [M + H]⁺ calcd 274.0975, found 274.0978.

2-(*p*-Tolyl)pyrimido[4,5-*b*]quinolin-4(3*H*)-one (**99b**)



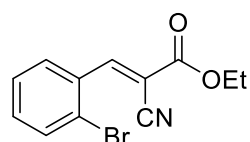
Orange solid (84 mg, 54%); mp 304–306 °C; ¹H NMR (400 MHz, DMSO-*d*₆) δ 12.62 (s, 1H), 9.29 (s, 1H), 8.26 (d, *J* = 8.1 Hz, 1H), 8.20 (d, *J* = 8.0 Hz, 2H), 8.08 (d, *J* = 8.6 Hz, 1H), 7.94 (t, *J* = 8.5 Hz, 1H), 7.66 (t, *J* = 7.3 Hz, 1H), 7.41 (d, *J* = 8.0 Hz, 2H), 2.42 (s, 3H); ¹³C NMR (100 MHz, DMSO-*d*₆) δ 163.7, 156.9, 156.1, 151.6, 142.8, 138.6, 133.3, 130.2, 130.0, 129.8, 128.9, 128.6, 126.8, 126.6, 116.0, 21.5; HRMS for C₁₈H₁₄N₃O [M + H]⁺ calcd 288.1131, found 288.1127.

2-(4-Chlorophenyl)pyrimido[4,5-*b*]quinolin-4(3*H*)-one (**99c**)



Yellow solid (72 mg, 43%); mp 376 – 378 °C; ¹H NMR (400 MHz, DMSO-*d*₆) δ 12.80 (s, 1H), 9.32 (s, 1H), 8.32 – 8.28 (m, 3H), 8.10 (d, *J* = 8.6 Hz, 1H), 7.96 (t, *J* = 7.4 Hz, 1H), 7.70 – 7.67 (m, 3H); ¹³C NMR (100 MHz, DMSO-*d*₆) δ 156.6, 151.5, 138.7, 137.5, 133.4, 132.0, 130.5, 130.1, 130.0, 129.3, 129.0, 128.9, 127.0, 126.7, 116.1; HRMS for C₁₇H₁₁ClN₃O [M + H]⁺ calcd 308.0585, found 308.0582.

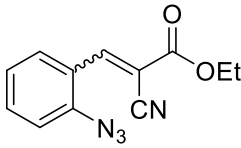
Ethyl 3-(2-bromophenyl)-2-cyanoacrylate (**97aa**)



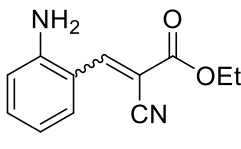
Colorless oil (118 mg, 78%); ¹H NMR (400 MHz, CDCl₃) δ 8.63 (s, 1H), 8.17 (dd, *J* = 7.8, 1.6 Hz, 1H), 7.71 (dd, *J* = 8.0, 1.2 Hz, 1H), 7.46 (td, *J* = 7.4, 0.8 Hz, 1H), 7.38 (td, *J* = 7.7, 1.7 Hz, 1H), 4.41 (q, *J* = 7.1 Hz, 1H), 1.41

(t, $J = 7.1$ Hz, 2H); ^{13}C NMR (100 MHz, CDCl_3) δ 161.8, 153.9, 133.7, 133.6, 131.7, 130.1, 128.1, 126.6, 114.7, 106.4, 63.0, 14.2; HRMS for $\text{C}_{12}\text{H}_{11}\text{BrNO}_2$ $[\text{M}+\text{H}]^+$ calcd 279.9968, found 279.9973 and 281.9954 $[\text{M}+2+\text{H}]^+$.

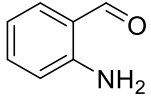
Ethyl 3-(2-azidophenyl)-2-cyanoacrylate (101)

 Yellow Oil (16 mg, 18%); ^1H NMR (400 MHz, CDCl_3) δ 8.79 (s, 1H), 8.78 (d, $J = 9.0$ Hz, 1H), 8.14 (dd, $J = 8.1, 1.1$ Hz, 1H), 8.04 (td, $J = 8.4, 7.9, 1.3$ Hz, 1H), 7.85 – 7.80 (m, 1H), 4.64 (q, $J = 7.1$ Hz, 2H), 1.55 (t, $J = 7.1$ Hz, 3H); ^{13}C NMR (100 MHz, CDCl_3) δ 162.6, 145.7, 138.1, 133.6, 132.0, 130.5, 128.6, 122.7, 117.2, 117.1, 62.7, 14.4. MS (ESI) m/z calcd for $\text{C}_{12}\text{H}_{11}\text{N}_4\text{O}_2$ $[\text{M}+\text{H}]^+$ 243.09, found 243.15.

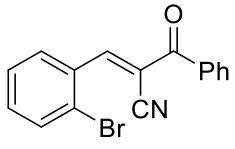
Ethyl 3-(2-aminophenyl)-2-cyanoacrylate (102)

 Brown solid (58 mg, 50%); mp 123–125 °C; ^1H NMR (400 MHz, $\text{DMSO}-d_6$) δ 8.55 (s, 1H), 8.32 (d, $J = 8.6$ Hz, 1H), 8.09 (d, $J = 7.9$ Hz, 1H), 7.84 (d, $J = 8.2$ Hz, 3H), 7.47 (t, $J = 7.4$ Hz, 1H), 4.42 (q, $J = 7.1$ Hz, 2H), 1.40 (t, $J = 7.1$ Hz, 3H); ^{13}C NMR (100 MHz, $\text{DMSO}-d_6$) δ 165.50, 147.65, 141.08, 133.74, 130.93, 130.68, 125.00, 120.86, 117.26, 110.72, 62.23, 14.54; ^1H NMR (400 MHz, $\text{DMSO}-d_6$, D_2O exchange) δ 8.58 (s, 1H), 8.26 (d, $J = 8.5$ Hz, 1H), 8.04 (d, $J = 7.7$ Hz, 1H), 7.85 (t, $J = 7.6$ Hz, 1H), 7.47 (t, $J = 7.3$ Hz, 1H), 4.39 (q, $J = 6.9$ Hz, 2H), 1.37 (t, $J = 7.0$ Hz, 3H); HRMS for $\text{C}_{12}\text{H}_{13}\text{N}_2\text{O}_2$ $[\text{M}+\text{H}]^+$ calcd 217.0972, found 217.0975.

2-Aminobenzaldehyde (103)

 Pale yellow liquid (42 mg, 64%); ^1H NMR (400 MHz, $\text{DMSO}-d_6$) δ 9.81 (d, $J = 0.4$ Hz, 1H), 7.53 (dd, $J = 7.8, 1.6$ Hz, 1H), 7.30 (ddd, $J = 8.5, 7.0, 1.7$ Hz, 1H), 7.12 (bs, 2H), 6.76 (d, $J = 8.4$ Hz, 1H), 6.64 (ddd, $J = 7.9, 7.0, 1.0$ Hz, 1H); ^{13}C NMR (100 MHz, $\text{DMSO}-d_6$) δ 194.5, 151.2, 136.0, 135.5, 118.2, 116.3, 115.4; HRMS for $\text{C}_7\text{H}_8\text{NO}$ $[\text{M}+\text{H}]^+$ calcd 122.0600, found 121.0581.

2-Benzoyl-3-(2-bromophenyl)acrylonitrile (104af)

 Crystalline off white solid (234 mg, 70%); mp 126–128 °C; ^1H NMR (400 MHz, CDCl_3) δ 8.37 (s, 1H), 8.25 (d, $J = 7.1$ Hz, 1H), 7.94 (d, $J = 7.3$ Hz, 2H), 7.73 (d, $J = 7.8$ Hz, 1H), 7.68 (t, $J = 7.4$ Hz, 1H), 7.57 (t, $J = 7.6$ Hz, 2H), 7.51 (t, $J = 7.6$ Hz, 1H), 7.42 (t, $J = 7.7$ Hz, 1H); ^{13}C NMR (100 MHz, CDCl_3) δ 188.8, 154.1, 135.3,

133.8, 133.7, 133.6, 132.1, 130.10, 129.6, 128.8, 128.2, 126.5, 115.7, 113.6; HRMS for $C_{16}H_{11}BrNO$ $[M+H]^+$ calcd 312.0019, found 312.0015.

Crystal Structure Report for 104af (CCDC 1433055)

Table 2A.4: Sample and crystal data of 104af

Identification code	vbchem114	
Chemical formula	CHBrNO	
Formula weight	122.94 g/mol	
Temperature	296(2) K	
Wavelength	0.71073 Å	
Crystal system	triclinic	
Space group	P -1	
Unit cell dimensions	a = 8.9523(11) Å	$\alpha = 83.854(10)^\circ$
	b = 10.8955(15) Å	$\beta = 89.882(9)^\circ$
	c = 13.2918(18) Å	$\gamma = 89.928(9)^\circ$
Volume	1289.0(3) Å ³	
Z	16	
Density (calculated)	2.534 g/cm ³	
Absorption coefficient	12.492 mm ⁻¹	
F(000)	912	

Table 2A.5: Data collection and structure refinement of 104af

Theta range for data collection	1.54 to 28.89°	
Index ranges	-12<=h<=12, -14<=k<=14, -17<=l<=17	
Reflections collected	41097	
Independent reflections	6642 [R(int) = 0.3862]	
Coverage of independent reflections	97.9%	
Absorption correction	multi-scan	
Refinement method	Full-matrix least-squares on F ²	
Refinement program	SHELXL-2014/7 (Sheldrick, 2014)	
Function minimized	$\Sigma w(F_o^2 - F_c^2)^2$	
Data / restraints / parameters	6642 / 0 / 343	
Goodness-of-fit on F ²	1.410	
Final R indices	2552 data; I>2 σ (I)	R1 = 0.1575, wR2 = 0.2795
	all data	R1 = 0.3435, wR2 = 0.3407
Weighting scheme	$w=1/[\sigma^2(F_o^2)+(0.1000P)^2+0.6035P]$ where $P=(F_o^2+2F_c^2)/3$	
Largest diff. peak and hole	1.172 and -2.442 eÅ ⁻³	

R.M.S. deviation from mean 0.342 eÅ⁻³

Table 2A.6: Atomic coordinates and equivalent isotropic atomic displacement parameters (Å²)
U(eq) is defined as one-third of the trace of the orthogonalized U_{ij} tensor.

	x/a	y/b	z/c	U(eq)
Br1	0.60369(15)	0.69560(14)	0.83172(11)	0.0500(5)
Br2	0.10329(15)	0.80468(14)	0.66867(11)	0.0506(5)
O1	0.9436(9)	0.6540(9)	0.9648(7)	0.054(3)
O2	0.4430(9)	0.8458(9)	0.5355(7)	0.051(3)
C26	0.8130(12)	0.9171(10)	0.5811(8)	0.023(3)
C11	0.4127(12)	0.4928(11)	0.8810(8)	0.025(3)
C24	0.6670(11)	0.9044(10)	0.5990(8)	0.022(3)
C27	0.9104(11)	0.0081(10)	0.6184(8)	0.021(3)
N2	0.5303(12)	0.0301(11)	0.7224(9)	0.053(3)
C10	0.3134(12)	0.5834(10)	0.9178(8)	0.025(3)
C28	0.0510(13)	0.9716(10)	0.6573(9)	0.027(3)
C1	0.1367(13)	0.7953(11)	0.9798(9)	0.031(3)
C6	0.2482(13)	0.8594(12)	0.9246(10)	0.037(3)
C25	0.5917(14)	0.9761(13)	0.6660(10)	0.040(3)
C7	0.0678(14)	0.6820(12)	0.9475(9)	0.034(3)
C8	0.1679(11)	0.5961(10)	0.9002(8)	0.022(3)
C12	0.5517(13)	0.5272(11)	0.8441(8)	0.027(3)
N1	0.0322(13)	0.4726(12)	0.7763(10)	0.058(4)
C16	0.3682(14)	0.3704(12)	0.8881(9)	0.038(3)
C29	0.1508(13)	0.0522(13)	0.6904(9)	0.037(3)
C9	0.0936(14)	0.5236(13)	0.8350(11)	0.042(3)
C32	0.8698(14)	0.1305(12)	0.6139(9)	0.039(3)
C18	0.7488(14)	0.6418(12)	0.5745(10)	0.039(3)
C23	0.5687(14)	0.8178(11)	0.5518(9)	0.033(3)
C31	0.9671(15)	0.2133(13)	0.6487(9)	0.040(3)
C17	0.6362(12)	0.7056(12)	0.5193(9)	0.030(3)
C15	0.4680(15)	0.2877(13)	0.8525(10)	0.044(3)
C13	0.6516(14)	0.4463(14)	0.8084(10)	0.041(3)
C30	0.1078(16)	0.1758(15)	0.6855(10)	0.053(4)

	x/a	y/b	z/c	U(eq)
C2	0.0718(15)	0.8384(14)	0.0669(10)	0.048(4)
C22	0.5754(15)	0.6607(13)	0.4332(10)	0.046(4)
C14	0.6106(16)	0.3280(15)	0.8148(9)	0.049(4)
C5	0.3053(15)	0.9665(12)	0.9598(12)	0.047(4)
C21	0.6369(18)	0.5529(14)	0.4033(11)	0.056(4)
C4	0.2500(18)	0.0126(14)	0.0420(13)	0.058(4)
C20	0.7503(18)	0.4885(14)	0.4563(12)	0.052(4)
C3	0.1345(18)	0.9483(16)	0.0979(12)	0.062(5)
C19	0.8027(16)	0.5314(13)	0.5392(12)	0.054(4)

Table 2A.7: Bond lengths (Å).

Br1-C12	1.884(11)	Br2-C28	1.868(11)
O1-C7	1.169(13)	O2-C23	1.179(14)
C26-C24	1.333(14)	C26-C27	1.449(15)
C11-C12	1.374(15)	C11-C16	1.387(17)
C11-C10	1.451(15)	C24-C25	1.415(17)
C24-C23	1.480(16)	C27-C32	1.377(16)
C27-C28	1.403(16)	N2-C25	1.141(16)
C10-C8	1.328(15)	C28-C29	1.360(17)
C1-C6	1.382(16)	C1-C2	1.418(17)
C1-C7	1.485(17)	C6-C5	1.400(18)
C7-C8	1.482(16)	C8-C9	1.403(18)
C12-C13	1.374(17)	N1-C9	1.147(17)
C16-C15	1.386(17)	C29-C30	1.40(2)
C32-C31	1.371(17)	C18-C17	1.390(17)
C18-C19	1.420(18)	C23-C17	1.468(16)
C31-C30	1.396(19)	C17-C22	1.403(17)
C15-C14	1.423(19)	C13-C14	1.33(2)
C2-C3	1.42(2)	C22-C21	1.39(2)
C5-C4	1.34(2)	C21-C20	1.38(2)
C4-C3	1.41(2)	C20-C19	1.33(2)

	x/a	y/b	z/c	U(eq)
Table 2A.8: Bond angles (°)				
C24-C26-C27	126.3(10)		C12-C11-C16	120.6(11)
C12-C11-C10	120.3(10)		C16-C11-C10	119.1(10)
C26-C24-C25	121.6(10)		C26-C24-C23	124.6(10)
C25-C24-C23	113.8(10)		C32-C27-C28	119.2(10)
C32-C27-C26	121.5(10)		C28-C27-C26	119.3(10)
C8-C10-C11	127.0(10)		C29-C28-C27	122.9(11)
C29-C28-Br2	117.8(10)		C27-C28-Br2	119.3(9)
C6-C1-C2	122.4(12)		C6-C1-C7	122.4(11)
C2-C1-C7	115.1(11)		C1-C6-C5	118.6(12)
N2-C25-C24	177.6(15)		O1-C7-C8	119.6(11)
O1-C7-C1	123.2(11)		C8-C7-C1	117.0(10)
C10-C8-C9	121.4(10)		C10-C8-C7	125.2(10)
C9-C8-C7	113.4(10)		C13-C12-C11	123.4(11)
C13-C12-Br1	117.6(9)		C11-C12-Br1	118.8(9)
C15-C16-C11	116.6(12)		C28-C29-C30	117.2(12)
N1-C9-C8	174.5(16)		C31-C32-C27	119.1(13)
C17-C18-C19	117.6(12)		O2-C23-C17	123.0(11)
O2-C23-C24	118.8(11)		C17-C23-C24	118.0(10)
C32-C31-C30	121.0(13)		C18-C17-C22	121.0(12)
C18-C17-C23	121.9(11)		C22-C17-C23	117.0(11)
C16-C15-C14	120.6(13)		C14-C13-C12	116.7(12)
C29-C30-C31	120.6(12)		C1-C2-C3	115.9(13)
C21-C22-C17	117.3(13)		C13-C14-C15	122.0(12)
C4-C5-C6	122.3(13)		C20-C21-C22	122.7(13)
C5-C4-C3	119.2(13)		C19-C20-C21	118.6(14)
C4-C3-C2	121.4(13)		C20-C19-C18	122.7(14)

Table 2A.9: Anisotropic atomic displacement parameters (\AA^2).

The anisotropic atomic displacement factor exponent takes the form: $-2\pi^2 [h^2 a^{*2} U_{11} + \dots + 2 h k a^* b^* U_{12}]$

	U_{11}	U_{22}	U_{33}	U_{23}	U_{13}	U_{12}
Br1	0.0527(9)	0.0466(10)	0.0521(10)	-0.0116(8)	0.0168(7)	-0.0195(7)
Br2	0.0509(9)	0.0492(10)	0.0538(10)	-0.0156(8)	-0.0135(7)	0.0197(7)
O1	0.022(5)	0.073(7)	0.073(7)	-0.028(6)	0.010(4)	-0.011(4)
O2	0.022(5)	0.065(7)	0.070(7)	-0.026(6)	-0.009(4)	0.014(4)
C26	0.029(6)	0.017(6)	0.023(6)	-0.007(5)	-0.002(5)	0.004(5)
C11	0.028(6)	0.030(8)	0.019(6)	-0.011(5)	0.001(5)	-0.004(5)
C24	0.029(6)	0.019(7)	0.020(6)	-0.012(5)	0.002(5)	0.005(5)
C27	0.024(6)	0.022(7)	0.019(6)	-0.013(5)	0.006(4)	0.003(5)
N2	0.042(7)	0.058(9)	0.064(9)	-0.033(7)	0.015(6)	0.004(6)
C10	0.038(7)	0.017(7)	0.022(7)	-0.006(5)	0.011(5)	-0.005(5)
C28	0.045(7)	0.012(6)	0.025(7)	-0.003(5)	0.014(5)	0.006(5)
C1	0.037(7)	0.034(8)	0.024(7)	-0.016(6)	-0.006(5)	0.009(6)
C6	0.034(7)	0.029(8)	0.046(8)	0.001(7)	0.009(6)	0.001(6)
C25	0.036(7)	0.048(10)	0.036(8)	-0.005(7)	-0.006(6)	-0.014(6)
C7	0.038(8)	0.032(8)	0.035(8)	-0.017(6)	0.001(6)	-0.001(6)
C8	0.025(6)	0.018(7)	0.022(6)	-0.005(5)	-0.001(5)	-0.004(5)
C12	0.043(7)	0.018(7)	0.022(7)	-0.012(5)	0.002(5)	-0.014(5)
N1	0.044(7)	0.065(9)	0.072(9)	-0.039(8)	-0.008(6)	-0.001(6)
C16	0.061(9)	0.024(8)	0.033(8)	-0.017(6)	-0.008(6)	0.005(6)
C29	0.033(7)	0.047(10)	0.033(8)	-0.011(7)	0.000(5)	-0.008(6)
C9	0.041(8)	0.034(9)	0.053(10)	-0.016(8)	0.017(7)	0.010(6)
C32	0.060(9)	0.034(9)	0.025(7)	-0.013(6)	0.016(6)	-0.014(7)
C18	0.042(8)	0.033(8)	0.043(8)	-0.004(7)	0.003(6)	0.005(6)
C23	0.046(8)	0.025(8)	0.028(7)	-0.013(6)	0.004(6)	-0.003(6)
C31	0.050(8)	0.043(9)	0.026(7)	-0.003(7)	-0.001(6)	-0.004(7)
C17	0.031(7)	0.040(8)	0.021(7)	-0.011(6)	0.003(5)	-0.007(6)
C15	0.055(9)	0.048(10)	0.029(8)	-0.010(7)	-0.006(6)	0.009(7)
C13	0.036(7)	0.047(10)	0.043(9)	-0.023(7)	0.002(6)	0.004(6)
C30	0.059(10)	0.069(12)	0.031(8)	-0.011(8)	0.013(7)	-0.037(8)
C2	0.052(9)	0.054(10)	0.041(9)	-0.025(8)	-0.008(6)	0.015(7)

C22	0.057(9)	0.050(10)	0.034(8)	-0.023(7)	0.008(6)	-0.022(7)
C14	0.056(9)	0.066(12)	0.023(8)	-0.005(7)	-0.006(6)	0.033(8)
C5	0.059(9)	0.021(8)	0.064(11)	-0.015(7)	-0.009(7)	-0.009(6)
C21	0.078(11)	0.047(10)	0.048(10)	-0.033(8)	0.015(8)	-0.016(8)
C4	0.076(11)	0.045(11)	0.058(11)	-0.026(9)	-0.014(8)	-0.005(8)
C20	0.077(11)	0.041(10)	0.043(9)	-0.021(8)	0.002(8)	0.004(8)
C3	0.078(11)	0.062(11)	0.052(10)	-0.039(9)	-0.018(8)	0.027(9)
C19	0.067(10)	0.032(9)	0.064(11)	-0.006(8)	0.014(8)	0.006(7)

2A.6 REFERENCES

- [1] J. P. Michael, *Natural Product Reports*, **2008**, *25*, 166-187.
- [2] B. Trofimov, N. Nedolya, *Comprehensive Heterocyclic Chemistry III*, Katritzky, AR, Ramsden, CA, Scriven, EFV, and Taylor, RJK, Eds, Amsterdam: Elsevier, **2008**.
- [3] R. H. Manske, *Chemical Reviews*, **1942**, *30*, 113-144.
- [4] J. A. Spicer, S. A. Gamage, G. J. Atwell, G. J. Finlay, B. C. Baguley, W. A. Denny, *Journal of Medicinal Chemistry*, **1997**, *40*, 1919-1929.
- [5] S. Vandekerckhove, M. D'hooghe, *Bioorganic & Medicinal Chemistry*, **2015**, *23*, 5098-5119.
- [6] Y.-Q. Hu, C. Gao, S. Zhang, L. Xu, Z. Xu, L.-S. Feng, X. Wu, F. Zhao, *European Journal of Medicinal Chemistry*, **2017**, *139*, 22-47.
- [7] R. A. Jones, S. S. Panda, C. D. Hall, *European Journal of Medicinal Chemistry*, **2015**, *97*, 335-355.
- [8] K. Kaur, M. Jain, R. P. Reddy, R. Jain, *European Journal of Medicinal Chemistry*, **2010**, *45*, 3245-3264.
- [9] A. Marella, O. P. Tanwar, R. Saha, M. R. Ali, S. Srivastava, M. Akhter, M. Shaquiquzzaman, M. M. Alam, *Saudi Pharmaceutical Journal*, **2013**, *21*, 1-12.
- [10] S. Jain, V. Chandra, P. Kumar Jain, K. Pathak, D. Pathak, A. Vaidya, *Arabian Journal of Chemistry*, **2016**.
- [11] O. Afzal, S. Kumar, M. R. Haider, M. R. Ali, R. Kumar, M. Jaggi, S. Bawa, *European Journal of Medicinal Chemistry*, **2015**, *97*, 871-910.
- [12] A. C. Shaikh, D. S. Ranade, S. Thorat, A. Maity, P. P. Kulkarni, R. G. Gonnade, P. Munshi, N. T. Patil, *Chemical Communications*, **2015**, *51*, 16115-16118.

- [13] Y. Liu, H. Ma, A. K. Y. Jen, *Journal of Materials Chemistry*, **2001**, *11*, 1800-1804.
- [14] T. Eicher, S. Hauptmann, A. Speicher, *The Chemistry of Heterocycles: Structures, Reactions, Synthesis, and Applications*, John Wiley & Sons, **2013**.
- [15] S. Yamashkin, E. Oreshkina, *Chemistry of Heterocyclic Compounds*, **2006**, *42*, 701-718.
- [16] B. E. Cohn, R. G. Gustavson, *Journal of the American Chemical Society*, **1928**, *50*, 2709-2711.
- [17] V. F. Batista, D. C. G. A. Pinto, A. M. S. Silva, *ACS Sustainable Chemistry & Engineering*, **2016**, *4*, 4064-4078.
- [18] L. F. Tietze, *Chemical Reviews*, **1996**, *96*, 115-136.
- [19] L. F. Tietze, G. Brasche, K. Gericke, *Domino Reactions in Organic Synthesis*, John Wiley & Sons, **2006**.
- [20] T.-L. Ho, *Tandem Organic Reactions*, John Wiley & Sons, **1992**.
- [21] C. S. Cho, B. T. Kim, T.-J. Kim, S. C. Shim, *Chemical Communications*, **2001**, 2576-2577.
- [22] R. Martinez, D. J. Ramon, M. Yus, *European Journal of Organic Chemistry*, **2007**, *2007*, 1599-1605.
- [23] L. Hui-Jing, W. Chen-Chao, Z. Shuai, D. Chun-Yang, W. Yan-Chao, *Advanced Synthesis & Catalysis*, **2015**, *357*, 583-588.
- [24] J. Horn, S. P. Marsden, A. Nelson, D. House, G. G. Weingarten, *Organic Letters*, **2008**, *10*, 4117-4120.
- [25] J. D. Neuhaus, S. M. Morrow, M. Brunavs, M. C. Willis, *Organic Letters*, **2016**, *18*, 1562-1565.
- [26] S. M. Prajapati, K. D. Patel, R. H. Vekariya, S. N. Panchal, H. D. Patel, *RSC Advances*, **2014**, *4*, 24463-24476.
- [27] H. Amii, Y. Kishikawa, K. Uneyama, *Organic Letters*, **2001**, *3*, 1109-1112.
- [28] Z. Min, R. Thierry, D. P. H., *Advanced Synthesis & Catalysis*, **2010**, *352*, 1896-1903.
- [29] G. Song, X. Gong, X. Li, *The Journal of Organic Chemistry*, **2011**, *76*, 7583-7589.
- [30] S. K. Gadakh, S. Dey, A. Sudalai, *Organic & Biomolecular Chemistry*, **2016**, *14*, 2969-2977.
- [31] X. Xu, Y. Yang, X. Zhang, W. Yi, *Organic Letters*, **2018**, *20*, 566-569.

- [32] L. Zhang, L. Zheng, B. Guo, R. Hua, *The Journal of Organic Chemistry*, **2014**, *79*, 11541-11548.
- [33] X.-F. Xia, G.-W. Zhang, D. Wang, S.-L. Zhu, *The Journal of Organic Chemistry*, **2017**, *82*, 8455-8463.
- [34] X. Yang, L. Li, Y. Li, Y. Zhang, *The Journal of Organic Chemistry*, **2016**, *81*, 12433-12442.
- [35] M. T. Stone, *Organic Letters*, **2011**, *13*, 2326-2329.
- [36] R. C. Larock, M.-Y. Kuo, *Tetrahedron Letters*, **1991**, *32*, 569-572.
- [37] J. Xu, J. Sun, J. Zhao, B. Huang, X. Li, Y. Sun, *RSC Advances*, **2017**, *7*, 36242-36245.
- [38] J. Xiaochen, H. Huawen, L. Yibiao, C. Huoqi, J. Huanfeng, *Angewandte Chemie International Edition*, **2012**, *51*, 7292-7296.
- [39] C. Li, J. Li, Y. An, J. Peng, W. Wu, H. Jiang, *The Journal of Organic Chemistry*, **2016**, *81*, 12189-12196.
- [40] G. C. Senadi, W.-P. Hu, A. M. Garkhedkar, S. S. K. Boominathan, J.-J. Wang, *Chemical Communications*, **2015**, *51*, 13795-13798.
- [41] W. Zhou, J. Lei, *Chemical Communications*, **2014**, *50*, 5583-5585.
- [42] G. Abbiati, A. Arcadi, V. Canevari, L. Capezzuto, E. Rossi, *The Journal of Organic Chemistry*, **2005**, *70*, 6454-6460.
- [43] J. W. Collet, K. Ackerman, J. Lambregts, B. U. W. Maes, R. V. A. Orru, E. Ruijter, *The Journal of Organic Chemistry*, **2018**, *83*, 854-861.
- [44] H. Z. Syeda Huma, R. Halder, S. Singh Kalra, J. Das, J. Iqbal, *Tetrahedron Letters*, **2002**, *43*, 6485-6488.
- [45] V. A. Peshkov, O. P. Pereshivko, E. V. Van der Eycken, *Chemical Society Reviews*, **2012**, *41*, 3790-3807.
- [46] F. Xiao, Y. Chen, Y. Liu, J. Wang, *Tetrahedron*, **2008**, *64*, 2755-2761.
- [47] C. E. Meyet, C. H. Larsen, *The Journal of Organic Chemistry*, **2014**, *79*, 9835-9841.
- [48] K.-M. Jiang, J.-A. Kang, Y. Jin, J. Lin, *Organic Chemistry Frontiers*, **2018**, *5*, 434-441.
- [49] Y. Li, X. Cao, Y. Liu, J.-P. Wan, *Organic & Biomolecular Chemistry*, **2017**, *15*, 9585-9589.
- [50] N. T. Patil, V. S. Raut, *The Journal of Organic Chemistry*, **2010**, *75*, 6961-6964.

- [51] H. Jing, L. Li, S. Yangyong, C. Jie, D. Hongmei, S. Min, L. Xuesheng, Z. Hui, C. Weiguo, *European Journal of Organic Chemistry*, **2013**, 2013, 8323-8329.
- [52] L. Kong, Y. Zhou, H. Huang, Y. Yang, Y. Liu, Y. Li, *The Journal of Organic Chemistry*, **2015**, 80, 1275-1278.
- [53] W. Xuesong, W. Xingyong, H. Dayun, L. Chulong, W. Xinyan, H. Yuefei, *Advanced Synthesis & Catalysis*, **2016**, 358, 2332-2339.
- [54] Y. Chi, H. Yan, W.-X. Zhang, Z. Xi, *Organic Letters*, **2017**, 19, 2694-2697.
- [55] A. C. S. Reddy, P. Anbarasan, *Journal of Catalysis*, **2018**, 363, 102-108.
- [56] G. Liu, J. Qian, J. Hua, F. Cai, X. Li, L. Liu, *Organic & Biomolecular Chemistry*, **2016**, 14, 1147-1152.
- [57] B. Jiang, Y.-G. Si, *The Journal of Organic Chemistry*, **2002**, 67, 9449-9451.
- [58] S. Cai, J. Zeng, Y. Bai, X.-W. Liu, *The Journal of Organic Chemistry*, **2012**, 77, 801-807.
- [59] A. Kumar, V. K. Rao, *Synlett*, **2011**, 2011, 2157-2162.
- [60] A.-H. Li, E. Ahmed, X. Chen, M. Cox, A. P. Crew, H.-Q. Dong, M. Jin, L. Ma, B. Panicker, K. W. Siu, A. G. Steinig, K. M. Stolz, P. A. R. Tavares, B. Volk, Q. Weng, D. Werner, M. J. Mulvihill, *Organic & Biomolecular Chemistry*, **2007**, 5, 61-64.
- [61] R. P. Rubén, S. P. Samuel, P. M. R., S. Roberto, *Advanced Synthesis & Catalysis*, **2018**, 360, 2216-2220.
- [62] S. Das, D. Maiti, S. De Sarkar, *The Journal of Organic Chemistry*, **2018**, 83, 2309-2316.
- [63] Y. Kim, M. R. Kumar, N. Park, Y. Heo, S. Lee, *The Journal of Organic Chemistry*, **2011**, 76, 9577-9583.
- [64] D. Dhar, W. B. Tolman, *Journal of the American Chemical Society*, **2015**, 137, 1322-1329.
- [65] T. Maejima, Y. Shimoda, K. Nozaki, S. Mori, Y. Sawama, Y. Monguchi, H. Sajiki, *Tetrahedron*, **2012**, 68, 1712-1722.
- [66] S. Cenini, E. Gallo, A. Penoni, F. Ragaini, S. Tollari, *Chemical Communications*, **2000**, 2265-2266.
- [67] Q. Nguyen, T. Nguyen, T. G. Driver, *Journal of the American Chemical Society*, **2013**, 135, 620-623.
- [68] F.-C. Jia, C. Xu, Z.-W. Zhou, Q. Cai, D.-K. Li, A.-X. Wu, *Organic Letters*, **2015**, 17, 2820-2823.
- [69] B. Li, C. Guo, X. Fan, J. Zhang, X. Zhang, *Tetrahedron Letters*, **2014**, 55, 5944-5948.

- [70] Y. Goriya, C. V. Ramana, *Chemical Communications*, **2013**, *49*, 6376-6378.
- [71] J. Shen, D. Yang, Y. Liu, S. Qin, J. Zhang, J. Sun, C. Liu, C. Liu, X. Zhao, C. Chu, R. Liu, *Organic Letters*, **2014**, *16*, 350-353.
- [72] K. Wang, K. Nguyen, Y. Huang, A. Dömling, *Journal of Combinatorial Chemistry*, **2009**, *11*, 920-927.

CHAPTER 2: PART-B

One-Pot Synthesis of Pyrido[2',1':2,3]imidazo[4,5-c]- quinolines and their Antimicrobial Activity

2B.1 INTRODUCTION

Compound with imidazo[1,2-*a*]pyridine scaffolds have found a wide range of application in the field of drug discovery, biological chemistry and in material science.^[1-4] For instance, imidazo[1,2-*a*:5,4-*b'*]dipyridin-2-amine (Glu-P1 and Glu-P2) act as anticancer agent, 5*H*-pyridio[1,2-*a*]imidazo[5,4-*b*]indole used as antihypertensive agent and 2-(imidazo[1,2-*a*]pyridin-2-yl)phenol display excited state intramolecular proton transfer (ESIPT) (**Figure 2B.1**). Several marketed drugs such as Zolpidem, Alpidem, Saripidem, and Olprinone, etc. are imidazo[1,2-*a*]pyridine derivatives used for the treatment of anxiety, insomnia, anxiolytic, and cardio related problems (**Figure 2B.1**).^[5-7] It is also an important scaffold for the synthesis of various fused-heterocyclic compounds.^[7-8] Among various fused-heterocycles, biologically intriguing imidazo[1,2-*a*]pyridine-fused quinoline system has attracted considerable attention of the organic chemists as quinoline is a well-established motif present in natural products^[9] and synthetic compounds that exhibit versatile application in medicinal chemistry.^[10-12]

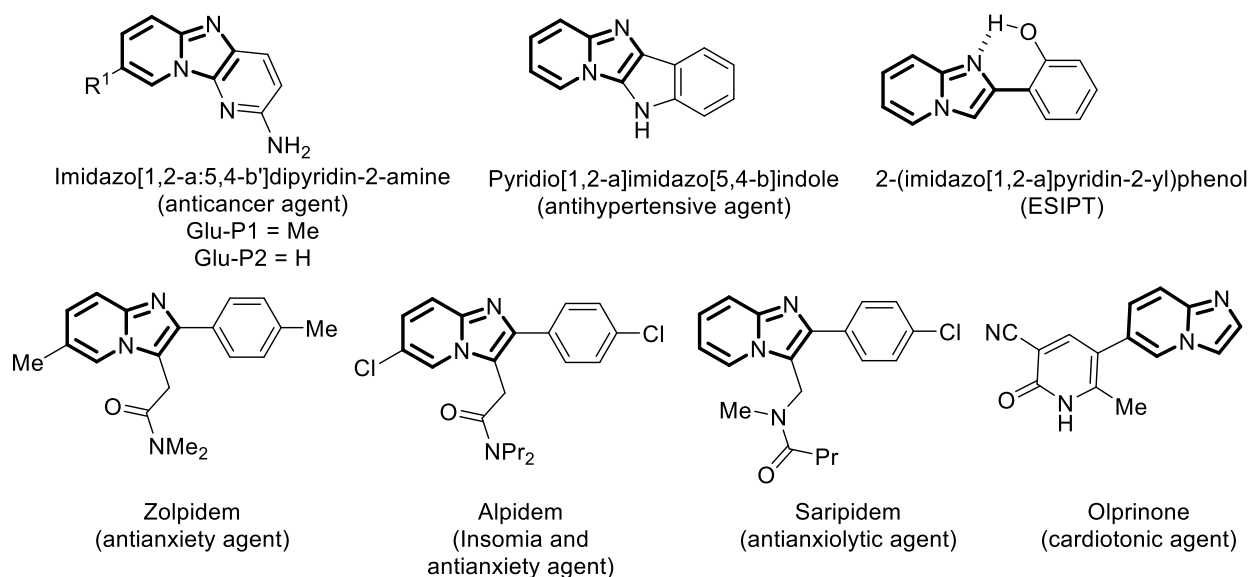
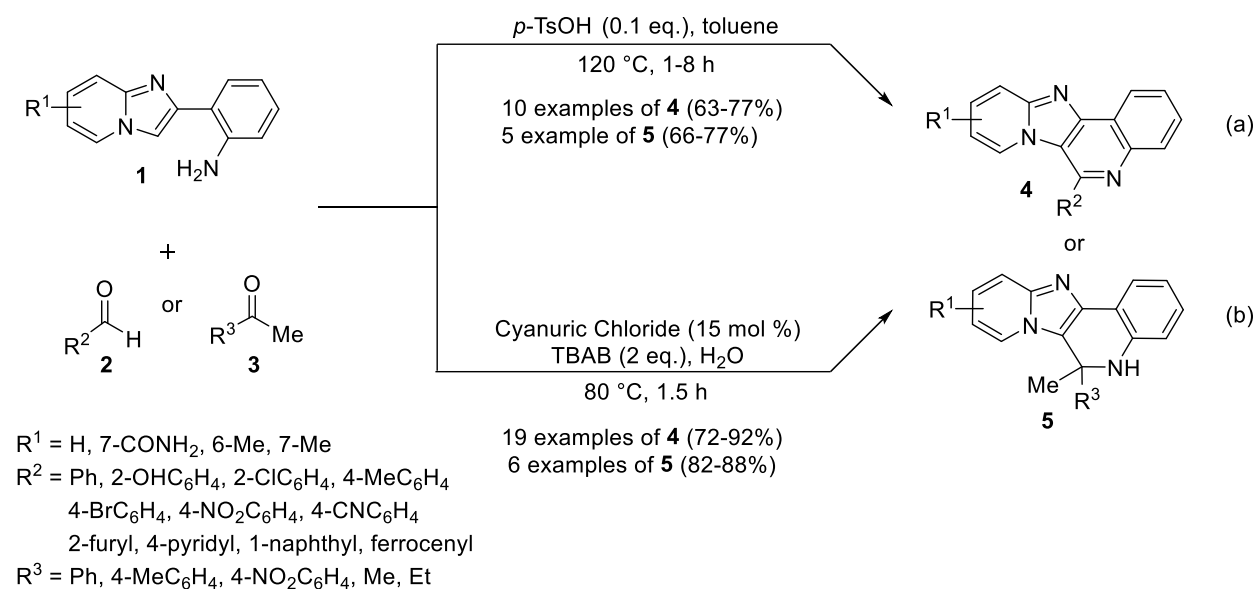


Figure 2B.1: Selective examples of imidazo[1,2-*a*]pyridine-based molecules

In this respect, Kundu group synthesized pyrido[2',1':2,3]imidazo[4,5-*c*]quinolines (**PIQ**) (**4** & **5**) from 2-(imidazo[1,2-*a*]pyridin-2-yl)anilines (**1**) and aldehydes (**2**)/ketones (**3**) via Pictet–Spengler reaction in the presence of *p*-TsOH as catalyst (**Scheme 2B.1a**).^[13] Chauhan and coworkers have also achieved the synthesis of PIQ derivatives (**4** & **5**) from 2-(imidazo[1,2-*a*]pyridin-2-yl)anilines

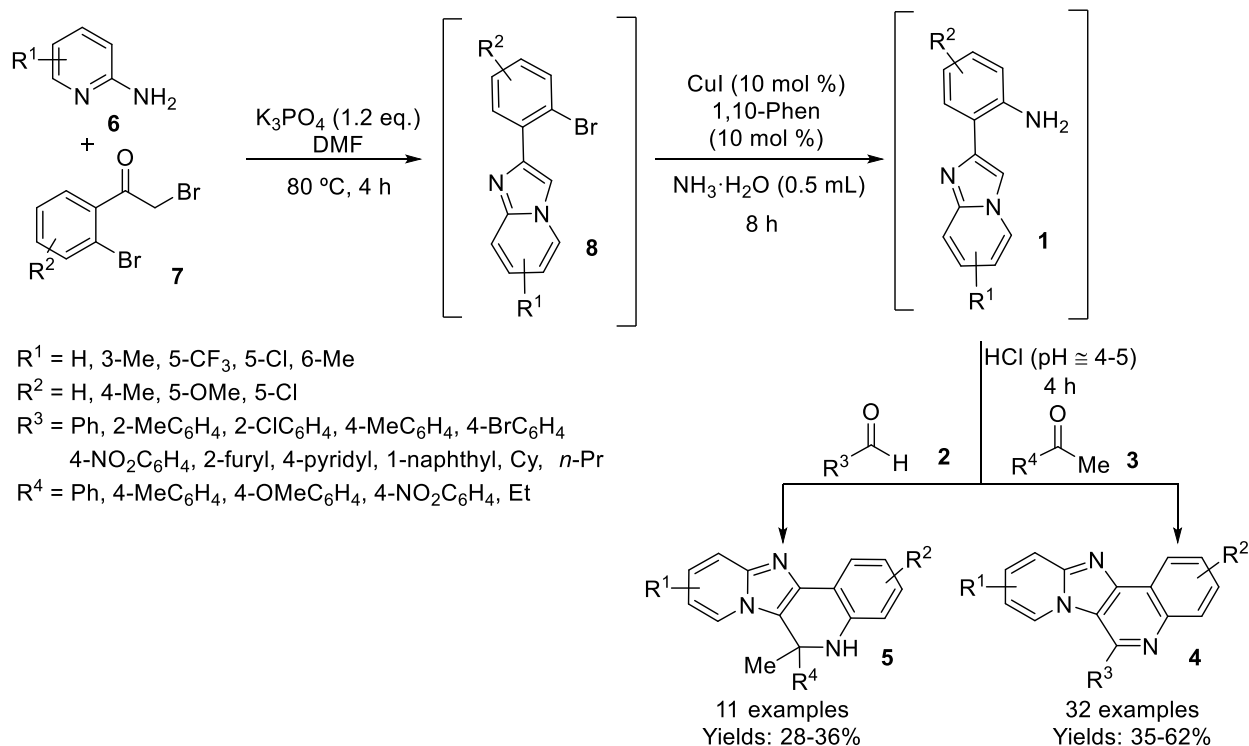
(1) and aldehydes (2)/ketone (3) by using cyanuric chloride in catalytic amount and *tetra-n*-butylammonium bromide (TBAB) as phase transfer catalyst **Scheme 2B.1b**).^[14]



Scheme 2B.1: Synthesis of pyrido[2',1':2,3]imidazo[4,5-*c*]quinolines from 2-(imidazo[1,2-*a*]pyridin-2-yl)anilines

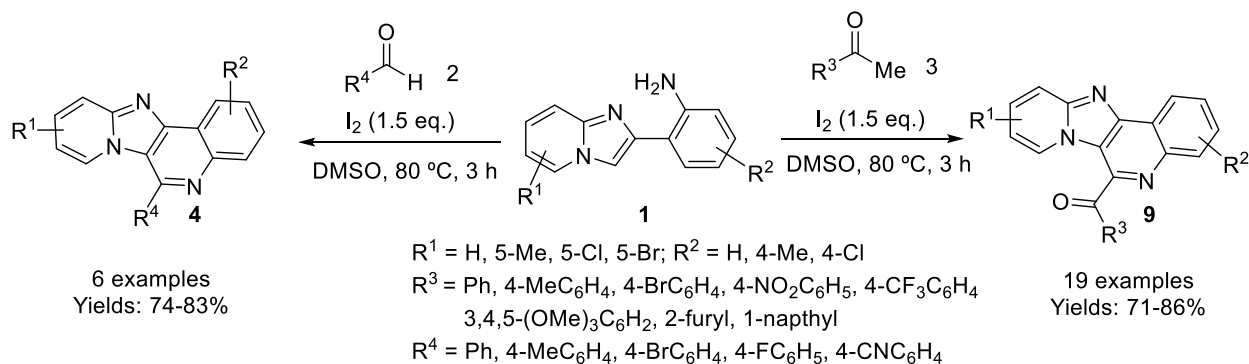
Various type of aryl/heteroaryl aldehydes (2) and ketones (3) reacted well under this protocol to give corresponding products in good yield (72-92%). Even ferrocene aldehyde also reacted smoothly and afforded product in 75% yield. The synthesized compounds were further evaluated for their antimalarial activity against CQ-S 3D7 and CQ-R K1 strains of *P. falciparum* and cytotoxicity towards the VERO cell line (1008; Monkey kidney fibroblast). All the synthesized compounds showed moderate antimalarial activity.

Zhang and coworkers reported the one-pot synthesis of PIQ analogues (4 & 5) starting from 2-aminopyridines (6). Initially, the reaction of 2-aminopyridines (6) and 2-bromophenacyl bromides (7) afforded 2-(2-bromophenyl)imidazo[1,2-*a*]pyridines (8) in the presence of a base. Subsequently, the addition of ammonia *via* copper-assisted amination reaction resulted in 2-(imidazo[1,2-*a*]pyridin-2-yl)anilines (1). Finally reaction of 1 with aldehydes (2) or ketones (3) produced desired imidazopyridine fused quinoline derivatives *via* Pictet–Spengler reaction in the presence of HCl (**Scheme 2B.2**).^[15] A series of 43 molecules synthesized by varying different aldehydes and ketones in moderate to good yields (28-62%).



Scheme 2B.2: Synthesis of PIQ derivatives from 2-aminopyridines and 2-bromophenacyl bromides

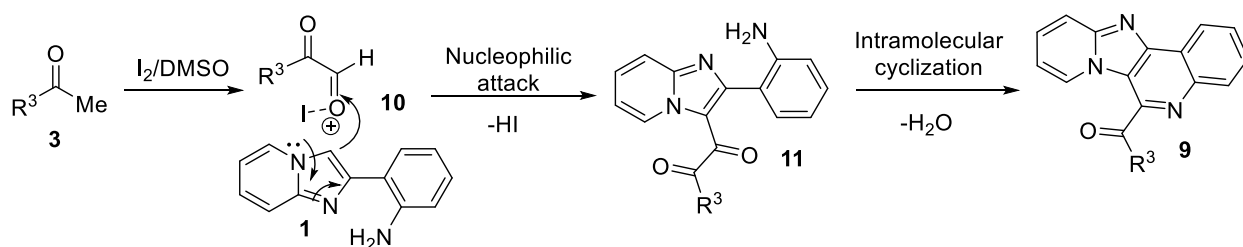
Atmakur group reported formation of substituted imidazo[1,2-*a*]pyridine-fused quinolines (**4**) and aroyl substituted imidazo[1,2-*a*]pyridine-fused quinolines (**9**) by I_2 -DMSO mediated oxidative cross coupling followed by intramolecular cyclization of 2-(imidazo[1,2-*a*]pyridin-2-yl)anilines (**1**) with aldehydes (**2**)/ketone (**3**) in one-pot fashion (**Scheme 2B.3**).^[16]



Scheme 2B.3: I_2 -DMSO promoted formation of substituted PIQ from 2-(imidazo[1,2-*a*]pyridin-2-yl)anilines

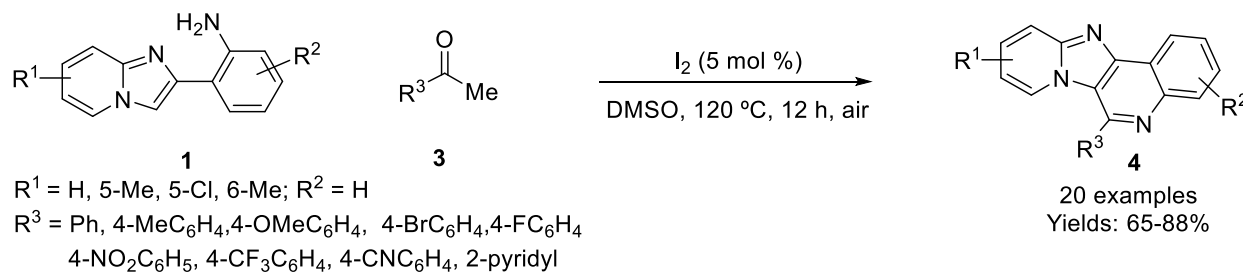
The developed strategy proceeded though initially formation of phenylglyoxal (**10**) in the presence of I_2 and DMSO (Kornblum reaction conditions). Subsequently, nucleophilic attack of

imidazopyridines on *in situ* formed phenylglyoxal was activated by I₂ to produce intermediate (11). Finally, intramolecular cyclization afforded the desired products (Scheme 2B.3a).



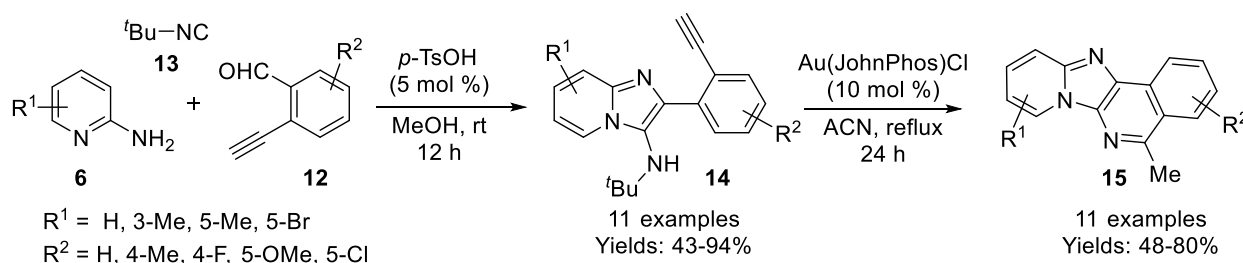
Scheme 2B.3a: Reaction pathway for I₂-DMSO mediated formation of PIQ

Interestingly, pyrido[2',1':2,3]imidazo[4,5-*c*]quinolines (4) were obtained when 2-(imidazo[1,2-*a*]pyridin-2-yl)anilines (1) were allowed to react with ketones (3) in the presence of I₂ in DMSO at 120 °C for 12 h (Scheme 2B.4). This transformation is believed to proceed through sequential condensation, Pictet–Spengler reaction, C_{sp}³-H functionalization, and cleavage of CO-C bond.



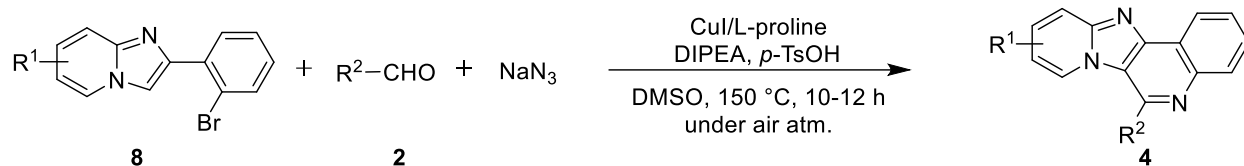
Scheme 2B.4: I₂-catalyzed synthesis of PIQ analogues

The group prepared structurally diverse imidazo[1,2-*a*]pyridine-fused isoquinolines by using the Groebke–Blackburn–Bienaymé reaction of 2-aminopyridines (6), isocyanide (13) and *o*-alkynylbenzaldehydes (12) followed by gold-catalyzed hydroamination. Imidazo[1,2-*a*]pyridine-fused isoquinolines (15) in good yields (48-80%) (Scheme 2B.5).^[17]



Scheme 2B.5: Synthesis of PIQs in two steps from 2-aminopyridines and 2-alkynylbenzaldehydes

Importance of imidazo[1,2-*a*]pyridine framework in various fields motivated us to develop a new simple and straightforward method for the synthesis of PIQ analogues. In this chapter of the thesis, we have synthesized PIQs from 2-(2-bromophenyl)imidazo[1,2-*a*]pyridine (**8**) and aldehydes (**2**) using sodium azide as a source of nitrogen in the presence of CuI as catalyst (**Scheme 2B.6**).



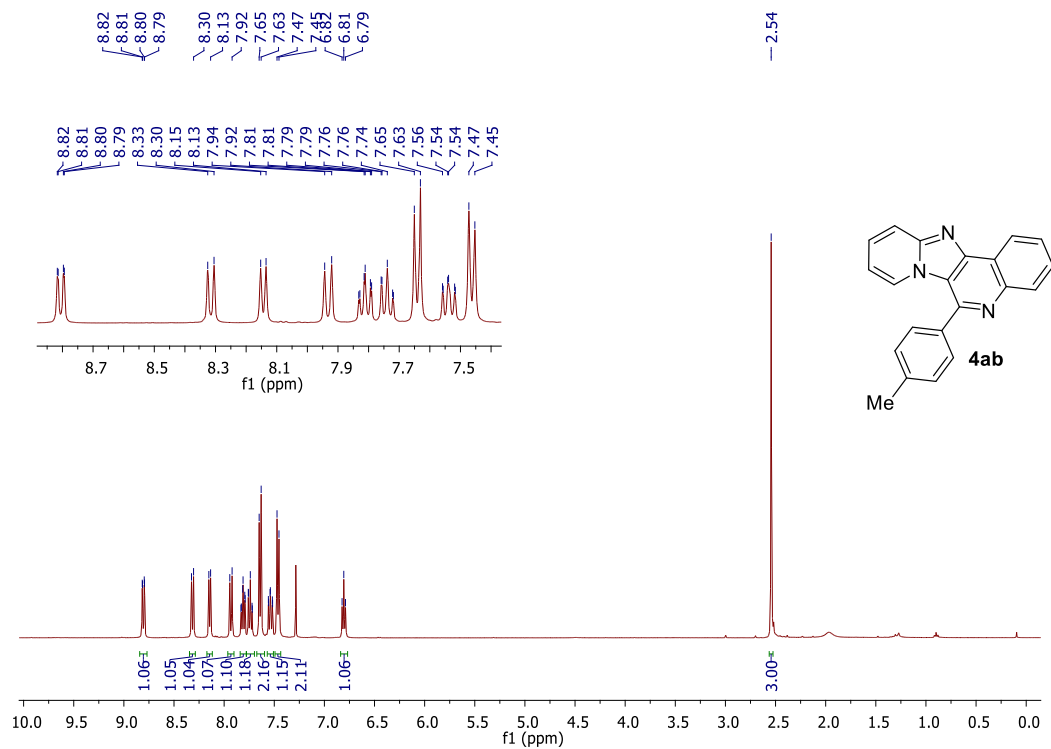
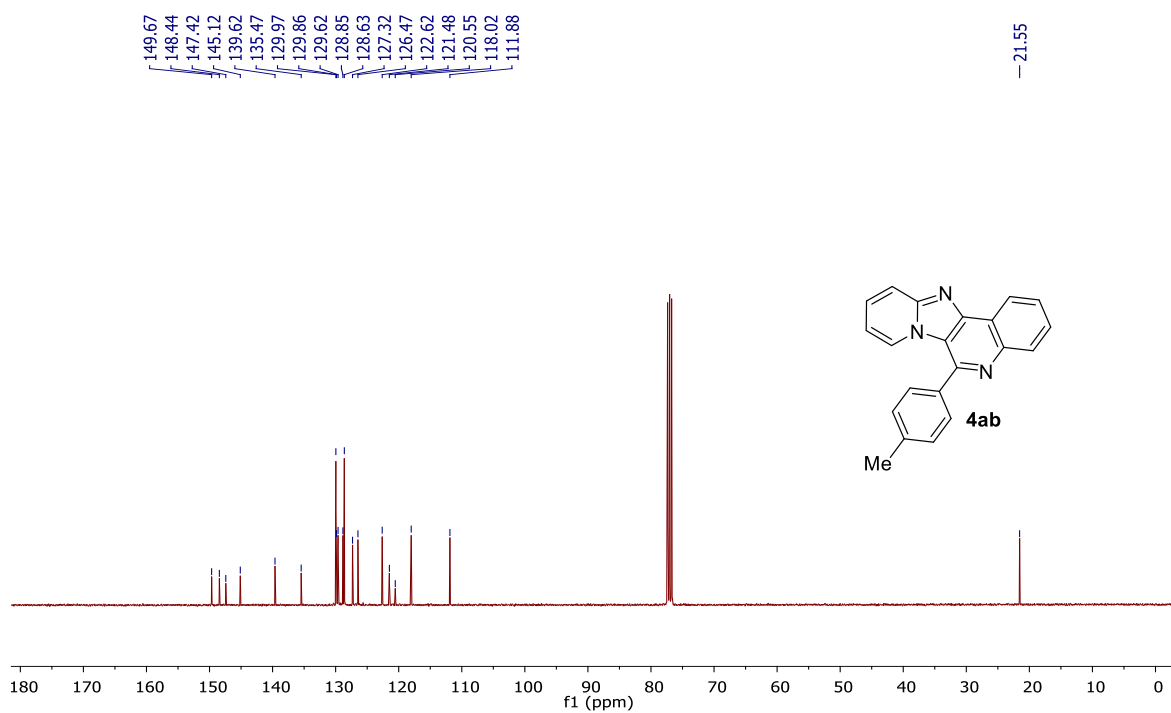
Scheme 2B.6: Synthesis of PIQ derivatives from 2-(2-bromophenyl)imidazo[1,2-*a*]pyridines

2B.2 RESULTS AND DISCUSSION

IB.2.1 Chemistry

The optimized conditions for this transformation were recognized by performing a series of experiments using 2-(2-bromophenyl)imidazo[1,2-*a*]pyridine (**8a**), 4-methylbenzaldehyde (**2b**) and sodium azide as model substrates (Table 2.1). Our initial efforts commenced with the reaction of **8a** with **2b** using NaN₃ in the presence of CuI (10 mol %), L-proline (20 mol %), trimethylamine (TEA) (1 eq.) and *p*-TsOH (0.1 eq.) in DMSO at 150 °C after 10 h. Expected product 6-(*p*-tolyl)pyrido[2',1':2,3]imidazo[4,5-*c*]quinoline (PIQ) (**4ab**) was obtained in 40% yield (entry 1, **Table 2B.1**).

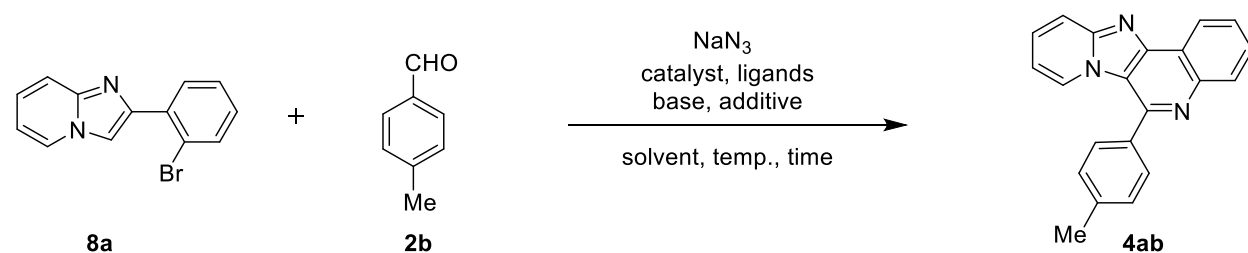
Structure of **4ab** is confirmed by ¹H & ¹³C NMR and mass analysis. In the ¹H NMR spectrum of **4ab**, a characteristic deshielded doublet of doublet appeared at δ 8.82 ppm for C₈-H of imidazopyridine ring, a singlet at δ 2.54 ppm for C₄-CH₃ aryl ring at the C₆ position of **4ab** along with other expected protons at their respective positions were observed (**Figure 2B.2**). The methyl carbons of aryl appeared at δ 21.55 along with all other expected peaks in the ¹³C NMR spectrum confirmed the structure of **4ab** (**Figure 2B.3**).

Figure 2B.2: ¹H NMR spectrum of 4abFigure 2B.3: ¹³C NMR spectrum of 4ab

To further improve the reaction yield, various bases such as DIPEA, DBU, and K_2CO_3 (entries 2-4, **Table 2B.1**) and found that DIPEA was most effective base for this protocol. Then we evaluated the different copper salts such as CuI, CuBr, $Cu(OAc)_2$ and $Cu(OTf) \cdot DCM$. It is found that CuI was the best catalyst among different copper salts for this transformation giving the highest yield of **4ab** (entries 7-9, **Table 2B.1**). Further, we found that 20 mol % of CuI gave the best yield of **4ab** by varying the catalyst loading from 10 mol % to 30 mol % (entries 2, 5-6, **Table 2B.1**)

Examine the effect of loading of additive for model reaction; it was found 0.5 eq. of *p*-TsOH afforded the highest yield of **4ab** (entries 2, 10-12, **Table 2B.1**). Use of different acid additive such as TFA AcOH, and, $BF_3 \cdot OEt_2$ did not improve the yield of **4ab** and *p*-TsOH was best among all tested additive (entries 13-15, **Table 2B.1**). Furthermore, we screened different ligands, and L-proline (30 mol %) provided the highest yield (entries 11 vs 16-18, **Table 2B.1**). We next examined the impact of solvents on reaction yield, use of other polar solvents such as DMF, DMA, and EtOH as well as non-polar solvents such as toluene instead of DMSO resulted in decreased yield (entries 19-22, **Table 2B.1**). Notably, the reaction did not work at all without the use of CuI (entry 25, **Table 2B.1**). It was also worth mentioning that the yield of desired product **4ab** decreased significantly when the model reaction is performed in the absence of *p*-TsOH or L-proline or DIPEA (entries, 23-24 and 26, **Table 2B.1**).

Table 2B.1: Optimization of reaction condition for copper-catalyzed one-pot reaction.^a



Entry	Catalyst (mol %)	Ligand (mol %)	Base (1.0 eq.)	Additive (eq.)	Solvent (2 mL)	Yield ^b (%)
1	CuI (10)	L-proline (20)	TEA	<i>p</i> -TsOH (0.1)	DMSO	40
2	CuI (10)	L-proline (20)	DIPEA	<i>p</i> -TsOH (0.1)	DMSO	56
3	CuI (10)	L-proline (20)	DBU	<i>p</i> -TsOH (0.1)	DMSO	32
4	CuI (10)	L-proline (20)	K_2CO_3	<i>p</i> -TsOH (0.1)	DMSO	10
5	CuI (20)	L-proline (30)	DIPEA	<i>p</i> -TsOH (0.1)	DMSO	64

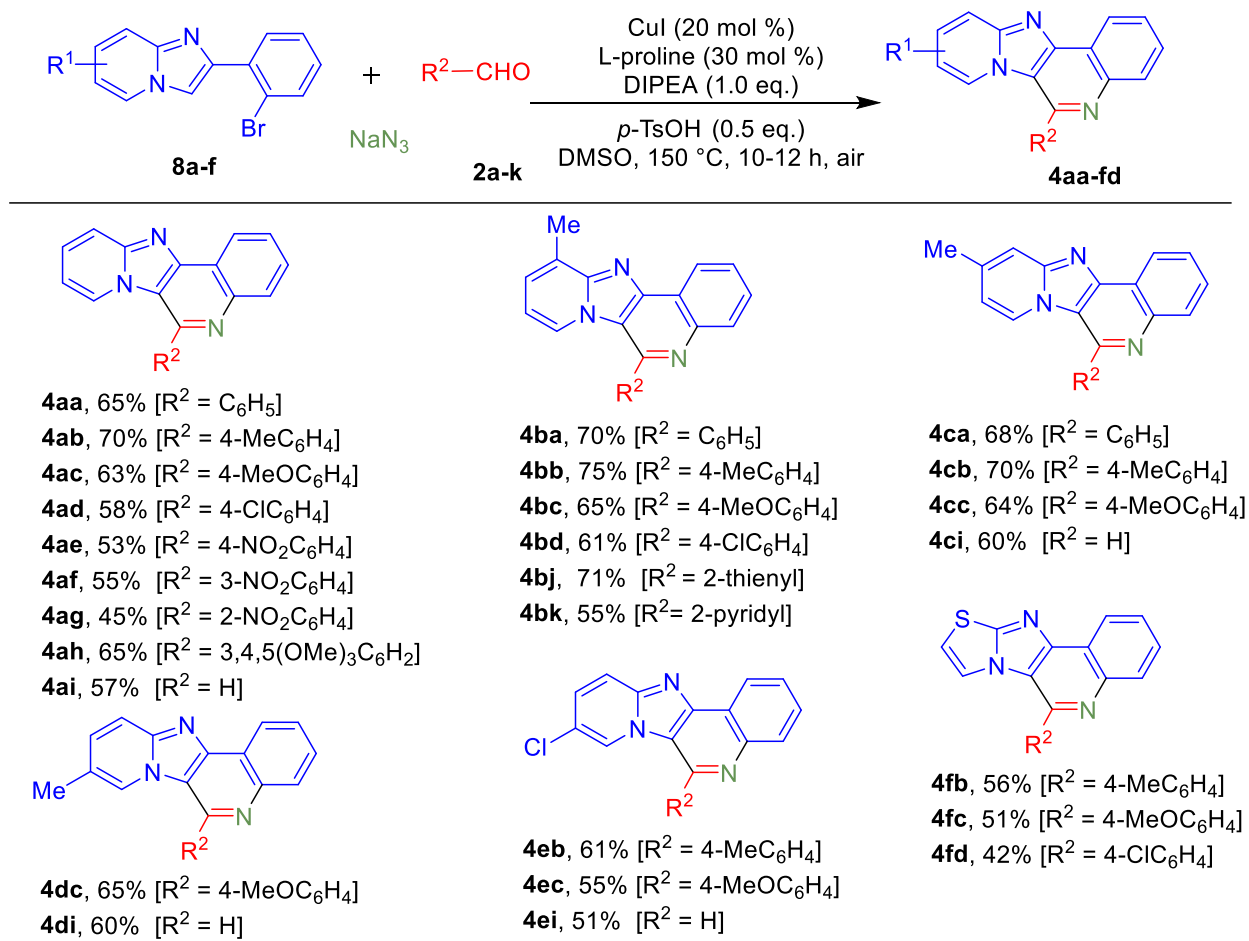
6	CuI (30)	L-proline (60)	DIPEA	<i>p</i> -TsOH (0.1)	DMSO	60
7	CuBr (20)	L-proline (30)	DIPEA	<i>p</i> -TsOH (0.1)	DMSO	55
8	Cu(OAc) ₂ (20)	L-proline (30)	DIPEA	<i>p</i> -TsOH (0.1)	DMSO	42
9	Cu(OTf)·DCM(20)	L-proline (30)	DIPEA	<i>p</i> -TsOH (0.1)	DMSO	61
10	CuI (20)	L-proline (30)	DIPEA	<i>p</i> -TsOH (0.3)	DMSO	66
11	CuI (20)	L-proline (30)	DIPEA	<i>p</i>-TsOH (0.5)	DMSO	70
12	CuI (20)	L-proline (30)	DIPEA	<i>p</i> -TsOH (1.0)	DMSO	72
13	CuI (20)	L-proline (30)	DIPEA	TFA ^c (0.5)	DMSO	43
14	CuI (20)	L-proline (30)	DIPEA	AcOH (0.5)	DMSO	51
15	CuI (20)	L-proline (30)	DIPEA	BF ₃ OEt ₂ (0.5)	DMSO	35
16	CuI (20)	Glycine (30)	DIPEA	<i>p</i> -TsOH (0.5)	DMSO	54
17	CuI (20)	DMEDA ^d (30)	DIPEA	<i>p</i> -TsOH (0.5)	DMSO	61
18	CuI (20)	1,10-Phen ^e (30)	DIPEA	<i>p</i> -TsOH (0.5)	DMSO	48
19	CuI (20)	L-proline (30)	DIPEA	<i>p</i> -TsOH (0.5)	DMF	42
20	CuI (20)	L-proline (30)	DIPEA	<i>p</i> -TsOH (0.5)	DMAc	38
21	CuI (20)	L-proline (30)	DIPEA	<i>p</i> -TsOH (0.5)	EtOH ^f	35
22	CuI (20)	L-proline (30)	DIPEA	<i>p</i> -TsOH (0.5)	Toluene ^g	20
23	CuI (20)	L-proline (30)	DIPEA	-	DMSO	25
24	CuI(20)	-	DIPEA	<i>p</i> -TsOH (0.5)	DMSO	53
25	-	L-proline (30)	DIPEA	<i>p</i> -TsOH (0.5)	DMSO	-
26	CuI(20)	L-proline (30)	-	<i>p</i> -TsOH (0.5)	DMSO	60

Reaction conditions: **8a** (0.366 mmol), **2a** (0.439 mmol), NaN₃ (0.549 mmol), CuI (20 mol %), L-proline (30 mol %), *p*-TsOH (0.183 mol %), base (1 eq.), 150 °C, air atmosphere, 10 h. ^bIsolated yields. ^cTFA = Trifluoro acetic acid. ^dDMEDA = *N,N*-Dimethylethylenediamine. ^e1,10-Phen = 1,10-Phenanthroline. ^fAt 90 °C for 10 h. ^gAt 120°C for 24 h.

With the optimized conditions in hand, we sought to evaluate the applicability of this methodology to synthesize imidazopyridine-fused quinolines (**Table 2B.2**). Pyrido[2',1':2,3]imidazo[4,5-*c*]quinolines (**4aa-ai**) were obtained in good to high (45-70%) yields from reaction of **8a** with aldehydes (**2a-i**). The yield of **4** was relatively poor from aldehydes having electron withdrawing groups. Similarly, other substituted imidazo[1,2-*a*]pyridines (**8b-e**) reacted with aldehydes (**2a-i**) to give corresponding pyrido[2',1':2,3]imidazo[4,5-*c*]quinolines (**4ba-ei**) in moderate to good

yields. Interestingly, heteroaryl-aldehydes such as thiophene-2-carbaldehyde (**2j**) and 2-picolinaldehyde (**2k**) were well tolerated under the optimized conditions and gave corresponding products (**4bj** and **4bk**) in 71% and 55% yield, respectively. In addition, 6-(2-bromophenyl)imidazo[2,1-b]thiazole (**8f**) also reacted well with aldehydes (**2b-d**) and gave corresponding desired products (**4fb-fd**) in good yield (42-56%).

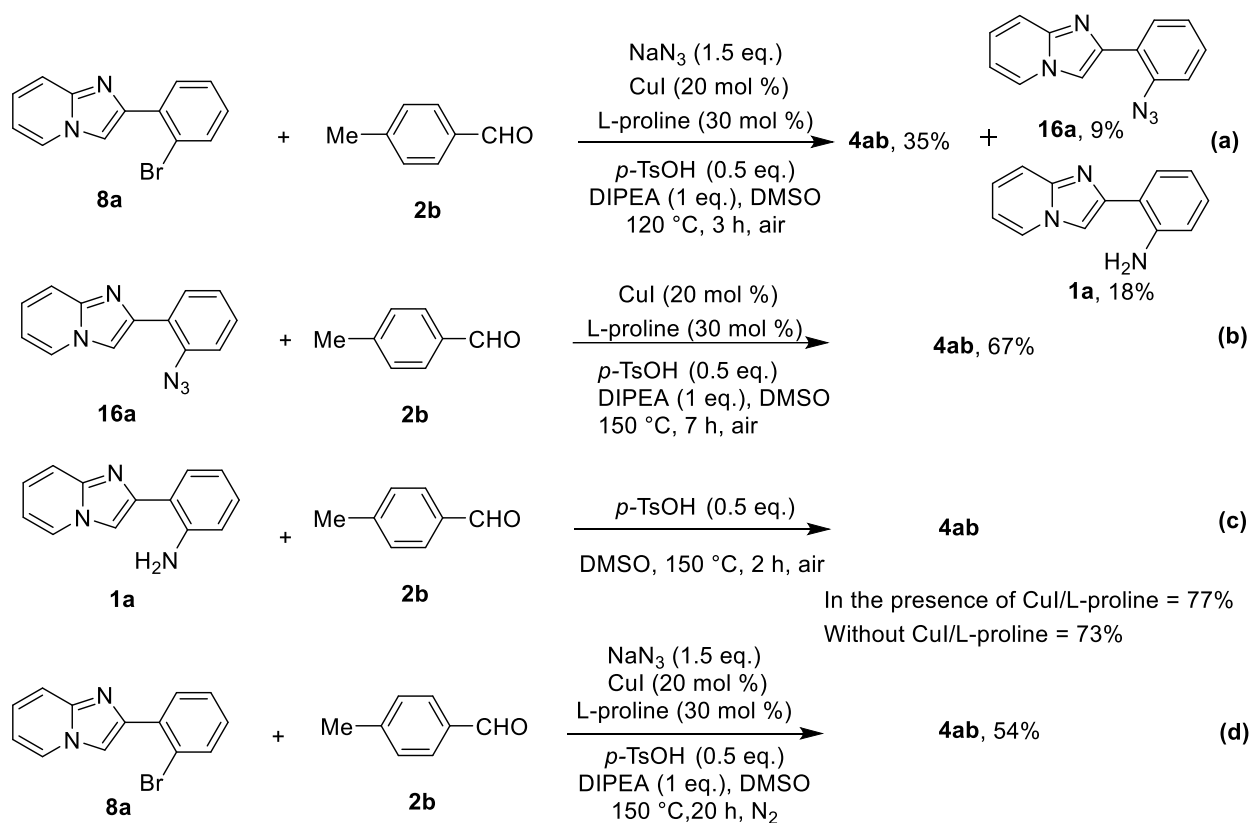
Table 2B.2: Substrate scope of PIQs (**4**)



^a**Reaction conditions:** **8** (0.366 mmol), **2** (0.439 mmol) NaN_3 (0.549 mmol), CuI (20 mol %), L-proline (30 mol %), *p*-TsOH (0.183 mmol), DIPEA (1 eq.), DMSO (2.0 mL), 150 °C, air atmosphere, 10 h; ^bIsolated yields.

To gain insight into the mechanism, a few control experiments were performed (**Scheme 2B.7**). On reacting **8a**, **2b** and NaN_3 in the presence of CuI (20 mol %), L-proline (30 mol %), DIPEA (1 eq.) and *p*-TsOH (0.5 eq.) in DMSO at 120 °C for 3 h, 2-(2-azidophenyl)imidazo[1,2-*a*]pyridine

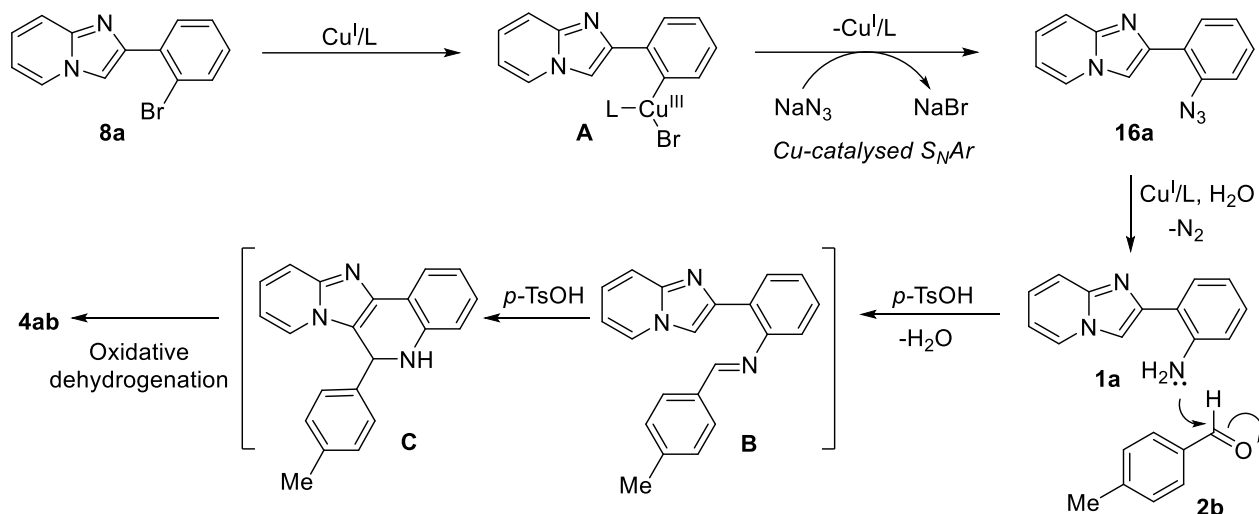
(**16a**), 2-(imidazo[1,2-*a*]pyridin-2-yl)aniline (**1a**) and **4ab** were obtained in 9%, 18% and 35% yields, respectively (**Scheme 2B.7a**). The reaction of **16a** with **2b** under optimized reaction conditions gave **4ab** in 67% yield (**Scheme 2B.7b**). On the other hand, reaction of **1a** with **2b** in the presence of CuI, L-proline and *p*-TsOH in DMSO at 150 °C resulted in the formation of **4ab** in 77%, While the yield of **4ab** was 73% when performed in the absence CuI (**Scheme 2B.7c**), indicating that CuI has no role in the second step of the reaction. The yield of **4ab** reduced significantly (54%) when the reaction of **8a**, **2b**, and NaN₃ was performed under nitrogen keeping other conditions same (**Scheme 2B.7d**).



Scheme 2B.7: Control experiments

Based on results of the control experiments and literature precedent,^[18-26] a plausible mechanism for the formation of **4** is depicted in **Scheme 2B.8**. Initially, copper-catalyzed S_NAr reaction results in the formation of 2-(2-azidophenyl)imidazo[1,2-*a*]pyridine (**16a**) via intermediate **A**. Extrusion of dinitrogen from **16a** in the presence of copper and traces of moisture provides (2-(imidazo[1,2-*a*]pyridin-2-yl)aniline (**1a**). Intermediate **1a** on reaction with aldehyde **2b** gives the desired product **4ab** via Pictet–Spengler cyclization in DMSO in the presence of *p*-TsOH. In this reaction,

condensation of aldehyde **2b** with **1a** generates Schiff base **B**, which then undergoes an intramolecular cyclization to afford cyclic intermediate **C**. Finally, intermediate **C** undergoes an oxidative dehydrogenation under air to give **4ab** as the final product (**Scheme 2B.8**).



Scheme 2B.8: Proposed mechanism of Cu(I)-catalyzed multicomponent reaction

2B.2.2 Biology

2B.2.2.1 Antibacterial activity

Quinoline derivatives are recognized to exhibit prominent antibacterial activity^[27-30], so to determine the antibacterial efficacy, synthesized compounds **4aa–4fd** were tested against three Gram-negative bacteria *S. typhi*, *K. pneumoniae*, and *P. putida*, or two Gram-positive bacteria *B. cereus* and *S. aureus* (**Table 2B.3**). The activity in terms of minimal inhibitory concentrations (MIC) and zone of inhibition (ZOI) of the compounds was determined *in vitro* using Streptomycin as standard drug. The observed results from **Table 2B.3** revealed that most of the compounds effectively inhibit the growth of tested pathogenic strains *in vitro*. Compounds **4ae**, **4ai**, and **4cc** showed considerable antibacterial activity with MIC of 12.5 $\mu\text{g}/\text{mL}$ as compared to all other tested compounds against Gram-negative bacterial strains.

Table 2B.3: *In vitro* antibacterial activity of pyrido[2',1':2,3]imidazo[4,5-*c*]quinolines (**4**).

Compound	<i>S. typhi</i>		<i>P. putida</i>		<i>K. pneumonia</i>		<i>B. cereus</i>		<i>S. aureus</i>	
	MIC μg/ml	ZOI mm	MIC μg/ml	ZOI mm	MIC μg/ml	ZOI mm	MIC μg/ml	ZOI mm	MIC μg/ml	ZOI mm
4aa	50	15	50	14	>25	14	50	15	50	14
4ab	100	13	100	13	100	13	>100	14	>100	14
4ac	50	15	>50	13	>50	13	50	14	50	13
4ad	100	15	50	15	50	14	50	13	50	13
4ae	12.5	18	12.5	18	25	15	>25	15	25	16
4af	150	15	150	14	150	14	-	-	-	-
4ag	50	14	50	12	100	12	>50	12	>50	13
4ah	50	13	50	15	>25	13	100	13	100	13
4ai	12.5	18	12.5	18	25	15	25	15	>25	14
4ba	25	15	25	16	>25	16	25	16	25	17
4bb	50	15	50	13	>25	14	>25	14	50	15
4bc	100	14	>50	12	>50	15	>50	13	100	13
4bd	25	14	25	14	>25	13	50	14	50	15
4bj	50	12	50	13	>25	13	50	14	50	12
4bk	50	15	>50	14	>50	14	50	14	50	15
4ca	100	13	>50	14	100	14	50	14	50	14
4cb	50	14	>25	14	50	15	100	15	100	15
3cc	12.5	19	12.5	19	25	16	25	16	25	15
4ci	-	-	-	-	-	-	-	-	-	-
4dc	100	14	100	14	100	15	>100	14	>100	14
4di	100	13	100	14	100	14	-	-	-	-
4eb	25	14	25	15	25	14	50	13	50	13
4ec	25	14	>25	15	50	14	50	14	50	14
4ei	>25	14	50	16	>25	14	>25	14	>25	14
4fb	100	14	>50	14	>50	12	50	13	100	14
4fc	50	14	>25	12	50	13	50	14	>25	13
4fd	>50	15	>25	15	25	14	>25	14	>50	14
Streptomycin	6.25	22	6.25	23	3.125	22	6.25	21	6.25	22

Zone of inhibition (ZOI in mm) and minimum inhibitory concentration (MIC, μg/mL) values for a compound with significant activity are shown in bold.

2B.2.2.2 Evaluation of cell death

The antibacterial activity gives useful information about the potential of chemically synthesized compounds against a wide range of pathogenic bacterial strains. However, the cell death assay provides better information about the killing efficacy of the compounds against the tested pathogenic bacteria. Three most effective compounds **4ae**, **4ai**, and **4cc** were selected to evaluate the reduction of the bacterial population (*S. typhi* and *P. putida*) with time at $3 \times \text{MIC}$ (**Figure 2B.4, A and B**). Compounds (**4ae**, **4ai**, and **4cc**) resulted in $>55\%$ reduction in the population of tested pathogenic bacteria after 4 h of incubation.

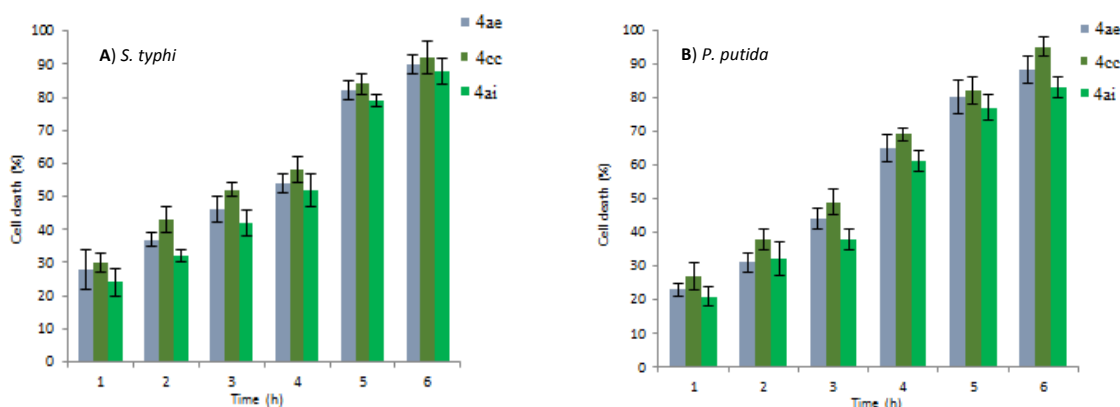


Figure 2B.4: A) and B) Killing efficacy of **4ae**, **4ai**, and **4cc** against *S. typhi* and *P. putida*, respectively

The reduction in the population of the pathogenic bacteria was $>85\%$ for all the selected compounds after 6 h of incubation. The killing efficiency of these compounds was slightly better against *S. typhi* as compared to *P. putida*.

2B.2.2.3 Bactericidal kinetics

To explore the killing behavior of most effective compounds **4ae**, **4ai**, and **4cc**, a kinetic study was performed against *S. typhi* and *P. putida* at $3 \times \text{MIC}$ (**Figure 2B.5, A and B**). The log phase culture of both the bacterial strains is incubated with the compounds and change in optical density (OD_{600}) was observed at different time intervals (1-6 h). Untreated bacterial culture is taken as a control. Significant reduction in the bacterial number is observed after 4 h of incubation. This indicates that the compounds are active to inhibit the bacterial growth in a short time. Compound **4cc** showed the highest reduction of bacterial cells as compared to **4ae** and **4ai**.

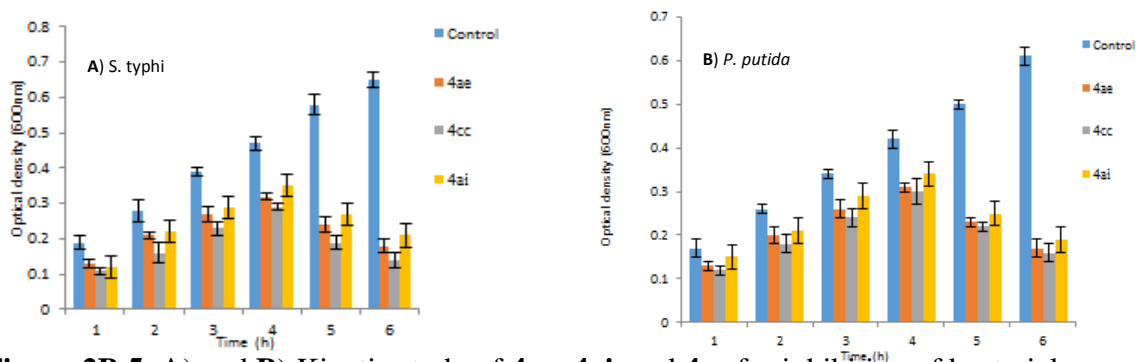


Figure 2B.5: A) and B) Kinetic study of **4ae**, **4ai**, and **4cc** for inhibition of bacterial growth of *S. typhi* and *P. putida*, respectively

2B.2.2.4 Live dead cell screening

The bacterial cell death caused by most effective compounds **4ae**, **4ai** and **4cc** were tested by dual staining of acridine orange/ethidium bromide (AO/EB). For the assay, untreated as well as treated *S. typhi* cells were stained with the mixture of AO/EB for 3 h. From the Figure 1B.7, it is evident that AO enters inside the untreated living cells to emit green fluorescence whereas EB enters only in the compromised cell membrane of dead cells to emit red fluorescence (**Figure 2B.6**). The observed results illustrate that the tested compounds are capable of disrupting the cell membrane integrity and causes cell death.

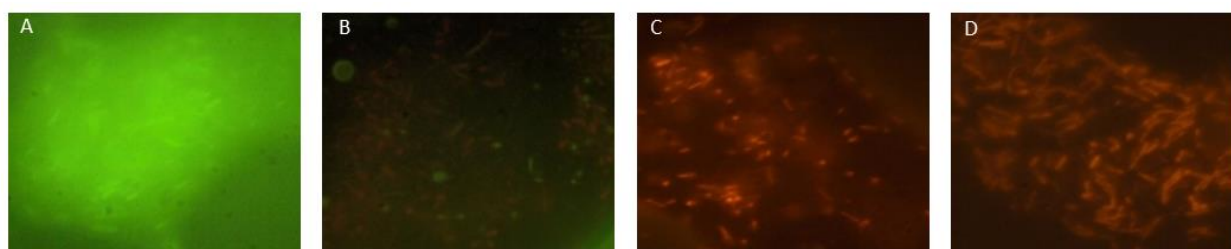


Figure 2B.6: Fluorescence images of *S. typhi* A) without treatment; B) on treatment with **4ae**; C) on treatment with **4cc**; (D) on treatment with **4ai**.

12B.3 CONCLUSIONS

We have developed an efficient and straightforward protocol for the synthesis of pyrido[2',1':2,3]imidazo[4,5-*c*]quinoline derivatives *via* copper catalyzed one-pot multicomponent reaction of 2-(2-bromophenyl)imidazo[1,2-*a*]pyridines, aldehydes, and sodium azide. The experimental procedure is simple and uses inexpensive copper catalyst and easily available starting materials to give moderate to good yields of products. All the synthesized compounds were evaluated for *in-vitro* antibacterial activities against three Gram-negative bacteria *S. typhi*, *K. pneumoniae*, *P. putida* and two Gram-positive bacteria *B. cereus*, *S. aureus*. Among all screened compounds, **4ae**, **4ai**, and **4cc** exhibited moderate antibacterial activity against Gram-negative bacteria *S. typhi* and *P. putida*. These compounds were further studied for cell death, bactericidal kinetics, and live cell screening.

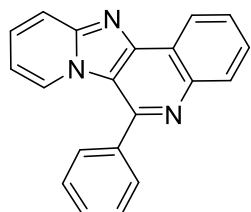
2B.4 EXPERIMENTAL SECTION

General information: Melting points were determined in open capillary tubes on an automated melting point apparatus and are uncorrected. Reactions are monitored by using thin layer chromatography (TLC) on 0.2 mm silica gel F₂₅₄ plates. The chemical structures of the final products were determined by their NMR and mass analysis. NMR spectra were recorded on Bruker Ascend 400. Chemical shifts are reported in parts per million (ppm) using tetramethylsilane (TMS) as an internal standard or deuterated solvent peak (CDCl₃ and DMSO-*d*₆). The HRMS data were recorded on Agilent 6545 mass spectrometer with electrospray ionization and TOF mass analyzer. 2-(2-Bromophenyl)imidazo-[1,2-*a*]pyridine derivatives (**8**) are synthesized according to the published procedure.^[31] All other chemicals were obtained from the commercial suppliers and used without further purification.

Representative procedure for synthesis of pyrido-[2',1':2,3]imidazo[4,5-*c*]quinoline derivatives (4ab): A mixture of 2-(2-bromophenyl)imidazo[1,2-*a*]pyridine (**8a**) (0.366 mmol), benzaldehyde (**2b**) (0.439 mmol), sodium azide (35 mg, 0.549 mmol), CuI (14 mg, 20 mol %), L-proline (12 mg, 30 mol %), DIPEA (1.0 eq.) and *p*-TsOH (35 mg, 0.5 eq.) was stirred in DMSO (2.0 mL) under air atmosphere at room temperature and then heated at 150 °C for 10 h. After cooling to ambient temperature, the reaction mass was quenched with ice-cold aqueous solution of NH₄Cl (30 mL), filtered through celite bed and washed with ethyl acetate (10 mL). Filtrate was

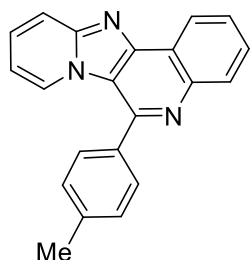
extracted with ethyl acetate (2×10 mL). Organic layers were combined, dried over anhydrous Na_2SO_4 and concentrated under reduced pressure. Desired product **4ab** was isolated by column chromatography on silica gel (100-200 mesh) using ethyl acetate/hexane (30%, v/v) as eluent.

6-Phenylpyrido[2',1':2,3]imidazo[4,5-c]quinoline (4aa)



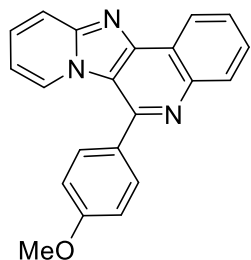
Off white solid (70 mg, 65%); mp 207–209 °C (Lit.^[15] 207–208 °C); ^1H NMR (400 MHz, CDCl_3) δ 8.82 (dd, $J = 8.0, 1.1$ Hz, 1H), 8.33 (dd, $J = 8.3, 0.4$ Hz, 1H), 8.07 (dt, $J = 7.0, 1.1$ Hz, 1H), 7.95 (dt, $J = 9.2, 1.1$ Hz, 1H), 7.86 – 7.80 (m, 1H), 7.78 – 7.73 (m, 3H), 7.70 – 7.63 (m, 3H), 7.58 – 7.52 (m, 1H), 6.81 (td, $J = 6.9, 1.2$ Hz, 1H); ^{13}C NMR (100 MHz, CDCl_3) δ 149.7, 148.2, 147.5, 145.0, 138.3, 130.0, 129.64, 129.62, 129.3, 128.9, 128.7, 127.2, 126.6, 122.6, 121.5, 120.5, 118.1, 112.0; HRMS calcd for $\text{C}_{20}\text{H}_{14}\text{N}_3$ $[\text{M}+\text{H}]^+$ 296.1182, found 296.1194

6-(*p*-Tolyl)pyrido[2',1':2,3]imidazo[4,5-c]quinoline (4ab)



Off white solid (79 mg, 70%); mp 237–239 °C (Lit.^[13] 239–240 °C); ^1H NMR (400 MHz, CDCl_3) δ 8.81 (dd, $J = 8.0, 1.1$ Hz, 1H), 8.32 (d, $J = 8.3$ Hz, 1H), 8.14 (d, $J = 7.0$ Hz, 1H), 7.93 (d, $J = 9.1$ Hz, 1H), 7.85 – 7.78 (m, 1H), 7.78 – 7.71 (m, 1H), 7.64 (d, $J = 8.0$ Hz, 2H), 7.57 – 7.51 (m, 1H), 7.46 (d, $J = 7.8$ Hz, 2H), 6.81 (t, $J = 6.9$ Hz, 1H), 2.54 (s, 3H); ^{13}C NMR (100 MHz, CDCl_3) δ 149.7, 148.4, 147.4, 145.1, 139.6, 135.5, 130.0, 129.9, 129.6, 128.8, 128.6, 127.3, 126.5, 122.6, 121.5, 120.5, 118.0, 111.9, 21.5; HRMS calcd for $\text{C}_{21}\text{H}_{16}\text{N}_3$ $[\text{M}+\text{H}]^+$ 310.1339, found 310.1347

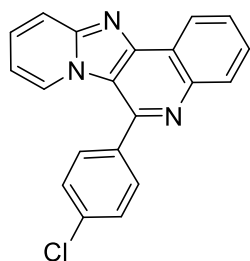
6-(4-Methoxyphenyl)pyrido[2',1':2,3]imidazo[4,5-c]-quinoline (4ac)



Off white solid (75 mg, 63%); mp 233–235 °C (Lit.^[15] 233–234 °C); ^1H NMR (400 MHz, CDCl_3) δ 8.79 (dd, $J = 8.0, 1.0$ Hz, 1H), 8.31 (d, $J = 8.3$ Hz, 1H), 8.18 (d, $J = 7.0$ Hz, 1H), 7.93 (d, $J = 9.1$ Hz, 1H), 7.84 – 7.78 (m, 1H), 7.76 – 7.71 (m, 1H), 7.69 (d, $J = 8.6$ Hz, 2H), 7.57 – 7.51 (m, 1H), 7.18 (d, $J = 8.6$ Hz, 2H), 6.82 (td, $J = 6.9, 1.0$ Hz, 1H), 3.97 (s, 3H); ^{13}C NMR (100 MHz, CDCl_3) δ 160.7, 149.6, 148.1, 147.4, 145.1, 130.7, 130.2, 129.9, 129.5, 128.8, 127.3,

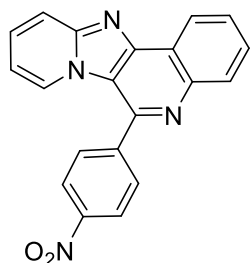
126.4, 122.6, 121.4, 120.6, 118.0, 114.7, 111.9, 55.5; HRMS calcd for $C_{21}H_{16}N_3O$ $[M+H]^+$ 326.1288, found 326.1300.

6-(4-Chlorophenyl)pyrido[2',1':2,3]imidazo[4,5-c]quinoline (4ad)



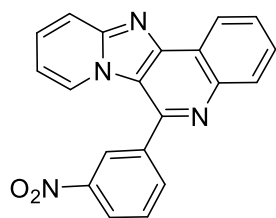
Off white solid (70 mg, 58%); mp 255–257 °C; 1H NMR (400 MHz, $CDCl_3$) δ 8.81 (dd, $J = 8.0, 1.1$ Hz, 1H), 8.30 (d, $J = 8.0$ Hz, 1H), 8.12 (d, $J = 7.0$ Hz, 1H), 7.96 (d, $J = 9.1$ Hz, 1H), 7.86–7.80 (m, 1H), 7.79–7.74 (m, 1H), 7.74–7.63 (m, 4H), 7.60–7.55 (m, 1H), 6.87 (td, $J = 6.9, 1.0$ Hz, 1H); ^{13}C NMR (100 MHz, $CDCl_3$) δ 149.7, 147.6, 146.9, 145.0, 136.8, 135.8, 130.3, 130.1, 129.6, 129.1, 127.0, 126.8, 122.7, 121.5, 120.3, 118.2, 112.2; HRMS calcd for $C_{20}H_{13}ClN_3$ $[M+H]^+$ 330.0793, found 330.0808.

6-(4-Nitrophenyl)pyrido[2',1':2,3]imidazo[4,5-c]quinoline (4ae)



Yellow solid (66 mg, 53%); mp 271–273 °C (Lit.^[15] 285–286 °C); 1H NMR (400 MHz, $CDCl_3$) δ 8.83 (dd, $J = 8.0, 1.2$ Hz, 1H), 8.55 (dt, $J = 8.7, 1.9$ Hz, 2H), 8.31 (dd, $J = 8.2, 0.7$ Hz, 1H), 8.05 (dt, $J = 7.0, 1.0$ Hz, 1H), 8.02–7.96 (m, 3H), 7.88–7.84 (m, 1H), 7.82–7.8 (m, 1H), 7.62–7.58 (m, 1H), 6.89 (td, $J = 6.9, 1.2$ Hz, 1H); ^{13}C NMR (100 MHz, $CDCl_3$) δ 149.9, 148.6, 147.8, 145.4, 144.9, 144.6, 130.3, 130.2, 129.7, 129.4, 127.3, 126.7, 124.5, 122.8, 121.6, 120.0, 118.5, 112.6; HRMS calcd for $C_{20}H_{13}N_4O_2$ $[M+H]^+$ 341.1033, found 341.1039.

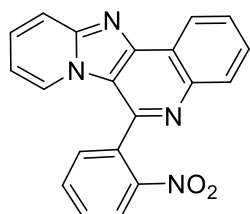
6-(3-Nitrophenyl)pyrido[2',1':2,3]imidazo[4,5-c]quinoline (4af)



Yellow solid (68 mg, 55%); mp 219–221 °C; 1H NMR (400 MHz, $CDCl_3$) δ 8.84 (dd, $J = 8.0, 1.2$ Hz, 1H), 8.71 (t, $J = 1.8$ Hz, 1H), 8.54–8.51 (m, 1H), 8.31 (dd, $J = 8.4, 0.8$ Hz, 1H), 8.16–8.13 (m, 1H), 8.06 (d, $J = 7.0$ Hz, 1H), 8.00 (d, $J = 9.2$ Hz, 1H), 7.91–7.84 (m, 2H), 7.82–7.80 (m, 1H), 7.63–7.58 (m, 1H), 6.89 (td, $J = 6.9, 1.1$ Hz, 1H); ^{13}C NMR (100 MHz, $CDCl_3$) δ 149.9, 148.7, 147.9, 145.1, 144.9, 140.1, 134.9, 130.4, 130.3, 129.6, 129.4, 127.3,

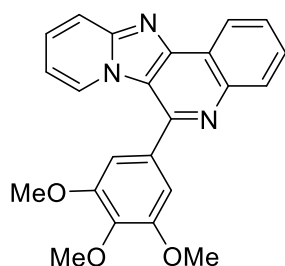
126.6, 124.4, 124.2, 122.8, 121.6, 120.1, 118.5, 112.6; HRMS calcd for $C_{20}H_{13}N_4O_2$ $[M+H]^+$ 341.1033, found 341.1040.

6-(2-Nitrophenyl)pyrido[2',1':2,3]imidazo[4,5-c]quinoline (4ag)



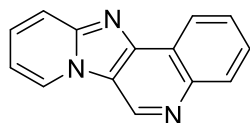
Yellow solid (56 mg, 45%); mp 219–221 °C; 1H NMR (400 MHz, $CDCl_3$) δ 8.84 (dd, $J = 7.8, 1.4$ Hz, 1H), 8.38 (dd, $J = 8.2, 1.1$ Hz, 1H), 8.23 – 8.22 (m, 1H), 7.98 (dt, $J = 9.2, 1.2$ Hz, 1H), 7.92 (td, $J = 7.5, 1.3$ Hz, 1H), 7.86 – 7.84 (m, 1H), 7.82 (dt, $J = 9.1, 1.8$ Hz, 1H), 7.72 – 7.76 (m, 1H), 7.71 (dd, $J = 7.5, 1.4$ Hz, 1H), 7.68 (dt, $J = 7.0, 1.0$ Hz, 1H), 7.58 – 7.53 (m, 1H), 6.81 (td, $J = 6.9, 1.1$ Hz, 1H); ^{13}C NMR (100 MHz, $CDCl_3$) δ 149.6, 148.1, 147.0, 144.8, 144.2, 134.4, 133.5, 131.7, 130.7, 130.1, 129.5, 129.1, 127.1, 125.9, 125.3, 122.8, 121.8, 120.8, 118.3, 112.7; HRMS calcd for $C_{20}H_{13}N_4O_2$ $[M+H]^+$ 341.1033, found 341.1039.

6-(3,4,5-Trimethoxyphenyl)pyrido[2',1':2,3]-imidazo[4,5-c]quinoline (4ah)



Off white solid (92 mg, 65%); mp 244–245 °C; 1H NMR (400 MHz, $CDCl_3$) δ 8.80 (dd, $J = 7.6, 0.8$ Hz, 1H), 8.32 (d, $J = 8.2$ Hz, 1H), 8.13 (d, $J = 7.0$ Hz, 1H), 7.95 (d, $J = 9.1$ Hz, 1H), 7.84 – 7.80 (m, 1H), 7.77 – 7.73 (m, 1H), 7.59 – 7.54 (m, 1H), 6.94 (s, 2H), 6.87 (t, $J = 6.5$ Hz, 1H), 3.98 (s, 3H), 3.92 (s, 6H); ^{13}C NMR (100 MHz, $CDCl_3$) δ 154.1, 149.7, 147.9, 147.4, 144.9, 138.9, 133.6, 130.1, 129.5, 129.02, 127.4, 126.7, 122.7, 121.5, 120.3, 118.0, 112.2, 105.5, 61.1, 56.3; HRMS calcd for $C_{23}H_{20}N_3O_3$ $[M+H]^+$ 386.1499, found 386.1514.

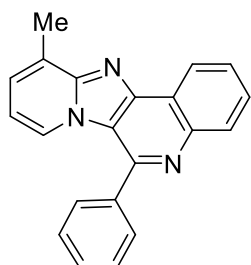
Pyrido[2',1':2,3]imidazo[4,5-c]quinoline (4ai)



Off white solid; 46 mg (57%); mp 253–255 °C; 1H NMR (400 MHz, $DMSO-d_6$) δ 9.77 (s, 1H), 9.31 (d, $J = 6.7$ Hz, 1H), 8.60 (d, $J = 7.7$ Hz, 1H), 8.16 (d, $J = 8.2$ Hz, 1H), 7.86 (d, $J = 9.1$ Hz, 1H), 7.74 (t, $J = 7.1$ Hz, 1H), 7.71 – 7.62 (m, 2H), 7.17 (t, $J = 6.7$ Hz, 1H); ^{13}C NMR (100 MHz, $DMSO-d_6 + CDCl_3$) δ 149.1, 145.9,

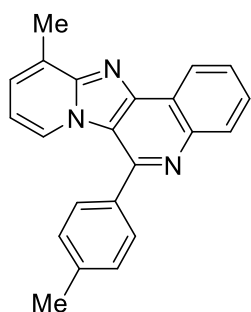
145.7, 137.9, 131.2, 129.8, 128.4, 127.6, 126.6, 122.7, 122.1, 117.5, 112.9; HRMS calculated for $C_{14}H_{10}N_3$ $[M+H]^+$ 220.0869, found 220.0876.

11-Methyl-6-phenylpyrido[2',1':2,3]imidazo[4,5-c]quinoline (4ba)



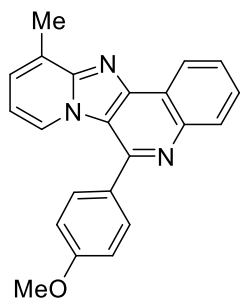
Off white solid (75 mg, 70%); mp 234–236 °C (Lit.^[15] 234–235 °C); 1H NMR (400 MHz, $CDCl_3$) δ 8.88 (dd, $J = 8.0, 1.2$ Hz, 1H), 8.33 (d, $J = 8.2$ Hz, 1H), 7.92 (d, $J = 6.9$ Hz, 1H), 7.83 – 7.79 (m, 1H), 7.78 – 7.69 (m, 3H), 7.70 – 7.58 (m, 3H), 7.34 (dt, $J = 6.9, 1.3$ Hz, 1H), 6.71 (t, $J = 6.9$ Hz, 1H), 2.85 (s, 3H); ^{13}C NMR (100 MHz, $CDCl_3$) δ 150.3, 148.3, 147.2, 144.7, 138.1, 129.6, 129.3, 129.3, 128.82, 128.79, 128.5, 128.1, 126.4, 124.9, 122.9, 121.6, 120.9, 112.0, 17.7; HRMS calcd for $C_{21}H_{16}N_3$ $[M+H]^+$ 310.1339, found 310.1349.

11-Methyl-6-(*p*-tolyl)pyrido[2',1':2,3]imidazo[4,5-c]-quinoline (4bb)



Off white solid (84 mg, 75%); mp 229–230 °C; 1H NMR (400 MHz, $CDCl_3$) δ 8.86 (dd, $J = 8.0, 1.2$ Hz, 1H), 8.31 (d, $J = 8.2$ Hz, 1H), 7.99 (d, $J = 6.9$ Hz, 1H), 7.83 – 7.77 (m, 1H), 7.76 – 7.69 (m, 1H), 7.63 (d, $J = 8.0$ Hz, 2H), 7.45 (d, $J = 7.8$ Hz, 2H), 7.36 – 7.30 (m, 1H), 6.71 (t, $J = 6.9$ Hz, 1H), 2.85 (s, 3H), 2.54 (s, 3H); ^{13}C NMR (100 MHz, $CDCl_3$) δ 150.2, 148.5, 147.1, 144.9, 139.5, 135.4, 129.9, 129.4, 128.7, 128.3, 128.0, 126.2, 125.0, 122.8, 121.6, 121.0, 111.8, 21.5, 17.7; HRMS calcd for $C_{22}H_{18}N_3$ $[M+H]^+$ 324.1495, found 324.1503.

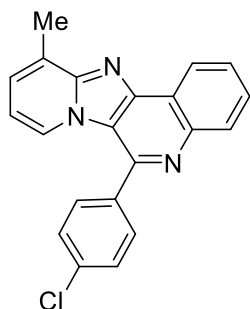
6-(4-Methoxyphenyl)-11-methylpyrido[2',1':2,3]-imidazo[4,5-c]quinoline (4bc)



Off white solid (77 mg, 65%); mp 188–190 °C; 1H NMR (400 MHz, $CDCl_3$) δ 8.87 (d, $J = 7.9$ Hz, 1H), 8.31 (d, $J = 8.3$ Hz, 1H), 8.05 (d, $J = 7.0$ Hz, 1H), 7.81 – 7.78 (m, 1H), 7.73 (t, $J = 7.1$ Hz, 1H), 7.69 (d, $J = 8.6$ Hz, 2H), 7.35 (d, $J = 6.8$ Hz, 1H), 7.18 (d, $J = 8.6$ Hz, 2H), 6.74 (t, $J = 6.9$ Hz, 1H), 3.97 (s, 3H), 2.86 (s, 3H). ^{13}C NMR (100 MHz, $CDCl_3$) δ 160.9, 149.1, 147.8, 147.6,

144.2, 133.5, 130.4, 129.0, 128.8, 126.5, 125.0, 122.6, 121.9, 121.3, 120.3, 117.3, 114.6, 55.6, 18.5; HRMS calcd for C₂₂H₁₈N₃O [M+H]⁺ 340.1444, found 340.1459.

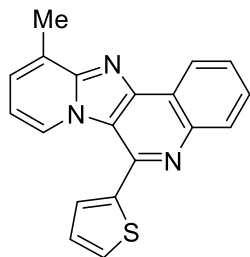
6-(4-Chlorophenyl)-11-methylpyrido[2',1':2,3]-imidazo[4,5-c]quinoline (4bd)



Off white solid (72 mg, 61 %); mp 269–270 °C; ¹H NMR (400 MHz, CDCl₃) δ 8.85 (dd, *J* = 8.0, 1.1 Hz, 1H), 8.28 (d, *J* = 7.8 Hz, 1H), 7.94 (d, *J* = 6.9 Hz, 1H), 7.84 – 7.77 (m, 1H), 7.76 – 7.69 (m, 3H), 7.68 – 7.61 (m, 2H), 7.38 – 7.30 (m, 1H), 6.74 (t, *J* = 6.9 Hz, 1H), 2.84 (s, 3H); ¹³C NMR (100 MHz, CDCl₃) δ 150.3, 147.2, 146.9, 144.8, 136.8, 135.7, 130.3, 129.5, 129.4, 128.8, 128.5, 128.2, 126.5, 124.7, 122.8, 121.7, 120.7, 112.1, 17.7; HRMS

calcd for C₂₁H₁₅ClN₃ [M+H]⁺ 344.0949, found 344.0959.

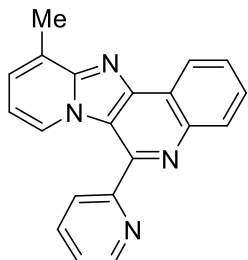
11-Methyl-6-(thiophen-2-yl)pyrido[2',1':2,3]-imidazo[4,5-c]quinoline (4bj)



Off white solid (78 mg, 71%); mp 215–217 °C; ¹H NMR (400 MHz, CDCl₃) δ 8.86 (dd, *J* = 8.0, 1.2 Hz, 1H), 8.30 (d, *J* = 8.1 Hz, 1H), 8.25 (d, *J* = 7.0 Hz, 1H), 7.82 – 7.78 (m, 1H), 7.76 – 7.72 (m, 1H), 7.66 (dd, *J* = 5.2, 1.2 Hz, 1H), 7.51 – 7.47 (m, 1H), 7.36 (dt, *J* = 6.9, 1.2 Hz, 1H), 7.33 – 7.31 (m, 1H), 6.79 (t, *J* = 6.9 Hz, 1H), 2.85 (s, 3H); ¹³C NMR (100 MHz, CDCl₃) δ 150.3, 147.2,

144.8, 141.6, 139.6, 129.52, 128.8, 128.5, 128.3, 128.2, 128.1, 127.6, 126.7, 125.0, 122.8, 121.8, 121.3, 112.0, 17.7; HRMS calcd for C₁₉H₁₄N₃S [M+H]⁺ 316.0903, found 316.0913.

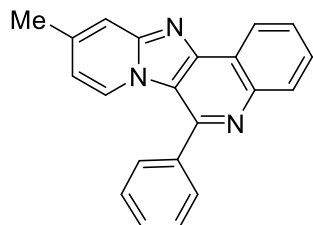
11-Methyl-6-(pyridin-2-yl)pyrido[2',1':2,3]imidazo[4,5-c]quinoline (4bk)



Light brown solid (60 mg, 55%); mp 231–233 °C; ¹H NMR (400 MHz, CDCl₃) δ 8.90 (dd, *J* = 8.0, 1.2 Hz, 1H), 8.88 – 8.85 (m, 1H), 8.82 (d, *J* = 7.0 Hz, 1H), 8.31 (d, *J* = 8.0 Hz, 2H), 8.06 (td, *J* = 7.7, 1.8 Hz, 1H), 7.84 – 7.79 (m, 1H), 7.78 – 7.73 (m, 1H), 7.57 – 7.53 (m, 1H), 7.38 (dt, *J* = 6.8, 1.3 Hz, 1H), 6.82 (t, *J* = 6.9 Hz, 1H), 2.86 (s, 3H); ¹³C NMR (100 MHz, CDCl₃) δ 157.3, 150.5, 148.6, 148.0, 146.7, 144.6, 137.8, 129.5, 128.7, 128.6, 127.6,

127.4, 126.8, 125.4, 124.4, 123.0, 122.1, 121.3, 111.5, 17.7; HRMS calcd for C₂₀H₁₅N₄ [M+H]⁺ 311.1291, found 311.1303.

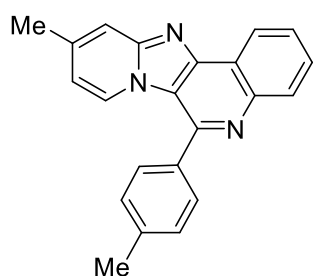
10-Methyl-6-phenylpyrido[2',1':2,3]imidazo[4,5-c]-quinoline (4ca)



Off white solid (73 mg, 68%); mp 223–225 °C; ¹H NMR (400 MHz, CDCl₃) δ 8.79 (dd, *J* = 8.0, 1.0 Hz, 1H), 8.31 (d, *J* = 8.2 Hz, 1H), 7.92 (d, *J* = 7.1 Hz, 1H), 7.83 – 7.78 (m, 1H), 7.77 – 7.71 (m, 3H), 7.68 (s, 1H), 7.67 – 7.62 (m, 3H), 6.62 (dd, *J* = 7.1, 1.5 Hz, 1H), 2.50 (s, 3H); ¹³C NMR (100 MHz, CDCl₃) δ 150.3, 147.9, 147.8, 145.1, 141.6, 138.4,

129.6, 129.5, 129.3, 128.7, 126.4, 126.2, 122.6, 121.5, 120.4, 116.3, 114.7, 21.8; HRMS calcd for C₂₁H₁₆N₃ [M+H]⁺ 310.1339, found 310.1345.

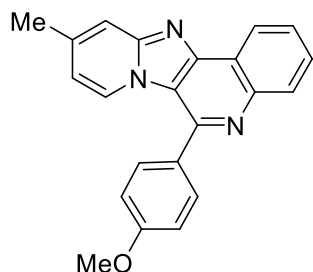
10-Methyl-6-(*p*-tolyl)pyrido[2',1':2,3]imidazo[4,5-c]-quinoline (4cb)



Off white solid (78 mg, 70%); mp 240–241 °C; ¹H NMR (400 MHz, CDCl₃) δ 8.77 (d, *J* = 7.6 Hz, 1H), 8.29 (d, *J* = 8.3 Hz, 1H), 7.98 (d, *J* = 7.1 Hz, 1H), 7.78 (t, *J* = 7.0 Hz, 1H), 7.71 (t, *J* = 7.3 Hz, 1H), 7.66 (s, 1H), 7.63 (d, *J* = 7.9 Hz, 2H), 7.44 (d, *J* = 7.7 Hz, 2H), 6.61 (d, *J* = 6.1 Hz, 1H), 2.53 (s, 3H), 2.47 (s, 3H); ¹³C NMR (100 MHz, CDCl₃) δ 150.2, 148.1, 147.5, 145.0, 141.6, 139.5, 135.4, 129.9, 129.5, 128.7,

128.6, 126.3, 126.2, 122.6, 121.4, 120.4, 116.2, 114.6, 21.8, 21.5; HRMS calcd for C₂₂H₁₈N₃ [M+H]⁺ 324.1495, found 324.1508.

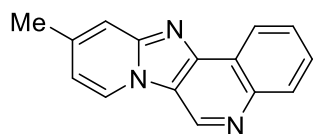
6-(4-Methoxyphenyl)-10-methylpyrido[2',1':2,3]-imidazo[4,5-c]quinoline (4cc)



Off white solid (76 mg, 64%); mp 248–250 °C; ¹H NMR (400 MHz, CDCl₃) δ 8.76 (d, *J* = 7.9 Hz, 1H), 8.28 (d, *J* = 8.3 Hz, 1H), 8.03 (d, *J* = 7.1 Hz, 1H), 7.81 – 7.75 (m, 1H), 7.74 – 7.63 (m, 4H), 7.16 (d, *J* = 8.6 Hz, 2H), 6.62 (dd, *J* = 7.1, 1.3 Hz, 1H), 3.96 (s, 3H), 2.48 (s, 3H); ¹³C NMR (100 MHz, CDCl₃) δ 160.6, 150.2, 147.8, 147.6, 145.1, 141.5,

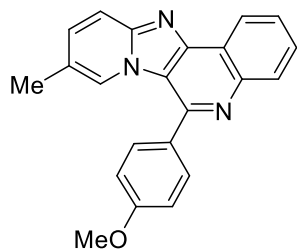
130.7, 130.2, 129.4, 128.7, 126.3, 126.2, 122.6, 121.4, 120.5, 116.2, 114.64, 114.61, 55.5, 21.8; HRMS calcd for C₂₂H₁₈N₃O [M+H]⁺ 340.1444, found 340.1459.

10-Methylpyrido[2',1':2,3]imidazo[4,5-c]quinoline (4ci)



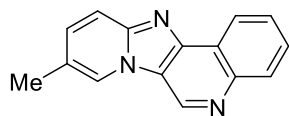
Off white solid (49 mg, 60%); mp 243–245 °C; ¹H NMR (400 MHz, CDCl₃) δ 9.41 (s, 1H), 8.70 (d, *J* = 7.6 Hz, 1H), 8.53 (d, *J* = 6.9 Hz, 1H), 8.25 (d, *J* = 8.2 Hz, 1H), 7.79 – 7.74 (m, 1H), 7.71 (t, *J* = 7.3 Hz, 1H), 7.61 (s, 1H), 6.85 (dd, *J* = 6.8, 0.8 Hz, 1H), 2.51 (s, 3H); ¹³C NMR (100 MHz, CDCl₃) δ 149.7, 146.7, 145.7, 142.1, 135.4, 129.7, 128.4, 126.6, 124.3, 122.7, 116.4, 115.3, 22.0; HRMS calcd for C₁₅H₁₂N₃ [M+H]⁺ 234.1026, found 234.1034.

6-(4-Methoxyphenyl)-9-methylpyrido[2',1':2,3]-imidazo[4,5-c]quinoline (4dc)



Pale Yellow solid (77 mg, 65%); mp 270–272 °C; ¹H NMR (400 MHz, CDCl₃) δ 8.75 (d, *J* = 8.0 Hz, 1H), 8.38 (d, *J* = 8.2 Hz, 1H), 7.97 (s, 1H), 7.85 – 7.76 (m, 2H), 7.76 – 7.68 (m, 3H), 7.40 (dd, *J* = 9.2, 1.3 Hz, 1H), 7.18 (d, *J* = 8.6 Hz, 2H), 3.97 (s, 3H), 2.25 (s, 3H); C NMR (100 MHz, CDCl₃) δ 160.9, 149.1, 147.8, 147.6, 144.2, 133.5, 130.4, 129.0, 128.8, 126.5, 125.0, 122.6, 121.9, 121.3, 120.3, 117.3, 114.6, 55.6, 18.5; HRMS calcd for C₂₂H₁₈N₃O [M+H]⁺ 340.1444, found 340.1452.

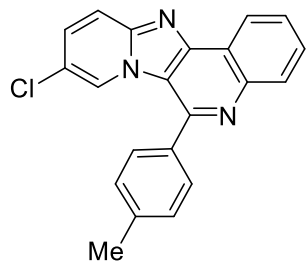
9-Methylpyrido[2',1':2,3]imidazo[4,5-c]quinoline (3di)



Off white solid (46 mg, 57%); mp 228–230 °C; ¹H NMR (400 MHz, CDCl₃) δ 9.28 (s, 1H), 8.62 (d, *J* = 7.7 Hz, 1H), 8.26 (s, 1H), 8.19 (d, *J* = 8.2 Hz, 1H), 7.72 (t, *J* = 7.0 Hz, 1H), 7.67 – 7.64 (m, 2H), 7.29 – 7.25 (m, 1H), 2.30 (s, 3H); ¹³C NMR (100 MHz, CDCl₃) δ 148.0, 146.1, 145.5, 135.6, 133.4, 129.6, 128.3,

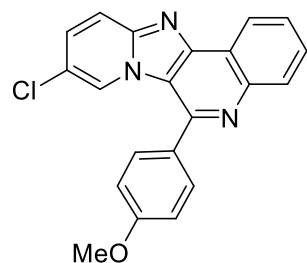
126.6, 122.7, 122.6, 122.5, 122.0, 121.7, 117.1, 18.1; HRMS calcd for $C_{15}H_{12}N_3$ $[M+H]^+$ 234.1026, found 234.1036.

9-Chloro-6-(*p*-tolyl)pyrido[2',1':2,3]imidazo[4,5-*c*]-quinoline (4eb)



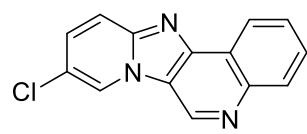
Off white solid (68 mg, 61%); mp 212–214 °C; 1H NMR (400 MHz, $CDCl_3$) δ 8.78 (dd, $J = 8.0, 1.1$ Hz, 1H), 8.32 (d, $J = 8.0$ Hz, 1H), 8.19 (d, $J = 1.2$ Hz, 1H), 7.89 (dd, $J = 9.6, 0.6$ Hz, 1H), 7.85 – 7.80 (m, 1H), 7.78 – 7.73 (m, 1H), 7.65 (d, $J = 8.0$ Hz, 2H), 7.53 – 7.48 (m, 3H), 2.56 (s, 3H); ^{13}C NMR (100 MHz, $CDCl_3$) δ 148.3, 147.8, 147.7, 145.1, 140.1, 134.8, 131.1, 130.1, 129.7, 129.1, 128.5, 126.8, 125.2, 122.6, 121.4, 120.5, 119.9, 118.3, 21.6; HRMS calcd for $C_{21}H_{15}ClN_3$ $[M+H]^+$ 344.0949, found 344.0959.

9-Chloro-6-(4-methoxyphenyl)pyrido[2',1':2,3]-imidazo[4,5-*c*]quinoline (4ec)



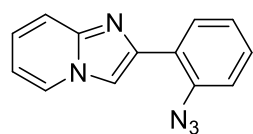
Off white solid (64 mg, 55%); mp 298–300 °C (Lit.^[151] 298–299 °C); 1H NMR (400 MHz, $CDCl_3$) δ 8.77 (d, $J = 7.7$ Hz, 1H), 8.31 (d, $J = 8.1$ Hz, 1H), 8.24 (bs, 1H), 7.88 (d, $J = 9.5$ Hz, 1H), 7.83 (t., 7.8 Hz, 1H), 7.78 – 7.67 (m, 3H), 7.51 (d, $J = 9.0$ Hz, 1H), 7.21 (d, $J = 8.0$ Hz, 2H), 3.99 (s, 3H); ^{13}C NMR (100 MHz, $CDCl_3$) δ 161.0, 148.0, 147.7, 146.4, 145.1, 137.6, 131.1, 130.1, 129.6, 129.1, 126.7, 125.2, 122.4, 121.3, 119.9, 118.3, 114.8, 109.4, 54.1; HRMS calcd for $C_{21}H_{15}ClN_3O$ $[M+H]^+$ 360.0898, found 360.0910.

9-Chloropyrido[2',1':2,3]imidazo[4,5-*c*]quinoline (4ei)



Off white solid (42 mg, 51%); mp 260–262 °C; 1H NMR (400 MHz, $CDCl_3$) δ 9.49 (s, 1H), 8.79 (d, $J = 1.1$ Hz, 1H), 8.74 (dd, $J = 8.0, 1.2$ Hz, 1H), 8.30 (d, $J = 7.9$ Hz, 1H), 7.90 (dd, $J = 9.7, 0.6$ Hz, 1H), 7.86 – 7.81 (m, 1H), 7.80 – 7.75 (m, 1H), 7.59 (dd, $J = 9.7, 2.0$ Hz, 1H); ^{13}C NMR (100 MHz, $CDCl_3$) δ 147.3, 146.8, 145.8, 135.7, 131.6, 129.9, 129.0, 127.2, 123.3, 122.7, 122.0, 120.9, 118.6; HRMS calcd for $C_{14}H_9ClN_3$ $[M+H]^+$ 254.0480, found 254.0492.

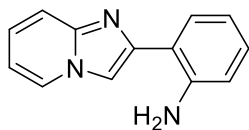
2-(2-Azidophenyl)imidazo[1,2-*a*]pyridine (16a)



Colorless oil (38 mg, 9%); 1H NMR (400 MHz, $DMSO-d_6$) δ 11.87 (s, 1H), 9.37 (d, $J = 6.6$ Hz, 1H), 8.27 (d, $J = 7.6$ Hz, 1H), 7.93 (d, $J = 9.0$ Hz, 1H), 7.71 (t, $J = 7.7$ Hz, 1H), 7.58 (t, $J = 7.2$ Hz, 1H), 7.52 (d, $J = 8.0$ Hz, 1H),

7.35 (t, $J = 7.3$ Hz, 1H), 7.28 (t, $J = 6.7$ Hz, 1H); ^{13}C NMR (100 MHz, DMSO- d_6) δ 156.0, 148.9, 147.6, 138.0, 130.4, 130.0, 128.0, 123.2, 122.7, 117.3, 116.8, 116.0, 114.3.

2-(Imidazo[1,2-*a*]pyridin-2-yl)aniline (1a)



Off white solid (69 mg, 18 %); mp 126–128 °C; ^1H NMR (400 MHz, DMSO- d_6 + CDCl_3) δ 8.53 (d, $J = 6.7$ Hz, 1H), 8.31 (CDCl_3), 8.29 (s, 1H), 7.62 – 7.54 (m, 2H), 7.28 – 7.22 (m, 1H), 7.05 – 6.99 (m, 1H), 6.94 – 6.89 (m, 1H), 6.75 (dd, $J = 8.1, 0.7$ Hz, 1H), 6.60 (bs, 2H), 6.57 (d, $J = 7.0$ Hz, 1H); ^{13}C NMR (100 MHz, DMSO- d_6 + CDCl_3) δ 147.1, 146.2, 144.0, 128.9, 128.1, 126.8, 124.9, 116.6, 116.5, 116.0, 115.6, 112.8, 109.2.

2B.4.1 Biological studies

MIC, ZOC, bactericidal and Cell death were determined by following the standard method reported in literature.^[32-33]

Antibacterial activity: The synthesized compounds were tested for antibacterial activity against the three Gram-negative bacteria *S. typhi*, *K. pneumoniae*, *P. putida*, and two Gram-positive bacteria *B. cereus*, *S. aureus*. The activity of the compounds in terms of minimal inhibitory concentrations (MIC) and zone of inhibition (ZOI) was determined *in vitro*. For activity assay, Muller-Hilton (Himedia, India) agar medium was sterilized by autoclaving and poured into sterile glass petri-dishes under aseptic conditions using a laminar air flow chamber. After solidification of the medium, suspension of each pathogenic microorganism (10^7 CFU/mL) was spread onto the individual media plates using a sterile glass spreader. Following adsorption of bacterial suspension, well the size of 6 mm diameter was made by the sterile metallic borer, and the solution of the working compound of different concentration was poured into the wells. The plates were incubated at 37 °C for 18-24 h under dark conditions. The determination as to whether the organism is susceptible, intermediate or resistant was made by measuring the size of the zone of inhibition in comparison with the standard antibiotic. For MIC assay, tested compounds were dissolved in dimethyl sulfoxide (DMSO), and serial dilution of each compound was prepared in the concentrations of 200, 100, 50, 25, 12.5, 6.25, 3.125, 1.56 $\mu\text{g}/\text{mL}$. For the MIC assay, serially diluted test samples of each compound (75 μL) were added in 96 well micro-trays. The same amount of each pathogenic microorganism was added to micro-trays well under the aseptic condition and incubated at 37 °C for 24 h. A control test with solvent DMSO at the same dilution

was also used to ensure that the solvent did not affect bacterial growth. All assays were performed in duplicate sets. A broad spectrum antibiotic streptomycin effective against Gram positive and Gram negative bacterium was used as positive control.

Bactericidal kinetics: Glass test tubes containing 400 μ l of nutrient broth is sterilized, and after cooling at room temperature, 50 μ l of freshly grown bacterial culture *S. typhi* and *P. putida* of 10^7 CFU ml^{-1} was added (3 tubes for single concentration). Afterward, 50 μ l of selected compounds **4ae**, **4ai** and **4cc** corresponding to $3 \times \text{MIC}$ was added to each tube and incubated at 37°C at different time intervals from 1-6 h with constant shaking speed at 150 rpm. Following incubation, the absorbance of the cultures was taken at 600 nm in a UV-visible spectrophotometer (Jasco Corporation, Japan). The experiment was repeated in triplicates and value was shown as mean \pm SD.

Cell death assay: The testing culture of *S. typhi* and *P. putida* were treated with compounds **4ae**, **4ai**, and **4cc** at concentration $3 \times \text{MIC}$ and kept for incubation for 1 to 6 h. After treatment, 100 μ L of 10-fold cell dilution were spread onto LB-agar plates and left to grow overnight at 37°C . Bacterial colonies were counted by colony counter and compared with those of control plates to calculate changes in cell-growth after compound treatment. For control, isotonic saline solution was used in place of the selected compound. All treatments were performed in triplicate sets and repeated at least in thrice independent experiments. The % death rate was calculated by the following formula: $\text{Death rate (\%)} = (\text{Bacterial no. in control} - \text{Bacterial no. after compound treatment}) / \text{Bacterial no. in control}$

Live/dead cell assay: To discriminate the live and dead bacterial cells, the overnight grown culture of *P. putida* (10^7 cfu/mL) was treated with selected compounds at $3 \times \text{MIC}$ for 3 h. The working solution of acridine orange (AO, 15 $\mu\text{g/mL}$) and ethidium bromide (EB, 50 $\mu\text{g/mL}$) were prepared in the PBS buffer ($1 \times \text{pH } 7.2$). After the compounds treatment, 5 μ L each of AO and EB was added to 500 μ L of *S. typhi* culture. The suspension was centrifuged at 5,000 g for 10 min, and the supernatant was discarded. The cell pellet was washed with $1 \times \text{PBS}$ buffer three times to remove any traces of unbound dyes. The washed cell pellet was streaked on the glass slide with a cover slip on top of it and viewed under an epi-fluorescence microscope (Olympus-CKX41, Olympus,

Japan) at an intensity between 450 and 490 nm using the 100X objective lens and 10X eyepiece lens.

2B.5 REFERENCES

- [1] R. Goel, V. Luxami, K. Paul, *Organic & Biomolecular Chemistry*, **2015**, *13*, 3525-3555.
- [2] O. N. Burchak, L. Mugherli, M. Ostuni, J. J. Lacapère, M. Y. Balakirev, *Journal of the American Chemical Society*, **2011**, *133*, 10058-10061.
- [3] L. Almirante, L. Polo, A. Mugnaini, E. Provinciali, P. Rugarli, A. Biancotti, A. Gamba, W. Murmann, *Journal of Medicinal Chemistry*, **1965**, *8*, 305-312.
- [4] G. C. Moraski, L. D. Markley, J. Cramer, P. A. Hipskind, H. Boshoff, M. A. Bailey, T. Alling, J. Ollinger, T. Parish, M. J. Miller, *ACS Medicinal Chemistry Letters*, **2013**, *4*, 675-679.
- [5] S. Z. Langer, S. Arbilla, J. Benavides, B. Scatton, *Adv Biochem Psychopharmacol*, **1990**, *46*, 61-72.
- [6] K. Mizushige, T. Ueda, K. Yukiiri, H. Suzuki, *Cardiovasc Drug Rev*, **2002**, *20*, 163-174.
- [7] K. Pericherla, P. Kaswan, K. Pandey, A. Kumar, *Synthesis*, **2015**, *47*, 887-912.
- [8] A. K. Bagdi, S. Santra, K. Monir, A. Hajra, *Chemical Communications*, **2015**, *51*, 1555-1575.
- [9] J. P. Michael, *Natural product reports*, **2007**, *24*, 223-246.
- [10] K. Kaur, M. Jain, R. P. Reddy, R. Jain, *European Journal of Medicinal Chemistry*, **2010**, *45*, 3245-3264.
- [11] O. Afzal, S. Kumar, M. R. Haider, M. R. Ali, R. Kumar, M. Jaggi, S. Bawa, *European Journal of Medicinal Chemistry*, **2015**, *97*, 871-910.
- [12] S. M. Prajapati, K. D. Patel, R. H. Vekariya, S. N. Panchal, H. D. Patel, *RSC Advances*, **2014**, *4*, 24463-24476.
- [13] S. Sharma, B. Saha, D. Sawant, B. Kundu, *Journal of Combinatorial Chemistry*, **2007**, *9*, 783-792.
- [14] A. K. Pandey, R. Sharma, A. Singh, S. Shukla, K. Srivastava, S. K. Puri, B. Kumar, P. M. S. Chauhan, *RSC Advances*, **2014**, *4*, 26757-26770.
- [15] X.-S. Fan, J. Zhang, B. Li, X.-Y. Zhang, *Chemistry – An Asian Journal*, **2015**, *10*, 1281-1285.

- [16] A. Kale, C. Bingi, N. C. Ragi, P. Sripadi, P. R. Tadikamalla, K. Atmakur, *Synthesis*, **2017**, *49*, 1603-1612.
- [17] T. Shao, Z. Gong, T. Su, W. Hao, C. Che, *Beilstein Journal of Organic Chemistry*, **2017**, *13*, 817-824.
- [18] S. Dhiman, H. K. Saini, N. K. Nandwana, D. Kumar, A. Kumar, *RSC Advances*, **2016**, *6*, 23987-23994.
- [19] Y. Kim, M. R. Kumar, N. Park, Y. Heo, S. Lee, *The Journal of Organic Chemistry*, **2011**, *76*, 9577-9583.
- [20] D. Dhar, W. B. Tolman, *Journal of the American Chemical Society*, **2015**, *137*, 1322-1329.
- [21] T. Maejima, Y. Shimoda, K. Nozaki, S. Mori, Y. Sawama, Y. Monguchi, H. Sajiki, *Tetrahedron*, **2012**, *68*, 1712-1722.
- [22] Q. Nguyen, T. Nguyen, T. G. Driver, *Journal of the American Chemical Society*, **2013**, *135*, 620-623.
- [23] F.-C. Jia, C. Xu, Z.-W. Zhou, Q. Cai, D.-K. Li, A.-X. Wu, *Organic Letters*, **2015**, *17*, 2820-2823.
- [24] F.-C. Jia, Z.-W. Zhou, C. Xu, Q. Cai, D.-K. Li, A.-X. Wu, *Organic Letters*, **2015**, *17*, 4236-4239.
- [25] Y. Goriya, C. V. Ramana, *Tetrahedron*, **2010**, *66*, 7642-7650.
- [26] Y. Goriya, C. V. Ramana, *Chemical Communications*, **2014**, *50*, 7790-7792.
- [27] S. Eswaran, A. V. Adhikari, I. H. Chowdhury, N. K. Pal, K. D. Thomas, *European Journal of Medicinal Chemistry*, **2010**, *45*, 3374-3383.
- [28] R. S. Upadhayaya, J. K. Vandavasi, N. R. Vasireddy, V. Sharma, S. S. Dixit, J. Chattopadhyaya, *Bioorganic & Medicinal Chemistry*, **2009**, *17*, 2830-2841.
- [29] S. Sabatini, F. Gosetto, G. Manfroni, O. Tabarrini, G. W. Kaatz, D. Patel, V. Cecchetti, *Journal of Medicinal Chemistry*, **2011**, *54*, 5722-5736.
- [30] R. Kharb, H. Kaur, *Int. Res. J. Pharm.*, **2013**, *4*, 63-69.
- [31] K. Pericherla, P. Khedar, B. Khungar, A. Kumar, *Chemical Communications*, **2013**, *49*, 2924-2926.
- [32] S. Agnihotri, S. Mukherji, S. Mukherji, *RSC Advances*, **2014**, *4*, 3974-3983.

- [33] S. Joshi, R. P. Dewangan, S. Yadav, D. S. Rawat, S. Pasha, *Organic & Biomolecular Chemistry*, **2012**, *10*, 8326-8335.

CHAPTER 2: PART-C

Cu(I)-Catalyzed Three-Component Cascade Synthesis of Quinazolin-4(3*H*)-Ones

2C.1 INTRODUCTION

Quinazolinone is an important structural motif which has been found in more than 150 natural products isolated from a variety of plants, microorganism, and animals.^[1-6] These natural products have exhibited a wide variety of biological activity for example Rutaecarpine isolated from fruit of Chinese and Korean plant *Euodia ruticarpa* inhibited the COX-2 enzyme responsible for inflammation and rheumatism,^[7] Luotonin A isolated from *Peganum nigellastrum* used in the treatment of rheumatism,^[8] and Tryptanthrin isolated from plant *Isatis tinctoria* also act as COX-2 inhibitor. Apart from naturally occurring quinazolinones, various quinazolinones derivatives have been extracted from a microorganism such as Schizocommunin isolated from the liquid culture medium of *Schizophyllum commune*. Schizocommunin has exhibited significant cytotoxic activity against murine lymphoma cells.^[9] Auranthine (**2**) has isolated from *Penicillium aurantiogriseum* and used as an anticancer agent (**Figure 2C.1**).^[10]

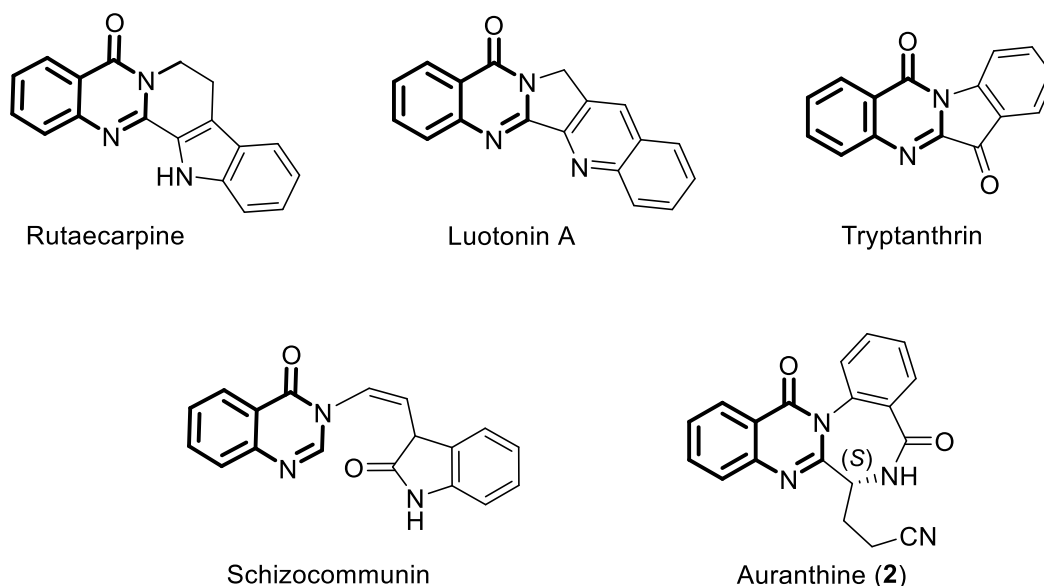


Figure 2C.1: Selected examples of a natural product containing quinazolin-4(3H)-one

Quinazolinone has attracted considerable attention of the scientific community due to their excellent pharmaceutical and biological profile. Several quinazolinones derivatives have been shown to exhibit antiviral, anticancer, antifungal, antimalarial, antihistamine, and antimicrobial activity.^[5, 11-17] Quinazolin-4(3H)-one based marketed drugs Afoqualone used in epileptic therapy, Raltitrexed Thymitaq are used for the treatment of cancer (**Figure 2C.2**).^[11, 18]

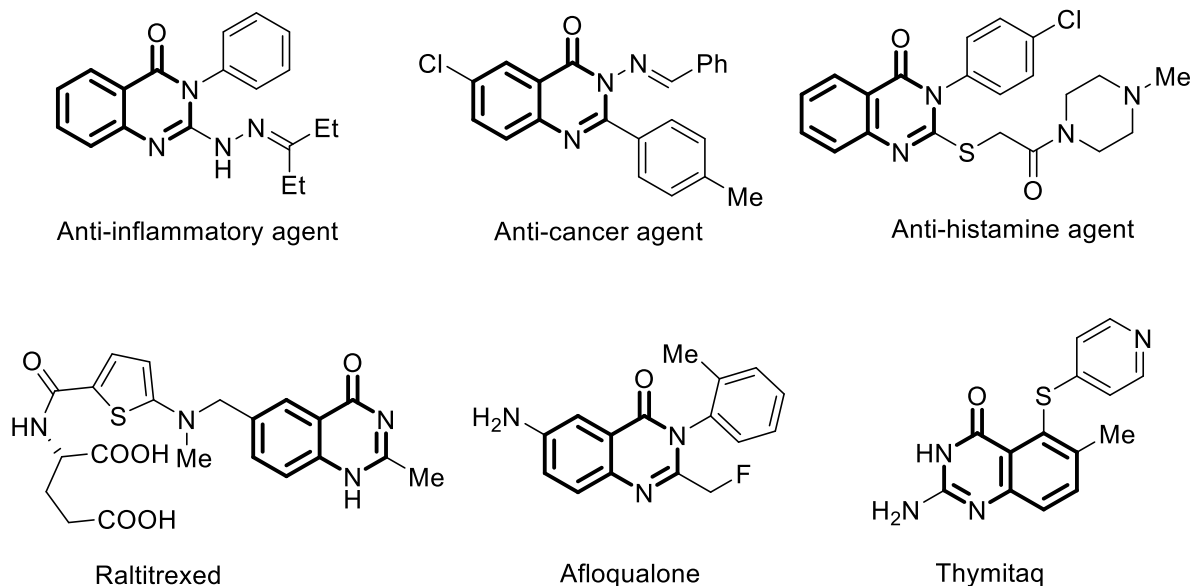
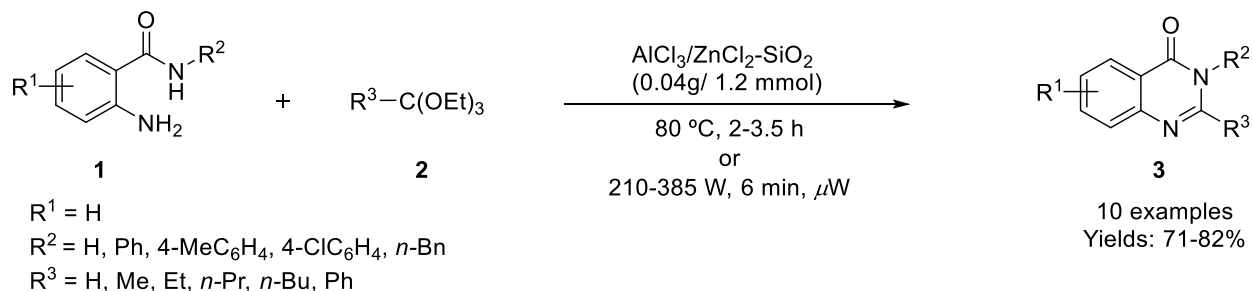


Figure 2C.2: Quinazolin-4(3*H*)-one based drugs and synthetic bioactive compounds

A great focus has been on the development of a synthetic method for quinazolinones because of wide range biological and pharmaceutical activities shown by these compounds. A summary of synthetic methods for quinazolinones is presented below.

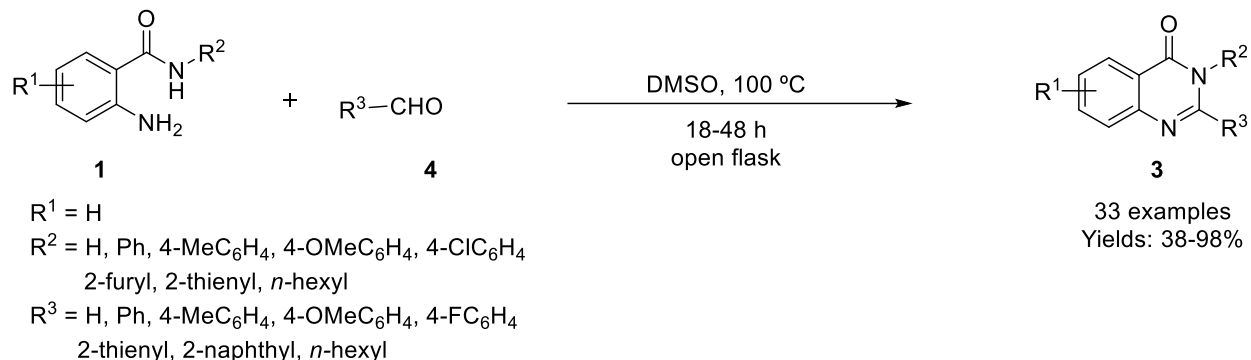
2C.1.1 Synthesis of quinazolinones from 2-aminobenzamides

Generally, quinazolinone derivatives are prepared using 2-aminobenzamides (anthranilamides) (**1**) as the most typical starting material.^[5-6, 17, 19] Dabiri group reported the synthesis of quinolinones derivatives (**3**) by using the mixture of AlCl_3 and ZnCl_2 supported on silica gel from 2-aminobenzamides (**1**) and ortho ester (**2**) under conventionally and microwave heating (**Scheme 2C.1**).^[20] Later on, Threadgill and coworkers also reported the metal-free synthesis of quinazolin-4(3*H*)-ones (**3**) using 2-aminobenzamides and orthoamides.^[21]



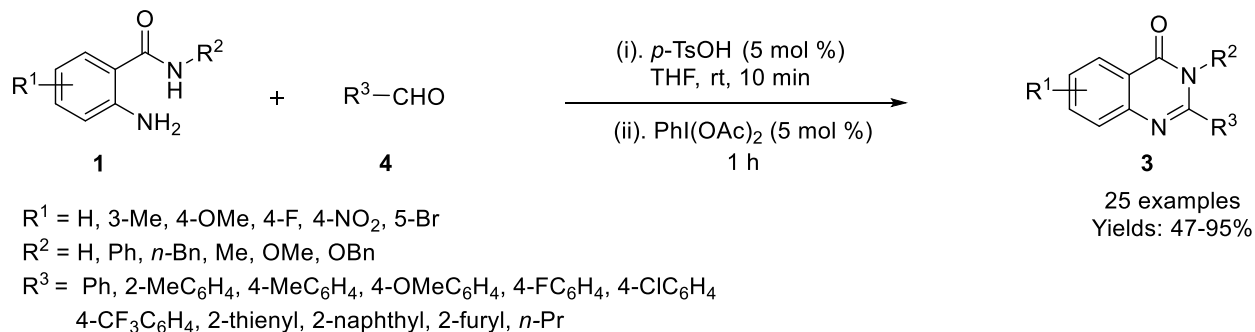
Scheme 2C.1: Synthesis of quinazolinones by $\text{AlCl}_3/\text{ZnCl}_2\text{-SiO}_2$

Cheon *et al.* disclosed a metal-free synthesis of quinazolinones (**3**) in good to excellent yields (38-98%) in DMSO from 2-aminobenzamides (**1**) and aldehydes (**4**) under aerobic condition. In this reaction, DMSO acted as oxidant as well as solvent media (**Scheme 2C.2**).^[22]



Scheme 2C.2: Metal-free synthesis of quinazolin-4(3*H*)-ones from 2-aminobenzamides and aldehydes

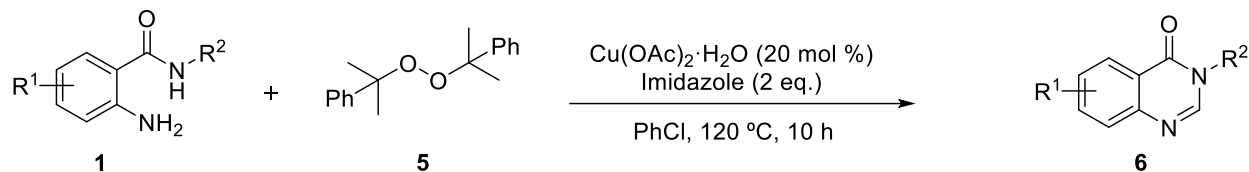
Zhao and co-workers described the metal-free synthesis of quinazolinone derivatives (**3**) by the reaction of anthranilamides (**1**) with various aldehydes (**4**) in the presence of *p*-toluenesulfonic acid (*p*-TsOH) and phenyliodine diacetate (**Scheme 2C.3**).^[23] This reaction proceeds in one-pot two steps; the first condensation took place between anthranilamides and aldehydes catalyzed by *p*-TsOH. Second, phenyliodine diacetate (PIDA) mediated cross dehydrogenative coupling produced quinazolinone derivatives. Various substituents either on 2-aminobenzamides or aldehydes transformed into corresponding products smoothly in good to excellent yields (42-95%).



Scheme 2C.3: Synthesis of quinazolinones in the presence of *p*-TsOH and PIDA

Wang group developed a new protocol for the synthesis of 3-substituted quinazolinones (**6**) by using anthranilamides (**1**) and dicumyl peroxides (DCP) (**5**) under copper catalysis (**Scheme 2C.4**).^[24] In the developed method DCP (**5**) acted as methyl source as well as an oxidant in the reaction. The reaction proposed to proceed through first thermally homolytic cleavage of DCP (**5**)

to generate *tert*-butoxy radical which subsequently used for *N*-methylation of anthranilamide followed by Csp³-H amidation. Finally, oxidation of dihydroquinazolinone by DCP afforded desired products (**6**).

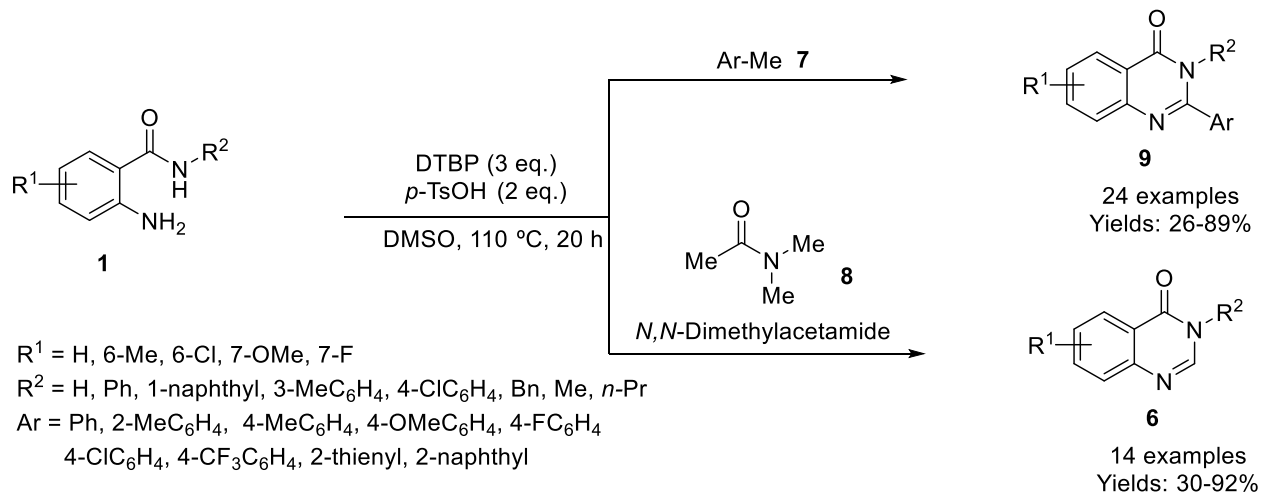


R¹ = H, 5-Me, 5-F, 5-Cl, 5-NO₂
 R² = Ph, 2-MeC₆H₄, 2-ClC₆H₄, 2-CF₃C₆H₄, 3-CF₃C₆H₄,
 4-MeC₆H₄, 4-OMeC₆H₄, 4-ClC₆H₄, 2-naphthyl, Bn, Cy, *n*-Bu

28 examples
 Yields: 35-82%

Scheme 2C.4: Cu(II)-catalyzed synthesis of quinazolinones using DCP as C-source

Zhao group also disclosed a DTBP-mediated synthesis of 2-aryl-quinazolin-4(3*H*)-ones (**9**) and quinazolinones (**6**) through dual amination of benzylic C-H bond from commercially readily accessible substrates 2-amino benzamides and methylarenes (**7**) or DMA (**8**) (*N,N*-dimethylacetamide) under acidic conditions in DMSO (**Scheme 2C.5**).^[25] The possible radical-mediated mechanism was proposed based on control experiments such as radical scavengers BHT (2,6-di-*tert*-butyl-4-methylphenol) or TEMPO (2,2,6,6-tetramethylpiperidine-*N*-oxyl).



R¹ = H, 6-Me, 6-Cl, 7-OMe, 7-F
 R² = H, Ph, 1-naphthyl, 3-MeC₆H₄, 4-ClC₆H₄, Bn, Me, *n*-Pr
 Ar = Ph, 2-MeC₆H₄, 4-MeC₆H₄, 4-OMeC₆H₄, 4-FC₆H₄,
 4-ClC₆H₄, 4-CF₃C₆H₄, 2-thienyl, 2-naphthyl

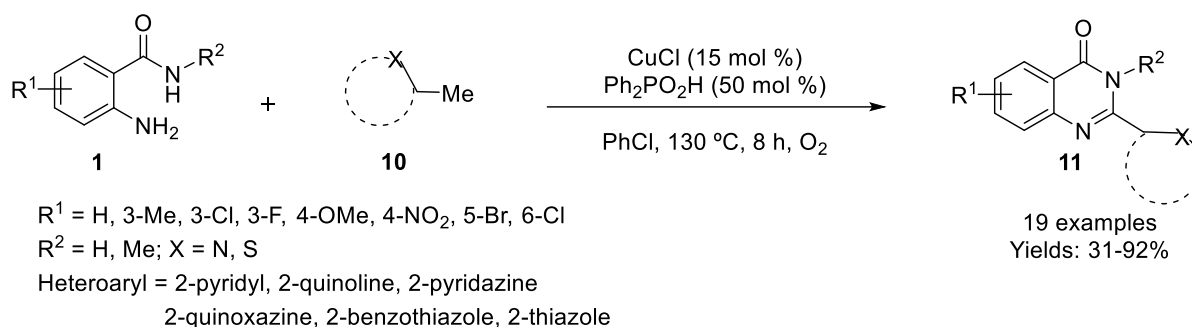
24 examples
 Yields: 26-89%

14 examples
 Yields: 30-92%

Scheme 2C.5: Formation of quinazolin-4(3*H*)-ones using DMA and methylaryl as C-source

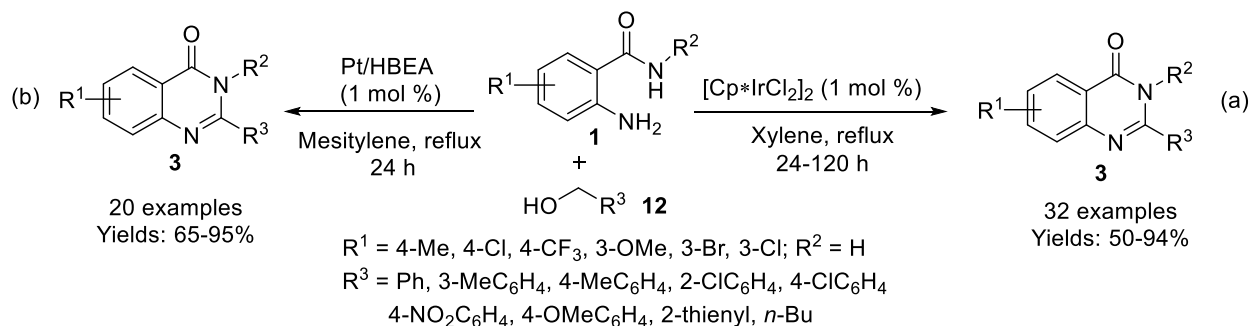
Han and coworkers applied Cu(I)-catalyzed aerobic oxidative amination (CDC) approach for the synthesis of 2-heteroarylquinazolin-4(3*H*)-ones (**11**) from easily available 2-aminobenzamides (**1**) and heteroarylmethanes (**10**) under O₂ atmosphere (**Scheme 2C.6**).^[26] In this strategy, three sp³

C–H and three N–H bonds were eliminated to produce medicinally interesting 2-hetarylquinazolin-4(3*H*)-ones (**11**).



Scheme 2C.6: Cu(I)-catalyzed synthesis of substituted quinazolin-4(3*H*)-ones from **1** and **10**

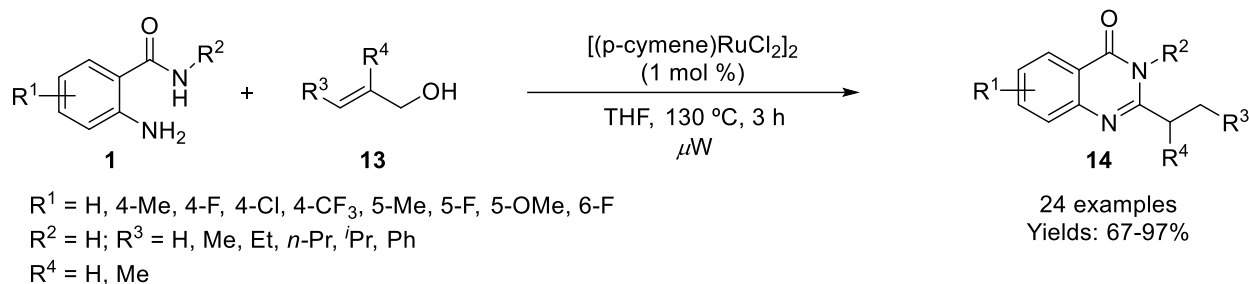
In the past few years, benzyl alcohols (**12**) have been employed instead of aldehydes (**4**) for the synthesis of substituted quinazolinones (**3**) using heavy transition metals. Generally this type of strategies not required any additional oxidant for the oxidation steps compared to other methods and generated H_2 -gas as a by-product.^[27-31] These approaches have been gained more attention towards organic chemist due to high atom-economy, minimal consumption of chemicals and energy. In this context, Zhou group developed a one-pot tandem approach for the synthesis of quinazolin-4(3*H*)-ones (**3**) from *o*-aminobenzamides (**1**) and benzyl alcohols (**12**) using Ir-catalyst in xylene under the refluxed condition for 24-120 h (**Scheme 2C.7a**).^[32] The series of 32 different quinazolinone derivatives (**3**) were synthesized in good to excellent yields (50-94%) by varying different substituents on benzyl alcohols (**12**) and 2-aminobenzamides (**1**). Siddki and co-worker reported HBEA zeolite-supported Pt-catalyzed synthesis of quinazolinones (**3**) using same starting precursors **1** and **12** (**Scheme 2C.7b**).^[33]



Scheme 2C.7: Synthesis of quinazolinones from benzyl alcohol

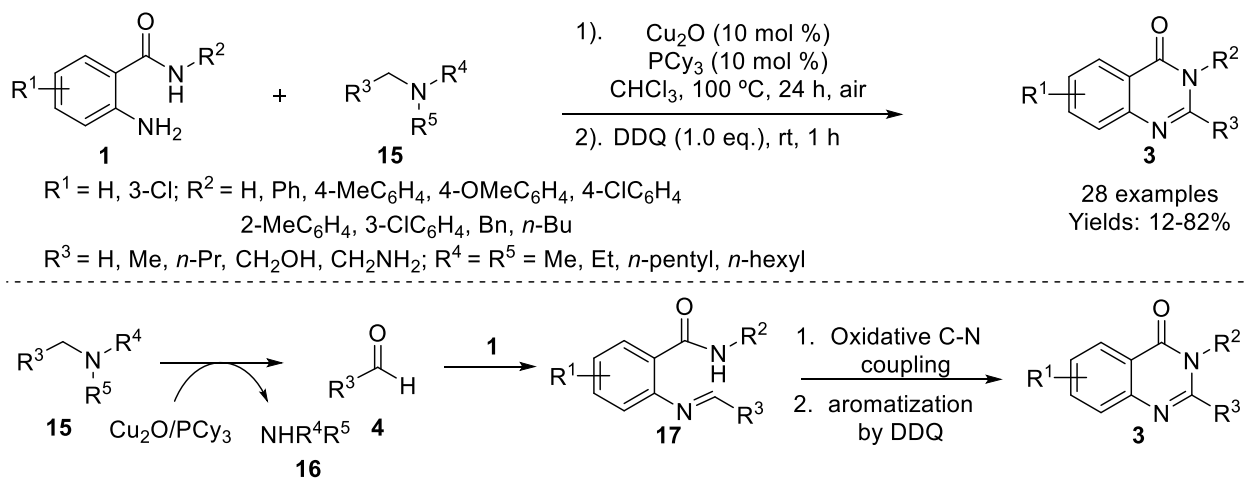
Very recently, Li group disclosed an alternative approach for the synthesis of substituted quinazolinone derivatives (**14**) from substituted allyl alcohols (**13**) using Ru-complex under

microwave radiation in THF at 130 °C for 3 h (**Scheme 2C.8**).^[34] The reaction pathway proposed by performing a series of control experiments and also performed a reaction in NMR to evaluate the reactive intermediate. Variety of allyl alcohols (**13**) were studied under optimal conditions and afforded the corresponding quinazolin-4(3*H*)-ones (**14**) in 67-97% yields



Scheme 2C.8: Synthesis of quinazolin-4(3*H*)-ones using allyl alcohols *via* Ru-complex

Deng and co-workers achieved the substituted quinazolin-4(3*H*)-ones (**3**) synthesis by one-pot sequential strategy from 2-aminobenzamides (**1**) and tertiary amines (**15**) as a carbon source in the presence of Cu_2O as a catalyst and DDQ as an oxidant (**Scheme 2C.9**).^[35] The reaction mechanism was elucidated on the basis of control experiments. Initially, the aldehydes (**4**) and *sec.* amines (**16**) were produced by the oxidative decomposition of tertiary amines (**15**) in the presence of copper-catalyst.

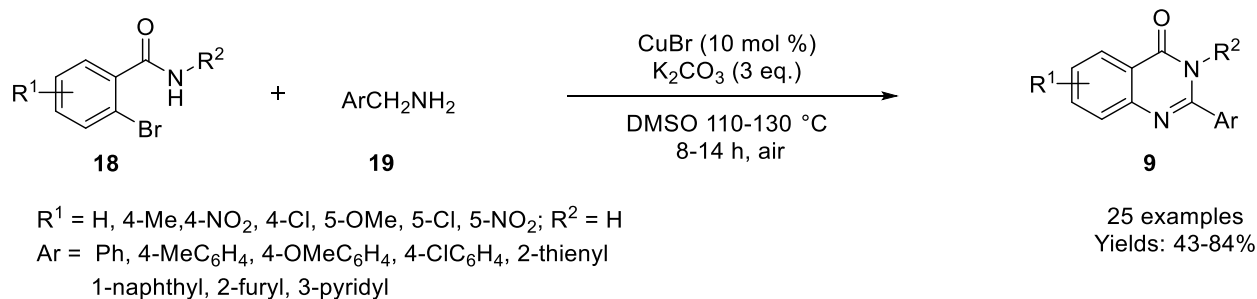


Scheme 2C.9: Cu_2O -catalyzed synthesis of quinazolines from 2-aminobenzamides and *tert.* amines

Subsequently, aldehyde (**4**) subjected to condensation with 2-aminobenzamides (**1**) to generate imines intermediate (**17**), which further led to the quinazolinone products (**3**) by oxidative C-N coupling

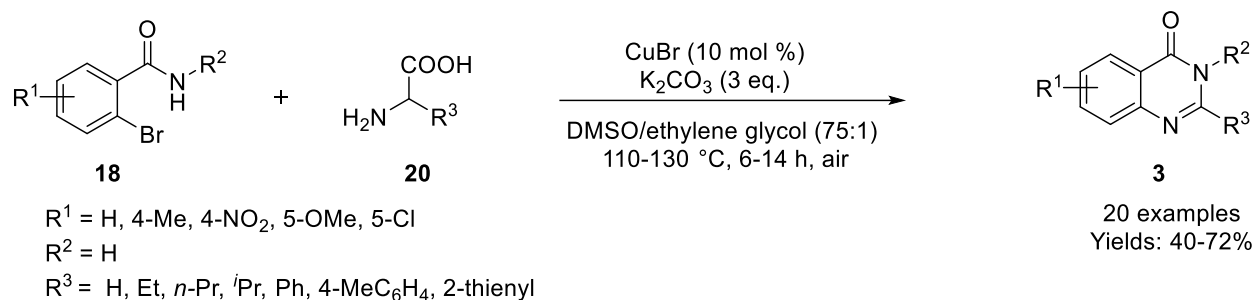
2C.1.2 Synthesis of Quinazolinones from 2-bromobenzamides

Various alternative approaches for the synthesis of quinazolinones (**3**) has been developed.^[24, 27, 32, 36-49] The most of methods use of *o*-amino benzamides (**1**) as starting materials, usually prepared from corresponding nitro-group through various reduction process.^[50] At present, the efforts for the synthesis of quinazolinones (**3**) are directed towards using 2-halobenzamides (**18**) substrates to avoid amine in the starting materials, which could be more efficient than classical methods. In this regard, Fu and coworkers have successfully reported the direct access of quinazolinones (**9**) from 2-bromobenzamides (**18**) and benzyl amines (**19**) in the presence of CuBr as catalyst (**Scheme 2C.10**).^[51] This developed protocol proceed through initially Ullmann type C-N coupling took place between 2-bromobenzamides (**18**) and benzyl amines (**19**) by CuBr-catalyst followed by oxidation. Finally, desired products (**9**) afforded by intramolecular nucleophilic attack of amidic NH₂-group and aromatization. Variety of quinazolin-4(3*H*)-ones (**9**) synthesized in moderate to good yields by this method which showed the high functional group tolerance.



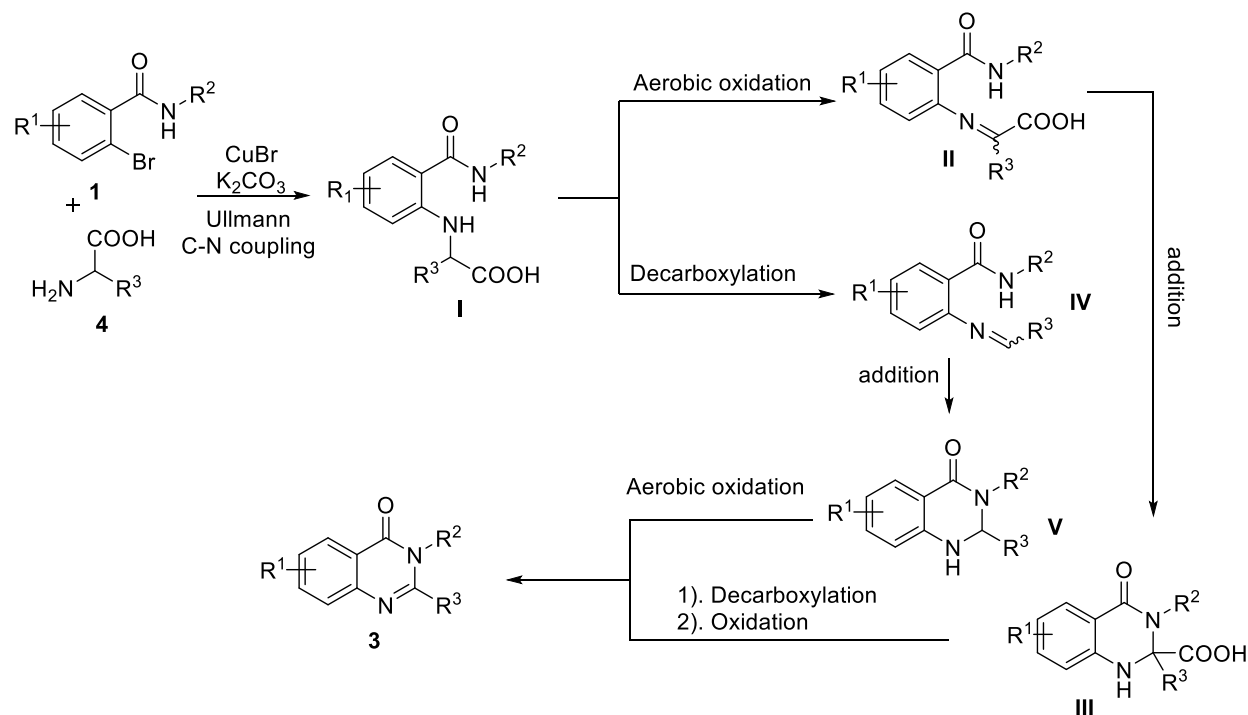
Scheme 2C.10: Cu-catalyzed synthesis of 2-aryl quinazolinones using 2-bromobenzamides

Subsequently, the same group realized the one-pot transformation of 2-bromobenzamide (**18**) to quinazolin-4(3*H*)-ones (**3**) using α -amino acids (**20**) as starting with CuBr as a catalyst in a mixture of DMSO and ethylene glycol (75:1)(**Scheme 2C.11**).^[52]



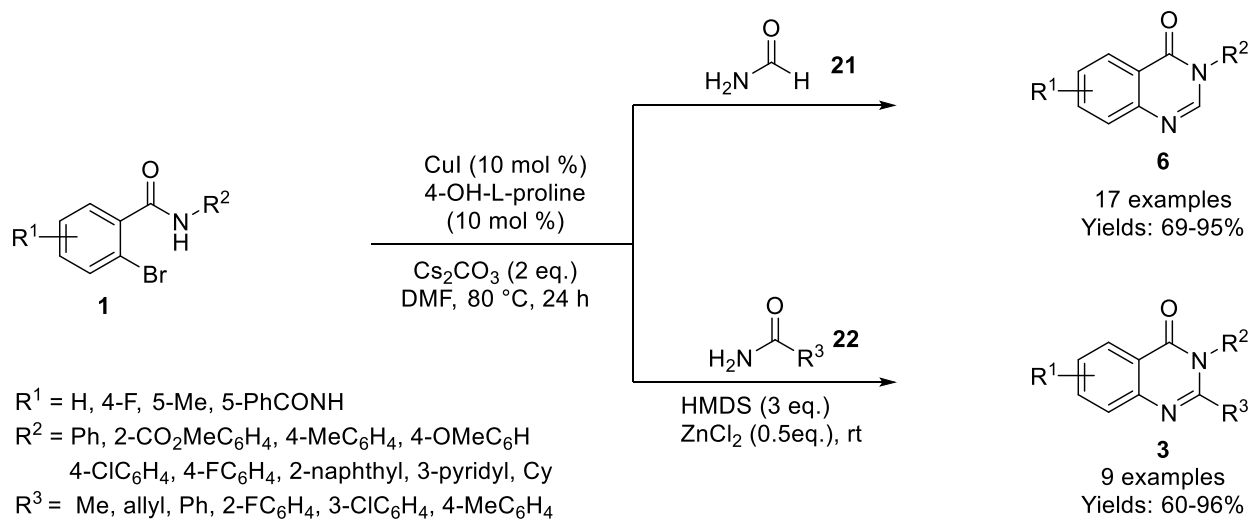
Scheme 2C.11: Synthesis of quinazolinones from amino acids by CuBr-catalyst

The developed reaction proposed to proceed in two pathway path A and B as shown in **scheme 2C.12**. In path A, initially C-N coupled product (**I**) formed by Cu(I)-catalyzed Ullmann-type coupling followed by aerobic oxidation produced intermediate (**II**). Then intramolecular nucleophilic addition produced dihydroquinazolinone intermediate (**III**), which subsequently underwent decarboxylation and oxidation led to the desired product (**3**). While in path B, the first decarboxylation took place and formed intermediate (**I**) followed by oxidation generated intermediate (**IV**). Then underwent intramolecular addition reaction produced dihydroquinazolinone intermediate (**V**). Finally, aerobic oxidation afforded the desired product (**3**).



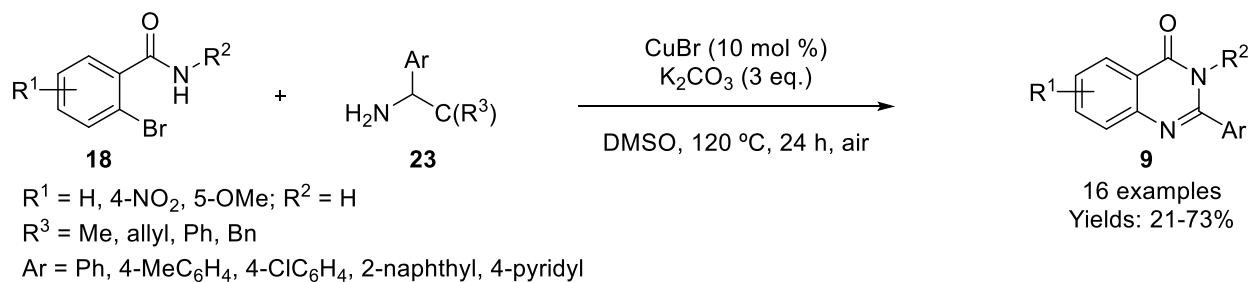
Scheme 2C.12: Proposed reaction mechanism for the synthesis of quinazolin-4(3H)-ones

In extension, Ma *et al.* have also developed a protocol for the preparation of quinazolin-4(3*H*)-ones (**6**) from 2-bromo *N*-arylbenzamides (**18**) and formamide (**21**) under copper catalysis in the presence of 4-hydroxy L-proline and Cs₂CO₃ in DMF at 80 °C for 24 h (**Scheme 2C.13**).^[53] In this protocol, the first amidation took place followed by a condensation reaction offered 2-hydroxy-dihydroquinazolinones. Subsequently, dehydration led to the formation of quinazolinones derivatives (**6**). Acetamides/benzamides (**22**) also produced desired products (**3**) smoothly. However, it required the combination of HMDS and ZnCl₂ for cyclization step at room temperature.



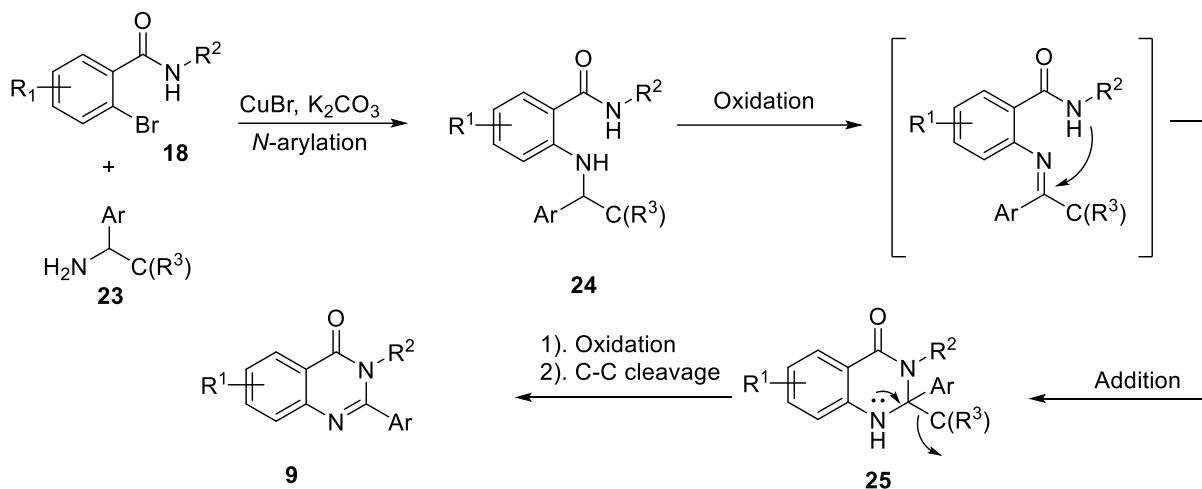
Scheme 2C.13: Synthesis of quinazolin-4(3*H*)-ones using formamide/acetamide/benzamide

Tang group also described the formation of 2-aryl-quinazolin-4(3*H*)-ones derivatives (**9**) via copper-catalyzed domino reaction of *o*-halobenzamides (**18**) with α -substituted aryl-methenamine (**23**) as starting materials through C–C bond cleavage in the presence of K₂CO₃ in DMSO at 120 °C for 24 h under aerobic condition (**Scheme 2C.14**).^[54]



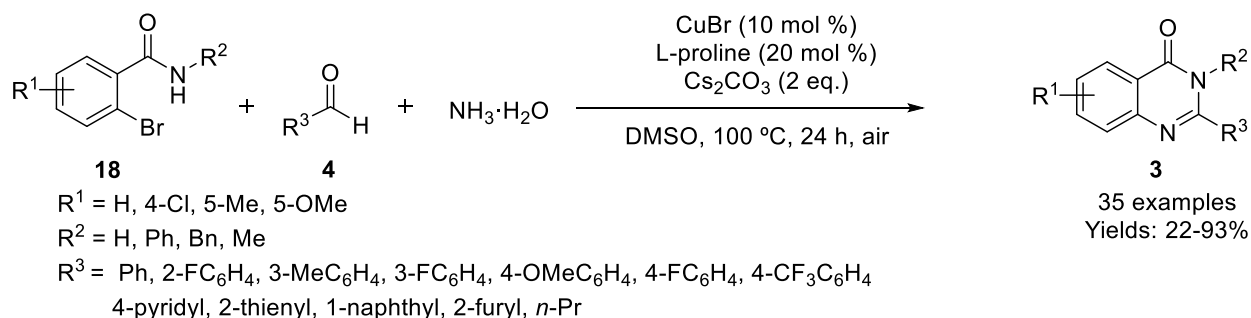
Scheme 2C.14: Synthesis of quinazolinones derivatives using *tert.*amines and 2-bromobenzamides

Variety of 2-halobenzamides (**18**) were used such as Cl, Br, I and reacted very well under the developed protocol. The proposed reaction pathway proceeds through initially, *N*-arylation via Ullmann-type C-N coupling followed by oxidation produced imine (**24**). Finally, nucleophilic addition, aromatization, and C-C bond cleavage led to desired products (**9**) (**Scheme 2C.15**).



Scheme 2C.15: Mechanism for the synthesis of quinazolinones derivatives using *tert.* amines

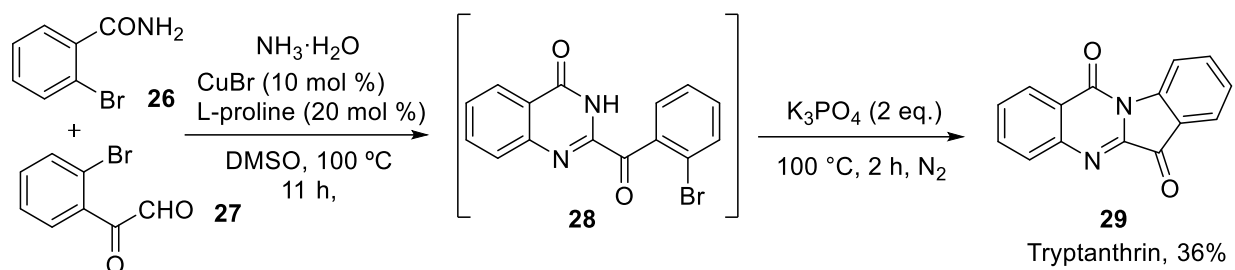
In the same year, Fan and co-workers disclosed the synthesis of substituted quinazolin-4(3*H*)-ones by copper-catalyzed multicomponent reaction of 2-bromo *N*-protected benzamides/benzamides (**18**), aldehydes (**1**) and ammonia used as nitrogen source (**Scheme 2C.16**).^[55] Benzaldehydes having electron-rich and poor substituents well tolerated in this protocol and transformed into the products in 67-83% yields. Sterically hindered, and heteroaldehydes were also reacted smoothly under the developed method.



Scheme 2C.16: Cu(I)-catalyzed multicomponent reaction for the synthesis of quinazolinones

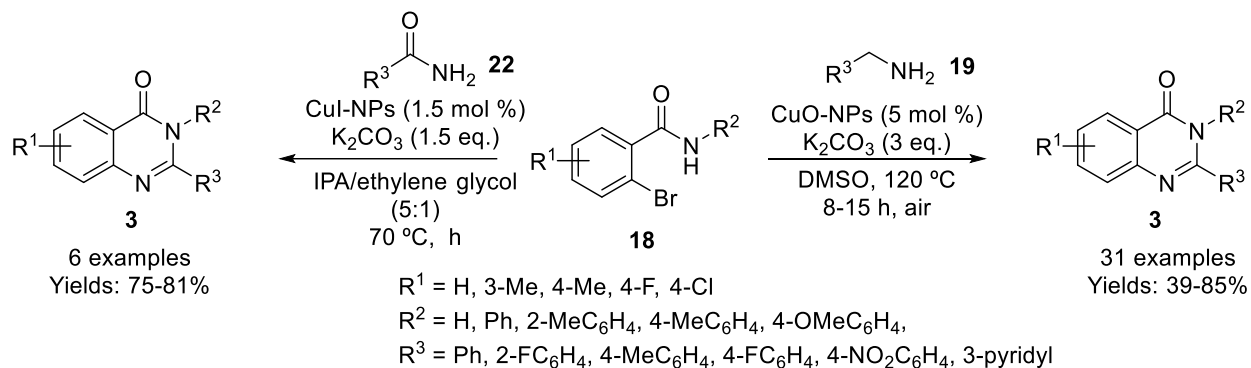
The developed strategy further applied for the synthesis of alkaloid tryptanthrin in one-pot sequential addition to showcase the synthetic application. First, 2-aminobenzamide was formed by Cu-catalyzed amination of **18** with aqueous ammonia followed by condensation with 2-(2-

bromophenyl)-2-oxoacetaldehyde (**27**), cyclization and finally, base-mediated intramolecular C-N coupling led to the formation of tryptanthrin (**29**) in 36% total yield (**Scheme 2C.17**).



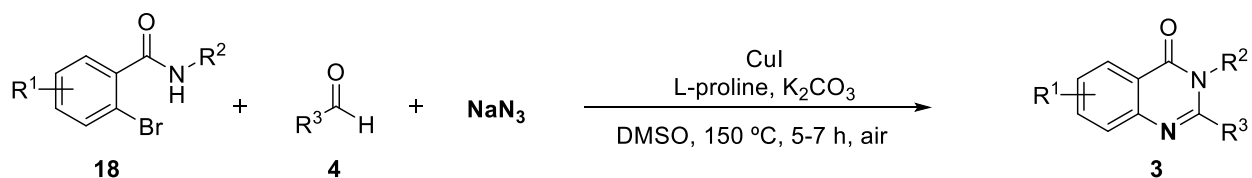
Scheme 2C.17: Total synthesis of alkaloid tryptanthrin (**29**)

Atul and Patel group independently reported this class of product by using benzamides (**22**) and benzylamines (**19**) respectively in the presence of Copper-nano particles (**Scheme 2C.18**).^[56-57]



Scheme 2C.18: Synthesis of quinazolin-4(3*H*)-ones by using Cu-NPs from 2-bromobenzamides

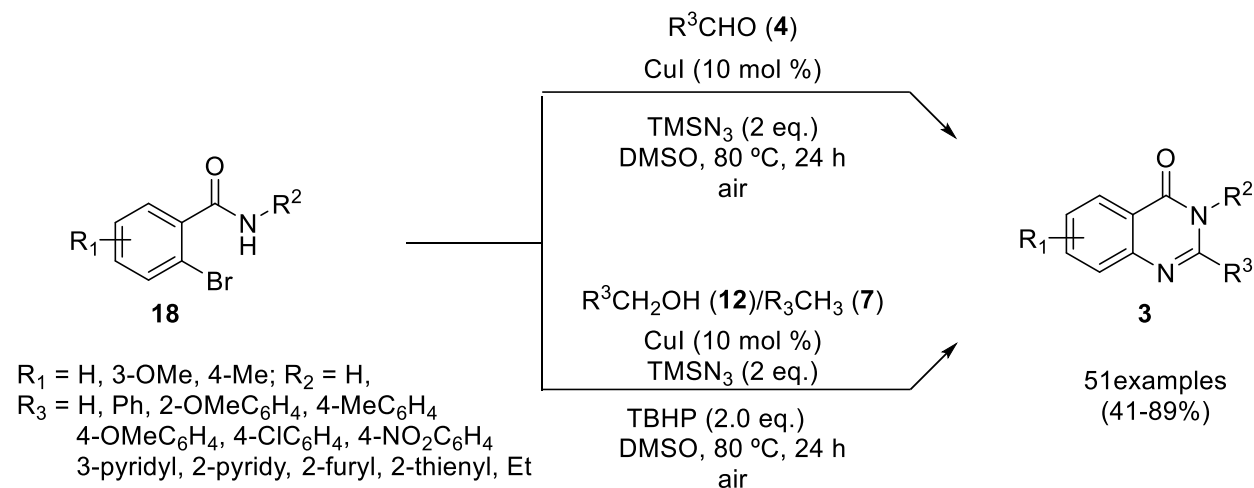
Encourage by existing methods and our ongoing research for developing new methodology in the construction of *N*-heterocycles by using sodium azide as a nitrogen source.^[58-62] We further motivated to construct quinazolin-4(3*H*)-ones from 2-bromobenzamides, aldehydes, and sodium azide as nitrogen source (**Scheme 2C.19**).



Scheme 2C.19: Our alternative approach for the synthesis of quinazolin-4(3*H*)-ones

During this work, Tripathi and team reported similar strategy *via* Cu(I)-catalyzed tandem reaction for the synthesis of 2-substituted quinazolinones (**3**) from 2-bromobenzamide (**18**), aldehydes (**4**)/alcohols (**12**)/methylarenes (**7**) in the presence TMSN₃ as a nitrogen source and TBHP as

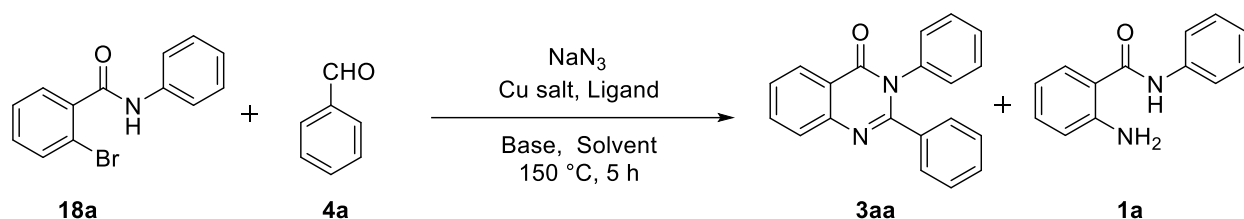
oxidant under ligand and base free condition (**Scheme 2C.20**).^[63] This strategy offered a diverse range of quinazolinones in good to high yields with large functional group tolerance and reaction proceed *via* radical mechanism confirmed by use of different loading of radical inhibitor TEMPO.



Scheme 2C.20: Synthesis of quinazolinones by using TMSN₃ and TBHP via Cu(I)-catalyst

2C.2 RESULTS AND DISCUSSION

In our initial investigation, 2-bromo-*N*-phenylbenzamide (**18a**), benzaldehyde (**4a**) and sodium azide were employed as substrates using 20 mol % CuI as a catalyst, 30 mol % L-proline as a ligand and 2.0 eq. of K₂CO₃ as a base in DMSO at 120 °C under air atmosphere for 10 h. Gratifyingly, expected 2,3-diphenylquinazolin-4(3*H*)-one (**3aa**) was isolated in 63% (entry 1, **Table 2C.1**). The structure of **3aa** was elucidated by various spectroscopic techniques (IR, NMR, and MS). Increase in reaction temperature to 150 °C further increased yield of **3aa** to 73% with reduced time (entry 2, **Table 2C.1**). Inspired by this result, we screened the different copper salt, such as CuBr, CuI, CuCl₂·H₂O and Cu(OAc)₂·H₂O. Among all, CuI showed the highest catalytic efficiency (entries 2-5, **Table 2C.1**). Furthermore, we tested the effect of ligands, and L-proline provided the highest yield (entries 6-9, **Table 2C.1**). Effect of bases was also evaluated, and K₂CO₃ proved to be an effective base for this methodology as compared to other strong bases (entries 10-15, **Table 2C.1**). We next examined the impact of solvents on reaction yield (entries 16-19, **Table 2C.1**). When DMF and DMA were employed to replace DMSO as the reaction medium, the yield was diminished slightly (entries 16-17, **Table 2C.1**).

Table 2C.1: Optimization of reaction condition for the synthesis of **3aa**.^a

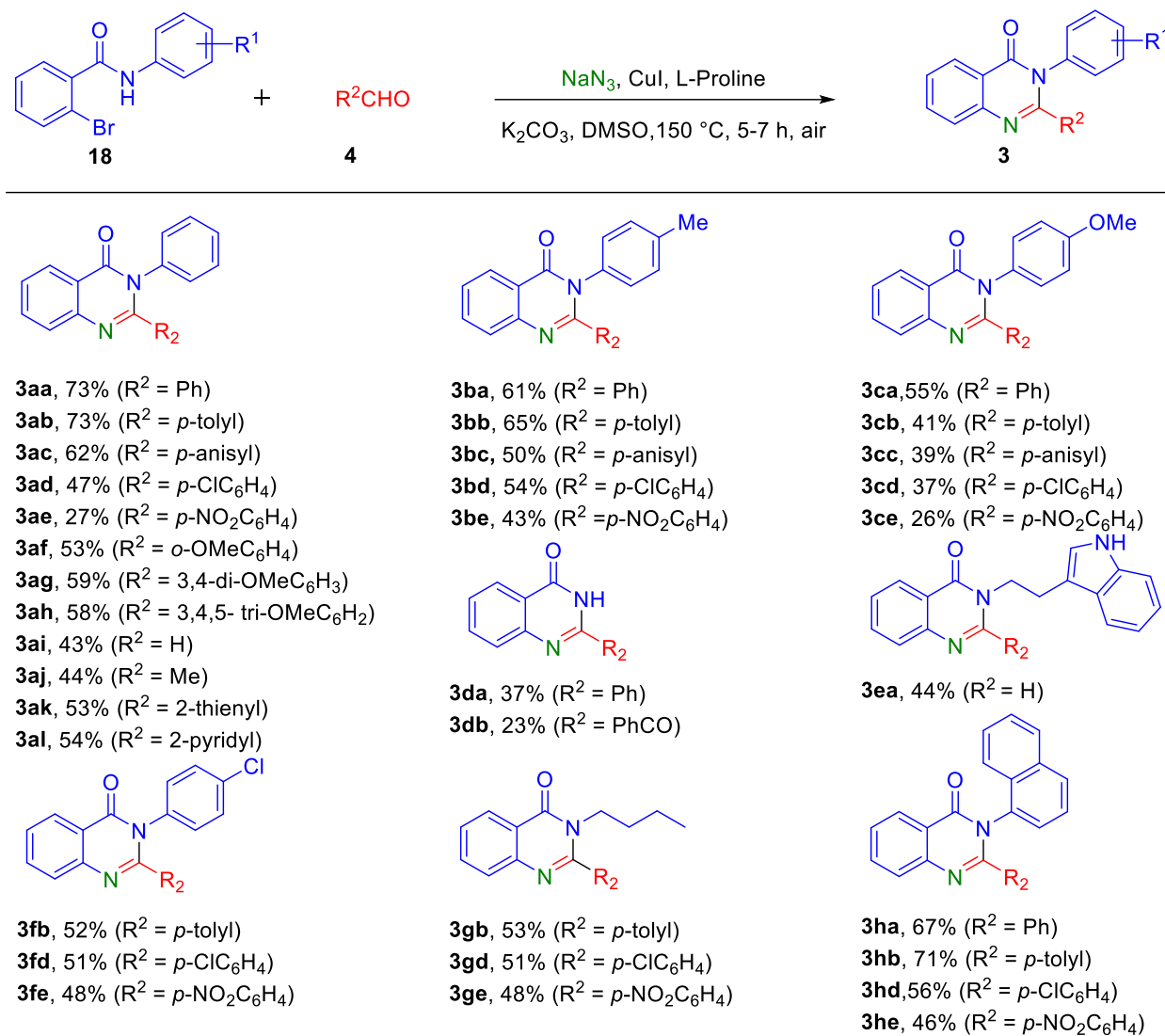
entry	catalyst (20 mol %)	ligand (30 mol %)	base (2.0 equiv.)	solvent (2 mL)	yield ^b (%)
1 ^c	CuI	L-Proline	K ₂ CO ₃	DMSO	63
2	CuI	L-Proline	K₂CO₃	DMSO	73
3	Cu(OAc) ₂ ·H ₂ O	L-Proline	K ₂ CO ₃	DMSO	50
4	CuCl ₂ ·H ₂ O	L-Proline	K ₂ CO ₃	DMSO	54
5	CuBr	L-Proline	K ₂ CO ₃	DMSO	58
6	CuI	Glycine	K ₂ CO ₃	DMSO	55
7	CuI	DMEDA ^d	K ₂ CO ₃	DMSO	51
8	CuI	N ³ -TMEDA ^e	K ₂ CO ₃	DMSO	48
9	CuI	Alanine	K ₂ CO ₃	DMSO	47
10	CuI	L-proline	^t BuOK	DMSO	54
11	CuI	L-proline	Cs ₂ CO ₃	DMSO	39
12	CuI	L-proline	Na ₂ CO ₃	DMSO	63
13	CuI	L-proline	NaHCO ₃	DMSO	67
14	CuI	L-proline	Et ₃ N	DMSO	54
15	CuI	L-proline	K ₃ PO ₄	DMSO	56
16	CuI	L-proline	K ₂ CO ₃	DMF	60
17	CuI	L-proline	K ₂ CO ₃	DMA	57
18 ^f	CuI	L-proline	K ₂ CO ₃	Toluene	20
19 ^g	CuI	L-proline	K ₂ CO ₃	1,4-dioxane	nr
20	CuI	-	K ₂ CO ₃	DMSO	37
21	-	L-proline	K ₂ CO ₃	DMSO	10
22	CuI	L-proline	-	DMSO	trace
23 ^h	CuI	L-proline	K ₂ CO ₃	DMSO	51%

^a**Reactions conditions:** **18a** (0.36 mmol), **4a** (0.40 mmol), NaN₃ (0.54 mmol), catalyst (20 mol %), ligand (30 mol %) and K₂CO₃ (0.72 mmol) in DMSO (2 mL) at 150 °C for 5 h under air.

^bIsolated yields. ^cat 120 °C for 10 h. ^dDMEDA= *N,N*-Dimethylethylenediamine. ^eN³-TMEDA= *N,N,N*-Trimethylethylenediamine. ^fat 120 °C for 16 h. ^gat 110 °C for 16 h. ^h10 mol % CuI and 20 mol % L-proline were used.

The yield of **3aa** was decreased significantly in a non-polar solvent as the reaction medium. By using toluene as solvent **3aa** was obtained in 20% yield along with 15% Schiff base intermediate and 22% of 2-amino-*N*-phenylbenzamide (**1a**) after 16 h while only 2-amino-*N*-phenylbenzamide (**1a**) was isolated in 40% yield by using 1,4-dioxane as solvent (entries 18–19, **Table 2C.1**). The yield of **3aa** decreased significantly when the model reaction was performed in the absence of either copper salt, ligand or base (entries 20–22, **Table 2C.1**). It was found that the best yield of **3aa** was obtained by using CuI (20 mol %) with L-proline (30 mol %) as ligand and K₂CO₃ (2 eq.) as a base in DMSO at 150 °C for 5 h. Moreover, we found that product yield was decreased with the use of 10 mol % CuI and 20 mol % L-proline (entry 23, **Table 2C.1**).

With optimized reaction conditions for the transformation of *o*-bromobenzamides to quinazolinones in hand, we turned our attention to explore the generality of this protocol as shown in **Table 2C.2**. 2-Bromo-*N*-phenylbenzamide (**18a**) was reacted with different aldehydes (**4a–k**) to give corresponding quinazolin-4(3*H*)-ones (**3aa–ak**) in moderate to good yield (27–73%). All aliphatic, aromatic and heterocyclic aldehydes reacted equally well. Aldehydes with electron withdrawing group gave a relatively lower yield of quinazolin-4(3*H*)-one (**3ad** and **3ae**). Next, 2-bromobenzamide with different *N*-substituents (**3b–h**) were allowed to react with different aldehydes in the presence of NaN₃ and CuI/L-proline to give corresponding quinazolin-4(3*H*)-one (**3ba–he**). As observed for **18a**, 4-nitrobenzaldehyde (**4e**) gave a lower yield of the corresponding quinazolin-4(3*H*)-one from other 2-bromobenzamides. Interestingly, 2-bromobenzamide (**18d**) also reacted to give corresponding quinazolin-4(3*H*)-ones (**3da**, **3db**) in moderate yields. Overall, a broad range of amides and aldehydes reacted smoothly to give corresponding quinazolin-4(3*H*)-ones in good to high yield. It is worth to mention that only 2-amino-*N*-(2-bromophenyl)benzamide (**3i'**) was observed in 50% yield by the reaction 2-bromo-*N*-(2-bromophenyl)benzamide with 4-methylbenzaldehyde under optimized reaction condition.

Table 2C.2: Substrate scope for the synthesis of 2,3-disubstituted quinazolin-4(3*H*)-ones.^{a,b}

^a**Reactions conditions:** **18a** (0.36 mmol), **4a** (0.40 mmol), NaN_3 (0.54 mmol), catalyst (20 mol %), ligand (30 mol %) and K_2CO_3 (0.72 mmol) in DMSO (2 mL) at $150\text{ }^\circ\text{C}$ for 5 h under air.

^bIsolated yields.

Structure of all the synthesized quinazolin-4(3*H*)-ones was elucidated by the ^1H , ^{13}C NMR, IR and HRMS data. The representative IR for **3ac** is shown in **Figure 2C.3**. The presence of amidic carbonyl group in **3ac** indicated by a strong peak at 1682 cm^{-1} of $\text{C}=\text{O}$ stretching in the IR spectrum. The peaks ranging from $1466\text{-}1605$ and 1250 cm^{-1} corresponding to aromatic $\text{C}=\text{C}$, and C-O stretching were also observed in the IR spectrum. In the ^1H NMR spectrum, characteristic deshielded doublet appeared at δ 8.38-8.36 ppm for $\text{C}_8\text{-H}$, and one singlet at δ 3.77 ppm for OMe-

group along with other expected protons at their respective positions were observed (**Figure 2C.4**). The amidic carbonyl carbon appeared at δ 167.49 ppm along with all other corresponding peaks in the ^{13}C NMR spectrum (**Figure 2C.5**).

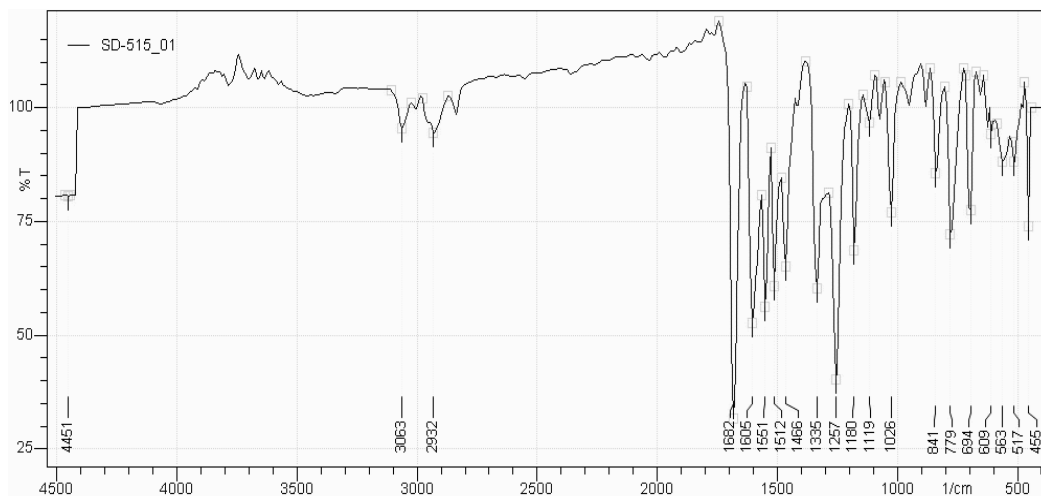


Figure 2C.3: IR spectrum of **3ac**

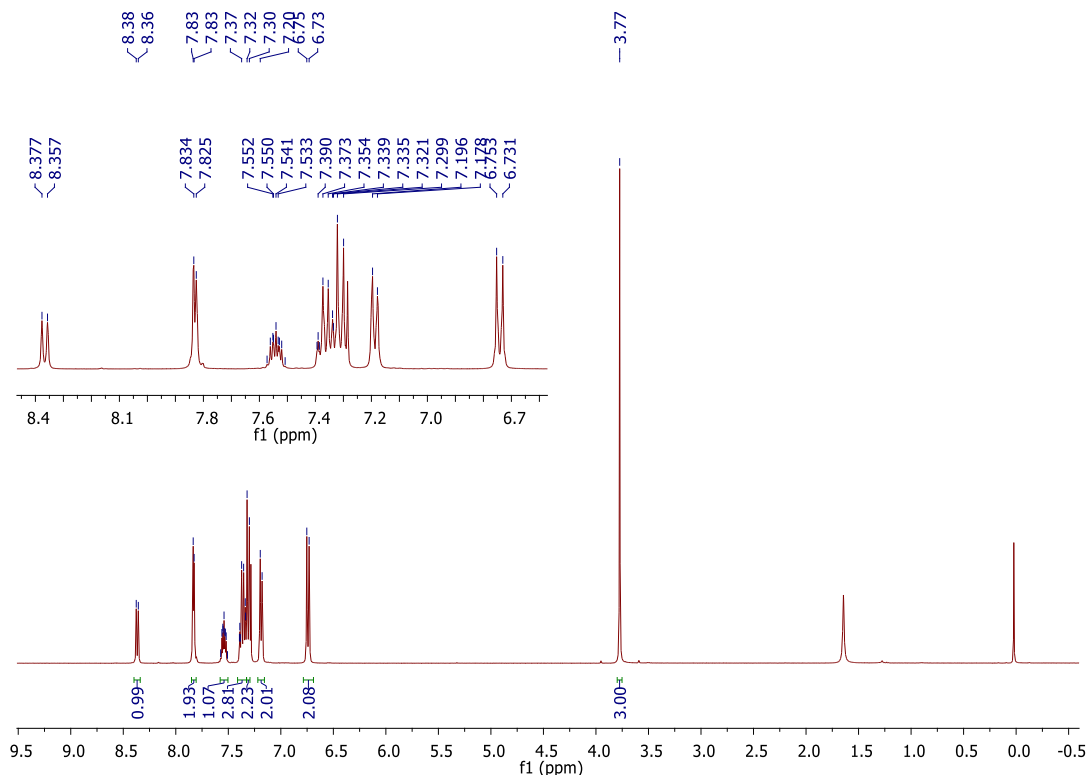


Figure 2C.4: ^1H NMR spectrum of **3ac**

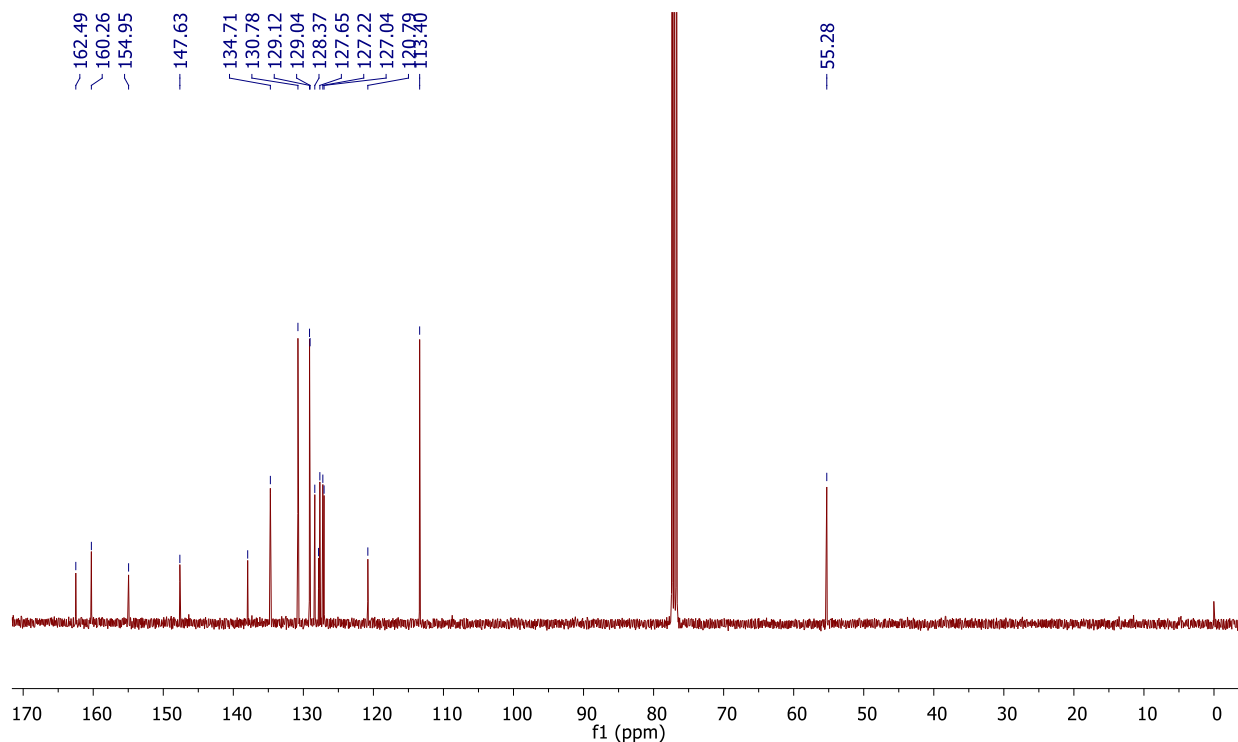
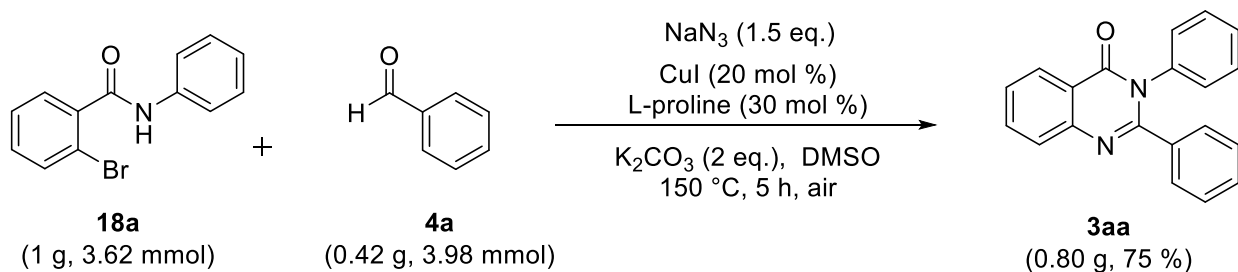


Figure 2C.5: ^{13}C NMR spectrum of **3ac**

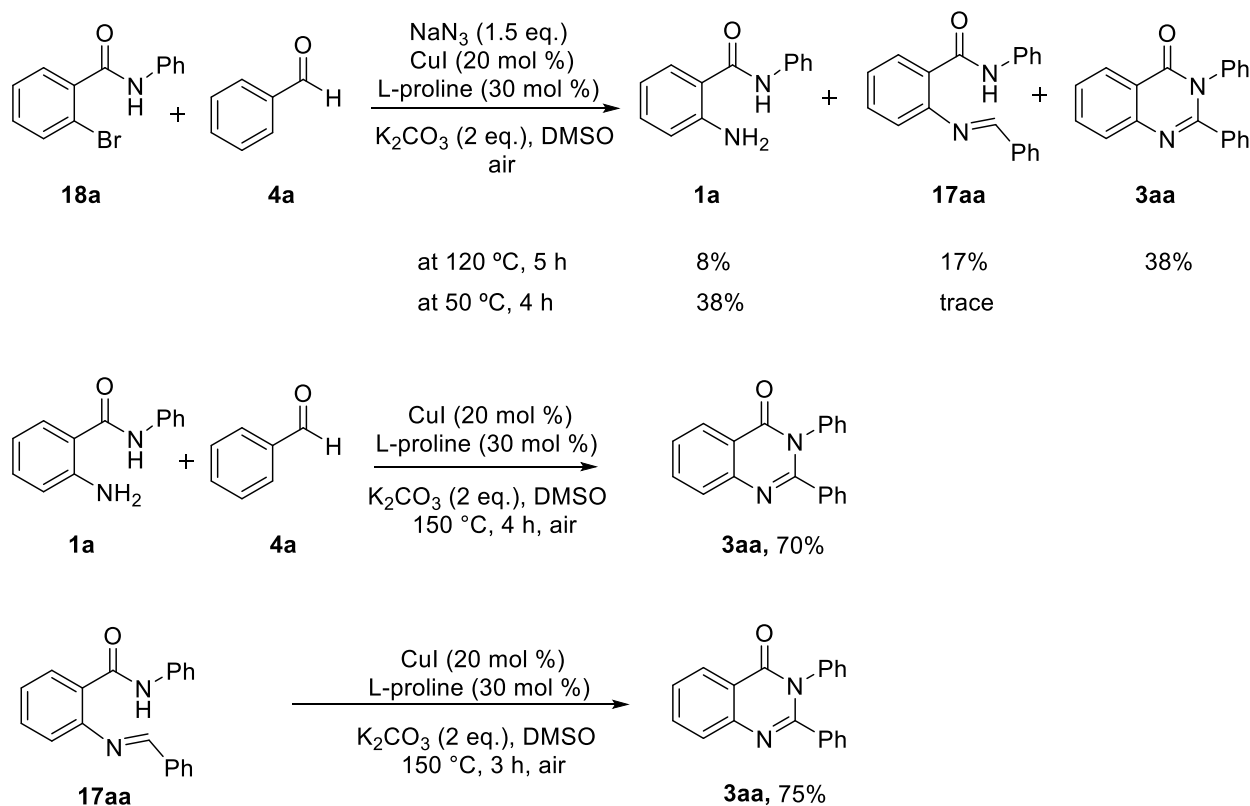
To explore the practicality of the developed method, a gram scale reaction of **18a** with **4a** using NaN_3 was performed under the optimized reaction conditions, and **3aa** was obtained in 75% (0.8 g) yield (**Scheme 2C.20**).



Scheme 2C.20: Gram scale reaction of **18a** with **4a**

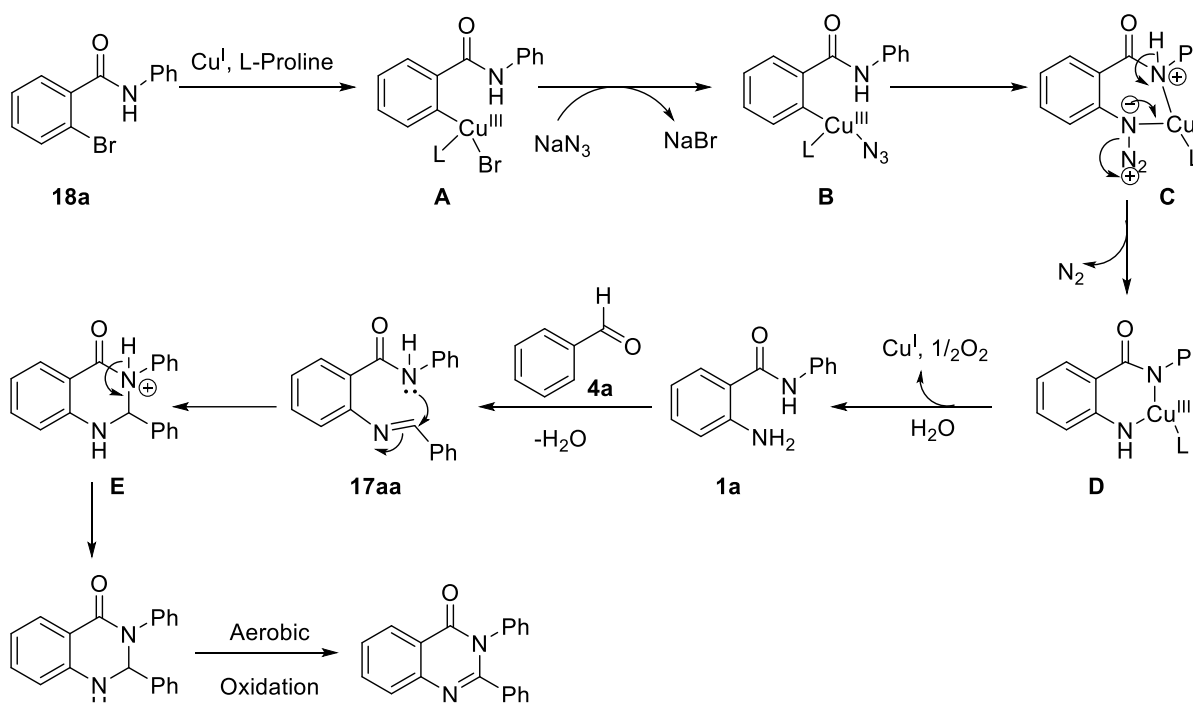
To gain insight into the mechanism of the reaction, several control experiments were performed (**Scheme 2C.21**). Initially, 2-bromo-*N*-phenylbenzamide (**18a**) was treated with benzaldehyde (**4a**) under optimal reaction condition at the lower temperature (120 °C) for 5 h. Desired product **3aa**, 2-amino-*N*-phenylbenzamide (**1a**) and un-cyclized intermediate (Schiff base, **17aa**) were isolated in 38%, 8%, and 17% yields, respectively. Intermediate **1a** was formed in 38% yield along with traces amount of **17aa** from the reaction of **18a** and **4a** with NaN_3 in the presence of CuI, L-proline

and K_2CO_3 in DMSO at 50 °C after 4 h. Next, on treating **1a** with benzaldehyde (**4a**) under optimized reaction conditions gave **3aa** in 70% yield after 4 h. Similarly, when intermediate **17aa** was heated at 150 °C for 3 h in the presence of CuI, L-proline and K_2CO_3 in DMSO under air the desired product **3aa** was obtained in 75% yield.



Scheme 2C.21: Control experiments

Based on the above results from control experiments and literature precedent,^[62, 64-69] plausible reaction mechanism for the formation of 2,3-diphenylquinazolin-4(3*H*)-one has been depicted in **Scheme 2C.22**. Initially, Cu(I) complex (**A**) was formed through the oxidative insertion of copper in aryl bromide (**18a**). Subsequently, aryl-azide Cu(I) complex (**B**) was formed by the exchange of Br^- with N_3^- which led to release of N_2 and formed a complex (**D**). The reductive amination of complex (**D**) generated intermediate (**1a**) with the help of moisture content in DMSO. 2-Amino-*N*-phenylbenzamide (**1a**) condensed with benzaldehyde (**4a**) to produce imine intermediate (**17a**). Subsequently, intramolecular nucleophilic attack of amidic nitrogen onto imine afforded the cyclized product (**F**). Finally, aerobic oxidation of **F** led to the formation of desired product quinazolin-4(3*H*)-one (**3aa**).



Scheme 2C.22: Plausible mechanism for the synthesis of quinazolin-4(3H)-one

2C.3 CONCLUSIONS

We have developed a simple and efficient copper-catalyzed one-pot, three-component tandem reaction to synthesize quinazolin-4(3H)-ones. The cascade reaction involves reductive amination, imine formation, C-N bond formation *via* intramolecular cyclization and aerobic oxidation. Good functional group tolerance, mild condition, readily available starting materials, and user-friendly procedure makes this protocol practically good and attractive method for the synthesis of quinazolin-4(3H)-ones.

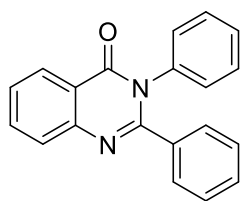
2C.4 EXPERIMENTAL SECTION

General information: Melting points were determined in open capillary tubes on an EZ-Melt Automated melting point apparatus and are uncorrected. Reactions were monitored by using thin layer chromatography (TLC) on 0.2 mm silica gel F254 plates (Merck). The chemical structures of final products were determined by their NMR spectra (^1H and ^{13}C NMR). Chemical shifts are reported in parts per million (ppm) using deuterated solvent peak or tetramethylsilane as an internal

standard. The HRMS data were recorded on a mass spectrometer with electrospray ionization and TOF mass analyzer. All starting materials were synthesized according to published literature.^[70-71] All other chemicals were obtained from the commercial suppliers and used without further purification.

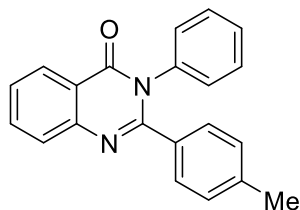
General procedure for the synthesis of quinazolin-4(3*H*)-ones (3): A mixture of 2-bromo-*N*-phenylbenzamide (**18a**) (100 mg, 0.362 mmol), benzaldehyde (**4a**) (42 mg, 0.398 mmol), sodium azide (35 mg, 0.543 mmol), CuI (20 mol %), L-proline (40 mol %) and K₂CO₃ (100 mg, 2.0 eq.) were stirred in DMSO (2 mL) under air atmosphere at room temperature and slowly warmed to 150 °C for 5 h. After completion reaction, cooling to ambient temperature and reaction mass was diluted with ice-cold aqueous solution of NH₄Cl (50 mL), filtered through celite bed and washed with ethyl acetate (20 mL). Filtrate was extracted by ethyl acetate (30 mL x 2). Organic layers were combined, dried over Na₂SO₄ and concentrated under reduced pressure. Desired product **3aa** (79 mg, 73%) was isolated by column chromatography on silica gel (100-200 mesh) using ethylacetate/hexane (15-17%) as eluant.

2,3-Diphenylquinazolin-4(3*H*)-one (3aa)



Off white solid (79 mg, 73%); mp 159–160 °C (Lit.^[72] 158–159 °C); ¹H NMR (400 MHz, DMSO-*d*₆) δ 8.21 (dd, *J* = 8.0, 1.2 Hz, 1H), 7.94 – 7.90 (m, 1H), 7.78 (d, *J* = 7.6 Hz, 1H), 7.64 – 7.60 (m, 1H), 7.38 (dd, *J* = 7.8, 1.7 Hz, 1H), 7.35 – 7.28 (m, 5H), 7.25 – 7.20 (m, 3H); ¹³C NMR (100 MHz, DMSO-*d*₆) δ 161.9, 155.7, 147.7, 138.3, 136.1, 135.3, 130.0, 129.4, 129.3, 129.0, 128.6, 128.0, 127.9, 127.7, 126.9, 121.2; IR (KBr): 3055, 1682, 1589, 1335, 1275 cm⁻¹; HRMS calcd for C₂₀H₁₅N₂O [M+H]⁺ 299.1179, found 299.1184.

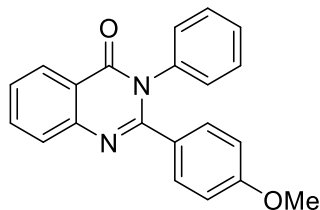
3-Phenyl-2-*p*-tolylquinazolin-4(3*H*)-one (3ab)



White solid (83 mg, 73%); mp 170–172 °C (Lit.^[72] 171–172 °C); ¹H NMR (400 MHz, DMSO-*d*₆) δ 8.20 (d, *J* = 6.9 Hz, 1H), 7.90 (t, *J* = 7.9 Hz, 1H), 7.77 (d, *J* = 8.7 Hz, 1H), 7.60 (t, *J* = 7.0 Hz, 1H), 7.33 (d, *J* = 4.4 Hz, 4H), 7.27 (d, *J* = 8.1 Hz, 3H), 7.03 (d, *J* = 7.9 Hz, 2H), 2.22 (s, 3H); ¹³C NMR (100 MHz, DMSO-*d*₆) δ 161.9, 155.7, 147.8, 138.9, 138.4, 135.2, 133.3, 130.0, 129.4, 129.1, 128.6, 128.5, 127.9, 127.5, 126.9, 121.1, 21.3; IR (KBr):

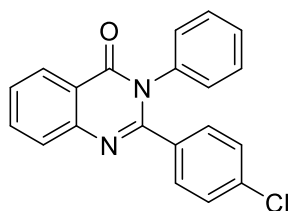
3055, 1682, 1582, 1335, 1265 cm^{-1} ; HRMS calcd for $\text{C}_{21}\text{H}_{17}\text{N}_2\text{O}$ $[\text{M}+\text{H}]^+$ 313.1335, found 313.1342.

2-(4-Methoxyphenyl)-3-phenylquinazolin-4(3H)-one (3ac)



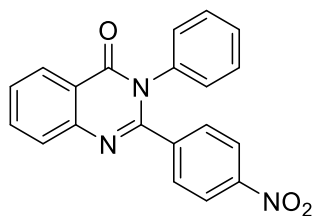
Off white solid (73 mg, 63%); mp 149–150 °C; ^1H NMR (400 MHz, CDCl_3) δ 8.37 (d, $J = 7.9$ Hz, 1H), 7.83 (d, $J = 3.5$ Hz, 2H), 7.56 – 7.52 (m, 1H), 7.37 – 7.30 (m, 3H), 7.31 (d, $J = 8.8$ Hz, 2H), 7.19 (d, $J = 7.0$ Hz, 2H), 6.74 (d, $J = 8.8$ Hz, 2H), 3.77 (s, 3H); ^{13}C NMR (100 MHz, CDCl_3) δ 162.5, 160.3, 154.9, 147.6, 137.9, 134.7, 130.8, 129.1, 129.0, 128.4, 127.8, 127.6, 127.2, 127.0, 120.8, 113.4, 55.3; IR (KBr): 3063, 1682, 1551, 1335, 1257 cm^{-1} ; HRMS calcd for $\text{C}_{21}\text{H}_{17}\text{N}_2\text{O}_2$ $[\text{M}+\text{H}]^+$ 329.1285, found 329.1290.

2-(4-Chlorophenyl)-3-phenylquinazolin-4(3H)-one (3ad)

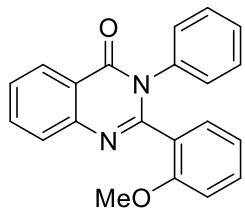


White solid (57 mg, 47%); mp 175–177 °C (Lit.^[72] 177–178 °C); ^1H NMR (400 MHz, CDCl_3) δ 8.38 (d, $J = 7.6$ Hz, 1H), 7.88 – 7.80 (m, 2H), 7.61 – 7.55 (m, 1H), 7.41 – 7.34 (m, 3H), 7.33 – 7.29 (m, 2H), 7.25 – 7.20 (m, 2H), 7.19 – 7.15 (m, 2H); ^{13}C NMR (100 MHz, CDCl_3) δ 162.2, 154.0, 147.3, 137.4, 135.6, 134.9, 133.9, 130.4, 129.2, 129.0, 128.7, 128.3, 127.7, 127.5, 127.3, 120.9; IR (KBr): 3055, 1682, 1589, 1342, 1265 cm^{-1} ; HRMS calcd for $\text{C}_{20}\text{H}_{14}\text{ClN}_2\text{O}$ $[\text{M}+\text{H}]^+$ 333.0789, found 333.0794.

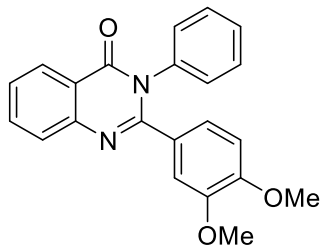
2-(4-Nitrophenyl)-3-phenylquinazolin-4(3H)-one (3ae)



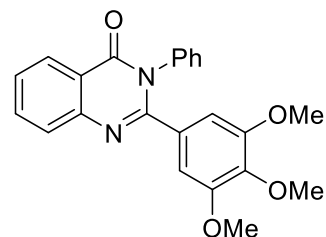
Light yellow solid (34 mg, 27%); mp 167–168 °C; ^1H NMR (400 MHz, CDCl_3) δ 8.40 (d, $J = 7.7$ Hz, 1H), 8.11 (d, $J = 8.8$ Hz, 2H), 7.921–7.84 (m, 2H), 7.64 – 7.60 (m, 1H), 7.57 (d, $J = 8.8$ Hz, 2H), 7.12 – 7.33 (m, 3H), 7.19 (dd, $J = 7.7, 1.5$ Hz, 2H); ^{13}C NMR (100 MHz, CDCl_3) δ 161.8, 152.9, 147.8, 147.1, 141.4, 137.0, 135.1, 130.2, 129.4, 129.1, 129.0, 128.1, 127.9, 127.5, 123.2, 121.1; IR (KBr): 3070, 1697, 1574, 1342, 1265 cm^{-1} ; HRMS calcd for $\text{C}_{20}\text{H}_{14}\text{N}_3\text{O}_3$ $[\text{M}+\text{H}]^+$ 344.1030, found 344.1037.

2-(2-Methoxyphenyl)-3-phenylquinazolin-4(3H)-one (3af)

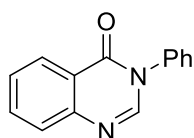
Off white solid (34 mg, 27%); mp 133–135 °C; ^1H NMR (400 MHz, CDCl_3) δ 8.40 (d, $J = 7.7$ Hz, 1H), 7.86 – 7.81 (m, 2H), 7.59 – 7.56 (m, 1H), 7.461–7.35 (m, 3H), 7.24 (t, $J = 7.8$ Hz, 2H), 7.17 (t, $J = 7.4$ Hz, 1H), 6.93 (t, $J = 7.4$ Hz, 2H), 6.62 (d, $J = 8.4$ Hz, 1H), 3.63 (s, 3H); ^{13}C NMR (100 MHz, CDCl_3) δ 162.2, 155.4, 154.1, 147.7, 137.1, 134.5, 131.1, 129.9, 128.8, 128.7, 128.4, 128.3, 127.9, 127.7, 127.2, 127.1, 124.9, 121.4, 120.4, 110.4, 54.9; IR (KBr): 3055, 1682, 1589, 1342, 1265 cm^{-1} ; HRMS calcd for $\text{C}_{21}\text{H}_{17}\text{N}_2\text{O}_2$ $[\text{M}+\text{H}]^+$ 329.1285, found 329.1290.

2-(3,4-Dimethoxyphenyl)-3-phenylquinazolin-4(3H)-one (3ag)

Off white solid (76 mg, 59%); mp 153–155 °C; ^1H NMR (400 MHz, CDCl_3) δ 8.35 (d, $J = 7.9$ Hz, 1H), 7.89 – 7.73 (m, 2H), 7.59 – 7.45 (m, 1H), 7.43 – 7.26 (m, 3H), 7.20 (d, $J = 7.2$ Hz, 2H), 7.05 (d, $J = 8.3$ Hz, 1H), 6.79 (s, 1H), 6.73 (d, $J = 8.4$ Hz, 1H), 3.83 (s, 3H), 3.66 (s, 3H); ^{13}C NMR (100 MHz, CDCl_3) δ 162.4, 154.7, 149.9, 148.1, 147.5, 138.1, 134.7, 129.1, 129.0, 128.4, 127.7, 127.6, 127.2, 127.1, 122.8, 120.8, 112.3, 110.4, 55.9, 55.8; IR (KBr): 3055, 1682, 1597, 1335, 1265 cm^{-1} ; HRMS calcd for $\text{C}_{22}\text{H}_{19}\text{N}_2\text{O}_3$ $[\text{M}+\text{H}]^+$ 359.1390, found 359.1395.

3-Phenyl-2-(3,4,5-trimethoxyphenyl)quinazolin-4(3H)-one (3ah)

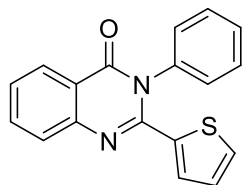
Off white solid (76 mg, 59%); mp 133–134 °C; ^1H NMR (400 MHz, CDCl_3) δ 8.38 (d, $J = 7.8$ Hz, 1H), 7.85 (d, $J = 2.8$ Hz, 2H), 7.56 (bs, 1H), 7.41 – 7.34 (m, 3H), 7.22 (d, $J = 7.2$ Hz, 2H), 6.60 (s, 2H), 3.80 (s, 3H), 3.70 (s, 6H); ^{13}C NMR (100 MHz, CDCl_3) δ 162.3, 154.6, 152.7, 147.4, 138.90, 138.0, 134.8, 130.3, 129.1, 128.9, 128.5, 127.7, 127.32, 127.2, 120.9, 106.9, 60.9, 56.1; IR (KBr): 2932, 1682, 1574, 1358, 1234 cm^{-1} ; HRMS calcd for $\text{C}_{23}\text{H}_{21}\text{N}_2\text{O}_4$ $[\text{M}+\text{H}]^+$ 389.1496, found 389.1501.

3-Phenylquinazolin-4(3H)-one (3ai)

Pale yellow solid (34 mg, 43%); mp 94–95 °C (Lit.^[73] 139–140 °C); ^1H NMR (400 MHz, CDCl_3) δ 8.39 (d, $J = 8.7$ Hz, 1H), 8.15 (s, 1H), 7.85 – 7.78 (m, 2H), 7.59 – 7.49 (m, 4H), 7.45 (d, $J = 7.2$ Hz, 2H); ^{13}C NMR (100 MHz, CDCl_3) δ

160.8, 147.9, 146.1, 137.5, 134.6, 129.7, 129.1, 127.7, 127.6, 127.2, 127.0, 122.4; IR (KBr): 3055, 1666, 1605, 1466, 1281 cm^{-1} ; HRMS calcd for $\text{C}_{14}\text{H}_{11}\text{N}_2\text{O}$ $[\text{M}+\text{H}]^+$ 223.0866, found 223.0870.

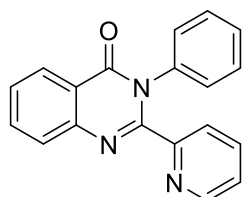
3-Phenyl-2-(thiophen-2-yl)quinazolin-4(3H)-one (3aj)



Pale white solid (58 mg, 53%); mp 172–174 °C; ^1H NMR (400 MHz, CDCl_3) δ 8.39 (dd, $J = 8.0, 0.9$ Hz, 1H), 8.11 (d, $J = 11.1$ Hz, 2H), 7.90 – 7.80 (m, 2H), 7.63 – 7.59 (m, 1H), 7.58 (t, $J = 1.9$ Hz, 1H), 7.56 (t, $J = 7.6$ Hz, 1H), 7.17 (d, $J = 8.0$ Hz, 2H), 7.05 (d, $J = 8.3$ Hz, 2H); ^{13}C NMR (100 MHz, CDCl_3) δ 162.0, 153.1, 147.8, 147.1, 141.5, 139.2, 135.0, 134.3, 130.3, 130.2, 130.1, 128.6, 128.0,

127.9, 127.4, 123.2, 121.1; IR (KBr): 3055, 1682, 1543, 1327, 1265 cm^{-1} ; HRMS calcd for $\text{C}_{18}\text{H}_{13}\text{N}_2\text{OS}$ $[\text{M}+\text{H}]^+$ 305.0743, found 305.0749.

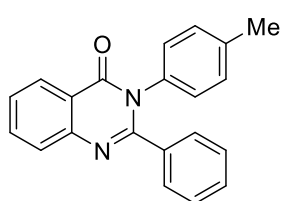
3-Phenyl-2-(pyridin-2-yl)quinazolin-4(3H)-one (3aj)



Light brown solid (58 mg, 53%); mp 153–155 °C; ^1H NMR (400 MHz, CDCl_3) δ 8.41 (d, $J = 7.1$ Hz, 2H), 7.89 – 7.83 (m, 2H), 7.65 (t, $J = 6.9$ Hz, 1H), 7.59 (t, $J = 7.3$ Hz, 1H), 7.53 (d, $J = 7.8$ Hz, 1H), 7.34 – 7.27 (m, 3H), 7.23 – 7.19 (m, 2H), 7.18 – 7.16 (m, 1H); ^{13}C NMR (100 MHz, CDCl_3) δ

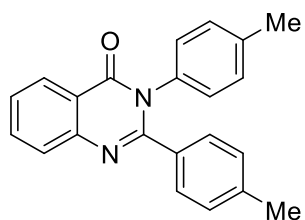
162.1, 153.4, 153.3, 148.9, 147.3, 137.4, 136.4, 134.8, 129.0, 128.8, 128.3, 128.0, 127.7, 127.3, 124.3, 123.7, 121.5; IR (KBr): 3055, 1681, 1589, 1342, 1281 cm^{-1} ; HRMS calcd for $\text{C}_{19}\text{H}_{14}\text{N}_3\text{O}$ $[\text{M}+\text{H}]^+$ 300.1131, found 300.1136.

2-Phenyl-3-*p*-tolylquinazolin-4(3H)-one (3ba)

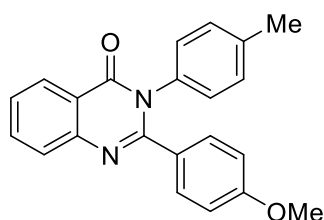


Off white solid (65 mg, 61%); mp 168–170 °C (Lit.^[72] 180–181 °C); ^1H NMR (400 MHz, CDCl_3) δ 8.38 (d, $J = 7.8$ Hz, 1H), 7.84 (dd, $J = 4.4, 1.6$ Hz, 2H), 7.58–7.54 (m, 1H), 7.37 (dd, $J = 7.8, 1.4$ Hz, 2H), 7.30 – 7.22 (m, 3H), 7.14 (d, $J = 8.1$ Hz, 2H), 7.05 (d, $J = 8.3$ Hz, 2H), 2.33 (s, 3H); ^{13}C

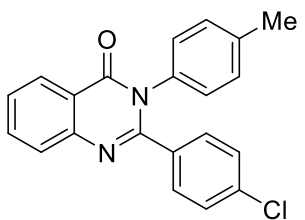
NMR (100 MHz, CDCl_3) δ 162.4, 155.4, 147.5, 138.4, 135.6, 135.0, 134.7, 129.7, 129.3, 129.0, 128.7, 128.0, 127.7, 127.2, 127.2, 121.0, 21.2; IR (KBr): 3040, 1682, 1589, 1342, 1250 cm^{-1} ; HRMS calcd for $\text{C}_{21}\text{H}_{17}\text{N}_2\text{O}$ $[\text{M}+\text{H}]^+$ 313.1335, found 313.1339.

2,3-Di-*p*-tolylquinazolin-4(3*H*)-one (3bb)

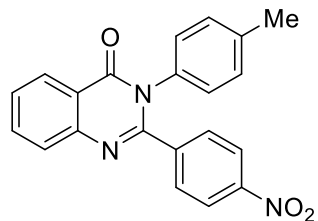
White solid (65 mg, 65%); mp 172–173 °C (Lit.^[72] 170–171 °C); ¹H NMR (400 MHz, CDCl₃) δ 8.37 (d, *J* = 7.7 Hz, 1H), 7.84 – 7.79 (m, 2H), 7.55 – 7.51 (m, 1H), 7.27 (d, *J* = 8.1 Hz, 2H), 7.15 (d, *J* = 8.1 Hz, 2H), 7.06 (d, *J* = 4.4 Hz, 2H), 7.04 (d, *J* = 4.1 Hz, 2H), 2.34 (s, 3H), 2.30 (s, 3H); ¹³C NMR (100 MHz, CDCl₃) δ 162.5, 155.5, 147.6, 139.4, 138.3, 135.2, 134.6, 132.7, 129.7, 129.0, 128.7, 128.7, 127.7, 127.2, 127.0, 120.9, 21.4, 21.2; IR (KBr): 3024, 1682, 1574, 1342, 1265 cm⁻¹; HRMS calcd for C₂₂H₁₉N₂O [M+H]⁺ 327.1492, found 327.1498.

2-(4-Methoxyphenyl)-3-*p*-tolylquinazolin-4(3*H*)-one (3bc)

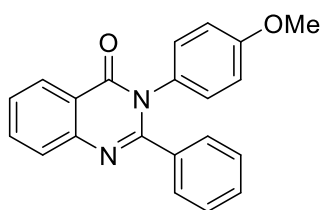
Off white solid (54 mg, 54 % yield); mp 154–155 °C; ¹H NMR (400 MHz, CDCl₃) δ 8.35 (d, *J* = 7.7 Hz, 1H), 7.83 – 7.78 (m, 2H), 7.55 – 7.50 (m, 1H), 7.32 (d, *J* = 8.9 Hz, 2H), 7.16 (d, *J* = 8.0 Hz, 2H), 7.06 (d, *J* = 8.3 Hz, 2H), 6.75 (d, *J* = 8.9 Hz, 2H), 3.77 (s, 3H), 2.35 (s, 3H); ¹³C NMR (100 MHz, CDCl₃) δ 162.6, 160.2, 155.1, 147.6, 138.3, 135.2, 134.6, 130.8, 129.7, 128.7, 128.0, 127.6, 127.2, 126.9, 120.8, 113.4, 55.3, 21.2; IR (KBr): 3055, 1682, 1589, 1341, 1265 cm⁻¹; HRMS calcd for C₂₂H₁₉N₂O₂ [M+H]⁺ 343.1441, found 343.1448.

2-(4-Chlorophenyl)-3-*p*-tolylquinazolin-4(3*H*)-one (3bd)

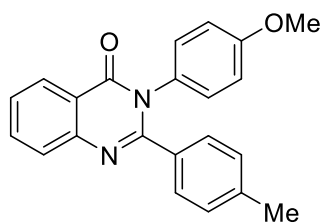
White solid (59 mg, 50%); mp 186–188 °C; ¹H NMR (400 MHz, CDCl₃) δ 8.35 (d, *J* = 7.9 Hz, 1H), 7.81 (d, *J* = 3.6 Hz, 2H), 7.56 – 7.52 (m, 1H), 7.32 (d, *J* = 8.5 Hz, 2H), 7.22 (d, *J* = 8.5 Hz, 2H), 7.16 (d, *J* = 8.0 Hz, 2H), 7.04 (d, *J* = 8.2 Hz, 2H), 2.35 (s, 3H); ¹³C NMR (100 MHz, CDCl₃) δ 162.3, 154.2, 147.3, 138.7, 135.5, 134.8, 134.7, 134.0, 130.5, 129.9, 128.7, 128.3, 127.7, 127.44, 127.3, 120.9, 21.2; IR (KBr): 3024, 1682, 1574, 1342, 1265 cm⁻¹; HRMS calcd for C₂₁H₁₆ClN₂O [M+H]⁺ 347.0946, found 347.0951.

2-(4-Nitrophenyl)-3-*p*-tolylquinazolin-4(3*H*)-one (3be)

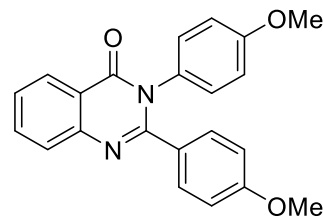
Pale yellow solid (59 mg, 43% yield); mp 166–168 °C; ¹H NMR (400 MHz, CDCl₃) δ 8.39 (d, *J* = 8.8 Hz, 1H), 8.12 (d, *J* = 8.9 Hz, 2H), 7.89 – 7.82 (m, 2H), 7.62 (d, *J* = 6.8 Hz, 1H), 7.57 (d, *J* = 8.9 Hz, 2H), 7.17 (d, *J* = 8.1 Hz, 2H), 7.05 (d, *J* = 8.3 Hz, 2H), 2.35 (s, 3H); ¹³C NMR (100 MHz, CDCl₃) δ 162.0, 153.1, 147.8, 147.1, 141.5, 139.2, 135.0, 134.3, 130.2, 130.1, 128.6, 128.0, 127.9, 127.4, 123.2, 121.1, 21.2; IR (KBr): 3069, 1695, 1572, 1344, 1266 cm⁻¹; HRMS calcd for C₂₁H₁₆N₃O₃ [M+H]⁺ 358.1186, found 358.1190.

3-(4-Methoxyphenyl)-2-phenylquinazolin-4(3*H*)-one (3ca)

Off white solid (59 mg, 55%); mp 198–200 °C (Lit.^[72] 199–200 °C); ¹H NMR (400 MHz, CDCl₃) δ 8.38 (d, *J* = 7.7 Hz, 1H), 7.86 – 7.80 (m, 2H), 7.57 – 7.54 (m, 1H), 7.39 – 7.35 (m, 2H), 7.29 – 7.23 (m, 3H), 7.08 (d, *J* = 7.1 Hz, 2H), 6.84 (d, *J* = 6.8 Hz, 2H), 3.79 (s, 3H); ¹³C NMR (100 MHz, CDCl₃) δ 162.6, 159.2, 155.5, 147.5, 135.6, 134.7, 130.3, 130.0, 129.2, 129.0, 128.1, 127.7, 127.2, 121.0, 114.2, 55.4; IR (KBr): 3040, 1682, 1558, 1342, 1250 cm⁻¹; HRMS calcd for C₂₁H₁₇N₂O₂ [M+H]⁺ 329.1285, found 329.1290.

3-(4-Methoxyphenyl)-2-*p*-tolylquinazolin-4(3*H*)-one (3cb)

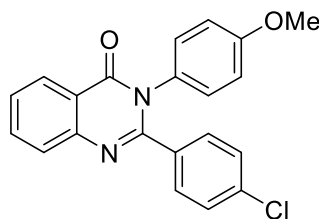
Off white solid (46 mg, 41%); mp 235–237 °C; ¹H NMR (400 MHz, CDCl₃) δ 8.37 (d, *J* = 7.8 Hz, 1H), 7.84 – 7.81 (m, 2H), 7.56 – 7.53 (m, 1H), 7.26 (d, *J* = 8.1 Hz, 2H), 7.08 (d, *J* = 8.9 Hz, 2H), 7.05 (d, *J* = 8.0 Hz, 2H), 6.86 (d, *J* = 8.9 Hz, 2H), 3.81 (s, 3H), 2.31 (s, 3H); ¹³C NMR (100 MHz, CDCl₃) δ 162.7, 159.1, 155.6, 147.6, 139.4, 134.6, 132.8, 130.5, 130.0, 129.0, 128.7, 127.7, 127.2, 127.1, 120.9, 114.2, 55.4, 21.3; IR (KBr): 3050, 1682, 1589, 1342, 1250 cm⁻¹; HRMS calcd for C₂₂H₁₉N₂O₂ [M+H]⁺ 343.1441, found 343.1444.

2,3-Bis(4-methoxyphenyl)quinazolin-4(3*H*)-one (3cc)

Off white solid (46 mg, 39%); mp 136–138 °C; ¹H NMR (400 MHz, CDCl₃) δ 8.35 (d, *J* = 7.7 Hz, 1H), 7.84 – 7.77 (m, 2H), 7.54 – 7.50 (m, 1H), 7.32 (d, *J* = 8.9 Hz, 2H), 7.09 (d, *J* = 9.0 Hz, 2H), 6.87 (d, *J* = 9.0 Hz, 2H), 6.76 (d, *J* = 8.9 Hz, 2H), 3.80 (s, 3H), 3.78 (s, 3H); ¹³C NMR (100 MHz, CDCl₃) δ 162.7, 160.2, 159.1, 155.3, 147.6, 134.6, 130.8,

130.5, 130.0, 127.9, 127.6, 127.2, 127.0, 120.8, 114.3, 113.4, 55.4, 55.3; IR (KBr) 3050, 1682, 1589, 1342, 1250 cm^{-1} ; HRMS calcd for $\text{C}_{22}\text{H}_{19}\text{N}_2\text{O}_3$ $[\text{M}+\text{H}]^+$ 359.1390, found 359.1394.

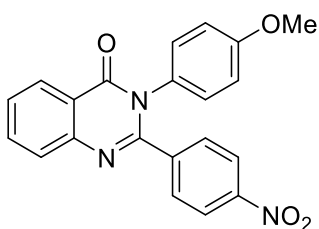
2-(4-Chlorophenyl)-3-(4-methoxyphenyl)quinazolin-4(3H)-one (3cd)



White solid (44 mg, 37%); mp 166–168 °C; ^1H NMR (400 MHz, CDCl_3) δ 8.37 (d, $J = 7.6$ Hz, 1H), 7.86–7.80 (m, 2H), 7.59–7.53 (m, $J = 8.2, 6.0, 2.4$ Hz, 1H), 7.32 (d, $J = 8.7$ Hz, 2H), 7.24 (d, $J = 8.7$ Hz, 2H), 7.07 (d, $J = 9.0$ Hz, 2H), 6.87 (d, $J = 8.9$ Hz, 2H), 3.82 (s, 3H); ^{13}C NMR (100 MHz, CDCl_3) δ 162.4, 159.7, 154.4, 147.4, 135.5, 134.8,

134.1, 130.4, 130.0, 129.9, 128.4, 127.7, 127.4, 127.3, 121.0, 114.4, 55.4; IR (KBr): 3055, 1682, 1570, 1342, 1265 cm^{-1} ; HRMS calcd for $\text{C}_{21}\text{H}_{16}\text{ClN}_2\text{O}_2$ $[\text{M}+\text{H}]^+$ 363.0895, found 363.0901.

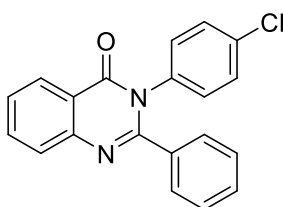
3-(4-Methoxyphenyl)-2-(4-nitrophenyl)quinazolin-4(3H)-one (3ce)



Pale yellow solid (32 mg, 26%); mp 151–152 °C; ^1H NMR (400 MHz, CDCl_3) δ 8.38 (d, $J = 7.6$ Hz, 1H), 8.12 (d, $J = 8.8$ Hz, 2H), 7.90–7.79 (m, 2H), 7.64–7.52 (m, 3H), 7.08 (d, $J = 8.8$ Hz, 2H), 6.86 (d, $J = 8.8$ Hz, 2H), 3.80 (s, 3H); ^{13}C NMR (101 MHz, CDCl_3) δ 162.1, 159.6, 153.2, 147.7, 147.1, 141.6, 135.0, 130.1, 129.9, 129.4, 128.0, 127.9,

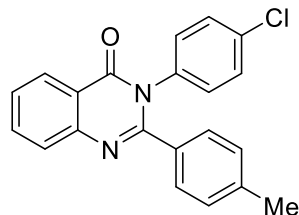
127.4, 123.3, 121.1, 114.6, 55.4; IR (KBr) 3070, 1697, 1574, 1342, 1265 cm^{-1} ; HRMS calcd for $\text{C}_{21}\text{H}_{16}\text{N}_3\text{O}_4$ $[\text{M}+\text{H}]^+$ 374.1135, found 374.1142.

3-(4-Chlorophenyl)-2-phenylquinazolin-4(3H)-one (3fa)

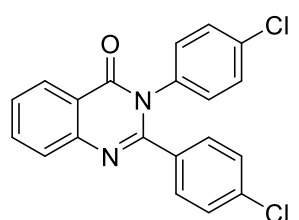


Off white solid (56 mg, 52%); mp 191–193 °C (Lit.^[72] 198–199 °C); ^1H NMR (400 MHz, CDCl_3) δ 8.36 (d, $J = 7.9$ Hz, 1H), 7.84 (d, $J = 3.6$ Hz, 2H), 7.58–7.54 (m, 1H), 7.38–7.23 (m, 7H), 7.12 (d, $J = 8.6$ Hz, 2H); ^{13}C NMR (100 MHz, CDCl_3) δ 162.2, 154.8, 147.4, 136.2, 135.2, 134.9, 134.4, 130.4, 129.6, 129.3, 129.0, 128.3, 127.8, 127.5, 127.2, 120.8; IR

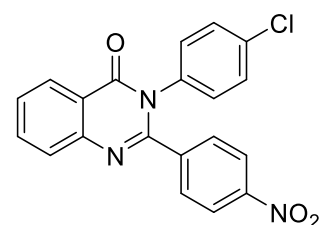
(KBr): 3065, 1691, 1562, 1342, 1265 cm^{-1} ; HRMS calcd for $\text{C}_{20}\text{H}_{14}\text{ClN}_2\text{O}$ $[\text{M}+\text{H}]^+$ 333.0789, found 333.0794.

3-(4-Chlorophenyl)-2-*p*-tolylquinazolin-4(3*H*)-one (3fb)

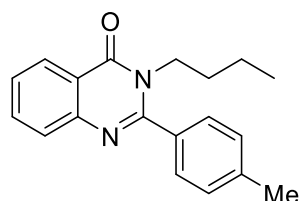
Off white solid (58 mg, 52%); mp 136–138 °C; ^1H NMR (400 MHz, CDCl_3) δ 8.35 (d, $J = 7.9$ Hz, 1H), 7.83 (d, $J = 3.6$ Hz, 2H), 7.57 – 7.53 (m, 1H), 7.32 (d, $J = 8.6$ Hz, 2H), 7.24 (d, $J = 8.1$ Hz, 2H), 7.12 (d, $J = 8.6$ Hz, 2H), 7.07 (d, $J = 8.0$ Hz, 2H), 2.32 (s, 3H). ^{13}C NMR (100 MHz, CDCl_3) δ 162.3, 154.9, 147.5, 139.8, 136.4, 134.9, 134.3, 132.3, 130.4, 129.2, 129.0, 128.9, 127.8, 127.3, 127.2, 120.7, 21.4; IR (KBr): 3065, 1691, 1562, 1342, 1265 cm^{-1} ; HRMS calcd for $\text{C}_{21}\text{H}_{16}\text{ClN}_2\text{O}$ $[\text{M}+\text{H}]^+$ 347.0946, found 347.0950.

2,3-Bis(4-chlorophenyl)quinazolin-4(3*H*)-one (3fd)

Off white solid (60 mg, 51%); mp 177–178 °C (Lit.^[72] 182–183 °C); ^1H NMR (400 MHz, CDCl_3) δ 8.35 (d, $J = 8.2$ Hz, 1H), 7.87 – 7.81 (m, 2H), 7.62 – 7.52 (m, 1H), 7.35 (d, $J = 8.6$ Hz, 2H), 7.31 (d, $J = 8.7$ Hz, 2H), 7.26 (d, $J = 8.6$ Hz, 2H), 7.12 (d, $J = 8.6$ Hz, 2H); ^{13}C NMR (100 MHz, CDCl_3) δ 162.0, 153.6, 147.2, 135.9, 135.9, 135.1, 134.7, 133.6, 130.4, 130.3, 129.5, 128.6, 127.8, 127.7, 127.3, 120.7; IR (KBr): 3064, 1691, 1566, 1343, 1268 cm^{-1} ; HRMS calcd for $\text{C}_{20}\text{H}_{13}\text{Cl}_2\text{N}_2\text{O}$ $[\text{M}+\text{H}]^+$ 367.0399, found 367.0404.

3-(4-Chlorophenyl)-2-(4-nitrophenyl)quinazolin-4(3*H*)-one (3fe)

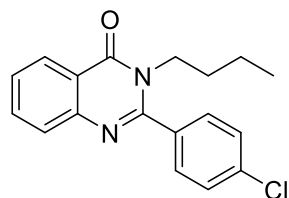
Off white solid (58 mg, 48%); mp 157–159 °C; ^1H NMR (400 MHz, CDCl_3) δ 8.36 (d, $J = 7.6$ Hz, 1H), 7.88 – 7.81 (m, 2H), 7.60 – 7.56 (m, 1H), 7.35 (d, $J = 8.6$ Hz, 2H), 7.31 (d, $J = 8.7$ Hz, 2H), 7.26 (d, $J = 8.7$ Hz, 2H), 7.12 (d, $J = 8.6$ Hz, 2H); ^{13}C NMR (100 MHz, CDCl_3) δ 162.1, 153.6, 147.2, 135.9, 135.9, 135.1, 134.7, 133.6, 130.4, 130.3, 129.5, 128.6, 127.8, 127.7, 127.3, 120.7; IR (KBr): 3070, 1696, 1589, 1380, 1271 cm^{-1} ; HRMS calcd for $\text{C}_{20}\text{H}_{13}\text{ClN}_3\text{O}_3$ $[\text{M}+\text{H}^+]$ 378.0640, found 378.0644.

3-Butyl-2-*p*-tolylquinazolin-4(3*H*)-one (3gb)

Pale yellow semisolid (61 mg, 53%); ^1H NMR (400 MHz, CDCl_3) δ 8.34 (d, $J = 8.4$ Hz, 1H), 7.79 – 7.72 (m, 1H), 7.53 – 7.49 (m, 1H), 7.43 (d, $J = 7.4$ Hz, 1H), 7.33 (d, $J = 7.9$ Hz, 1H), 4.053– 3.99 (m, 2H), 2.46 (s, 3H), 1.65 – 1.57 (m, 2H), 1.21 – 1.14 (m, 2H), 0.79 (t, $J = 7.4$ Hz, 3H); ^{13}C NMR (100 MHz, CDCl_3) δ 162.3, 156.5, 147.2, 139.9, 134.2, 132.7,

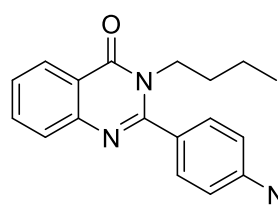
129.4, 127.7, 127.4, 126.8, 126.7, 120.9, 45.8, 30.8, 21.4, 19.9, 13.5; IR (KBr): 3055, 1681, 1561, 1373, 1265 cm^{-1} ; HRMS calcd for $\text{C}_{19}\text{H}_{21}\text{N}_2\text{O}$ $[\text{M}+\text{H}]^+$ 293.1648, found 293.1652.

3-Butyl-2-(4-chlorophenyl)quinazolin-4(3H)-one (3gd)



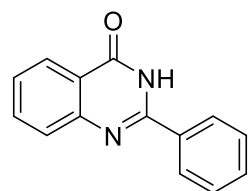
Pale yellow oil (62 mg, 51%); ^1H NMR (400 MHz, CDCl_3) δ 8.43 (d, $J = 8.8$ Hz, 2H), 8.37 (d, $J = 6.9$ Hz, 1H), 7.85 – 7.80 (m, 1H), 7.78 (d, $J = 8.8$ Hz, 2H), 7.73 (d, $J = 8.7$ Hz, 1H), 7.58 (d, $J = 7.6$ Hz, 1H), 3.99 – 3.95 (m, 2H), 1.64 – 1.57 (m, 2H), 1.26 – 1.18 (m, 2H), 0.81 (t, $J = 7.4$ Hz, 3H); ^{13}C NMR (100 MHz, CDCl_3) δ 162.0, 155.1, 147.0, 136.0, 134.4, 133.9, 129.3, 129.0, 127.4, 127.2, 126.8, 120.9, 45.7, 30.8, 19.9, 13.45; IR (KBr) 3062, 1684, 1589, 1366, 1250 cm^{-1} ; HRMS calcd for $\text{C}_{18}\text{H}_{18}\text{ClN}_2\text{O}$ $[\text{M}+\text{H}]^+$ 313.1102, found 313.1108.

3-Butyl-2-(4-nitrophenyl)quinazolin-4(3H)-one (3ge)



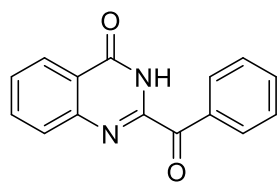
Pale yellow solid (61 mg, 48%); mp 133 – 136 $^{\circ}\text{C}$; ^1H NMR (400 MHz, CDCl_3) δ 8.43 (d, $J = 8.8$ Hz, 2H), 8.37 (d, $J = 6.9$ Hz, 1H), 7.85 – 7.80 (m, 1H), 7.78 (d, $J = 8.8$ Hz, 2H), 7.73 (d, $J = 8.7$ Hz, 1H), 7.58 (d, $J = 7.6$ Hz, 1H), 3.99 – 3.95 (m, 2H), 1.64 – 1.57 (m, 2H), 1.26 – 1.18 (m, 2H), 0.81 (t, $J = 7.4$ Hz, 3H); ^{13}C NMR (100 MHz, CDCl_3) δ 161.7, 153.9, 148.5, 146.8, 141.4, 134.6, 129.3, 127.7, 127.5, 126.9, 124.1, 121.0, 45.8, 30.9, 19.9, 13.5; IR (KBr): 3068, 1693, 1579, 1382, 1271; HRMS calcd for $\text{C}_{18}\text{H}_{18}\text{N}_3\text{O}_3$ $[\text{M}+\text{H}]^+$ 324.1343, found 324.1348.

2-Phenylquinazolin-4(3H)-one (3da)



White solid (41 mg, 37%); mp 238–240 $^{\circ}\text{C}$; ^1H NMR (400 MHz, $\text{DMSO}-d_6$) δ 12.58 (s, 1H), 8.21 – 8.16 (m, 3H), 7.85 (t, $J = 8.4$ Hz, 1H), 7.76 (d, $J = 7.6$ Hz, 1H), 7.63 – 7.52 (m, 4H); ^{13}C NMR (100 MHz, $\text{DMSO}-d_6$) δ 162.7, 152.8, 149.2, 135.1, 133.2, 131.9, 129.1, 128.2, 128.0, 127.1, 126.3, 121.4; IR (KBr): 3055, 1670, 1565, 1348, 1265 cm^{-1} ; HRMS calcd for $\text{C}_{14}\text{H}_{11}\text{N}_2\text{O}$ $[\text{M}+\text{H}]^+$ 223.0866, found 223.0869.

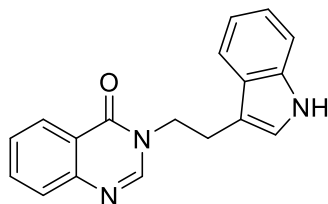
2-Benzoylquinazolin-4(3H)-one (3db)



Off white solid (25 mg, 23%); mp 178–180 $^{\circ}\text{C}$; ^1H NMR (400 MHz, $\text{DMSO}-d_6$) δ 12.73 (bs, 1H), 8.23 (d, $J = 8.2$ Hz, 1H), 8.17 (dd, $J = 8.3, 1.2$ Hz, 2H), 7.92 – 7.88 (m, 1H), 7.79 (d, $J = 7.6$ Hz, 1H), 7.77 – 7.73 (m, 1H), 7.67 (t, $J = 7.5$ Hz, 1H), 7.61 (t, $J = 7.8$ Hz, 2H); ^{13}C NMR (100 MHz,

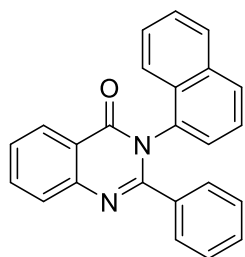
DMSO-*d*₆) δ 187.7, 161.5, 149.5, 147.6, 135.3, 134.8, 134.5, 131.3, 129.1, 128.8, 126.5, 123.3; IR (KBr): 3062, 1696, 1578, 1335, 1265 cm⁻¹; HRMS calcd for C₁₅H₁₁N₂O₂ [M+H]⁺ 251.0815, found 251.0820.

3-(2-(1*H*-Indol-3-yl)ethyl)quinazolin-4(3*H*)-one (3ea)



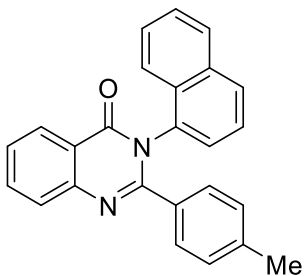
Pale yellow solid (37 mg, 44%); mp 170–171 °C; ¹H NMR (400 MHz, CDCl₃) δ 8.39 (d, *J* = 7.4 Hz, 1H), 8.29 (bs, 1H), 7.77 (t, *J* = 7.0 Hz, 1H), 7.68 (d, *J* = 7.7 Hz, 1H), 7.66 (d, *J* = 7.7 Hz, 1H), 7.56 (s, 1H), 7.53 (s, *J* = 7.6 Hz, 1H), 7.37 (d, *J* = 8.1 Hz, 1H), 7.23 (t, *J* = 7.3 Hz, 1H), 7.15 (t, *J* = 7.3 Hz, 1H), 6.87 (d, *J* = 6.9 Hz, 1H), 4.32 (t, *J* = 6.7 Hz, 3H), 3.29 (t, *J* = 6.7 Hz, 3H); ¹³C NMR (100 MHz, CDCl₃) δ 161.1, 148.1, 146.8, 136.5, 134.2, 127.3, 127.2, 126.8, 126.7, 122.8, 122.4, 122.1, 119.8, 118.4, 111.6, 111.3, 47.6, 25.0; IR (KBr): 3371, 3055, 1674, 1612, 1373, 1327 cm⁻¹; HRMS calcd for C₁₈H₁₆N₃O [M+H]⁺ 290.1288, found 290.1295.

3-(Naphthalen-1-yl)-2-phenylquinazolin-4(3*H*)-one (3ha)



Light pink solid (71 mg, 67%); mp 212–213 °C; ¹H NMR (400 MHz, CDCl₃) δ 8.43 (dd, *J* = 7.9, 1.0 Hz, 1H), 7.93 (t, *J* = 8.3 Hz, 1H), 7.91 – 7.84 (m, 2H), 7.82 (d, *J* = 8.3 Hz, 1H), 7.71 (d, *J* = 7.9 Hz, 1H), 7.62 – 7.52 (m, 3H), 7.38 (t, *J* = 7.4 Hz, 1H), 7.27 (dd, *J* = 7.2, 1.4 Hz, 3H), 7.15 (t, *J* = 6.9 Hz, 1H), 7.05 (t, *J* = 7.5 Hz, 2H); ¹³C NMR (100 MHz, CDCl₃) δ 162.3, 156.2, 147.7, 135.3, 135.0, 134.6, 134.0, 130.5, 129.5, 129.4, 128.6, 128.1, 127.9, 127.7, 127.6, 127.5, 127.4, 127.4, 126.5, 125.1, 122.4, 121.0; IR (KBr): 3055, 1682, 1588, 1340, 1265 cm⁻¹; HRMS calcd for C₂₄H₁₇N₂O [M+H]⁺ 349.1335, found 349.1341.

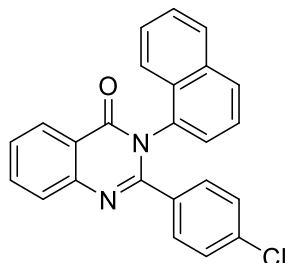
3-(Naphthalen-1-yl)-2-*p*-tolylquinazolin-4(3*H*)-one (3hb)



Light pink solid (79 mg, 71%); mp 208–209 °C; ¹H NMR (400 MHz, CDCl₃) δ 8.40 (dd, *J* = 8.0, 0.8 Hz, 1H), 7.93 – 7.86 (m, 3H), 7.84 (d, *J* = 8.3 Hz, 1H), 7.69 (d, *J* = 9.0 Hz, 1H), 7.61 – 7.56 (m, 1H), 7.55 – 7.49 (m, 2H), 7.40 (t, *J* = 7.8 Hz, 1H), 7.26 (t, *J* = 7.3 Hz, 2H), 7.15 (d, *J* = 8.1 Hz, 2H), 6.85 (d, *J* = 8.0 Hz, 2H), 2.20 (s, 3H). ¹³C NMR (100 MHz, CDCl₃) δ 162.4, 156.3, 147.8, 139.5, 134.8, 134.7, 134.0, 132.4, 130.5, 129.4, 128.6, 128.4, 128.1, 127.8, 127.5, 127.5, 127.3, 127.2, 126.5, 125.2, 122.4, 120.8,

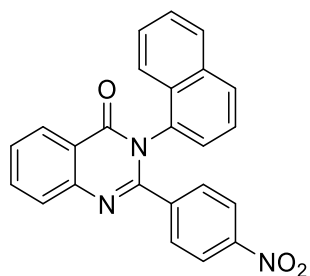
21.2. IR (KBr): 3055, 1682, 1589, 1342, 1265 cm^{-1} ; HRMS calcd for $\text{C}_{25}\text{H}_{19}\text{N}_2\text{O}$ [$\text{M}+\text{H}^+$] 363.1492, found 363.1496.

2-(4-Chlorophenyl)-3-(naphthalen-1-yl)quinazolin-4(3H)-one (3hd)



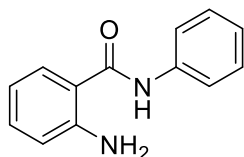
Off white solid (66 mg, 56%); mp 216–218 $^{\circ}\text{C}$; ^1H NMR (400 MHz, CDCl_3) δ 8.41 (d, $J = 7.2$ Hz, 1H), 7.91 (s, 4H), 7.73 – 7.50 (m, 4H), 7.41 (t, $J = 7.4$ Hz, 1H), 7.24 (dd, $J = 19.0, 7.2$ Hz, 3H), 7.04 (d, $J = 7.5$ Hz, 2H); ^{13}C NMR (100 MHz, CDCl_3) δ 162.2, 155.1, 147.6, 135.6, 135.0, 134.3, 134.04, 133.7, 130.4, 129.8, 129.5, 128.8, 128.1, 127.9, 127.8, 127.6, 127.5, 127.4, 126.7, 125.2, 122.1, 120.9; IR (KBr): 3055, 1682, 1590, 1327, 1265 cm^{-1} ; HRMS calcd for $\text{C}_{24}\text{H}_{16}\text{ClN}_2\text{O}$ [$\text{M}+\text{H}^+$] 383.0946, found 383.0951.

3-(Naphthalen-1-yl)-2-(4-nitrophenyl)quinazolin-4(3H)-one (3he)

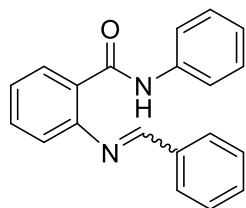


Pale yellow solid (55 mg, 46%); mp 256–257 $^{\circ}\text{C}$; ^1H NMR (400 MHz, CDCl_3) δ 8.43 (d, $J = 8.1$ Hz, 1H), 7.96 – 7.89 (m, 5H), 7.87 (d, $J = 8.3$ Hz, 1H), 7.71 – 7.62 (m, 2H), 7.61 – 7.52 (m, 2H), 7.46 (d, $J = 8.8$ Hz, 2H), 7.40 (t, $J = 7.8$ Hz, 1H), 7.28 (d, $J = 7.2$ Hz, 2H); ^{13}C NMR (100 MHz, CDCl_3) δ 161.9, 154.0, 147.9, 147.3, 141.1, 135.2, 134.1, 133.8, 130.2, 130.2, 129.2, 129.0, 128.1, 128.0, 127.9, 127.6, 127.5, 127.0, 125.2, 122.9, 122.0, 121.0; IR (KBr): 3070, 1694, 1574, 1342, 1265 cm^{-1} ; HRMS calcd for $\text{C}_{24}\text{H}_{16}\text{N}_3\text{O}_3$ [$\text{M}+\text{H}^+$] 394.1186, found 394.1190.

2-Amino-N-phenylbenzamide (1a)



White solid (58 mg, 38%); mp 127–129 $^{\circ}\text{C}$ (Lit.^[19] 130–132 $^{\circ}\text{C}$); ^1H NMR (400 MHz, $\text{DMSO}-d_6$) δ 10.00 (s, 1H), 7.72 (d, $J = 7.6$ Hz, 2H), 7.62 (dd, $J = 7.9, 1.1$ Hz, 1H), 7.33 (t, $J = 7.9$ Hz, 2H), 7.21 (t, $J = 8.3$ Hz, 1H), 7.08 (t, $J = 7.4$ Hz, 1H), 6.76 (d, $J = 8.8$ Hz, 1H), 6.60 (t, $J = 8.0$ Hz, 1H), 6.33 (s, 2H); ^{13}C NMR (100 MHz, $\text{DMSO}-d_6$) δ 168.3, 150.2, 139.7, 132.5, 129.2, 129.0, 123.8, 121.0, 116.8, 115.7, 115.2; IR (KBr): 3472, 3294, 1643, 1528, 1319, 1257 cm^{-1} .

2-(Benzylideneamino)-N-phenylbenzamide (17aa)

Off white solid (37 mg, 17%); mp 216–217 °C; ^1H NMR (400 MHz, DMSO- d_6) δ 7.73 (dd, $J = 7.8, 1.5$ Hz, 1H), 7.66 (d, $J = 2.6$ Hz, 1H), 7.39 (dd, $J = 8.1, 1.1$ Hz, 2H), 7.36 – 7.23 (m, 7H), 7.22 – 7.16 (m, 1H), 6.77 (d, $J = 8.1$ Hz, 1H), 6.72 (t, $J = 7.5$ Hz, 1H), 6.29 (d, $J = 2.7$ Hz, 1H); ^{13}C NMR (100 MHz, DMSO- d_6) δ 162.7, 147.0, 141.3, 141.2, 134.2, 129.1, 128.8, 128.8, 128.4, 127.0, 126.7, 126.5, 118.0, 115.8, 115.3, 73.1; IR (KBr): 3294, 1636, 1512, 1311, 1250 cm^{-1} .

2-Amino-N-(2-bromophenyl)benzamide (3i'): White solid (41 mg, 50%); mp 116 – 117 °C; ^1H NMR (400 MHz, CDCl_3) δ 8.46 (dd, $J = 8.2, 1.0$ Hz, 1H), 8.37 (bs, 1H), 7.60 (t, $J = 6.8$ Hz, 2H), 7.39 (t, $J = 7.8$ Hz, 1H), 7.31 (t, $J = 7.8$ Hz, 1H), 7.06 – 7.01 (m, 1H), 6.77 (t, $J = 7.7$ Hz, 2H), 5.65 (bs, 2H); ^{13}C NMR (100 MHz, CDCl_3) δ 167.29, 149.45, 135.91, 133.13, 132.3, 128.4, 127.2, 125.1, 122.0, 117.7, 117.0, 115.5, 114.1; IR (cm^{-1}) 3475, 3292, 1627, 1527, 1321, 1267. HRMS for $\text{C}_{13}\text{H}_{12}\text{BrN}_2\text{O}$ [$\text{M}+\text{H}^+$] calcd 291.0128, found 292.0125 and [$\text{M}+2+\text{H}^+$] 293.0107.

2C.5 REFERENCES

- [1] S. Lee, J.-K. Son, B. Jeong, T.-C. Jeong, H. Chang, E.-S. Lee, Y. Jahng, *Molecules*, **2008**, *13*, 272.
- [2] J. P. Michael, *Natural Product Reports*, **2008**, *25*, 166-187.
- [3] U. A. Kshirsagar, *Organic & Biomolecular Chemistry*, **2015**, *13*, 9336-9352.
- [4] Z.-Z. H. Ma, Y.; Nomura, T.; Chen, Y.-J., *Heterocycles*, **1997**, *46*, 541-546.
- [5] I. Khan, A. Ibrar, N. Abbas, A. Saeed, *European Journal of Medicinal Chemistry*, **2014**, *76*, 193-244.
- [6] I. Khan, A. Ibrar, W. Ahmed, A. Saeed, *European Journal of Medicinal Chemistry*, **2015**, *90*, 124-169.
- [7] R. Manske, in *The alkaloids: Chemistry and Physiology, Vol. 1*, Elsevier, **1950**, pp. 1-14.
- [8] Z.-Z. Ma, Y. Hano, T. Nomura, Y.-J. Chen, *Heterocycles*, **1997**, 541-546.
- [9] K. Uehata, N. Kimura, K. Hasegawa, S. Arai, M. Nishida, T. Hosoe, K.-i. Kawai, A. Nishida, *Journal of Natural Products*, **2013**, *76*, 2034-2039.
- [10] S. A. Kalinina, D. V. Kalinin, Y. Hövelmann, C. G. Daniliuc, C. Mück-Lichtenfeld, B. Cramer, H.-U. Humpf, *Journal of Natural Products*, **2018**.
- [11] V. G. Ugale, S. B. Bari, *European Journal of Medicinal Chemistry*, **2014**, *80*, 447-501.

- [12] V. Alagarsamy, V. Raja Solomon, K. Dhanabal, *Bioorganic & Medicinal Chemistry*, **2007**, *15*, 235-241.
- [13] M. S. Mohamed, M. M. Kamel, E. M. M. Kassem, N. Abotaleb, S. I. Abd El-moez, M. F. Ahmed, *European Journal of Medicinal Chemistry*, **2010**, *45*, 3311-3319.
- [14] Y. Xia, Z.-Y. Yang, M.-J. Hour, S.-C. Kuo, P. Xia, K. F. Bastow, Y. Nakanishi, P. Nampoothiri, T. Hackl, E. Hamel, K.-H. Lee, *Bioorganic & Medicinal Chemistry Letters*, **2001**, *11*, 1193-1196.
- [15] P. Pospisil, H. Korideck, K. Wang, Y. Yang, L. K. Iyer, A. I. Kassis, *Chemical Biology & Drug Design*, **2012**, *79*, 926-934.
- [16] V. Alagarsamy, U. S. Pathak, *Bioorganic & Medicinal Chemistry*, **2007**, *15*, 3457-3462.
- [17] R. Noel, N. Gupta, V. Pons, A. Goudet, M. D. Garcia-Castillo, A. Michau, J. Martinez, D.-A. Buisson, L. Johannes, D. Gillet, J. Barbier, J.-C. Cintrat, *Journal of Medicinal Chemistry*, **2013**, *56*, 3404-3413.
- [18] N. M. Abdel Gawad, H. H. Georgey, R. M. Youssef, N. A. El-Sayed, *European Journal of Medicinal Chemistry*, **2010**, *45*, 6058-6067.
- [19] A. R. Oveisi, M. Honarmand, *Synthetic Communications*, **2010**, *40*, 1231-1242.
- [20] M. Dabiri, P. Salehi, A. A. Mohammadi, M. Baghbanzadeh, *Synthetic Communications*, **2005**, *35*, 279-287.
- [21] A. Nathubhai, R. Patterson, T. J. Woodman, H. E. C. Sharp, M. T. Y. Chui, H. H. K. Chung, S. W. S. Lau, J. Zheng, M. D. Lloyd, A. S. Thompson, M. D. Threadgill, *Organic & Biomolecular Chemistry*, **2011**, *9*, 6089-6099.
- [22] N. Y. Kim, C.-H. Cheon, *Tetrahedron Letters*, **2014**, *55*, 2340-2344.
- [23] R. Cheng, T. Guo, D. Zhang-Negrerie, Y. Du, K. Zhao, *Synthesis*, **2013**, *45*, 2998-3006.
- [24] Y. Bao, Y. Yan, K. Xu, J. Su, Z. Zha, Z. Wang, *The Journal of Organic Chemistry*, **2015**, *80*, 4736-4742.
- [25] D. Zhao, T. Wang, J.-X. Li, *Chemical Communications*, **2014**, *50*, 6471-6474.
- [26] Q. Li, Y. Huang, T. Chen, Y. Zhou, Q. Xu, S.-F. Yin, L.-B. Han, *Organic Letters*, **2014**, *16*, 3672-3675.
- [27] H. Hikawa, Y. Ino, H. Suzuki, Y. Yokoyama, *The Journal of Organic Chemistry*, **2012**, *77*, 7046-7051.

- [28] M. L. Buil, M. A. Esteruelas, M. P. Gay, M. Gómez-Gallego, A. I. Nicasio, E. Oñate, A. Santiago, M. A. Sierra, *Organometallics*, **2018**, *37*, 603-617.
- [29] C. Schleppehorst, B. Maji, F. Glorius, *ACS Catalysis*, **2016**, *6*, 4184-4188.
- [30] N. J. Oldenhuis, V. M. Dong, Z. Guan, *Journal of the American Chemical Society*, **2014**, *136*, 12548-12551.
- [31] W. Zhao, W. Ma, T. Xiao, F. Li, *ChemistrySelect*, **2017**, *2*, 3608-3612.
- [32] J. Zhou, J. Fang, *The Journal of Organic Chemistry*, **2011**, *76*, 7730-7736.
- [33] S. H. Siddiki, K. Kon, A. S. Touchy, K.-i. Shimizu, *Catalysis Science & Technology*, **2014**, *4*, 1716-1719.
- [34] W. Zhang, C. Meng, Y. Liu, Y. Tang, F. Li, *Advanced Synthesis & Catalysis*, **2018**, *360*, 3751-3759.
- [35] W. Xu, X.-R. Zhu, P.-C. Qian, X.-G. Zhang, C.-L. Deng, *Synlett*, **2016**, *27*, 2851-2857.
- [36] T. M. M. Maiden, S. Swanson, P. A. Procopiou, J. P. A. Harrity, *Chemistry – A European Journal*, **2015**, *21*, 14342-14346.
- [37] Y. Feng, Y. Li, G. Cheng, L. Wang, X. Cui, *The Journal of Organic Chemistry*, **2015**, *80*, 7099-7107.
- [38] S. Mohammed, R. A. Vishwakarma, S. B. Bharate, *The Journal of Organic Chemistry*, **2015**, *80*, 6915-6921.
- [39] Y. Yan, Y. Xu, B. Niu, H. Xie, Y. Liu, *The Journal of Organic Chemistry*, **2015**, *80*, 5581-5587.
- [40] L. He, H. Li, H. Neumann, M. Beller, X.-F. Wu, *Angewandte Chemie*, **2014**, *126*, 1444-1448.
- [41] X. Jiang, T. Tang, J.-M. Wang, Z. Chen, Y.-M. Zhu, S.-J. Ji, *The Journal of Organic Chemistry*, **2014**, *79*, 5082-5087.
- [42] X.-F. Wu, L. He, H. Neumann, M. Beller, *Chemistry – A European Journal*, **2013**, *19*, 12635-12638.
- [43] H. Wang, X. Cao, F. Xiao, S. Liu, G.-J. Deng, *Organic Letters*, **2013**, *15*, 4900-4903.
- [44] D. K. Sreenivas, N. Ramkumar, R. Nagarajan, *Organic & Biomolecular Chemistry*, **2012**, *10*, 3417-3423.
- [45] J. E. R. Sadig, R. Foster, F. Wakenhut, M. C. Willis, *The Journal of Organic Chemistry*, **2012**, *77*, 9473-9486.

- [46] M. Sharma, S. Pandey, K. Chauhan, D. Sharma, B. Kumar, P. M. S. Chauhan, *The Journal of Organic Chemistry*, **2012**, *77*, 929-937.
- [47] C. L. Yoo, J. C. Fettinger, M. J. Kurth, *The Journal of Organic Chemistry*, **2005**, *70*, 6941-6943.
- [48] X. Liu, H. Fu, Y. Jiang, Y. Zhao, *Angewandte Chemie*, **2009**, *121*, 354-357.
- [49] M. Kumar, Richa, S. Sharma, V. Bhatt, N. Kumar, *Advanced Synthesis & Catalysis*, **2015**, *357*, 2862-2868.
- [50] S. A. Lawrence, Cambridge University Press, Cambridge, **2004**.
- [51] W. Xu, Y. Jin, H. Liu, Y. Jiang, Fu, Hua, *Organic Letters*, **2011**, *13*, 1274-1277.
- [52] W. Xu, H. Fu, *The Journal of Organic Chemistry*, **2011**, *76*, 3846-3852.
- [53] L. Xu, Y. Jiang, D. Ma, *Organic Letters*, **2012**, *14*, 1150-1153.
- [54] L.-X. Wang, J.-F. Xiang, Y.-L. Tang, *European Journal of Organic Chemistry*, **2014**, *2014*, 2682-2685.
- [55] S. Guo, Y. Li, L. Tao, W. Zhang, X. Fan, *RSC Advances*, **2014**, *4*, 59289-59296.
- [56] A. Modi, W. Ali, P. R. Mohanta, N. Khatun, B. K. Patel, *ACS Sustainable Chemistry & Engineering*, **2015**, *3*, 2582-2590.
- [57] A. Kumar, A. K. Bishnoi, *RSC Advances*, **2014**, *4*, 41631-41635.
- [58] S. Dhiman, H. K. Saini, N. K. Nandwana, D. Kumar, A. Kumar, *RSC Advances*, **2016**, *6*, 23987-23994.
- [59] N. K. Nandwana, S. Dhiman, H. K. Saini, I. Kumar, A. Kumar, *European Journal of Organic Chemistry*, **2017**, *2017*, 514-522.
- [60] K. Pericherla, A. Jha, B. Khungar, A. Kumar, *Organic Letters*, **2013**, *15*, 4304-4307.
- [61] C. Xu, F.-C. Jia, Z.-W. Zhou, S.-J. Zheng, H. Li, A.-X. Wu, *The Journal of Organic Chemistry*, **2016**, *81*, 3000-3006.
- [62] F.-C. Jia, C. Xu, Z.-W. Zhou, Q. Cai, D.-K. Li, A.-X. Wu, *Organic Letters*, **2015**, *17*, 2820-2823.
- [63] K. Upadhyaya, R. K. Thakur, S. K. Shukla, R. P. Tripathi, *The Journal of Organic Chemistry*, **2016**, *81*, 5046-5055.
- [64] D. Dhar, W. B. Tolman, *Journal of the American Chemical Society*, **2015**, *137*, 1322-1329.
- [65] Y. Kim, M. R. Kumar, N. Park, Y. Heo, S. Lee, *The Journal of Organic Chemistry*, **2011**, *76*, 9577-9583.

-
- [66] F.-C. Jia, Z.-W. Zhou, C. Xu, Q. Cai, D.-K. Li, A.-X. Wu, *Organic Letters*, **2015**, *17*, 4236-4239.
- [67] Y. Goriya, C. V. Ramana, *Chemical Communications*, **2014**, *50*, 7790-7792.
- [68] Y. Goriya, C. V. Ramana, *Tetrahedron*, **2010**, *66*, 7642-7650.
- [69] S. Cenini, E. Gallo, A. Penoni, F. Ragaini, S. Tollari, *Chemical Communications*, **2000**, 2265-2266.
- [70] J. Shen, D. Yang, Y. Liu, S. Qin, J. Zhang, J. Sun, C. Liu, C. Liu, X. Zhao, C. Chu, R. Liu, *Organic Letters*, **2014**, *16*, 350-353.
- [71] P. Cheng, J. Zhou, Z. Qing, W. Kang, S. Liu, W. Liu, H. Xie, J. Zeng, *Bioorganic & Medicinal Chemistry Letters*, **2014**, *24*, 2712-2716.
- [72] Z. Zheng, H. Alper, *Organic Letters*, **2008**, *10*, 829-832.
- [73] H. B. Jalani, A. N. Pandya, D. H. Pandya, J. A. Sharma, V. Sudarsanam, K. K. Vasu, *Tetrahedron Letters*, **2012**, *53*, 4062-4064.

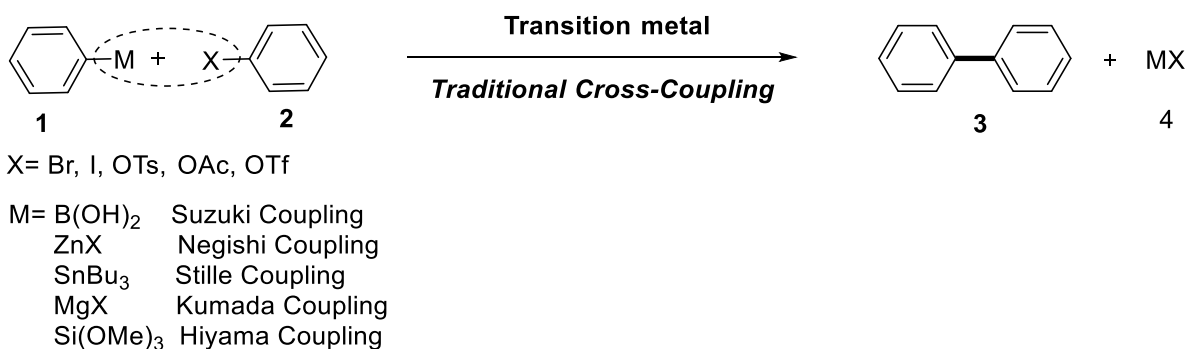
CHAPTER 3

Pd(II)-Catalyzed One-Pot Synthesis of Benzimidazo/Imidazo[2,1-*a*]isoquinolines

3.1 INTRODUCTION

In chemistry, access of the *N*-heterocyclic compounds is always desirable because of their occurrence in natural products and significant demand in pharmaceuticals.^[1-3] Over the centuries, the synthesis of these privilege compounds *via* functional group interconversion approach has been in tradition. Based on these traditional approaches as numerous routes were developed for the synthesis of various heterocycles which often include multiple synthetic steps and harsh reaction conditions.^[4]

In the last few decades, the evolution of transition metal catalyzed reactions has proven a paradigm shift in organic synthesis.^[5-8] The construction of direct C-C and C-X bonds has been very much convenient after the discovery of these metal catalyzed cross-coupling reactions.^[9] Among these, the Suzuki,^[10-11] Negishi,^[12-13] Stille,^[14-15] Kumada,^[16] and Hiyama^[17-18] are the examples of classical cross coupling which require both the coupling partners to be functionalized (**Scheme 3.1**). In this regard, one of the substrates must be functionalized with metallic functionality (**1**) as necessary coupling partner such as borane, zinc, tin, magnesium, and silane, respectively whereas, other can be halogenated/pseudo-halogenated (**2**).^[9, 19] The difficult procedure to access organometallic reagent as well as the waste generation of a stoichiometric amount of metallic salts limits their applications greatly.



Scheme 3.1: Transition metal-catalyzed traditional cross-coupling reaction

The utilization of an unfunctionalized substrate is an alternate choice to overcome abovementioned limitations. With this advent, the cleavage of direct C-H bond (C-H activation) has emerged as an alternative approach for constructing a new C-C bond. The inert C-H bond cleaves under transition metal-catalysis and forms reactive C-M bond to lead functionalization (**Figure 3.1**).^[5, 20-21]

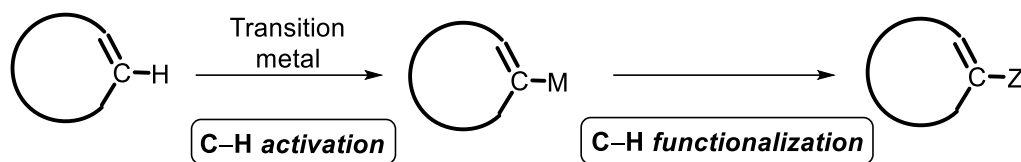
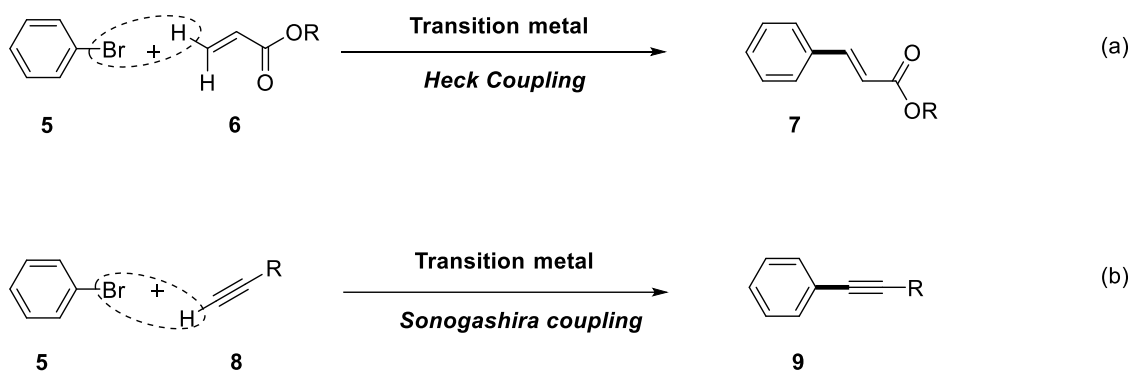


Figure 3.1: General strategy of C-H activation and functionalization

The landmark achievement, C-H activation, in organic synthesis has earned significant attention of organic researcher's which rendered various fused heterocyclic compounds with an efficient and straightforward manner. In reference to the C-H activation strategy, Heck coupling (**Scheme 3.2a**) and Sonogashira coupling (**Scheme 3.2b**) are the excellent examples which showed wide application in heterocyclic synthesis.^[22-24]



Scheme 3.2: Example of transition metal-catalyzed Heck and Sonogashira coupling

In the last decade, a variety of strategies, alkylation, arylation, heteroarylation, using C-H activation has been developed to access fused azaheterocycles.^[25-26] Among these, more focus has been on arylation reactions due to the deliverance of extended conjugated *N*-heterocycles. For example, aryl-fused pyrenoimidazoles, possess large π -conjugated systems, display attractive optical applications and used as fluorescent probes (**Figure 3.2**).^[9] Apart from this, the enriched π -electrons *N*-heterocycles containing aryl-aryl bonds are frequently encountered in biological systems.^[7, 27-28] Many natural products and drug candidates comprise these arylated fused *N*-heterocycles.^[27] For example, natural product Cryptautoline and Rosettacin are exhibit tubulin polymerization inhibitor and a cytotoxic agent, respectively.^[29-30] Indole/imidazole-fused isoquinoline core displays a variety of intriguing biological properties such as anticancer, analgesic, anti-inflammatory and treatment against CNS diseases (**Figure 3.2**).^[31-32]

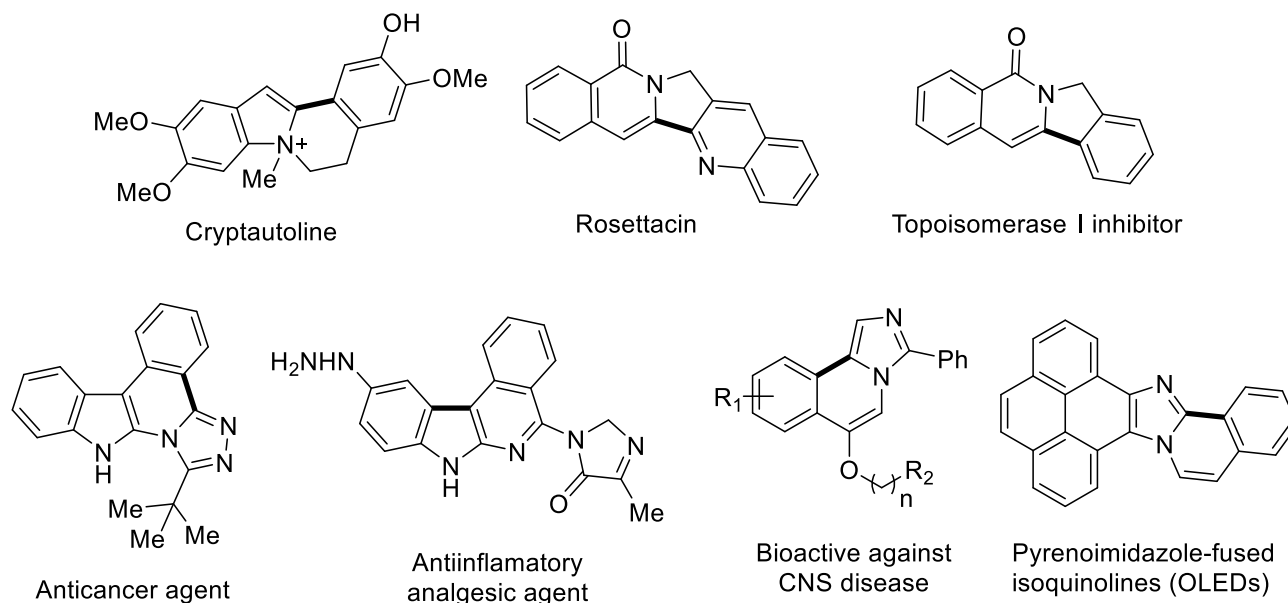
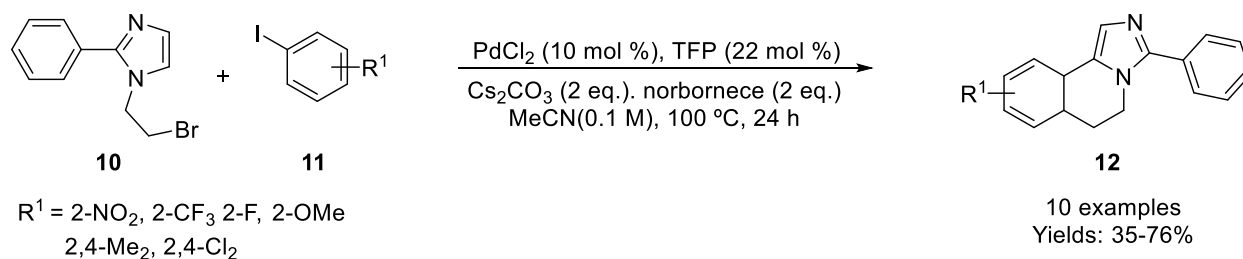


Figure 3.2: Representative molecules containing isoquinoline framework

Owing to intriguing applications of arylation in fused azaheterocycles, special attention has been toward synthesis and functionalization of isoquinolines by various research groups. The variety of routes have been described where transition metal catalyzed arylation has been employed to access these frameworks.

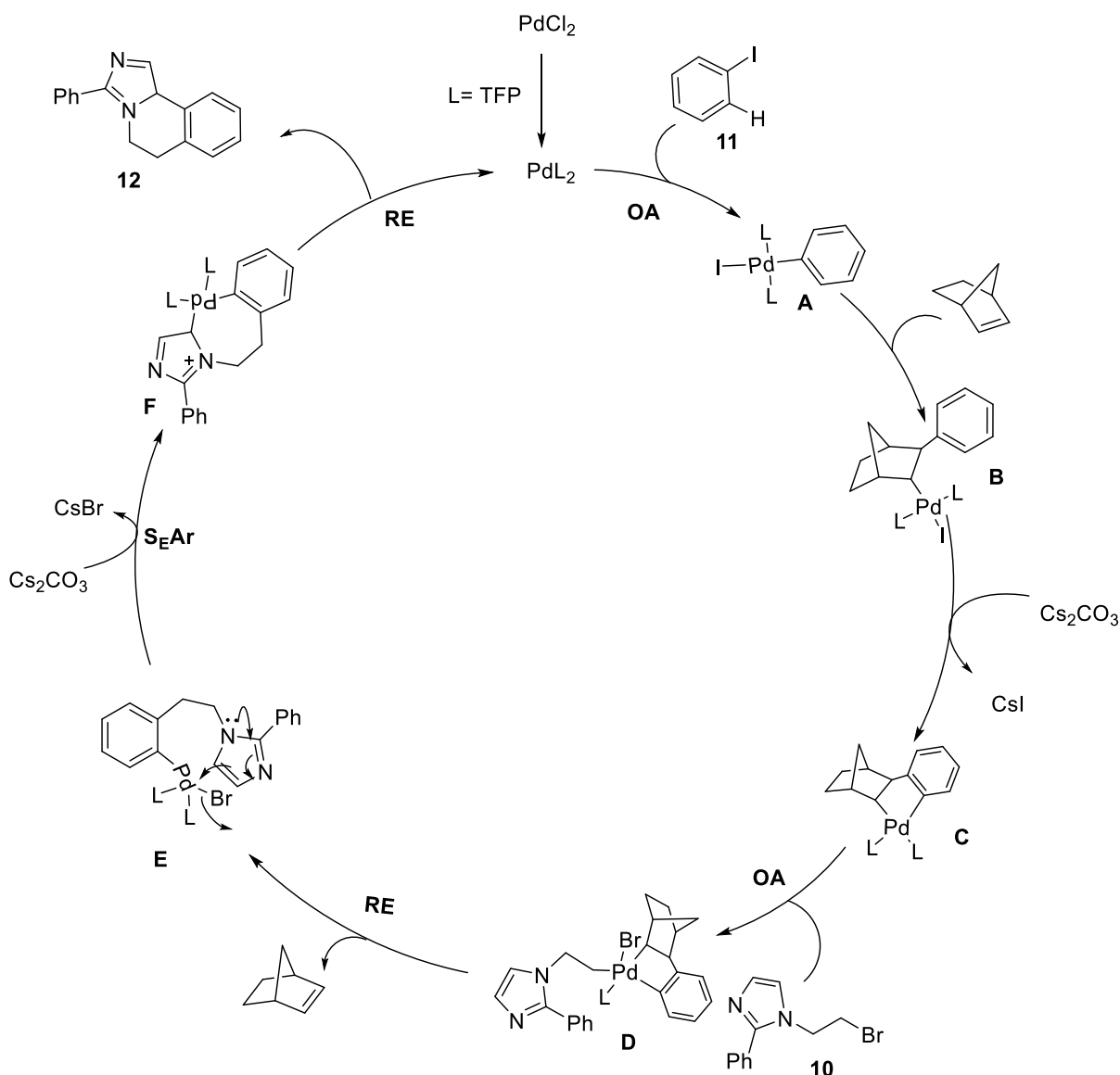
An early report described by Jafarpour group for the synthesis of imidazole fused isoquinolines (**12**) *via* direct C-H arylation from *N*-bromoalkyl 2-phenylimidazole (**10**) and iodoarenes (**11**) using the combination of PdCl₂/TFP (**Scheme 3.3**).^[33] Variety of substrates showed that aryl iodides are having *ortho* nitro and chloro-substitutents gave quantitative yields of corresponding 3-phenyl-5,6-dihydroimidazo[5,1-*a*]isoquinolines.



Scheme 3.3: Synthesis of 3-phenyl-5,6-dihydroimidazo[5,1-*a*]isoquinolines

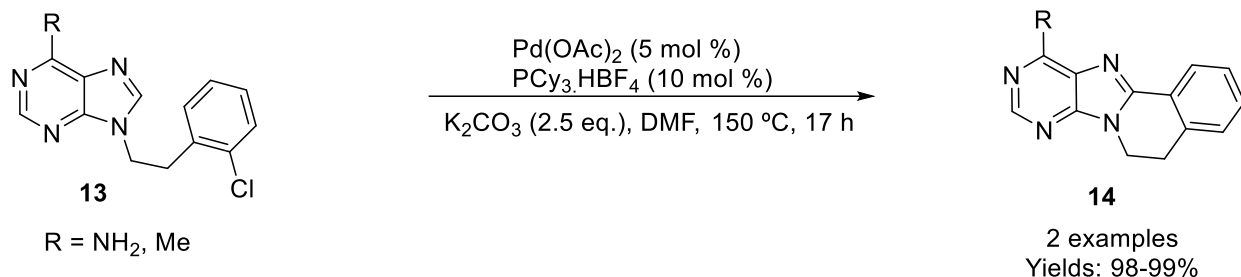
The mechanistic study for the synthesis of 3-phenyl-5,6-dihydroimidazo[5,1-*a*] isoquinolines (**12**) is depicted in **Scheme 3.4**. Initially, Pd(0) generated *via* the reduction of Pd(II) underwent oxidative addition (OA) with aryl iodide (**11**) to produce arylpalladium iodide complex (**A**). Then,

insertion of norbornene into **A** formed Pd complex **B** which upon basic conditions converted into palladacycle **C**. Further palladacycle **C** underwent oxidative addition (OA) with *N*-bromoalkylimidazole (**10**) and formed Pd(IV) species **D**. Reductive elimination (RE), extrusion of norbornene and rearrangement in Pd-complex of **D** gave intermediate **E** which further underwent electrophilic aromatic substitution reaction on imidazole to give palladacycle **F**. Eventually, the desired product 3-phenyl-5,6-dihydroimidazo[5,1-*a*]isoquinolines (**12**) could be achieved from palladium complex **F** via a reductive elimination reaction.



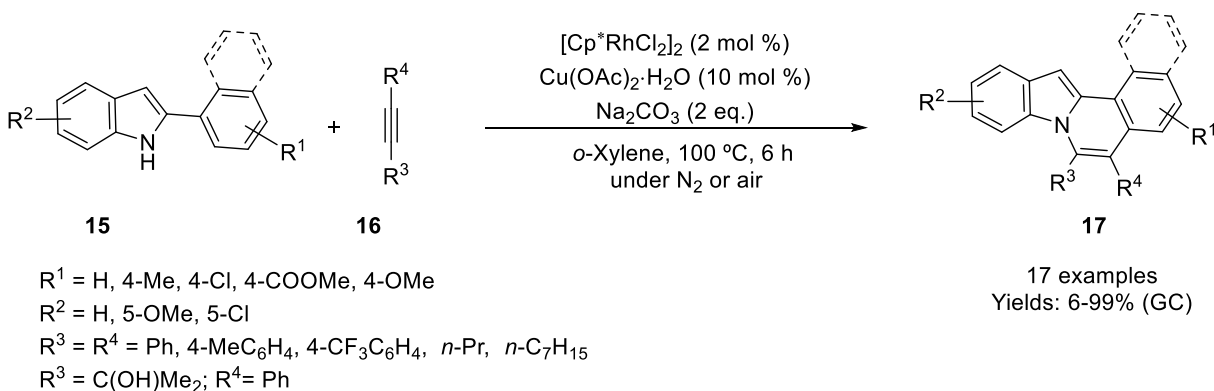
Scheme 3.4: Pd(II)-catalytic cycle for the synthesis of imidazole-fused isoquinolines via intramolecular direct C-H arylation

Hocek and co-workers reported the synthesis of 5,6-dihydropurino[8,9-*a*]isoquinolines (**14**) via Pd(II)-catalyzed intramolecular direct arylation in excellent yields (**Scheme 3.5**)^[34] and studied their luminescent properties and biological activities. Electronic absorption-emission spectra and cytostatic activity of these purines fused isoquinoline compounds (**14**) revealed that the adenine derivative (R = NH₂) of isoquinoline exhibited good quantum yield. The compounds were found to possess poor cytostatic activity against cancer as well as leukemia cell lines.



Scheme 3.5: Synthesis of 5,6-dihydropurino[8,9-*a*]isoquinolines via Pd(II)-catalyzed intramolecular C-H arylation

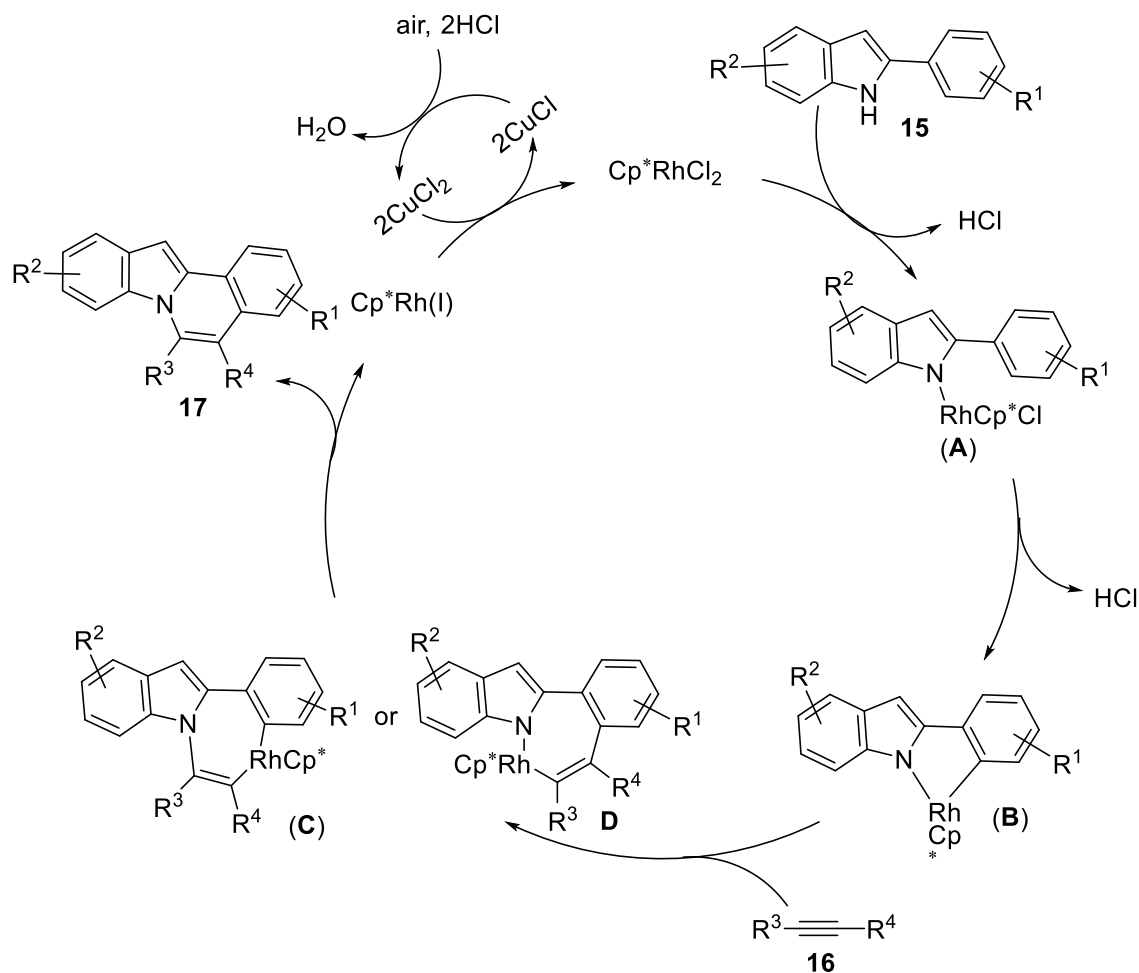
Miura and coworkers achieved indolo[2,1-*a*]isoquinoline framework (**17**) through Rh(III)-catalyzed oxidative C-H/N-H coupling with internal alkynes. The fused isoquinolines were obtained in poor to excellent yields (6-99%) by reacting 2-arylindoles (**15**) and alkynes (**16**) in the presence of [Cp**Rh*Cl₂]₂ and Cu(OAc)₂ (**Scheme 3.6**).^[35] Solid-state fluorescence was investigated for all synthesized compounds and found some of the indolo[2,1-*a*]isoquinoline derivatives (**17**) exhibited fluorescence in the range of 460-510 nm.



Scheme 3.6: The construction of indolo[2,1-*a*]isoquinolines derivatives under Rh(III)-catalysis

The proposed reaction pathway for the synthesis of indolo[2,1-*a*]isoquinolines (**17**) is illustrated in **Scheme 3.7**. Initially, NH-group of indole coordinated with Rh(III)-complex to generate Rh-

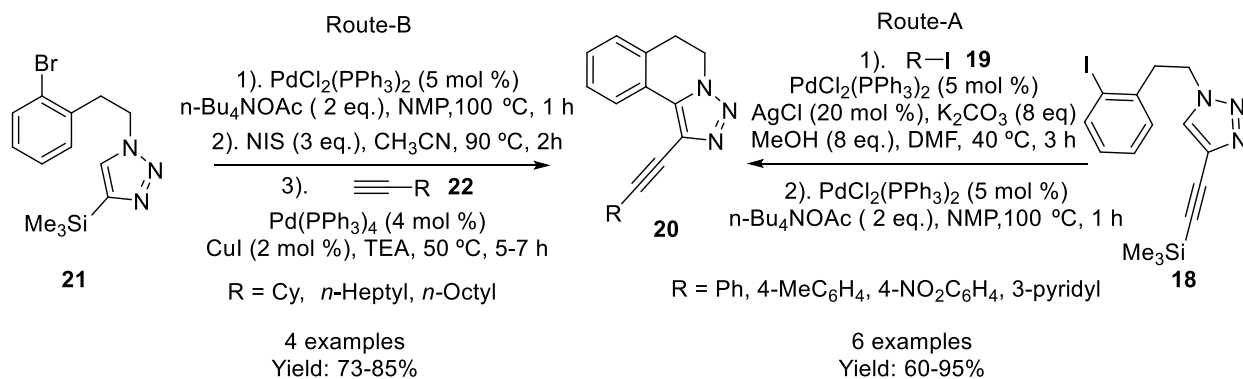
complex (A) which subsequently produced five-membered rhodacycle (B). Insertion of internal alkynes to rhodacycle (B) *via* N-Rh or C-Rh formed seven-membered rhodacycle (C) or (D), respectively. Finally, the reductive elimination of intermediate (C) or (D) facilitated the desired product (17). Eliminated Cp^{*}Rh(I)-complex further oxidized in the presence of air with co-catalyst Cu(II) and regenerated the active Rh(III)-complex to complete the catalytic cycle.



Scheme 3.7: Rh-catalytic cycle for the synthesis of indolo[2,1-a]isoquinolines

Fiandanese *et al.* reported the sequential synthesis of alkyl- and arylethynyl-1,2,3-triazole-fused dihydroisoquinolines (20) through two different routes (a & b) using precursors as 1-(2-iodophenyl)-4-((trimethylsilyl)ethynyl)-1*H*-1,2,3-triazoles (18) and 1-(2-bromophenethyl)-4-((trimethylsilyl)-1*H*-1,2,3-triazoles (21) (Scheme 3.8).^[36] In route A, first intermolecular arylation in between 1-(2-iodophenethyl)-4-((trimethylsilyl)ethynyl)-1*H*-1,2,3-triazoles (18) and iodoarenes (19) by using $\text{PdCl}_2(\text{PPh}_3)_2$ with AgCl produced arylated product in 61-95% yields.

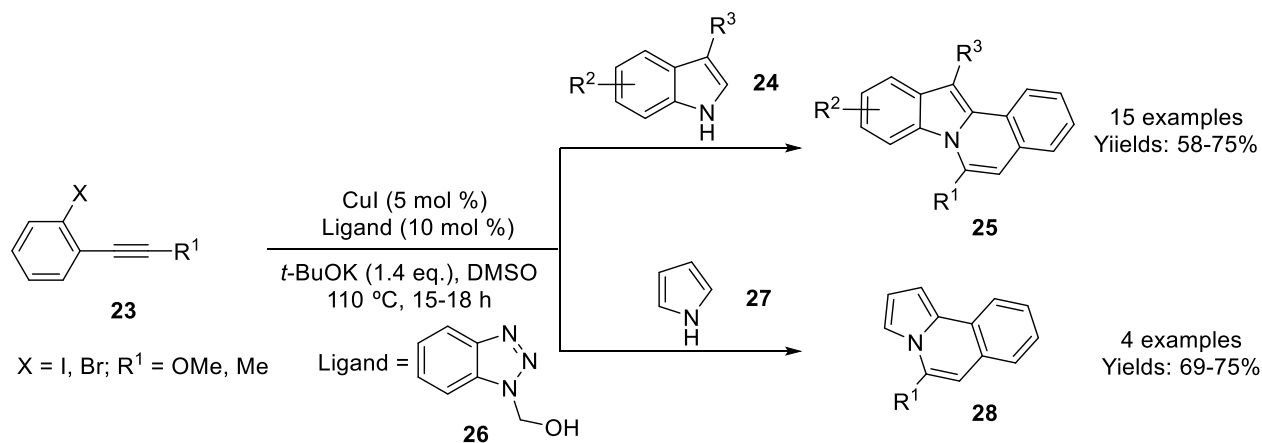
Then arylated product subjected to intramolecular arylation under Pd-catalysis took place targeted 1-(arylethynyl)-5,6-dihydro-[1,2,3]triazolo[5,1-*a*]isoquinoline derivatives (**20**) in 60-95% yields (**Scheme 3.8, Route-A**).



Scheme 3.8: Synthesis of 1-(aryl/alkylethynyl)-5,6-dihydro-[1,2,3]triazolo[5,1-*a*]isoquinoline derivatives in multiple steps

Similarly, in case of route B first, palladium-catalyzed intramolecular strategy was applied to produce functionalize triazole fused isoquinolines which further underwent iodination using *N*-iodosuccinamide followed by Sonogashira coupling to give alkyne tethered triazole fused isoquinolines (**20**) in 73-85% yields (**Scheme 3.8, Route-B**).

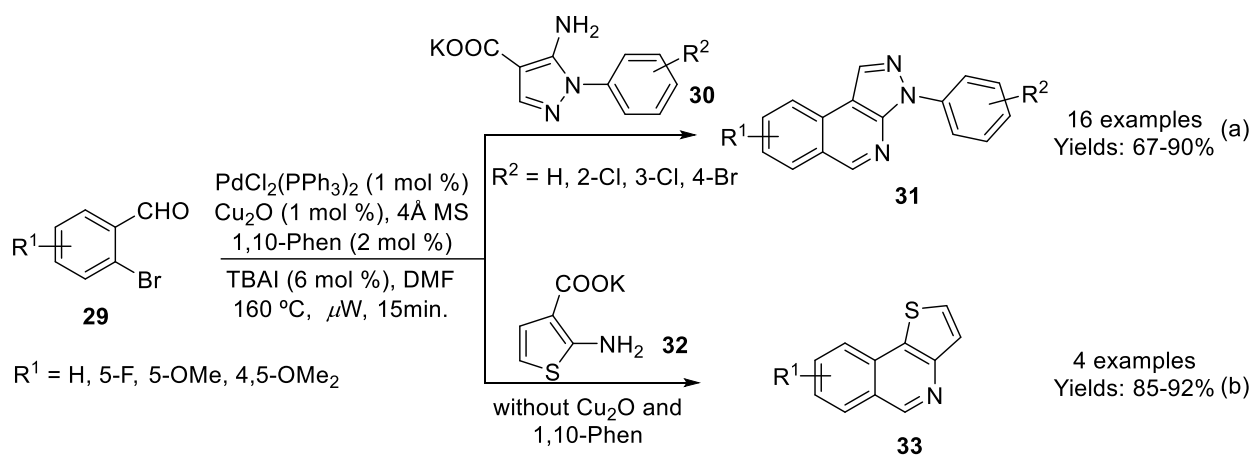
Verma and coworkers disclosed tandem reaction of substituted indoles (**24**) or pyrrole (**27**) with internal alkynes (**23**) which afforded indolo[2,1-*a*]isoquinolines (**25**) and pyrrolo[2,1-*a*]isoquinolines (**28**) in good to moderate yields in the presence Cu(I)-catalyst using (1*H*-benzo[*d*][1,2,3]triazol-1-yl)methanol (**26**) as ligand and *tert*-BuOK as base (**Scheme 3.9**).^[37]



Scheme 3.9: Synthesis of indolo/pyrrolo[2,1-*a*]isoquinolines from 1-halo-2-(arylethynyl)benzene

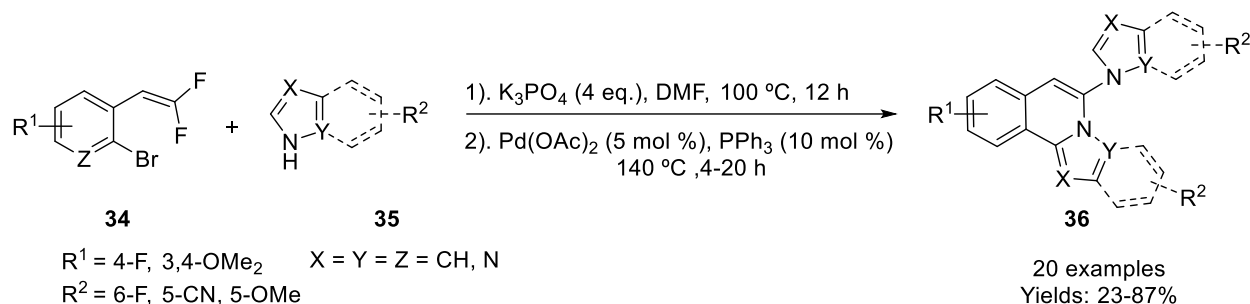
Various electron releasing and withdrawing substituents on both indoles and internal alkynes were evaluated and revealed that electron releasing substituents gave corresponding indole fused isoquinolines (**25**) in good yields as compared to electron-withdrawing substituents.

The construction of 3*H*-pyrazolo[3,4-*c*]isoquinolines (**31**) was described in a one-pot tandem reaction of 2-bromobenzaldehydes (**29**) with potassium 5-amino-1-aryl-1*H*-pyrazole-4-carboxylates (**30**) under Pd-Cu co-catalyst system by Batra group (**Scheme 3.10a**). They also, synthesized thieno[3,4-*c*]isoquinolines (**33**) using potassium 2-aminothiophene-3-carboxylate (**32**) with 2-bromo benzaldehydes (**29**) under Pd catalyst (**Scheme 3.10b**). The developed strategy involved tandem condensation followed by decarboxylative arylation process to achieve thieno/pyrazolo[3,4-*c*]isoquinoline derivatives (**31** and **33**).



Scheme 3.10: Synthesis of thieno/pyrazolo[3,4-*c*]isoquinolines from 2-bromobenzaldehydes

Langer group described the sequential one-pot process for the assembly of aza-fused isoquinoline derivatives (**36**) by the reaction of 1-bromo-2-(2,2-difluorovinyl)benzenes (**34**) with various heterocycles (**35**) having NH functionality in the ring such as indole, imidazole, pyrazole, benzimidazole, pyrrole (**Scheme 3.11**).^[38] In the described methodology, initially, base-mediated C-N bond formation occurred between NH-heterocycles (**35**) and *gem*-difluoroalkenes (**34**) followed by intramolecular C-H arylation took place through palladium catalyst to afford aza-fused isoquinolines (**36**).



Scheme 3.11: Synthesis of aza-fused isoquinolines from 1-bromo-2-(2,2-difluorovinyl)benzenes

All the synthesized compounds (**36**) were also tested for their inhibitory potential towards human nucleotide pyrophosphatase h-NPP-1 and human nucleotide phosphodiesterase 3 (h-NPP-3). The results revealed that 6-(1*H*-indol-1-yl)indolo[2,1-*a*]isoquinoline derivative (**36a**) showed highest inhibitory potential of h-NPP-1 and 6-(5-cyano-1*H*-indol-1-yl)indolo[2,1-*a*]isoquinoline-10-carbonitrile (**36b**) exhibited significant inhibitory activity of h-NPP-3 (**Figure 3.3**).

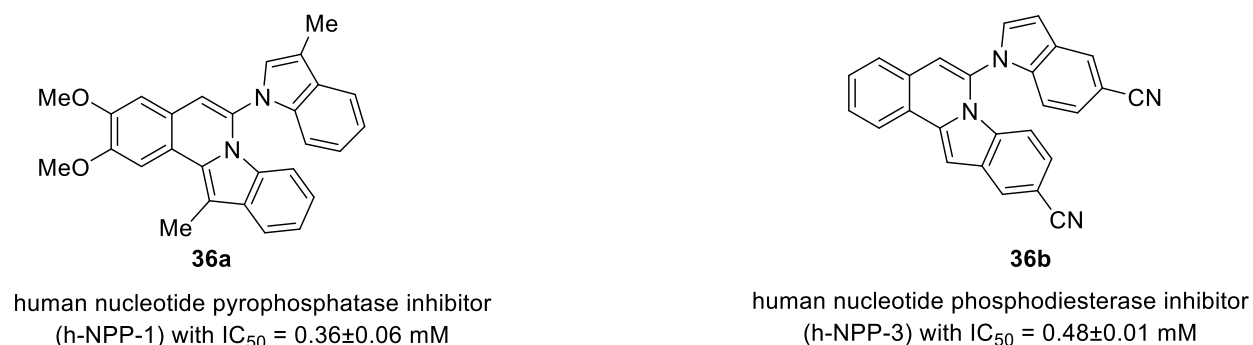
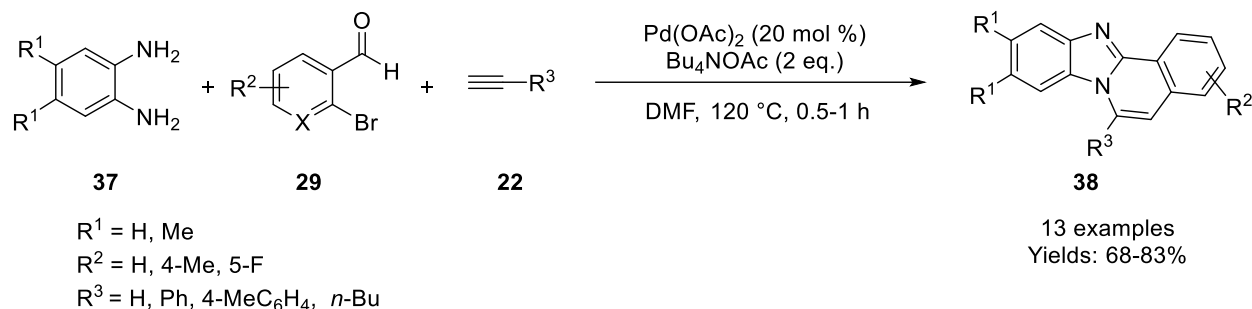


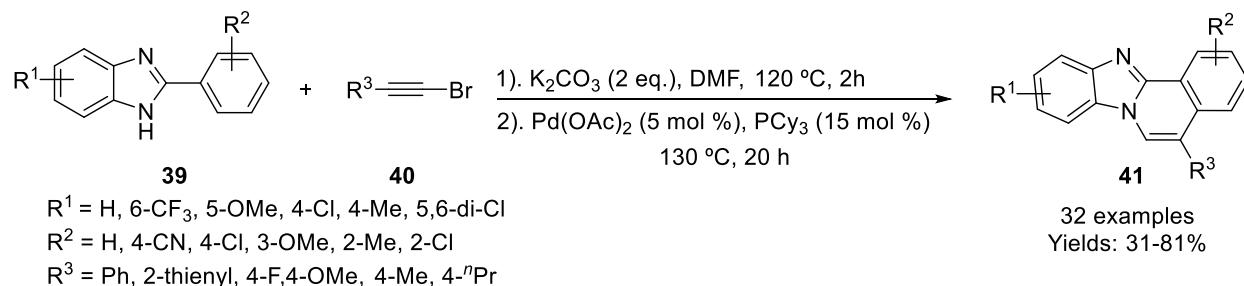
Figure 3.3: Inhibition against h-NPP-1 and h-NPP-3 by compounds **36a** and **36b**, respectively

Benzimidazo/imidazo[2,1-*a*]isoquinolines are an important framework which is found in various pharmacophore and bioactive molecules such as antiasthmatic, antihypertensive, anticancer, antianxiolytic agent and also used in material science for fluorescent probes.^[39-43] In this respect, Yanada group synthesized benzimidazo/imidazo[2,1-*a*]isoquinolines (**38**) via multicomponent reactions of *o*-phenylenediamines (**37**), 2-haloarylaldehydes (**29**), and alkynes (**16**) under microwave radiation in the presence of palladium catalyst (**Scheme 3.12**).^[44] This developed methodology involved Sonogashira coupling, 5-endo-cyclization, oxidative aromatization and finally, 6-endo-cyclization to afford desired product in 68-83% yields.



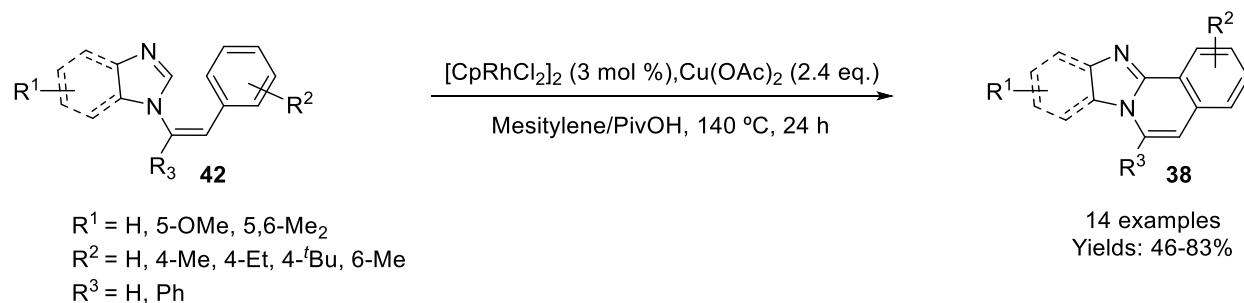
Scheme 3.12: Pd-catalyzed multicomponent synthesis of benzimidazo[2,1-*a*]isoquinolines

Alternatively, Li and colleagues disclosed efficient tandem approach to access benzimidazo[2,1-*a*]isoquinoline derivatives (**41**) by employing 2-arylbenzimidazoles (**39**) and alkynyl bromides (**40**) under palladium catalyst (**Scheme 3.13**).^[45] In this approach, initially, hydroamination reaction took place between benzimidazoles (**39**) and alkynyl bromides (**40**) in the presence of a base to form (*Z*)-alkenyl bromide followed by palladium catalyzed intramolecular direct C-H arylation produced imidazole fused isoquinolines (**41**) in good to moderate yields (31-81%).



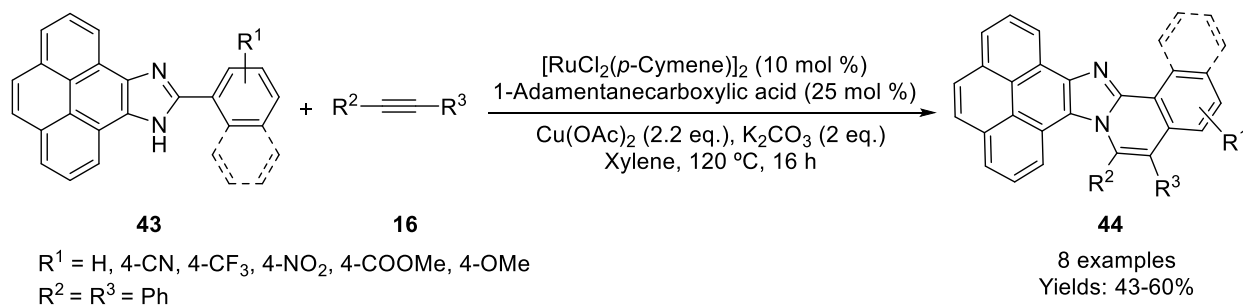
Scheme 3.13: Pd(II)-catalyzed synthesis of benzimidazo[2,1-*a*]isoquinolines from 2-arylbenzimidazoles

Later on, Kambe group reported the synthesis of benzimidazo/imidazo[2,1-*a*]isoquinolines (**38**) via Rh(III)-catalyzed intramolecular cross dehydrogenative coupling (CDC) of (*Z*)-1-styryl-1*H*-imidazoles (**Scheme 3.14**).^[42]



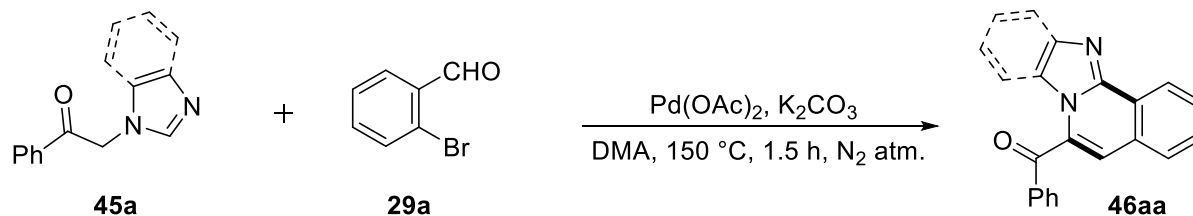
Scheme 3.14: Synthesis of imidazo[2,1-*a*]isoquinolines via Rh-catalyzed CDC

The assembly of π -extended pyrenoimidazole-fused isoquinolines (**44**) was disclosed by Gandhi group using rhodium-catalyzed oxidative C-H coupling from pyrenoimidazoles (**43**) and internal alkynes (**16**) (Scheme 3.15).^[43] All synthesized derivatives were investigated about electrochemical and photophysical properties. The single crystal X-ray structures of trifluoromethyl and carboxylate substituted derivatives revealed the near coplanarity of pyrene and imidazole moiety. The molecular packing diagram showed that the presence of twisted conformation led intermolecular C-H... π interaction, which was responsible for significant solid-state fluorescence than solution state.



Scheme 3.15: Ru(III)-catalyzed synthesis of pyrenoimidazole-fused isoquinolines from 2-arylpirenoimidazoles

As a part of our ongoing research on the synthesis of imidazole-fused heterocycles *via* C-H functionalization, we motivated to develop a new methodology for the synthesis of benzimidazo/imidazole[2,1-*a*]isoquinolines by that involve the formation of two C-C bonds in one-pot using traditional Knoevenagel condensation and direct C-H arylation (Scheme 3.16).



Scheme 3.16: Our alternate approach for the synthesis of benzimidazo/imidazole[2,1-*a*]isoquinolines

3.2 RESULTS AND DISCUSSION

Our initial investigations commenced by recognizing a suitable catalytic system for the envisioned domino approach and results are summarized in **Table 3.1**. Initially, 2-(1*H*-imidazol-1-yl)-1-phenylethanone (**45a**) was treated with 2-bromobenzaldehyde (**29a**) in the presence of Pd(OAc)₂ (5 mol %), Cs₂CO₃ (2.5 equiv) in *N,N*-dimethylacetamide (DMA) at 150 °C for 1.5 h. Gratifyingly, imidazo[2,1-*a*]isoquinolin-5-yl(phenyl)methanone (**46aa**) was isolated in 59% yield (entry 1, **Table 3.1**). The structure of **46aa** was characterized by its spectral data (IR, MS, and NMR). In the IR spectrum of **46aa**, a strong peak appeared at 1636 cm⁻¹ for C=O stretching (**Figure 3.4**). In the ¹H NMR spectrum of **46aa**, a singlet appeared at δ 9.20 ppm for highly deshielded C₆-H along with other protons at their respective positions (**Figure 3.5**). The ketonic carbon of **46aa** appeared at δ 190.42 along with all other expected carbons in the ¹³C NMR spectrum (**Figure 3.6**). The peak at 273.1023 for [M+H]⁺ ion in the mass spectrum of **46aa** further confirmed its structure (**Figure 3.7**).

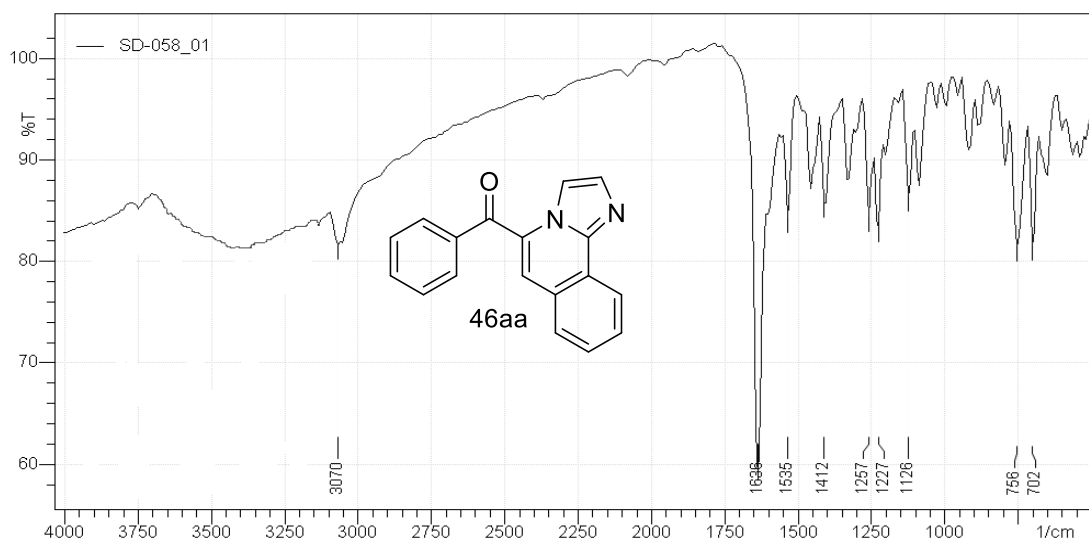
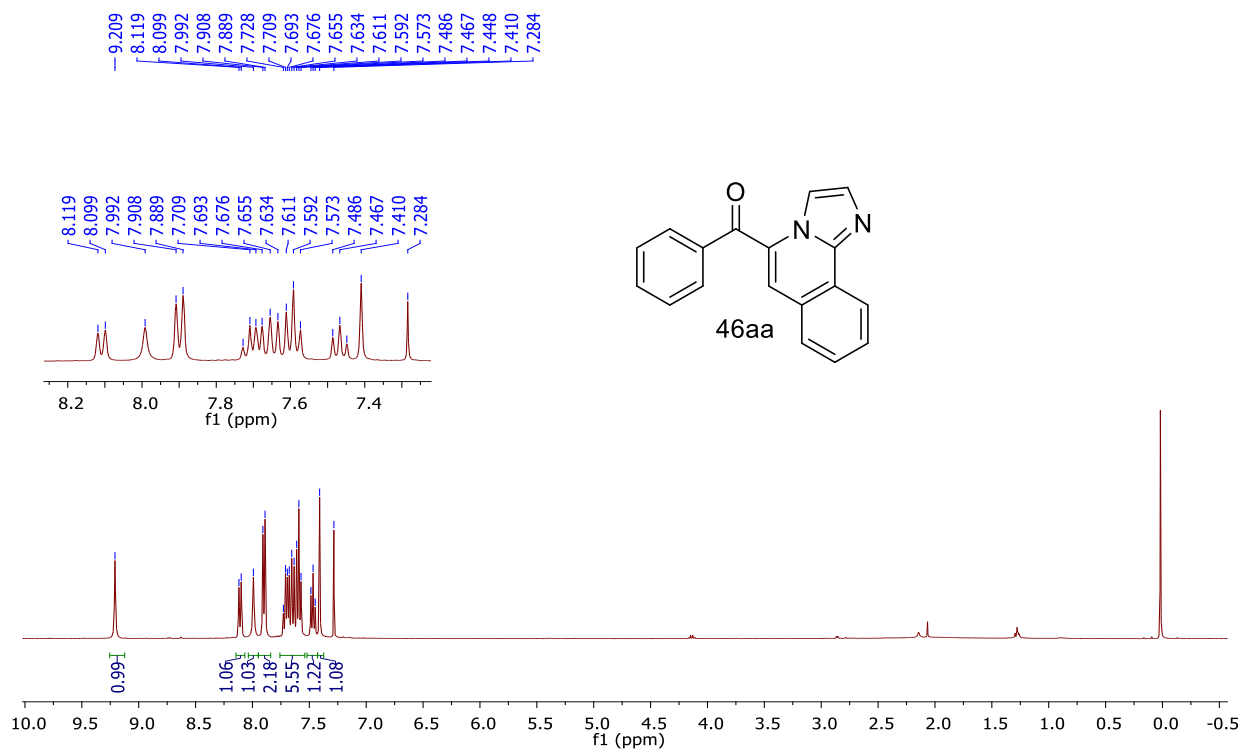
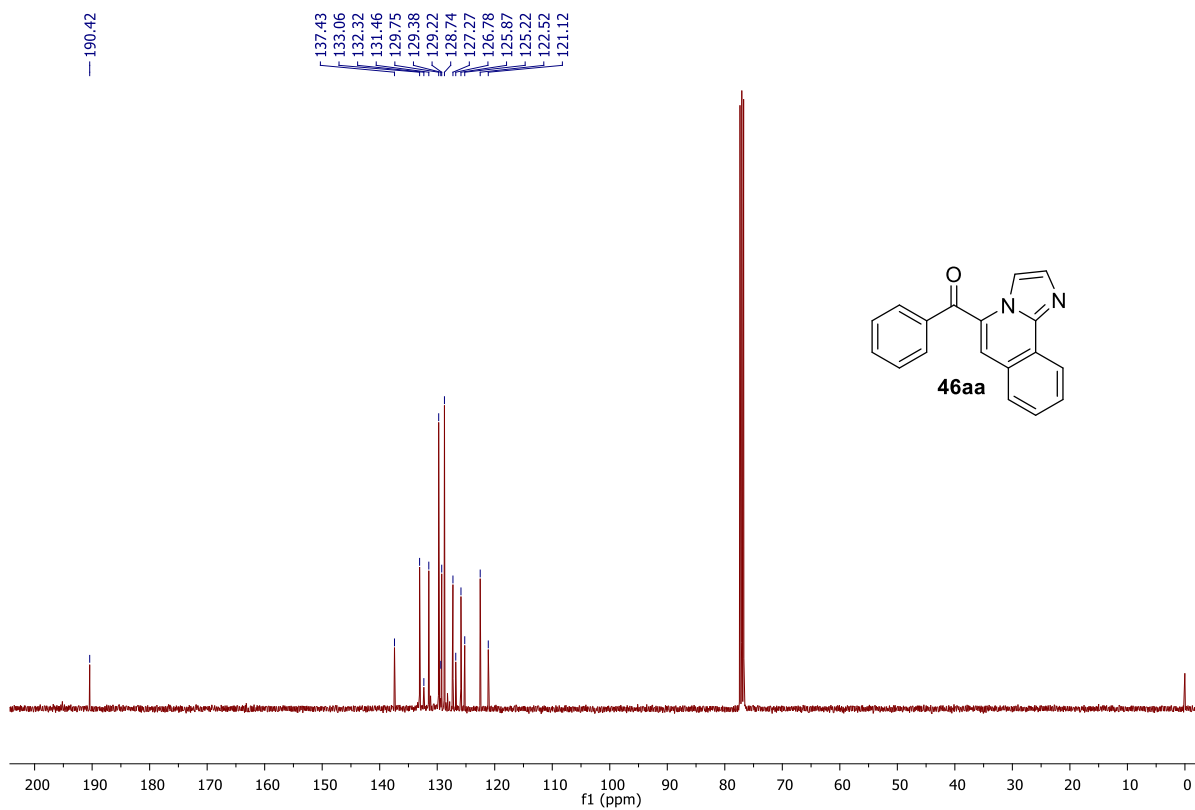


Figure 3.4: IR spectrum of **46aa**

Figure 3.5: ^1H NMR spectrum of 46aaFigure 3.6: ^{13}C NMR spectrum of 46aa

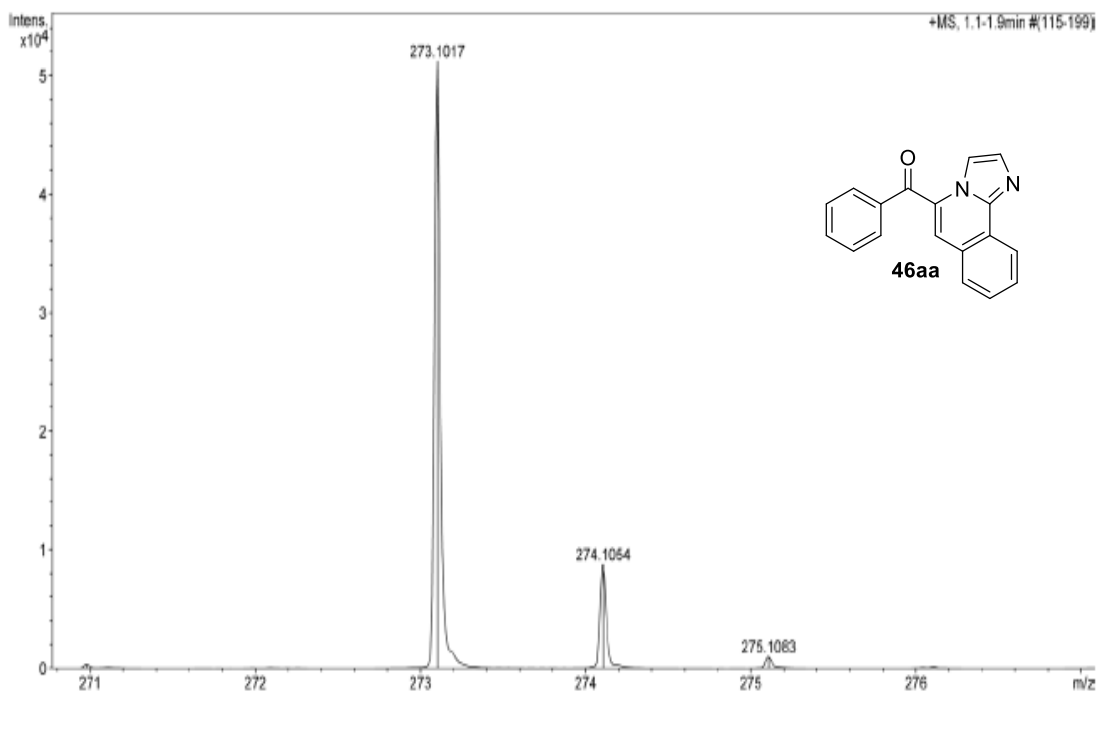
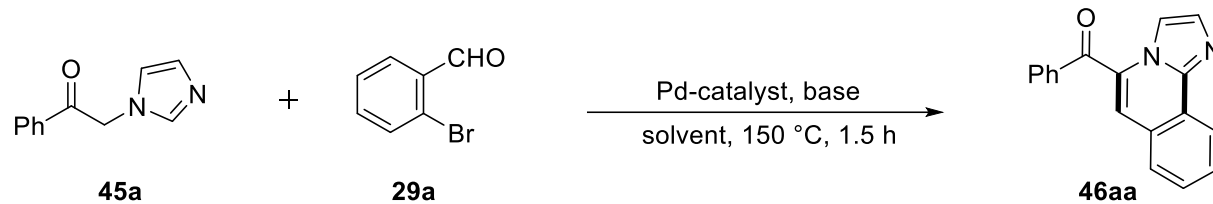


Figure 3.7: HRMS spectrum of **46aa**

Encouraged by this result, we further screened various palladium catalysts, bases and solvents to improve the yield of tandem product **46aa**. Survey of various bases such as K_2CO_3 , $t\text{BuOK}$, and KOH suggested that K_2CO_3 is suitable for the present methodology, which afforded 68% of **46aa** (entries 2-4, **Table 3.1**).

Among all palladium-catalysts *viz* $\text{Pd}(\text{OAc})_2$, $\text{Pd}(\text{PPh}_3)_4$, PdCl_2 , $\text{Pd}(\text{PPh}_3)_2\text{Cl}_2$, and $\text{Pd}(\text{PCy}_3)_2\text{Cl}_2$ screened for the reaction, highest yield for **46aa** was obtained using $\text{Pd}(\text{OAc})_2$ (entries 2 and 5-8, **Table 3.1**). Surprisingly, changing the reaction solvent to toluene or 1,4-dioxane failed to produce **46aa**, whereas with DMF or DMSO yields were diminished (entries 9-12, **Table 3.1**). The reaction was restricted to an intermediate stage (knoevengel adduct) without Pd catalyst and only starting materials were recovered with traces of **46aa** in the absence of a base (entries 13-14, **Table 3.1**). The use of PPh_3 as a ligand and pivalic acid as an additive also did not improve the yield of **46aa** (entries 15-16, **Table 3.1**).

Table 3.1: Optimization of reaction conditions.^a

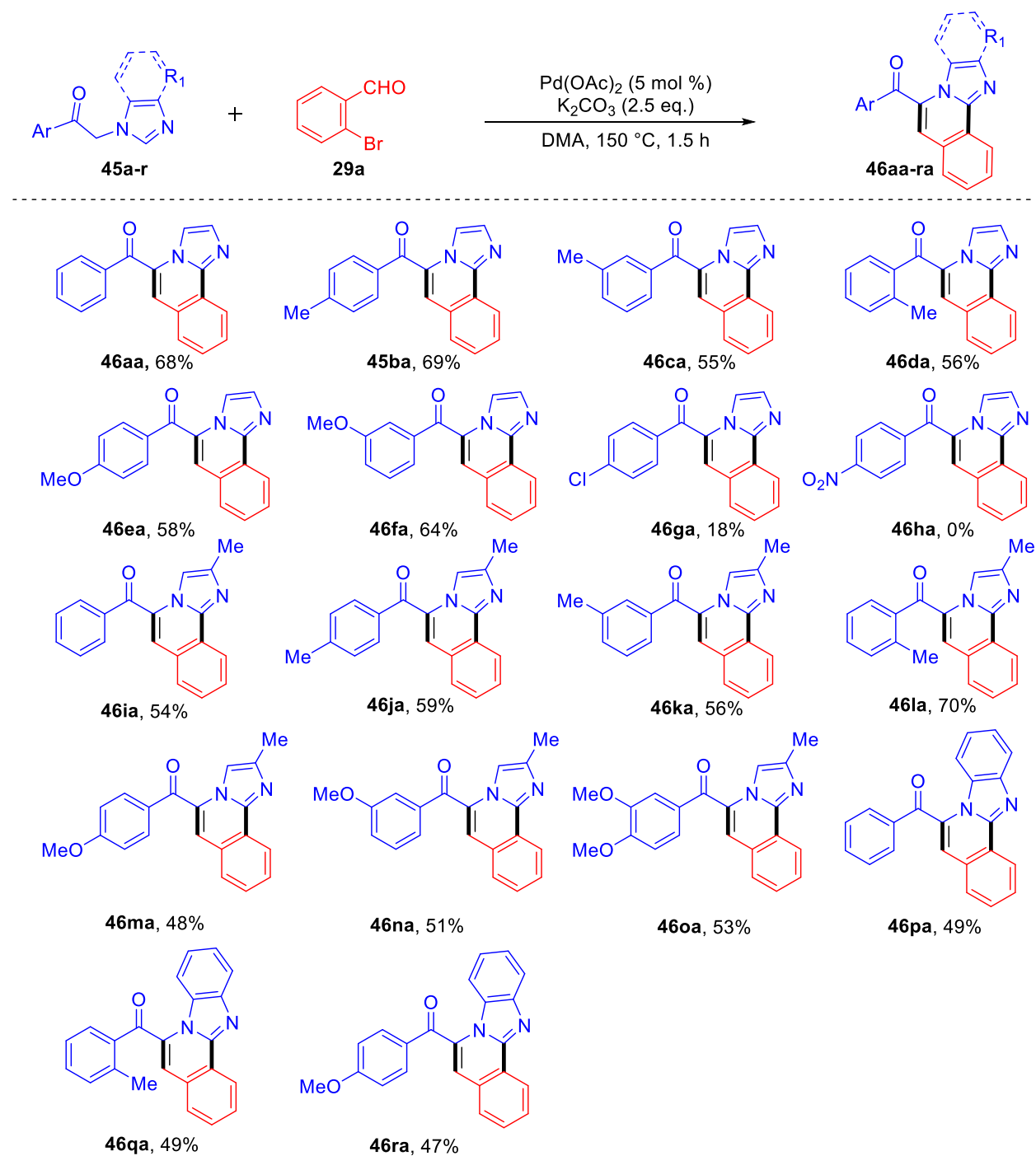
entry	catalyst	base	solvent	yield (%) ^b
1	Pd(OAc) ₂	Cs ₂ CO ₃	DMA	59
2	Pd(OAc)₂	K₂CO₃	DMA	68
3	Pd(OAc) ₂	^t BuOK	DMA	Traces
4	Pd(OAc) ₂	KOH	DMA	52
5	Pd(PPh ₃) ₄	K ₂ CO ₃	DMA	22
6	PdCl ₂	K ₂ CO ₃	DMA	25
7	Pd(PPh ₃) ₂ Cl ₂	K ₂ CO ₃	DMA	20
8	Pd(PCy ₃) ₂ Cl ₂	K ₂ CO ₃	DMA	33
9	Pd(OAc) ₂	K ₂ CO ₃	DMF	40
10	Pd(OAc) ₂	K ₂ CO ₃	DMSO	17
11 ^c	Pd(OAc) ₂	K ₂ CO ₃	toluene	– ^e
12 ^d	Pd(OAc) ₂	K ₂ CO ₃	1,4-dioxane	– ^e
13	–	K ₂ CO ₃	DMA	– ^e
14	Pd(OAc) ₂	–	DMA	Traces
15 ^f	Pd(OAc) ₂	K ₂ CO ₃	DMA	49
16 ^g	Pd(OAc) ₂	K ₂ CO ₃	DMA	58

Reaction conditions: **45a** (0.53 mmol), **29a** (0.55 mmol), catalyst (5 mol %), base (1.25 mmol), solvent (2 mL), 1.5 h, 150 °C, N₂ atmosphere. ^bIsolated yields. ^cAt 120 °C. ^dAt 110 °C. ^eOnly aldol product was isolated after 16 h. ^f10 mol % of PPh₃ was used. ^g30 mol % of pivalic acid was used.

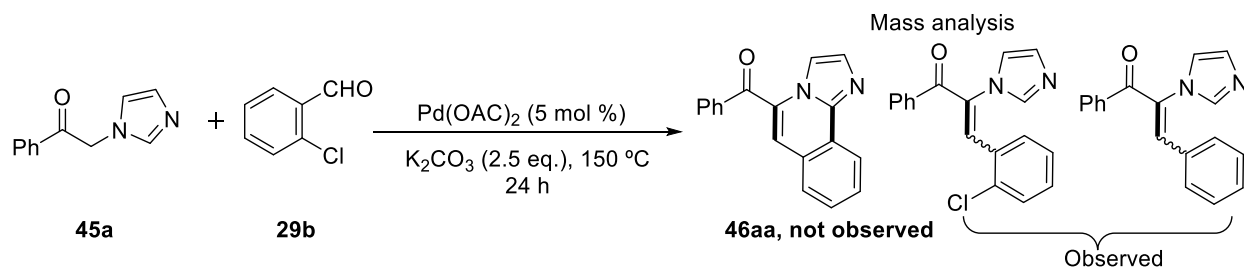
With the established reaction conditions in hand (entry 2, **Table 3.1**), we further investigated the scope of the cascade reaction. As shown in **Table 3.2**, diversely substituted azolyl aryl ethanones (**45a-r**) produced **46aa-ra** in moderate to good yields under the optimized reaction conditions. Though, the aryl group in substrate **45** is not in the vicinity of reactive sites, however, substituents on aryl moiety greatly influenced the outcome of the cascade process.

For example, substrates with electron-rich arenes (**45a-f**) resulted in higher yields (55-69%) of corresponding tandem products (**46aa-fa**) when compared to arenes with electron-withdrawing groups (**46ga-ha**). It is important to mention that 4-chlorophenyl substituted azole (**45g**) gave **46ga** in poor yield (18%), whereas only starting material was recovered in the case of 4-nitrophenyl substituted azole (**45h**). Aryl groups with electron-rich substituents at *ortho*-, *meta*-, *para*-positions were well tolerated under the reaction conditions to give good yields of the cascade products. Similarly, 4-methyl imidazole analogue (**45i-o**) underwent smooth conversion to afford the corresponding tandem products (**46ia-oa**) in good yields. To our delight, substrates with benzimidazole moieties (**45p-r**) also smoothly participated in domino process and provided good yields of corresponding benzimidazo-fused isoquinolines (**46pa-ra**).

When 2-chlorobenzaldehyde (**29b**) was allowed to react with **45a** under optimized reaction condition, only aldol adduct was detected in the reaction mass analysis through LC-MS (**Figure 3.8**). No improvement was observed when the reaction was continued overnight.

Table 3.2: Substrate scope for the Pd-catalyzed tandem synthesis of azole-fused isoquinolines^a

^a**Reaction conditions:** **45** (0.53 mmol), **29** (0.55 mmol), K₂CO₃ (1.25 mmol), Pd(OAc)₂ (5 mol %), DMA (2 mL), 150 °C, 1.5 h. ^bYields of the isolated products



Scheme 3.17: Reaction of 2-chlorobenzaldehyde under the optimized reaction condition

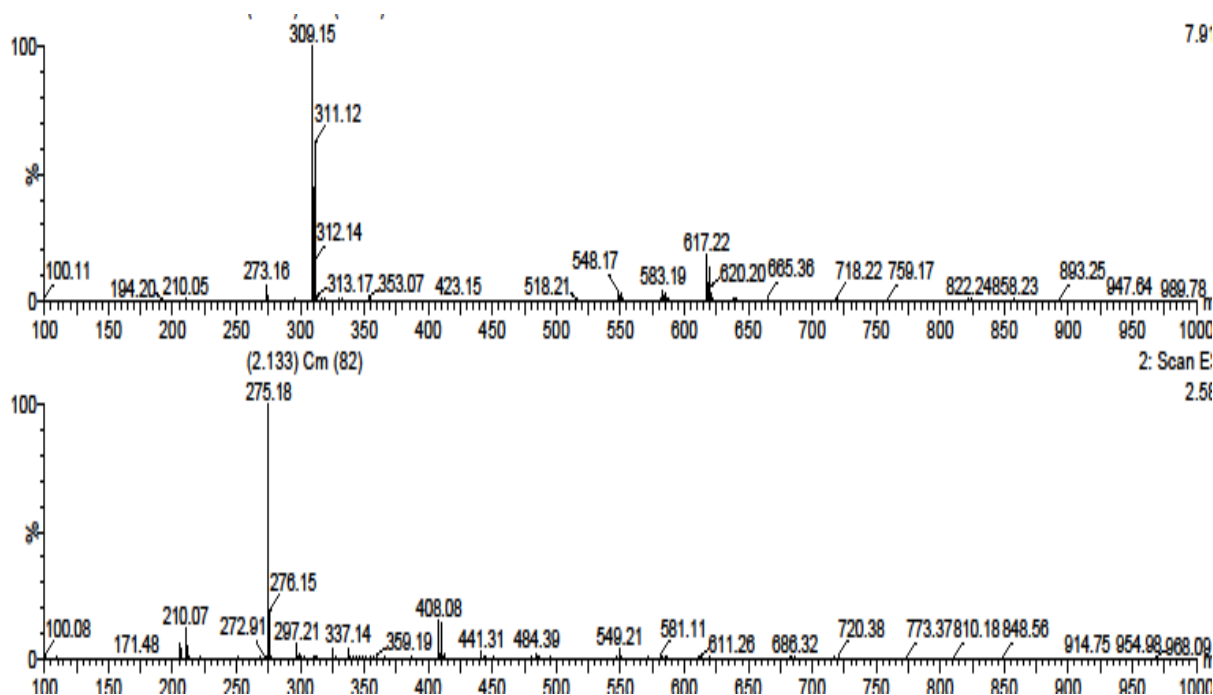
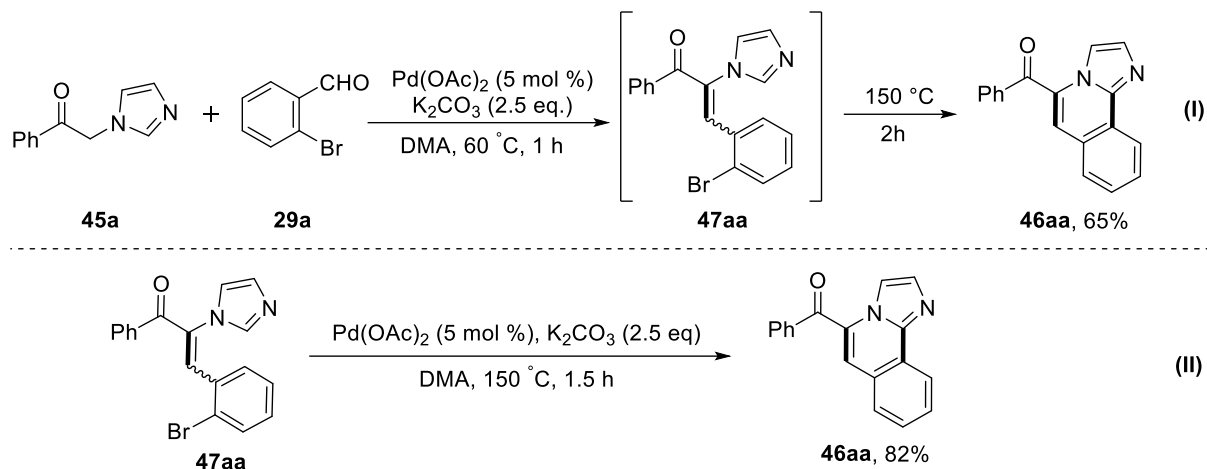


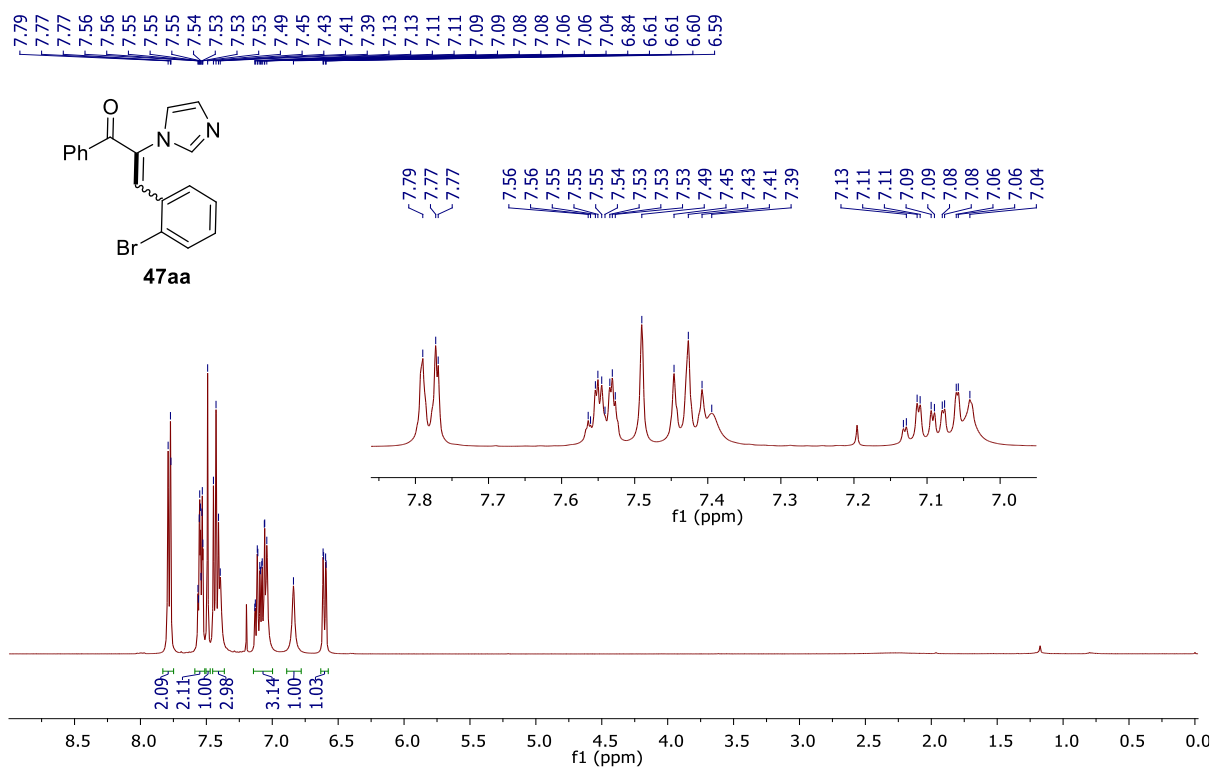
Figure 3.8: Mass analysis of the reaction mixture

Control experiments were performed to investigate the likely synthetic pathway of designed tandem sequences (**Scheme 3.18**). When the standard reaction was performed at 60 °C, only Knoevenagel adduct **47aa** was detected as a major product after 1 h, confirmed by ^1H and ^{13}C -NMR (**Figure 3.9 & 3.10**). Further continuation of the reaction for 2 h at 150 °C led to **46aa** which confirms that the Knoevenagel adduct **47aa** is the key intermediate in this tandem reaction (**Scheme 3.18I**). To further validate this pathway, the isolated Knoevenagel adduct **47aa** was treated under similar reaction conditions to afford the tandem product **46aa** in 82% yields (**Scheme 3.18II**).



Scheme 3.17: Control experiments

In the ^1H NMR spectrum, singlet peak appeared at δ 7.49 ppm for $\text{C}_3\text{-H}$ with all other peaks at their respective place (**Figure 3.9**). The carbonyl carbon of **47aa** appeared at δ 191.4 ppm along with all other expected carbons in the ^{13}C NMR spectrum (**Figure 3.10**) further confirmed the structure of **47aa**.

Figure 3.9: ^1H NMR spectrum of **47aa**

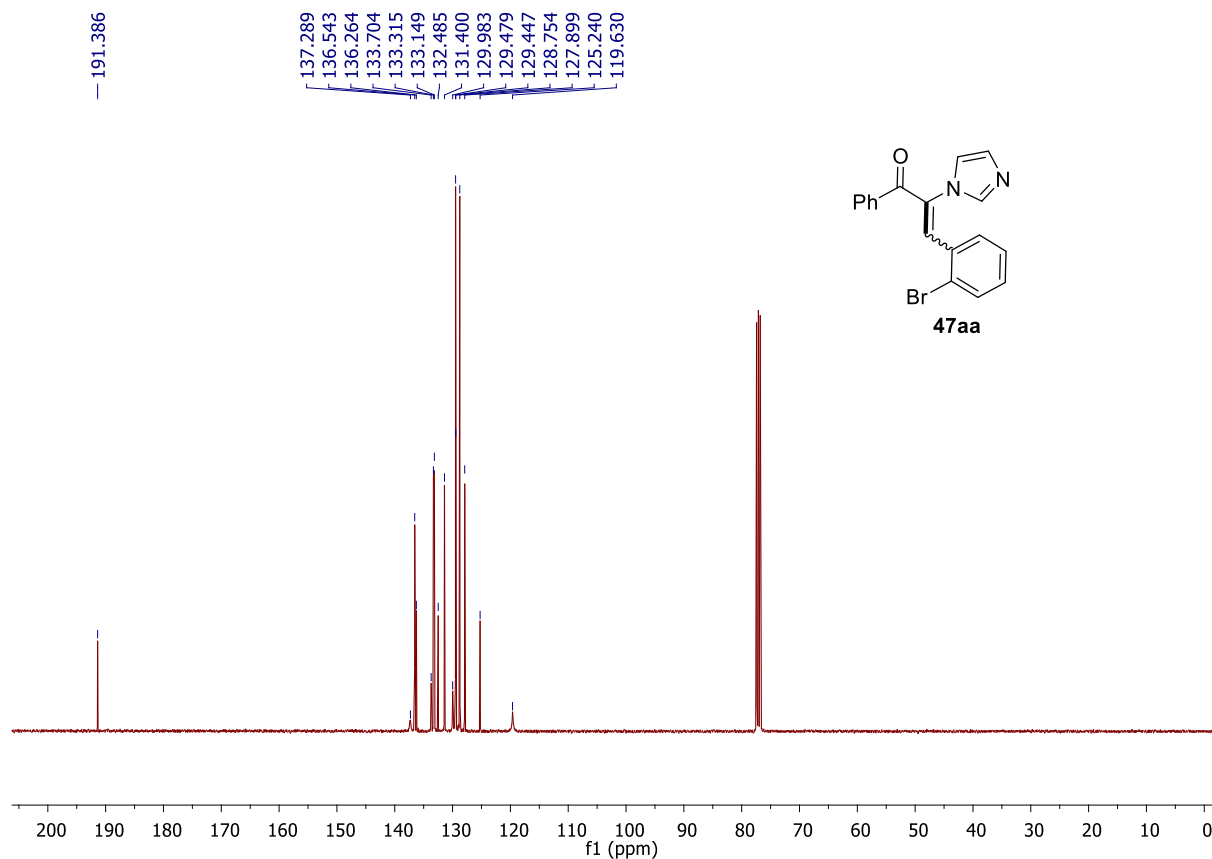


Figure 3.10: ^{13}C NMR spectrum of **47aa**

To check the unambiguous structure of Knoevenagel adduct, we performed the 2D correlation experiments. First, we conducted $^1\text{H} - ^{13}\text{C}$ Heteronuclear Multiple Bond Correlation (HMBC) experiment and we observed that singlet peak at δ 7.49 ppm in ^1H -NMR showed the correlation with carbonyl carbon at δ 191.3 ppm in ^{13}C -NMR which confirmed that peak at δ 7.49 ppm in ^1H -NMR corresponds to $\text{C}_3 - \text{H}$ of propanone (**47aa**). The multiplet peak from δ 7.79 – 7.77 ppm in ^1H -NMR also showed the correlation with carbonyl carbon in HMBC spectrum, confirmed that multiplet peak from δ 7.79 – 7.77 ppm correspond to $\text{C}_{2/6} - \text{H}$ of aroyl ring (**Figure 3.11**). Then we performed the 2D NOESY experiment; this experiment showed that the correlation of $\text{C}_3 - \text{H}$ (at 7.49 ppm) with $\text{C}_2 - \text{H}$ (δ 7.79 – 7.77 ppm) of aroyl ring (**Figure 3.12**). By HMBC and 2D-NOESY experiments confirmed that Knoevenagel adduct has *Z*-configuration.

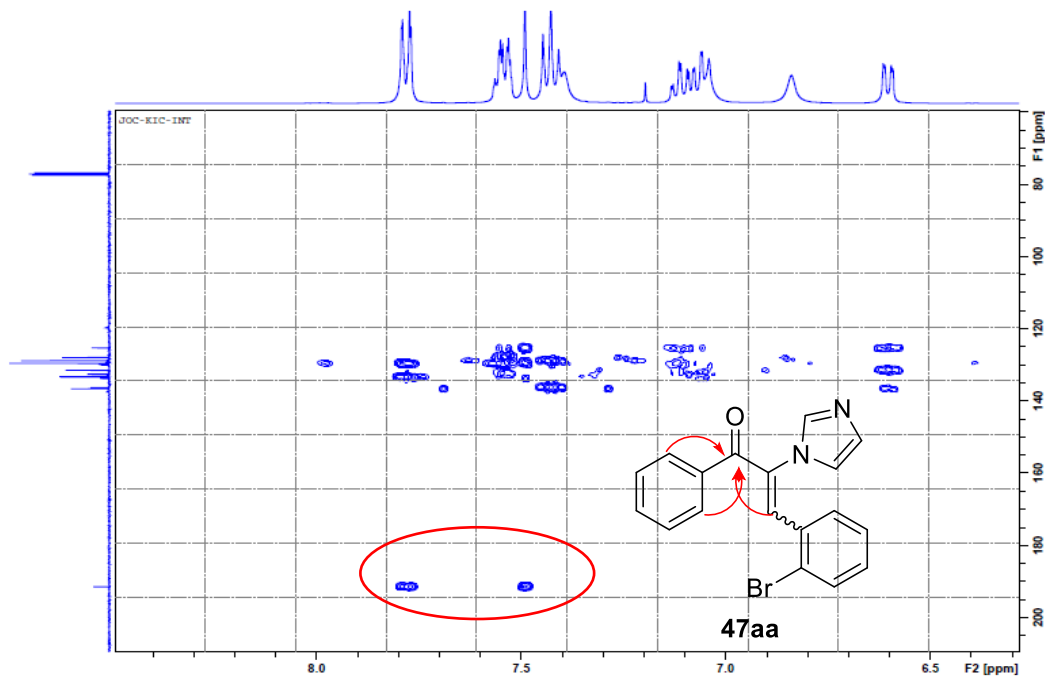


Figure 3.11: HMBC spectrum of 47aa

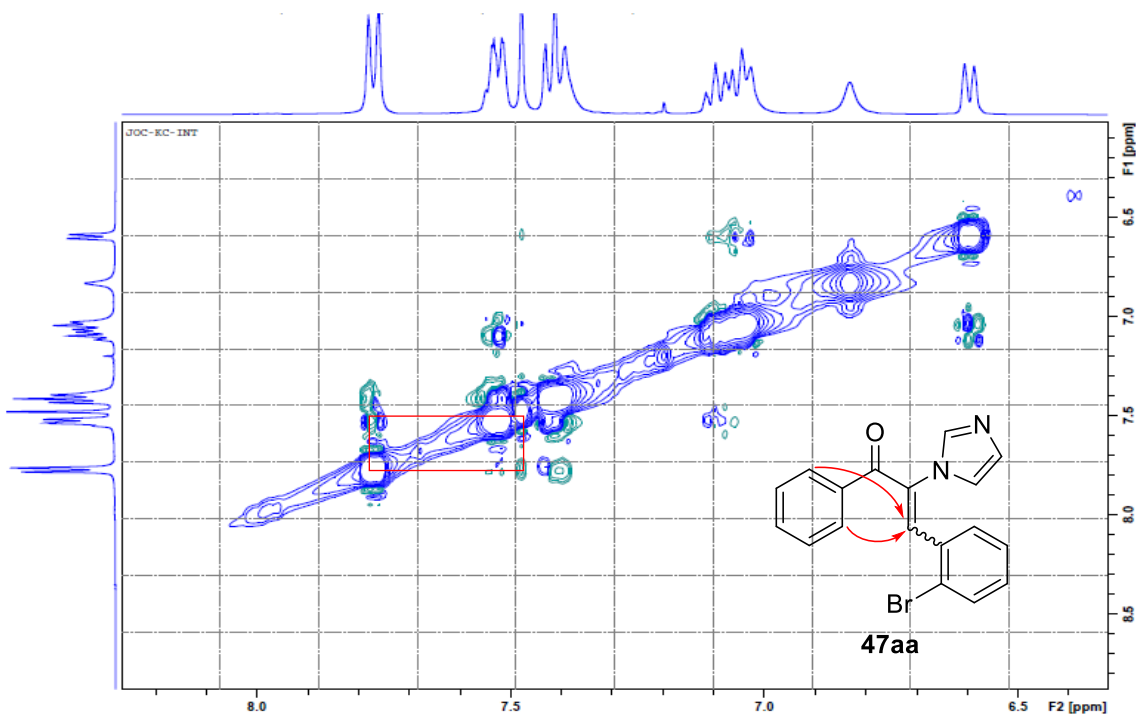
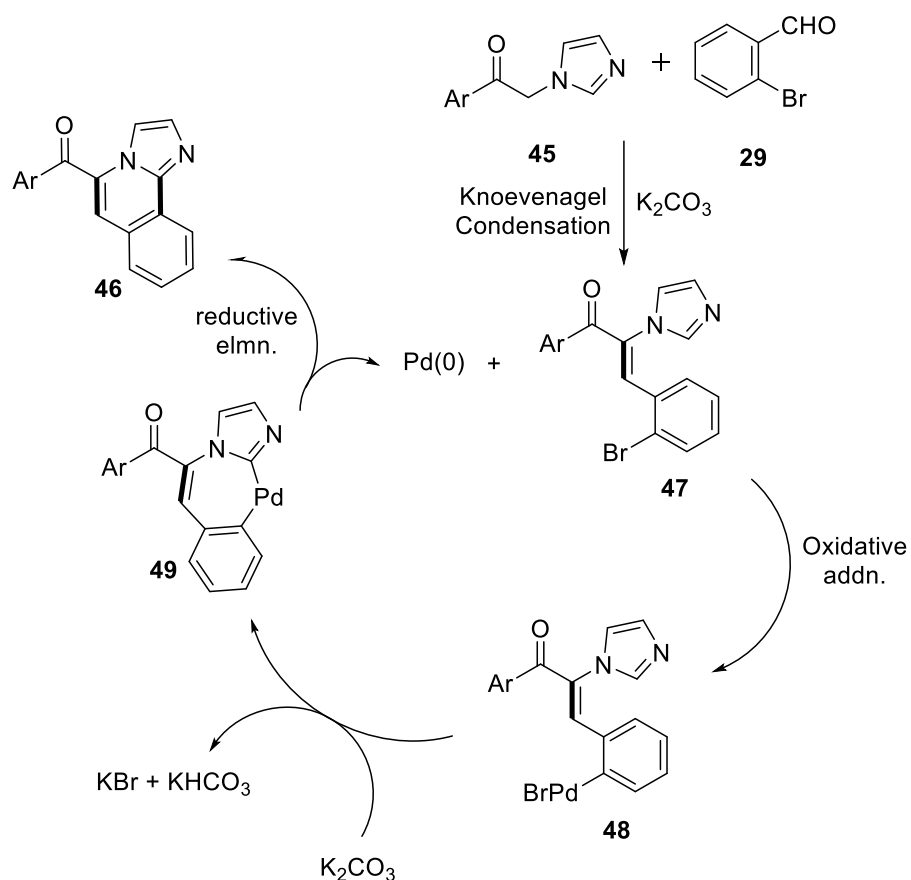


Figure 3.12: 2D NOESY spectrum of 47aa

Based on previous literature reports^[46-47] and our experimental results, we believe that the reaction proceeds *via* initial Knoevenagel adduct (**47**) was formed by the reaction of **45** and **29** in the presence of a base. Oxidative insertion of palladium (0) into **47** gives arylpalladium(II) bromide intermediate **48**. The Pd(II) intermediate **48** is believed to be responsible for the intramolecular C–H activation of azole C₂-position to give palladacycle intermediate **49**. Finally, reductive elimination of **49** affords the domino product, azole fused isoquinolines (**46**) with the regeneration of active palladium (0) for the next cycle (**Scheme 3.19**).



Scheme 3.19. A plausible mechanism for the formation of **46**

3.3 CONCLUSIONS

In conclusion, we have demonstrated a straightforward cascade approach for the synthesis of benzimidazo/imidazo[2,1-*a*]isoquinolines (**46**) *via* Knoevenagel condensation and palladium-catalyzed intramolecular C–H functionalization. This method allows an alternative route for the assembly of benzimidazo/imidazo[2,1-*a*]isoquinolines (**46**) with hitherto unknown aroyl moiety at

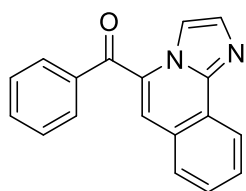
the C-5 position. The precursor, 2-(1*H*-imidazol/benzimidazolyl-1-yl)-1-arylethanones (**45**) are readily available from corresponding methyl ketones and azoles in a single step.^[48]

3.4 EXPERIMENTAL SECTION

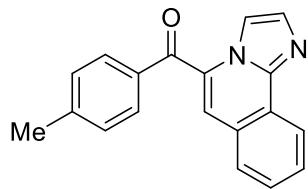
General information: Melting points were determined in open capillary tubes on a EZ-Melt automated melting point apparatus and are uncorrected. Reactions were monitored by using thin layer chromatography (TLC) on 0.2 mm silica gel F254 plates (Merck). The chemical structures of final products were determined by their NMR spectra (¹H and ¹³C NMR). Chemical shifts are reported in parts per million (ppm) using deuterated solvent peak or tetramethylsilane as an internal standard. The HRMS data were recorded on a mass spectrometer with electrospray ionization and QTOF mass analyzer. 2-(1*H*-imidazol/benzimidazolyl-1-yl)-1-arylethanones (**45a**) were synthesized from phenacyl bromides. All other chemicals were obtained from the commercial suppliers and used without further purification.

General procedure for synthesis of 46aa: A clean oven-dried 10 mL RB-flask was charged with **45a** (93 mg, 0.5 mmol), 2-bromobenzaldehyde **29a** (102 mg, 0.55 mmol), K₂CO₃ (172 mg, 1.25 mmol), Pd(OAc)₂ (11 mg, 5 mol %) and DMA (2 mL). The resulting solution was stirred at 150 °C for 1.5 h under N₂ atmosphere. On completion, the reaction mass was allowed to cool to ambient temperature, diluted with water (5 mL) and extracted with EtOAc (2 × 5 mL). The combined organic layer was dried over anhydrous Na₂SO₄ and evaporated to dryness. The crude residue so obtained was purified by column chromatography (EtOAc: hexanes) to afford **46aa** in 68% (93 mg) yield.

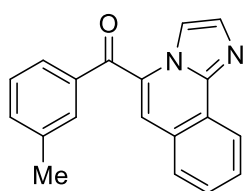
Imidazo[2,1-*a*]isoquinolin-5-yl(phenyl)methanone (**46aa**)



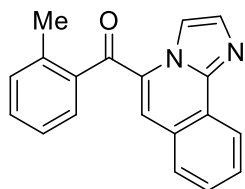
Yellow solid (93 mg, 68%); mp 164–166 °C; ¹H NMR (400 MHz, CDCl₃) δ 9.21 (s, 1H), 8.11 (d, *J* = 8.0 Hz, 1H), 7.99 (s, 1H), 7.90 (d, *J* = 7.5 Hz, 2H), 7.76 – 7.55 (m, 5H), 7.47 (t, *J* = 7.6 Hz, 1H), 7.41 (s, 1H); ¹³C NMR (100 MHz, CDCl₃) δ 190.4, 137.4, 133.0, 132.3, 131.4, 129.7, 129.3, 129.2, 128.7, 127.2, 126.7, 125.8, 125.2, 122.5, 121.1; IR(KBr): 3070, 1636, 1412, 1227 cm⁻¹; HRMS calcd for C₁₈H₁₃N₂O [M+H]⁺ 273.1022, found 273.1017.

Imidazo[2,1-*a*]isoquinolin-5-yl(*p*-tolyl)methanone (46ba)

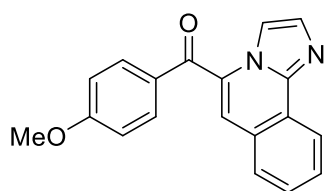
Yellow solid (99 mg, 69%); mp 201–202 °C; ^1H NMR (400 MHz, DMSO-*d*₆) δ 8.92 (s, 1H), 8.28 (d, J = 8.0 Hz, 1H), 8.11 (s, 1H), 7.94 (d, J = 7.7 Hz, 1H), 7.86 (d, J = 8.1 Hz, 2H), 7.76 – 7.69 (m, 1H), 7.58 (s, 1H), 7.55 – 7.49 (m, 1H), 7.45 (d, J = 7.9 Hz, 2H), 2.46 (s, 3H); ^{13}C NMR (100 MHz, CDCl₃) δ 190.1, 144.2, 134.6, 132.2, 131.2, 130.0, 129.5, 129.4, 129.1, 127.2, 126.7, 125.3, 125.0, 122.5, 121.1, 21.8; IR(KBr): 3055, 2924, 1643, 1458, 1257 cm⁻¹; HRMS calcd for C₁₉H₁₅N₂O [M+H]⁺ 287.1179, found 287.1189.

Imidazo[2,1-*a*]isoquinolin-5-yl(*m*-tolyl)methanone (45ca)

Yellow solid (79 mg, 55%); mp 141–143 °C; ^1H NMR (400 MHz, CDCl₃) δ 9.18 (s, 1H), 8.10 (d, J = 8.0 Hz, 1H), 7.98 (s, 1H), 7.71 (s, 1H), 7.70 – 7.62 (m, 3H), 7.53 – 7.43 (m, 3H), 7.40 (s, 1H), 2.49 (s, 3H); ^{13}C NMR (100 MHz, CDCl₃) δ 190.6, 138.8, 137.4, 133.8, 132.3, 131.3, 130.1, 129.5, 129.2, 128.7, 128.5, 127.2, 126.9, 126.7, 125.6, 125.2, 122.5, 121.0, 21.4; IR (KBr): 2916, 2854, 1643, 1458, 1265 cm⁻¹; HRMS calcd for C₁₉H₁₅N₂O [M+H]⁺ 287.1179, found 287.1155.

Imidazo[2,1-*a*]isoquinolin-5-yl(*o*-tolyl)methanone (46da)

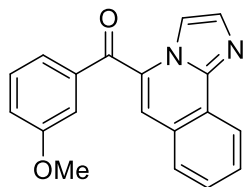
Yellow solid (80 mg, 59%); mp 156–158 °C; ^1H NMR (400 MHz, CDCl₃) δ 9.50 (s, 1H), 8.10 (d, J = 8.0 Hz, 1H), 8.00 (s, 1H), 7.71 – 7.63 (m, 1H), 7.59 (d, J = 7.6 Hz, 1H), 7.54 – 7.47 (m, 1H), 7.44 – 7.42 (m, 2H), 7.40 – 7.31 (m, 2H), 7.29 (s, 1H), 2.42 (s, 3H); ^{13}C NMR (100 MHz, CDCl₃) δ 192.6, 137.6, 137.0, 132.7, 131.7, 131.3, 130.9, 130.2, 129.4, 128.7, 128.4, 127.5, 127.1, 127.1, 125.5, 125.1, 122.4, 121.2, 19.7. IR (KBr): 3186, 3055, 1651, 1458, 1211 cm⁻¹; HRMS calcd for C₁₉H₁₅N₂O [M+H]⁺ 287.1187, found 287.1168.

Imidazo[2,1-*a*]isoquinolin-5-yl(4-methoxyphenyl)methanone (46ea)

Yellow solid (88 mg, 58%); mp 165–167 °C; ^1H NMR (400 MHz, CDCl₃) δ 9.03 (s, 1H), 8.10 (d, J = 7.9 Hz, 1H), 7.97 – 7.93 (m, 3H), 7.66 (t, J = 8.3 Hz, 2H), 7.47 (t, J = 7.3 Hz, 1H), 7.34 (s, 1H), 7.06 (d, J = 8.8 Hz, 2H), 3.95 (s, 3H); ^{13}C NMR (100 MHz, CDCl₃) δ 188.9, 163.9, 132.3, 131.0, 129.7, 128.9, 127.2, 126.5, 125.4, 123.8, 122.5, 121.1, 114.0, 55.6; IR (KBr):

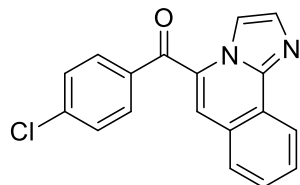
3065, 2948, 1631, 1482, 1278, 1221 cm^{-1} ; HRMS calcd for $\text{C}_{19}\text{H}_{15}\text{N}_2\text{O}_2$ $[\text{M}+\text{H}]^+$ 303.1128, found 303.1152.

Imidazo[2,1-*a*]isoquinolin-5-yl(3-methoxyphenyl)methanone (46fa)



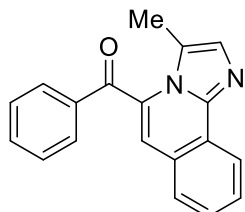
Yellow solid (97 mg, 64%); mp 147–149 °C; ^1H NMR (400 MHz, CDCl_3) δ 9.18 (d, $J = 2.6$ Hz, 1H), 8.08 (t, $J = 7.8$ Hz, 1H), 7.96 (d, $J = 6.3$ Hz, 1H), 7.70–7.57 (m, 2H), 7.52–7.36 (m, 5H), 7.22 (s, 1H), 3.90 (s, 3H); ^{13}C NMR (100 MHz, CDCl_3) δ 190.1, 159.8, 138.6, 132.2, 131.4, 129.6, 129.3, 129.2, 128.6, 127.2, 126.7, 125.8, 125.1, 122.4, 122.2, 121.0, 119.3, 114.2, 55.5; IR (KBr): 3070, 2962, 1628, 1466, 1285, 1126 cm^{-1} ; HRMS calcd for $\text{C}_{19}\text{H}_{15}\text{N}_2\text{O}_2$ $[\text{M}+\text{H}]^+$ 303.1128, found 303.1112.

(4-chlorophenyl)(imidazo[2,1-*a*]isoquinolin-5-yl)methanone (46ga)



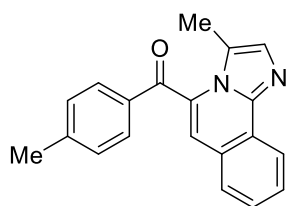
Yellow solid (27 mg, 18%); mp 160–162 °C; ^1H NMR (400 MHz, CDCl_3) δ 9.17 (s, 1H), 8.11 (d, $J = 8.0$ Hz, 1H), 7.99 (s, 1H), 7.85 (d, $J = 8.5$ Hz, 2H), 7.71–7.61 (m, 2H), 7.57 (d, $J = 8.5$ Hz, 2H), 7.51–7.43 (m, 1H), 7.37 (s, 1H); ^{13}C NMR (100 MHz, CDCl_3) δ 189.1, 139.6, 135.7, 131.6, 131.1, 129.2, 129.1, 129.1, 127.3, 126.8, 125.7, 125.1, 122.5, 121.3; IR (KBr): 2926, 2864, 1651, 1459, 1255 cm^{-1} ; HRMS calcd for $\text{C}_{18}\text{H}_{12}\text{ClN}_2\text{O}$ $[\text{M}+\text{H}]^+$ 307.0633, found 307.0612.

(2-Methylimidazo[2,1-*a*]isoquinolin-5-yl)(phenyl)methanone (46ia)



Orange solid (77 mg, 54%); mp 135–137 °C; ^1H NMR (400 MHz, CDCl_3) δ 9.08 (s, 1H), 8.17–8.12 (m, 1H), 7.88 (d, $J = 8.1$ Hz, 2H), 7.73–7.64 (m, 2H), 7.61–7.55 (m, 3H), 7.41 (t, $J = 7.5$ Hz, 1H), 7.31 (d, $J = 1.4$ Hz, 1H), 2.85 (s, 3H); ^{13}C NMR (100 MHz, CDCl_3) δ 190.4, 137.5, 133.0, 131.7, 131.3, 129.9, 129.7, 129.3, 129.0, 128.7, 128.3, 126.1, 126.0, 125.4, 123.3, 122.6, 16.6; IR (KBr): 3055, 2916, 1636, 1458, 1257 cm^{-1} ; HRMS calcd for $\text{C}_{19}\text{H}_{15}\text{N}_2\text{O}$ $[\text{M}+\text{H}]^+$ 287.1179, found 287.1192.

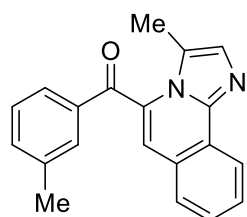
(2-Methylimidazo[2,1-*a*]isoquinolin-5-yl)(*p*-tolyl)methanone (46ja)



Orange solid (88 mg, 59%); mp 155–156 °C; ^1H NMR (400 MHz, CDCl_3) δ 9.06 (s, 1H), 8.14 (d, $J = 7.7$ Hz, 1H), 7.73–7.62 (m, 3H), 7.60 (d, $J = 7.3$ Hz, 1H), 7.53–7.34 (m, 3H), 7.29 (s, 1H), 2.85 (s, 3H), 2.47 (s, 3H); ^{13}C NMR (100 MHz, CDCl_3) δ 190.6, 138.7, 137.5, 133.8, 131.7,

131.2, 130.1, 129.9, 129.4, 129.3, 128.4, 128.2, 126.9, 126.0, 125.7, 125.4, 123.2, 122.5, 21.4, 16.6; IR(KBr): 2916, 2854, 1643, 1456, 1265 cm^{-1} ; HRMS calcd for $\text{C}_{20}\text{H}_{17}\text{N}_2\text{O}$ $[\text{M}+\text{H}]^+$ 301.1335, found 301.1326.

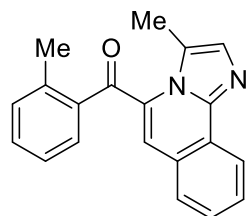
(2-Methylimidazo[2,1-*a*]isoquinolin-5-yl)(*m*-tolyl)methanone (46ka)



Orange solid (84 mg, 56%); mp 151–152 °C; ^1H NMR (400 MHz, CDCl_3) δ 9.01 (s, 1H), 8.14 (d, $J = 8.1$ Hz, 1H), 7.79 (d, $J = 8.1$ Hz, 2H), 7.69 – 7.63 (m, 1H), 7.59 (d, $J = 7.5$ Hz, 1H), 7.44 – 7.34 (m, 3H), 7.27 (s, 1H), 2.85 (s, 3H), 2.50 (s, 3H); ^{13}C NMR (100 MHz, CDCl_3) δ 190.0, 144.1, 134.7, 131.6, 131.0, 129.9, 129.8, 129.5, 129.4, 129.1, 128.1, 126.0, 125.5, 125.1, 123.2,

122.5, 21.7, 16.6; IR (KBr): 2916, 2854, 1643, 1458, 1257 cm^{-1} ; HRMS calcd for $\text{C}_{20}\text{H}_{17}\text{N}_2\text{O}$ $[\text{M}+\text{H}]^+$ 301.1335, found 301.1362.

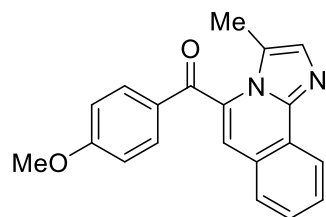
(2-Methylimidazo[2,1-*a*]isoquinolin-5-yl)(*o*-tolyl)methanone (46la)



Orange solid (110 mg, 70%); mp 142–143 °C; ^1H NMR (400 MHz, CDCl_3) δ 9.40 (s, 1H), 8.16 (d, $J = 8.1$ Hz, 1H), 7.68 (t, 1H), 7.56 (d, $J = 7.6$ Hz, 1H), 7.49 (t, 1H), 7.46 – 7.31 (m, 4H), 7.21 (s, 1H), 2.87 (s, 3H), 2.41 (s, 3H); ^{13}C NMR (100 MHz, CDCl_3) δ 192.6, 137.8, 137.0, 131.8, 131.6, 131.2, 130.8,

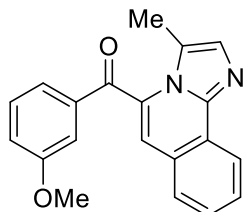
130.4, 130.1, 129.5, 128.6, 128.4, 127.7, 126.0, 125.5, 125.3, 123.3, 122.5, 19.7, 16.7; IR (KBr): 3163, 3032, 1651, 1458, 1250 cm^{-1} ; HRMS calcd for $\text{C}_{20}\text{H}_{17}\text{N}_2\text{O}$ $[\text{M}+\text{H}]^+$ 301.1335, found 301.1312.

(4-Methoxyphenyl)(2-methylimidazo[2,1-*a*]isoquinolin-5-yl)methanone (46ma)

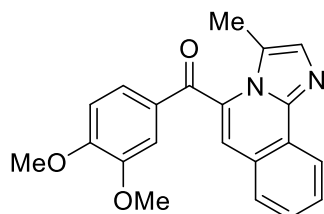


Orange solid (76 mg, 48%); mp 141–143 °C; ^1H NMR (400 MHz, CDCl_3) δ 8.89 (s, 1H), 8.13 (d, $J = 7.9$ Hz, 1H), 7.91 (d, $J = 8.4$ Hz, 2H), 7.64 (t, $J = 7.5$ Hz, 1H), 7.59 (d, $J = 7.6$ Hz, 1H), 7.40 (t, $J = 7.3$ Hz, 1H), 7.22 (s, 1H), 7.03 (d, $J = 8.4$ Hz, 2H), 3.93 (s, 3H), 2.84 (s,

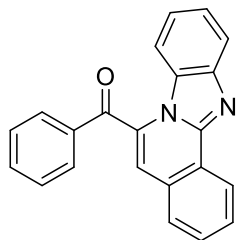
3H); ^{13}C NMR (100 MHz, CDCl_3) δ 188.8, 163.8, 132.2, 131.5, 130.8, 129.7, 129.7, 129.5, 129.0, 127.9, 126.0, 125.6, 123.9, 123.2, 122.5, 114.0, 55.6, 16.6; IR (KBr): 2952, 2928, 1647, 1461, 1261, 1189 cm^{-1} ; HRMS calcd for $\text{C}_{20}\text{H}_{17}\text{N}_2\text{O}_2$ $[\text{M}+\text{H}]^+$ 317.1285, found 317.1268.

(3-Methoxyphenyl)(2-methylimidazo[2,1-*a*]isoquinolin-5-yl)methanone (46na)

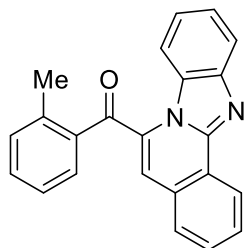
Orange solid (80 mg, 51%); mp 153–155 °C; ^1H NMR (400 MHz, CDCl_3) δ 9.06 (s, 1H), 8.15 (d, $J = 8.1$ Hz, 1H), 7.70 – 7.65 (m, 1H), 7.61 (d, $J = 7.4$ Hz, 1H), 7.49 – 7.39 (m, 4H), 7.34 (s, 1H), 7.22 (ddd, $J = 7.9, 2.5, 1.5$ Hz, 1H), 3.90 (s, 3H), 2.86 (s, 3H); ^{13}C NMR (100 MHz, CDCl_3) δ 190.1, 159.8, 138.8, 131.7, 131.3, 129.9, 129.6, 129.3, 128.3, 126.1, 125.9, 125.4, 123.2, 122.6, 122.2, 119.3, 114.2, 55.5, 16.6; IR(KBr): 2962, 2924, 1643, 1458, 1257, 1180 cm^{-1} ; HRMS calcd for $\text{C}_{20}\text{H}_{17}\text{N}_2\text{O}_2$ $[\text{M}+\text{H}]^+$ 317.1285, found 317.1298.

(3,4-Dimethoxyphenyl)(2-methylimidazo[2,1-*a*]isoquinolin-5-yl)methanone (46oa)

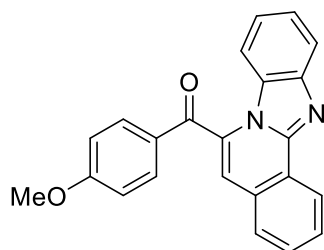
Orange solid (80 mg, 53%); mp 174–175 °C; ^1H NMR (400 MHz, CDCl_3) δ 8.86 (s, 1H), 8.18 (d, $J = 8.0$ Hz, 1H), 7.71 – 7.65 (m, 1H), 7.63 (d, $J = 7.8$ Hz, 1H), 7.55 (s, 1H), 7.46–7.39 (m, 1H), 7.28 (s, 2H), 6.98 (d, $J = 8.1$ Hz, 1H), 4.03 (s, 3H), 3.99 (s, 2H), 2.87 (s, 2H); ^{13}C NMR (100 MHz, CDCl_3) δ 191.4, 156.4, 152.0, 134.2, 133.4, 132.4, 132.2, 132.1, 131.5, 130.6, 128.7, 128.2, 127.4, 126.3, 125.8, 125.2, 114.5, 112.6, 58.8, 58.7, 19.1; IR (KBr): 3070, 2962, 1628, 1466, 1288, 1211 cm^{-1} ; HRMS calcd for $\text{C}_{21}\text{H}_{19}\text{N}_2\text{O}_3$ $[\text{M}+\text{H}]^+$ 343.1390, found 303.1376

Benzo[4,5]imidazo[2,1-*a*]isoquinolin-6-yl(phenyl)methanone (46pa)

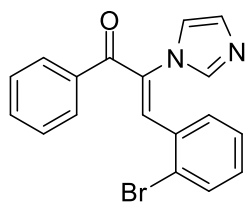
Yellow solid (79 mg, 49%); mp 148–150 °C; ^1H NMR (400 MHz, CDCl_3) δ 8.93 (d, $J = 7.9$ Hz, 1H), 8.15 (d, $J = 7.2$ Hz, 2H), 8.04 (d, $J = 8.2$ Hz, 1H), 7.84 – 7.68 (m, 4H), 7.61 (t, $J = 7.7$ Hz, 2H), 7.56 – 7.47 (m, 2H), 7.31 – 7.25 (m, 2H); ^{13}C NMR (100 MHz, CDCl_3) δ 189.0, 147.6, 144.1, 135.9, 134.6, 133.5, 130.6, 130.3, 130.0, 129.8, 129.5, 129.0, 127.9, 125.3, 124.7, 124.6, 122.2, 120.0, 116.9, 114.1; IR (KBr): 2924, 2854, 1651, 1450, 1288 cm^{-1} ; HRMS calcd for $\text{C}_{22}\text{H}_{15}\text{N}_2\text{O}$ $[\text{M}+\text{H}]^+$ 323.1179, found 323.1156.

Benzo[4,5]imidazo[2,1-*a*]isoquinolin-6-yl(*o*-tolyl)methanone (46qa)

Yellow solid (87 mg, 49%); mp 158–160 °C; ¹H NMR (400 MHz, CDCl₃) δ 8.91 (d, *J* = 8.0 Hz, 1H), 8.06 (d, *J* = 8.2 Hz, 1H), 7.82 – 7.73 (m, 2H), 7.72 – 7.67 (m, 3H), 7.59 – 7.50 (m, 2H), 7.45 (d, *J* = 7.6 Hz, 1H), 7.38 – 7.31 (m, 2H), 7.18 (s, 1H), 2.66 (s, 3H); ¹³C NMR (100 MHz, CDCl₃) δ 190.6, 147.6, 144.1, 140.3, 135.9, 135.3, 132.9, 132.1, 131.4, 130.3, 130.2, 130.1, 129.5, 128.1, 125.8, 125.3, 124.9, 124.7, 122.2, 120.0, 118.5, 114.6, 21.1; IR (KBr): 3055, 2924, 1659, 1450, 1211 cm⁻¹; HRMS calcd for C₂₃H₁₇N₂O [M+H]⁺ 337.1335, found 337.1362.

Benzo[4,5]imidazo[2,1-*a*]isoquinolin-6-yl(4-methoxyphenyl)methanone (46ra)

Yellow solid (86 mg, 47%); mp 172–173 °C; ¹H NMR (400 MHz, CDCl₃) δ 8.92 (d, *J* = 7.8 Hz, 1H), 8.12 (d, *J* = 8.8 Hz, 2H), 8.04 (d, *J* = 8.1 Hz, 1H), 7.81 – 7.68 (m, 3H), 7.55 – 7.44 (m, 2H), 7.31 – 7.24 (m, 1H), 7.21 (s, 1H), 7.05 (d, *J* = 8.9 Hz, 2H), 3.94 (s, 3H); ¹³C NMR (100 MHz, CDCl₃) δ 187.8, 165.0, 147.6, 144.1, 133.6, 133.1, 130.3, 129.8, 129.7, 129.6, 128.6, 127.7, 125.3, 124.6, 124.4, 122.2, 119.9, 115.4, 114.4, 114.0, 55.7; IR (KBr): 2924, 2847, 1643, 1450, 1257, 1165 cm⁻¹; HRMS calcd for C₂₃H₁₇N₂O₂ [M+H]⁺ 353.1285, found 353.1256.

(3-(2-Bromophenyl)-2-(1*H*-imidazol-1-yl)-1-phenylprop-2-en-1-one (47aa)

Yellow oil (75 mg, 40%); ¹H NMR (400 MHz, CDCl₃) δ 7.82 – 7.75 (m, 2H), 7.58 – 7.51 (m, 2H), 7.49 (s, 1H), 7.46 – 7.36 (m, 3H), 7.14 – 7.01 (m, 3H), 6.84 (s, 1H), 6.60 (dd, *J* = 7.6, 1.6 Hz, 1H). ¹³C NMR (100 MHz, CDCl₃) δ 191.4, 137.3, 136.5, 136.3, 133.7, 133.3, 133.1, 132.5, 131.4, 130.0, 129.5, 129.4, 128.7, 127.9, 125.2, 119.6; MS-ES for C₁₈H₁₄BrN₂O [M+H]⁺ 353.03, found 353.10 and [M+H+2]⁺ 355.11.

3.5 REFERENCES

- [1] A. F. Pozharskii, A. T. Soldatenkov, A. R. Katritzky, *Heterocycles in Life and Society: An Introduction to Heterocyclic Chemistry, Biochemistry and Applications*, John Wiley & Sons, **2011**.
- [2] P. M. Dewick, *Medicinal Natural Products: A Biosynthetic Approach*, John Wiley & Sons, **2002**.
- [3] A. Gomtsyan, *Chemistry of Heterocyclic Compounds*, **2012**, 48, 7-10.
- [4] A. R. Katritzky, S. V. Ley, O. Meth-Cohn, C. W. Rees, *Comprehensive Organic Functional Group Transformations: Synthesis: Carbon with One Heteroatom Attached by a Single Bond, Vol. 2*, Elsevier, **1995**.
- [5] J. Yamaguchi, A. D. Yamaguchi, K. Itami, *Angewandte Chemie International Edition*, **2012**, 51, 8960-9009.
- [6] T. Brückl, R. D. Baxter, Y. Ishihara, P. S. Baran, *Accounts of Chemical Research*, **2012**, 45, 826-839.
- [7] L. McMurray, F. O'Hara, M. J. Gaunt, *Chemical Society Reviews*, **2011**, 40, 1885-1898.
- [8] K. Godula, D. Sames, *Science*, **2006**, 312, 67-72.
- [9] S. Xu, E. H. Kim, A. Wei, E.-i. Negishi, *Science and Technology of Advanced Materials*, **2014**, 15, 044201.
- [10] K. L. Billingsley, K. W. Anderson, S. L. Buchwald, *Angewandte Chemie International Edition*, **2006**, 45, 3484-3488.
- [11] N. Miyaura, A. Suzuki, *Chemical Reviews*, **1995**, 95, 2457-2483.
- [12] C. Han, S. L. Buchwald, *Journal of the American Chemical Society*, **2009**, 131, 7532-7533.
- [13] E. Negishi, *Accounts of Chemical Research*, **1982**, 15, 340-348.
- [14] W.-J. Zhou, K.-H. Wang, J.-X. Wang, *The Journal of Organic Chemistry*, **2009**, 74, 5599-5602.
- [15] D. Milstein, J. Stille, *Journal of the American Chemical Society*, **1979**, 101, 4981-4991.
- [16] K. Tamao, K. Sumitani, M. Kumada, *Journal of the American Chemical Society*, **1972**, 94, 4374-4376.
- [17] L. Zhang, J. Wu, *Journal of the American Chemical Society*, **2008**, 130, 12250-12251.

- [18] T. Hiyama, *Journal of Organometallic Chemistry*, **2002**, 653, 58-61.
- [19] A. Kumar, G. K. Rao, S. Kumar, A. K. Singh, *Dalton Transactions*, **2013**, 42, 5200-5223.
- [20] T. W. Lyons, M. S. Sanford, *Chemical Reviews*, **2010**, 110, 1147-1169.
- [21] J. Wencel-Delord, F. Glorius, *Nature Chemistry*, **2013**, 5, 369.
- [22] T. Mizoroki, K. Mori, A. Ozaki, *Bulletin of the Chemical Society of Japan*, **1971**, 44, 581-581.
- [23] R. Heck, J. Nolley Jr, *The Journal of Organic Chemistry*, **1972**, 37, 2320-2322.
- [24] K. Mori, T. Mizoroki, A. Ozaki, *Bulletin of the Chemical Society of Japan*, **1973**, 46, 1505-1508.
- [25] L.-C. Campeau, K. Fagnou, *Chemical Communications*, **2006**, 1253-1264.
- [26] O. Baudoin, *Angewandte Chemie International Edition*, **2007**, 46, 1373-1375.
- [27] J. Yamaguchi, A. D. Yamaguchi, K. Itami, *Angewandte Chemie International Edition*, **2012**, 51, 8960-9009.
- [28] W. R. Gutekunst, P. S. Baran, *Chemical Society Reviews*, **2011**, 40, 1976-1991.
- [29] Y.-Q. Xia, L. Dong, *Organic Letters*, **2017**, 19, 2258-2261.
- [30] L. Song, G. Tian, Y. He, E. V. Van der Eycken, *Chemical Communications*, **2017**, 53, 12394-12397.
- [31] F. Jafarpour, P. T. Ashtiani, *The Journal of Organic Chemistry*, **2009**, 74, 1364-1366.
- [32] S. M. Allin, W. R. Bowman, M. R. Elsegood, V. McKee, R. Karim, S. S. Rahman, *Tetrahedron*, **2005**, 61, 2689-2696.
- [33] F. Jafarpour, P. T. Ashtiani, *The Journal of Organic Chemistry*, **2009**, 74, 1364-1366.
- [34] I. Čerňa, R. Pohl, B. Klepetářová, M. Hocek, *The Journal of Organic Chemistry*, **2010**, 75, 2302-2308.
- [35] K. Morimoto, K. Hirano, T. Satoh, M. Miura, *Organic Letters*, **2010**, 12, 2068-2071.
- [36] V. Fiandanese, S. Maurantonio, A. Punzi, G. G. Rafaschieri, *Organic & Biomolecular Chemistry*, **2012**, 10, 1186-1195.
- [37] A. K. Verma, R. R. Jha, R. Chaudhary, R. K. Tiwari, K. S. K. Reddy, A. Danodia, *The Journal of Organic Chemistry*, **2012**, 77, 8191-8205.
- [38] E. Ausekle, S. A. Ejaz, S. U. Khan, P. Ehlers, A. Villinger, J. Lecka, J. Sévigny, J. Iqbal, P. Langer, *Organic & Biomolecular Chemistry*, **2016**, 14, 11402-11414.

- [39] I. R. Ager, A. C. Barnes, G. W. Danswan, P. W. Hairsine, D. P. Kay, P. D. Kennewell, S. S. Matharu, P. Miller, P. Robson, *Journal of Medicinal Chemistry*, **1988**, *31*, 1098-1115.
- [40] S. M. Rida, S. A. El-Hawash, H. T. Fahmy, A. A. Hazzaa, M. M. El-Meligy, *Archives of Pharmacal Research*, **2006**, *29*, 826-833.
- [41] T. K. Chaitanya, K. S. Prakash, R. Nagarajan, *Tetrahedron*, **2011**, *67*, 6934-6938.
- [42] V. P. Reddy, T. Iwasaki, N. Kambe, *Organic & Biomolecular Chemistry*, **2013**, *11*, 2249-2253.
- [43] S. Karthik, J. Ajantha, C. M. Nagaraja, S. Easwaramoorthi, T. Gandhi, *Organic & Biomolecular Chemistry*, **2016**, *14*, 10255-10266.
- [44] N. Okamoto, K. Sakurai, M. Ishikura, K. Takeda, R. Yanada, *Tetrahedron Letters*, **2009**, *50*, 4167-4169.
- [45] J. Peng, G. Shang, C. Chen, Z. Miao, B. Li, *The Journal of Organic Chemistry*, **2013**, *78*, 1242-1248.
- [46] D. Alberico, M. E. Scott, M. Lautens, *Chemical Reviews*, **2007**, *107*, 174-238.
- [47] T. Wesch, A. Berthelot-Bréhier, F. R. Leroux, F. Colobert, *Organic Letters*, **2013**, *15*, 2490-2493.
- [48] I. C. Lennon, J. A. Ramsden, *Organic Process Research & Development*, **2005**, *9*, 110-112.

CHAPTER 4

Nickel-Catalyzed One-Pot Cascade Synthesis of Pyrazolo[5,1-*a*]isoquinolines

4.1 INTRODUCTION

Pyrazolo[5,1-*a*]isoquinolines is an azaheterocycle scaffold embedded with two bioactive isoquinoline and pyrazolo[1,5-*a*]pyridine frameworks, which is present in a significant number of pharmaceutically relevant molecules that exhibit remarkable biological activities (**Figure 4.1**). The pyrazole fused isoquinolines derivatives are used as an antagonist for dopamine D4 receptor, CB1 cannabinoid receptor, adenosine receptor and also used as the antibacterial agent.^[1-4] It is also showing potential inhibition of CDC25B, TC-PTP, PTP1B and phosphodiesterase 10A.^[5-7]

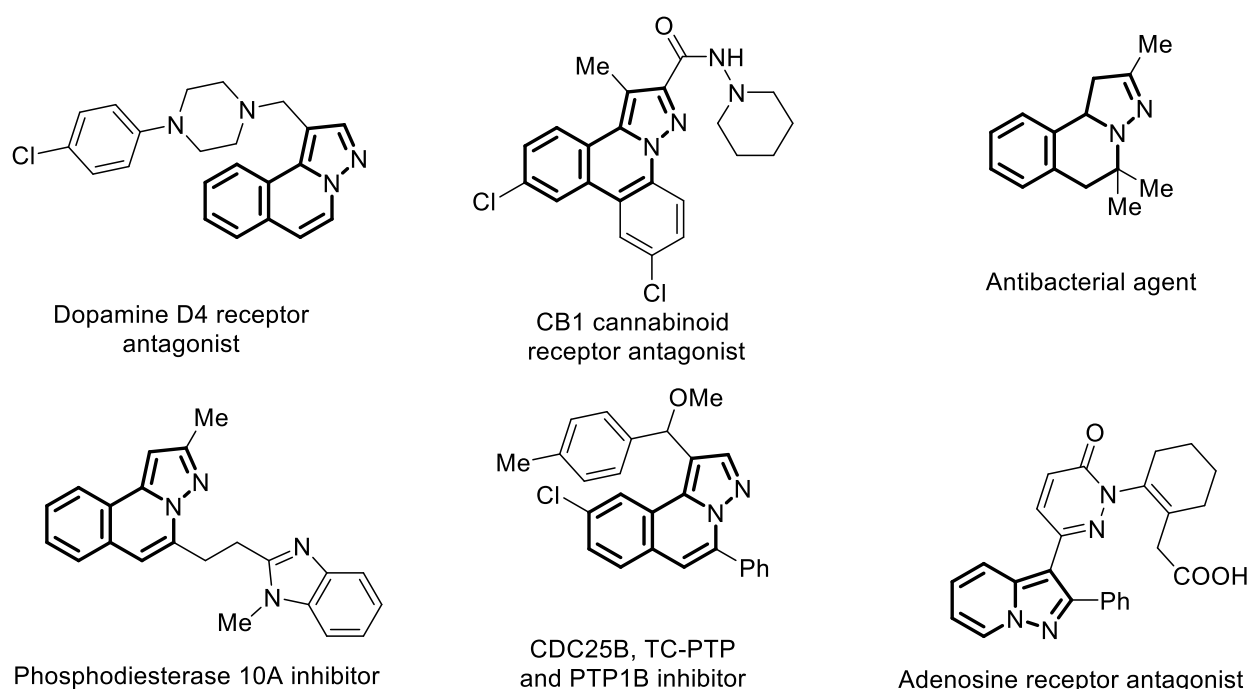
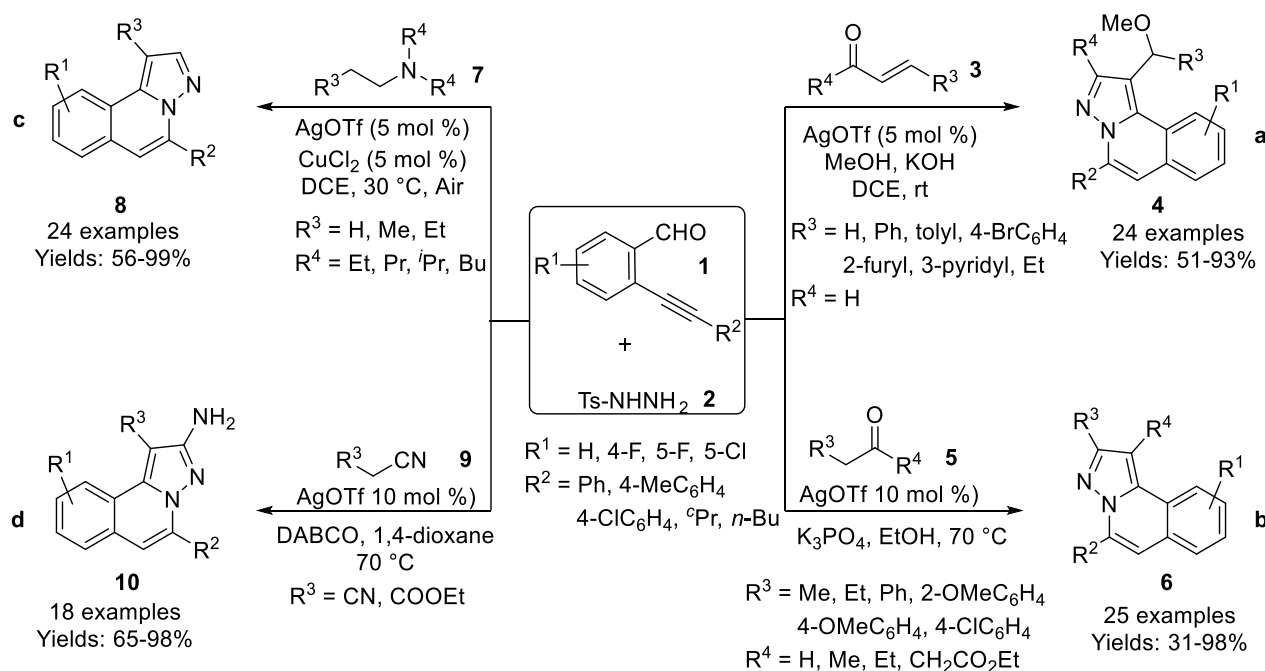


Figure 4.1: Representative examples of some bioactive pyrazolo[5,1-*a*]isoquinolines

4.1.1 Synthetic routes for the construction of pyrazolo[5,1-*a*]isoquinolines

Due to their great biological importance, the synthesis of pyrazolo[5,1-*a*]isoquinoline has special attention of organic chemists. In this regard, Wu and coworkers consecutively developed variety of synthetic route for the construction of pyrazolo[5,1-*a*]isoquinoline derivatives (**4**, **6**, **8** and **10**) *via* multicomponent reactions using 2-alkynylbenzaldehyde (**1**) and *N*-tosylhydrazides (**2**) as key precursor with different α , β -unsaturated aldehydes or ketones (**3**) (**Scheme 4.1a**),^[8] α -methylene aldehydes/ketones (**5**) (**Scheme 4.1b**),^[9] tertiary amines (**7**) (**Scheme 4.1c**),^[10] and α -methylene

nitriles (**9**) (Scheme 4.1d),^[7] under AgOTf catalyst or with the combination of CuCl₂ catalyst in the presence of base.



Scheme 4.1: Synthesis pyrazolo[5,1-*a*]isoquinoline derivatives under AgOTf catalyst

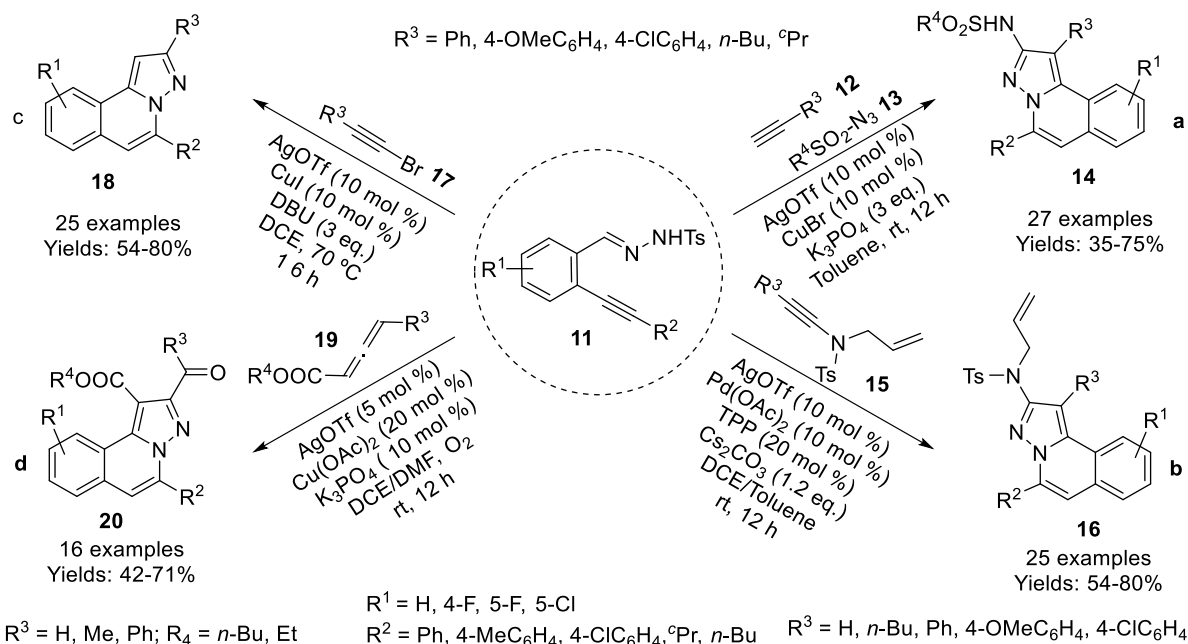
Later on, the same group further synthesized 2-amino-pyrazole fused isoquinoline derivatives (**14**) *via* multicomponent reaction of *N'*-(2-alkynylbenzylidene)-hydrazides (**11**), alkynes (**12**), and sulfonyl azides (**13**) with combination AgOTf and CuBr as catalyst system (Scheme 4.2a).^[11] Notably, 4-nitrophenylacetylene and 4-pyridylacetylene did not work in this protocol. Aliphatic alkyne reacted well and afforded corresponding products in slightly less yield. The transformation proposed to proceed through *6-end* cyclization, [3+2] cycloaddition followed by aromatization.

Peng group have also described synthesis of 2-amino-1*H*-pyrazolo[5,1-*a*]isoquinolines (**16**) synthesis in moderate to good yield (54-80%) using a similar precursor with *N*-allylhydrazides (**15**) in the presence of AgOTf and Pd(OAc)₂ co-catalyst (Scheme 4.2b).^[12]

Subsequently, the same group further developed a protocol in the construction pyrazole fused isoquinolines (**18**) by the reaction of *N'*-(2-alkynylbenzylidene)-hydrazides (**11**) with bromoalkynes (**17**) using AgOTf/CuI co-catalyst system (Scheme 4.2c).^[13]

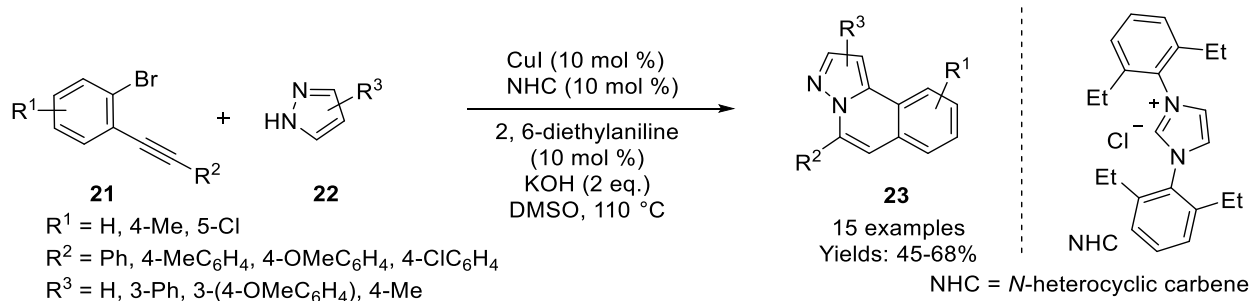
Wu group reported the synthesis of 2-carbonyl-1*H*-pyrazolo[5,1-*a*]isoquinolines (**20**) from *N'*-(2-alkynylbenzylidene)-hydrazides (**11**) and allenoates (**19**) in the presence of co-catalyst AgOTf and Cu(OAc)₂ under O₂ atmosphere (Scheme 4.2d).^[14] In this protocol, the carbonyl oxygen in the

product was formed through peroxy-Cu(III) intermediate which is formed by the reaction of $\text{Cu}(\text{OAc})_2$ and molecular oxygen. The rest of the steps were the same as aforementioned in the synthesis of 2-amino-1*H*-pyrazolo[5,1-*a*]isoquinolines.



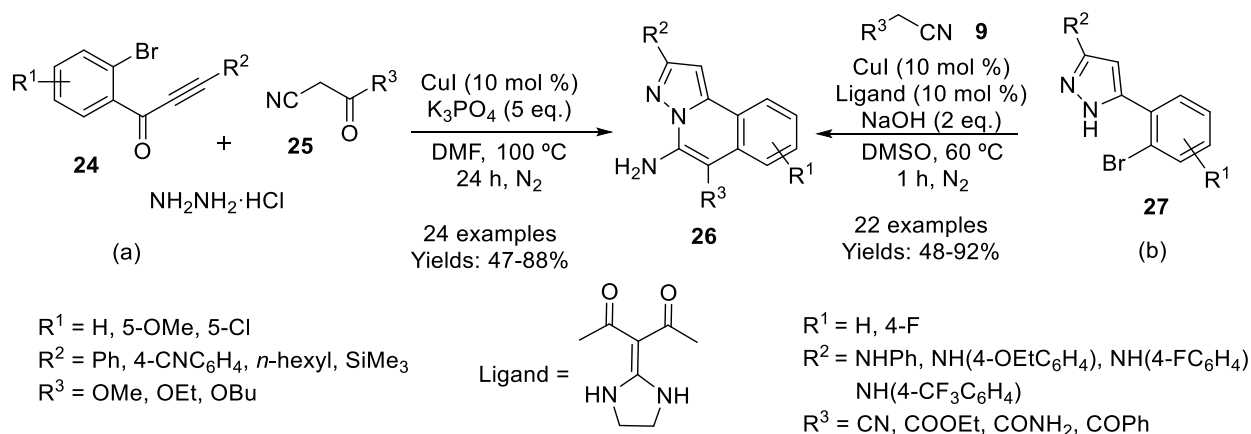
Scheme 4.2: Synthesis of [5,1-*a*]isoquinolines from *N'*-(2-alkynylbenzylidene)-hydrazides

Wu group also discovered an efficient and facile pathway towards the synthesis of pyrazolo[5,1-*a*]isoquinolines (**23**) *via* Cu(I)-catalyzed domino reaction of 2-alkynylbromobenzenes (**21**) and pyrazoles (**22**) (**Scheme 4.3**).^[15] The reaction was proposed to proceed *via* hydroamination of pyrazoles (**22**) with alkynylbromobenzenes (**21**) took place in the presence of CuI, NHC (*N*-heterocyclic carbene), and KOH. Followed by Cu(I)-catalyzed intramolecular direct C-H arylation led to pyrazolo[5,1-*a*]isoquinolines (**23**). Various *o*-alkynylbromobenzenes (**21**) bearing both electron-rich and poor substituents reacted smoothly under this protocol and afforded the desired product in moderate to good yields (45-68%).



Scheme 4.3: Cu(I)-catalyzed synthesis of pyrazole fused isoquinolines from **21** and **22**

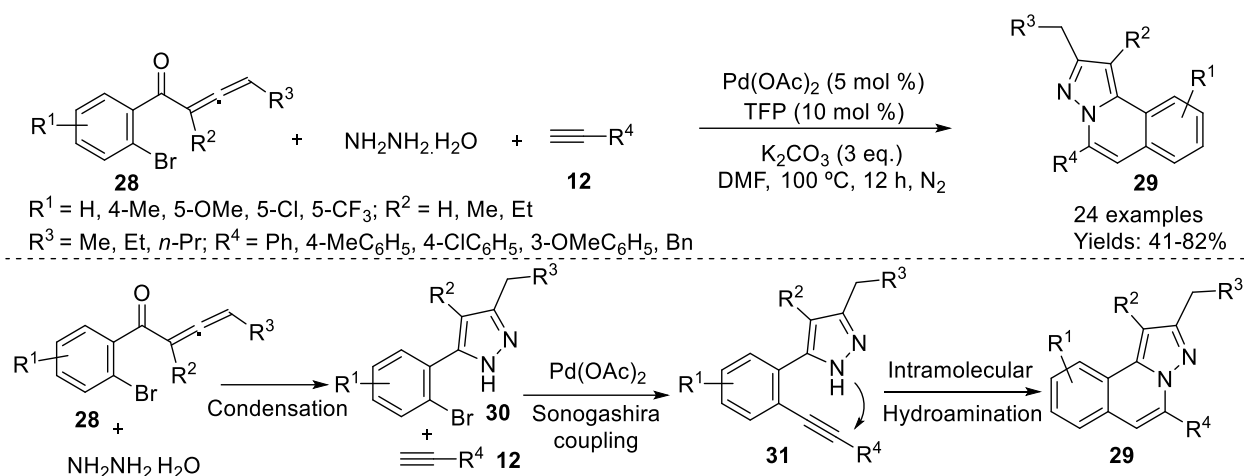
Fu group disclosed the synthesis of 5-amino-1*H*-pyrazolo[5,1-*a*]isoquinolines (**26**) via multicomponent reaction of 1-(2-bromophenyl)-3-arylprop-2-yn-1-one (**24**), ethyl-2-cyanoacetate/ β -keto nitriles (**25**) and hydrazine hydrochloride in the presence of copper-catalyst (**Scheme 4.4a**).^[16] Li and coworkers further improved the synthesis of 5-amino-1*H*-pyrazolo[5,1-*a*]isoquinolines (**26**) by the domino reaction of 5-(2-bromophenyl)-1*H*-pyrazoles (**27**) with active methylene nitriles (**9**) via copper-catalyst in the presence of heterocyclic ketene aminals (HKAs) as ligand under mild reaction condition (**Scheme 4.4b**).^[17]



Scheme 4.4: Synthesis of 5-amino-1*H*-pyrazolo[5,1-*a*]isoquinolines via Cu(I)-catalyzed C-C/C-N bond formation

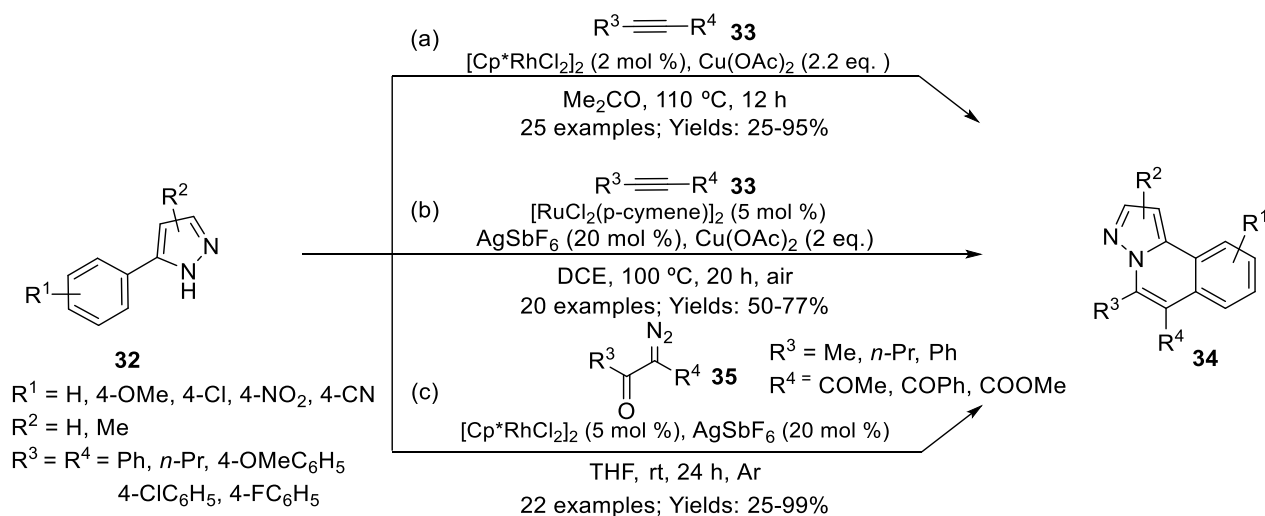
Zhang *et al.* have also documented the synthesis of pyrazolo [5,1-*a*]isoquinolines (**29**) by palladium catalyzed three-component reaction of 1-(2-bromophenyl)buta-2,3-dien-1-ones (**28**), hydrazine hydrate and alkynes (**12**) (**Scheme 4.5**).^[18] In this methodology, initially, condensation reaction took place between 1-(2-bromophenyl)buta-2,3-dien-1-ones and hydrazine hydrate to produce 5-(2-bromophenyl)-1*H*-pyrazole (**30**). $\text{Pd}(\text{OAc})_2$ mediated Sonogashira coupling of 5-

(2-bromophenyl)-1*H*-pyrazole (**30**) with alkynes (**12**) led to intermediate (**31**) which on further intramolecular 6-*endo* hydroamination afforded pyrazolo[5,1-*a*]isoquinolines (**29**).



Scheme 4.5: Scheme: Pd(II)-catalyzed synthesis of pyrazolo[5,1-*a*]isoquinoline analogues

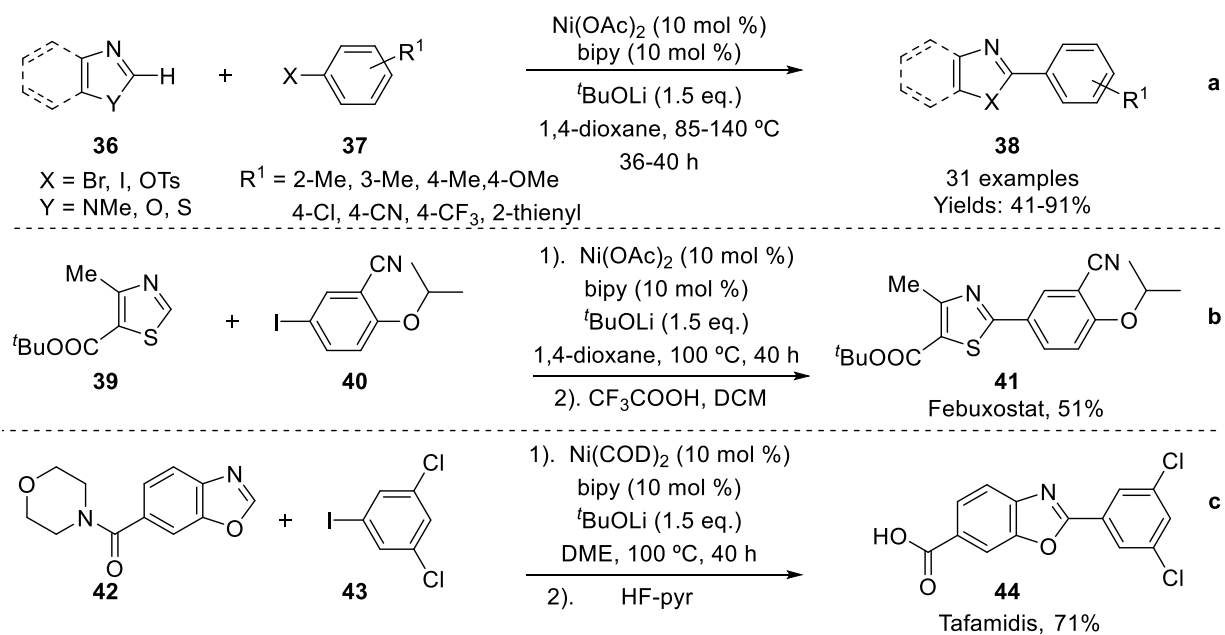
Ackermann and Li group independently reported the synthesis of pyrazolo[5,1-*a*]isoquinoline analogues (**34**) by Rh/Ru-catalyzed oxidative annulation using 5-aryl-1*H*-pyrazoles (**32**) and internal alkynes (**33**) as starting materials (**Scheme 4.6a & b**).^[19-20] Yang group reported the synthesis of pyrazolo[5,1-*a*]isoquinolines from 5-aryl-1*H*-pyrazoles (**32**) using α -diazocarbonyl compounds (**35**) under $[\text{Cp}^*\text{RhCl}_2]_2$ -catalysis (**Scheme 4.6c**).^[21]



Scheme 4.6: Ru/Rh-catalyzed preparation of pyrazole fused isoquinolines from 5-arylpyrazoles

4.1.2 Nickel-catalyzed direct C-H arylation by using haloarenes/pseudoaldehydearenes

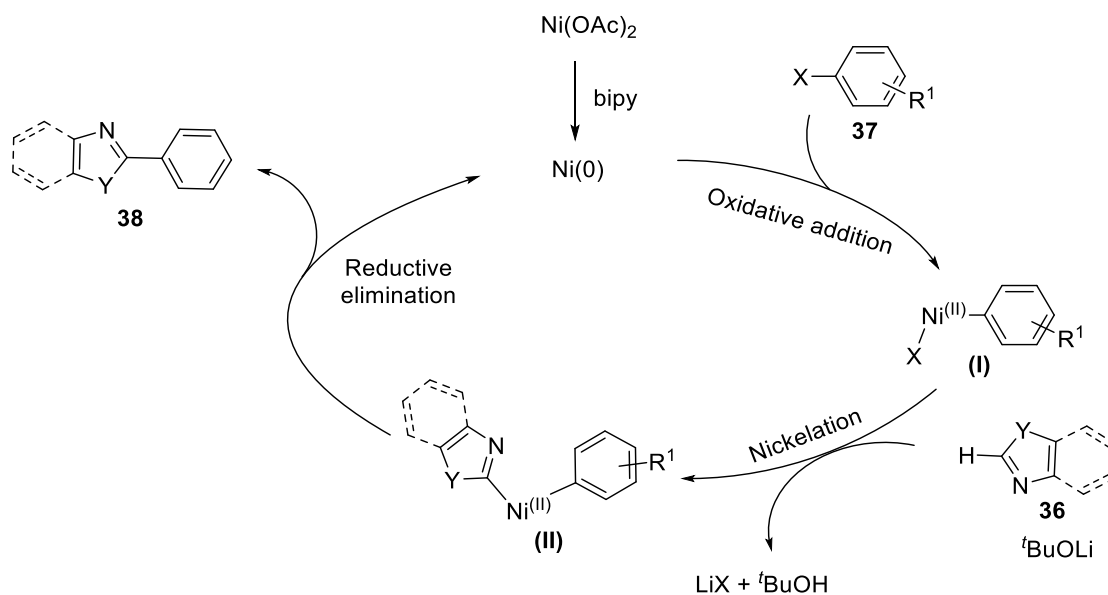
As discussed in previous, direct C-H arylation reactions have been emerged as an important tool for the construction of *N*-heterocycles. The majority of direct C-H arylation reactions have been documented by Pd, Ru, Rh, and Cu.^[22-29] Nickel catalyzed arylation reaction recently has gained significant focus due to the same chemical feature as Pd/Pt catalyst. Also, nickel is abundant, inexpensive, possess low toxicity and has small atomic radii than Pd/Pt which facilitates the activation of unreactive C–H bond.^[30-36] Several methods have been reported for intermolecular direct arylation reaction in the presence of nickel catalyst by using pre-activated substrate for example boronic acid/ester, Grignard reagent, organozinc compounds, carboxylic acid derivatives.^[30-31, 37] However, C-H arylation in the presence of a nickel-based catalyst by using haloarenes and arenes are less explored. In this regard, Itami group reported the direct arylation reactions on azoles (**36**) such as imidazole, oxazole, and thiazole by using aryl halides (**37**) in the presence of Ni(OAc)₂ as a catalyst, bipyridine as a ligand (**Scheme 4.7a**).^[38-39]



Scheme 4.7: Nickel-catalyzed direct C-H arylation of azoles

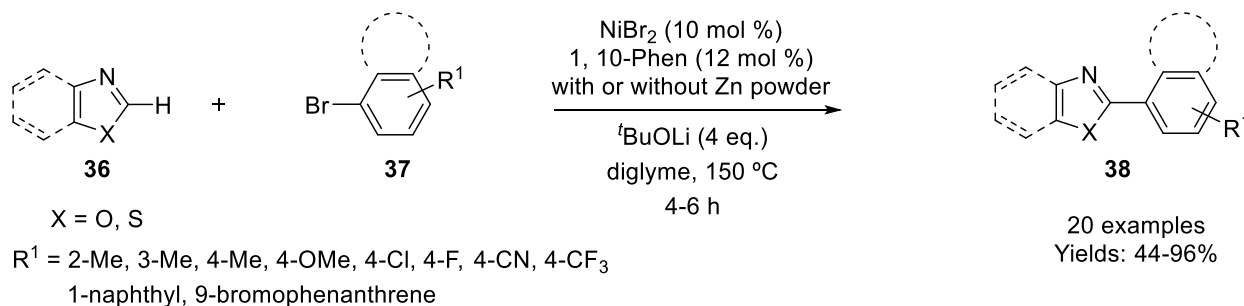
The developed method was utilized for the synthesis of drug candidate febuxostat (**41**) (**Scheme 4.7b**) and tafamidis (**44**) (**Scheme 4.7c**).

The proposed mechanism of Ni(II)-catalyzed arylation is shown in **Scheme 4.8**. Initially, active Ni(0)-species was produced by coordination of Ni(II) with bipyridine which on oxidative addition with aryl halides formed nickel complex (I). Insertion of azoles in nickel complex (I) generated nickel complex (II) in the presence of a base. Finally, reductive elimination led arylated product **38** and generated a Ni(0) for further catalytic cycle.



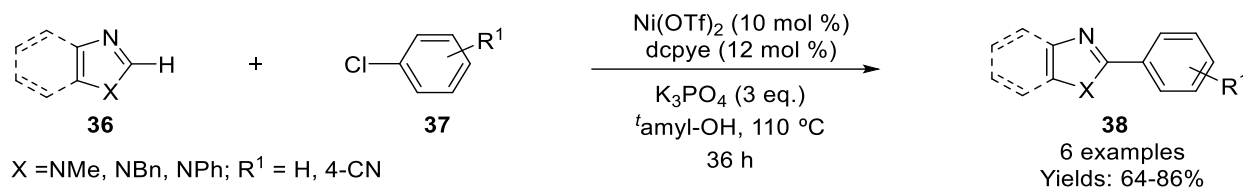
Scheme 4.8: Catalytic cycle of nickel-catalyzed C-H arylation

Miura *et al.* described nickel catalyzed direct arylation of oxazoles and thiazole with arylbromide (**Scheme 4.9**)^[40] It was found that addition of 0.5 eq. of Zinc powder increased the yields in case of oxazole and benzoxazoles.



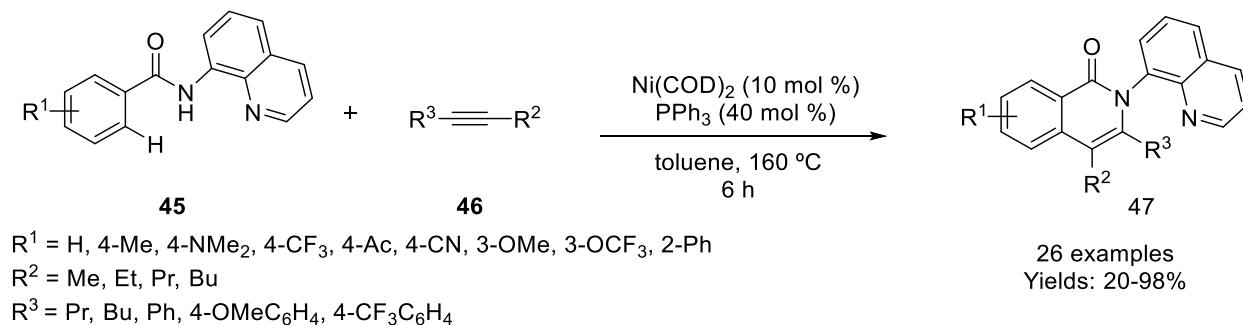
Scheme 4.9: NiBr₂-catalyzed direct arylation of oxazoles and thiazoles

Itami and coworkers also disclosed Ni(II)-catalyzed direct arylation of benzimidazoles/imidazoles using chlorobenzenes in the presence of dcppe (1,2-bis(dicyclohexylphosphino)ethane)) as a ligand, K_3PO_4 as a base in *tert*-Amyl alcohol at 110 °C for 36 h (**Scheme 4.10**).^[41]



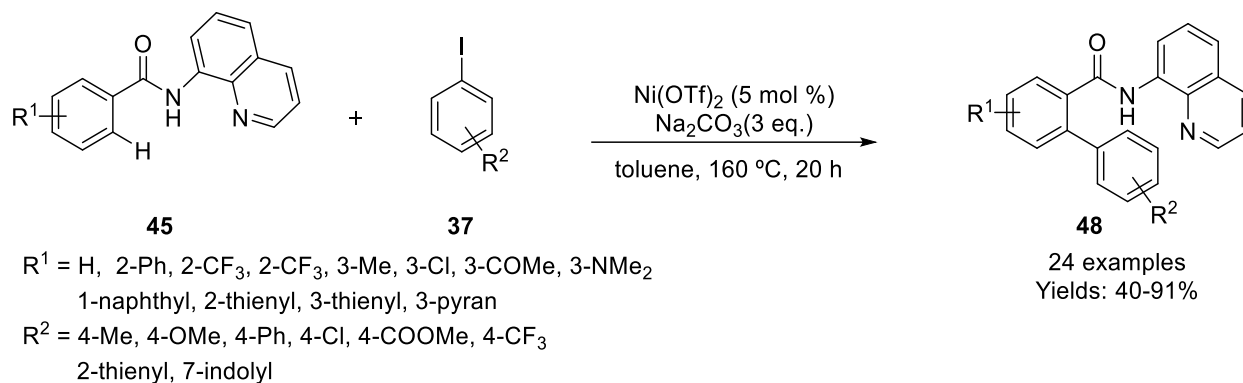
Scheme 4.10: Ni(OTf)₂-catalyzed direct arylation of imidazoles using chlorobenzenes

Chatani group described the first time nickel-catalyzed *ortho*-C-H arylation of amide bearing 8-aminoquinoline as a bidentate group (**45**) and led to the formation of isoquinolinones (**47**) without the use of any oxidant (**Scheme 4.11**).^[42] This reaction proceeds through the first insertion of internal alkynes (**46**) to *ortho* C-H of amides (**45**) facilitated by nickel catalyst followed by intramolecular hydroamination to give isoquinolinones (**47**).



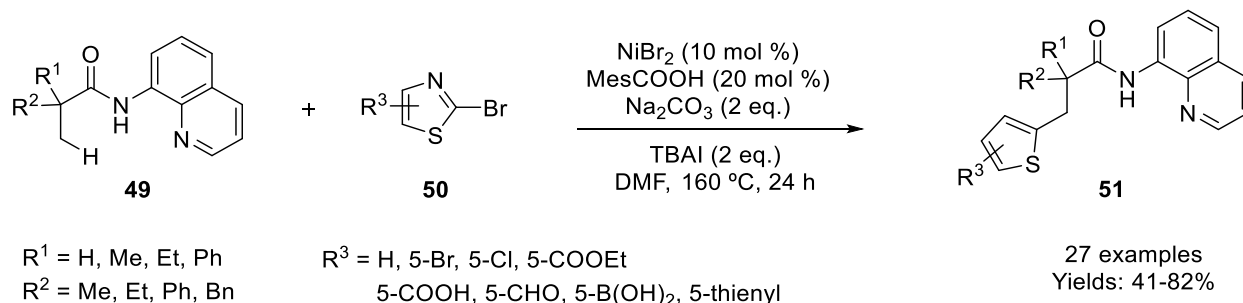
Scheme 4.11: Synthesis of isoquinolinones *via* chelation assistant Ni(II)-catalyzed arylation

Similarly, the same group also documented arylation at *ortho* C-H of amides having quinoline as directing group (**48**) from aryl iodides (**49**) in the presence of nickel triflate as catalyst (**Scheme 4.12**).^[43]



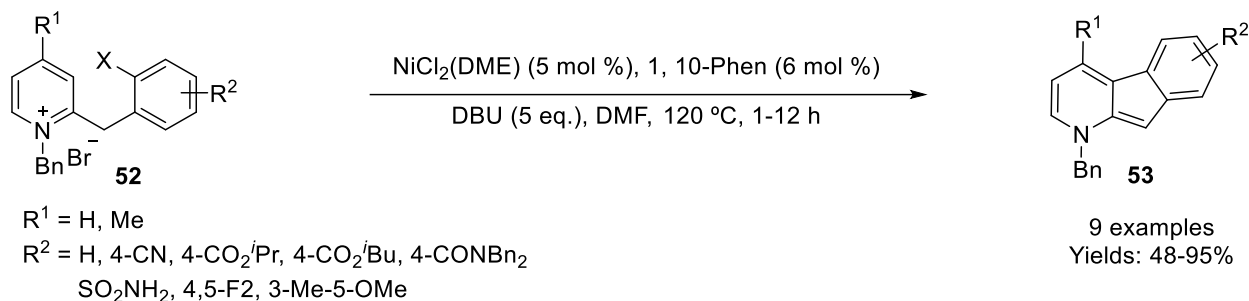
Scheme 4.12: Nickel-catalyzed direct arylation using bidentate-auxiliary

Qiu and team demonstrated nickel-catalyzed direct thienylation of inert $\text{Csp}^3\text{-H}$ aliphatic amide containing 8-aminoquinoline auxiliary (**Scheme 4.13**).^[44] Variety of thiophenes having electron-releasing and electron-withdrawing substituents reacted smoothly and delivered the desired product in moderate to good yields. Heteroaryl bromides such as 2-bromopyridine and 5-bromoindole also reacted well under this protocol.



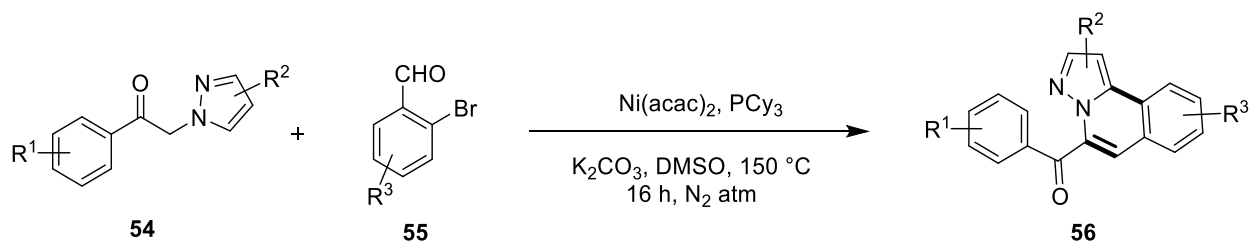
Scheme 4.13: Nickel-catalyzed heteroarylation of an aliphatic amide having bidentate-auxiliary

Kozłowski and co-worker described Ni(II)-catalyzed intramolecular direct C-3 arylation of pyridinium ion (**52**) for the synthesis of azafluorenes (**53**) (**Scheme 4.14**).^[45] The electron withdrawing substituents on arylbromides (**52**) reacted very well and afforded corresponding products (**53**) in high yield as compared to electron-releasing substituents. This protocol was limited to aza-fluorenes (**52**), and it did not work for the synthesis of a fused 6-membered ring. DFT-calculation supported the proposed mechanism of this reaction.



Scheme 4.14: Synthesis of azafluorenes *via* Ni(II)-catalyzed intramolecular arylation

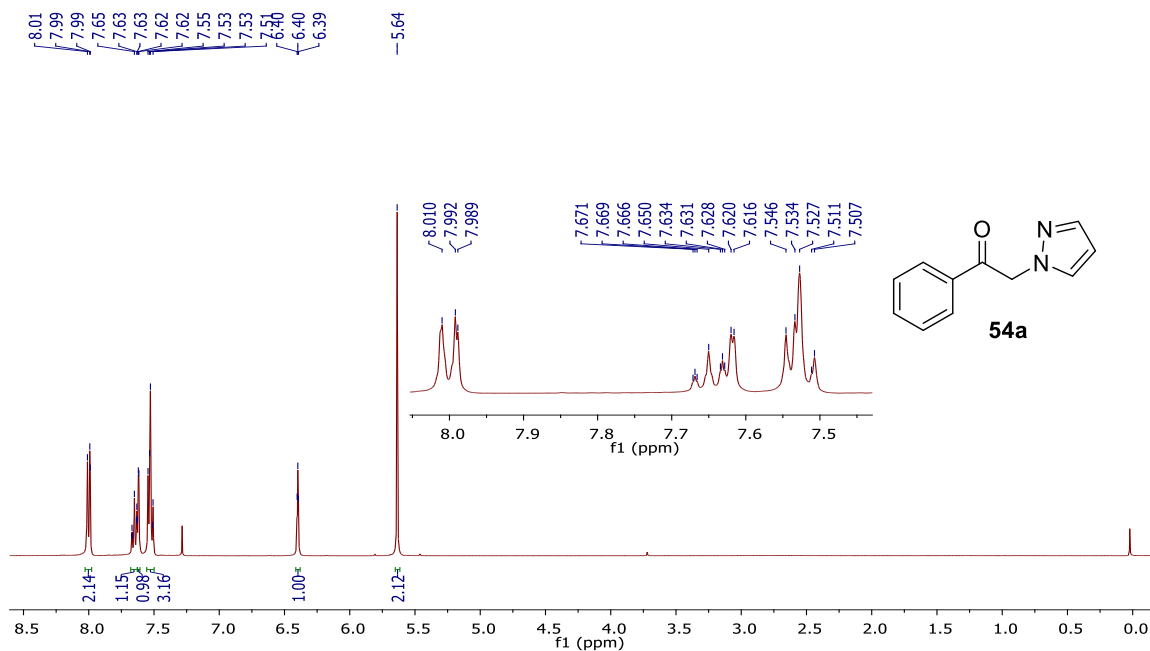
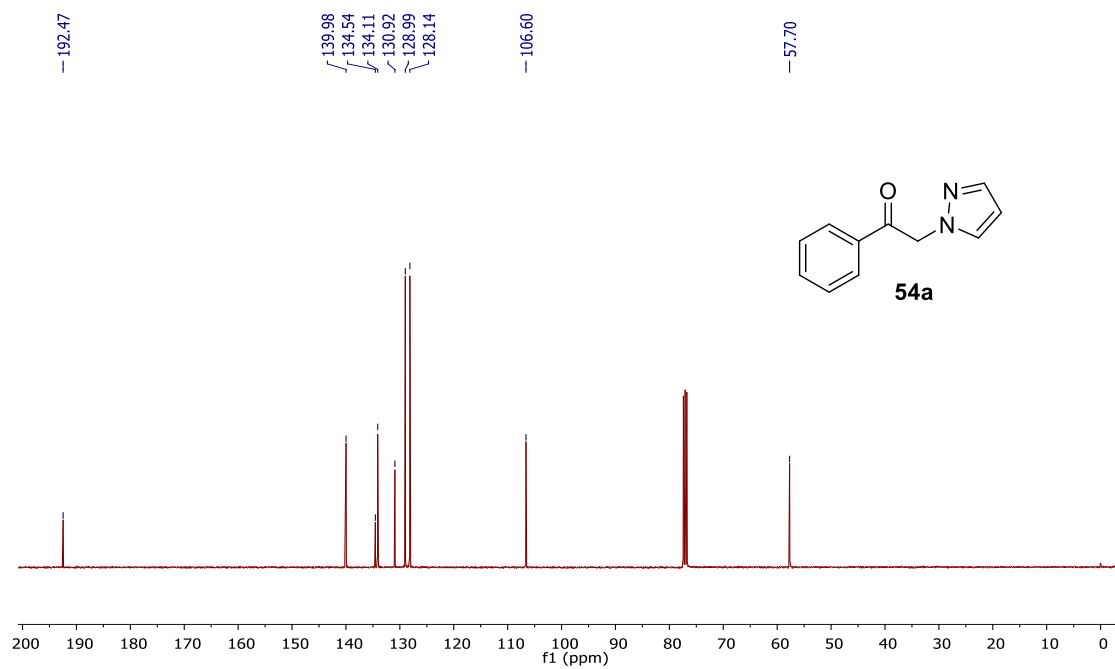
Inspired from the biological importance, existing methods for the synthesis of pyrazolo[5,1-*a*]isoquinolines and nickel-catalyzed C-H arylation, we aimed to synthesize pyrazolo[5,1-*a*]isoquinoline framework (**56**) from *N*-alkylated pyrazoles (**54**) and 2-bromobenzaldehydes (**55**) under Ni(II)-catalysis (**Scheme 4.15**)



Scheme 4.15: Synthesis of aryl substituted pyrazole fused isoquinolines

4.2 RESULTS AND DISCUSSION

To examine the feasibility of our designed tandem reaction, initially 1-aryl-2-(1*H*-pyrazol-1-yl)ethan-1-one (**54a-m**) were synthesized by the reaction of pyrazoles (**22**) with 2-bromo-1-arylethanones (**57**) in the presence of K_2CO_3 in 1,4-dioxane at 60 °C for 5 h. The compound **54a** was characterized by NMR and IR. In the ^1H NMR spectrum of **54a**, a singlet appeared at δ 5.64 for CH_2 of ethanone, a triplet at δ 6.40 and doublet at δ 7.62 for $\text{C}_4\text{-H}$ and $\text{C}_3\text{-H}$ of pyrazole, respectively along with other peaks at their respective position (**Figure 4.2**). In the ^{13}C -NMR of **54a**, a peak at 192 of a ketonic group along with all other expected carbon confirmed the structure of **54a** (**Figure 4.3**). A strong peak appeared at 1697 cm^{-1} for $\text{C}=\text{O}$ stretching in the IR spectrum of **54aa**, (**Figure 4.4**).

Figure 4.2: ^1H NMR spectrum of 54aFigure 4.3: ^{13}C NMR spectrum of 54a

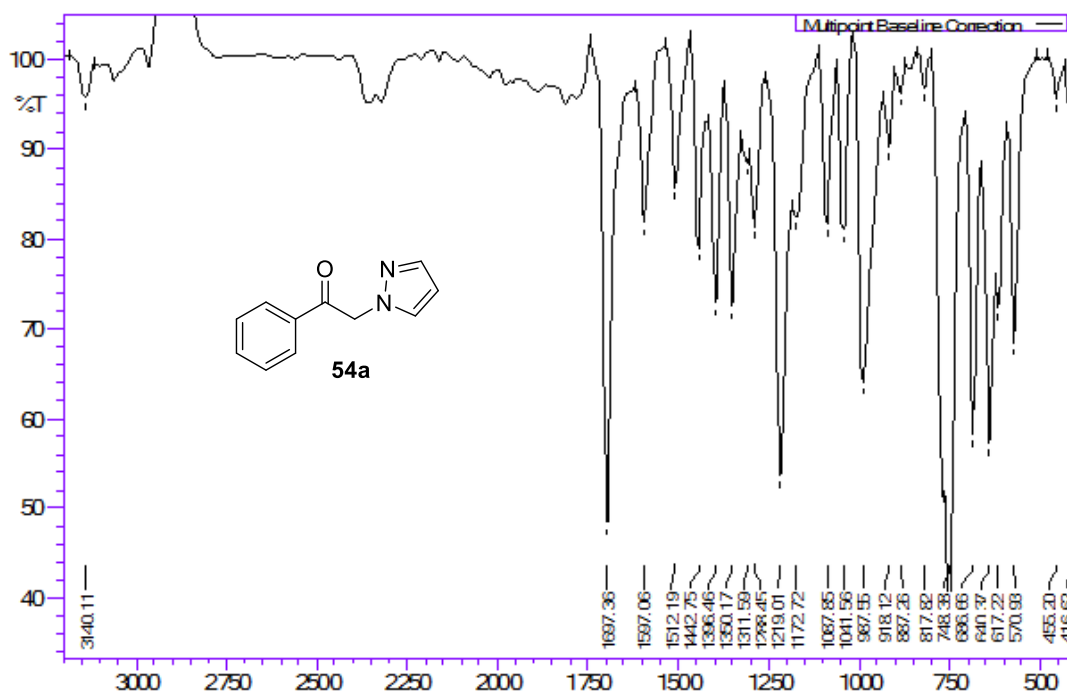


Figure 4.4: IR spectrum of **54a**

At the outset, we chose 1-phenyl-2-(1*H*-pyrazol-1-yl)ethan-1-one (**54a**) and 2-bromobenzaldehyde (**55a**) as model substrates to optimize the reaction conditions for the proposed tandem reaction. The results of the optimization experiments are summarized in **Table 4.1**. The reaction of **54a** and **55a** was initiated in the presence of Pd(OAc)₂ and K₂CO₃ in *N,N*-dimethyl acetamide (DMA) at 150 °C under a nitrogen atmosphere (entry 1, **Table 4.1**) by following our previous work on the synthesis of aza-fused isoquinolines.^[46] However, only traces of phenyl(pyrazolo[1,5-*a*]isoquinolin-5yl)methanone (**56aa**) was observed on TLC which was confirmed by HRMS. We then examined Co(acac)₂ and Ni(acac)₂ under similar conditions and to our satisfaction both resulted in **56aa** in 28% and 35% yield, respectively (entries 2-3, **Table 4.1**). The structure of **56aa** was characterized by using various spectroscopic techniques such as NMR, IR, and MS. In the ¹H NMR spectrum, characteristic singlet appeared at δ 7.25 ppm for C₆-H, and two doublets at δ 8.00 and 7.10 ppm for C₁-H and C₂-H, respectively along with other expected protons at their respective positions were observed (**Figure 4.5**). The carbonyl carbon of ketone appeared at δ 189.44 ppm along with all other expected peaks in the ¹³C NMR spectrum (**Figure 4.6**). In the IR spectrum of **56aa**, strong peaks appeared at 1668 which confirmed the presence of C=O functionality in the

molecule (**Figure 4.7**). In the HRMS spectrum, peak at m/z 273.1023 for the $[M+H]^+$ ion further confirms the structure of **56aa** (**Figure 4.8**).

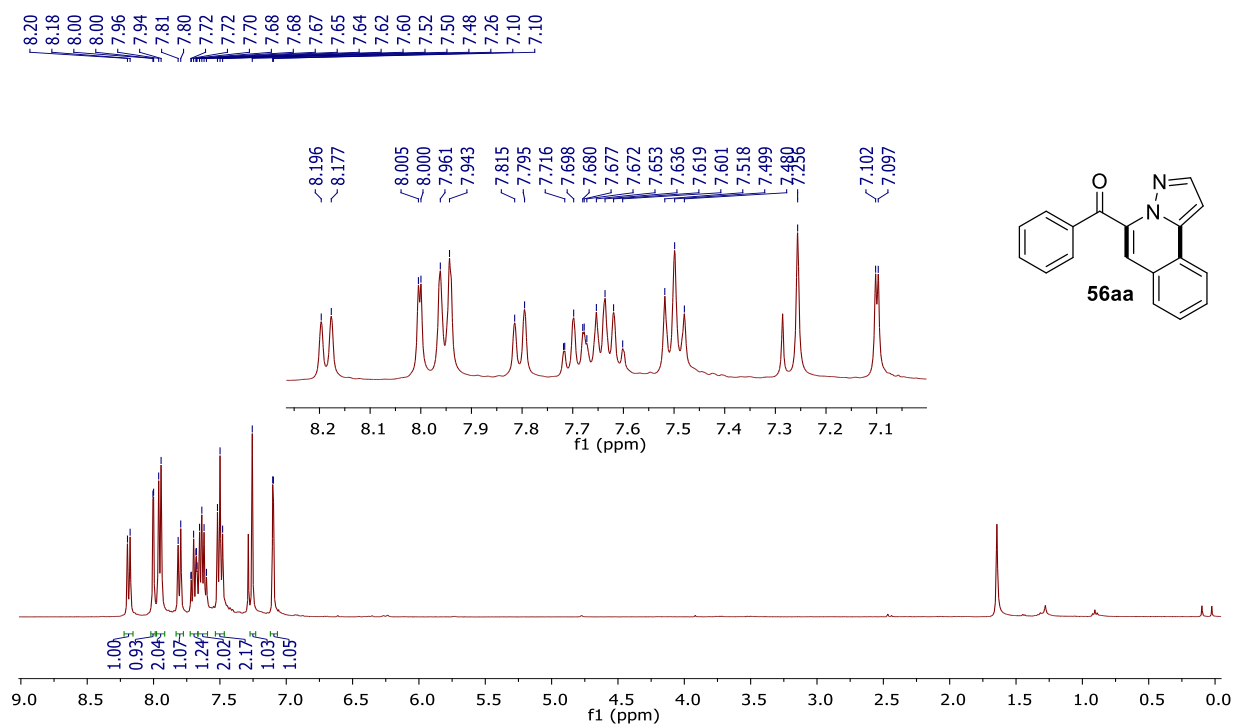


Figure 4.5: ^1H NMR spectrum of **56aa**

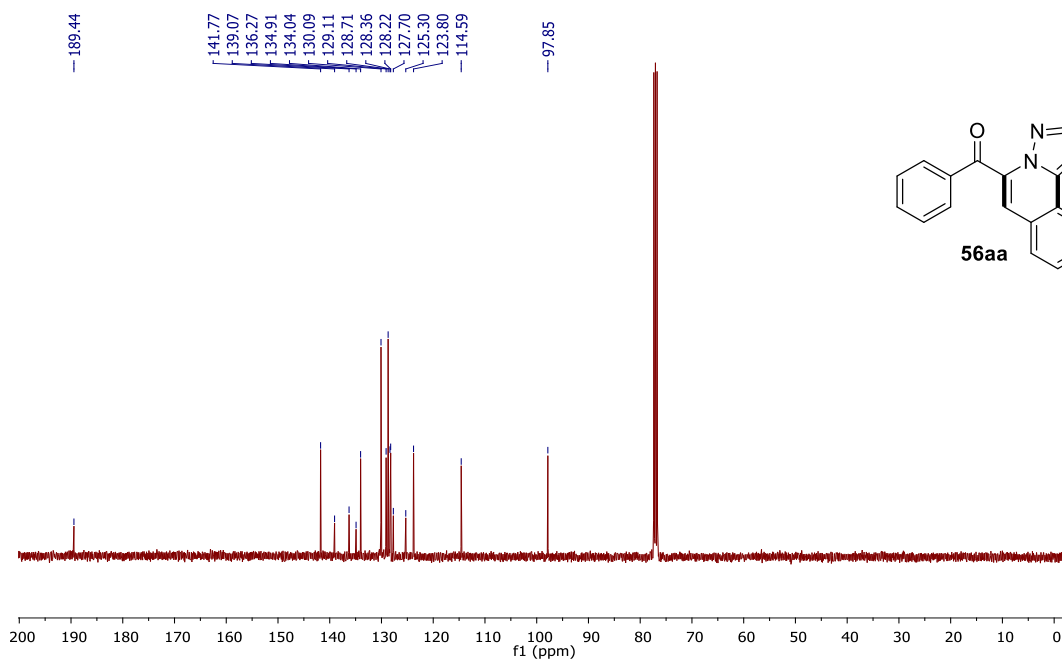
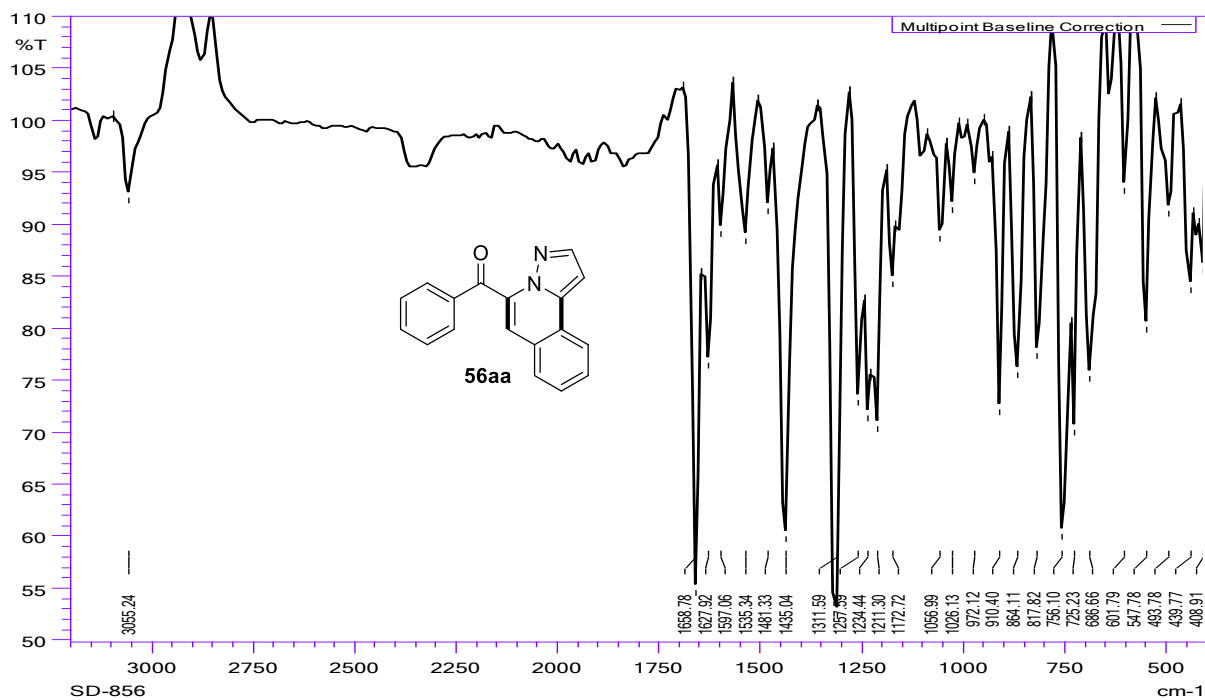
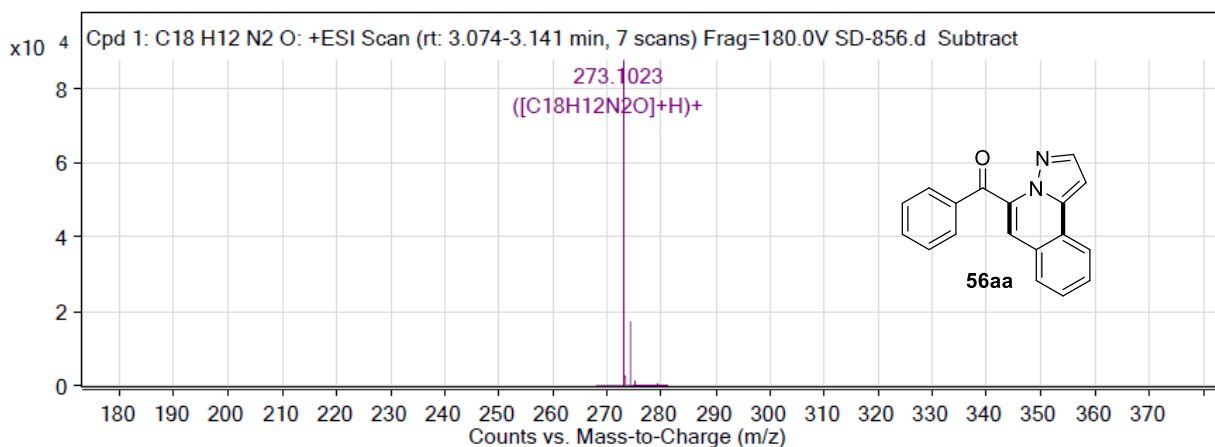


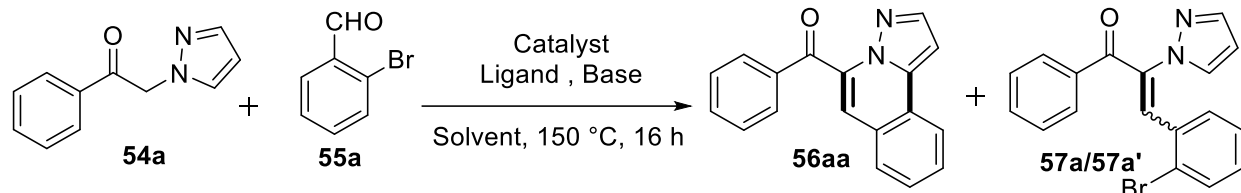
Figure 4.6: ^{13}C NMR spectrum of **56aa**

Figure 4.7: IR spectrum of **56aa**

MS Zoomed Spectrum

Figure 4.8: HRMS spectrum of **56aa**

With our initial success in the synthesis of **56aa**, we proceeded to examine the effect of solvents on the yield of **56aa** using Ni(acac)₂ as a catalyst of choice. The best yield of **56aa** (52%) was obtained in DMSO (entries 4-6, **Table 4.1**). In the case of toluene, only the Knoevenagel product **57a/57a'** (45%) was isolated from the reaction mixture (entry 6, **Table 4.1**). Next, we studied a series of potential ligands such as PCy₃, 1,10-phenanthroline, xantphos, PCy₃HBF₄ and PPh₃ in the catalysis of the reaction under investigation (entries 7-11, **Table 4.1**).

Table 4.1: Optimization of reaction condition for the synthesis of pyrazolo[5,1-*a*]isoquinoline.^a

Entry	Catalyst	Ligand	Base	Solvent	% Yield of 56aa ^b
1	Pd(OAc) ₂	-	K ₂ CO ₃	DMA	trace
2	Co(acac) ₂	-	K ₂ CO ₃	DMA	28
3	Ni(acac) ₂	-	K ₂ CO ₃	DMA	35
4	Ni(acac) ₂	-	K ₂ CO ₃	DMSO	52
5	Ni(acac) ₂	-	K ₂ CO ₃	DMF	39
6	Ni(acac) ₂	-	K ₂ CO ₃	Toluene	45 ^c
7	Ni(acac)₂	PCy₃^d	K₂CO₃	DMSO	68^{e-h}
8	Ni(acac) ₂	1,10-Phen ^d	K ₂ CO ₃	DMSO	40
9	Ni(acac) ₂	PCy ₃ ·HBF ₄	K ₂ CO ₃	DMSO	20
10	Ni(acac) ₂	Xanthphos	K ₂ CO ₃	DMSO	12
11	Ni(acac) ₂	PPh ₃	K ₂ CO ₃	DMF	34
12	Ni(OAc) ₂ ·4H ₂ O	PCy ₃	K ₂ CO ₃	DMSO	15
13	Ni(PPh ₃) ₂ Cl ₂	PCy ₃	K ₂ CO ₃	DMSO	trace
14	NiCl ₂ ·6H ₂ O	PCy ₃	K ₂ CO ₃	DMSO	12
15	Ni(acac) ₂	PCy ₃	K ₃ PO ₄	DMSO	7
16	Ni(acac) ₂	PCy ₃	CS ₂ CO ₃	DMSO	19
17	Ni(acac) ₂	PCy ₃	NaOMe	DMSO	15
18	Ni(acac) ₂	PCy ₃	DIPEA ^d	DMSO	28 ^c
19	Ni(acac) ₂	PCy ₃	K ₂ CO ₃	DMSO	18 ^e
20	Ni(acac) ₂	PCy ₃	K ₂ CO ₃	DMSO	40 ^f
21	Ni(acac) ₂	PCy ₃	K ₂ CO ₃	DMSO	10 ^g
22	Ni(acac) ₂	PCy ₃	K ₂ CO ₃	DMSO	trace ^h
23	Ni(acac) ₂	PCy ₃	-	DMSO	NR ⁱ
24	-	PCy ₃	K ₂ CO ₃	DMSO	- ^c

^aReaction conditions: **54a** (0.537 mmol), **55a** (0.590 mmol), base (3 eq.), catalyst (20 mol %), ligand (30 mol %) at 150 °C, 16 h under N₂ atmosphere. ^bIsolated yield. ^cYield for the mixture of **57a/57a'**. ^dPCy₃ = tricyclohexyl phosphine, 1,10-Phen = 1,10-Phenanthroline, DIPEA = *N,N*-Diisopropylethylamine. ^eAt 80 °C **56aa** was obtained in 18% yield along with **57a/57a'** in 61% yield after 24 h. ^fYield of **56aa** was 40% when 10 mol % Ni(acac)₂ and 20 mol % PCy₃ were used.

^g**56aa** was obtained in 10% yield along with **57a/57a'** under air atm. after 16 h. ^h**56aa** was observed in traces along with **57a/57a'** under oxygen atm. after 16 h. ⁱNR = no reaction.

We noticed that the reaction efficiency improved significantly with the use of PCy₃ compared to the other ligands, furnishing **56aa** in 68% yield (entry 7, **Table 4.1**). Subsequently, a variety of nickel salts (Ni(OAc)₂•4H₂O, Ni(PPh₃)₂Cl₂ and NiCl₂•6H₂O) were examined, however, somewhat disappointing results were obtained (entries 12-14, **Table 4.1**). The efficacy of the reaction was found to decrease in the presence of these salts dramatically. To further fine-tune the reaction conditions, we then shifted our focus on the effect of base and temperature on the reaction outcome. Several inorganics (K₃PO₄, Cs₂CO₃, NaOMe) and organic (DIPEA) bases were screened in the presence of the Ni(acac)₂ catalyst and PCy₃ ligand mixture (entries 15-18, **Table 4.1**).

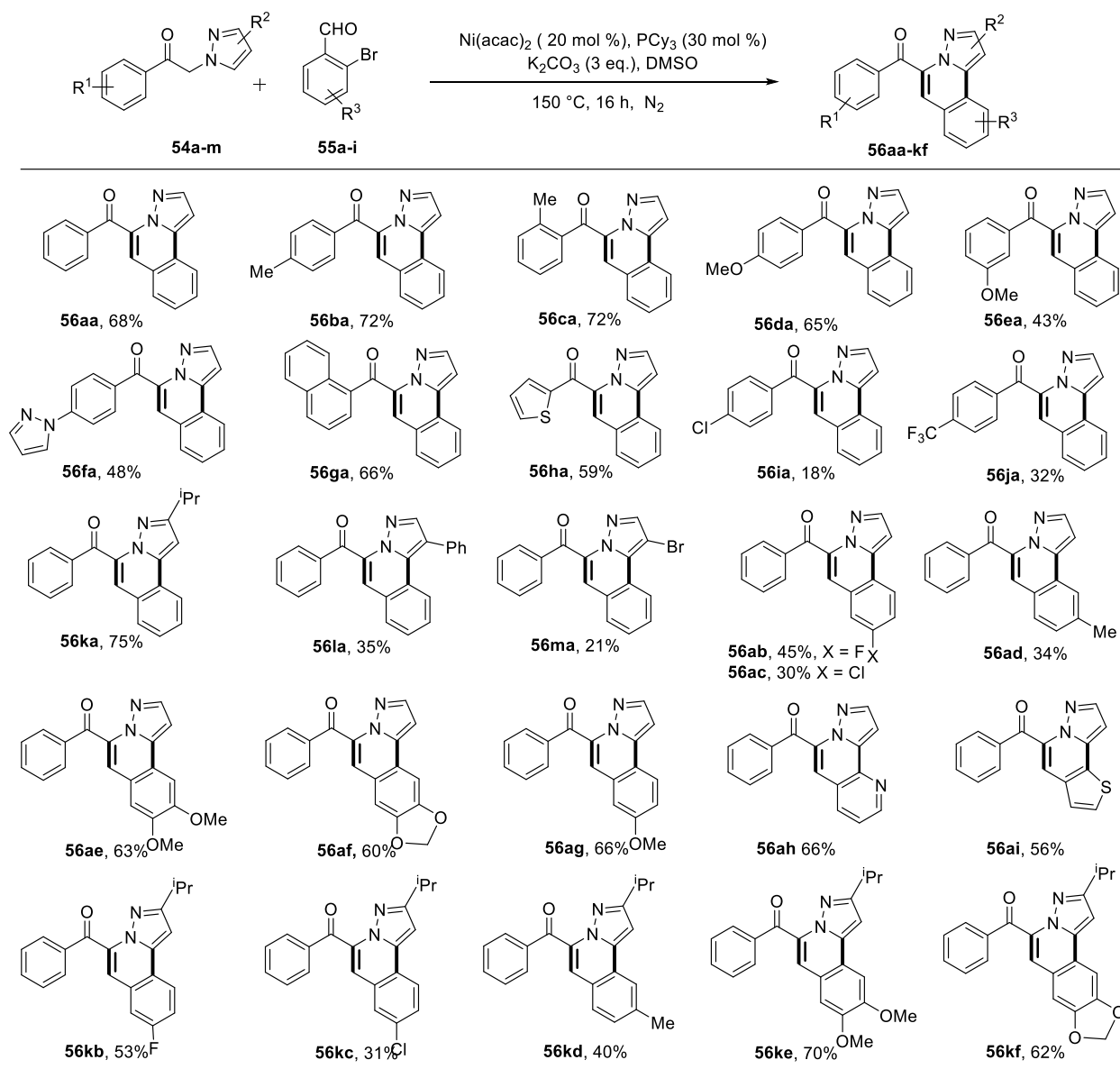
As indicated in **Table 4.1**, poor yields of the desired product **56aa** were obtained in the presence of other inorganic bases (entries 15-17, **Table 4.1**), while the reaction failed to afford desired product in the presence of the DIPEA and only the Knoevenagel product was obtained in 28% yield (entry 18, **Table 4.1**). Decreasing the reaction temperature to 80 °C resulted in the formation of **56aa** in low yield (18%) along with the Knoevenagel adduct (**57a/57a'**) in 61% yield after 24 h (entry 19, **Table 4.1**). It is worthwhile to mention that decreasing the catalyst loading to 10 mol % and the ligand to 20 mol % diminished the yield of **56aa** (entry 20, **Table 4.1**). Notably, desired product was formed in very less amount, when reaction was performed in the presence of air or oxygen atmosphere (entries 21-22 **Table 4.1**). The reaction did not take place in the absence of a base (entry 23, **Table 4.1**). Formation of **56aa** was not detected in the absence of Ni(acac)₂ under the optimized conditions and only Knoevenagel product was obtained in 68% yield (entry 24, **Table 4.1**).

Having optimized the reaction conditions to prepare pyrazolo[5,1-*a*]isoquinoline, we turned our attention to study the scope and limitations of this methodology. Initial efforts were made to explore the reactions of 2-bromobenzaldehyde (**55a**) with variously substituted 1-aryl-2-(1*H*-pyrazol-1-yl)ethan-1-ones (**54a-m**) to furnish the corresponding pyrazolo[5,1-*a*]isoquinolines. As depicted in **Table 4.2**, we were delighted to achieve the synthesis of the compounds **56aa-ma** in decent yields using the optimized reaction conditions. Our results suggested that 1-aryl-2-(1*H*-pyrazol-1-yl)ethan-1-ones (**54a-h**) with neutral or electron-releasing substituents on the 1-aryl ring reacted smoothly to furnish corresponding pyrazolo[5,1-*a*]isoquinolines (**56aa-ha**) in moderate to

good (43-72%) yields. However, 1-aryl-2-(1*H*-pyrazol-1-yl)ethan-1-ones **54i** and **54j** with electron-withdrawing on the 1-aryl ring gave the corresponding products **56ia** (18%) and **56ja** (32%) in poor yields.

The reactions of **54** having substituents on the pyrazole ring with **55a** yielded some interesting results. 1-Aryl-2-(1*H*-pyrazol-1-yl)ethan-1-ones (**54k** and **54l**) with bulky substituents ($R_2 =$ isopropyl and Ph) at the C-3 and C-4 positions of the pyrazole ring reacted with **55a** to give the corresponding pyrazolo[5,1-*a*]isoquinolines **56ka** and **56la** in 75% and 35% yields, respectively. 1-Aryl-2-(1*H*-pyrazol-1-yl)ethan-1-one (**54m**) with a bromo and (**54n**) with chloro substituent at the C-4 position of the pyrazole ring gave corresponding product **56ma** and **56na** in 21% and 18% yields, respectively. In the next series of experiments, we investigated the reactions of **54a** and **54k** with substituted 2-bromobenzaldehydes (**55b-i**) under the optimized reaction conditions (**Table 4.2**).

It was found that 2-bromobenzaldehydes having either electron-releasing or electron-withdrawing substituents participated well in the reaction to furnish corresponding pyrazolo[5,1-*a*]isoquinolines (**56ab-kf**) in moderate to good yields (30-70%). Interestingly, 2-bromo heteroaromatic aldehydes such as 2-bromo-3-pyridinecarboxaldehyde (**55h**) and 2-bromothiophene-3-carbaldehyde (**55i**) also reacted smoothly with **54a** to give corresponding products **56ah** and **56ai** in 66% and 56% yield, respectively. It is worth mentioning that the reaction of 1-(2-bromophenyl)ethanone with **54a** under the optimized reaction and resulted in a complex reaction mixture along with corresponding desired product which enable to purified by column chromatography. The peak at m/z 287.1166 $[M+H]^+$ in HRMS analysis of the reaction mixture confirmed the formation of the desired product.

Table 4.2: Substrate scope of pyrazolo[5,1-*a*]isoquinolines (**56**)

Reaction conditions: **54** (0.537 mmol), **55** (0.590 mmol), K₂CO₃ (3 eq.), Ni(acac)₂ (20 mol %) and PCy₃ (30 mol %), 150 °C, 16 h, under N₂ atmosphere

The structural confirmation of all synthesized molecules was done by ¹H & ¹³C NMR, IR, and HRMS. The single crystal X-ray analysis unambiguously confirmed the structure of **56ae**, the single crystal structure ORTEP diagram of **56ae** with 50% thermal ellipsoids is given in **Figure 4.9** (CCDC No. 1569506). The three fused cyclic rings of the pyrazolo[5,1-*a*]isoquinoline moiety are nearly planar. However, the phenyl ring of the benzoyl group (-COPh) substitution deviates by 73.04° concerning the main heterocyclic plane. The torsion angles of N1-C11- C12-C13, and C11-

C12-C13-C18 are 43.77° and 29.27° , respectively. The carbonyl group C=O is not in the plane of either of the two adjacent rings and deviates from these planes with torsion angles of C10-C11-C12-O1 = 39.01° , and C14-C13-C12-O1 = 27.35° .

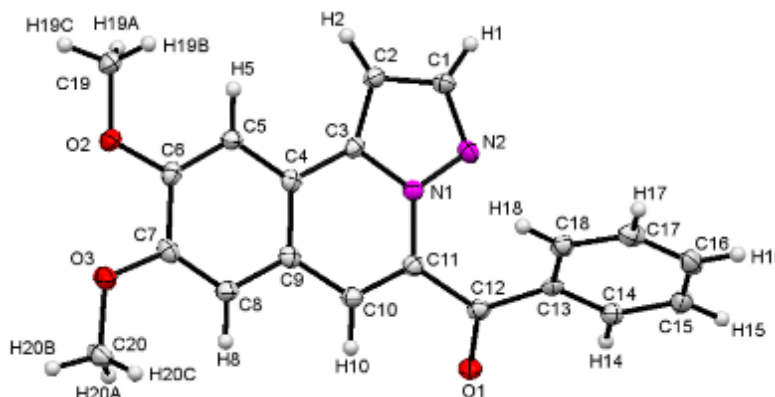
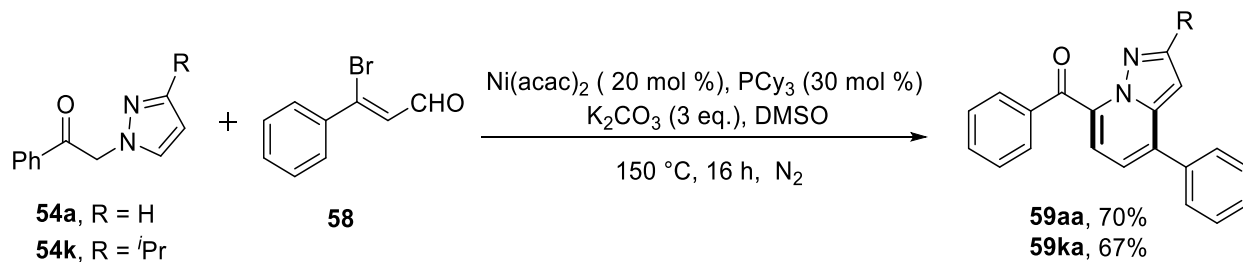


Figure 4.9: ORTEP diagram of **56ae**

The compatibility of the developed method was further explored by reacting **54a** and **54k** with 3-bromo-3-phenylacrylaldehydes (**58**) to give pyrazolo[1,5-*a*]pyridines **59aa** and **59ak** in 70% and 67% yields, respectively (**Scheme 4.16**).



Scheme 4.16: Synthesis of pyrazolo[1,5-*a*]pyridine derivatives

Next, to obtain experimental support to elucidate the reaction pathway, some control experiments were performed (**Scheme 4.17**). Initially, the reaction of **54a** with **55a** was carried out under the optimized reaction conditions but at a lower temperature (80 °C). This resulted in a mixture of two isomeric Knoevenagel condensation products **57a** (*E*-isomer, 47%) and **57a'** (*Z*-isomer, 19%) (**Scheme 4.17A**). The configuration of **57a'** was confirmed by X-ray crystallography and the crystal structure ORTEP diagram with 50% thermal ellipsoids is given in **Figure 4.10** (CCDC 1575940).

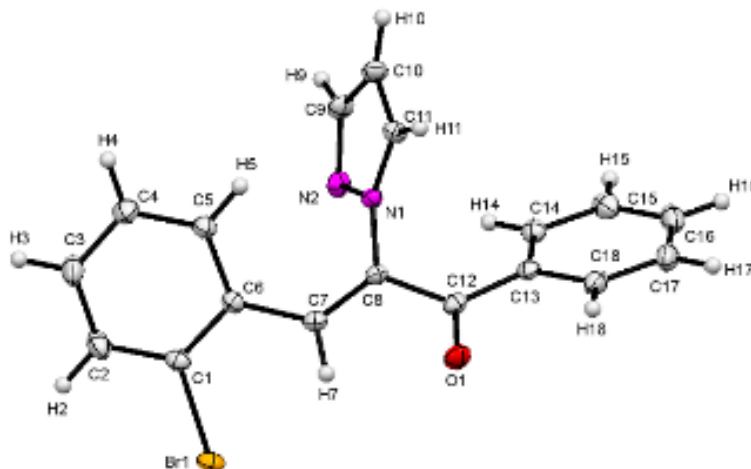
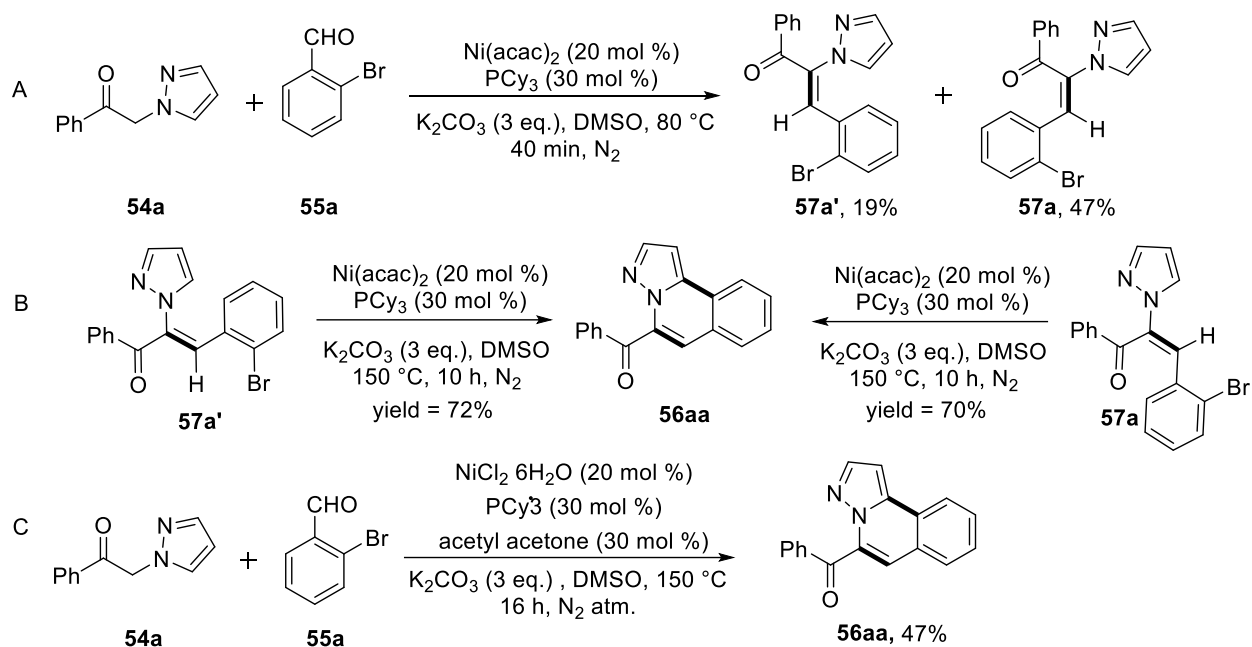


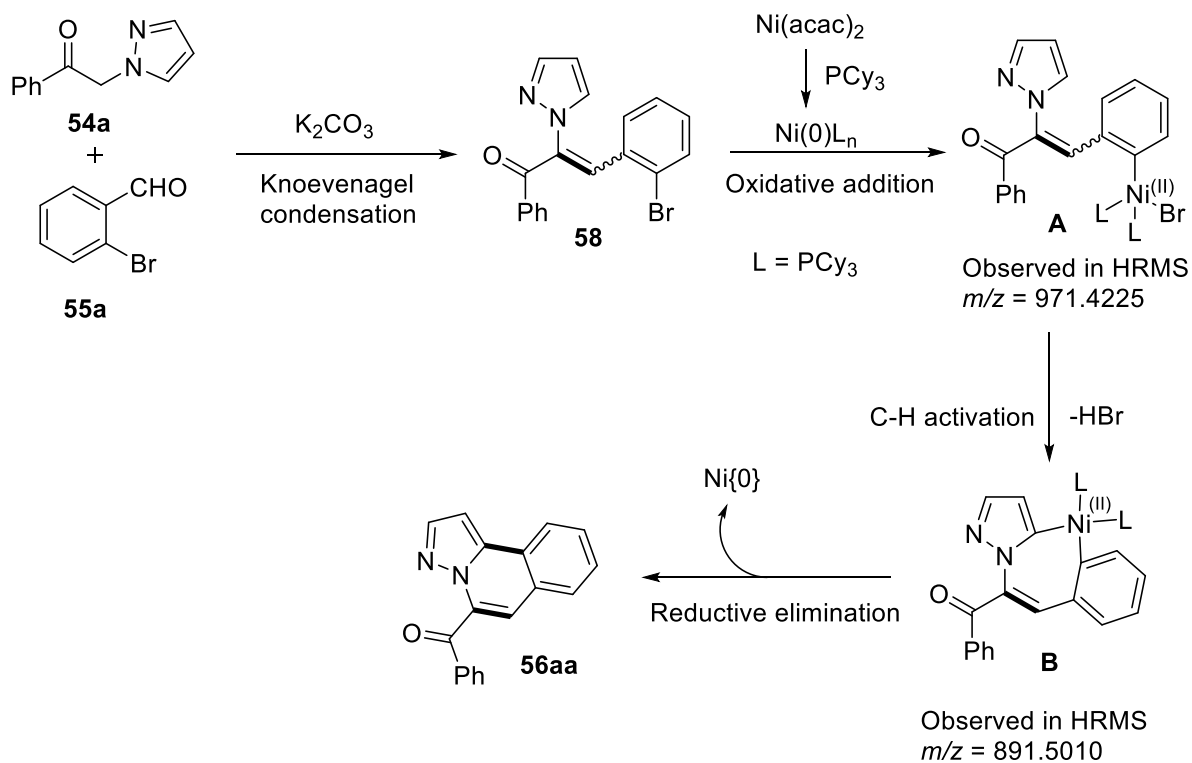
Figure 4.10: ORTEP diagram of **57a'**

Further, pure forms of both of these isomers, **57a** and **57a'** were heated separately in the presence of $\text{Ni}(\text{acac})_2$ under the optimized conditions, and cyclized product **56aa** was observed from both the isomers in good yields (**Scheme 4.17B**). It is quite likely that intramolecular cyclization might be happening *via* **57a'** (*Z-isomer*) due to the spatial proximity of the reaction sites. It appears that high temperature not only aids the catalytic process but also facilitates the isomerization of **57a** (*E-isomer*) to **57a'**. In another experiment, the reaction of **54a** with **55a** was carried out in the presence of $\text{NiCl}_2 \cdot 6\text{H}_2\text{O}$, PCy_3 and acetylacetone (30 mol %) under conditions analogous to the optimized conditions, which afforded **56aa** in 47% yield (**Scheme 4.17C**). The increase in the yield of **56aa** from 12% (**Table 4.1**, entry 14) to 47% when using acetylacetone along with $\text{NiCl}_2 \cdot 6\text{H}_2\text{O}$ suggests the involvement of $\text{Ni}(0)$ in the catalysis of the reaction under investigation.^[47]

Based on the current results and literature reports,^[48-49] a plausible mechanism invoking a cascade-type cyclization is presented in **Scheme 4.18**. Firstly, the reaction of **54a** with **56a** in the presence of K_2CO_3 generates the Knoevenagel condensation product **57**. Simultaneously, $\text{Ni}(\text{acac})_2$ reacts with PCy_3 to form the active catalyst $\text{Ni}(0)$, which undergoes oxidative addition with the Knoevenagel product **57** to form the organo-nickel complex **A**. The formation of complex **A**, in turn, leads to intramolecular C–H activation at the C–5 position of the azole to produce the cyclic complex **B**. Finally, the reductive elimination of the complex **B** affords the product **56aa**, along with the concomitant release of the active $\text{Ni}(0)$ for the next catalytic cycle.



Scheme 4.17: Control experiments



Scheme 4.18: Proposed reaction mechanism for Ni(II)-catalyzed arylation

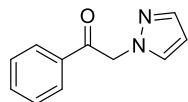
4.3 CONCLUSIONS

In conclusion, we have successfully developed a simple one-pot synthesis of 5-substituted pyrazolo[5,1-*a*]isoquinolines from 1-aryl-2-(1*H*-pyrazol-1-yl)ethan-1-ones *via* nickel-catalyzed tandem cross aldol condensation and intramolecular carbon-carbon bond formation through C–H activation. The easily accessible substrates, cheaper catalyst, ease of operation and good yields make this method very practical for the synthesis of the biologically useful 5-substituted pyrazolo[5,1-*a*]isoquinolines derivatives.

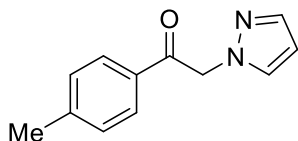
4.4 EXPERIMENTAL SECTION

General Information: Melting points were measured using an automatic melting point apparatus and are uncorrected. The thin layer chromatography to monitor the progress of the reactions was performed on 0.25 mm silica gel 60-F254. The ¹H and ¹³C NMR spectra were obtained on a 400 MHz spectrometer. Coupling constant and chemical shifts were reported in Hertz (Hz) and parts per million (ppm) respectively, downfield from tetramethylsilane as an internal with CDCl₃. IR spectral values are expressed in cm⁻¹. The HRMS spectra were recorded on a Q-TOF mass spectrometer in ESI mode. 3-bromo-3-phenylacrylaldehydes was synthesized by the reported procedure.^[50] All reagents and solvents were commercial grade and used as such without further purification.

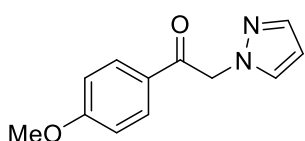
Representative procedure for the synthesis of 1-aryl-2-(1*H*-pyrazol-1-yl)ethan-1-one: An oven-dried RB flask was charged with 1*H*-pyrazole (0.500 g, 7.34 mmol) and K₂CO₃ (2.02 g, 14.68 mmol) and was kept under a nitrogen atmosphere. Phenacyl bromide (1.46 g, 7.35 mmol) was added portion wise. The reaction mixture was heated at 60 °C for 5 h. Reaction progress was monitored by TLC. After completion of the reaction, 1,4-dioxane was evaporated, and the reaction mixture was diluted with water (100 mL) and extracted by ethyl acetate (20 mL × 2). The combined organic layer was dried over anhydrous Na₂SO₄, filtered and evaporated the ethyl acetate layer. Crude solid compound was triturated with cold diethyl ether to provide pure 1-phenyl-2-(1*H*-pyrazol-1-yl)ethan-1-one (**1a**) in 67% (0.92 g) yield as off white solid.

1-Phenyl-2-(1*H*-pyrazol-1-yl)ethan-1-one (54a)

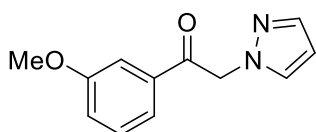
Off white solid (0.92 g, 67%); mp 90–91 °C; ¹H NMR (400 MHz, CDCl₃) δ 8.01 – 7.99 (m, 2H), 7.67 – 7.63 (m, 1H), 7.62 (d, *J* = 1.6 Hz, 1H), 7.55 – 7.51 (m, 3H), 6.40 (t, *J* = 2.1 Hz, 1H), 5.64 (s, 2H); ¹³C NMR (100 MHz, CDCl₃) δ 192.5, 140.0, 134.5, 134.1, 130.9, 129.0, 128.1, 106.6, 57.7; FT-IR (neat) 3140, 1697, 1597, 1211, 1087, 748 cm⁻¹.

2-(1*H*-pyrazol-1-yl)-1-(*p*-tolyl)ethan-1-one (54b)

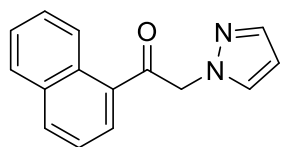
White crystalline solid (1.04 g, 71%); mp 136–138 °C; ¹H NMR (400 MHz, CDCl₃) δ 7.90 (d, *J* = 8.3 Hz, 2H), 7.62 (d, *J* = 1.6 Hz, 1H), 7.53 (d, *J* = 2.2 Hz, 1H), 7.32 (d, *J* = 8.0 Hz, 2H), 6.40 (t, *J* = 2.1 Hz, 1H), 5.61 (s, 2H), 2.45 (s, 3H); ¹³C NMR (100 MHz, CDCl₃) δ 192.0, 145.1, 139.9, 132.0, 130.9, 129.7, 128.2, 106.5, 57.6, 21.8; FT-IR (neat) 3124, 1689, 1597, 1288, 1188, 756 cm⁻¹.

1-(4-Methoxyphenyl)-2-(1*H*-pyrazol-1-yl)ethan-1-one (54d)

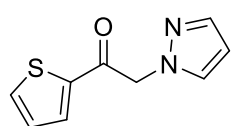
White crystalline solid (1.08 g, 68%); mp 140–141 °C; ¹H NMR (400 MHz, CDCl₃) δ 8.01 – 7.98 (m, 2H), 7.61 (d, *J* = 1.6 Hz, 1H), 7.54 (d, *J* = 2.2 Hz, 1H), 7.01 – 6.98 (m, 2H), 6.39 (t, *J* = 2.1 Hz, 1H), 5.59 (s, 2H), 3.91 (s, 3H); ¹³C NMR (100 MHz, CDCl₃) δ 190.8, 164.2, 139.9, 130.8, 130.5, 127.5, 114.2, 106.5, 57.4, 55.6; FT-IR (neat) 3140, 1681, 1597, 1265, 1066, 756 cm⁻¹.

1-(3-Methoxyphenyl)-2-(1*H*-pyrazol-1-yl)ethan-1-one (54e)

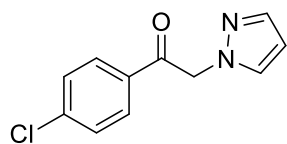
Light yellow solid (114 mg, 61%); mp 67–68 °C; ¹H NMR (400 MHz, CDCl₃) δ 7.61 (d, *J* = 1.1 Hz, 1H), 7.56 (d, *J* = 7.6 Hz, 1H), 7.52 (d, *J* = 2.1 Hz, 1H), 7.50 (bs, 1H), 7.42 (t, *J* = 7.9 Hz, 1H), 7.18 (dd, *J* = 8.2, 2.2 Hz, 1H), 6.39 (s, 1H), 5.60 (s, 2H), 3.86 (s, 3H); ¹³C NMR (100 MHz, CDCl₃) δ 192.3, 160.0, 139.9, 135.8, 130.9, 129.9, 120.6, 112.4, 106.6, 57.8, 55.5; FT-IR (neat) 2933, 1689, 1597, 1257, 1165, 756 cm⁻¹.

1-(Naphthalen-2-yl)-2-(1H-pyrazol-1-yl)ethan-1-one (54g)

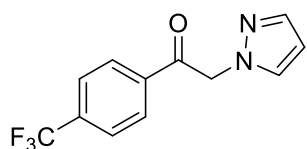
Off white solid (0.89 g, 52%); mp 134–136 °C; ^1H NMR (400 MHz, CDCl_3) δ 8.54 (s, 1H), 8.04 (dd, $J = 8.6, 1.7$ Hz, 1H), 8.01 (d, $J = 8.1$ Hz, 1H), 7.97 – 7.90 (m, 2H), 7.69 – 7.61 (m, 3H), 7.58 (d, $J = 2.2$ Hz, 1H), 6.42 (t, $J = 2.1$ Hz, 1H), 5.77 (s, 2H); ^{13}C NMR (100 MHz, CDCl_3) δ 192.4, 140.0, 136.0, 132.4, 131.9, 130.9, 130.1, 129.7, 129.1, 129.0, 127.9, 127.1, 123.5, 106.6, 57.8; FT-IR (neat) 3084, 1662, 1455, 1288, 1107, 730 cm^{-1} .

2-(1H-Pyrazol-1-yl)-1-(thiophen-2-yl)ethan-1-one (54h)

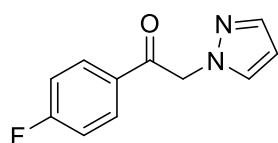
Brown oil (0.86 g, 60%); ^1H NMR (400 MHz, CDCl_3) δ 7.75 – 7.74 (m, 1H), 7.73 (bs, 1H), 7.61 (d, $J = 1.7$ Hz, 1H), 7.55 (d, $J = 2.3$ Hz, 1H), 7.19 – 7.16 (m, 1H), 6.39 (t, $J = 2.1$ Hz, 1H), 5.51 (s, 2H); ^{13}C NMR (100 MHz, CDCl_3) δ 185.6, 141.0, 140.1, 135.1, 132.8, 130.9, 128.5, 106.7, 57.9; FT-IR (neat) 3086, 1662, 1450, 1292, 1099, 729 cm^{-1} .

1-(4-Chlorophenyl)-2-(1H-pyrazol-1-yl)ethan-1-one (54i)

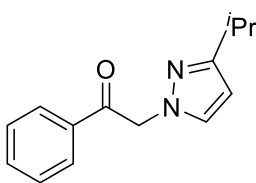
White crystalline solid (1.10 g, 68 %); mp 134–136 °C; ^1H NMR (400 MHz, CDCl_3) δ 7.96 – 7.93 (m, 2H), 7.62 (d, $J = 1.6$ Hz, 1H), 7.53 – 7.51 (m, 2H), 7.50 – 7.49 (m, 1H), 6.40 (t, $J = 2.1$ Hz, 1H), 5.60 (s, 2H); ^{13}C NMR (100 MHz, CDCl_3) δ 191.4, 140.7, 140.1, 132.8, 130.8, 129.6, 129.4, 106.8, 57.6; FT-IR (neat) 3109, 1705, 1581, 1211, 1087, 763 cm^{-1} .

2-(1H-Pyrazol-1-yl)-1-(4-(trifluoromethyl)phenyl)-ethan-1-one (54j)

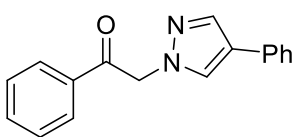
White crystalline (152 mg, 32%); mp 140–141 °C; ^1H NMR (400 MHz, CDCl_3) δ 8.11 (d, $J = 8.2$ Hz, 2H), 7.80 (d, $J = 8.3$ Hz, 2H), 7.63 (d, $J = 1.7$ Hz, 1H), 7.54 (d, $J = 2.3$ Hz, 1H), 6.41 (t, $J = 2.1$ Hz, 1H), 5.64 (s, 2H); ^{13}C NMR (100 MHz, CDCl_3) δ 191.7, 140.3, 137.2, 137.2, 135.3 (q, $J = 33$ Hz), 130.8, 128.6, 126.0 (q, $J = 3.7$ Hz), 123.3 (q, $J = 271$ Hz), 106.9, 57.9; ^{19}F NMR (375 MHz, CDCl_3) δ -63.3; FT-IR (neat) 3109, 1705, 1404, 1327, 1111, 763 cm^{-1} .

1-(4-Fluorophenyl)-2-(1*H*-pyrazol-1-yl)ethan-1-one (54g)

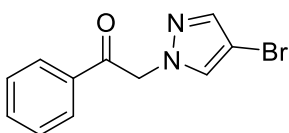
Brown solid (0.91 g, 61%); mp 110–111 °C; ¹H NMR (400 MHz, CDCl₃) δ 8.05 – 8.01 (m, 2H), 7.61 (d, *J* = 1.6 Hz, 1H), 7.52 (d, *J* = 2.2 Hz, 1H), 7.22 – 7.17 (m, 2H), 6.39 (t, *J* = 2.1 Hz, 1H), 5.59 (s, 2H); ¹³C NMR (100 MHz, CDCl₃) δ 191.0, 166.3 (d, *J* = 256.7 Hz), 140.1, 130.9 (d, *J* = 9.5 Hz), 130.8, 116.23 (d, *J* = 22.1 Hz), 106.7, 57.6; FT-IR (neat) 3109, 1705, 1442, 1234, 1141, 761 cm⁻¹.

2-(3-Isopropyl-1*H*-pyrazol-1-yl)-1-phenylethan-1-one (54k)

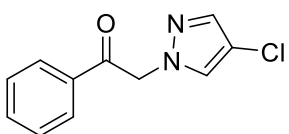
Yellow solid (0.71 g, 69%); mp 95–96 °C; ¹H NMR (400 MHz, CDCl₃) δ 8.01 – 7.99 (m, 2H), 7.67 – 7.62 (m, 1H), 7.54 – 7.50 (m, 2H), 7.43 (d, *J* = 2.3 Hz, 1H), 6.21 (d, *J* = 2.3 Hz, 1H), 5.59 (s, 2H), 3.10 – 2.99 (m, 1H), 1.31 (d, *J* = 6.9 Hz, 6H); ¹³C NMR (100 MHz, CDCl₃) δ 192.7, 159.7, 134.6, 134.0, 131.40, 128.9, 128.1, 103.4, 57.5, 27.8, 22.9; FT-IR (neat) 3209, 2970, 1705, 1257, 1211, 1026, 717 cm⁻¹.

1-Phenyl-2-(4-phenyl-1*H*-pyrazol-1-yl)ethan-1-one (54l)

Off white solid (0.232 g, 64%); mp 121–122 °C; ¹H NMR (400 MHz, CDCl₃) δ 8.06 – 8.01 (m, 2H), 7.90 (s, 1H), 7.79 (s, 1H), 7.67 (t, *J* = 7.4 Hz, 1H), 7.58 – 7.51 (m, 4H), 7.39 (t, *J* = 7.7 Hz, 2H), 7.26 (d, *J* = 8.0 Hz, 1H), 5.65 (s, 2H); ¹³C NMR (100 MHz, CDCl₃) δ 192.2, 137.5, 134.5, 134.2, 132.4, 129.0, 128.8, 128.2, 127.8, 126.5, 125.7, 124.1, 57.9; FT-IR (neat) 3102, 1658, 1450, 1282, 1078, 728 cm⁻¹.

2-(4-Bromo-1*H*-pyrazol-1-yl)-1-phenylethan-1-one (54m)

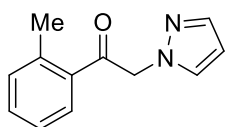
White crystalline solid (0.54 g, 60%); mp 138–139 °C; ¹H NMR (400 MHz, CDCl₃) δ 8.02 – 7.99 (m, 2H), 7.71 – 7.65 (m, 1H), 7.57 (s, 2H), 7.57 – 7.52 (m, 2H), 5.61 (s, 2H); ¹³C NMR (100 MHz, CDCl₃) δ 191.7, 140.6, 134.4, 134.2, 131.1, 129.1, 128.1, 94.1, 58.2; FT-IR (neat) 3125, 1697, 1597, 1219, 1088, 687 cm⁻¹.

2-(4-Chloro-1*H*-pyrazol-1-yl)-1-phenylethan-1-one (54n)

White crystalline solid (0.225 g, 52%); mp 129–130 °C; ¹H NMR (400 MHz, CDCl₃) δ 8.00 (dd, *J* = 8.4, 1.2 Hz, 2H), 7.68 (tt, *J* = 7.6, 1.2 Hz, 1H), 7.57 – 7.53 (m, 4H), 5.58 (s, 2H); ¹³C NMR (101 MHz, CDCl₃) δ

191.7, 138.5, 134.3, 134.2, 129.1, 129.0, 128.9, 128.2, 58.3; FT-IR (neat) 3124, 1697, 1597, 1219, 1087, 748 cm^{-1}

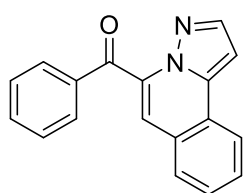
Procedure for the synthesis of 2-(1*H*-Pyrazol-1-yl)-1-(*o*-tolyl)ethan-1-one (54c)



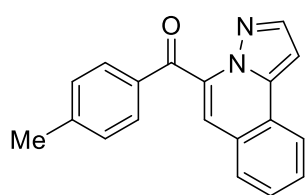
An oven-dried RB flask was charged with 1*H*- pyrazole (**22a**) (200 mg, 2.94 mmol), DMF (5 mL) and stirred at room temperature. To the reaction mixture was added KOH (247 mg, 4.4 mmol) portion wise and after 20 min, 2-bromo-1-(*o*-tolyl)ethan-1-one (0.751 g, 3.52 mmol) was added portion wise. Reaction progress was monitored by TLC. After completion of the reaction, reaction mixture was diluted with ice-cold water (50 mL) and extracted with ethyl acetate (2 × 20 mL). Combined organic layer was dried over anhydrous Na_2SO_4 , filtered and evaporated the ethyl acetate layer. Crude solid compound was purified by column chromatography over silica (25% v/v EtOAc: Hexane) to obtain 2-(1*H*-pyrazol-1-yl)-1-(*o*-tolyl)ethan-1-one (**54j**) as light yellow solid (59%, 110 mg); mp. 75–77 °C; ^1H NMR (400 MHz, CDCl_3) δ 7.78 (d, $J = 7.7$ Hz, 1H), 7.62 (d, $J = 1.4$ Hz, 1H), 7.52 (d, $J = 2.1$ Hz, 1H), 7.47 (t, $J = 7.5$ Hz, 1H), 7.34 (t, $J = 8.5$ Hz, 2H), 6.40 (t, $J = 2.0$ Hz, 1H), 5.54 (s, 2H), 2.56 (s, 3H); ^{13}C NMR (100 MHz, CDCl_3) δ 195.4, 140.0, 139.8, 134.3, 132.5, 130.9, 128.5, 125.9, 106.5, 59.2, 21.6; FT-IR (neat) 2927, 1666, 1597, 1242, 1035, 742 cm^{-1} .

General procedure for the synthesis of pyrazolo[5,1-*a*]isoquinoline derivatives (56aa–56kf):

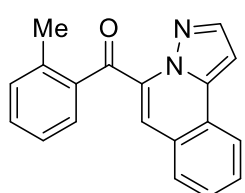
An oven-dried sealed tube with a rubber septum was charged with 1-aryl-2-(1*H*-pyrazol-1-yl)ethan-1-one (**54a**) (0.537 mmol), 2-bromoarylbenzaldehydes (**55a**) (0.590 mmol), K_2CO_3 (1.61 mmol), PCy_3 (0.161 mmol) and dry DMSO (2 mL). The resulting slurry was evacuated and backfilled with nitrogen gas. After 10 min, $\text{Ni}(\text{acac})_2$ (0.027 g, 0.107 mmol) was added then septum was replaced with a screw cap to sealed vial tightly, and the reaction mixture was heated at 150 °C for 16 h. The reaction mass was allowed to cool to ambient temperature, diluted with ice-cold water (20 mL) and extracted by EtOAc (2 × 30 mL). The combined organic layer was dried over anhydrous Na_2SO_4 and evaporated to dryness under reduced pressure on a rotatory evaporator. The crude residue was purified by column chromatography (12% EtOAc: Hexane) to afford corresponding pyrazolo[5,1-*a*]isoquinoline derivatives.

Phenyl(pyrazolo[5,1-*a*]isoquinolin-5-yl)methanone (56aa)

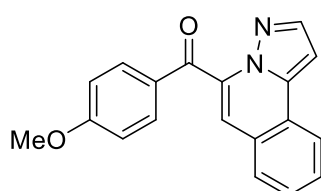
Light yellow solid (100 mg, 68%); mp 134–136 °C; ^1H NMR (400 MHz, CDCl_3) δ 8.19 (d, $J = 7.9$ Hz, 1H), 8.00 (d, $J = 2.0$ Hz, 1H), 7.95 (d, $J = 7.3$ Hz, 2H), 7.80 (d, $J = 7.8$ Hz, 1H), 7.72 – 7.67 (m, 1H), 7.67 – 7.59 (m, 2H), 7.50 (t, $J = 7.7$ Hz, 2H), 7.26 (s, 1H), 7.10 (d, $J = 2.1$ Hz, 1H); ^{13}C NMR (100 MHz, CDCl_3) δ 189.4, 141.8, 139.1, 136.3, 134.9, 134.0, 130.1, 129.1, 128.7, 128.4, 128.2, 127.7, 125.3, 123.8, 114.6, 97.8; FT-IR (neat) 3055, 1659, 1435, 1257, 1172, 756 cm^{-1} ; HRMS (ESI) calcd. for $\text{C}_{18}\text{H}_{13}\text{N}_2\text{O}$ $[\text{M}+\text{H}]^+$ 273.1022, found 273.1023.

Pyrazolo[5,1-*a*]isoquinolin-5-yl(*p*-tolyl)methanone (56ba)

Light yellow solid (102 mg, 72%); mp 158–159 °C; ^1H NMR (400 MHz, CDCl_3) δ 8.16 (d, $J = 8.0$ Hz, 1H), 7.99 (d, $J = 2.0$ Hz, 1H), 7.85 (d, $J = 8.2$ Hz, 2H), 7.77 (d, $J = 7.9$ Hz, 1H), 7.69 – 7.63 (m, 1H), 7.62 – 7.56 (m, 1H), 7.28 (d, $J = 8.0$ Hz, 2H), 7.21 (s, 1H), 7.08 (d, $J = 2.1$ Hz, 1H), 2.44 (s, 3H); ^{13}C NMR (100 MHz, CDCl_3) δ 189.1, 145.2, 141.7, 139.0, 135.1, 133.7, 130.2, 129.5, 129.0, 128.3, 128.1, 127.8, 125.2, 123.8, 114.1, 97.8, 21.9; FT-IR (neat) 3140, 1657, 1435, 1249, 1173, 740 cm^{-1} ; HRMS (ESI) calcd. for $\text{C}_{19}\text{H}_{15}\text{N}_2\text{O}$ $[\text{M}+\text{H}]^+$ 287.1179, found 287.1203.

(Pyrazolo[5,1-*a*]isoquinolin-5-yl(*o*-tolyl)methanone (56ca)

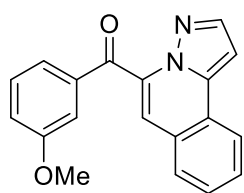
Light yellow solid (103 mg, 72%); mp 154–156 °C; ^1H NMR (400 MHz, CDCl_3) δ 8.13 (d, $J = 7.9$ Hz, 1H), 8.02 (bs, 1H), 7.74 (d, $J = 7.8$ Hz, 1H), 7.66 (t, $J = 7.4$ Hz, 1H), 7.56 (t, $J = 7.5$ Hz, 1H), 7.52 (d, $J = 7.7$ Hz, 1H), 7.45 (t, $J = 7.4$ Hz, 1H), 7.35 (d, $J = 7.5$ Hz, 1H), 7.24 – 7.19 (m, 2H), 7.07 (s, 1H), 2.61 (s, 3H); ^{13}C NMR (100 MHz, CDCl_3) δ 191.0, 141.8, 139.6, 139.2, 136.6, 135.8, 132.1, 131.9, 130.8, 129.4, 128.4, 128.3, 127.5, 125.6, 125.6, 123.7, 116.5, 97.8, 21.0; FT-IR (neat) 3016, 1659, 1589, 1265, 1033, 741 cm^{-1} ; HRMS (ESI) calcd. for $\text{C}_{19}\text{H}_{15}\text{N}_2\text{O}$ $[\text{M}+\text{H}]^+$ 287.1179, found 287.1194.

(4-Methoxyphenyl)(pyrazolo[5,1-*a*]isoquinolin-5-yl)methanone (56da)

Light yellow solid (91 mg, 65%); mp 132–134 °C; ^1H NMR (400 MHz, CDCl_3) δ 8.16 (d, $J = 7.9$ Hz, 1H), 7.99 (d, $J = 2.1$ Hz, 1H), 7.96 – 7.90 (m, 2H), 7.77 (d, $J = 7.6$ Hz, 1H), 7.69 – 7.63 (m, 1H), 7.61 – 7.56 (m, 1H), 7.19 (s, 1H), 7.08 (d, $J = 2.1$ Hz, 1H), 6.98 – 6.92 (m, 2H), 3.88

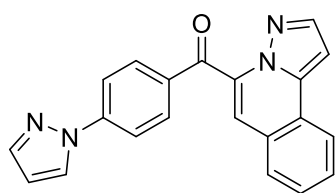
(s, 3H); ^{13}C NMR (100 MHz, CDCl_3) δ 188.0, 164.4, 141.7, 139.0, 135.3, 132.6, 129.1, 128.8, 128.3, 128.0, 127.8, 125.1, 123.8, 114.0, 113.6, 97.8, 55.6; FT-IR (neat) 3132, 1659, 1435, 1257, 1172, 756 cm^{-1} ; HRMS (ESI) calcd. for $\text{C}_{19}\text{H}_{15}\text{N}_2\text{O}_2$ $[\text{M}+\text{H}]^+$ 303.1128, found 303.1149.

(3-Methoxyphenyl)(pyrazolo[5,1-*a*]isoquinolin-5-yl)methanonemethanone (56ea)



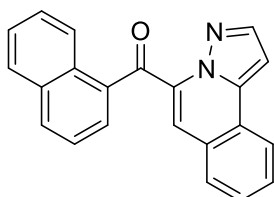
Light yellow solid (60 mg, 43%); mp 186–187 °C; ^1H NMR (400 MHz, CDCl_3) δ 8.18 (d, $J = 7.9$ Hz, 1H), 8.00 (d, $J = 2.0$ Hz, 1H), 7.80 (d, $J = 7.8$ Hz, 1H), 7.71 – 7.67 (m, 1H), 7.63 – 7.59 (m, 1H), 7.58 – 7.57 (m, 1H), 7.43 (d, $J = 7.7$ Hz, 1H), 7.36 (t, $J = 7.9$ Hz, 1H), 7.24 (s, 1H), 7.21 – 7.18 (m, 1H), 7.09 (d, $J = 2.1$ Hz, 1H), 3.87 (s, 3H); ^{13}C NMR (101 MHz, CDCl_3) δ 189.19, 141.75, 139.0, 137.5, 134.9, 129.6, 129.0, 128.3, 128.2, 127.7, 125.3, 123.8, 123.1, 120.8, 114.4, 113.6, 97.8, 55.5; FT-IR (neat) 3132, 1651, 1597, 1311, 1041, 748 cm^{-1} ; HRMS (ESI) calcd. for $\text{C}_{19}\text{H}_{15}\text{N}_2\text{O}_2$ $[\text{M}+\text{H}]^+$ 303.1128, found 303.1145.

(4-(1*H*-Pyrazol-1-yl)phenyl)(pyrazolo[5,1-*a*]isoquinolin-5-yl)methanone (56fa)

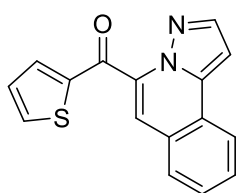


Yellow solid (78 mg, 48%); mp 135–137 °C; ^1H NMR (400 MHz, CDCl_3) δ 8.18 (d, $J = 7.9$ Hz, 1H), 8.04 – 8.02 (m, 3H), 7.99 (d, $J = 1.9$ Hz, 1H), 7.84 – 7.78 (m, 4H), 7.70 (t, $J = 7.6$ Hz, 1H), 7.62 (t, $J = 7.5$ Hz, 1H), 7.28 (s, 1H), 7.10 (d, $J = 2.0$ Hz, 1H), 6.53 (t, $J = 1.6$ Hz, 1H); ^{13}C NMR (100 MHz, CDCl_3) δ 188.1, 143.9, 142.2, 141.7, 139.1, 134.8, 133.9, 131.8, 129.1, 128.4, 128.2, 127.7, 126.9, 125.32, 123.8, 118.4, 114.5, 108.7, 97.9; FT-IR (neat) 3016, 1659, 1435, 1265, 1033, 741 cm^{-1} ; HRMS (ESI) calcd. for $\text{C}_{21}\text{H}_{15}\text{N}_4\text{O}$ $[\text{M}+\text{H}]^+$ 339.1240, found 339.1244.

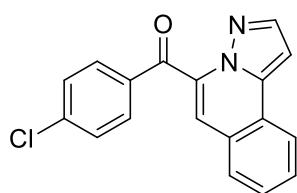
Naphthalen-2-yl(pyrazolo[5,1-*a*]isoquinolin-5-yl)methanone (56ga)



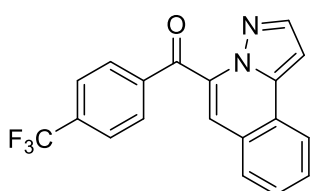
Light yellow solid (90 mg, 66%); mp 156–158 °C; ^1H NMR (400 MHz, CDCl_3) δ 8.42 (s, 1H), 8.21 (d, $J = 7.9$ Hz, 1H), 8.08 (d, $J = 8.5$ Hz, 1H), 8.00 (s, 1H), 7.98 – 7.85 (m, 3H), 7.82 (d, $J = 7.8$ Hz, 1H), 7.72 (t, $J = 7.5$ Hz, 1H), 7.64 (t, $J = 6.5$ Hz, 2H), 7.58 – 7.51 (m, 1H), 7.31 (s, 1H), 7.12 (s, 1H); ^{13}C NMR (100 MHz, CDCl_3) δ 189.4, 141.8, 139.1, 136.1, 135.1, 133.7, 132.6, 132.4, 129.8, 129.1, 129.0, 128.7, 128.4, 128.2, 127.9, 127.8, 126.9, 125.3, 124.9, 123.8, 114.6, 98.0; FT-IR (neat) 3059, 1678, 1469, 1257, 1184, 744 cm^{-1} ; HRMS (ESI) calcd. for $\text{C}_{22}\text{H}_{15}\text{N}_2\text{O}$ $[\text{M}+\text{H}]^+$ 323.1179, found 323.1158.

Pyrazolo[5,1-*a*]isoquinolin-5-yl(thiophen-2-yl)methanone (56ha)

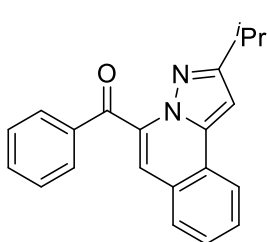
Light yellow oil (85 mg, 59%); ^1H NMR (400 MHz, CDCl_3) δ 8.16 (d, $J = 7.9$ Hz, 1H), 8.04 (d, $J = 2.0$ Hz, 1H), 7.82 (dd, $J = 4.9, 0.8$ Hz, 1H), 7.79 (d, $J = 7.9$ Hz, 1H), 7.71 – 7.66 (m, 2H), 7.60 (t, $J = 7.5$ Hz, 1H), 7.32 (s, 1H), 7.16 (t, $J = 4.0$ Hz, 1H), 7.09 (d, $J = 2.1$ Hz, 1H); ^{13}C NMR (100 MHz, CDCl_3) δ 181.0, 143.30, 141.8, 139.2, 136.2, 135.7, 134.4, 129.2, 128.4, 128.2, 127.5, 125.3, 123.8, 114.4, 98.0; FT-IR (neat) 3059, 1666, 1477, 1242, 1108, 725 cm^{-1} ; HRMS (ESI) calcd. for $\text{C}_{16}\text{H}_{11}\text{N}_2\text{OS}$ $[\text{M}+\text{H}]^+$ 279.0587, found 279.0587.

(4-Chlorophenyl)(pyrazolo[5,1-*a*]isoquinolin-5-yl)methanone (56ia)

Light yellow oil (25 mg, 18%); ^1H NMR (400 MHz, CDCl_3) δ 8.18 (d, $J = 8.0$ Hz, 1H), 7.99 (d, $J = 1.8$ Hz, 1H), 7.86 (d, $J = 8.6$ Hz, 2H), 7.81 (d, $J = 7.8$ Hz, 1H), 7.72 – 7.68 (m, 1H), 7.64 – 7.60 (m, 1H), 7.46 (d, $J = 8.6$ Hz, 2H), 7.26 (s, 1H), 7.10 (d, $J = 1.9$ Hz, 1H); ^{13}C NMR (100 MHz, CDCl_3) δ 188.2, 141.8, 140.5, 139.0, 134.7, 134.6, 131.3, 129.3, 129.1, 128.4, 128.3, 127.6, 125.3, 123.8, 114.7, 97.9; FT-IR (neat) 2954, 1666, 1597, 1249, 1165, 694 cm^{-1} ; HRMS (ESI) calcd. for $\text{C}_{18}\text{H}_{12}\text{ClN}_2\text{O}$ $[\text{M}+\text{H}]^+$ 307.0633, found 307.0639.

Pyrazolo[5,1-*a*]isoquinolin-5-yl(4-(trifluoromethyl)-phenyl)methanone (56ja)

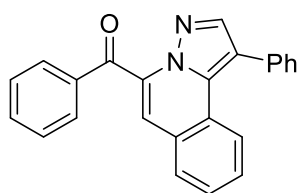
Off white solid (43 mg, 32%); mp 143–145 $^{\circ}\text{C}$; ^1H NMR (400 MHz, CDCl_3) δ 8.20 (d, $J = 7.8$ Hz, 1H), 8.01 – 7.98 (m, 3H), 7.83 (d, $J = 7.7$ Hz, 1H), 7.76 – 7.71 (m, 3H), 7.64 (t, $J = 7.3$ Hz, 1H), 7.30 (s, 1H), 7.11 (s, 1H); ^{13}C NMR (100 MHz, CDCl_3) δ 188.4, 141.8, 139.2, 139.1, 135.1 (q, $J = 33$ Hz), 134.4, 130.1, 129.5, 128.5, 128.4, 125.7 (q, $J = 3.6$ Hz), 125.5, 124.9, 123.5 (q, $J = 271$ Hz), 115.5, 98.0; ^{19}F NMR (375 MHz, CDCl_3) δ -63.2; FT-IR (neat) 2954, 1674, 1442, 1319, 1111, 748 cm^{-1} ; HRMS (ESI) calcd. for $\text{C}_{19}\text{H}_{12}\text{F}_3\text{N}_2\text{O}$ $[\text{M}+\text{H}]^+$ 341.0896, found 341.0901.

(2-Isopropylpyrazolo[5,1-*a*]isoquinolin-5-yl)(phenyl)methanone (56ka)

Off white solid (103 mg, 75%); mp 140–142 $^{\circ}\text{C}$; ^1H NMR (400 MHz, CDCl_3) δ 8.13 (d, $J = 8.0$ Hz, 1H), 7.94 (d, $J = 7.3$ Hz, 2H), 7.75 (d, $J = 7.8$ Hz, 1H), 7.70 – 7.60 (m, 2H), 7.57 (t, $J = 7.5$ Hz, 1H), 7.48 (t, $J = 7.7$ Hz, 2H), 7.16 (s, 1H), 6.91 (s, 1H), 3.22 – 3.12 (m, 1H), 1.31 (d, $J = 6.9$ Hz, 6H); ^{13}C NMR (100 MHz, CDCl_3) δ 189.6, 161.9, 139.6, 136.5, 134.9,

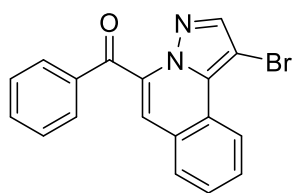
133.7, 130.2, 128.8, 128.4, 128.1, 128.0, 127.7, 125.2, 123.6, 113.6, 94.4, 28.1, 23.0; FT-IR (neat) 3132, 2970, 1659, 1234, 1080, 679 cm^{-1} ; HRMS (ESI) calcd. for $\text{C}_{21}\text{H}_{19}\text{N}_2\text{O}$ $[\text{M}+\text{H}]^+$ 315.1492, found 315.1494.

Phenyl(1-phenylpyrazolo[5,1-*a*]isoquinolin-5-yl)methanone (56la)



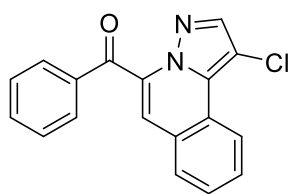
Light yellow solid (46 mg, 35%); mp 162–164 °C; ^1H NMR (400 MHz, CDCl_3) δ 8.10 (d, $J = 8.2$ Hz, 1H), 8.01 – 7.93 (m, 2H), 7.93 (s, 1H), 7.78 (d, $J = 7.8$ Hz, 1H), 7.67 – 7.61 (m, 1H), 7.61 – 7.57 (m, 2H), 7.57 – 7.51 (m, 4H), 7.51 – 7.49 (m, 1H), 7.48 – 7.45 (m, 1H), 7.46 – 7.42 (m, 1H), 7.24 (s, 1H); ^{13}C NMR (100 MHz, CDCl_3) δ 189.5, 142.5, 136.2, 135.0, 134.3, 134.1, 133.7, 130.1, 130.0, 128.8, 128.7, 128.6, 128.4, 128.3, 128.2, 127.7, 125.8, 123.5, 117.0, 114.4; FT-IR (neat) 3059, 1643, 1408, 1238, 1091, 725 cm^{-1} ; HRMS (ESI) calcd. for $\text{C}_{24}\text{H}_{17}\text{N}_2\text{O}$ $[\text{M}+\text{H}]^+$ 349.1335, found 349.1358.

(1-Bromopyrazolo[5,1-*a*]isoquinolin-5-yl)(phenyl)-methanone (56ma)

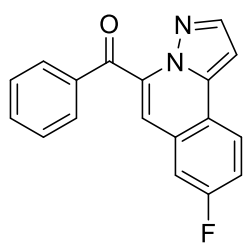


Yellow solid (28 mg, 21%); mp 183–185 °C; ^1H NMR (400 MHz, CDCl_3) δ 9.10 (d, $J = 8.1$ Hz, 1H), 7.94 (s, 1H), 7.92 – 7.90 (m, 2H), 7.81 (d, $J = 7.8$ Hz, 1H), 7.76 – 7.72 (m, 1H), 7.68 – 7.63 (m, 2H), 7.49 (t, $J = 7.8$ Hz, 2H), 7.26 (s, 1H); ^{13}C NMR (100 MHz, CDCl_3) δ 188.9, 142.9, 136.1, 134.9, 134.2, 133.8, 129.9, 129.0, 128.8, 128.7, 128.3, 128.2, 125.1, 123.4, 115.0, 87.4; FT-IR (neat) 2924, 1659, 1435, 1311, 1249, 679 cm^{-1} ; HRMS (ESI) calcd. for $\text{C}_{18}\text{H}_{12}\text{BrN}_2\text{O}$ $[\text{M}+\text{H}]^+$ 351.0128, found 351.0143 and $[\text{M}+\text{H}+2]^+$ 353.0124.

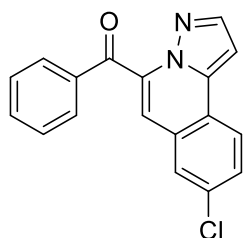
(1-Chloropyrazolo[5,1-*a*]isoquinolin-5-yl)(phenyl)-methanone (56na)



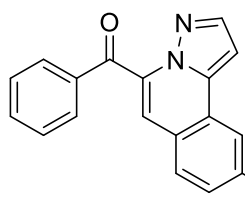
Yellow solid (25 mg, 18%); mp 170–172 °C; ^1H NMR (400 MHz, CDCl_3) δ 8.93 (d, $J = 8.1$ Hz, 1H), 7.93 – 7.91 (m, 3H), 7.82 (d, $J = 8.1$ Hz, 1H), 7.77 – 7.73 (m, 1H), 7.69 – 7.64 (m, 2H), 7.50 (t, $J = 7.8$ Hz, 2H), 7.25 (s, 1H); ^{13}C NMR (100 MHz, CDCl_3) δ 188.9, 140.6, 136.1, 134.9, 134.2, 132.8, 129.9, 129.1, 128.8, 128.2, 128.1, 125.0, 123.4, 115.0, 104.3; FT-IR (neat) 3055, 1659, 1435, 1319, 1249, 756 cm^{-1} ; HRMS (ESI) calcd. for $\text{C}_{18}\text{H}_{12}\text{ClN}_2\text{O}$ $[\text{M}+\text{H}]^+$ 307.0633, found 307.0627.

(8-Fluoropyrazolo[5,1-*a*]isoquinolin-5-yl)(phenyl)methanone (56ab)

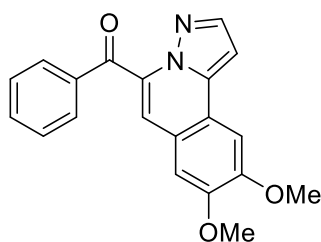
Yellow solid (70 mg, 45%); mp 154–155 °C; ^1H NMR (400 MHz, CDCl_3) δ 8.16 (dd, $J = 8.2, 5.3$ Hz, 1H), 7.98 (s, 1H), 7.93 (d, $J = 7.5$ Hz, 2H), 7.65 (t, $J = 7.1$ Hz, 1H), 7.49 (t, $J = 7.5$ Hz, 2H), 7.42 (dd, $J = 16.4, 8.5$ Hz, 2H), 7.16 (s, 1H), 7.03 (s, 1H); ^{13}C NMR (100 MHz, CDCl_3) δ 189.2, 162.1 (d, $J = 249.0$ Hz), 142.1, 138.7, 136.0, 135.9, 134.2, 130.0, 129.5 (d, $J = 9.2$ Hz), 128.8, 126.12 (d, $J = 8.9$ Hz), 121.7 (d, $J = 2.0$ Hz), 117.7 (d, $J = 23.8$ Hz), 113.10, 113.07, 113.0 (d, $J = 22.0$ Hz), 97.6; ^{19}F NMR (375 MHz, CDCl_3) δ -111.2; FT-IR (neat) 3124, 1659, 1442, 1234, 1141, 679 cm^{-1} ; HRMS (ESI) calcd. for $\text{C}_{18}\text{H}_{12}\text{FN}_2\text{O}$ $[\text{M}+\text{H}]^+$ 291.0928, found 291.0929.

(8-Chloropyrazolo[5,1-*a*]isoquinolin-5-yl)(phenyl)methanone (56ac)

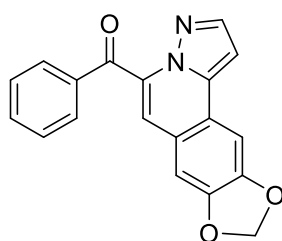
Off white solid (50 mg, 30%); mp 172–174 °C; ^1H NMR (400 MHz, CDCl_3) δ 8.10 (d, $J = 8.5$ Hz, 1H), 7.99 (s, 1H), 7.93 (d, $J = 7.4$ Hz, 2H), 7.77 (s, 1H), 7.69 – 7.60 (m, 2H), 7.49 (t, $J = 7.6$ Hz, 2H), 7.14 (s, 1H), 7.07 (d, $J = 1.7$ Hz, 1H); ^{13}C NMR (100 MHz, CDCl_3) δ 189.1, 142.1, 138.5, 135.9, 135.9, 134.2, 134.2, 130.0, 129.4, 128.9, 128.8, 127.3, 125.2, 123.5, 112.9, 98.1; FT-IR (neat) 3063, 1662, 1435, 1288, 1083, 721 cm^{-1} ; HRMS (ESI) calcd. for $\text{C}_{18}\text{H}_{12}\text{ClN}_2\text{O}$ $[\text{M}+\text{H}]^+$ 307.0633, found 307.0631.

(9-Methylpyrazolo[5,1-*a*]isoquinolin-5-yl)(phenyl)methanone (56ad)

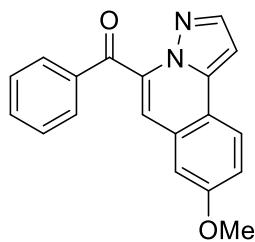
Off white solid (52 mg, 34%); mp 173–175 °C; ^1H NMR (400 MHz, CDCl_3) δ 7.98 (d, $J = 6.7$ Hz, 2H), 7.94 (d, $J = 7.5$ Hz, 2H), 7.68 (d, $J = 8.0$ Hz, 1H), 7.64 (t, $J = 7.4$ Hz, 1H), 7.49 (t, $J = 7.6$ Hz, 2H), 7.43 (d, $J = 7.8$ Hz, 1H), 7.23 (s, 1H), 7.06 (d, $J = 1.4$ Hz, 1H), 2.60 (s, 3H); ^{13}C NMR (100 MHz, CDCl_3) δ 189.5, 141.6, 139.6, 139.0, 136.5, 134.1, 133.9, 130.1, 130.0, 128.7, 128.1, 125.4, 125.4, 123.6, 115.0, 97.6, 21.9; FT-IR (neat) 3063, 1665, 1447, 1226, 1187, 663 cm^{-1} ; HRMS (ESI) calcd. for $\text{C}_{19}\text{H}_{15}\text{N}_2\text{O}$ $[\text{M}+\text{H}]^+$ 287.1179, found 287.1201.

(8,9-Dimethoxypyrazolo[5,1-*a*]isoquinolin-5-yl)(phenyl)methanone (56ae)

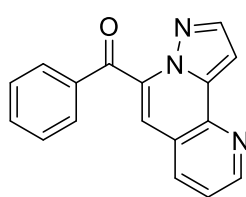
Yellow solid (112 mg, 63%); mp 144–146 °C; ^1H NMR (400 MHz, CDCl_3) δ 7.99 (s, 1H), 7.94 (d, $J = 7.4$ Hz, 2H), 7.64 (t, $J = 7.6$ Hz, 1H), 7.53 – 7.46 (m, 3H), 7.21 (s, 1H), 7.16 (s, 1H), 6.95 (s, 1H), 4.12 (s, 3H), 4.02 (s, 3H); ^{13}C NMR (100 MHz, CDCl_3) δ 189.4, 151.2, 150.3, 141.6, 138.9, 136.7, 133.7, 133.3, 130.1, 128.6, 122.1, 120.2, 115.3, 108.4, 104.3, 96.3, 56.3, 56.1; FT-IR (neat) 3132, 1651, 1496, 1242, 1157, 732 cm^{-1} ; HRMS (ESI) calcd. for $\text{C}_{20}\text{H}_{17}\text{N}_2\text{O}_3$ $[\text{M}+\text{H}]^+$ 333.1234, found 333.1230.

[1,3]Dioxolo[4,5-*g*]pyrazolo[5,1-*a*]isoquinolin-5-yl(phenyl)methanone (56af)

Yellow solid (102 mg, 60%); mp 172–173 °C; ^1H NMR (400 MHz, CDCl_3) δ 7.94 (d, $J = 2.0$ Hz, 1H), 7.91 (d, $J = 7.4$ Hz, 2H), 7.62 (t, $J = 7.4$ Hz, 1H), 7.49 – 7.46 (m, 3H), 7.14 (s, 1H), 7.10 (s, 1H), 6.89 (d, $J = 2.0$ Hz, 1H), 6.12 (s, 2H); ^{13}C NMR (100 MHz, CDCl_3) δ 189.4, 149.6, 148.8, 141.6, 139.1, 136.5, 133.8, 133.4, 130.0, 128.6, 123.5, 121.5, 115.1, 106.0, 102.2, 102.0, 96.6; FT-IR (neat) 3063, 1666, 1450, 1219, 1039, 687 cm^{-1} ; HRMS (ESI) calcd. for $\text{C}_{19}\text{H}_{13}\text{N}_2\text{O}_3$ $[\text{M}+\text{H}]^+$ 317.0921, found 317.0944.

(8-Methoxypyrazolo[5,1-*a*]isoquinolin-5-yl)(phenyl)methanone (56ag)

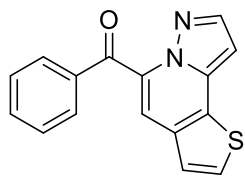
Light yellow solid (107 mg, 66%); mp 176–177 °C; ^1H NMR (400 MHz, CDCl_3) δ 8.09 (d, $J = 8.8$ Hz, 1H), 7.95 (d, $J = 8.0$ Hz, 3H), 7.65 (t, $J = 7.2$ Hz, 1H), 7.50 (t, $J = 7.5$ Hz, 2H), 7.30 (d, $J = 8.2$ Hz, 1H), 7.18 (s, 2H), 6.97 (s, 1H), 3.95 (s, 3H); ^{13}C NMR (100 MHz, CDCl_3) δ 189.5, 159.6, 141.9, 139.2, 136.2, 135.3, 134.0, 130.1, 129.3, 128.7, 125.4, 119.4, 118.9, 114.2, 109.0, 96.6, 55.6; FT-IR (neat) 3063, 1666, 1604, 1242, 1165, 687 cm^{-1} ; HRMS (ESI) calcd. for $\text{C}_{19}\text{H}_{15}\text{N}_2\text{O}_2$ $[\text{M}+\text{H}]^+$ 303.1128, found 303.1154.

Phenyl(pyrazolo[1,5-*h*][1,7]naphthyridin-6-yl)methanone (56ah)

Light yellow solid (96 mg, 66%); mp 161–162 °C; ^1H NMR (400 MHz, CDCl_3) δ 8.97 (dd, $J = 4.5, 1.5$ Hz, 1H), 8.11 (dd, $J = 8.0, 1.5$ Hz, 1H), 8.05 (d, $J = 2.0$ Hz, 1H), 7.93 (d, $J = 7.3$ Hz, 2H), 7.66 (t, $J = 7.4$ Hz, 1H), 7.55 (dd, $J = 8.0, 4.6$ Hz, 1H), 7.50 (t, $J = 7.8$ Hz, 2H), 7.44 (d, $J = 2.1$ Hz, 1H), 7.19 (s, 1H); ^{13}C NMR (100 MHz, CDCl_3) δ 189.0, 150.9, 142.7, 142.3, 139.7, 135.9, 135.8, 135.5,

134.3, 130.0, 128.8, 123.6, 123.2, 112.2, 100.2; FT-IR (neat) 3062, 1659, 1473, 1273, 1180, 729 cm^{-1} ; HRMS (ESI) calcd. for $\text{C}_{17}\text{H}_{12}\text{N}_3\text{O}$ $[\text{M}+\text{H}]^+$ 274.0975, found 274.0977.

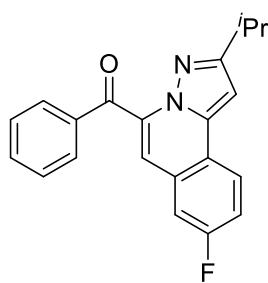
Phenyl(pyrazolo[1,5-*a*]thieno[2,3-*c*]pyridin-5-yl)methanone (56ai)



Light brown oil (86 mg, 56%); ^1H NMR (400 MHz, CDCl_3) δ 8.01 (d, $J = 1.6$ Hz, 1H), 7.90 (d, $J = 7.5$ Hz, 2H), 7.68 (dd, $J = 19.5, 5.3$ Hz, 2H), 7.63 (t, $J = 7.6$ Hz, 1H), 7.48 (t, $J = 7.6$ Hz, 2H), 7.43 (s, 1H), 6.85 (d, $J = 1.8$ Hz, 1H); ^{13}C NMR (100 MHz, CDCl_3) δ 189.3, 142.0, 137.7, 136.3, 133.9, 133.3,

133.1, 130.3, 130.0, 129.8, 128.7, 122.5, 109.7, 95.9; FT-IR (neat) 3059, 1655, 1446, 1276, 1180, 725 cm^{-1} ; HRMS (ESI) calcd. for $\text{C}_{16}\text{H}_{11}\text{N}_2\text{OS}$ $[\text{M}+\text{H}]^+$ 279.0587, found 279.0588.

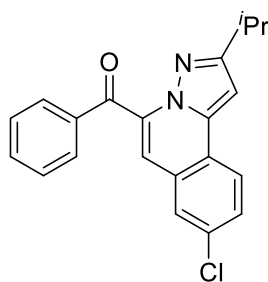
(8-Fluoro-2-isopropylpyrazolo[5,1-*a*]isoquinolin-5-yl)(phenyl)methanone (56kb)



Light yellow solid (77 mg, 53%); mp 151–152 $^{\circ}\text{C}$; ^1H NMR (400 MHz, CDCl_3) δ 8.13 – 8.10 (m, 1H), 7.92 (d, $J = 7.3$ Hz, 2H), 7.64 (t, $J = 7.4$ Hz, 1H), 7.48 (t, $J = 7.7$ Hz, 2H), 7.39 (ddd, $J = 15.8, 8.9, 2.4$ Hz, 2H), 7.07 (s, 1H), 6.86 (s, 1H), 3.20 – 3.10 (m, 1H), 1.30 (d, $J = 6.9$ Hz, 6H); ^{13}C NMR (100 MHz, CDCl_3) δ 189.4, 162.3, 161.9 (d, $J = 248.3$ Hz), 139.3, 136.2,

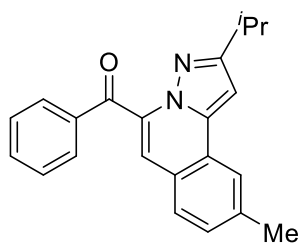
135.9, 133.9, 130.1, 129.5 (d, $J = 9.2$ Hz), 128.5, 125.9 (d, $J = 8.9$ Hz), 121.8 (d, $J = 2.1$ Hz), 117.3 (d, $J = 23.8$ Hz), 112.9 (d, $J = 21.9$ Hz), 112.2, 112.1, 94.2, 28.1, 22.9; ^{19}F NMR (375 MHz, CDCl_3) δ -111.9; FT-IR (neat) 3132, 2947, 1659, 1234, 1141, 687 cm^{-1} ; HRMS (ESI) calcd. for $\text{C}_{21}\text{H}_{18}\text{FN}_2\text{O}$ $[\text{M}+\text{H}]^+$ 333.1398, found 333.1420.

(8-Chloro-2-isopropylpyrazolo[5,1-*a*]isoquinolin-5-yl)(phenyl)methanone (56kc)

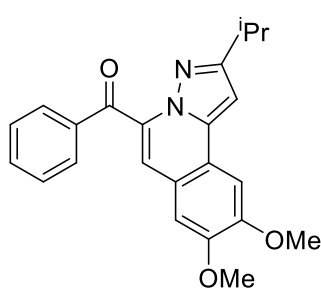


Off white solid (52 mg, 34%); mp 164–166 $^{\circ}\text{C}$; ^1H NMR (400 MHz, CDCl_3) δ 8.05 (d, $J = 8.6$ Hz, 1H), 7.92 (dd, $J = 8.3, 1.1$ Hz, 2H), 7.73 (d, $J = 2.0$ Hz, 1H), 7.66 – 7.61 (m, 1H), 7.58 (dd, $J = 8.6, 2.1$ Hz, 1H), 7.47 (t, $J = 7.8$ Hz, 2H), 7.04 (s, 1H), 6.88 (s, 1H), 3.21 – 3.10 (m, 1H), 1.30 (d, $J = 6.9$ Hz, 6H); ^{13}C NMR (100 MHz, CDCl_3) δ 189.1, 162.3, 139.1, 136.1,

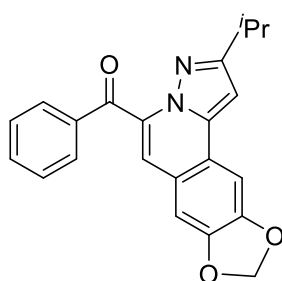
135.9, 133.9, 133.7, 130.1, 129.1, 129.0, 128.5, 127.2, 125.1, 123.4, 111.9, 94.7, 28.1, 22.9; FT-IR (neat) 3130, 2960, 1662, 1253, 1053, 725 cm^{-1} ; HRMS (ESI) calcd. for $\text{C}_{21}\text{H}_{18}\text{ClN}_2\text{O}$ $[\text{M}+\text{H}]^+$ 349.1102, found 349.1092.

(2-Isopropyl-9-methylpyrazolo[5,1-*a*]isoquinolin-5-yl)(phenyl)methanone (56kd)

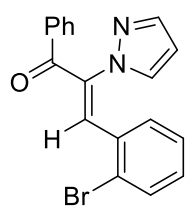
Off white solid (57 mg, 40%); mp 173–175 °C; ^1H NMR (400 MHz, CDCl_3) δ 7.94 – 7.92 (m, 2H), 7.66 – 7.61 (m, 2H), 7.48 (t, $J = 7.4$ Hz, 2H), 7.40 (d, $J = 7.9$ Hz, 1H), 7.29 (s, 1H), 7.15 (s, 1H), 6.89 (s, 1H), 3.23 – 3.12 (m, 1H), 2.59 (s, 3H), 1.31 (d, $J = 6.8$ Hz, 6H); ^{13}C NMR (100 MHz, CDCl_3) δ 189.6, 161.7, 139.5, 139.2, 136.7, 134.1, 133.6, 130.3, 129.6, 128.4, 128.0, 125.4, 125.3, 123.4, 114.2, 94.3, 28.1, 23.0, 21.9; FT-IR (neat) 3155, 2955, 1658, 1235, 1187, 671 cm^{-1} ; HRMS (ESI) calcd. for $\text{C}_{22}\text{H}_{21}\text{N}_2\text{O}$ $[\text{M}+\text{H}]^+$ 329.1648, found 329.1672.

(2-Isopropyl-8,9-dimethoxy pyrazolo[5,1-*a*]isoquinolin-5-yl)(phenyl)methanone (56ke)

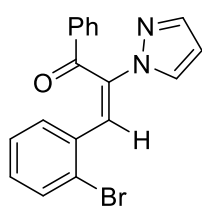
Yellow solid (115 mg, 70%); mp 154–155 °C; ^1H NMR (400 MHz, CDCl_3) δ 7.93 – 7.92 (m, 2H), 7.62 (t, $J = 7.6$ Hz, 1H), 7.49 – 7.45 (m, 3H), 7.12 (s, 2H), 6.78 (s, 1H), 4.11 (s, 3H), 4.01 (s, 3H), 3.20 – 3.15 (m, 1H), 1.32 (d, $J = 6.5$ Hz, 6H); ^{13}C NMR (100 MHz, CDCl_3) δ 189.5, 161.8, 151.0, 150.0, 139.4, 136.8, 133.4, 133.3, 130.2, 128.3, 122.1, 120.0, 114.4, 108.3, 104.2, 92.8, 56.2, 56.1, 28.1, 23.1; FT-IR (neat) 3155, 2962, 1667, 1242, 1149, 686 cm^{-1} ; HRMS (ESI) calcd. for $\text{C}_{23}\text{H}_{23}\text{N}_2\text{O}_3$ $[\text{M}+\text{H}]^+$ 375.1703, found 375.1730.

(2-Isopropyl-[1,3]dioxolo[4,5-*g*]pyrazolo[5,1-*a*]isoquinolin-5-yl)(phenyl)methanone (56kf)

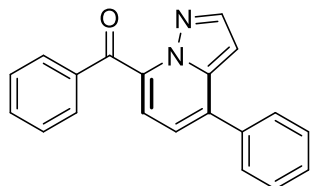
Off white solid (97 mg, 62%); mp 160–162 °C; ^1H NMR (400 MHz, CDCl_3) δ 7.91 (d, $J = 7.4$ Hz, 2H), 7.62 (t, $J = 7.4$ Hz, 1H), 7.48 – 7.45 (m, 3H), 7.09 (s, 1H), 7.06 (s, 1H), 6.72 (s, 1H), 6.13 (s, 2H), 3.21 – 3.10 (m, 1H), 1.30 (d, $J = 6.9$ Hz, 6H); ^{13}C NMR (100 MHz, CDCl_3) δ 189.5, 161.8, 149.4, 148.5, 139.7, 136.7, 133.5, 133.4, 130.1, 128.3, 123.5, 121.4, 114.2, 105.9, 102.1, 101.8, 93.1, 28.1, 23.0; FT-IR (neat) 3130, 2950, 1662, 1258, 1061, 728 cm^{-1} ; HRMS (ESI) calcd. for $\text{C}_{22}\text{H}_{19}\text{N}_2\text{O}_3$ $[\text{M}+\text{H}]^+$ 359.1390, found 359.1364.

(Z)-3-(2-Bromophenyl)-1-phenyl-2-(1H-pyrazol-1-yl)prop-2-en-1-one (57a')

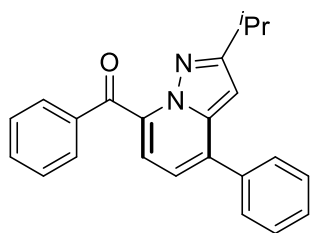
Light yellow solid (0.18 g, 19%); mp 104–105°C; ^1H NMR (400 MHz, CDCl_3) δ 7.86 – 7.82 (m, 2H), 7.66 (d, $J = 1.7$ Hz, 1H), 7.64 – 7.62 (m, 1H), 7.61 – 7.57 (m, 1H), 7.55 (s, 1H), 7.46 (t, $J = 7.8$ Hz, 2H), 7.41 (d, $J = 2.4$ Hz, 1H), 7.20 (td, $J = 7.7, 1.8$ Hz, 1H), 7.14 (td, $J = 7.6, 1.3$ Hz, 1H), 6.72 (dd, $J = 7.6, 1.7$ Hz, 1H), 6.35 (t, $J = 2.0$ Hz, 1H); ^{13}C NMR (100 MHz, CDCl_3) δ 191.1, 141.2, 137.2, 136.7, 134.3, 133.1, 133.0, 132.9, 131.5, 131.0, 130.1, 129.3, 128.5, 127.4, 125.3, 107.4; HRMS (ESI) calcd. for $\text{C}_{18}\text{H}_{14}\text{BrN}_2\text{O}$ $[\text{M}+\text{H}]^+$ 353.0284, found 353.0301 $[\text{M} + \text{H}]^+$ and 355.0280. $[\text{M} + \text{H} + 2]^+$.

(E)-3-(2-Bromophenyl)-1-phenyl-2-(1H-pyrazol-1-yl)prop-2-en-1-one (57a)

Light brown oil (0.45 g, 47%); ^1H NMR (400 MHz, CDCl_3) δ 7.93 (d, $J = 7.2$ Hz, 2H), 7.71 (d, $J = 2.4$ Hz, 2H), 7.58 (s, 1H), 7.45 (t, $J = 7.6$ Hz, 2H), 7.33 (t, $J = 7.7$ Hz, 2H), 7.23 (dd, $J = 7.5, 1.2$ Hz, 1H), 7.03 (td, $J = 7.4, 1.0$ Hz, 1H), 6.98 (td, $J = 7.6, 1.6$ Hz, 1H), 6.43 (t, $J = 2.0$ Hz, 1H); ^{13}C NMR (100 MHz, CDCl_3) δ 191.8, 141.8, 136.6, 136.0, 134.1, 133.9, 132.6, 130.7, 129.8, 129.4, 128.7, 128.6, 127.3, 124.3, 120.8, 107.8; HRMS (ESI) calcd. for $\text{C}_{18}\text{H}_{14}\text{BrN}_2\text{O}$ $[\text{M}+\text{H}]^+$ 353.0284, found 353.0295 $[\text{M} + \text{H}]^+$ and 355.0272 $[\text{M} + \text{H} + 2]^+$.

Phenyl(4-phenylpyrazolo[1,5-a]pyridin-7-yl)methanone (59aa)

Light yellow solid (112 mg, 70%); mp 104–105 °C; ^1H NMR (400 MHz, CDCl_3) δ 8.03 (d, $J = 1.8$ Hz, 1H), 7.94 (d, $J = 7.4$ Hz, 2H), 7.74 (d, $J = 7.1$ Hz, 2H), 7.65 (t, $J = 7.4$ Hz, 1H), 7.57 (t, $J = 6.9$ Hz, 2H), 7.50 (t, $J = 7.7$ Hz, 3H), 7.25 (d, $J = 7.1$ Hz, 1H), 7.10 (d, $J = 7.1$ Hz, 1H), 6.81 (d, $J = 1.9$ Hz, 1H); ^{13}C NMR (100 MHz, CDCl_3) δ 189.4, 142.5, 140.4, 137.5, 136.2, 135.5, 134.8, 134.0, 130.0, 129.0, 128.9, 128.7, 128.1, 121.3, 114.6, 97.9; FT-IR (neat) 3055, 1659, 1450, 1296, 1180, 721 cm^{-1} ; HRMS (ESI) calcd. for $\text{C}_{20}\text{H}_{15}\text{N}_2\text{O}$ $[\text{M}+\text{H}]^+$ 299.1179, found 299.1183.

(2-Isopropyl-4-phenylpyrazolo[1,5-a]pyridin-7-yl)(phenyl)methanone (59ka)

Light yellow solid (99 mg, 67%); mp 76–78 °C; ^1H NMR (400 MHz, CDCl_3) δ 7.93 (d, $J = 7.4$ Hz, 2H), 7.74 (d, $J = 7.2$ Hz, 2H), 7.63 (t, $J = 7.4$ Hz, 1H), 7.56 (t, $J = 7.4$ Hz, 2H), 7.52 – 7.47 (m, 3H), 7.17 (d, $J = 7.1$ Hz, 1H), 7.02 (d, $J = 7.1$ Hz, 1H), 6.59 (s, 1H), 3.21 – 3.11 (m, 1H), 1.28 (d, $J = 6.9$ Hz, 6H); ^{13}C NMR (100 MHz, CDCl_3) δ 189.6, 162.9, 141.2, 137.9, 136.4, 135.2, 134.1, 133.7, 130.1, 128.9, 128.7, 128.4, 128.1, 120.9, 113.8, 94.2, 28.1, 23.0; FT-IR (neat) 3059, 2962, 1666, 1477, 1253, 1176, 698 cm^{-1} ; HRMS (ESI) calcd. for $\text{C}_{23}\text{H}_{21}\text{N}_2\text{O}$ $[\text{M}+\text{H}]^+$ 341.1648, found 341.1658.

X-ray crystallography data for 56ae and 57a'**Table 4.3:** Crystal data and structure refinement for **56ae**

Identification code	56ae
Empirical formula	C ₂₀ H ₁₆ N ₂ O ₃
Formula weight	332.35
Temperature/K	93(2)
Crystal system	monoclinic
Space group	P2 ₁ /c
a/Å	10.9507(7)
b/Å	9.2147(5)
c/Å	16.0716(10)
α/°	90
β/°	105.156(6)
γ/°	90
Volume/Å ³	1565.34(17)
Z	4
ρ _{calc} /cm ³	1.410
μ/mm ⁻¹	0.096
F(000)	696.0
Crystal size/mm ³	0.2 × 0.1 × 0.03
Radiation	MoKα (λ = 0.71073)
2Θ range for data collection/°	10.208 to 49.996
Index ranges	-12 ≤ h ≤ 13, -10 ≤ k ≤ 10, -19 ≤ l ≤ 19
Reflections collected	10374
Independent reflections	2717 [R _{int} = 0.0251, R _{sigma} = 0.0223]
Data/restraints/parameters	2717/0/228
Goodness-of-fit on F ²	1.031
Final R indexes [I ≥ 2σ (I)]	R ₁ = 0.0318, wR ₂ = 0.0808
Final R indexes [all data]	R ₁ = 0.0427, wR ₂ = 0.0867
Largest diff. peak/hole / e Å ⁻³	0.19/-0.26

Table 4.4: Crystal data and structure refinement for 57a'

Identification code	MJ-001
Empirical formula	$C_{18}H_{13}BrN_2O$
Formula weight	353.21
Temperature	125(2) K
Wavelength	0.71073 Å
Crystal system	Monoclinic
Space group	$P2_1/c$
Unit cell dimensions	$a = 9.5950(6)$ Å $\alpha = 90^\circ$ $b = 9.1037(5)$ Å $\beta = 95.184(3)^\circ$ $c = 17.4692(10)$ Å $\gamma = 90^\circ$
Volume	1519.69(15) Å ³
Z	4
Density (calculated)	1.544 Mg/m ³
Absorption coefficient	2.708 mm ⁻¹
F(000)	712
Crystal size	0.380 x 0.300 x 0.250 mm ³
Theta range for data collection	2.131 to 28.954°
Index ranges	-12 ≤ h ≤ 12, -12 ≤ k ≤ 11, -23 ≤ l ≤ 22
Reflections collected	25082
Independent reflections	3801 [R(int) = 0.0461]
Completeness to theta = 25.242°	100.0 %
Absorption correction	Semi-empirical from equivalents
Max. and min. transmission	0.7458 and 0.5584
Refinement method	Full-matrix least-squares on F ²
Data / restraints / parameters	3801 / 0 / 199
Goodness-of-fit on F ²	1.061
Final R indices [I > 2σ(I)]	R1 = 0.0234, wR2 = 0.0629
R indices (all data)	R1 = 0.0257, wR2 = 0.0640
Extinction coefficient	n/a
Largest diff. peak and hole	0.594 and -0.332 e.Å ⁻³

4.5 REFERENCES

- [1] S. Löber, H. Hübner, P. Gmeiner, *Bioorganic & Medicinal Chemistry Letters*, **1999**, *9*, 97-102.
- [2] X.-H. Liu, P. Cui, B.-A. Song, P. S. Bhadury, H.-L. Zhu, S.-F. Wang, *Bioorganic & Medicinal Chemistry*, **2008**, *16*, 4075-4082.
- [3] C. Custodi, R. Nuti, T. I. Oprea, A. Macchiarulo, *Journal of Molecular Graphics and Modelling*, **2012**, *38*, 70-81.
- [4] W. J. Begley, J. Grimshaw, J. Trocha-Grimshaw, *Journal of the Chemical Society, Perkin Transactions 1*, **1974**, 2633-2637.
- [5] A. Dore, B. Asproni, A. Scampuddu, G. A. Pinna, C. T. Christoffersen, M. Langgård, J. Kehler, *European Journal of Medicinal Chemistry*, **2014**, *84*, 181-193.
- [6] Z. Chen, J. Wu, *Organic Letters*, **2010**, *12*, 4856-4859.
- [7] X. Yu, Q. Yang, H. Lou, Y. Peng, J. Wu, *Organic & Biomolecular Chemistry*, **2011**, *9*, 7033-7037.
- [8] Z. Chen, J. Wu, *Organic Letters*, **2010**, *12*, 4856-4859.
- [9] X. Yu, S. Ye, J. Wu, *Advanced Synthesis & Catalysis*, **2010**, *352*, 2050-2056.
- [10] S. Li, J. Wu, *Organic Letters*, **2011**, *13*, 712-715.
- [11] S. Li, Y. Luo, J. Wu, *Organic Letters*, **2011**, *13*, 4312-4315.
- [12] P. Huang, Z. Chen, Q. Yang, Y. Peng, *Organic Letters*, **2012**, *14*, 2790-2793.
- [13] P. Huang, Q. Yang, Z. Chen, Q. Ding, J. Xu, Y. Peng, *The Journal of Organic Chemistry*, **2012**, *77*, 8092-8098.
- [14] Z. Chen, L. Gao, S. Ye, Q. Ding, J. Wu, *Chemical Communications*, **2012**, *48*, 3975-3977.
- [15] X. Pan, Y. Luo, J. Wu, *The Journal of Organic Chemistry*, **2013**, *78*, 5756-5760.
- [16] X. Yang, Y. Luo, Y. Jin, H. Liu, Y. Jiang, H. Fu, *RSC Advances*, **2012**, *2*, 8258-8261.
- [17] L.-R. Wen, X.-J. Jin, X.-D. Niu, M. Li, *The Journal of Organic Chemistry*, **2015**, *80*, 90-98.
- [18] X. Fan, M. Yan, Y. Wang, X. Zhang, *The Journal of Organic Chemistry*, **2015**, *80*, 10536-10547.
- [19] X. Li, M. Zhao, *The Journal of Organic Chemistry*, **2011**, *76*, 8530-8536.
- [20] W. Ma, K. Graczyk, L. Ackermann, *Organic Letters*, **2012**, *14*, 6318-6321.

- [21] J. Jie, H. Li, S. Wu, Q. Chai, H. Wang, X. Yang, *RSC Advances*, **2017**, 7, 20548-20552.
- [22] O. Daugulis, H.-Q. Do, D. Shabashov, *Accounts of Chemical Research*, **2009**, 42, 1074-1086.
- [23] J. C. Lewis, R. G. Bergman, J. A. Ellman, *Accounts of Chemical Research*, **2008**, 41, 1013-1025.
- [24] P. Nareddy, F. Jordan, M. Szostak, *ACS Catalysis*, **2017**, 7, 5721-5745.
- [25] A. Biffis, P. Centomo, A. Del Zotto, M. Zecca, *Chemical Reviews*, **2018**, 118, 2249-2295.
- [26] Y. Yang, J. Lan, J. You, *Chemical Reviews*, **2017**, 117, 8787-8863.
- [27] P. B. Arockiam, C. Bruneau, P. H. Dixneuf, *Chemical Reviews*, **2012**, 112, 5879-5918.
- [28] D. Alberico, M. E. Scott, M. Lautens, *Chemical Reviews*, **2007**, 107, 174-238.
- [29] C. Liu, J. Yuan, M. Gao, S. Tang, W. Li, R. Shi, A. Lei, *Chemical Reviews*, **2015**, 115, 12138-12204.
- [30] B. M. Rosen, K. W. Quasdorf, D. A. Wilson, N. Zhang, A.-M. Resmerita, N. K. Garg, V. Percec, *Chemical Reviews*, **2011**, 111, 1346-1416.
- [31] J. Yamaguchi, K. Muto, K. Itami, *European Journal of Organic Chemistry*, **2013**, 2013, 19-30.
- [32] M. Tobisu, N. Chatani, *Accounts of Chemical Research*, **2015**, 48, 1717-1726.
- [33] D. J. Weix, *Accounts of Chemical Research*, **2015**, 48, 1767-1775.
- [34] S. Z. Tasker, E. A. Standley, T. F. Jamison, *Nature*, **2014**, 509, 299-309.
- [35] W. Song, L. Ackermann, *Chemical Communications*, **2013**, 49, 6638-6640.
- [36] M. I. Lipschutz, T. D. Tilley, *Angewandte Chemie International Edition*, **2014**, 53, 7290-7294.
- [37] K. Amaike, K. Muto, J. Yamaguchi, K. Itami, *Journal of the American Chemical Society*, **2012**, 134, 13573-13576.
- [38] J. Canivet, J. Yamaguchi, I. Ban, K. Itami, *Organic Letters*, **2009**, 11, 1733-1736.
- [39] T. Yamamoto, K. Muto, M. Komiyama, J. Canivet, J. Yamaguchi, K. Itami, *Chemistry – A European Journal*, **2011**, 17, 10113-10122.
- [40] H. Hachiya, K. Hirano, T. Satoh, M. Miura, *Organic Letters*, **2009**, 11, 1737-1740.
- [41] K. Muto, T. Hatakeyama, J. Yamaguchi, K. Itami, *Chemical Science*, **2015**, 6, 6792-6798.
- [42] H. Shiota, Y. Ano, Y. Aihara, Y. Fukumoto, N. Chatani, *Journal of the American Chemical Society*, **2011**, 133, 14952-14955.

-
- [43] A. Yokota, Y. Aihara, N. Chatani, *The Journal of Organic Chemistry*, **2014**, *79*, 11922-11932.
- [44] X. Wang, L. Zhu, S. Chen, X. Xu, C.-T. Au, R. Qiu, *Organic Letters*, **2015**, *17*, 5228-5231.
- [45] J.-N. Desrosiers, X. Wei, O. Gutierrez, J. Savoie, B. Qu, X. Zeng, H. Lee, N. Grinberg, N. Haddad, N. K. Yee, F. Roschangar, J. J. Song, M. C. Kozlowski, C. H. Senanayake, *Chemical Science*, **2016**, *7*, 5581-5586.
- [46] S. Dhiman, K. Pericherla, N. K. Nandwana, D. Kumar, A. Kumar, *The Journal of Organic Chemistry*, **2014**, *79*, 7399-7404.
- [47] M. N. Bhattacharjee, M. K. Chaudhuri, S. K. Ghosh, Z. Hiese, N. Roy, *Journal of the Chemical Society, Dalton Transactions*, **1983**, 2561-2562.
- [48] X.-h. Cai, B. Xie, *ARKIVOC*, **2015**, 184-211.
- [49] S. Z. Tasker, E. A. Standley, T. F. Jamison, *Nature*, **2014**, *509*, 299-309.
- [50] L. A. Hardegger, J. Habegger, T. J. Donohoe, *Organic Letters*, **2015**, *17*, 3222-3225.

CHAPTER 5

Conclusions

5.1 GENERAL CONCLUSIONS

Over the last few years, much attention has been focused towards the development of biologically relevant *N*-heterocycles such as indoles, quinolines, isoquinolines, and quinazolines with high molecular diversity from simple commercially available starting materials by minimizing the number of steps. Compound with *N*-heterocyclic framework exhibits a variety of biological activity, found in various natural products, marketed drugs and in material science. In this context, the development of highly complex molecules in a one-step by utilizing the multiple bond formation strategies, for example, multicomponent reaction, one-pot sequential, and domino or tandem reactions have gained importance in organic synthesis. Moreover, these strategies coupled with transition metal-catalyzed coupling reactions have become a most powerful tool for the synthesis of biological importance *N*-heterocyclic compound by the formation C-C and C-X (X= N, O, S) bond without pre-functionalization of starting precursor. Such protocols deliver potent *N*-heterocycles with tremendous regioselectivity, high molecular diversity, and functional group tolerance as compared to traditional organic synthesis. In this respect, we have developed a new methodology for the synthesis of *N*-heterocycles by exploring transition metal-catalysts.

The current thesis entitled “**Design and Synthesis of Quinoline and Quinazolinone Derivatives through Transition Metal-Catalyzed Cascade Protocols**” deals with the synthesis of selected *N*-heterocycles such as quinolines, imidazopyridine fused quinoline, quinazolines, and aza-fused isoquinolines by using transition metal-catalysts. The thesis is divided into four chapters (**Figure 5.1**).

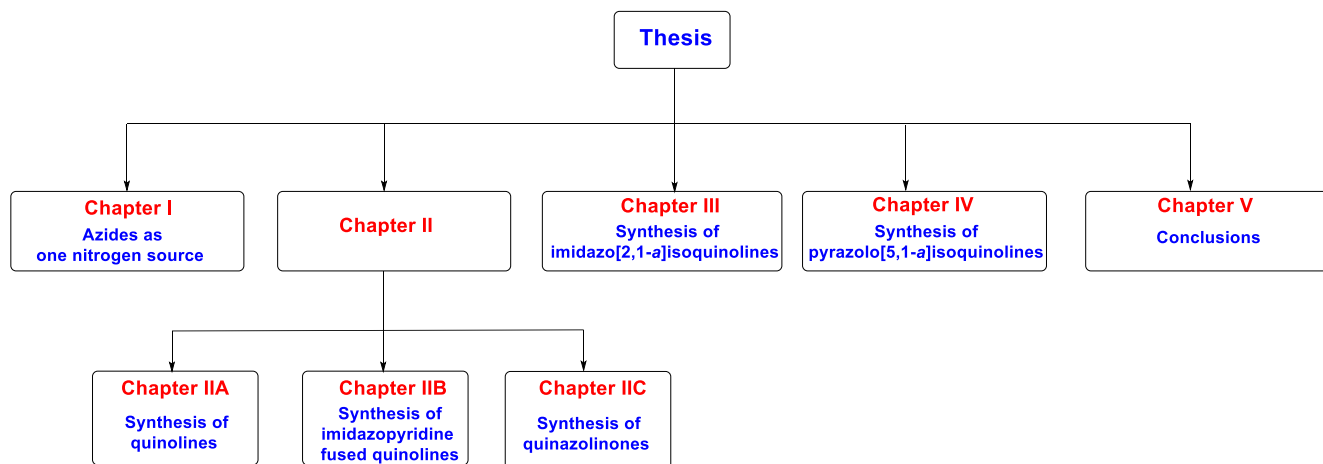


Figure 5.1: Systematically representation of thesis

5.2 SPECIFIC CONCLUSIONS

Chapter I: Synthesis of *N*-Heterocycles Using Azides as One Nitrogen Source: An Overview

In **Chapter, I** of the thesis, a brief review of azide as one nitrogen source in the synthesis of various nitrogen-containing heterocycles has been provided (**Figure 5.2**). Overall, this chapter discussed new innovative strategies towards the synthesis of *N*-heterocycles in the presence of transition metal-catalysts

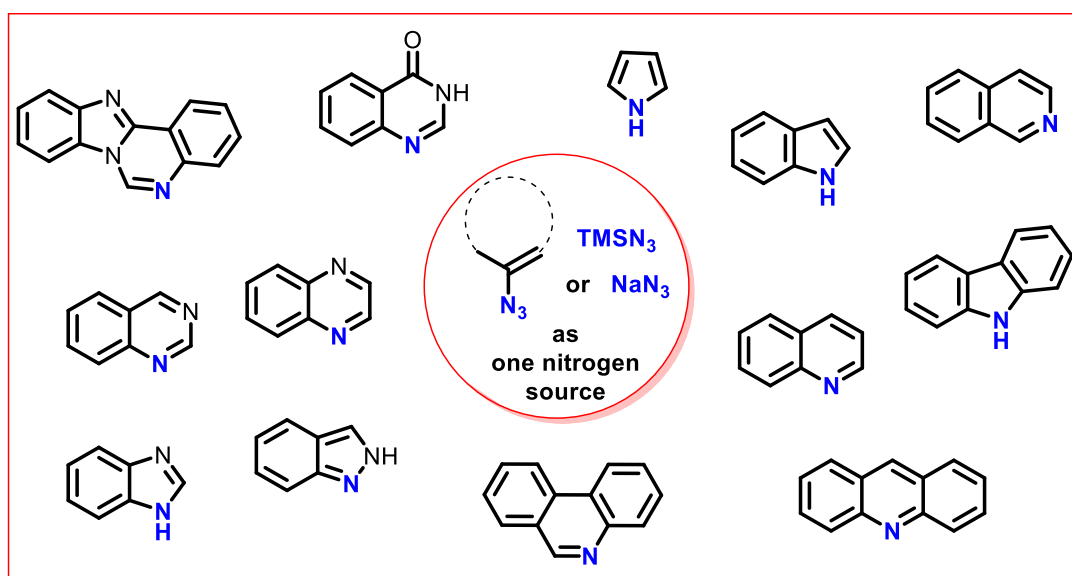


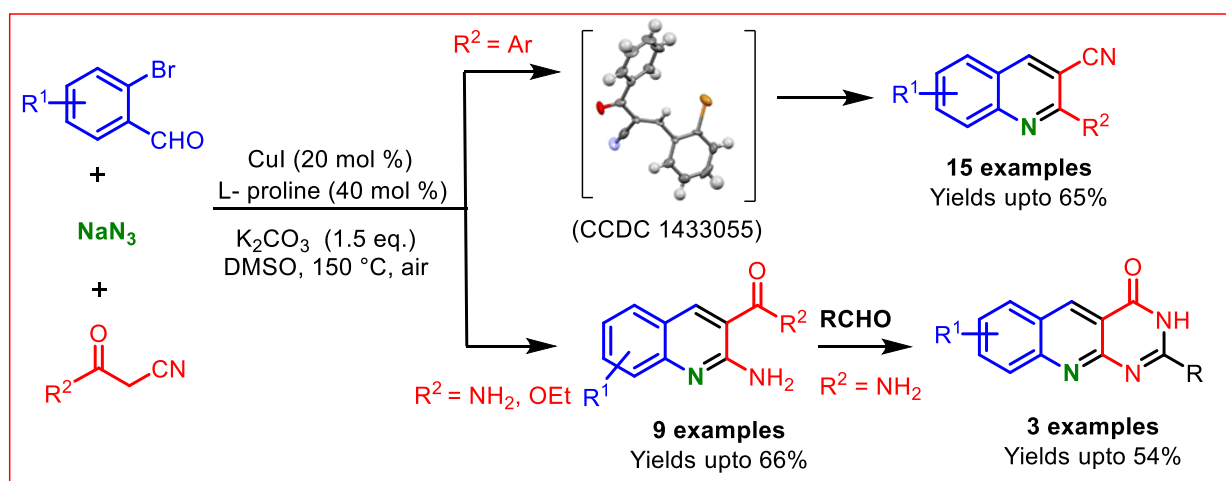
Figure 5.2: A Graphical representation to access various *N*-heterocycles using azides

Chapter II of the thesis describes the synthesis of *N*-heterocycles using sodium azide as one nitrogen source and divided into three parts.

Chapter IIA: Copper-Catalyzed One-Pot Synthesis of Quinoline Derivatives

Chapter IIA of the thesis deals with the synthesis of functionalized quinolines using transition metal-catalyst with some advance examples. The several methods for the synthesis of quinoline derivatives have been developed since extensively studies for antimalarial drugs. Most of these developed methods use *o*-aminocarbonyl compounds which are easily self-condensed over a time and restrict the molecular diversity in the molecules. In this chapter, we described synthesis of 2-aminoquinoline-3-carboxylates and 2-arylquinoline-3-carbonitriles by multicomponent reaction of 2-bromobenzaldehydes, active methylene nitriles and sodium azide as a nitrogen source in the

presence of copper-catalyst. The developed one-pot tandem three-component protocol displays broad substrate scope with good functional group tolerance and gives quinoline derivatives in moderate to good yield. We have performed a series of control experiments to elucidate the reaction pathway. The developed methodology was further utilized for one-pot synthesis of pyrimido[4,5-*b*]quinolin-4(3*H*)-ones in good yield *via* sequential addition of aldehydes (**Scheme 5.1**). All of the synthesized quinoline and pyrimido[4,5-*b*]quinolin-4(3*H*)-one derivatives were characterized by using spectroscopic analysis such as ^1H NMR, ^{13}C NMR and HRMS. The Knoevenagel adduct further confirmed by single crystal X-ray analysis.

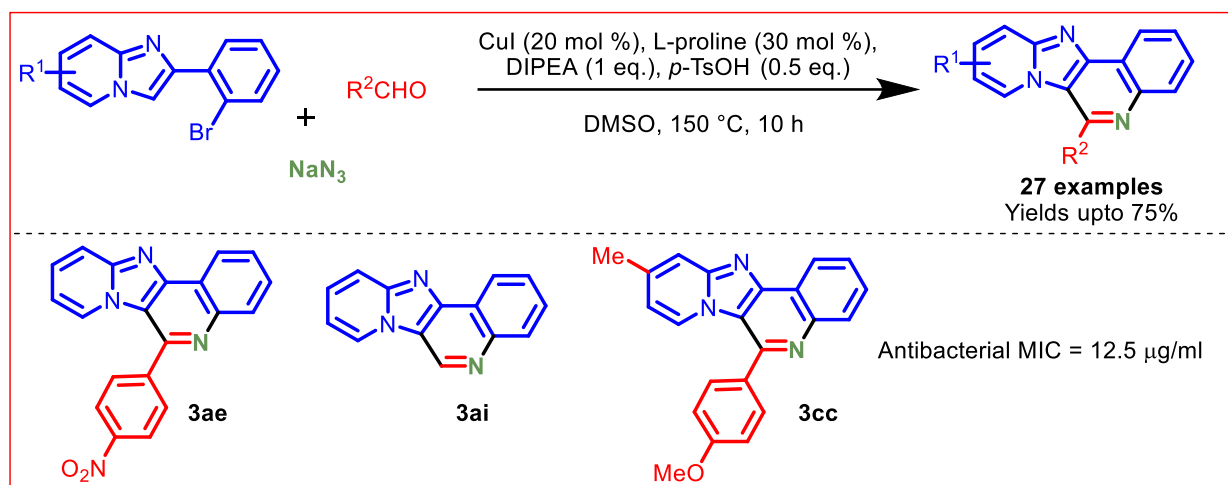


Scheme 5.1: Synthesis of 2-aminoquinoline-3-carboxylates and 2-arylquinoline-3-carbonitriles from 2-bromobenzaldehydes

Chapter IIB: One-Pot Synthesis of Pyrido[2,1:2,3]imidazo[4,5-*c*]quinoline Derivatives and their Antimicrobial Activity

Chapter IIB of the thesis described the simple and efficient protocol for the rapid synthesis of pyrido[2',1':2,3]imidazo[4,5-*c*]quinolines through Cu(I)-catalyzed three component, one-pot reaction of 2-(2-bromophenyl)imidazo[1,2-*a*]pyridines, aldehydes, and sodium azide. A series of twenty-seven compounds were prepared by varying different substituents on substrates in moderate to good yields (45-75%) (**Scheme 4.2**). All the synthesized compounds were evaluated for their *in-vitro* antibacterial activity against three Gram-negative bacteria *S. typhi*, *K. pneumoniae*, *P. putida* and two Gram-positive bacteria *B. cereus*, *S. aureus*. Compounds, **3ae**, **3ai** and **3cc**, exhibited moderate antibacterial activity against Gram-negative bacteria *S. typhi* and *P.*

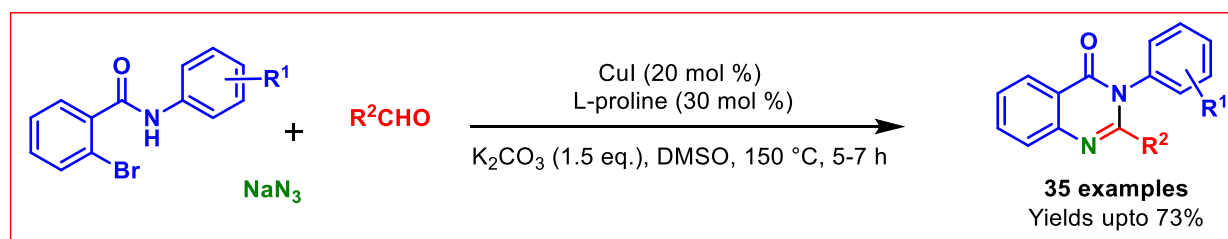
putida. All of the synthesized compounds were well characterized by ^1H NMR, ^{13}C NMR and HRMS spectroscopic analysis.



Scheme 5.2: Synthesis of imidazopyridine fused-quinoline derivatives

Chapter IIC: Cu(I)-Catalyzed Three-Component Cascade Synthesis of Quinazolin-4(3H)-Ones

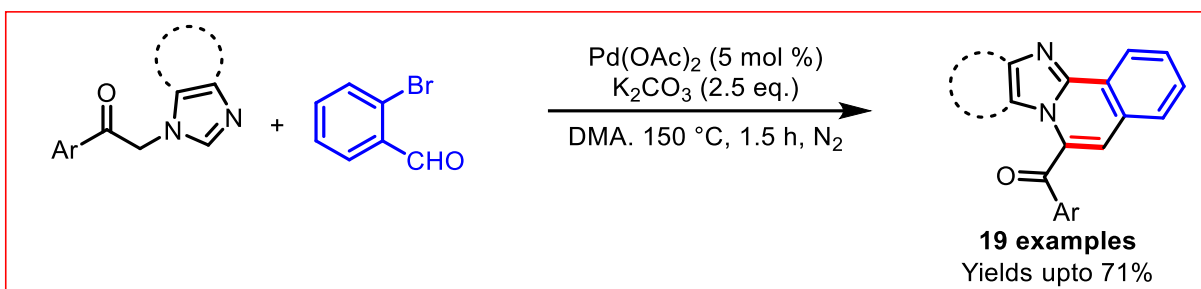
Encouraged from the valuable medicinal importance of quinazolinones, and the superficial biological profile of quinazolinone derivatives. **Chapter IIC** of the thesis involved the same methodology of the previous chapters and facilitates quinazolinone heterocycles (**Scheme 5.3**). The developed cascade reaction proposed to proceed through copper-mediated nucleophilic aromatic substitution with sodium azide, reductive amination, condensation with aldehydes, and C-N bond formation *via* intramolecular oxidative amidation followed by aerobic oxidation. Good functional group tolerance, mild condition, readily available starting materials, and user-friendly procedure makes this protocol practically good and attractive method for the synthesis of quinazolin-4(3H)-ones.



Scheme 5.3: Copper-catalyzed multicomponent synthesis of quinazolinone derivatives

Chapter III: Pd(II)-Catalyzed One-Pot Synthesis of Benzimidazo/Imidazo[1,2-*a*]isoquinolines

Chapter III of the thesis described a concise overview of the transition metal-catalyzed arylation strategies towards the synthesis of non-benzodiazepine drug azole-fused isoquinolines. Thereafter, this chapter focus on the synthesis of imidazole and benzimidazole-fused isoquinolines *via* Pd(II)-catalyzed intramolecular C-H arylation from 2-bromobenzaldehydes and 2-(1*H*-imidazol-1-yl/benzimidazolyl-1-yl)-1-arylethanones. The developed method proceeded initially *via* cross knoevenagel condensation of 2-(1*H*-imidazol-1-yl/benzimidazolyl-1-yl)-1-arylethanones with 2-bromobenzaldehyde followed by Pd(II)-catalyzed intramolecular C–H arylation. This approach offers series of biologically interest aroyl functionalized imidazo/benzimidazo[2,1-*a*]isoquinolines in moderate to good yields (**Scheme 5.4**). All the synthesized aroyl substituted imidazo/benzimidazo[2,1-*a*]isoquinolines were well characterized by ¹H NMR, ¹³C NMR and HRMS analysis.

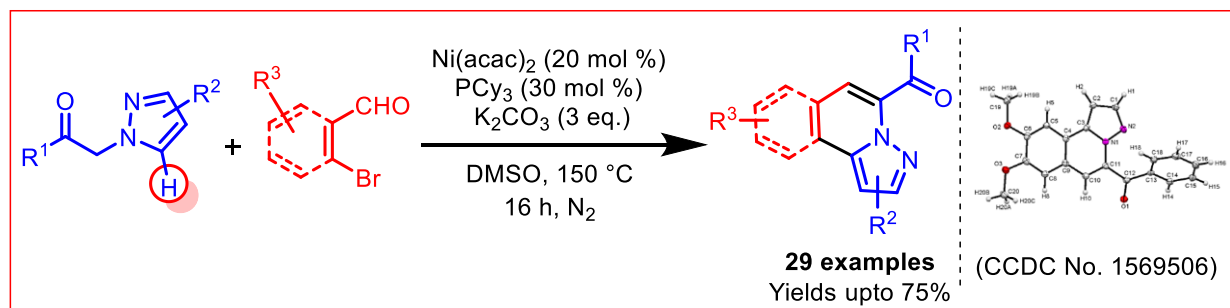


Scheme 5.4: Synthesis of benzimida/imidazole-fused isoquinolines *via* Pd-catalyzed arylation

Chapter IV: Nickel-Catalyzed One-Pot Cascade Synthesis of Pyrazolo[5,1-*a*]isoquinolines

Chapter IV deals with different synthetic routes for the synthesis of pyrazolo[5,1-*a*]isoquinoline scaffolds. The pyrazolo[5,1-*a*]isoquinolines is an azaheterocycle scaffold contains two bioactive isoquinoline and pyrazolo[1,5-*a*]pyridine framework, which is present in a significant number of pharmaceutically relevant molecules that exhibit remarkable biological activities. Later on, this chapter describes the significant exploration of nickel-catalyzed strategies towards the direct arylation of heterocycles. After that, disclose the synthesis of aroyl functionalized pyrazolo[5,1-*a*]isoquinolines by reaction of 1-aryl-2-(1*H*-pyrazol-1-yl)ethan-1-ones and 2-bromo aldehydes under Ni(II)-catalysis. This process involves. Initially Knoevenagel condensation followed by Ni(II)-catalyzed intramolecular arylation at C5 of pyrazole. The reaction pathway proposed by

conducting a series of control experiments and observing reaction mixture by ESI-MS analysis. The easily obtainable starting materials, simple procedure, and good yields make this protocol very practical for the assembly of biologically useful 5-aryl pyrazolo[5,1-*a*]isoquinolines (**Scheme 5.5**). All synthesized pyrazolo[5,1-*a*]isoquinoline derivatives were well characterized by detailed ¹H NMR, ¹³C NMR, and HRMS analysis. Also, a single X-ray crystal structure of one of the synthesized pyrazolo[5,1-*a*]isoquinoline compound further confirmed the structure of the product.



Scheme 5.5: Ni(II)-catalyzed synthesis of pyrazolo[5,1-*a*]isoquinolines *via* C-H arylation

5.3 Future scope of the research work

In recent years, transition metal-catalyzed cross oxidative coupling has become a more powerful tool in organic synthesis to access *N*-fused heterocycles from easily obtainable starting materials. The current thesis reflects the development of new strategy for the synthesis of biologically relevant quinolines, imidazo[1,2-*a*]pyridine-fused quinolines, quinazolines and azole-fused isoquinoline derivatives through transition metal-catalyzed cascade C-C and C-N bond formation. There exist a great scope for the synthesis of various complex quinoline and isoquinoline based-heterocycles by employing developed protocols. In this respect, target molecules given in **Figure 5.3** can be synthesized and can be evaluated for their biological activity such as anticancer, anti-HIV, antibacterial, and photophysical properties (**Figure 5.3**).

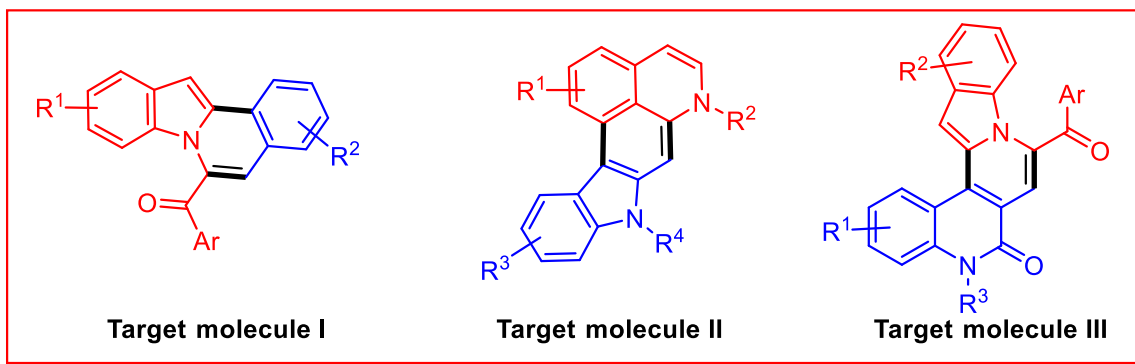


Figure 5.3: Some novel quinoline-base heterocycles

Appendices

List of Publications

1. **Shiv Dhiman**, Om P. S. Patel, Shahid Khan, Vikki N. Shinde, Sonam Jaswal, Manu R. Srivathsa, Prabhat N. Jha, and Anil Kumar, A straightforward TBHP-mediated synthesis of anthranilic acids from 2-arylindoles and their antibacterial activity, *Org. Biomol. Chem.* **2019**, *17*, 5962-5970.
2. **Shiv Dhiman**, Hitesh K. Saini, Nitesh K. Nandwana, Krishnan Rangan and Anil Kumar, Copper and palladium-catalyzed sequential reactions: one-pot synthesis of isoindolo[2,1-*b*]isoquinolin-7(5*H*)-ones, *Org. Biomol. Chem.* **2019**, *17*, 4281–4290.
3. Nitesh K. Nandwana, Rajnish P. Singh, Om P.S. Patel, **Shiv Dhiman**, Hitesh K. Saini, Prabhat N. Jha, and Anil Kumar, Design and synthesis of imidazo/benzimidazo[1,2-*c*]quinazoline derivatives and evaluation of their antimicrobial activity, *ACS Omega* **2018**, *3*, 16338–16346.
4. Raghuram Gujjarappa, Suvik K. Maity, Chinmoy K. Hazra, Nagaraju Vodnala, **Shiv Dhiman**, Anil Kumar, Uwe Beifuss, and Chandi C. Malakar, Divergent synthesis of quinazolines using organocatalytic domino strategies under aerobic conditions, *Eur. J. Org. Chem.* **2018**, 4628–4638.
5. **Shiv Dhiman**, Vikki N. Shinde, Krishnan Rangan, Dalip Kumar, and Anil Kumar, Synthesis of imidazopyridine-fused indoles *via* one-pot sequential Knoevenagel condensation and cross dehydrogenative coupling, *Org. Biomol. Chem.* **2018**, *16*, 6123–6132.
6. **Shiv Dhiman**, Nitesh K. Nandwana, Hitesh K. Saini, Krishnan Rangan, Katherine N. Robertson, Mukund Jha, Dalip Kumar, and Anil Kumar, Nickel-catalyzed tandem Knoevenagel condensation and intramolecular direct arylation: synthesis of pyrazolo[5,1-*a*]isoquinoline derivatives, *Adv. Synth. Catal.* **2018**, *360*, 360, 1973–1983.
7. **Shiv Dhiman**, Steven Rhodes, Dalip Kumar, Anil Kumar, and Mukund Jha, Copper-catalyzed tandem imine formation, Sonogashira coupling and intra-molecular hydroamination: a facile synthesis of 3-aryl- γ -carboline, *ChemistrySelect* **2017**, *2*, 8922–8926.
8. **Shiv Dhiman**, Nitesh K. Nandwana, Shreemala Dhayal, Hitesh K. Saini, Dalip Kumar, and Anil Kumar, A facile synthesis of quinazolin-4(3*H*)-ones *via* copper-catalyzed one-pot, three-component tandem reaction, *ChemistrySelect* **2017**, *2*, 8016–8019.

9. Mukund Jha, **Shiv Dhiman**, T. Stanley Cameron, Dalip Kumar, and Anil Kumar, Au-catalyzed synthesis of thiopyrano[2,3-*b*]indoles featuring tandem rearrangement and hydroarylation, *Org. Lett.* **2017**, 19, 2038–2041.
10. Hitesh K. Saini, Nitesh K. Nandwana, **Shiv Dhiman**, and Anil Kumar, Sequential copper-catalyzed Sonogashira coupling, hydroamination and palladium-catalyzed intramolecular direct arylation: synthesis of azepino-fused isoindolinones, *Eur. J. Org. Chem.* **2017**, 7277–7282.
11. Nitesh K. Nandwana, **Shiv Dhiman**, Hitesh K. Saini, Indresh Kumar and Anil Kumar, Synthesis of quinazolinones, imidazo[1,2-*c*]quinazolines and imidazo[4,5-*c*]quinolines through tandem reductive amination of aryl halides and oxidative amination of C(sp³)-H bond, *Eur. J. Org. Chem.* **2017**, 514–522.
12. **Shiv Dhiman**, Hitesh K. Saini, Nitesh K. Nandwana, Dalip Kumar and Anil Kumar, Copper-catalyzed synthesis of quinoline derivatives *via* tandem Knoevenagel condensation, amination and cyclization, *RSC Adv.* **2016**, 6, 23987–23994.
13. Nitesh K. Nandwana, **Shiv Dhiman**, Ganesh M. Shelke and Anil Kumar, Copper-catalyzed tandem Ullmann type C–N coupling and dehydrative cyclization: synthesis of imidazo[1,2-*c*]quinazolines, *Org. Biomol. Chem.* **2016**, 14, 1736-1741.
14. Hitesh Kumar Saini, **Shiv Dhiman**, Kasiviswanadharaju Pericherla, and Anil Kumar, Synthesis of imidazo[1,2-*f*]phenanthridines through palladium-catalyzed intramolecular C–C bond formation, *Synthesis* **2015**, 47, 3727–3732.
15. **Shiv Dhiman**, Kasiviswanadharaju Pericherla, Nitesh K. Nandwana, Dalip Kumar, and Anil Kumar, Synthesis of aza-fused isoquinolines through domino Cross-Aldol condensation and palladium-catalyzed intramolecular direct arylation, *J. Org. Chem.* **2014**, 79, 7399–7404.
16. **Shiv Dhiman**, Rajnish P. Singh, Prabhat N. Jha, Dalip Kumar, and Anil Kumar, Copper catalyzed multicomponent one-pot synthesis of pyrido[2',1':2,3]imidazo[4,5-*c*]quinoline derivatives and evaluation of their antimicrobial activity (Communicated).
17. **Shiv Dhiman**, Srijita P. Chowdhuri, Neha Meena, Benu Brata Das, and Anil Kumar, Design and synthesis of imidazopyridine fused quinolines and study of their leishmania parasite activity (Manuscript under preparation).

Org. Biomol. Chem. 2019, 17, 5962–5970

Organic & Biomolecular Chemistry



PAPER

[View Article Online](#)
[View Journal](#)

Cite this: DOI: 10.1039/c9ob00797k

A straightforward TBHP-mediated synthesis of 2-amidobenzoic acids from 2-arylindoles and their antimicrobial activity†

Om P. S. Patel,^{‡a} Shiv Dhiman,^{‡a} Shahid Khan,^b Vikki N. Shinde,^a Sonam Jaspal,^a Manu R. Srivathsa,^a Prabhat N. Jha^b and Anil Kumar^{ib**a}

A simple and highly efficient strategy has been developed for the synthesis of 2-amidobenzoic acids through the *tert*-butyl hydroperoxide (TBHP)-mediated oxygenation and sequential ring opening of 2-arylindoles in a one-pot fashion under metal-free aerobic conditions. The developed synthetic protocol is operationally simple, tolerates a wide range of functional groups, and is amenable to the gram-scale. Radical trapping experiments revealed that the reaction involves a radical pathway. The synthesized compounds (**2a–s**) were tested for *in vitro* antimicrobial activity. Among all screened compounds, **2d** showed the maximum antibacterial activity against *P. aeruginosa* (ZOI = 17 mm, MIC = 32 µg mL⁻¹) and compounds **2d** and **2p** showed the maximum (32 µg mL⁻¹) antifungal activity against *A. flavus* and *C. albicans*.

Received 7th April 2019,
Accepted 20th May 2019
DOI: 10.1039/c9ob00797k
rsc.li/obc

Org. Biomol. Chem. 2019, 17, 4281–4230

Organic & Biomolecular Chemistry



PAPER

[View Article Online](#)
[View Journal](#) | [View Issue](#)Cite this: *Org. Biomol. Chem.*, 2019, 17, 4281

Copper and palladium-catalyzed sequential reactions: one-pot synthesis of isoindolo[2,1-*b*]isoquinolin-7(5*H*)-ones†

Hitesh Kumar Saini,^{‡a} Shiv Dhiman,^{‡a} Nitesh Kumar Nandwana,^a Rangan Krishnan^b and Anil Kumar^{ib**a}

A highly efficient protocol has been developed for the synthesis of diversely substituted isoindolo[2,1-*b*]isoquinolin-7(5*H*)-ones through sequential Cu(i)-catalyzed Sonogashira coupling, intramolecular hydroamidation followed by palladium-catalyzed ligand-free Heck reaction. Good to excellent yields (41–94% were observed with excellent substrate scope and functional group tolerance. The developed method represents a practical strategy for the construction of bioactive isoindolo[2,1-*b*]isoquinolin-7(5*H*)-ones.

Received 21st February 2019,
Accepted 26th March 2019
DOI: 10.1039/c9ob00440h
rsc.li/obc

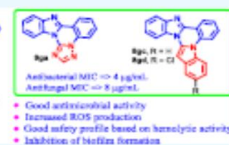
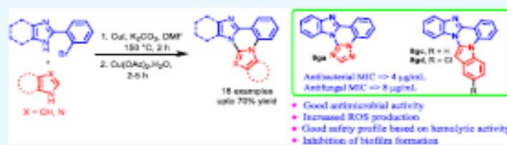
Design and Synthesis of Imidazo/Benzimidazo[1,2-c]quinazoline Derivatives and Evaluation of Their Antimicrobial Activity

Nitesh Kumar Nandwana,[†] Rajnish Prakash Singh,[‡] Om P. S. Patel,[†] Shiv Dhiman,[†] Hitesh Kumar Saini,[†] Prabhat N. Jha,[‡] and Anil Kumar^{*,†,‡}[†]Department of Chemistry and [‡]Department of Biological Sciences, Birla Institute of Technology and Science, Pilani 333031, Rajasthan, India

Supporting Information

ABSTRACT: A new class of fused quinazolines has been designed and synthesized via copper-catalyzed Ullmann type C–N coupling followed by intramolecular cross-dehydrogenative coupling reaction in moderate to good yields. The synthesized compounds were tested for in vitro antibacterial activity against three Gram negative (*Escherichia coli*, *Pseudomonas putida*, and *Salmonella typhi*) and two Gram positive (*Bacillus subtilis*, and *Staphylococcus aureus*) bacteria.

Among all tested compounds, 8ga, 8gc, and 8gd exhibited promising minimum inhibitory concentration (MIC) values (4–8 $\mu\text{g}/\text{mL}$) for all bacterial strains tested as compared to the positive control ciprofloxacin. The synthesized compounds were also evaluated for their in vitro antifungal activity against *Aspergillus niger* and *Candida albicans* and compounds 8ga, 8gc, and 8gd having potential antibacterial activity also showed pronounced antifungal activity (MIC values 8–16 $\mu\text{g}/\text{mL}$) against both strains. The bactericidal assay by propidium iodide and live–dead bacterial cell screening using a mixture of acridine orange/ethidium bromide (AO/Et-Br) showed considerable changes in the bacterial cell membrane, which might be the cause or consequence of cell death. Moreover, the hemolytic activity for most potent compounds (8ga, 8gc, and 8gd) showed their safety profile toward human blood cells.



- Good antibacterial activity
- Increased ROS production
- Good safety profile based on hemolytic activity
- Inhibition of biofilm formation

Nitrogen Heterocycles

Divergent Synthesis of Quinazolines Using Organocatalytic Domino Strategies under Aerobic Conditions

Raghuram Gujjarappa,^{[a][‡]} Suvik K. Maity,^{[a][‡]} Chinmoy K. Hazra,^[b] Nagaraju Vodnala,^[a] Shiv Dhiman,^[c] Anil Kumar,^[c] Uwe Beifuss,^[d] and Chandi C. Malakar^{*,[a]}

Abstract: An easy and efficient organocatalytic approach to the synthesis of 2-substituted quinazolines is described based on the reaction between 2-aminobenzylamines and aldehydes or alcohols or amines. Three organocatalytic platforms were investigated, using 3-nitropyridine, pyridine *N*-oxide, and vitamin B₃. Having established the new catalytic systems, the tandem transformations of 2-aminobenzylamines to give substituted quinazolines were achieved in excellent yields and with a broad substrate scope, with no formation of toxic side-products. The investigated conditions are not restricted to the use of alde-

hydes; the protocol also works well with alcohols or amines as substrates. These are oxidized in situ to the corresponding aldehydes to achieve the successful transformation. A mechanistic proposal has been drawn up based on control experiments. We found that under aerobic conditions, catalytic amounts of H₂O₂ can be generated; this plays a key role in the efficacy of the described approach. The green chemistry metrics of the developed method are also presented. The *E* factor of 0.18 mg/1 mg demonstrates that the reported method is an excellent complement to previous protocols.



Cite this: *Org. Biomol. Chem.*, 2018, 16, 6123

Synthesis of imidazopyridine-fused indoles via one-pot sequential Knoevenagel condensation and cross dehydrogenative coupling†

Vikki N. Shinde,^{‡a} Shiv Dhiman,^{‡a} Rangan Krishnan,^b Dalip Kumar^{†a} and Anil Kumar^{†*a}

A simple and efficient strategy for the synthesis of imidazopyridine-fused indoles has been developed that involves one-pot sequential Knoevenagel condensation of readily available active methylene azoles with *N*-substituted-1*H*-indole-3-carboxaldehydes or *N*-substituted-1*H*-indole-2-carboxaldehydes followed by palladium-catalyzed intramolecular cross dehydrogenative coupling reaction. A series of 36 derivatives was prepared by using this strategy. The products were obtained in moderate to excellent (32–94%) yields and showed broad substrate scope with tolerance of various functional groups and was amiable for gram scale preparation without problems.

Received 20th June 2018,
Accepted 3rd August 2018
DOI: 10.1039/c8ob01449c
rsc.li/obc



Nickel-Catalyzed Tandem Knoevenagel Condensation and Intramolecular Direct Arylation: Synthesis of Pyrazolo[5,1-*a*]-isoquinoline Derivatives

Shiv Dhiman,^a Nitesh Kumar Nandwana,^a Hitesh Kumar Saini,^a Dalip Kumar,^a Krishnan Rangan,^b Katherine N. Robertson,^c Mukund Jha,^d and Anil Kumar^{a,*}

^a Department of Chemistry, BITS Pilani, Pilani Campus, Pilani 333031, Rajasthan, India
E-mail: anilkumar@pilani.bits-pilani.ac.in

^b Department of Chemistry, BITS Pilani, Hyderabad Campus, Secunderabad 500078, Telangana, India

^c Department of Chemistry, Saint Mary's University, Halifax, NS, B3H 3C3, Canada

^d Department of Biology and Chemistry, Nipissing University, North Bay, ON, P1B 8L7, Canada

Received: November 28, 2017; Revised: February 23, 2018; Published online: March 23, 2018

† Supporting information for this article is available on the WWW under <https://doi.org/10.1002/adsc.201701519>

Abstract: A simple and efficient method for the synthesis of pyrazolo[5,1-*a*]isoquinoline derivatives has been developed using the nickel-catalyzed reaction of 1-aryl-2-(1*H*-pyrazol-1-yl)ethan-1-ones and 2-bromo aldehydes. The overall transformation involves tandem Knoevenagel condensation and intramolecular direct arylation *via* activation of the C5–H bond of the pyrazole ring. A series of 27 drug-like aryl-substituted pyrazolo[5,1-*a*]isoquinolines has been synthesized in moderate to good yields.

■ Organic & Supramolecular Chemistry

Copper-Catalyzed Tandem Imine Formation, Sonogashira Coupling and Intramolecular Hydroamination: A Facile Synthesis of 3-Aryl- γ -carbolines

Shiv Dhiman,^[a, b] Steven Rhodes,^[a] Dalip Kumar,^[b] Anil Kumar,^{*, [b]} and Mukund Jha^{*, [a]}

A one-pot, atom-economical multicomponent reaction of 2-bromoindole-3-carbaldehydes, alkynes and ammonia was developed in the presence of copper catalyst for the synthesis of a series of 3-aryl- γ -carboline derivatives in good to high yields. The developed reaction involved formation of imine followed by copper-catalyzed directed Sonogashira coupling and intramolecular hydroamination sequence of reactions. This multicomponent approach features mild reaction conditions and good functional group tolerance to access variety of 3-aryl γ -carbolines.

incorporate two privileged heterocycles, indole and pyridine, which elicit promising bioactivities.^[5] Among carbolines, γ -carboline has been shown to exhibit wide range of bioactivities such as antipsychotic,^[6] antiviral,^[7] antiallergic,^[8] antialzheimer^[9] and anticancer.^[10] Tetrahydro- γ -carboline selectively binds to human 5-HT_{5A} receptors which regulates the cardiovascular system^[11] and certain γ -carboline derivatives act as BET bromodomain inhibitor.^[12] Because of their importance in biological and medicinal field, development of simple and efficient protocols for the construction of carbolines and their derivatives under mild conditions is a continued area of

■ Organic & Supramolecular Chemistry

A Facile Synthesis of Quinazolin-4(3H)-ones via Copper-Catalyzed One-Pot, Three-Component Tandem Reaction

Shiv Dhiman, Nitesh K. Nandwana, Shreemala Dhayal, Hitesh K. Saini, Dalip Kumar, and Anil Kumar^{*, [a]}

A simple and convenient one-pot, three-component tandem reaction has been developed for the synthesis of substituted quinazolin-4(3H)-ones using Cu/L-proline as catalytic system. A series of 35 quinazolin-4(3H)-ones was synthesized in good to high yield. The method involves copper-catalyzed double C–N

coupling, reductive amination, condensation, cyclization and aerobic oxidation. Good functional group tolerance, mild reaction condition, readily available starting materials and user friendly procedure makes this protocol practically good and attractive method for the synthesis of quinazolin-4(3H)-ones.

Au-Catalyzed Synthesis of Thiopyrano[2,3-*b*]indoles Featuring Tandem Rearrangement and Hydroarylation

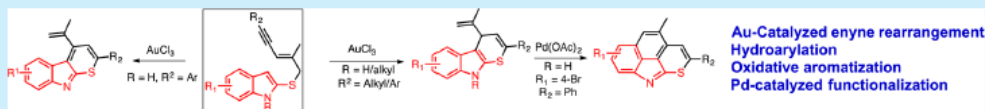
Mukund Jha,^{*,†} Shiv Dhiman,^{†,‡} T. Stanley Cameron,[§] Dalip Kumar,[‡] and Anil Kumar^{‡,§}

[†]Department of Biology and Chemistry, Nipissing University, North Bay, ON P1B 8L7, Canada

[‡]Department of Chemistry, Birla Institute of Technology and Science, Pilani, Pilani 333031, India

[§]Department of Chemistry, Dalhousie University, Halifax, NS B3H 4J3, Canada

Supporting Information



ABSTRACT: Gold(III)-catalyzed synthesis of 14- π electron heteroaromatic thiopyrano[2,3-*b*]indole is reported using conjugated enyne tethered indole sulfides, featuring skeletal rearrangement conjoined with intramolecular hydroarylation (via C3–H functionalization of the indole core) and oxidative aromatization. Subsequent Pd-catalyzed C–C coupling resulted in a 16- π electron heteroaromatic isothiochromeno[1,8,7-*bcd*]indole.

Sequential Reaction

Sequential Copper-Catalyzed Sonogashira Coupling, Hydroamination and Palladium-Catalyzed Intramolecular Direct Arylation: Synthesis of Azepino-Fused Isoindolinones

Hitesh Kumar Saini,^[a] Nitesh Kumar Nandwana,^[a] Shiv Dhiman,^[a] Krishnan Rangan,^[b] and Anil Kumar^{*[a]}

Abstract: A sequential copper-catalyzed Sonogashira coupling followed by an intramolecular hydroamination and palladium-catalyzed intramolecular direct arylation reaction was developed to provide a convenient and modular approach for the synthesis of useful azepino-fused isoindolinones. Nineteen azepino-fused isoindolinones were prepared in moderate to

high (22–90 %) yields. The developed protocol tolerated various functional groups and involved the formation of one carbon–nitrogen and two carbon–carbon bonds in a one-pot fashion. The palladium-catalyzed intramolecular direct arylation step involved formation of an unusual eight-membered palladacycle.

Nitrogen Heterocycles

Synthesis of Quinazolinones, Imidazo[1,2-*c*]quinazolines and Imidazo[4,5-*c*]quinolines through Tandem Reductive Amination of Aryl Halides and Oxidative Amination of C(sp³)-H Bonds

Nitesh Kumar Nandwana,^[a] Shiv Dhiman,^[a] Hitesh Kumar Saini,^[a] Indresh Kumar,^[a] and Anil Kumar*^[a]

Abstract: A tandem multicomponent approach has been described for the synthesis of quinazolinones, imidazo[1,2-*c*]quinazolines and imidazo[4,5-*c*]quinolines. The reaction involves a copper-catalyzed reductive amination through azidation followed by reduction and oxidative amination of C(sp³)-H bonds of *N,N*-dimethylacetamide in the presence of TBHP (*tert*-butyl-

hydroperoxide) as oxidant. The method uses the easily available sodium azide as a nitrogen source and DMA (*N,N*-dimethylacetamide) as a one-carbon source for the synthesis of these *N*-fused heterocycles in good to excellent yields. The reaction can also be used for gram-scale synthesis.

RSC Advances



PAPER



Cite this: RSC Adv., 2016, 6, 23987

Received 10th February 2016
Accepted 17th February 2016

DOI: 10.1039/c6ra03798d

www.rsc.org/advances

Copper-catalyzed synthesis of quinoline derivatives via tandem Knoevenagel condensation, amination and cyclization†‡

Shiv Dhiman, Hitesh Kumar Saini, Nitesh Kumar Nandwana, Dalip Kumar and Anil Kumar*

A novel regioselective synthesis of 2-aminoquinolines and 2-arylquinoline-3-carbonitriles is described via copper-mediated tandem reaction. Formation of substituted quinolines involves Knoevenagel condensation of *ortho*-bromobenzaldehyde with active methylene nitriles followed by copper-catalyzed reductive amination and intramolecular cyclization.



Cite this: *Org. Biomol. Chem.*, 2016, 14, 1736

Copper-catalyzed tandem Ullmann type C–N coupling and dehydrative cyclization: synthesis of imidazo[1,2-*c*]quinazolines†

Nitesh K. Nandwana, Shiv Dhiman, Ganesh M. Shelke and Anil Kumar*

A simple and efficient one-pot protocol has been demonstrated for the synthesis of imidazo[1,2-*c*]quinazoline derivatives through a copper catalyzed tandem reaction between substituted 2-(2-bromophenyl)-1*H*-imidazoles and formamide. The synthetic protocol involves initial Ullmann-type C–N coupling followed by intramolecular dehydrative cyclization. The method uses readily available 2-(2-bromophenyl)-1*H*-imidazoles as the starting materials to afford imidazo[1,2-*c*]quinazolines in moderate to good yields and provided 610 mg (71%) yield of **3a** from a gram scale reaction.

Received 2nd December 2015,

Accepted 22nd December 2015

DOI: 10.1039/c5ob02469b

www.rsc.org/obc

Synthesis 2015, 47, 3727–3732

Synthesis

H. K. Saini et al.

Paper

Synthesis of Imidazo[1,2-*f*]phenanthridines through Palladium-Catalyzed Intramolecular C–C Bond Formation

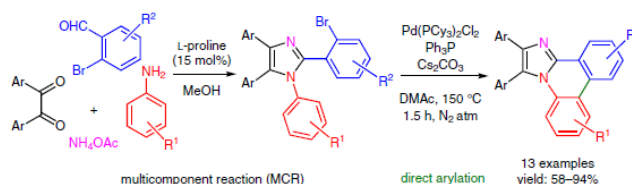
Hitesh Kumar Saini

Shiv Dhiman

Kasiviswanadharaju Pericherla

Anil Kumar*

Department of Chemistry, Birla Institute of Technology and Science, Pilani, Rajasthan 333031, India
anilkumar@pilani.bits-pilani.ac.in



Received: 25.05.2015

Accepted after revision: 27.07.2015

Published online: 28.08.2015

DOI: 10.1055/s-0035-1560177; Art ID: ss-2015-z0329-op

Abstract A simple and convenient approach is developed for the synthesis of the imidazo[1,2-*f*]phenanthridine framework via post-functionalization of imidazoles obtained through four-component reactions of 1,2-dicarbonyl compounds, anilines, aldehydes and ammonium acetate. The methodology involves palladium-catalyzed direct arylation through sp^2 C–H activation. The reported procedure delivers good to high yields of imidazo[1,2-*f*]phenanthridine derivatives (58–94%) starting from readily available precursors.

Key words C–H activation, C–C bond formation, direct arylation, palladium catalysis, imidazo[1,2-*f*]phenanthridines

arynes with haloarenes, intramolecular direct arylations⁷ and tandem couplings of dihalo-olefins with azoles^{8b} are examples of excellent methods for the synthesis of these fused heterocycles. The synthesis of imidazo[1,2-*f*]phenanthridines has also been achieved by palladium-catalyzed cascade reactions of dihalobenzenes with 2-phenylimidazoles through N–H/C–H bonding (Scheme 1, a, b).^{2a,8} Specifically, the synthesis of 2,3-diarylimidazo[1,2-*f*]phenanthridines was achieved through intramolecular Buchwald coupling (Scheme 1, c).^{2d} It is worth mentioning that the synthetic precursors for this process have been obtained in two steps, in which a palladium-catalyzed Suzuki–Miyaura reaction was involved as one of the key reactions. The synthetic methods developed for heteroaryl fused phenanthri-

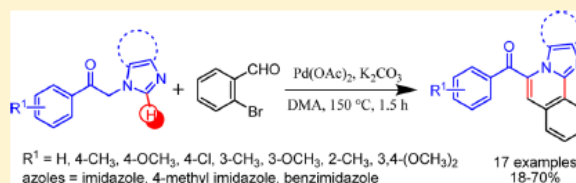
Synthesis of Aza-Fused Isoquinolines through Domino Cross-Aldol Condensation and Palladium-Catalyzed Intramolecular Direct Arylation

Shiv Dhiman, Kasiviswanadharaju Pericherla, Nitesh K. Nandwana, Dalip Kumar, and Anil Kumar*

Department of Chemistry, Birla Institute of Technology and Science, Pilani, 333031 Rajasthan, India

Supporting Information

ABSTRACT: A straightforward method has been developed for the synthesis of aryl-substituted imidazo-/benzimidazo-fused isoquinolines. The cascade reaction proceeds via a cross-aldol condensation of 2-(1*H*-imidazol-1-yl/benzimidazolyl-1-yl)-1-arylethanones and 2-bromobenzaldehyde followed by palladium-catalyzed intramolecular C–H functionalization. This approach offers a simple and efficient alternative one-pot protocol for the assembly of imidazo/benzimidazo[2,1-*a*]isoquinolines in moderate to good yields.



List of Poster Presented in Conferences/Workshop

[A-3]

1. **Shiv Dhiman**, Mukund Jha, Dalip Kumar, and Anil Kumar, Gold-mediated synthesis of thiopyrrolo[2,3-*b*]indoles from indoline-2-thione involving tandem rearrangement and hydroarylation, Contemporary Facets in Organic Synthesis (CFOS-2017), Department of Chemistry, IIT-Roorkee, Roorkee, Uttarakhand, India, Dec 22-24, 2017. (RSC Sponsered Best Poster Award)
2. **Shiv Dhiman**, Shreemala Dayal, Dalip Kumar, Rajnish Singh, P.N Jha, and Anil Kumar, Copper-catalyzed multicomponent one-pot synthesis of pyrido[2',1':2,3]imidazo[4,5-*c*]quinoline derivatives and evaluation of their antibacterial activity, International Conference on Frontiers at the Chemistry-Allied Science Interface (FCASI-2016), Department of Chemistry, University of Rajasthan, Jaipur, Rajasthan, India, April 25-26, 2016. (Best Poster Award)
3. **Shiv Dhiman**, Hitesh K. Saini, Nitesh. K. Nandwana, Dalip Kumar and Anil Kumar, One-pot copper catalyzed tandem Knoevenagel condensation, amination and cyclization: a facile regioselective synthesis of quinoline derivatives, National conference on New Frontiers in Chemistry-From fundamental to Application (NFCFA-2015), Department of Chemistry, BITS Pilani KK Birla Goa Campus, India, Dec 18-19, 2015.
4. **Shiv Dhiman**, Hitesh Kumar Saini, Nitesh K. Nandwana, Dalip Kumar and Anil Kumar, One-pot copper catalyzed tandem Knoevenagel condensation, amination and cyclization: a facile regioselective synthesis of quinoline derivatives, International Conference on Nascent Developments in Chemical Science: Oppertunities for Academia-Industry Collabratorion (NDCS-2015), Department of Chemistry, BITS Pilani, Pilani Campus, Rajasthan, India, Oct 16-18, 2015. (RSC Sponsered Best Poster award)
5. **Shiv Dhiman**, Kasiviswanadharaju Pericherla, Dalip Kumar and Anil Kumar, Palladium-catalyzed Cross Aldol/intramolecular direct arylation: an easy access to aza-fused isoquinoline, International Symposium on Recent Advances in Medicinal Chemistry 2014 (ISRAM-2014), NIPER, S.A.S Nagar (Mohali), Punjab, India, Sept 8-10, 2014.
6. **Shiv Dhiman**, Kasiviswanadharaju Pericherla, Dalip Kumar, and Anil Kumar, Synthesis of imidazo[2,1-*a*]isoquinoline derivatives *via* domino Aldol condensation and palladium catalyzed C-H bond functionalization, 20th Indian Society of Chemist and Biologist

International conference (ISCB-2014), Department of Chemistry, University of Delhi, Delhi India, March 1-4, 2014.

7. National Workshop on Nuclear Magnetic Resonance (**NMR**) Spectroscopy organized by the Sophisticated Analytical Instrument Facility (SAIF) at IIT Madras, Chennai, India, Feb 25-27, 2016.

Brief Biography of the Candidate

[A-4]

Shiv Dhiman was born in Punjab, India. He obtained his B.Sc (Industrial Chemistry) from Guru Nanak Khalsa College, Yamunanagar, India in 2007 and completed his M.Sc. (specialization in Pharmaceutical Chemistry) from the same institute in 2009. He secured 3rd in B.Sc and 2nd in M.Sc, at Guru Nanak Khalsa College. After his postgraduation studies, he worked as project fellow for six months at Department of Chemistry, Guru Nanak Dev University, Amritsar, under the supervision



of Prof. Subodh Kumar. He joined Jubilant Chemsys Ltd., Noida, India in June 2010, where he received best employee award in May 2011 and On Spot Chemsy'ian Champ award in June 2013. In Nov 2013, he joined as project fellow in Department of Chemistry, BITS Pilani, Pilani Campus as Ranbaxy Sponsored Project Fellow under the guidance of Prof. Anil Kumar and Prof. Dalip Kumar and later registered for the PhD program in Jan 2014. During his Ph.D tenure he visited Prof. Mukund Jha research lab at Nipissing University, ON, Canada from June 2016 – Dec 2016. He received Council of scientific and Industrial Research-Senior Research Fellow (CSIR-SRF) in Jan 2018. He has also qualified the GATE-2018 held by IIT, India in March 2018. He has published thirteen research paper in the peer-reviewed international journals and presented research works in two national and four international conferences in form of poster. Mr. Dhiman has received three best poster presentation award in national/international conferences (NDCS-2015, FCASI-2016, and CFOS-2017). He has attended one national workshop on Nuclear Magnetic Resonance (NMR) Spectroscopy at IIT-Madras, Chennai, India.

His research interests include medicinal chemistry, development of new reaction methodologies for the synthesis of *N*-fused heterocyclic molecules like quinolines, quinazolines, indoles and imidazopyridines by forming C-C and C-N bonds using transition metal-catalyzed C-H activation, tandem, and multicomponent reactions.

Brief Biography of the Supervisor

[A-5]

Dr. Anil Kumar is Professor of Chemistry at the Birla Institute of Technology and Science, Pilani. He obtained his PhD degree from Department of Chemistry, University of Delhi, India, under the guidance of Professor S. M. S. Chauhan in 2004. After a two year of postdoctoral fellow at Department of Biomedical and Pharmaceutical Sciences, University of Rhode Island, Kingston, USA in Prof. Keykavous Parang research group, he joined Department of Chemistry, Birla Institute of Technology and Science, Pilani, Pilani Campus, India, as Assistant Professor in 2006 and was promoted to Associate Professor in February 2013 and to full Professor in August 2018. He served as Associate Dean, Work Integrated Learning Programmes (WILP) (2014 – 2018) and Head of Department of Chemistry (2014 – 2016). Prof. Kumar has visited University of Rhode Island, Kingston, Chapman University, Irvine, USA, and Acadia University, Wolfville, Canada.



Prof. Kumar is recipient of Prof. S. Venkateswaran Faculty Excellence Award from BITSAA for 2017, Harrison McCain Foundation award from Acadia University, Canada for 2012, ISCB Young Scientist award in Chemical Sciences from Indian Society of Chemists and Biologists, Lucknow for 2013 and Dr. Aravind Kumar memorial award from Indian Council of Chemist for 2014. He has 20 year of research experience and 13 year of teaching experience. He has published over 150 research papers in international journals of repute in the area of synthetic organic chemistry, green chemistry and medicinal chemistry and contributed two book chapter and one US patent. He has participated in several national and international symposia/conferences and delivered more than 40 invited lectures. He has guided nine PhD students as supervisor and three students as co-supervisor. Currently, six PhD students, one NPDF research fellow and one INSPIRE faculty are working with him. He is member of editorial advisory board for The Open Catalysis Journal. He has completed four sponsored research projects as Principle Investigator from DST, CSIR and UGC and one as Co-PI sponsored by Ranbaxy. He has also served as a reviewer for several journals. He is life member of Chemical Research Society of India, Bangalore; Indian Society of Chemists and Biologists, Lucknow and Indian Council of Chemists, Agra.

His research interest lies in transition metal-catalyzed C–H activation/functionalization, tandem reactions, multicomponent reaction, development of new reaction methodology, green chemistry, medicinal chemistry, and design and synthesis of task-specific ionic liquids.

Brief Biography of the Co-Supervisor

[A-6]

Dr. Dalip Kumar is a Professor of Chemistry at Department of Chemistry, Birla Institute of Technology and Science, Pilani. He obtained his Ph.D degree from Department of Chemistry, Kurukshetra University, Kurukshetra, Haryana, India in 1997 under the supervision of Prof. Shiv P. Singh. During his doctoral studies Prof. Kumar worked around of heterocyclic chemistry. He was postdoctoral fellow (1997 – 1999) at Sam Houston State University, TX, USA in Prof. Rajender S. Varma research group. He was also postdoctoral associated (1999 –



2000) in Prof. Sean M. Kerwin, College of Pharmacy, University of Texas, Austin, TX, USA. He joined BITS Pilani, Pilani campus, as a lecturer in Dec 2000. In Dec 2002, he joined, University of Maryland, College Park, MD, USA as a Research Associate. In 2004, Prof. Kumar re-joined as an Assistant Professor at Department of Chemistry, BITS Pilani, Pilani campus. He was promoted to professor in year 2012. He served as Head of Department of Chemistry from 2004 to 2013.

Prof. Kumar is recipient of Honorary Diploma for Scientific Achievements and International Scientific Collaboration by Russian International Charitable Foundation “Scientific Partnership”, Moscow, Russia in March 2013. He received the Prof. R. D. Desai 80th Birthday Commemoration Medal and Prize from Indian Chemical Society in 2015. Prof. Kumar has been involved in research for the last 20 years and in teaching for 13 years. He has published over 120 research paper in the peer-reviewed journals in the area of medicinal chemistry and synthetic organic chemistry. Prof. Kumar has guided nine Ph.D students and currently he is supervising five Ph.D. students. He has one US patent, one Indian patent and successfully completed several sponsored research projects from DRDO, DST, DBT, CSIR, UGC, and DST-JSPS (Indo-Japan) project. Currently, he has two Government of India sponsored projects from CSIR and DST and a collaborative industrial project from Ranbaxy Research Laboratory Ltd.

He is an Associate Editor of Chemistry & Biology Interface (CBI) Journal published by Indian Society of Chemists and Biologists (ISCB), Lucknow. Prof. Kumar is life member of Indian Chemical Society, Indian Society of Chemists and Biologists, and Indian Council of Chemists. His research area include the synthesis of porphyrin and indole derived potential anticancer agents, functionalization of quinoline derivatives by employing organoiodine reagents and transition metal-catalysts.